Arthritis & Rheumatology

An Official Journal of the American College of Rheumatology
www.arthritisrheum.org and wileyonlinelibrary.com

Cover design: Todd Machen

This journal is printed on acid-free paper.

Arthritis & Rheumatology

An Official Journal of the American College of Rheumatology
www.arthritisrheum.org and wileyonlinelibrary.com

VOLUME 74 • February 2022 • NO. 2

Cover image: The figure on the cover (from Seoane-Collazo et al, pages 212–222) is an infrared thermal image of the interscapular brown adipose tissue area of a standard diet–fed rat that was treated intradermally with Freund's complete adjuvant and injected stereotaxically with an adenovirus encoding a constitutively active isoform of AMP-activated protein kinase α1 (AMPKα1-CA) within the ventromedial nucleus of the hypothalamus (VMH). "Cold colors" (purple, blue, and green) represent lower temperature and "warm colors" (yellow and red) represent higher temperature (for example, in the interscapular brown adipose tissue area). Stereotaxic treatment with the AMPKα1-CA adenovirus promoted a decrease in the brown adipose tissue temperature when compared with rats treated intradermally with Freund's complete adjuvant and injected stereotaxically with an adenovirus encoding green fluorescence protein within the VMH.

Arthritis & Rheumatology

An Official Journal of the American College of Rheumatology
www.arthritisrheum.org and wileyonlinelibrary.com

GENERAL INFORMATION

TO SUBSCRIBE

Institutions and Non-Members

Email: wileyonlinelibrary.com
Phone: (201) 748-6645
Write: Wiley Periodicals LLC
Attn: Journals Admin Dept UK
111 River Street
Hoboken, NJ 07030

Volumes 74, 2022:
Institutional Print Only: **Arthritis & Rheumatology and Arthritis Care & Research:** $2,603 in US, Canada, and Mexico; $2,603 outside North America
Institutional Online Only: $2,495 in US, Canada, Mexico, and outside North America
Institutional Print and Online Only: $2,802 in US, Canada, and Mexico; $2,802 outside North America

For submission instructions, subscription, and all other information visit: wileyonlinelibrary.com.

Arthritis & Rheumatology accepts articles for Open Access publication. Please visit https://authorservices.wiley.com/author-resources/Journal-Authors/open-access/hybrid-open-access.html for further information about OnlineOpen.

Wiley's Corporate Citizenship initiative seeks to address the environmental, social, economic, and ethical challenges faced in our business and which are important to our diverse stakeholder groups. Since launching the initiative, we have focused on sharing our content with those in need, enhancing community philanthropy, reducing our carbon impact, creating global guidelines and best practices for paper use, establishing a vendor code of ethics, and engaging our colleagues and other stakeholders in our efforts.
Follow our progress at www.wiley.com/go/citizenship.

Access to this journal is available free online within institutions in the developing world through the HINARI initiative with the WHO. For information, visit www.healthinternetwork.org.

Disclaimer

The Publisher, the American College of Rheumatology, and Editors cannot be held responsible for errors or any consequences arising from the use of information contained in this journal; the views and opinions expressed do not necessarily reflect those of the Publisher, the American College of Rheumatology and Editors, neither does the publication of advertisements constitute any endorsement by the Publisher, the American College of Rheumatology and Editors of the products advertised.

Members:

American College of Rheumatology/Association of Rheumatology Professionals

For membership rates, journal subscription information, and change of address, please write:
American College of Rheumatology
2200 Lake Boulevard
Atlanta, GA 30319-5312
(404) 633-3777

ADVERTISING SALES AND COMMERCIAL REPRINTS

Sales: Kathleen Malseed, National Account Manager
E-mail: kmalseed@pminy.com
Phone: (215) 852-9824
Pharmaceutical Media, Inc.
30 East 33rd Street, New York, NY 10016

Production: Patti McCormack
E-mail: pmccormack@pminy.com
Phone: (212) 904-0376
Pharmaceutical Media, Inc.
30 East 33rd Street, New York, NY 10016

Publisher: Arthritis & Rheumatology is published by Wiley Periodicals LLC, 101 Station Landing, Suite 300, Medford, MA 02155
Production Editor: Ramona Talantor, artprod@wiley.com

ARTHRITIS & RHEUMATOLOGY (Print ISSN 2326-5191; Online ISSN 2326-5205 at Wiley Online Library, wileyonlinelibrary.com) is published monthly on behalf of the American College of Rheumatology by Wiley Periodicals LLC, a Wiley Company, 111 River Street, Hoboken, NJ 07030-5774. Periodicals postage paid at Hoboken, NJ and additional offices. POSTMASTER: Send all address changes to Arthritis & Rheumatology, Wiley Periodicals LLC, c/o The Sheridan Press, PO Box 465, Hanover, PA 17331. **Send subscription inquiries care of** Wiley Periodicals LLC, Attn: Journals Admin Dept UK, 111 River Street, Hoboken, NJ 07030, (201) 748-6645 (nonmember subscribers only; American College of Rheumatology/Association of Rheumatology Health Professionals members should contact the American College of Rheumatology). **Subscription Price:** (Volumes 74, 2022: Arthritis & Rheumatology and Arthritis Care & Research) Print only: $2,603.00 in U.S., Canada and Mexico, $2,603.00 rest of world. For all other prices please consult the journal's website at wileyonlinelibrary.com. All subscriptions containing a print element, shipped outside U.S., will be sent by air. Payment must be made in U.S. dollars drawn on U.S. bank. Prices are exclusive of tax. Asia-Pacific GST, Canadian GST and European VAT will be applied at the appropriate rates. For more information on current tax rates, please go to www.wileyonlinelibrary.com/tax-vat. The price includes online access to the current and all online backfiles to January 1st 2018, where available. For other pricing options including access information and terms and conditions, please visit https://onlinelibrary.wiley.com/library-info/products/price-lists. Terms of use can be found here: https://onlinelibrary.wiley.com/terms-and-conditions. **Delivery Terms and Legal Title:** Where the subscription price includes print issues and delivery is to the recipient's address, delivery terms are Delivered at Place (DAP); the recipient is responsible for paying any import duty or taxes. Title to all issues transfers Free of Board (FOB) our shipping point, freight prepaid. We will endeavor to fulfill claims for missing or damaged copies within six months of publication, within our reasonable discretion and subject to availability. **Change of Address:** Please forward to the subscriptions address listed above 6 weeks prior to move; enclose present mailing label with change of address. **Claims** for undelivered copies will be accepted only after the following issue has been received. Please enclose a copy of the mailing label or cite your subscriber reference number in order to expedite handling. Missing copies will be supplied when losses have been sustained intransit and where reserve stock permits. Send claims care of Wiley Periodicals LLC, Attn: Journals Admin Dept UK, 111 River Street, Hoboken, NJ 07030. If claims are not resolved satisfactorily, please write to Subscription Distribution c/o Wiley Periodicals LLC, 111 River Street, Hoboken, NJ 07030. **Cancellations:** Subscription cancellations will not be accepted after the first issue has been mailed. **Journal Customer Services:** For ordering information, claims and any enquiry concerning your journal subscription please go to https://wolsupport.wiley.com/s/contactsupport?tabset-a7d10=2 or contact your nearest office. **Americas:** Email: cs-journals@wiley.com; Tel: +1 877 762 2974. **Europe, Middle East and Africa:** Email: cs-journals@wiley.com; Tel: +44 (0) 1865 778315; 0800 1800 536 (Germany). **Asia Pacific:** Email: cs-journals@wiley.com; Tel: +65 6511 8000. **Japan:** For Japanese speaking support, Email: cs-japan@wiley.com. **Visit our Online Customer Help** at https://wolsupport.wiley.com/s/contactsupport?tabset-a7d10=2. **Back Issues:** Single issues from current and prior year volumes are available at the current single issue price from csjournals@wiley.com. Earlier issues may be obtained from Periodicals Service Company, 351 Fairview Avenue-Ste 300, Hudson, NY 12534, USA. Tel: + 1 518 822-9300, Fax: +1 518 822-9305, Email: psc@periodicals.com. Printed in the USA by The Sheridan Group.

In this Issue

Highlights from this issue of *A&R* | By Lara C. Pullen, PhD

Presence of Structural Entheseal Lesions Predicts Progression from Psoriasis to PsA

In this issue, Simon et al (p. 253) report that the presence of structural entheseal lesions and low cortical volumetric bone mineral density (vBMD) at entheseal segments in patients with psoriasis is associated with an increased risk of developing psoriatic arthritis (PsA), and thus represents a robust and independent marker predictive of the development of PsA.

p. 253

The study included 114 psoriasis patients, 24 of whom developed PsA during a mean ± SD follow-up of 28.2 ± 17.7 months. At baseline, the patients had a mean ± SD age of 45.3 ± 13.9 years, duration of psoriasis of 15.8 ± 14.8 years, and psoriasis area and severity index (PASI) score of 7.3 ± 6.5. The 24 patients who developed PsA did so after a mean ± SD duration of 17.5 ± 10.0 months.

At baseline, 36% of patients had ≥1 structural entheseal lesion at the metacarpophalangeal joints, with a mean ± SD grade of 0.73 ± 1.37. The investigators found that patients with psoriasis progressing to PsA had localized reduction in bone mass at the entheseal region of the joints. In contrast, a higher vBMD at entheseal segments was associated with a lower risk of developing PsA. The association remained robust after multiple imputation of missing data. The investigators found no positive association, however, between PsA and nail involvement. The researchers next explored whether the risk of development of PsA in patients with structural entheseal lesions could be further stratified by cortical vBMD at entheseal segments and found this to be true. The study highlights the early phase of musculoskeletal involvement in a subset of patients with psoriatic disease and substantiates the concept of mechanoinflammation in the pathogenesis of psoriatic disease.

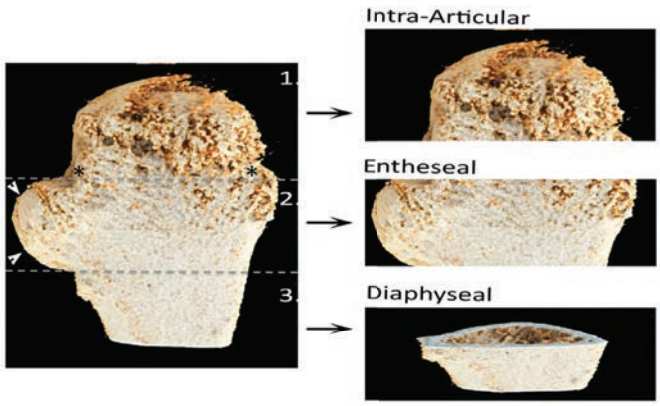

Figure 1. Anatomic orientation of the metacarpophalangeal joint for high-resolution peripheral quantitative computed tomography.

More Data about Mepolizumab for EGPA

The MIRRA (mepolizumab or placebo for the treatment of eosinophilic granulomatosis with polyangiitis [EGPA]) administered mepolizumab 300 mg every 4 weeks, despite this dosage not being based on a specific dose range–finding study for EGPA. However, in clinical practice, most patients with EGPA receive mepolizumab at the dose approved for severe eosinophilic asthma: 100 mg every 4 weeks. Even this dose may incur a risk of systemic disease flare in patients receiving anti–interleukin-5 treatments at the dose used for asthma control.

p. 295

In this issue, Bettiol et al (p. 295) report that mepolizumab, at both 100 mg every 4 weeks and 300 mg every 4 weeks, is effective for the treatment of EGPA. Their retrospective study revealed that both doses were associated with effective control of respiratory EGPA manifestations and an improvement in systemic disease. The study was conducted in multiple centers in Europe and is the largest series of mepolizumab-treated patients with EGPA reported to date.

In their real-world study, investigators found that the proportion of complete responses steadily increased throughout follow-up and reached, at 24 months, 33.3% for mepolizumab 100 mg every 4 weeks and 58.3% for mepolizumab 300 mg every 4 weeks. Only a small proportion of patients in the cohort experienced disease relapse. The patients receiving both mepolizumab regimens experienced not only disease control but also improvement in asthma and lung function. Mepolizumab was generally well tolerated.

These results also suggest that mepolizumab may be able to treat systemic manifestations of EGPA. The authors note that, although the subgroups were too small to draw conclusions, complete response rate appeared to be higher among patients negative for antineutrophil cytoplasmic antibodies. The authors conclude by calling for the 2 doses to be compared in the setting of a controlled trial.

Peripheral Blood B Cell Subsets in Patients with RA Remain Stable During Treatment

Although previous studies have demonstrated that peripheral blood B cells are abnormal in rheumatoid arthritis (RA) the results have not been entirely consistent, possibly due to variability in disease phenotypes, duration, activity, and therapy. Perhaps for this reason, researchers have been unsuccessful in identifying markers that can predict response to anti–tumor necrosis factor (anti-TNF) therapy. This has led some to propose that such biomarkers may exist in discrete cell populations.

p. 200

In this issue, Meednu et al (p. 200) describe several peripheral B cell flow cytometry–based biomarkers associated with inadequate response to TNF blockade. Their results are consistent with the notion that peripheral blood B cell subsets are remarkably stable in patients with RA. However, activated B cells do associate with a less robust response to therapy.

When the investigators examined peripheral blood B cell subsets of individuals with active RA, they found no difference between the effects of dual blockade of TNF and lymphotoxin (LT) with etanercept and single blockade of TNF with adalimumab. The results suggest that agents that block both TNF and LT are not necessarily more efficacious than those that block TNF alone. They also found that TNF blockade was not associated with a decrease in total peripheral blood memory B cells and propose that this may be because most peripheral blood memory B cells are longer-lived and not susceptible to alteration during a short period of treatment. This builds upon the team's previous research, which showed that lymphoid tissue from RA patients receiving etanercept display a paucity of follicular dendritic cell networks and germinal center structures, and highlights the importance of examining tissue in addition to blood.

Journal Club

A monthly feature designed to facilitate discussion on research methods in rheumatology.

Contribution of Rare Genetic Variation to Disease Susceptibility in a Large Scandinavian Myositis Cohort

Bianchi et al, Arthritis Rheumatol 2022;74:342–352

Idiopathic inflammatory myopathies (IIMs) are a family of rare heterogenous systemic inflammatory diseases characterized by a type I interferon (IFN) signature and complex etiology. Besides environmental and common genetic risk factors shared among other autoimmune diseases, rare genetic variation has been implicated in the genetic susceptibility of IIM, but it has remained largely unexplored. To investigate the role of this class of variation in the genetic landscape of IIM and subgroups of this disease, Bianchi et al performed targeted next-generation sequencing to mine coding and potentially regulatory regions of immune-related genes in a large Scandinavian cohort of patients and controls, followed by gene-based aggregate testing of all variants, including rare variants. Consistent with previous findings based on gene expression profiling, the authors found a specific genetic signature of type I IFN pathway activation in IIM, which was functionally linked in silico to potentially novel candidate genes and disease mechanisms. This signature also appeared to be less marked in the clinically and serologically defined subgroup with antisynthetase syndrome. Additionally, they discovered that distinct functional rare genetic variant categories contribute to disease susceptibility in IIM and specific IIM patient subgroups.

Next-generation sequencing allowed detection of genetic variation covering the full spectrum of allele frequencies for the assessed gene set. Noncoding potentially regulatory gene elements captured by the targeted array were defined based on mammalian evolutionary constraint, which can be leveraged to prioritize regions that are key in complex autoimmune diseases. Despite the wealth of genetic information obtained, classical single-variant and variant-aggregating association methods pinpointed only previously detected large-effect genetic signals (i.e., HLA). The authors therefore used an enhanced gene-based aggregate testing method that weights variants based not only on their minor allele frequency but on their functional potential. Along with in silico functional dissection of the associated locus, this method highlighted *IFI35* and *PTGES3L* as potentially novel IIM genetic risk loci. Evaluation of the burden of different variant functional classes in patients and controls showed that rare synonymous variants are associated with increased disease predisposition.

Questions

1. **What is currently known about the genetic architecture underlying the development of IIM?**
2. **Would the results be refined using the most recent disease clinical classification criteria, and/or a greater sample size, and/or a more accurate variant functional annotation?**
3. **Could whole-genome sequencing of this study cohort and/or a different cohort add more knowledge?**
4. **What might be a sensible functional validation experiment to follow up the findings related to the *IFI35–PTGES3L* locus?**

In this Issue

Highlights from this issue of *A&R* | By Lara C. Pullen, PhD

Presence of Structural Entheseal Lesions Predicts Progression from Psoriasis to PsA

In this issue, Simon et al (p. 253) report that the presence of structural entheseal lesions and low cortical volumetric bone mineral density (vBMD) at entheseal segments in patients with psoriasis is associated with an increased risk of developing psoriatic arthritis (PsA), and thus represents a robust and independent marker predictive of the development of PsA.

p. 253

The study included 114 psoriasis patients, 24 of whom developed PsA during a mean ± SD follow-up of 28.2 ± 17.7 months. At baseline, the patients had a mean ± SD age of 45.3 ± 13.9 years, duration of psoriasis of 15.8 ± 14.8 years, and psoriasis area and severity index (PASI) score of 7.3 ± 6.5. The 24 patients who developed PsA did so after a mean ± SD duration of 17.5 ± 10.0 months.

At baseline, 36% of patients had ≥1 structural entheseal lesion at the metacarpophalangeal joints, with a mean ± SD grade of 0.73 ± 1.37. The investigators found that patients with psoriasis progressing to PsA had localized reduction in bone mass at the entheseal region of the joints. In contrast, a higher vBMD at entheseal segments was associated with a lower risk of developing PsA. The association remained robust after multiple imputation of missing data. The investigators found no positive association, however, between PsA and nail involvement. The researchers next explored whether the risk of development of PsA in patients with structural entheseal lesions could be further stratified by cortical vBMD at entheseal segments and found this to be true. The study highlights the early phase of musculoskeletal involvement in a subset of patients with psoriatic disease and substantiates the concept of mechanoinflammation in the pathogenesis of psoriatic disease.

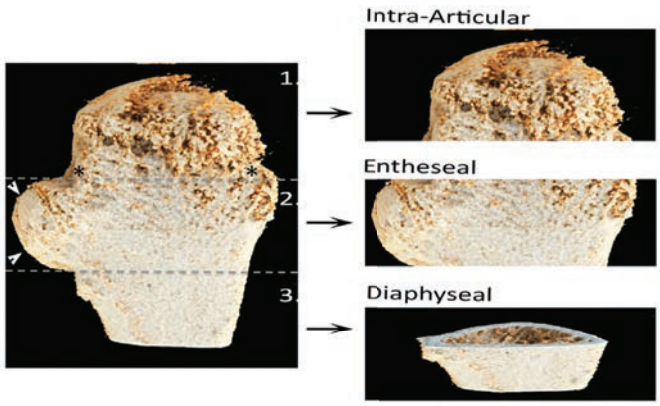

Figure 1. Anatomic orientation of the metacarpophalangeal joint for high-resolution peripheral quantitative computed tomography.

More Data about Mepolizumab for EGPA

The MIRRA (mepolizumab or placebo for the treatment of eosinophilic granulomatosis with polyangiitis [EGPA]) administered mepolizumab 300 mg every 4 weeks, despite this dosage not being based on a specific dose range–finding study for EGPA. However, in clinical practice, most patients with EGPA receive mepolizumab at the dose approved for severe eosinophilic asthma: 100 mg every 4 weeks. Even this dose may incur a risk of systemic disease flare in patients receiving anti–interleukin-5 treatments at the dose used for asthma control.

p. 295

In this issue, Bettiol et al (p. 295) report that mepolizumab, at both 100 mg every 4 weeks and 300 mg every 4 weeks, is effective for the treatment of EGPA. Their retrospective study revealed that both doses were associated with effective control of respiratory EGPA manifestations and an improvement in systemic disease. The study was conducted in multiple centers in Europe and is the largest series of mepolizumab-treated patients with EGPA reported to date.

In their real-world study, investigators found that the proportion of complete responses steadily increased throughout follow-up and reached, at 24 months, 33.3% for mepolizumab 100 mg every 4 weeks and 58.3% for mepolizumab 300 mg every 4 weeks. Only a small proportion of patients in the cohort experienced disease relapse. The patients receiving both mepolizumab regimens experienced not only disease control but also improvement in asthma and lung function. Mepolizumab was generally well tolerated.

These results also suggest that mepolizumab may be able to treat systemic manifestations of EGPA. The authors note that, although the subgroups were too small to draw conclusions, complete response rate appeared to be higher among patients negative for antineutrophil cytoplasmic antibodies. The authors conclude by calling for the 2 doses to be compared in the setting of a controlled trial.

Peripheral Blood B Cell Subsets in Patients with RA Remain Stable During Treatment

Although previous studies have demonstrated that peripheral blood B cells are abnormal in rheumatoid arthritis (RA) the results have not been entirely consistent, possibly due to variability in disease phenotypes, duration, activity, and therapy. Perhaps for this reason, researchers have been unsuccessful in identifying markers that can predict response to anti–tumor necrosis factor (anti-TNF) therapy. This has led some to propose that such biomarkers may exist in discrete cell populations.

p. 200

In this issue, Meednu et al (p. 200) describe several peripheral B cell flow cytometry–based biomarkers associated with inadequate response to TNF blockade. Their results are consistent with the notion that peripheral blood B cell subsets are remarkably stable in patients with RA. However, activated B cells do associate with a less robust response to therapy.

When the investigators examined peripheral blood B cell subsets of individuals with active RA, they found no difference between the effects of dual blockade of TNF and lymphotoxin (LT) with etanercept and single blockade of TNF with adalimumab. The results suggest that agents that block both TNF and LT are not necessarily more efficacious than those that block TNF alone. They also found that TNF blockade was not associated with a decrease in total peripheral blood memory B cells and propose that this may be because most peripheral blood memory B cells are longer-lived and not susceptible to alteration during a short period of treatment. This builds upon the team's previous research, which showed that lymphoid tissue from RA patients receiving etanercept display a paucity of follicular dendritic cell networks and germinal center structures, and highlights the importance of examining tissue in addition to blood.

Journal Club

A monthly feature designed to facilitate discussion on research methods in rheumatology.

Contribution of Rare Genetic Variation to Disease Susceptibility in a Large Scandinavian Myositis Cohort

Bianchi et al, Arthritis Rheumatol 2022;74:342–352

Idiopathic inflammatory myopathies (IIMs) are a family of rare heterogenous systemic inflammatory diseases characterized by a type I interferon (IFN) signature and complex etiology. Besides environmental and common genetic risk factors shared among other autoimmune diseases, rare genetic variation has been implicated in the genetic susceptibility of IIM, but it has remained largely unexplored. To investigate the role of this class of variation in the genetic landscape of IIM and subgroups of this disease, Bianchi et al performed targeted next-generation sequencing to mine coding and potentially regulatory regions of immune-related genes in a large Scandinavian cohort of patients and controls, followed by gene-based aggregate testing of all variants, including rare variants. Consistent with previous findings based on gene expression profiling, the authors found a specific genetic signature of type I IFN pathway activation in IIM, which was functionally linked in silico to potentially novel candidate genes and disease mechanisms. This signature also appeared to be less marked in the clinically and serologically defined subgroup with antisynthetase syndrome. Additionally, they discovered that distinct functional rare genetic variant categories contribute to disease susceptibility in IIM and specific IIM patient subgroups.

Next-generation sequencing allowed detection of genetic variation covering the full spectrum of allele frequencies for the assessed gene set. Noncoding potentially regulatory gene elements captured by the targeted array were defined based on mammalian evolutionary constraint, which can be leveraged to prioritize regions that are key in complex autoimmune diseases. Despite the wealth of genetic information obtained, classical single-variant and variant-aggregating association methods pinpointed only previously detected large-effect genetic signals (i.e., HLA). The authors therefore used an enhanced gene-based aggregate testing method that weights variants based not only on their minor allele frequency but on their functional potential. Along with in silico functional dissection of the associated locus, this method highlighted *IFI35* and *PTGES3L* as potentially novel IIM genetic risk loci. Evaluation of the burden of different variant functional classes in patients and controls showed that rare synonymous variants are associated with increased disease predisposition.

Questions

1. **What is currently known about the genetic architecture underlying the development of IIM?**
2. **Would the results be refined using the most recent disease clinical classification criteria, and/or a greater sample size, and/or a more accurate variant functional annotation?**
3. **Could whole-genome sequencing of this study cohort and/or a different cohort add more knowledge?**
4. **What might be a sensible functional validation experiment to follow up the findings related to the *IFI35–PTGES3L* locus?**

Clinical Connections

Defective Early B Cell Tolerance Checkpoints in Patients With SSc Allow the Production of Self Antigen–Specific Clones

Glauzy et al, *Arthritis Rheumatol* 2022;74:307–317

CORRESPONDENCE
Eric Meffre, PhD: eric.meffre@yale.edu

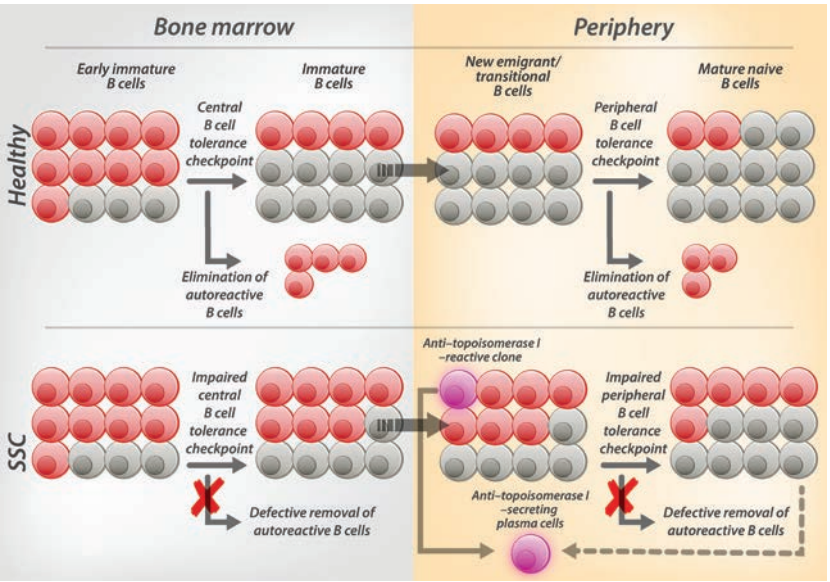

KEY POINTS

- Central and peripheral B cell tolerance checkpoints are impaired in SSc.
- Autoreactive naive B cells accumulate in the blood of patients with SSc.
- Failure in early B cell tolerance checkpoints is common in most patients with autoimmune disease.
- Anti–topoisomerase I–reactive clones have been identified in transitional B cells in SSc.

SUMMARY

Early selection steps, preventing the production of autoreactive naive B cells generated by random V(D)J recombination, are often impaired in patients with autoimmune diseases. Glauzy et al used an in vitro polymerase chain reaction–based approach that allows for the expression of recombinant antibodies cloned from single B cells. They demonstrated that patients with systemic sclerosis (SSc) displayed elevated proportions of autoreactive new emigrant/transitional and mature naive B cells that are characteristic of impaired central and peripheral B cell tolerance checkpoints, respectively. Therefore, the dysregulated removal of developing autoreactive naive B cells continuously produced throughout life correlates with autoimmunity, likely by favoring self antigen presentation to T cells and autoantibody secretion. However, the reservoir of naive B cells at the origin of the production of potentially pathogenic antibodies in patients with autoimmune diseases remains poorly characterized. The identification of anti–topoisomerase I–reactive clones devoid of somatic hypermutation in the new emigrant/transitional B cell compartment of patients with SSc supports a direct involvement of transitional B cells in autoantibody secretion in autoimmune diseases. Since autoreactive antibodies promote fibrosis in SSc through the formation of immune complexes, defective early B cell tolerance mechanisms appear to play an essential role in disease pathophysiology. Restoring early B cell tolerance checkpoints may thus represent an attractive therapeutic strategy to prevent the production of autoreactive naive B cells and thwart autoimmunity.

Activation of Hypothalamic AMPK Ameliorates Metabolic Complications of Experimental Arthritis

Seoane-Collazo et al, *Arthritis Rheumatol* 22022;74:212–222

CORRESPONDENCE
Oreste Gualillo, PharmD, PhD: oreste.gualillo@sergas.es
Miguel López, PhD: m.lopez@usc.es

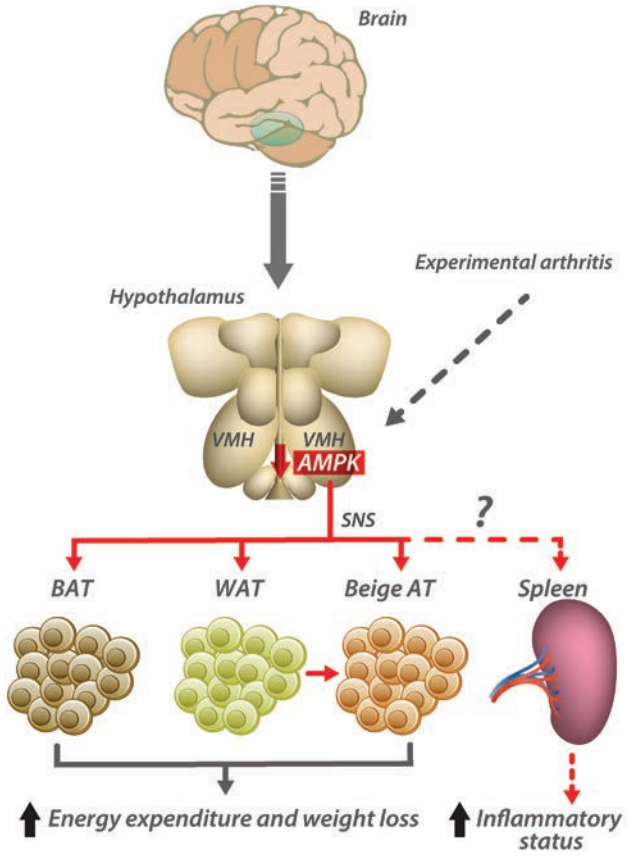

KEY POINTS

- EA induces inflammation and negative energy balance, which is associated with increased BAT thermogenesis and browning of WAT.
- EA inhibits hypothalamic AMPK.
- Activation of hypothalamic AMPK reverses the effect of EA on energy balance and inflammation.
- EA promotes a central catabolic state that can be targeted by the activation of hypothalamic AMPK.

SUMMARY

The AMP-activated protein kinase (AMPK) is a cellular gauge that is activated in conditions of low energy to increase energy production and reduce energy-wasting. Current findings have linked hypothalamic AMPK with the homeostatic regulation of peripheral metabolism by modulating food intake and energy expenditure, the latter via the sympathetic nervous system (SNS) regulation of brown adipose tissue (BAT) thermogenesis and white adipose tissue (WAT) browning. Seoane-Collazo et al demonstrated that experimental arthritis (EA), induced by intradermal injection of Freund's complete adjuvant (CFA) in rats, increased BAT thermogenesis and browning of WAT, promoting energy expenditure and weight loss. These effects were associated with the inhibition of hypothalamic AMPK. Virogenetic activation of AMPK, specifically in the ventromedial nucleus of the hypothalamus (VMH; a main brain site regulating metabolism), blunted the effects of EA on BAT and WAT and led to reversion of the catabolic status, to weight gain, and, notably, to amelioration of the inflammatory condition. Further work will be needed to address whether EA-induced inhibition of hypothalamic AMPK might directly impact immune function, for example, by SNS-mediated activation of the spleen lymphocytes.

These data demonstrate that the metabolic consequences of EA go far beyond peripheral tissues and target the hypothalamus to affect a key mechanism, namely AMPK, modulating energy balance. This provides new mechanistic insight into the pathophysiology of rheumatoid arthritis (and possibly of other autoimmune inflammatory diseases), which might offer new alternatives to current clinical management and the treatment of associated comorbidities.

Arthritis & Rheumatology
Vol. 74, No. 2, February 2022, pp 181–183
DOI 10.1002/art.42032

American College of Rheumatology
Empowering Rheumatology Professionals

EDITORIAL

Are Intraarticular Glucocorticoids Safe in Osteoarthritis?

Joel A. Block

The treatment of osteoarthritis (OA) pain remains an intractable clinical problem. Although in the inflammatory arthritides, dramatic advances have yielded therapeutics that have altered the course and clinical severity of many diseases, parallel advances have not yet occurred in the field of OA. Hence, despite decades of effort and the expenditure of enormous resources by the pharmaceutical industry, government, and private foundations, treatment of the chronic pain of OA remains a substantial unmet medical need. Although OA can involve any synovial joint, knee OA dominates clinical trials and epidemiologic studies because it is common, easily diagnosed, and remains a source of enormous public cost.

Intraarticular glucocorticoids have been used for many decades for short-term relief of painful knee OA and they continue to represent a widely employed strategy. Nonetheless, their overall utility remains a subject of controversy, as their risks and benefits have still not been fully elucidated. A study by Bucci et al, which is published in this issue of *Arthritis & Rheumatology* (1), may provide additional insight into this difficult clinical issue.

In the 1950s intraarticular glucocorticoids were believed to be dramatically effective for inflammatory and degenerative arthritis (2,3). Initial enthusiasm, however, appeared to be tempered by findings in animal studies suggesting that there may be some cartilage toxicity from the glucocorticoids (4), as well as the possibility of accidental hyaline cartilage trauma resulting from needle sticks. Human adult cartilage is a non-healing tissue, and thus there was concern that such trauma could accelerate the process of cartilage degeneration. Throughout this era, OA was considered to be primarily a disease of degenerative articular cartilage (5), and hence such accidental trauma was thought to represent a potential risk factor for progressive cartilage loss, and thus for OA disease progression.

The glucocorticoids have extraordinarily complex effects on the biology of cartilage. Studies using animal models, cartilage explants, and cultured chondrocytes suggest contradictory results, depending on the model system employed and on the dose and duration of exposure to the steroid. Whereas glucocorticoids potently inhibit cartilage matrix degradative enzymes, they also affect cellular remodeling and synthesis, and may disrupt cartilage matrix homeostasis (6). The net effect of therapeutic glucocorticoids on cartilage in animals and humans remains unclear. OA, however, is now widely recognized to be a disease of the entire joint, rather than merely a disease of degenerative cartilage. Nonetheless, concerns about potential adverse effects of intraarticular glucocorticoid injections have remained, and there are no conclusive data that either implicate these agents in or clear them from mediating OA disease progression in humans.

In contrast to the controversy surrounding the potential risks of intraarticular glucocorticoids, a consensus has emerged that they may provide pain palliation, but that this is of relatively short duration. Hence, patients typically require repeated injections over time. However, the magnitude of benefit that they provide remains debated; although treatment with intraarticular glucocorticoids is strongly recommended in the new American College of Rheumatology guidelines for the management of knee OA (7), it is only conditionally recommended by the updated guidelines published by the Osteoarthritis Research Society International (8). The continued popularity of these agents is likely largely a result of the paucity of highly effective alternative options to palliate OA pain, because the strategy is clearly neither particularly durable nor overwhelmingly effective.

The conventional method to approach clinical questions of efficacy and safety would be to perform well-powered prospective clinical trials and to maintain prospective registries of adverse events among patients exposed to the agent of interest. However, such definitive trials are unlikely ever to be performed for these drugs in OA, for several reasons. First, OA is a very slowly progressive disease, and progression in OA can be stuttering and unpredictable in the knee. Hence, to discern whether a seemingly benign procedure, such as the intraarticular injection of glucocorticoids, has an adverse effect on joint structure, it would

Joel A. Block, MD: Rush University Medical Center, Chicago, Illinois.

Author disclosures are available at https://onlinelibrary.wiley.com/action/downloadSupplement?doi=10.1002%2Fart.42032&file=art42032-sup-0001-Disclosureform.pdf.

Address correspondence to Joel A. Block, MD, Division of Rheumatology, Rush University Medical Center, 1611 West Harrison Street, Suite 510, Chicago, IL 60612. Email: jblock@rush.edu.

Submitted for publication November 5, 2021; accepted in revised form November 18, 2021.

take huge group sizes with many years' follow-up. Such a study design would be both impractically expensive and incompatible with the career demands of modern faculty advancement.

Second, and as important, there is no universally agreed upon definition of OA disease progression, nor is there clarity regarding the utility of surrogate end points. Structural progression of OA is conventionally defined as progressive narrowing of the radiographic joint space, and the demonstration of slowing of the rate of quantitative radiographic joint space narrowing using standardized views remains the accepted regulatory standard to assess the delay of knee OA structural progression. However, it is well recognized that this is an insensitive measure and correlates poorly with symptomatic disease (9). More sensitive techniques of imaging joint structures, such as longitudinal magnetic resonance imaging (MRI), have poorer standardization and have not been accepted by regulatory authorities as meaningful outcomes to demonstrate OA progression (10). Importantly, however, even the demonstration of unambiguous progression of structural joint degeneration is not reliably accompanied by worsening of symptoms, and conversely, agents that may retard the loss of articular cartilage have not been shown to have significant clinical benefit (10). It is widely acknowledged that progression of structural joint degeneration in OA is not at all synonymous with "disease" progression, because, to date, treatments that appear to reduce structural progression have not been shown to palliate symptoms, and conversely, advanced structural joint disease itself is not reliably accompanied by worse symptoms (11). Clinically, disease progression must involve both structural degeneration and symptomatic worsening. Thus, the clinical significance of structural progression, such as joint space narrowing, remains unclear.

With regard to the effect of intraarticular glucocorticoids on OA structural or disease progression, a large literature has developed in OA of the knee, and the reports tend to be contradictory. Earlier prospective clinical trials suggested safety and efficacy. For example, Raynauld et al (12) reported in a 2-year study that there was significant improvement without change in joint space narrowing in a small trial. In this case, joint space narrowing was assessed using conventional radiography and the quantitative semiflexed view of the knee. In contrast, in a more recent larger prospective trial, McAlindon et al (13) reported that intraarticular glucocorticoids had no benefit clinically after 2 years of quarterly injections, yet they resulted in accelerated cartilage loss by MRI criteria. As described above, however, the actual clinical significance of such MRI-defined cartilage loss remains uncertain, as does the meaning of the lack of observed joint space narrowing in the earlier studies. Moreover, the short follow-up relative to the known natural history of OA and the small group sizes further limit the potential interpretation.

In contrast to the ambiguity of surrogate outcomes, one clear measure of progression to end-stage disease is the choice to undergo arthroplasty; although there is no standardization, either by surgical indication or by patient preference, there is at least agreement that this represents a clinically significant end point, the timing of which is well defined.

Because there are not likely to be any prospective controlled trials that will definitively provide insight into the potential harm of intraarticular glucocorticoids, large observational studies may provide our best chance of approaching these questions. Bucci and colleagues (1) leveraged 2 large longitudinal data sets of well-characterized individuals with or at risk of knee OA, and they assessed knee OA progression among those patients who received intraarticular glucocorticoid injections, using both a structural surrogate (radiographic joint space narrowing) and a functional end point (progression to knee replacement). In addition, they compared this group to a parallel group that had received intraarticular hyaluronic acid as a control, assuming that intraarticular hyaluronic acid does not have potential toxicity similar to glucocorticoids. Importantly, they found that there were no differences in the rates of radiographic progression, nor were there differences in the progression to total knee replacement, among individuals in either group. If anything, there may have been a signal suggesting a trend toward fewer joint replacements in the glucocorticoid group than the hyaluronic acid group. While there was an attempt to control for the effects of multiple glucocorticoid injections, it is unfortunate that the safety of regularly repeated glucocorticoid injections was not addressed. It must be conceded, however, that even when combining some of the largest longitudinal data sets available for knee OA, the total number of events was still too small to obtain granularity in the conclusions. Nonetheless, these findings offer reassurance of the relative safety of intraarticular glucocorticoids in patients with knee OA.

Intraarticular glucocorticoids are widely used to palliate knee OA pain. Despite more than 50 years of widespread use, there is still concern about the potential toxicity of these agents, and especially about their potential adverse effect on progression of structural joint degeneration. The findings of Bucci et al provide some assurance that whatever risk there is with the use of these agents, it is likely quite small, and in any case is likely negligible relative to the risks associated with other intraarticular therapies. It is only unfortunate that comparable conclusions could not be formed regarding frequently repeated injections.

AUTHOR CONTRIBUTIONS

Dr. Block drafted the article, revised it critically for important intellectual content, and approved the final version to be published.

REFERENCES

1. Bucci J, Chen X, LaValley M, Nevitt M, Torner J, Lewis CE, et al. Progression of knee osteoarthritis with use of intraarticular glucocorticoids versus hyaluronic acid. Arthritis Rheumatol 2022;74: 223–6.

2. Bilka PJ. Intra-articular use of hydrocortisone in rheumatic diseases. Minn Med 1952;35:938–43.
3. Davison S. The treatment of degenerative joint disease (osteoarthritis) by the intra-articular instillation of hydrocortisone (Compound F). N Y State J Med 1953;53:975–7.
4. Behrens F, Shepard N, Mitchell N. Alterations of rabbit articular cartilage by intra-articular injections of glucocorticoids. J Bone Joint Surg Am 1975;57:70–6.
5. Dobson GP, Letson HL, Grant A, McEwen P, Hazratwala K, Wilkinson M, et al. Defining the osteoarthritis patient: back to the future [review]. Osteoarthritis Cartilage 2018;26:1003–7.
6. Black R, Grodzinsky AJ. Dexamethasone: chondroprotective corticosteroid or catabolic killer? Eur Cell Mater 2019;38: 246–63.
7. Kolasinski SL, Neogi T, Hochberg MC, Oatis C, Guyatt G, Block J, et al. 2019 American College of Rheumatology/Arthritis Foundation guideline for the management of osteoarthritis of the hand, hip, and knee. Arthritis Rheumatol 2020;72:220–33.
8. Bannuru RR, Osani MC, Vaysbrot EE, Arden NK, Bennell K, Bierma-Zeinstra SM, et al. OARSI guidelines for the non-surgical management of knee, hip, and polyarticular osteoarthritis. Osteoarthritis Cartilage 2019;27:1578–89.
9. Conaghan PG, Hunter DJ, Maillefert JF, Reichmann WM, Losina E. Summary and recommendations of the OARSI FDA Osteoarthritis Assessment of Structural Change Working Group. Osteoarthritis Cartilage 2011;19:606–10.
10. Katz JN, Neogi T, Callahan LF, Block JA, Conaghan PG, Simon LS, et al. Disease modification in osteoarthritis; pathways to drug approval. Osteoarthritis Cartilage Open 2020;2:100059.
11. Hannan MT, Felson DT, Pincus T. Analysis of the discordance between radiographic changes and knee pain in osteoarthritis of the knee. J Rheumatol 2000;27:1513–7.
12. Raynauld JP, Buckland-Wright C, Ward R, Choquette D, Haraoui B, Martel-Pelletier J, et al. Safety and efficacy of long-term intraarticular steroid injections in osteoarthritis of the knee: a randomized, double-blind, placebo-controlled trial. Arthritis Rheum 2003;48:370–7.
13. McAlindon TE, LaValley MP, Harvey WF, Price LL, Driban JB, Zhang M, et al. Effect of intra-articular triamcinolone vs saline on knee cartilage volume and pain in patients with knee osteoarthritis: a randomized clinical trial. JAMA 2017;317:1967–75.

American College of Rheumatology
Empowering Rheumatology Professionals

Arthritis & Rheumatology
Vol. 74, No. 2, February 2022, pp 184–199
DOI 10.1002/art.41979

REVIEW

Myocardial Dysfunction and Heart Failure in Rheumatoid Arthritis

Elizabeth Park, Jan Griffin, and Joan M. Bathon

Rheumatoid arthritis (RA) patients have almost twice the risk of heart failure (HF) as individuals without RA, even with adjustment for the presence of ischemic heart disease. Moreover, RA patients remain at a 2-fold higher risk of mortality from HF compared to non–RA patients. These observations suggest that RA-specific inflammatory pathways are significant contributors to this increased risk of HF. Herein we summarize the epidemiology of HF in RA patients, the differences in myocardial structure or function between RA patients and non–RA patients without clinical signs of HF, and data on the role of systemic and local inflammation in RA HF pathophysiology. We also discuss the impact of subduing inflammation through the use of RA disease-modifying therapies on HF and myocardial structure and function, emphasizing gaps in the literature and areas needing further research.

Introduction

Rheumatoid arthritis (RA) is a systemic inflammatory disease affecting ~0.5–1% of the population. RA patients have almost twice the risk of heart failure (HF) of individuals without RA, even after adjustment for conventional cardiovascular (CV) risk factors and coronary artery disease (CAD) (1,2). This observation suggests that RA-specific immune/inflammatory pathways are significant contributors to this increased risk of HF. In this review we 1) summarize the epidemiology of clinical HF in RA; 2) delineate differences in myocardial structure and function in RA patients without clinical heart failure compared to non–RA patients; 3) examine data in RA patients that support the notion that systemic and local inflammation play pathophysiologic roles in driving HF and subclinical myocardial dysfunction; 4) review available data on the effect of RA disease-modifying antirheumatic drugs (DMARDs) on HF and subclinical myocardial structure and function in RA; and 5) discuss future areas for additional research.

Epidemiology of HF in patients with RA

RA patients are at an almost 50% higher risk of incident CV disease (CVD) than non–RA patients (pooled relative risk [RR] 1.48) (3). Table 1 summarizes the incidence rates of HF specifically, revealing hazard ratios (HRs) of 1.21–1.87 in RA compared to non-RA (2,4–6). While several of the more recent epidemiologic studies (7–9) suggest declining overall CV event rates and CV-associated mortality rates in RA patients diagnosed after 2000 versus those diagnosed prior to 2000, these studies did not include or clearly distinguish HF as an outcome measure. HF-associated mortality is also increased 2-fold, and time to onset of HF is shorter, in RA versus non-RA groups (1,5,10) (Table 1). However, despite the higher incidence of HF, RA patients were less likely to report orthopnea and paroxysmal nocturnal dyspnea than non-RA controls (10). These data raise the possibility that RA-associated HF may be underdiagnosed and that aggressive screening for abnormalities in myocardial structure and function, while RA patients are still without HF symptoms, could present an opportunity for early intervention and prevention of HF.

The etiology of the increased risk of HF in RA has not been well delineated. While higher rates of CAD pose a large risk of HF in RA (4), the relative contribution of CAD to HF is attenuated in RA compared to non–RA patients (HR 3.25 [95% confidence interval (95% CI) 2.35, 4.51] and 4.94 [95% CI 3.30, 7.38], respectively) (1). Likewise, the attributable risk of HF due to conventional CV risk factors was only 54% in RA, compared to 77% in non–RA patients ($P < 0.01$) (1). This suggests that CAD and CV risk factors cannot solely account for the increased risk of HF

The content is solely the responsibility of the authors and does not necessarily represent the official views of the National Institutes of Health.

Supported by the National Institute of Arthritis and Musculoskeletal and Skin Diseases, NIH (award R01-AR-050026).

Elizabeth Park, MD, Jan Griffin, MD, Joan M. Bathon, MD: Columbia University Irving Medical Center and New York Presbyterian Hospital, New York, New York.

No potential conflicts of interest relevant to this article were reported.

Author disclosures are available at https://onlinelibrary.wiley.com/action/downloadSupplement?doi=10.1002%2Fart.41979&file=art41979-sup-0001-Disclosureform.pdf.

Address correspondence to Joan M. Bathon, MD, Division of Rheumatology, Department of Medicine, Columbia University, Vagelos College of Physicians and Surgeons, 630 West 168th Street, P&S 3-450, New York, NY 10032. Email: jmb2311@cumc.columbia.edu.

Submitted for publication April 23, 2021; accepted in revised form September 9, 2021.

Table 1. Epidemiologic studies of HF in RA patients versus non–RA patients*

Author, year (ref.)	Study design	n, RA vs. non-RA	HR/OR (95% CI), RA vs. non-RA	Incidence of HF (95% CI) [*P*], RA vs. non-RA	Statistical adjustments
Incidence of HF in RA					
Wolfe et al, 2003 (12)	Retrospective longitudinal cohort	9,093 vs. 2,479, RA vs. OA	OR 1.43 (1.28, 1.59), RA vs. OA	Not reported	Demographics, CV risk factors
Wolfe and Michaud, 2004 (11)	Retrospective longitudinal cohort	13,171 vs. 2,568, RA vs. OA	Not reported	3.9% (3.4, 4.3) vs. 2.3% (1.6, 3.3), RA vs. OA	Demographics, CV risk factors
Crowson et al, 2005 (1)	Retrospective longitudinal cohort	575 vs. 583	Not reported	36.3% vs. 20.4% [$P < 0.001$]	Sex, CV risk factors, alcohol use
Nicola et al, 2005 (2); 2006 (4)	Retrospective longitudinal cohort	575 vs. 583; 603 vs. 603	HR 1.87 (1.47, 2.39)	37.1% vs. 27.7% [$P < 0.001$]	Age, sex, CV risk factors, CAD
Mantel et al, 2017 (5)	Prospective cohort	12,943 vs. 113,884	Overall HF: HR 1.22 (1.09, 1.37); ischemic HF: HR 1.27 (1.07, 1.51); nonischemic HF: HR 1.22 (1.04, 1.42)	Rates per 1,000 person-years, overall HF: 5.8 vs. 3.1; ischemic HF: 3.5 vs. 1.9; non-ischemic HF: 2.7 vs. 1.4	Age, sex
Ahlers et al, 2020 (6)	Prospective cohort	9,889 vs. 9,889	Cumulative HR (HFpEF and HFrEF) 1.21 (1.03, 1.42)	HFpEF 64% vs. 62% [$P = 0.67$]	Age, sex, race, CAD, CV treatment
HF mortality in RA vs. non-RA					
Nicola et al, 2006 (4)	Retrospective longitudinal cohort	603 vs. 603	Not reported	39.0 vs. 29.2 per 1,000 person-years [$P < 0.001$]	Age, sex, calendar year
Davis et al, 2008 (10)	Prospective cohort	103 vs. 852	HR 1.89 (1.26, 2.84)	35% vs. 19%	Age, sex, calendar year, CV treatment, CAD
Ahlers et al, 2020 (6)	Prospective cohort	323 vs. 443	HR 1.68 (1.45, 1.95)	22.6% vs. 14.6% [$P = 0.006$]	Age, sex, race

* HF = heart failure; RA = rheumatoid arthritis; HR = hazard ratio; OR = odds ratio; 95% CI = 95% confidence interval; OA = osteoarthritis; CV = cardiovascular; CAD = coronary artery disease; HFpEF = HF with preserved ejection fraction; HFrEF = HF with reduced ejection fraction; EHR = electronic health record.

in RA. Of note, most of the cohort studies listed in Table 1 (1,2,4,6,11,12) did not distinguish ischemic versus nonischemic HF. However, Mantel et al (5) recently found similar HRs for incident ischemic and nonischemic HF in RA patients versus non–RA patients (1.27 [95% CI 1.07, 1.51] and 1.22 [95% CI 1.04, 1.42]). Taken together, these data suggest that a significant proportion of RA patients develop HF independently of CAD.

HF comprises a heterogeneous group of disorders that may be primarily cardiac in nature or secondary to systemic disease. It can be stratified according to whether left ventricular (LV) ejection fraction (EF) is reduced (EF <40%), midrange (EF 40–49%), or preserved (EF ≥50%) (13). HF with reduced EF (HFrEF) is characterized by systolic dysfunction, often with chamber dilation and eccentric remodeling, and is most commonly associated with ischemia, hypertension, and valvular disease. In contrast, previously "diastolic HF" (HFpEF) is characterized by normal EF and LV volumes, but concentric remodeling or LV hypertrophy (14). HFpEF is commonly associated with systemic proinflammatory states such as obesity, aging, and diabetes mellitus (14). With regard to RA, Davis and colleagues (10) reported that among patients with clinical HF, the mean EF in RA patients was higher than that in non–RA patients (50% versus 43%; $P = 0.007$) and the RA group was twice as likely to have preserved EF (odds ratio [OR] 1.90 [95% CI 0.98, 3.67]). Schau et al (15) reported that of 38 RA patients with clinical HF, nearly all (n = 36 [95%]) had a diastolic phenotype with preserved EF. These observations suggest that RA may be added

Table 2. Left ventricular structural and functional parameters in RA patients versus non–RA patients without HF*

Author, year (ref.)	Study design	n, RA vs. non-RA	RA vs. non-RA, (95% CI) [*P*]	Statistical adjustments
LVMI, TTE studies				
Aslam et al, 2013 (22)	Meta-analysis; cross-sectional	1,614 vs. 4,222	Mean difference in LVMI +6.2 gm/m^2 (1.08, 11.33)	None
Rudominer et al, 2009 (33)	Cross-sectional	89	LVMI and RA status, OR 3.24 (1.05, 5.42), $\beta = 0.177$ [$P = 0.004$]	Age, BMI, hypertension
Myasoedova et al, 2013 (24)	Cross-sectional	200 vs. 600	Mean ± SD LVMI 84.6 ± 15.9 gm/m^2 vs. 91.7 ± 22.2 gm/m^2 [$P < 0.001$]	CV risk factors, comorbidities
Corrao et al, 2015 (23)	Meta-analysis of case–control studies; cross-sectional	401 vs. 383	Mean difference in LVMI +0.47 gm/m^2 (0.32, 0.62)	None
Midtbø et al, 2017 (25)	Cross-sectional	119 vs. 46	Mean ± SD LVMI, active RA 34.5 ± 12.1 gm/m$^{2.7}$; remission RA 33.2 ± 10.2 gm/m$^{2.7}$; no RA 31.1 ± 8.1 gm/m$^{2.7}$: no significant differences among 3 groups	None
Davis et al, 2017 (31)	Prospective longitudinal cohort	160 vs. 1391	Mean difference in LVMI per year −0.0004% (−8.917, −0.199)	Age, sex, CV risk factors
LVMI, CMR studies				
Giles et al, 2010 (26)	Cross-sectional	75 vs. 225	Mean difference in LVMI −14.7 gm/m^2 [$P < 0.001$]	Demographics, CV risk factors
Ahlers et al, 2020 (6)	Cross-sectional	59 vs. 56	Median LVMI 44 gm/m^2 vs. 42 g/m^2 [$P = 0.19$]	None
Bissell et al, 2020 (27)	Cross-sectional	76 vs. 26	Mean difference in LVMI −4.558 gm/m^2 [$P < 0.001$]	Age, sex, CV risk factors
Plein et al, 2020 (28)	Cross-sectional: RA vs. controls	81 vs. 30	Mean LVM 78.2 gm (74.0, 82.6) vs. 92.9 gm (84.8, 101.7) [$P < 0.01$], RA vs. non-RA	Age, sex, systolic blood pressure, smoking
	Prospective: RA only		Mean LVM (RA only) 78.2 (73.7, 82.9) at baseline vs. 81.4 (76.3, 86.9) after 1 year of treatment [$P = 0.01$]	
Systolic strain, TTE studies				
Fine et al, 2014 (35)	Cross-sectional	59 vs. 59	Mean ± SD systolic strain −15.7 ± 3 .2% vs. −18.1 ± 2.4% [$P < 0.001$]	None
Cioffi et al, 2017 (36)	Prospective cohort	209 vs. 52	Mean ± SD systolic strain −18.4 ± 3.4% vs. −19.9 ± 2.6% [$P < 0.005$]	None
Midtbø et al, 2017 (25)	Cross-sectional	78 vs. 46	Mean ± SD global longitudinal strain −18.9 ± 3.1% vs. −20.6 ± 3.5% [$P = 0.02$], active RA vs. remission RA; no significant difference between active RA and controls or between remission RA and controls	None
Lo Gullo et al, 2018 (40)	Cross-sectional	41 vs. 58	Mean ± SD systolic strain −18.13 ± 1.36% vs. −23.25 ± 1.80% [$P < 0.001$]	None
Systolic strain, CMR studies				
Ntusi et al, 2019 (37)	Cross-sectional	69 vs. 63	Mean ± SD mid short axis circumferential strain rate −17.4 ± 1.3 vs. −19.2 ± 1.0 without CV risk factors; −16.8 ± 1.1 vs. −18.2 ± 1.2 with CV risk factors	None
Yokoe et al, 2020 (80)	Cross-sectional	80 vs. 20	Systolic strain −16.5% (−14.0, −18.6) vs. −18.2% (−16.2, −19.6) [$P < 0.055$]	None
Diastolic function, TTE studies				
Aslam et al, 2013 (22)	Meta-analysis; cross-sectional	1,614 vs. 4,222	Mean difference, LAD +0.09 cm (0.01, 0.17); IVRT +9.67 msec (5.78, 13.56); E/A ratio −0.17 (−0.25, −0.09); DT +6.38 msec (−2.76, 15.51)	None

(Continued)

Table 2. (*Cont'd*)

Author, year (ref.)	Study design	n, RA vs. non-RA	RA vs. non-RA, (95% CI) [*P*]	Statistical adjustments
Davis et al, 2017 (31)	Prospective longitudinal cohort	160 vs. 1,391	Mean difference (annualized rate of change), LAVI +0.251 [$P < 0.001$]; E/A ratio −0.307 [$P < 0.001$]; E/e′ ratio −0.038 [$P = 0.16$]; DT −0.009 msec [$P = 0.90$]	Age, sex, hypertension, obesity, diabetes, CAD, smoking

* RA = rheumatoid arthritis; HF = heart failure; LVMI = left ventricular mass index; TTE = transthoracic echocardiography; OR = odds ratio; 95% CI = 95% confidence interval; BMI = body mass index; CV = cardiovascular; CMR = cardiac magnetic resonance; LAD = left atrial dimension; IVRT = isovolumetric relaxation time; E/A ratio = ratio between peak early (E) and late (A) velocity of mitral flow; DT =deceleration time; E/e′ ratio = ratio between peak early (E) velocity of mitral flow and peak early diastolic velocities of lateral/septal mitral annulus (averaged); LAVI = left atrial volume index; CAD = coronary artery disease.

to the list of chronic inflammatory states that predispose to HFpEF.

Due to the retrospective nature of most of the HF studies in RA, there are limited available data on the relationship of RA-associated factors to the risk of developing HF, particularly HFpEF. However, in the study by Mantel and colleagues (5), non-ischemic HF was associated more potently than ischemic HF with an erythrocyte sedimentation rate (ESR) >40 mm/hour and with a Disease Activity Score in 28 joints (DAS28) (16) >5.1 (HR 3.03 [95% CI 1.69, 2.73] for ESR >40 mm/hour; HR 3.35 [95% CI 1.84, 6.09] for DAS28 >5.1). Moreover, rheumatoid factor (RF)–positive RA patients had a 40% higher risk of incident HF than RF-negative patients. Investigators at the Mayo Clinic (2,4,17) also observed an elevated risk of HF with RF positivity (HR 1.6 [95% CI 1.0, 2.5]), as well as with elevated ESR (HR 2.1 [95% CI 1.2, 3.5]) and extraarticular disease (HR 3.1 [95% CI 1.9, 5.1]). Taken together, these data suggest that rheumatoid inflammation represents an independent risk factor for incident HF, and perhaps more strongly for the HFpEF phenotype.

Traditional diagnostic and prognostic CVD biomarkers include N-terminal pro–B-type natriuretic peptide (NT-proBNP), BNP, and troponin. BNP, released with atrial contraction, has long been heralded as a biomarker for predicting systolic, decompensated HF risk and all-cause mortality (18). And a gradient increase in cumulative incidence of CV death per every unit increase in troponin was noted in a large population of patients with stable CAD in the general population (19). However, diagnostic/prognostic biomarkers for HF in RA patients are understudied. An association between NT-proBNP level and all-cause mortality in RA (HR 2.36 [95% CI 1.42, 3.94]) was reported, but HF-associated mortality was not separately identified (20). The elevated mortality of HF in RA adds urgency to the identification of sensitive measures to detect early myocardial dysfunction in patients with RA.

Measures of myocardial structure and function in RA patients without clinical HF

It is useful to examine whether echocardiographic parameters, known to predict the development of clinical HF, are overrepresented in RA patients *without* clinical HF compared to non–RA patients.

LV structure. In the general population, values of LV mass above defined cutoffs have been linked to an increased risk of composite CV end points, including HF (21). LV mass in RA patients without symptoms of HF has been compared to LV mass in non-RA controls in cross-sectional transthoracic echocardiographic (TTE) studies, summarized and analyzed in 2 meta-analyses (Table 2). In these meta-analyses (22,23), comprising 25 and 16 individual studies, respectively, higher mean differences in LV mass index (LVMI) of +6.2 gm/m^2 and +0.47 gm/m^2, respectively, were reported in the RA compared to non-RA groups. In contrast, findings of 2 more recent TTE studies showed lower average LVMI in the RA group (24), or no significant difference in LVMI between groups (25).

Other studies have utilized cardiac magnetic resonance (CMR) imaging to measure LV mass in RA. In 3 cross-sectional CMR studies of RA patients versus non-RA controls (26–28), all without clinical HF, LVMI was lower among RA patients (differences of −14.7 gm/m^2, −4.558 g/m^2, and −14.7 gm, respectively), while a fourth CMR study (6) showed no significant group difference (Table 2). CMR is considered the gold standard for assessing LV mass and volumes (29) because of its high spatial and temporal resolution that is not limited by body habitus or ventricular geometry, and thus, the ventricles can be imaged in their entirety without the necessity for geometric assumptions. Yang et al showed that adequate visualization of LV wall segments could be obtained by CMR in 97% of patients, versus only 38% with TTE (30). Thus, observed differences in LVMI may be attributable to technology. Other considerations include lack of statistical adjustment for potential confounders in the TTE meta-analyses, and differences among all studies in levels of severity or duration of RA. Indeed, positive associations of C-reactive protein (CRP) level and RA disease duration with LVMI, and association of current glucocorticoid use with lower LVMI, have been reported (28).

Additional insight might be gained from investigating differential rates of change in LVMI in RA versus non-RA groups over time. However, in a prospective observational TTE study

in RA patients without clinical HF (31), while LVMI in both RA and non-RA groups declined significantly over 4–5 years, the rates were not significantly different between groups. In a CMR study by Plein et al (28), patients with early untreated RA had a lower mean LVM at baseline than non-RA controls, but after 1 year of treatment, mean LVM increased in the RA group from 78.2 gm to 81.4 gm ($P = 0.01$). These CMR studies suggest that RA itself may be associated with a decline in LVM, perhaps similar to the sarcopenia seen in peripheral muscle in RA, and that treatment of RA may facilitate the regaining of some muscle mass. However, proof of this hypothesis will require longer follow-up with carefully performed sequential CMR or TTE, and adjustment for treatment effect and CV risk factors. Until then, associations of lower or higher LV mass with RA therapies, found in cross-sectional studies, are difficult to interpret.

Other descriptions of LV geometry (32), such as concentric remodeling (normal LVMI and relative wall thickness [RWT] >0.42 cm), concentric hypertrophy (increased LVMI and RWT >0.42 cm), and eccentric hypertrophy (increased LVMI and RWT ≤0.42 cm), have been used to categorize phenotypes of LV remodeling. Descriptions of LV geometry in RA patients versus non–RA patients have been reported in 3 TTE studies. Rudominer et al (33) observed that of 16 RA patients without clinical HF but with LV hypertrophy, 15 had eccentric hypertrophy. In contrast, Myasoedova and colleagues (24) reported that among individuals without HF, concentric remodeling was more prevalent in patients with RA compared to the non-RA group (44% versus 19.2%; P <0.001). Cioffi et al (34) also reported a significantly higher prevalence of concentric geometry in patients with RA versus non-RA subjects without HF (47% versus 10%; $P < 0.001$). Thus, the current evidence suggests a concentric geometry phenotype in RA patients without clinical HF, which would be consistent with the presumed nonischemic nature of RA-associated HFpEF.

LV function. *Systolic function.* Among subjects without clinical CVD with RA versus those without RA, the conventional measure of systolic function, EF, does not differ significantly between those with and without RA, as measured by either TTE (22,25,35,36) or CMR (37). However, systolic strain, assessed by speckle tracking echocardiography or by tagging in CMR, is a more sensitive predictor of systolic dysfunction and of CV clinical end points, including mortality (38), in general population studies. While EF reflects change in LV volume only, systolic strain is an assessment of myocardial deformation during systole coupled with LV volume. Global longitudinal strain (GLS) is reported as a negative value, reflecting shortening of the LV axis during contraction; a more negative value reflects greater contraction, with normal values in the −15.9% to −22.1% range (39). Systolic strain has been examined in RA patients without clinical HF (Table 2). All TTE studies (35,36,40) and 1 CMR study (37) demonstrated lower GLS (i.e., less negative, worse function) in RA patients versus non–RA patients. In an RA cohort without clinical CVD (36), low GLS predicted future CV hospitalizations for congestive heart failure, myocardial infarction, limb ischemia, or atrial fibrillation (HR 4.50 [95% CI 1.40, 13.70]).

Diastolic function. LV diastolic dysfunction (DD) is a characteristic finding in HFpEF and is manifested by increased myocardial stiffness, impaired relaxation, and impaired systolic reserve (41). DD is assessed by Doppler echocardiography, with measurement of transmitral blood flow velocities in early (E) and late (A) diastole, septal and/or lateral mitral valve annular velocities (e′), and tricuspid regurgitant jet velocity (42). Twenty-five case–control studies of DD in RA patients versus non-RA controls, all without clinical HF, were analyzed in a meta-analysis (22) (Table 2). DD (≥2 abnormal diastolic parameters) was reported in 26–36% of the RA patients versus 15–21.7% of the non–RA patients. In a prospective TTE study by Davis et al (31) comparing RA patients (n = 160) versus non–RA patients (n = 1,391) without HF, more rapid decreases in E/A, E/e′, and deceleration time, and a more rapid increase in left atrial volume index, all reflecting decline in diastolic function, occurred in the RA group (in contrast to no difference in rate of change in LVMI). Whether these changes in diastolic function herald the onset of HFpEF in RA is as yet unknown.

Biomarkers of myocardial dysfunction

There are few reports of CVD biomarkers in RA patients without clinical HF. BNP, as a screening tool for asymptomatic DD in RA patients, had low positive predictive value (25%), sensitivity of only 40%, and specificity of 89% (43). BNP and troponin measurements may both be confounded by systemic inflammation. In fact, although there are no reported studies of associations of troponin T or I levels with subclinical LV remodeling in RA, RA patients were reported to have higher levels of high-sensitivity troponin I (cTn-I) than non–RA patients, and DAS28-CRP was independently associated with cTn-I levels in RA patients (44). The paucity of data and potentially limited utility of conventional CV biomarkers in detection of subclinical LV dysfunction in RA underscore the need to incorporate novel biomarker studies into prospective investigations of the natural history of LV remodeling in RA.

Pathophysiologic roles of systemic and local inflammation in HF and subclinical myocardial remodeling in RA

There is substantial evidence of an association of RA characteristics, such as RA duration, disease activity, and seropositivity (45–47), with baseline biomarkers of inflammation (interleukin-6 [IL-6] and CRP levels) (31,45–48), with both baseline and

longitudinal changes in LV structure and function (Table 3). However, investigations of specific molecular mechanisms that drive these changes in RA are few. In this section, we consider the following: 1) What is the body of evidence suggesting that circulating inflammatory molecules critical to synovial inflammation and joint destruction also *cause* LV dysfunction in RA? 2) Can local (myocardial) inflammation be demonstrated and does it contribute to LV dysfunction in RA? and 3) Does endothelial dysfunction occur locally in the RA myocardium, is it associated with systemic and/or local myocardial inflammation, and does it contribute to LV remodeling and dysfunction? These hypotheses are represented graphically in Figure 1.

Systemic inflammation and LV structure/function in RA. Several inflammatory molecules that play a key role in RA synovitis and joint destruction, such as tumor necrosis factor (TNF), IL-1, IL-6, and matrix metalloproteases (MMPs), have also been implicated in the pathogenesis of HF in the general population. Inflammatory cytokines critical to HF pathophysiology can be broadly categorized into those implicated in negative LV inotropy (TNF, IL-1, IL-6, IL-18) (49) or in LV remodeling (TNF, tissue inhibitor of metalloproteinases 1, MMP-3, MMP-9, monocyte chemotactic protein 1, IL-8, IL-17) (50,51).

Given the limited number of studies in RA patients and in experimental RA models, we will focus on TNF, IL-1, and MMPs. Higher levels of TNF have been reported in both blood and myocardia of patients with HF in the general population compared to those without HF (52). Animal studies further support the notion that TNF has a direct role in HF pathophysiology. Infusion of TNF causes acute hemodynamic collapse and inflammatory infiltration in the LV, which are reversed with cessation of infusion (53). In mice with cardiac-restricted overexpression of a human TNF transgene, depression of LV function, LV dilatation, marked myocardial inflammation, and ultimately myocardial fibrosis, HF, and death were observed (51).

IL-1 levels are also elevated in patients with chronic HF (54). IL-1 acutely depresses myocyte contractility, due in part to impairments in cytoplasmic calcium handling and β-adrenergic receptor signaling (54). At the histologic level, IL-1 is implicated in cardiac myocyte hypertrophy, and ultimately in myocardial fibrosis, via NF-κB and JAK/STAT pathways (54). Although evidence is lacking in RA, it can be hypothesized that TNF and IL-1, circulating in high levels in RA patients, bathe the myocardium and engage cognate receptors on myocardial cells, inducing the types of deleterious effects outlined above.

Myocardial inflammation and LV structure/function in RA. Just as the RA synovium becomes infiltrated with inflammatory/immune cells including monocyte/macrophages, T cells, and B cells, there has been interest in whether a similar process occurs in RA myocardia. In early autopsy studies (55), higher prevalence rates of inflammatory cell infiltration and myofiber degeneration in the hearts of subjects with RA versus those without RA were reported. However, there is almost no modern literature on histopathology of the heart in RA. Moreover, given the risks involved in endomyocardial biopsy and its potential diagnostic inaccuracy due to sampling error (as myocarditis tends to be patchy), the research field has turned to noninvasive cardiac imaging, including CMR and cardiac positron emission tomography (PET)/computed tomography (CT) scanning, as alternative methods for identifying myocardial inflammation and fibrosis.

Several studies in RA patients have utilized CMR with late gadolinium enhancement (LGE) to identify myocardial fibrosis/inflammation (Table 3). Kobayashi et al (56,57) reported a prevalence of LGE of up to 38.9% in RA patients without clinical CVD. Moreover, LGE was associated with DAS28 in a multivariable model adjusted for CV risk factors. Ntusi and colleagues (58) found a significantly higher prevalence of LGE on CMR in RA patients versus non–RA patients without HF (46% versus 0%), and confirmed an association of LGE with disease activity in the RA patients. They further demonstrated moderate correlation between DAS28-CRP and LV extracellular volume estimation, a quantitative measure that is postulated to reflect the extent of myocardial fibrosis ($R = 0.61$, $P < 0.001$).

A limitation to the interpretation of LGE is that it can represent inflammation, edema, necrosis or fibrosis, or any combination thereof. Use of ^{18}F-fluorodeoxyglucose (^{18}F-FDG)–PET with CT has emerged as a potentially more specific method for detecting myocardial inflammation. The notion that myocardial FDG uptake reflects inflammation is supported by studies demonstrating accumulation of ^{18}F-FDG in monocyte/macrophages in mice post–myocardial infarction (59), and high association ($R^2 = 0.92$) between localization of CD68+ macrophages and ^{18}F-FDG signaling in rat models of autoimmune myocarditis (60). Cardiac FDG–PET-CT scans require careful pre-scan preparation with a very-low-carbohydrate diet to down-regulate glucose receptors on cardiomyocytes, thus hypothetically isolating inflammatory cells as the only residual glucose receptor–expressing cells. In the only myocardial PET/CT study in RA (61), nearly 40% of patients without clinical CVD (46 of 119) had visually detected myocardial FDG uptake. Using a quantitative software package and scans from healthy controls, a cutoff value for elevated FDG uptake was derived. According to this metric, 18% of RA patients had significantly elevated mean myocardial standardized uptake values, and myocardial standardized uptake values were correlated with RA disease activity ($P = 0.005$) in multivariable analyses. The weight of evidence suggests that subclinical myocarditis and/or fibrosis may be present in a significant proportion of RA patients without clinically evident CVD.

Mechanisms by which inflammatory myocarditis is initiated and/or propagated in RA are unknown. Antibodies to proteins that have a posttranslational modification called citrullination, termed anti–citrullinated protein antibodies, are highly specific for

Table 3. Associations of inflammatory biomarkers and RA characteristics with HF incidence (RA versus non-RA) and with subclinical LV structure/function (RA without HF)*

Author, year (ref.)	Study design	n, RA or RA vs. non-RA	Biomarkers, HR/OR (95% CI)	RA characteristics, HR/OR (95% CI) [*P*]	Statistical adjustments
Incidence of HF in RA vs. non-RA					
Nicola et al, 2005 (2)	Retrospective longitudinal cohort	575 vs. 583	None	HR 2.59 (1.95, 3.43), RF+ RA vs. non-RA	Age, sex, CV risk factors, CAD
Mantel et al, 2017 (5)	Prospective cohort	12,943 vs. 113,884	ESR ≥40 mm/hour vs. ESR ≤40 mm/hour, nonischemic HF: HR 3.03 (1.69, 2.73); ischemic HF: HR 2.41 (1.15, 5.08)	DAS28 ≥5.1 vs. DAS28 <5.1, nonischemic HF: HR 3.35 (1.84, 6.09); ischemic HF: HR 2.68 (1.24, 5.78)	None
Ahlers et al, 2020 (6)	Prospective cohort	9,889 vs. 9,889	OR 1.24 (1.11, 1.38), HFpEF and CRP; OR 1.17 (1.03, 1.33), HFrEF and CRP	Not reported	Age, sex, race, CAD, CV treatment, DMARDs
Myocardial measures (LVMI) in RA patients without HF					
Rudominer et al, 2009 (33)	Cross-sectional TTE	89	No significant associations	No significant associations	Age, BMI, hypertension
Giles et al, 2010 (26)	Cross-sectional CMR	75	No significant associations between LVMI and CRP, IL-6	LVMI associated with bDMARDs ($\beta = -5.75$) [$P < 0.05$] and CCP ($\beta = -0.46$) [$P < 0.05$]	Age, sex, BSA, systolic blood pressure, DMARDs, smoking
Myasoedova et al, 2013 (24)	Cross-sectional TTE	200	No significant associations between LVMI and CRP, IL-6, TNF	LVMI associated with glucocorticoid use ($\beta = -0.082$) [$P = 0.002$]	None
Ntusi et al, 2015 (58)	Cross-sectional CMR	39	Not reported	R = 0.6 [$P < 0.001$], ECV and DAS28	None
Bissell et al, 2020 (27)	Cross-sectional CMR	76	Not reported	No significant associations between LVMI and DAS28, ACPA, HAQ DI, RA duration	Age, sex, CV risk factors, ACPA
Diastolic function in RA patients without HF					
Di Franco et al, 2000 (47)	Cross-sectional TTE	32	Not reported	r = 0.40 [$P = 0.01$], E/A ratio and RA duration	None
Arslan et al, 2006 (46)	Cross-sectional TTE	52	Not reported	r =0.40 [$P = 0.004$], E/A ratio and RA duration	None
Udayakumar et al, 2007 (48)	Cross-sectional TTE	45	Not reported	r = −0.56 [$P = 0.001$], E/A ratio and RA duration	None
Liang et al, 2010 (45)	Cross-sectional TTE	244	OR 1.2 (1.01, 1.4), DD and median (IQR) IL-6 level	OR 3.3 (1.8, 5.9), DD and median (IQR) RA duration	Age, sex, CV risk factors

(Continued)

Table 3. (*Cont'd*)

Author, year (ref.)	Study design	n, RA or RA vs. non-RA	Biomarkers, HR/OR (95% CI)	RA characteristics, HR/OR (95% CI) [*P*]	Statistical adjustments
Davis et al, 2017 (31)	Prospective longitudinal cohort (5-year changes)	160	r = −0.16 [*P* = 0.047], E/A ratio and CRP; r = 0.19 [*P* = 0.02], E′ and IL-6	A velocity associated with glucocorticoid use [*P* = 0.04]; E/e′ ratio associated with patient global score [*P* = 0.005] and RAPID3 score [*P* = 0.02]	None
Systolic function in RA patients without HF					
Fine et al, 2014 (35)	Cross-sectional TTE	87	No significant associations between systolic longitudinal strain and ESR	β = 1.84 [*P* = 0.062], longitudinal strain and glucocorticoid use; β = 1.46 [*P* = 0.054], longitudinal strain and MTX use	Age, sex, systolic blood pressure, BMI, heart rate, LVMI
Cioffi et al, 2017 (36)	Prospective cohort TTE	209	No significant associations between GCS/GLS and CRP	No significant associations between GCS/GLS and RA duration, RF/CCP, CDAI, glucocorticoid use	None
Midtbø et al, 2017 (25)	Cross-sectional TTE	78	Not reported	β = 0.21 [*P* = 0.02], GLS and DAS28	Age, sex, BMI, systolic blood pressure, LVEF
Lo Gullo et al, 2018 (40)	Cross-sectional TTE	41	Not reported	β = 8.075 [*P* < 0.0001], GLS and DAS28; β = 7.214 [*P* = 0.002], GCS and DAS28	Age, BMI, CRP, ESR, systolic blood pressure, diastolic blood pressure, others
Ntusi et al, 2019 (37)	Cross-sectional CMR	69	β = 0.02 (0.01, 0.04) [*P* = 0.06], circumferential strain rate and CRP	None	Age, CV risk factors, aortic distensibility

* LV = left ventricular; RF = rheumatoid factor; ESR = erythrocyte sedimentation rate; DAS28 = Disease Activity Score in 28 joints; CRP = C-reactive protein; HFpEF = heart failure with preserved ejection fraction; HFrEF = heart failure with reduced ejection fraction; DMARDs = disease-modifying antirheumatic drugs; IL-6 = interleukin-6; bDMARDs = biologic DMARDS; CCP = cyclic citrullinated peptide; BSA = body surface area; TNF = tumor necrosis factor; ECV = extracellular volume; ACPA = anti–citrullinated protein antibody; HAQ DI = Health Assessment Questionnaire disability index; IQR = interquartile range; DD = diastolic dysfunction; RAPID3 = Routine Assessment of Patient Index Data 3; MTX = methotrexate; GCS = global circumferential strain; GLS = global longitudinal strain; CDAI = Clinical Disease Activity Index; LVEF = left ventricular ejection fraction (see Table 2 for other definitions).

RA (62). Data from autopsied hearts of patients with RA indicate that levels of myocardial citrullination are higher in RA compared to control hearts (63). It is possible that in RA, antibodies are generated not just to synovial, but also to cardiac-specific, citrullinated antigens, triggering an autoimmune response within the heart. In RA patients without clinical CVD, levels of seroreactivity against citrullinated fibrinogen and citrullinated vimentin correlated with higher LVMI ($P < 0.05$) (64). These putative immune complexes may lead to local myocardial inflammation and remodeling, but this conjecture requires further investigation and confirmation.

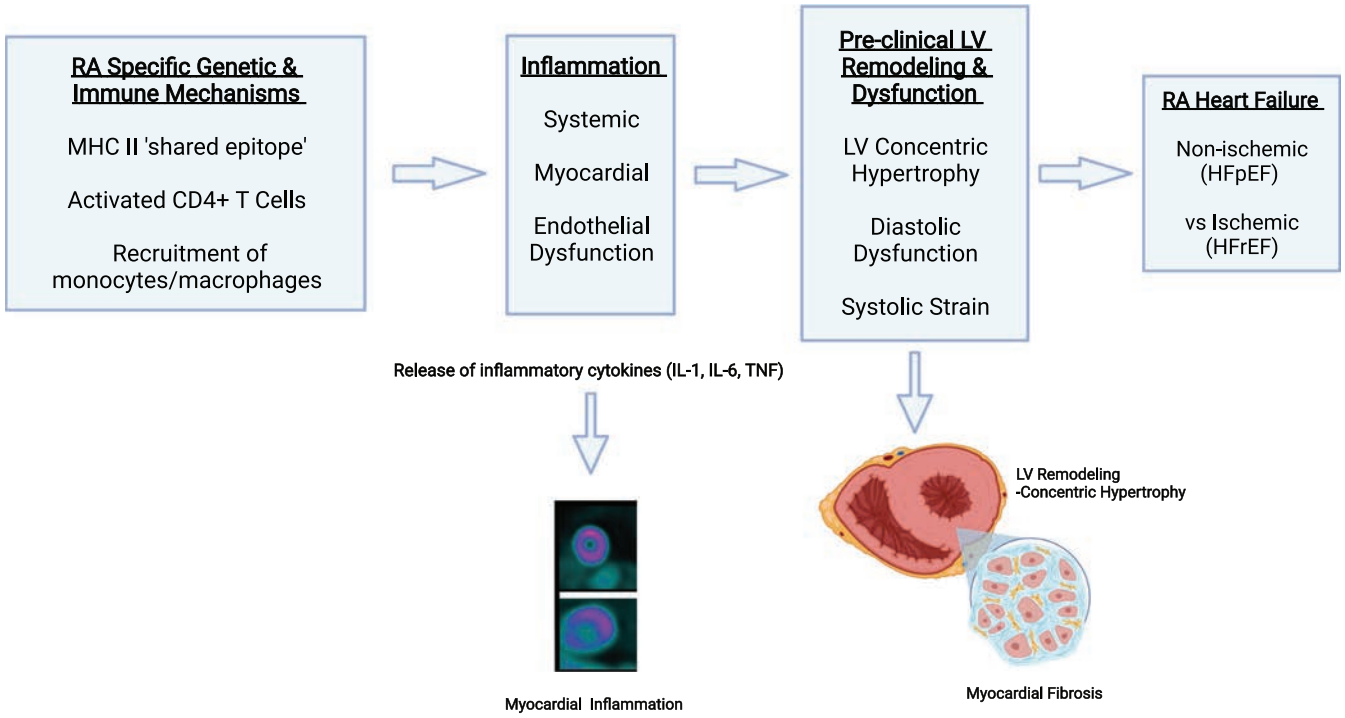

Figure 1. Mechanisms driving left ventricular (LV) dysfunction and heart failure (HF) in patients with rheumatoid arthritis (RA). Antigen-presenting cells expressing major histocompatibility complex (MHC) type II alleles that encode RA-specific "shared epitopes" interact with and select CD4+ T cells. Activated antigen-specific CD4+ T cells interact, in turn, with circulating monocytes and/or tissue macrophages to induce release of key inflammatory cytokines (interleukin-1 [IL-1], IL-6, tumor necrosis factor [TNF]). These cytokines, possibly coupled with anti–citrullinated protein antibody–containing immune complexes, induce myocardial inflammation with subsequent endothelial damage and microvascular dysfunction. In addition, inflammatory cytokines activate local myofibroblasts that promote myocardial fibrosis and LV remodeling (concentric hypertrophy), which results in diastolic dysfunction and/or systolic strain. These changes in turn may lead to clinical HF with preserved ejection fraction (HFpEF). Since RA also promotes accelerated atherosclerosis through similar mechanisms, ischemic damage to the myocardium may also contribute to HF resulting in a reduced EF (HFrEF).

Myocardial endothelial (microvascular) dysfunction and LV structure/function in RA. Another potential mechanism of HF in RA is inflammation-induced endothelial dysfunction, leading to impaired vasodilation of the microvasculature and decreased perfusion of the surrounding territory (65). This is also thought to be a mechanism contributing to the enhanced risk of HFpEF in mildly inflammatory conditions such as obesity and diabetes mellitus (66). Indeed, in RA, studies utilizing diverse methodologies—e.g., brachial artery reactivity, laser Doppler imaging, peripheral arterial tonometry—have demonstrated *microvascular* (defined by arteries smaller than 500 mm) dysfunction in RA patients and its association with disease activity, circulating cytokines, and future atherosclerosis (65). However, few studies have directly investigated *myocardial* microvascular function in RA. The intramyocardial arterioles and capillaries of the heart account for 75% of the resistance in the coronary circulation; thus, dysfunction in these vessels can lead to ischemia even in the absence of significant CAD (66). Microvascular disease is quantified by myocardial flow reserve (MFR), also called coronary flow reserve, i.e., the ratio of myocardial blood flow at peak vasodilatory stress to blood flow at rest. In the absence of significant CAD, this ratio is thought to represent the vasodilatory reserve of the microvascular circulation. MFR cutoffs of <1.5 or <2.0 have been suggested to represent microvascular dysfunction (66,67). In the general population, impaired MFR has been linked with subclinical DD and with HFpEF (67). Decreased nitric oxide bioavailability resulting from microvascular dysfunction has been suggested as a mechanism leading to concentric LV modeling and myocardial stiffness (67).

There have been few investigations of myocardial microvascular perfusion in RA patients without clinical CVD. Using TTE techniques, investigators have found significantly lower MFRs in RA patients without HF compared to controls (68,69). Recio-Mayoral et al (70) also reported lower (impaired) MFR in RA and systemic lupus erythematosus patients versus controls ($P < 0.001$) as demonstrated by cardiac PET-CT, and MFR correlated inversely with disease activity ($r = -0.65$, $P < 0.001$). Microvascular dysfunction is a well-documented complication of diabetes mellitus; Liao et al reported similar rates of impaired MFR in RA patients and diabetes mellitus patients (54% and 64%, respectively), and MFR <2 was significantly associated with all-cause mortality (HR 2.43 [95% CI 1.40, 4.22]) (71). Amigues

and colleagues (72) reported a mean MFR of <2.5 in 29% of RA patients without clinical CVD, and a mean MFR of <2.0 in 12%. In multivariable analyses, TNF inhibitor (TNFi) use was associated with higher (better) MFR ($P = 0.023$), while lower (worse) MFR was associated with higher IL-6 levels and higher LVMI, suggesting a relationship of depressed MFR with inflammation and myocardial remodeling. Longitudinal studies examining the potential role of microvascular disease in the development of clinical HF in RA are needed.

In summary, RA-specific autoimmune mechanisms that trigger release of inflammatory cytokines may lead to local activation of macrophages and myofibroblasts in the myocardium, subsequent myocardial inflammation, endothelial damage, and decreased perfusion, and ultimately, LV remodeling and clinical HF. However, much work is needed to confirm these events and elucidate causative molecular pathways.

Effect of DMARDs on HF and on subclinical measures of LV structure and function in RA

Demonstration of the association of inflammatory cytokines with LV remodeling in experimental models generated considerable interest in cytokine blockade as a therapy for HF. However, clinical trials of TNFi for treatment of moderate-to-severe HF in the general population yielded disappointing results. In the Randomized Etanercept Worldwide Evaluation (RENEWAL) trial (73), there was neither significant benefit nor increased risk in all-cause-mortality or HF hospitalizations in etanercept-treated versus placebo-treated patients (RR 1.10 [95% CI 0.9, 1.33], $P = 0.33$). In contrast, in the Anti-TNF Therapy Against Congestive Heart Failure (ATTACH) trial (74), a higher risk of death and/or hospitalization for HF was reported with infliximab versus placebo treatment (HR 2.84 [95% CI 1.01, 7.97], $P = 0.043$). Subsequently, 38 cases of new-onset HF in patients receiving etanercept or infliximab for conditions other than HF were reported (75), raising further concern. As a result, the US Food and Drug Administration issued a warning regarding use of TNFi in individuals with HF.

Consequently, no randomized controlled trials (RCTs) of TNF inhibitors to treat HF in RA patients have been conducted. However, several observational studies of the association of TNFi with HF incidence or prevalence in RA have been published (Table 4). In the prospective Rheumatoid Arthritis—Observation of Biologic Therapy (RABBIT) cohort study, a non–statistically significant increase in risk of incident HF with TNFi treatment versus conventional synthetic DMARD (csDMARD) treatment was observed (adjusted HR 1.66 [95% CI 0.67, 4.1]) (76). In a retrospective cohort study of RA patients age >65 years, the HR for new hospitalizations for HF in patients treated with TNFi versus those treated with methotrexate was also numerically elevated but not statistically significant (HR 1.61 [95% CI 0.75, 3.49]) (77). Using a combined Medicaid/Medicare database of >10,000 RA patients, Solomon et al (78) found no statistically significant difference in risk of incident HF with TNFi versus csDMARDs (HR 0.84 [95% CI 0.62, 1.12]). Finally, lower rates of incident HF in TNFi-treated versus csDMARD-treated RA patients were observed in 2 studies (11,79). Taken together, these findings suggest that TNFi treatment may reduce, or at least not elevate, risk of HF in RA. While an RCT would provide more definitive evidence, it seems unlikely that such a trial will be forthcoming, given the number of patients and extended length of follow-up needed.

In RA patients *without* HF, the effect of TNFi on measures of LV structure and function has been examined in studies with small sample sizes and with variable outcomes, and the results, taken together, do not offer a clear conclusion (Table 4). In a cross-sectional study, Giles et al (26) demonstrated an association of treatment with a biologic DMARD (bDMARD) (most were receiving TNFi agents) with lower LVMI compared to no bDMARD use. In an RCT, Plein et al (28) showed a modest increase in geometric mean LV mass in 81 RA patients after 1 year of treatment with etanercept plus methotrexate. In a cross sectional study, Yokoe and colleagues (80) reported better global circumferential strain in patients treated with bDMARDs than in those who received csDMARDs. In a study of 23 patients with RA, Kotyla et al (81) found an increase in EF, and a decrease in LVM, after 1 year of infliximab treatment. Other small and/or very-short-duration echocardiographic studies are listed in Table 4 (82–84). In the absence of an RCT to discern the effects of TNFi treatment on HF risk in RA, the American College of Rheumatology 2021 guidelines for the treatment of RA continue to recommend non-TNFi biologics over TNFi in RA patients with HF, and switching from a TNFi to a non-TNFi DMARD if HF develops during treatment with a TNFi.

Despite the success of the Canakinumab Antiinflammatory Thrombosis Outcome Study (CANTOS) RCT (85), in which an IL-1 antagonist was shown to reduce nonfatal myocardial infarction, stroke, and CV death in CAD patients in the general population, there are few studies of IL-1 inhibition in patients with HF. In a clinical trial of patients with HFrEF and HFpEF in the general population, incidence of readmission for or death due to HF after 24 weeks did not differ between the anakinra group and the placebo group (86). However, in experimental RA, IL-1 blockade was associated with improvements in LVEF, LV dilatation, and fractional shortening (50). Since IL-1 inhibitors are only modestly efficacious for the treatment of RA, data on the effect of IL-1 on LV function in RA are also scant. In a short-term study with a small sample size, Ikonomidis et al (87) reported significant improvements in flow-mediated dilation, MFR, and strain measures in RA patients treated with IL-1 inhibitors.

There have been even fewer studies on the impact of IL-6 blockade on HF or LV structure/function or cardiac biomarkers in patients with RA. In a post hoc analysis of RA patients receiving tocilizumab versus placebo, there were no statistically significant differences between groups in decreases in troponin or NT-

Table 4. Effects of anticytokine therapy on incidence/prevalence of clinical HF, and on subclinical LV structure and function, in RA patients*

Author, year (ref.)	Study design	n, TNF or DMARD use	Primary HF outcomes or LV structure/function outcomes (95% CI)	Statistical adjustments
Studies of incident or prevalent HF				
Wolfe et al, 2003 (12)	Retrospective review of longitudinal survey	5,832 vs. 7,339, TNFi (IFX, ETN) vs. no TNFi	Adjusted proportions of HF 2.8 vs. 3.4–3.9 [$P = 0.03$], TNFi vs. no TNFi; 2.6 vs. 2.9 vs. 3.4–3.9, IFX vs. ETN vs. no TNFi	Propensity score matched
Bernatsky et al, 2005 (78)	Nested case–control	187 vs. 3,656, TNFi (IFX, ETN) vs. csDMARDs	Adjusted RR for HF hospitalization 0.7 (0.6, 0.9), any DMARD vs. no DMARD	Age, sex, cohort, ischemic heart disease, stroke, peripheral arterial disease, hypertension, DM, hyperlipidemia, RA treatment
Listing et al, 2008 (75)	Prospective cohort; RABBIT study	2,757 vs. 1,491, TNFi (ADA, IFX, ETN) vs. csDMARDs	Adjusted HR for prevalent HF 1.49 (0.70, 3.18), TNFi vs. csDMARDs	Age, male sex, CVD, BMI, DAS28, functional capacity
			Adjusted HR for incident HF 1.66 (0.67, 4.1), TNFi vs. csDMARDs	Age, sex, CVD, BMI, functional capacity, disease activity at follow-up
			Adjusted HR for worsening HF 1.18 (0.30, 4.73), TNFi vs. csDMARDs	Age, male sex, glucocorticoids >10 mg/day
Setoguchi et al, 2008 (77)	Retrospective cohort; Medicare	1,002 vs. 5,593, TNFi (ADA, IFX, ETN) vs. MTX	Adjusted HR for new HF hospitalization 1.50 (0.41, 4.79), TNFi vs. MTX with previous HF; 3.41 (0.73, 16.05), TNFi vs. MTX without previous HF; 1.61 (0.75, 3.49), TNFi vs. MTX combined (with or without previous HF)	Age, sex, race, CV comorbidities including CAD, other DMARDs, ESR, CRP, CKD, DM, hyperlipidemia
Solomon et al, 2013 (78)	Cohort; Medicaid and Medicare	11,587 vs. 8,656, TNFi (ADA, IFX, ETN) vs. csDMARDs	HR for new or recurrent HF hospitalizations 0.85 (0.63, 1.14), TNFi vs. csDMARDs	Propensity score matched
Studies of LV structure and function in patients without HF				
Kotyla et al, 2012 (81)	Prospective cohort TTE	23, TNFi (IFX)	Median EF 58.5% vs. 63% [$P < 0.05$], before and 1 year after IFX	None

(Continued)

Table 4. (*Cont'd*)

Author, year (ref.)	Study design	n, TNF or DMARD use	Primary HF outcomes or LV structure/function outcomes (95% CI)	Statistical adjustments
Santos et al, 1992 (82)	Prospective cohort TTE	14, TNFi (IFX)	Mean ± SD CO 7.04 ± 2.3 liters/minute vs. 6.12 ± 2.1 liters/minute [$P <$ 0.001] before and 2 hours after IFX; mean ± SD SV 91 ± 29.0 ml/beat vs. 83 ± 28.8 ml/beat [$P <$ 0.001] before and 2 hours after IFX	None
Daien et al, 2013 (84)	Prospective cohort TTE	28 vs. 20, TNFi (ETN) vs. csDMARDs	Mean ± SD change in LVMI at 3 and 6 months −6.3 ± 7.6 and −14.2 ± 9.3 gm/m^2 with ETN; −2.2 ± 10.9 and −2.7 ± 10.2 gm/m^2 with csDMARD	None
Vizzardi et al, 2016 (83)	Prospective cohort TTE	13,TNFi (ADA, IFX, ETN)	No significant changes in EF or GLS 1 year after TNFi vs. baseline	None
Giles et al, 2010 (26)	Cross-sectional CMR	53 vs. 37, non-bDMARD (MTX) vs. bDMARDs (ADA, IFX, ETN, rituximab)	β = −5.75 [$P <$ 0.05], LVM and any bDMARD use	Age, sex, BSA, systolic blood pressure, smoking
Plein et al, 2020 (28)	RCT CMR	81, TNFi (ETN) + MTX	Geometric mean LVM 78.2 gm (73.7, 82.9) and 81.4 gm (76.3, 86.9) [$P =$ 0.01], baseline vs. 1 year after treatment	None
Yokoe et al, 2020 (80)	Cross-sectional CMR	80, csDMARDs or bDMARDs	β = 0.26 [$P =$ 0.021], GCS and bDMARD use	ACPA, SJC, SDAI, MMP-3

* HF = heart failure; RA = rheumatoid arthritis; 95% CI = 95% confidence interval; TNFi = TNF inhibitor; ETN = etanercept; IFX = infliximab; csDMARDs = conventional synthetic DMARDs; RR = relative risk; 95% CI = 95% confidence interval; DM = diabetes mellitus; RABBIT = Rheumatoid Arthritis—Observation of Biologic Therapy; ADA = adalimumab; HR = hazard ratio; CVD = cardiovascular disease; BMI = body mass index; CAD = coronary artery disease; CKD = chronic kidney disease; TTE = transthoracic echocardiography; CO = cardiac output; SV = stroke volume; LVMI = LV mass index; EF = ejection fraction; RCT = randomized controlled trial; CMR = cardiac magnetic resonance; SJC = swollen joint count; SDAI = Simplified Disease Activity Index; MMP-3 = matrix metalloproteinase 3 (see Table 3 for other definitions).

proBNP levels (88). However, Kobayashi et al (89) reported a significant reduction in LVMI ($P <$ 0.001) after 52 weeks of tocilizumab treatment in RA patients, and a significant correlation between the change in the Clinical Disease Activity Index (90) and change in LVMI (ρ = –0.580, $P =$ 0.007). However, as noted above, it is not clear which direction of change in LVMI (higher versus lower; increasing versus decreasing over time) is considered to be beneficial in RA HF pathophysiology and its natural progression.

In summary, the risk/benefit of TNFi treatment in RA patients with comorbid HF remains unclear and requires further investigation. Likewise, insufficient data preclude conclusions about use of IL-1 or IL-6 inhibitors in clinical HF or to slow or prevent subclinical LV remodeling in RA patients.

As glucocorticoids and nonsteroidal antiinflammatory drugs (NSAIDs) are both well-recognized factors in triggering or worsening of acute HF, current European Society of Cardiology guidelines (13) recommend against their use in patients with HF in the general population. Limited data are available on RA patients with HF, however, with regard to the contribution of glucocorticoid and/or NSAID treatment to the incidence or prevalence of HF or to abnormal echocardiographic measures of LV structure/function (such as LVMI). In a prospective cohort study of RA patients by Mantel et al (5), use of glucocorticoids was strongly

associated with nonischemic HF (HR 3.12 [95% CI 1.30, 7.44]) but not statistically significantly associated with ischemic HF or overall HF. However, in another prospective study of RA patients (6), the use of glucocorticoids was not a significant risk factor for incident HFpEF (OR 0.99 [95% CI 0.64, 1.54]).

With regard to the association of glucocorticoid use and abnormal measures of LV structure and function in RA patients without clinical HF, the data are somewhat conflicting. Each study focuses on a different outcome (LVMI [24], systolic longitudinal strain [36], diastolic function [31,45]), and both positive and negative associations with glucocorticoid use have been reported. None of the reviewed studies in RA patients specifically evaluated the association between NSAID use and myocardial measures or HF risk. Given the small number of studies and heterogeneity of findings in this area, clear conclusions are not possible, but clinicians are wise to exercise caution in the use of these medications in RA patients with HF.

Future directions

A keener awareness of the increased risk of HF in RA is needed, particularly given the reports of higher mortality in RA. Typical symptoms and physical examination findings of HF could be misinterpreted as RA-associated interstitial lung disease, and a normal EF on echocardiography may be dismissed before considering the possibility of HFpEF. The development of guidelines for screening RA patients to identify those at high risk of developing HF would be beneficial, but prospective imaging and biomarker data in RA are currently too scarce to inform guidelines. Davis et al (91) reported that a multicytokine immune response score discriminated between normal diastolic function and moderate-to-severe DD, but this cell-based assay may be too unwieldy to translate into clinical use. Longitudinal studies that delineate the natural history from preclinical echocardiographic findings to clinical HF, and that incorporate novel biomarker investigations, are critically needed in RA.

To supplement RA clinical studies, expanded investigation of in vitro HF models specific to RA should be pursued. A promising development in this regard, particularly given the limited availability of RA myocardial tissue, is the generation of engineered human cardiac tissue from an RA patient's own induced pluripotent stem cells (iPSCs). Rim and colleagues (92) derived iPSCs from RA fibroblast-like synoviocytes, and Lee et al (93) demonstrated successful differentiation of cardiomyocytes from those iPSCs. HF may also be investigated as a potential comorbidity of the induction of experimental inflammatory arthritis. Zhou and colleagues (94) reported myocardial inflammation and fibrosis, up-regulated expression of TNF, IL-6, IL-17, and MMP-3 genes in cardiomyocytes and cardiac fibroblasts, and a decline in LV function in mice with collagen-induced arthritis. Additional work in animal models with concurrent inflammatory arthritis and HF could aid in defining shared molecular pathways between the two processes.

A critical area for further study is investigation of the direct effect of cytokine inhibitors on parameters of LV structure and function in RA patients without clinical HF. If these studies were to indicate absence of a detrimental effect on LV function, then further study of the safety of these agents in RA patients with clinical HF could conceivably progress.

Conclusions

In conclusion, the morbidity and mortality burden of HF in RA patients is higher than in the general population and appears to be predominantly of the HFpEF phenotype. There is substantial evidence supporting the notion that chronic inflammation plays a role in driving HF in RA. Whether DMARDs prevent or worsen HF and/or subclinical LV dysfunction in RA remains unclear.

AUTHOR CONTRIBUTIONS

Drs. Park, Griffin, and Bathon drafted the article, revised it critically for important intellectual content, and approved the final version to be published.

REFERENCES

1. Crowson CS, Nicola PJ, Kremers HM, O'Fallon WM, Therneau TM, Jacobsen SJ, et al. How much of the increased incidence of heart failure in rheumatoid arthritis is attributable to traditional cardiovascular risk factors and ischemic heart disease? Arthritis Rheum 2005;52: 3039–44.
2. Nicola PJ, Maradit-Kremers H, Roger VL, Jacobsen SJ, Crowson CS, Ballman KV, et al. The risk of congestive heart failure in rheumatoid arthritis: a population-based study over 46 years. Arthritis Rheum 2005;52:412–20.
3. Avina-Zubieta JA, Thomas J, Sadatsafavi M, Lehman AJ, Lacaille D. Risk of incident cardiovascular events in patients with rheumatoid arthritis: a meta-analysis of observational studies. Ann Rheum Dis 2012;71:1524–9.
4. Nicola PJ, Crowson CS, Maradit-Kremers H, Ballman KV, Roger VL, Jacobsen SJ, et al. Contribution of congestive heart failure and ischemic heart disease to excess mortality in rheumatoid arthritis. Arthritis Rheum 2006;54:60–7.
5. Mantel Ä, Holmqvist M, Andersson DC, Lund LH, Askling J. Association between rheumatoid arthritis and risk of ischemic and nonischemic heart failure. J Am Coll Cardiol 2017;69:1275–85.
6. Ahlers MJ, Lowery BD, Farber-Eger E, Wang TJ, Bradham W, Ormseth MJ, et al. Heart failure risk associated with rheumatoid arthritis–related chronic inflammation. JAHA 2020;9:e014661.
7. Myasoedova E, Gabriel SE, Matteson EL, Davis JM III, Therneau TM, Crowson CS. Decreased cardiovascular mortality in patients with incident rheumatoid arthritis (RA) in recent years: dawn of a new era in cardiovascular disease in RA? J Rheumatol 2017;44:732–9.
8. Myasoedova E, Davis JM, Roger VL, Achenbach SJ, Crowson CS. Improved incidence of cardiovascular disease in patients with incident rheumatoid arthritis in the 2000s: a population-based cohort study. J Rheumatol 2021;48:1379–87.
9. Lacaille D, Avina-Zubieta JA, Sayre EC, Abrahamowicz M. Improvement in 5-year mortality in incident rheumatoid arthritis compared with the general population—closing the mortality gap. Ann Rheum Dis 2017;76:1057–63.

10. Davis JM III, Roger VL, Crowson CS, Kremers HM, Therneau TM, Gabriel SE. The presentation and outcome of heart failure in patients with rheumatoid arthritis differs from that in the general population. Arthritis Rheum 2008;58:2603–11.
11. Wolfe F, Michaud K. Heart failure in rheumatoid arthritis: rates, predictors, and the effect of anti–tumor necrosis factor therapy. Am J Med 2004;116:305–11.
12. Wolfe F, Freundlich B, Straus WL. Increase in cardiovascular and cerebrovascular disease prevalence in rheumatoid arthritis. J Rheumatol 2003:30:36–40.
13. Ponikowski P, Voors AA, Anker SD, Bueno H, Cleland JG, Coats AJ, et al, the Task Force for the Diagnosis and Treatment of Acute and Chronic Heart Failure of the European Society of Cardiology (ESC) developed with the special contribution of the Heart Failure Association (HFA) of the ESC. 2016 ESC guidelines for the diagnosis and treatment of acute and chronic heart failure. Eur Heart J 2016;37:2129–200.
14. Redfield MM. Heart failure with preserved ejection fraction [review]. N Engl J Med 2016;375:1868–77.
15. Schau T, Gottwald M, Arbach O, Seifert M, Schöpp M, Neuß M, et al. Increased prevalence of diastolic heart failure in patients with rheumatoid arthritis correlates with active disease, but not with treatment type. J Rheumatol 2015;42:2029–37.
16. Prevoo ML, van't Hof MA, Kuper HH, van Leeuwen MA, van de Putte LB, van Riel PL. Modified disease activity scores that include twenty-eight–joint counts: development and validation in a prospective longitudinal study of patients with rheumatoid arthritis. Arthritis Rheum 1995;38:44–8.
17. Myasoedova E, Crowson CS, Nicola PJ, Maradit-Kramers H, Davis JM III, Roger VL, et al. The influence of rheumatoid arthritis disease characteristics on heart failure. J Rheumatol 2011;38:1601–6.
18. Khanam SS, Son JW, Lee JW, Youn YJ, Yoon J, Lee SH, et al. Prognostic value of short-term follow-up BNP in hospitalized patients with heart failure. BMC Cardiovasc Disord 2017;17:215.
19. Omland T, de Lemos JA, Sabatine MS, Christophi CA, Rice MM, Jablonski KA, et al. A sensitive cardiac troponin T assay in stable coronary artery disease. N Engl J Med 2009;361:2538–47.
20. Mirjafari H, Welsh P, Verstappen SM, Wilson P, Marshall T, Edlin H, et al. N-terminal pro-brain-type natriuretic peptide (NT-pro-BNP) and mortality risk in early inflammatory polyarthritis: results from the Norfolk Arthritis Registry (NOAR). Ann Rheum Dis 2014;73:684–90.
21. Lieb W, Gona P, Larson MG, Aragam J, Zile MR, Cheng S, et al. The natural history of left ventricular geometry in the community: clinical correlates and prognostic significance of change in LV geometric pattern. JACC Cardiovasc Imaging 2014;7:870–8.
22. Aslam F, Bandeali SJ, Khan NA, Alam M. Diastolic dysfunction in rheumatoid arthritis: a meta-analysis and systematic review. Arthritis Care Res (Hoboken) 2013;65:534–43.
23. Corrao S, Argano C, Pistone G, Messina S, Calvo L, Perticone F. Rheumatoid arthritis affects left ventricular mass: systematic review and meta-analysis [review]. Eur J Intern Med 2015;26:259–67.
24. Myasoedova E, Davis JM III, Crowson CS, Roger VL, Karon BL, Borgeson DD, et al. Rheumatoid arthritis is associated with left ventricular concentric remodeling: results of a population-based cross-sectional study. Arthritis Rheum 2013;65:1713–8.
25. Midtbø H, Semb AG, Matre K, Kvien TK, Gerdts E. Disease activity is associated with reduced left ventricular systolic myocardial function in patients with rheumatoid arthritis. Ann Rheum Dis 2017;76:371–6.
26. Giles JT, Malayeri AA, Fernandes V, Post W, Blumenthal RS, Bluemke D, et al. Left ventricular structure and function in patients with rheumatoid arthritis, as assessed by cardiac magnetic resonance imaging. Arthritis Rheum 2010;62:940–51.
27. Bissell LA, Erhayiem B, Hensor EM, Fent G, Burska A, McDiarmid AK, et al. Cardiovascular MRI evidence of reduced systolic function and reduced LV mass in rheumatoid arthritis: impact of disease phenotype. Int J Cardiovasc Imaging 2020;36:491–501.
28. Plein S, Erhayiem B, Fent G, Horton S, Dumitru RB, Andrews J, et al. Cardiovascular effects of biological versus conventional synthetic disease-modifying antirheumatic drug therapy in treatment-naïve, early rheumatoid arthritis. Ann Rheum Dis 2020;79:1414–22.
29. Keenan NG, Pennell DJ. CMR of ventricular function [review]. Echocardiography 2007;24:185–93.
30. Yang PC, Kerr AB, Liu AC, Liang DH, Hardy C, Meyer CH, et al. New real-time interactive cardiac magnetic resonance imaging system complements echocardiography. J Am Coll Cardiol 1998;32: 2049–56.
31. Davis JM III, Lin G, Oh JK, Crowson CS, Achenback SJ, Therneau TM, et al. Five-year changes in cardiac structure and function in patients with rheumatoid arthritis compared with the general population. Int J Cardiol 2017;240:379–85.
32. Lang RM, Badano LP, Mor-Avi V, Afilalo J, Armstrong A, Ernande L, et al. Recommendations for cardiac chamber quantification by echocardiography in adults: an update from the American Society of Echocardiography and the European Association of Cardiovascular Imaging. J Am Soc Echocardiogr 2015;28:1–39.
33. Rudominer RL, Roman MJ, Devereux RB, Paget SA, Schwartz JE, Lockshin MD, et al. Independent association of rheumatoid arthritis with increased left ventricular mass but not with reduced ejection fraction. Arthritis Rheum 2009;60:22–9.
34. Cioffi G, Ognibeni F, Dalbeni A, Giollo A, Orsolini G, Gatti D, et al. High prevalence of occult heart disease in normotensive patients with rheumatoid arthritis. Clin Cardiol 2018;41:736–43.
35. Fine NM, Crowson CS, Lin G, Oh JK, Villarraga HR, Gabriel SE. Evaluation of myocardial function in patients with rheumatoid arthritis using strain imaging by speckle-tracking echocardiography. Ann Rheum Dis 2014;73:1833–9.
36. Cioffi G, Viapiana O, Ognibeni F, Dalbeni A, Giollo A, Gatti D, et al. Prognostic role of subclinical left ventricular systolic dysfunction evaluated by speckle-tracking echocardiography in rheumatoid arthritis. J Am Soc Echocardiogr 2017;30:602–11.
37. Ntusi NA, Francis JM, Gumedze F, Karvounis H, Matthews PM, Wordsworth PB, et al. Cardiovascular magnetic resonance characterization of myocardial and vascular function in rheumatoid arthritis patients. Hellenic J Cardiol 2019;60:28–35.
38. Sengeløv M, Jørgensen PG, Jensen JS, Bruun NE, Olson FJ, Fritz-Hansen T, et al. Global longitudinal strain is a superior predictor of all-cause mortality in heart failure with reduced ejection fraction. JACC Cardiovasc Imaging 2015;8:1351–9.
39. Yingchoncharoen T, Agarwal S, Popović ZB, Marwick TH. Normal ranges of left ventricular strain: a meta-analysis. J Am Soc Echocardiogr 2013;26:185–91.
40. Lo Gullo A, Rodríguez-Carrio J, Aragona CO, Dattilo G, Zito C, Suárez A, et al. Subclinical impairment of myocardial and endothelial functionality in very early psoriatic and rheumatoid arthritis patients: association with vitamin D and inflammation. Atherosclerosis 2018; 271:214–22.
41. Sharma K, Kass DA. Heart failure with preserved ejection fraction: mechanisms, clinical features, and therapies [review]. Circ Res 2014; 115:79–96.
42. Nagueh SF, Smiseth OA, Appleton CP, Byrd BF III, Dokainish H, Edvardsen T, et al. Recommendations for the evaluation of left ventricular diastolic function by echocardiography: an update from the American Society of Echocardiography and the European Association of Cardiovascular Imaging. J Am Soc Echocardiogr 2016;29:277–314.
43. Crowson CS, Myasoedova E, Davis JM III, Roger VL, Karon BL, Borgeson D, et al. Use of B-type natriuretic peptide as a screening tool for left ventricular diastolic dysfunction in rheumatoid arthritis

patients without clinical cardiovascular disease. Arthritis Care Res (Hoboken) 2011;63:729–34.

44. Avouac J, Meune C, Chenevier-Gobeaux C, Dieudé P, Borderie D, Lefevre G, et al. Inflammation and disease activity are associated with high circulating cardiac markers in rheumatoid arthritis independently of traditional cardiovascular risk factors. J Rheumatol 2014;41: 248–55.
45. Liang KP, Myasoedova E, Crowson CS, Davis JM, Rogwer VL, Karon BL, et al. Increased prevalence of diastolic dysfunction in rheumatoid arthritis. Ann Rheum Dis 2010;69:1665–70.
46. Arslan Ş, Bozkurt E, Ali Sari R, Erol MK. Diastolic function abnormalities in active rheumatoid arthritis evaluation by conventional Doppler and tissue Doppler: relation with duration of disease. Clin Rheumatol 2006;25:294–9.
47. Di Franco M, Paradiso M, Mammarella A, Paoletti V, Labbadia G, Coppotelli L, et al. Diastolic function abnormalities in rheumatoid arthritis. Evaluation by echo Doppler transmitral flow and pulmonary venous flow: relation with duration of disease. Ann Rheum Dis 2000;59:227–9.
48. Udayakumar N, Venkatesan S, Rajendiran C. Diastolic function abnormalities in rheumatoid arthritis: relation with duration of disease. Singapore Med J 2007;48:537–42.
49. Mann DL. Inflammatory mediators and the failing heart: past, present, and the foreseeable future [review]. Circ Res 2002;91:988–98.
50. Hartman MH, Groot HE, Leach IM, Karper JC, van der Harst P. Translational overview of cytokine inhibition in acute myocardial infarction and chronic heart failure [review]. Trends Cardiovasc Med 2018;28:369–79.
51. Sivasubramanian N, Coker ML, Kurrelmeyer KM, MacLellan WR, DeMayo FJ, Spinale FG, et al. Left ventricular remodeling in transgenic mice with cardiac restricted overexpression of tumor necrosis factor. Circulation 2001;104:826–31.
52. Levine B, Kalman J, Mayer L, Fillit HM, Packer M. Elevated circulating levels of tumor necrosis factor in severe chronic heart failure. N Engl J Med 1990;323:236–41.
53. Bozkurt B, Kribbs SB, Clubb FJ, Michael LH, Didenko VV, Hornsby PJ, et al. Pathophysiologically relevant concentrations of tumor necrosis factor-α promote progressive left ventricular dysfunction and remodeling in rats. Circulation 1998;97:1382–91.
54. Buckley LF, Abbate A. Interleukin-1 blockade in cardiovascular diseases: a clinical update [review]. Eur Heart J 2018;39:2063–9.
55. Bonfiglio T. Heart disease in patients with seropositive rheumatoid arthritis; a controlled autopsy study and review. Arch Intern Med 1969;124:714–9.
56. Kobayashi Y, Giles JT, Hirano M, Yokoe I, Nakajima Y, Bathon JM, et al. Assessment of myocardial abnormalities in rheumatoid arthritis using a comprehensive cardiac magnetic resonance approach: a pilot study. Arthritis Res Ther 2010;12:R171.
57. Kobayashi H, Kobayashi Y, Yokoe I, Akashi Y, Takei M, Giles JT. Magnetic resonance imaging–detected myocardial inflammation and fibrosis in rheumatoid arthritis: associations with disease characteristics and N-terminal pro–brain natriuretic peptide levels. Arthritis Care Res (Hoboken) 2017;69:1304–11.
58. Ntusi NA, Piechnik SK, Francis JM, Ferreira VM, Matthews PM, Robson MD, et al. Diffuse myocardial fibrosis and inflammation in rheumatoid arthritis. JACC Cardiovasc Imaging 2015;8:526–36.
59. Lee WW, Marinelli B, van der Laan AM, Sena BF, Gorbatov R, Leuschner F, et al. PET/MRI of inflammation in myocardial infarction. J Am Coll Cardiol 2012;59:153–63.
60. Werner RA, Wakabayashi H, Bauer J, Schütz C, Zechmeister C, Hayakawa N, et al. Longitudinal 18F-FDG PET imaging in a rat model of autoimmune myocarditis. Eur Heart J Cardiovasc Imaging 2019;20: 467–74.
61. Amigues I, Tugcu A, Russo C, Giles JT, Morgenstein R, Zartoshti A, et al. Myocardial inflammation, measured using 18-fluorodeoxyglucose positron emission tomography with computed tomography, is associated with disease activity in rheumatoid arthritis. Arthritis Rheumatol 2019;71:496–506.
62. Willemze A, Trouw LA, Toes RE, Huizinga TW. The influence of ACPA status and characteristics on the course of RA. Nat Rev Rheumatol 2012;8:144–52.
63. Giles JT, Fert-Bober J, Park J, Bingham CO III, Andrade F, Fox-Talbot K, et al. Myocardial citrullination in rheumatoid arthritis: a correlative histopathologic study. Arthritis Res Ther 2012;14:R39.
64. Geraldino-Pardilla L, Russo C, Sokolove J, Robinson WH, Zartoshi A, van Eyk J, et al. Association of anti-citrullinated protein or peptide antibodies with left ventricular structure and function in rheumatoid arthritis. Rheumatology (Oxford) 2017;56:534–40.
65. Bordy R, Totoson P, Prati C, Marie C, Wendling D, Demougeot C. Microvascular endothelial dysfunction in rheumatoid arthritis [review]. Nat Rev Rheumatol 2018;14:404–20.
66. Taqueti VR, Di Carli MF. Coronary microvascular disease pathogenic mechanisms and therapeutic options. J Am Coll Cardiol 2018;72: 2625–41.
67. Taqueti VR, Solomon SD, Shah AM, Desai AS, Groarke JD, Osborne MT, et al. Coronary microvascular dysfunction and future risk of heart failure with preserved ejection fraction. Eur Heart J 2018;39:840–9.
68. Ciftci O, Yilmaz S, Topcu S, Caliskan M, Gullu H, Erdogan D, et al. Impaired coronary microvascular function and increased intima-media thickness in rheumatoid arthritis. Atherosclerosis 2008;198:332–7.
69. Turiel M, Atzeni F, Tomasoni L, de Portu S, Delfino L, Bodini BD, et al. Non-invasive assessment of coronary flow reserve and ADMA levels: a case-control study of early rheumatoid arthritis patients. Rheumatology (Oxford) 2009;48:834–9.
70. Recio-Mayoral A, Mason JC, Kaski JC, Rubens MB, Harari OA, Camici PG. Chronic inflammation and coronary microvascular dysfunction in patients without risk factors for coronary artery disease. Eur Heart J 2009;30:1837–43.
71. Liao KP, Huang J, He Z, Cremone G, Lam E, Hainer JM, et al. Coronary microvascular dysfunction in rheumatoid arthritis compared to diabetes mellitus and association with all-cause mortality. Arthritis Care Res (Hoboken) 2021;73:159–65.
72. Amigues I, Russo C, Giles JT, Tugcu A, Weinberg R, Bokhari S, et al. Myocardial microvascular dysfunction in rheumatoid arthritis: quantitation by ^{13}N-ammonia positron emission tomography/computed tomography. Circ Cardiovasc Imaging 2019;12:e007495.
73. Mann DL, McMurray JJ, Packer M, Swedberg K, Borer JS, Colucci WS, et al. Targeted anticytokine therapy in patients with chronic heart failure: results of the Randomized Etanercept Worldwide Evaluation (RENEWAL). Circulation 2004;109:1594–602.
74. Chung ES, Packer M, Lo KH, Fasanmade AA, Willerson JT. Randomized, double-blind, placebo-controlled, pilot trial of infliximab, a chimeric monoclonal antibody to tumor necrosis factor-α, in patients with moderate-to-severe heart failure: results of the Anti-TNF Therapy Against Congestive Heart failure (ATTACH) Trial. Circulation 2003; 107:3133–40.
75. Kwon HJ, Cot TR, Cuffe MS, Kramer JM, Braun MM. Case reports of heart failure after therapy with a tumor necrosis factor antagonist. Ann Intern Med 2003;138:807.
76. Listing J, Strangfeld A, Kekow J, Schneider M, Kapelle A, Wassenberg S, et al. Does tumor necrosis factor α inhibition promote or prevent heart failure in patients with rheumatoid arthritis? Arthritis Rheum 2008;58:667–77.
77. Setoguchi S, Schneeweiss S, Avorn J, Katz JN, Weinblatt ME, Levin R, et al. Tumor necrosis factor-α antagonist use and heart failure in elderly patients with rheumatoid arthritis. Am Heart J 2008;156: 336–41.

78. Solomon DH, Rassen JA, Kuriya B, Chen L, Harrold LR, Graham DJ, et al. Heart failure risk among patients with rheumatoid arthritis starting a TNF antagonist. Ann Rheum Dis 2013;72:1813–8.
79. Bernatsky S, Hudson M, Suissa S. Anti-rheumatic drug use and risk of hospitalization for congestive heart failure in rheumatoid arthritis. Rheumatology (Oxford) 2005;44:677–80.
80. Yokoe I, Kobayashi H, Kobayashi Y, Nishikawa A, Sugiyama K, Nagasawa Y, et al. Impact of biological treatment on left ventricular dysfunction determined by global circumferential, longitudinal and radial strain values using cardiac magnetic resonance imaging in patients with rheumatoid arthritis. Int J Rheum Dis 2020;23:1363–71.
81. Kotyla PJ, Owczarek A, Rakoczy J, Lewicki M, Kucharz EJ, Emery P. Infliximab treatment increases left ventricular ejection fraction in patients with rheumatoid arthritis: assessment of heart function by echocardiography, endothelin 1, interleukin 6, and NT-pro brain natriuretic peptide. J Rheumatol 2012;39:701–6.
82. Santos RC, Figueiredo VN, Martins LC, Moraes CH, Quinaglia T, Boer-Martins L, et al. Infliximab reduces cardiac output in rheumatoid arthritis patients without heart failure. Rev Assoc Med Bras 1992;58:698–702.
83. Vizzardi E, Cavazzana I, Franceschini F, Bonadei I, Sciatti E, Lombardi CM, et al. Left ventricular function in rheumatoid arthritis during anti-TNF-α treatment: a speckle tracking prospective echocardiographic study. Monaldi Arch Chest Dis 2016;84:716.
84. Daïen CI, Fesler P, du Cailar G, Daïen V, Mura T, Dupuy AM, et al. Etanercept normalises left ventricular mass in patients with rheumatoid arthritis. Ann Rheum Dis 2013;72:881–7.
85. Ridker PM, Everett BM, Thuren T, MacFadyen JG, Chang WH, Ballantyne C, et al. Antiinflammatory therapy with canakinumab for atherosclerotic disease. N Engl J Med 2017;377:1119–31.
86. Van Tassell BW, Trankle CR, Canada JM, Carbone S, Buckley L, Kadariya D, et al. IL-1 blockade in patients with heart failure with preserved ejection fraction: results from DHART2. Circ Heart Fail 2018;11:e005036.
87. Ikonomidis I, Tzortzis S, Andreadou I, Paraskevaidis I, Katseli C, Katsimbri P, et al. Increased benefit of interleukin-1 inhibition on vascular function, myocardial deformation, and twisting in patients with coronary artery disease and coexisting rheumatoid arthritis. Circ Cardiovasc Imaging 2014;7:619–28.
88. Welsh P, Tuckwell K, McInnes IB, Sattar N. Effect of IL-6 receptor blockade on high-sensitivity troponin T and NT-proBNP in rheumatoid arthritis. Atherosclerosis 2016;254:167–71.
89. Kobayashi H, Kobayashi Y, Giles JT, Yoneyama K, Nakajima Y, Takei M. Tocilizumab treatment increases left ventricular ejection fraction and decreases left ventricular mass index in patients with rheumatoid arthritis without cardiac symptoms: assessed using 3.0 Tesla cardiac magnetic resonance imaging. J Rheumatol 2014;41:1916–21.
90. Aletaha D, Nell VP, Stamm T, Uffmann M, Pflugbeil S, Machold K, et al. Acute phase reactants add little to composite disease activity indices for rheumatoid arthritis: validation of a clinical activity score. Arthritis Res Ther 2005;7:R796–806.
91. Davis JM, Knutson KL, Strausbauch MA, Crowson CS, Therneau TM, Wettstein PJ, et al. A signature of aberrant immune responsiveness identifies myocardial dysfunction in rheumatoid arthritis. Arthritis Rheum 2011;63:1497–506.
92. Rim YA, Park N, Nam Y, Ju JH. Generation of induced-pluripotent stem cells using fibroblast-like synoviocytes isolated from joints of rheumatoid arthritis patients. J Vis Exp 2016;116:54072.
93. Lee J, Jung SM, Ebert AD, Wu H, Diecke S, Kim Y, et al. Generation of functional cardiomyocytes from the synoviocytes of patients with rheumatoid arthritis via induced pluripotent stem cells. Sci Rep 2016;6:32669.
94. Zhou Z, Miao Z, Luo A, Zhi D, Lu Y, Li P, et al. Identifying a marked inflammation mediated cardiac dysfunction during the development of arthritis in collagen-induced arthritis mice. Clin Exp Rheumatol 2020;38:203–211.

American College of Rheumatology
Empowering Rheumatology Professionals

Arthritis & Rheumatology
Vol. 74, No. 2, February 2022, pp 200–211
DOI 10.1002/art.41941

Activated Peripheral Blood B Cells in Rheumatoid Arthritis and Their Relationship to Anti–Tumor Necrosis Factor Treatment and Response: A Randomized Clinical Trial of the Effects of Anti–Tumor Necrosis Factor on B Cells

Nida Meednu,[1] Jennifer Barnard,[1] Kelly Callahan,[1] Andreea Coca,[1] Bethany Marston,[1] Ralf Thiele,[1] Darren Tabechian,[1] Marcy Bolster,[2] Jeffrey Curtis,[3] Meggan Mackay,[4] Jonathan Graf,[5] Richard Keating,[6] Edwin Smith,[2] Karen Boyle,[7] Lynette Keyes-Elstein,[7] Beverly Welch,[8] Ellen Goldmuntz,[8] and Jennifer H. Anolik[1]

Objective. B cells can become activated in germinal center (GC) reactions in secondary lymphoid tissue and in ectopic GCs in rheumatoid arthritis (RA) synovium that may be tumor necrosis factor (TNF) and lymphotoxin (LT) dependent. This study was undertaken to characterize the peripheral B cell compartment longitudinally during anti-TNF therapy in RA.

Methods. Participants were randomized in a 2:1 ratio to receive standard dosing regimens of etanercept (n = 43) or adalimumab (n = 20) for 24 weeks. Eligible participants met the American College of Rheumatology 1987 criteria for RA, had clinically active disease (Disease Activity Score in 28 joints >4.4), and were receiving stable doses of methotrexate. The primary mechanistic end point was the change in switched memory B cell fraction from baseline to week 12 in each treatment group.

Results. B cell subsets remained surprisingly stable over the course of the study regardless of treatment group, with no significant change in memory B cells. Blockade of TNF and LT with etanercept compared to blockade of TNF alone with adalimumab did not translate into significant differences in clinical response. The frequencies of multiple activated B cell populations, including CD21− double-negative memory and activated naive B cells, were higher in RA nonresponders at all time points, and CD95+ activated B cell frequencies were increased in patients receiving anti-TNF treatment in the nonresponder group. In contrast, frequencies of transitional B cells—a putative regulatory subset—were lower in the nonresponders.

Conclusion. Overall, our results support the notion that peripheral blood B cell subsets are remarkably stable in RA and not differentially impacted by dual blockade of TNF and LT with etanercept or single blockade of TNF with adalimumab. Activated B cells do associate with a less robust response.

INTRODUCTION

Rheumatoid arthritis (RA) is an inflammatory joint disease that affects 1.5 million people in the US and is associated with substantial morbidity and mortality (1). Although multiple cell types play a role in the pathogenesis of RA, the key participation of B cells has long been appreciated since the discovery of rheumatoid factor (RF) and has been re-highlighted over the past several years. Thus, RF and anti–cyclic citrullinated peptide (anti-CCP) autoantibodies are well-established indicators of disease and disease severity and may precede the onset of disease by many years (2–4). The efficacy of B cell depletion therapy further

ClinicalTrials.gov identifier: NCT00837434.

Supported by grant U19-AI-563262 from the National Institute of Allergy and Infectious Diseases, NIH to the Autoimmunity Centers of Excellence.

[1]Nida Meednu, PhD, Jennifer Barnard, BS, Kelly Callahan, BSW, Andreea Coca, MD, MPH, Bethany Marston, MD, Ralf Thiele, MD, Darren Tabechian, MD, Jennifer H. Anolik, MD, PhD: University of Rochester Medical Center, Rochester, New York; [2]Marcy Bolster, MD, Edwin Smith, MD: Medical University of South Carolina, Charleston; [3]Jeffrey Curtis, MD, MS, MPH: University of Alabama at Birmingham; [4]Meggan Mackay, MD, MS: Feinstein Institute for Medical Research, Manhasset, New York; [5]Jonathan Graf, MD: University of California, San Francisco; [6]Richard Keating, MD: University of Chicago, Chicago, Illinois; [7]Karen Boyle, MS, Lynette Keyes-Elstein, DrPH: Rho Federal Systems Division, Chapel Hill, North Carolina; [8]Beverly Welch, RN, MSN, Ellen Goldmuntz, MD, PhD: National Institute of Allergy and Infectious Diseases, NIH, Bethesda, Maryland.

Author disclosures are available at https://onlinelibrary.wiley.com/action/downloadSupplement?doi=10.1002%2Fart.41941&file=art41941-sup-0001-Disclosureform.pdf.

Address correspondence to Jennifer H. Anolik, MD, PhD, Department of Medicine, Division of Allergy, Immunology and Rheumatology, University of Rochester, 601 Elmwood Avenue, Box 695, Rochester, NY 14642. Email: jennifer_anolik@urmc.rochester.edu.

Submitted for publication November 18, 2020; accepted in revised form July 29, 2021.

highlights the pathogenic significance of B cells in RA (5–7). B cells may provide a critical link between the development of tertiary lymphoid structure within the inflamed synovium and the propagation of the autoimmune process. This connection is supported by the finding of germinal center (GC)–like structures within the inflamed RA synovium and the observation that T cell activation in the RA synovium is dependent on the presence of B cells within these active GCs (8,9).

Tumor necrosis factor (TNF) is also clearly established as a central player in the pathogenesis of RA. The current paradigm regarding the mechanism of action of TNF blockade in RA focuses on the proinflammatory effects of TNF. Indeed, TNF is a sentinel proinflammatory cytokine in normal immune responses and in pathologic immune responses in the RA synovium. Along with interleukin-1 (IL-1), it orchestrates many of the pathophysiologic abnormalities that characterize RA, including the local effects of inflammation and the development of joint damage (10). Inhibiting TNF interrupts the disease process by blocking the activation of T cells, macrophages, and synovial fibroblasts.

In addition to TNF, lymphotoxin α (LTα) and LTβ are 2 related TNF superfamily members whose levels have been shown to be increased in RA serum and synovial tissue (11–13). Notably, in mice, LT signaling is particularly critical for the development and maintenance of normal spleen and lymph node microarchitecture (14). LT signaling has also been associated with lymphoid aggregates in the synovium of RA patients (11,12). Signaling by TNF and LT is required for the development of follicular dendritic cells (FDCs), the cells that are responsible for the initiation of secondary lymphoid GC structures (15,16). Despite the potential for TNF and LT to directly signal through TNF receptor type I (TNFRI) and TNFRII expressed on B cells and indirectly impact B cell activation via promotion of tissue lymphoid aggregates, the effect of TNF blockade on B cells in RA is not well characterized.

We have previously reported in an observational cross-sectional study that RA patients receiving anti-TNF (etanercept) display a paucity of tonsil FDC networks and GC structures accompanied by a reduction in peripheral blood memory B cells compared with healthy controls and RA patients receiving methotrexate (MTX), suggesting that the combination of TNF and LT blockade may disrupt GC reactions at least in part via effects on FDCs (17). Despite these findings, the precise in vivo effects of blockade of TNF and LTα signaling pathways on human B cells remain unclear, since few careful longitudinal studies after anti-TNF initiation have been conducted (18). Moreover, the potential relationship between B cell changes and the efficacy of TNF blockade requires better elucidation. This study of patients with active RA receiving concurrent MTX was undertaken to evaluate the hypothesis that, due to the ability of etanercept to block both TNF and LTα, it would have more profound effects on B cell populations relative to adalimumab, which blocks only TNF.

PATIENTS AND METHODS

Study design. The study was a phase IV, multicenter, randomized, partially blinded trial. Eligible participants were randomized in a 2:1 ratio to receive standard dosing regimens of etanercept or adalimumab for 24 weeks. Participants were randomized to receive either 1 subcutaneous (SC) injection of etanercept 50 mg (or 2 injections of etanercept 25 mg on the same day) every week for 24 weeks or 1 SC injection of adalimumab 40 mg every other week. The drug was either self-administered or administered by a trained designated caregiver and was administered at approximately the same time of the same day every week for etanercept or every other week for adalimumab, in the form of 1 or 2 injections (per the dosage regimen). Randomization was conducted through a web-based system, RhoRAND, and was stratified based on the presence or absence of antibodies to RF and/or CCP with a block size of 3. Participants met the American College of Rheumatology (ACR) 1987 revised criteria for the classification of RA (19) beginning at least 3 months before study entry, had active disease with a Disease Activity Score in 28 joints (DAS28) of >4.4, and had been receiving stable doses of MTX for ≥8 weeks. Participants were clinically evaluated and blood was drawn for processing at baseline, 12 weeks, and 24 weeks.

Disease end points were evaluated by assessors who were blinded with regard to treatment status. The DAS28 response was determined as follows: patients with a DAS28 of ≤3.2 and a decrease in the DAS28 of ≥1.2 were considered good responders, patients with a DAS28 of >5.1 or a decrease in the DAS28 of <0.6 were considered nonresponders, and those with DAS28 scores falling between the scores for good responders and nonresponders were considered moderate responders. Responses according to the ACR criteria for 20% improvement (ACR20), ACR50, and ACR70 were also determined (20,21).

This trial was conducted between July 2009 and January 2014. Participants were recruited at the University of Rochester Medical Center (URMC) and other Autoimmunity Centers of Excellence participating sites (Medical University of South Carolina, Charleston; University of Alabama at Birmingham; Feinstein Institute for Medical Research; University of California, San Francisco; and University of Chicago). Detailed written informed consent was obtained from all participants. Age-matched healthy donors were included from a separate URMC protocol in accordance with protocols specifically approved by the respective Human Subjects Institutional Review Board. Full details of the trial protocol can be found in the Supplementary Methods, available on the *Arthritis & Rheumatology* website at http://onlinelibrary.wiley.com/doi/10.1002/art.41941/abstract.

Peripheral blood mononuclear cell (PBMC) isolation and flow cytometric analysis. Peripheral blood samples were collected in heparin tubes and shipped overnight to URMC. PBMCs were then immediately isolated from heparinized blood

by Ficoll–Hypaque density-gradient centrifugation (Pharmacia Biotech) and frozen in freezing medium until analyzed. Immunofluorescence staining for flow cytometric analysis was performed. We used 2 different 12-color, 14-parameter core B cell flow cytometry panels with well-validated Standard Operating Procedures that incorporate extensive Quality Assessment and Quality Controls as previously described (22,23).

B cells were identified based on CD19 expression, exclusion of CD3, and gating out cell aggregates and dead cells. Naive B cells were distinguished from transitional cells and memory B cells by the expression of ABCB1 transporter activity and MitoTracker dye extrusion as previously described (24). CD21 and CD95 were incorporated to evaluate activation status (25,26). B cells in PBMCs were additionally classified by multiparameter flow cytometry along a developmental pathway based on the expression of defined surface markers, as shown in Supplementary Figure 1, available on the *Arthritis & Rheumatology* website at http://onlinelibrary.wiley.com/doi/10.1002/art.41941/abstract. T cell subsets were gated using a separate panel from B cells with the focus on CD4 T cells. CD45RA separates T cells into memory T cells (CD45RA−) and naive T cells (CD45RA+). CCR6, CXCR3, and CCR4 are important markers for classifying Th1 cells (CD4+ CD45RA−CXCR3+CCR6+), Th2 cells (CD4+CD45RA−CCR6− CCR4+), and Th17 cells (CD4+CD45RA−CCR4+CCR6+) (25,26). Circulating follicular helper T (Tfh) cells were classified as CD4+CD45RA−CXCR5+ICOS+PD1+ (27). In addition, we used CD25 and CD127 to identify naturally occurring regulatory T (Treg) cells in blood as CD4+CD25+CD127$^{low/-}$ (28).

Cytokine assays and Ki-67 expression. PBMCs were aliquoted into 1 million per 100 μl of RPMI and stimulated with 200 ng/ml phorbol myristate acetate and 2 mg/ml ionomycin with the addition of 1 ml/ml GolgiPlug and 0.68 ml/ml GolgiStop at 37°C for 4 hours. The PBMCs were surface stained for CD19, followed by Live/Dead staining. Cells were fixed and internally stained for TNF, IL-17, interferon-γ (IFNγ), IL-2, IL-6, IL-10, CD3, CD4, and FoxP3 (eBioscience). Cells were analyzed on a 3-laser, 12-color LSRII flow cytometer (BD Biosciences).

In a subset of participants who had samples with enough cells available, unstimulated PBMCs were surface stained for IgD, IgG, IgA, IgM, CD24, CD21, CD38, CD19, CD20, CD27, CD95, CD86, and CD3, followed by Live/Dead staining, fixation (0.1% formalin), and staining for antibody against Ki-67. Cells were analyzed on a 3-laser, 12-color LSRII flow cytometer.

Statistical analysis. The study was powered for the primary analysis to test for a difference between treatment groups in the change in percentage of memory B cells in the peripheral blood at week 12. Assumptions for the sample size calculation were based on data collected from individuals treated in Rochester. It was assumed that the change in the mean percentage of peripheral memory B cells would differ between the 2 treatment groups by between 8% and 12% and that the within-treatment standard deviation (pooled across arms) would be ~10%. Sixty participants, randomized 2:1 with $\alpha = 0.05$, were needed in order to attain power between 81% and 95%. Participants who withdrew prior to week 12 were to be replaced.

The primary end point was the change from day 0 to week 12 in CD27+ switched memory B cells expressed as a percent of B cells. Primary mechanistic analyses were conducted on the per-protocol population, which consisted of participants who had day 0 and week 12 assessments, completed ≥75% of planned injections prior to week 12, and had no serious protocol deviations. Missing data were not imputed. An analysis of covariance (ANCOVA) model was used for the primary analysis comparing the percentage of CD27+ switched memory B cells between treatment groups at week 12, adjusted for the day 0 value. Because we hypothesized that the percentage of CD27+ switched memory B cells would not be impacted by adalimumab but would decline after treatment with etanercept, a key secondary analysis was the comparison of slopes for the regression lines describing the relationship between CD27+ switched memory B cells at week 12 and day 0 between treatment arms. To test for the equivalence of slopes, the day 0–by-treatment interaction term was added to the ANCOVA model from the primary analysis. These analyses were repeated for the subset of moderate and good DAS28 responders at week 12.

Secondary analyses to support the primary and secondary objectives were considered exploratory and included all randomized participants, regardless of treatment group and analysis population, for whom blood samples were available. *P* values are presented without adjustment for multiple comparisons. A *t*-test was performed to test for differences in cell subsets between treatment groups and between DAS28 response groups and to compare healthy controls to study participants at each visit. Three-group comparisons were conducted using ordinary one-way analysis of variance (ANOVA) and Tukey's multiple comparisons test. Statistical analyses were performed using Prism or SAS software.

RESULTS

Participant clinical characteristics and response. Sixty-three participants were randomized in the trial, 43 to receive etanercept and 20 to receive adalimumab. There were 49 participants in the per-protocol population. Fourteen randomized participants were excluded from the per-protocol population: 8 terminated the study early, 9 received <75% of the planned injections, 5 reported significant protocol deviations, and 2 participants had the week 12 visit more than 1 week from the expected visit date (Figure 1). Some participants were excluded from the per-protocol population for more than 1 criterion. Baseline participant characteristics are summarized in Table 1. The treatment

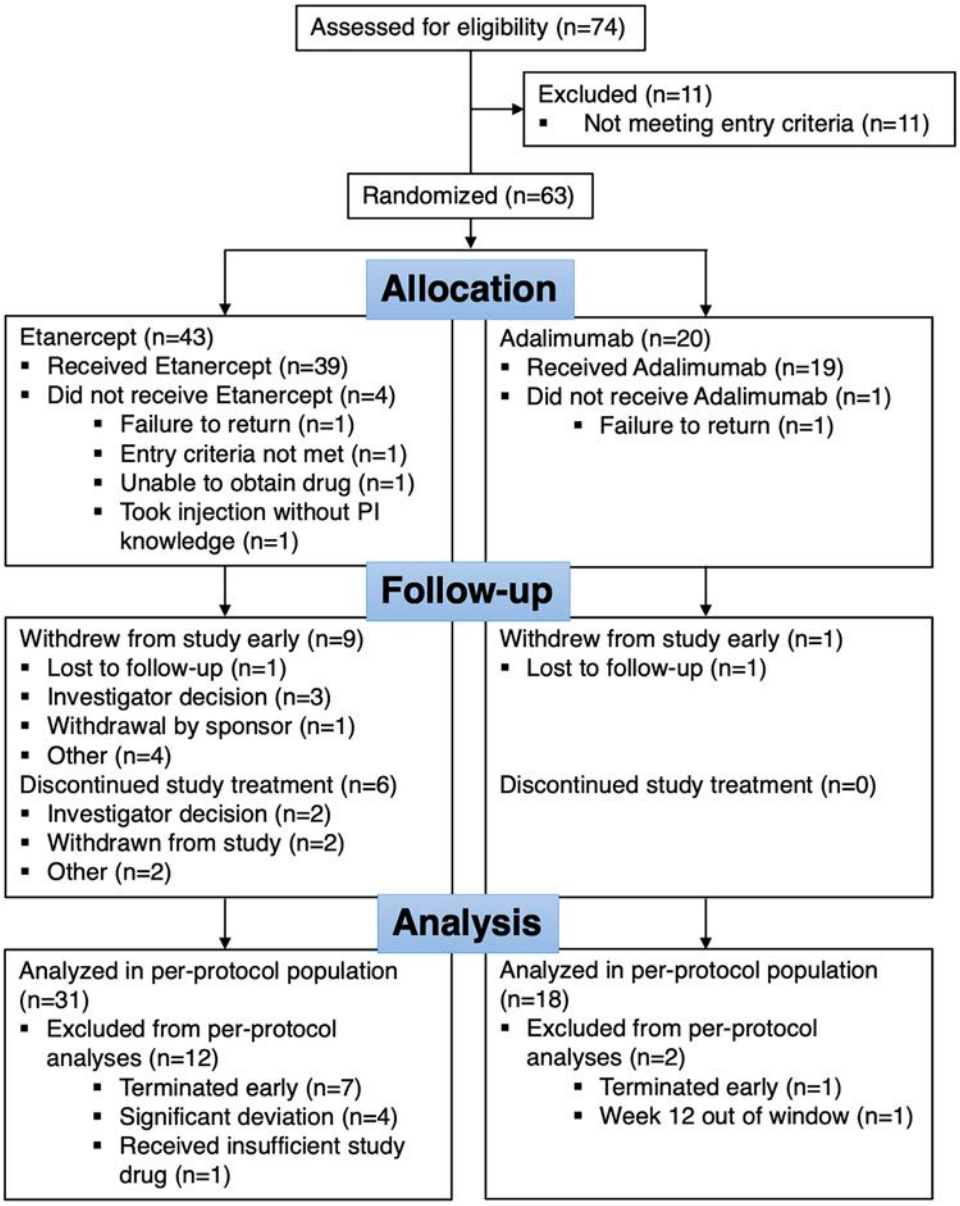

Figure 1. Flow chart showing the disposition of the study participants. PI = principal investigator.

groups were similar with respect to CCP status and disease activity. Overall, disease activity was high at study entry, with a mean DAS28 of 5.3, a mean number of swollen joints of 10, and a mean number of tender joints of 13, typical of an RA cohort clinically failing to respond to MTX and starting biologic therapy.

As shown in Figure 2, clinical responses were high, with 90% of etanercept-treated participants and 89% of adalimumab-treated participants achieving a good or moderate DAS28 response by 12 weeks and ~45% of participants achieving low disease activity (DAS28 ≤3.2) by 12 weeks, with numbers increasing further by 24 weeks. There were 7 DAS28 nonresponders at week 12. DAS28 results over time were similar between the 2 treatment arms (Figure 2A). Although the study was not designed to test for a difference between treatment arms based on disease activity end points, responder indexes appeared modestly higher in the adalimumab group at 12 weeks, with further increases at 24 weeks (Figure 2B).

Stable percentages of memory B cells in the peripheral blood over 24 weeks of anti-TNF treatment. The primary end point, the change in percentage of CD27+ switched memory B cells from day 0 to week 12, was not significantly different between treatment groups ($P = 0.301$) (Supplementary Table 1, available on the *Arthritis & Rheumatology* website at http://onlinelibrary.wiley.com/doi/10.1002/art.41941/abstract). The slopes describing the relationship between the percentage of CD27+ switched memory B cells at week 12 and the percentage at day 0 were also not significantly different between

Table 1. Baseline characteristics of the participants with RA in the per-protocol population*

	Etanercept (n = 31)	Adalimumab (n = 18)
Age, mean ± SD years	52 ± 10.0	52 ± 13.8
Sex, no, (%) female	25 (81)	14 (78)
White, no. (%)	26 (84)	17 (94)
Disease duration, mean ± SD years	4.5 ± 6.5	4.4 ± 5.4
CCP+, no. (%)	19 (61)	10 (56)
RF positive, no. (%)	17 (55)	8 (44)
DAS28, mean ± SD	5.2 ± 1.1	5.4 ± 0.7
MTX dosage, mean ± SD mg	16.8 ± 4.0	18.4 ± 3.5
No. of swollen joints, mean ± SD (28 assessed)	9.5 ± 5.9	9.6 ± 6.0
No. of tender joints, mean ± SD (28 assessed)	12.6 ± 6.8	12.9 ± 7.2
CRP, mean ± SD mg/liter	11.0 ± 25.9	13.6 ± 25.0

* RA = rheumatoid arthritis; CCP = cyclic citrullinated peptide; RF = rheumatoid factor; DAS28 = Disease Activity Score in 28 joints; MTX = methotrexate; CRP = C-reactive protein.

treatment groups ($P = 0.996$). Results were analogous for the subset of moderate and good DAS28 responders ($P = 0.286$; data not shown) and regardless of autoantibody status.

As a further analysis of the B cell compartment, we examined the other canonical B cell subsets identified by CD27 and IgD expression (see Supplementary Figure 1 [for gating strategy] and Supplementary Figure 2A, available on the *Arthritis & Rheumatology* website at http://onlinelibrary.wiley.com/doi/10.1002/art.41941/abstract) and further refined B cell populations. Overall, B cell subsets did not change over the course of the study regardless of treatment arm (Figures 3A and B, Supplementary Table 1, and Supplementary Figures 2B and C) or responder status (Figure 3C, Supplementary Tables 2 and 3, and Supplementary Figure 3C, available on the *Arthritis & Rheumatology* website at http://onlinelibrary.wiley.com/doi/10.1002/art.41941/abstract). Nonresponders did have higher frequencies of CD27− double-negative memory (IgD−CD27−) cell subsets at baseline

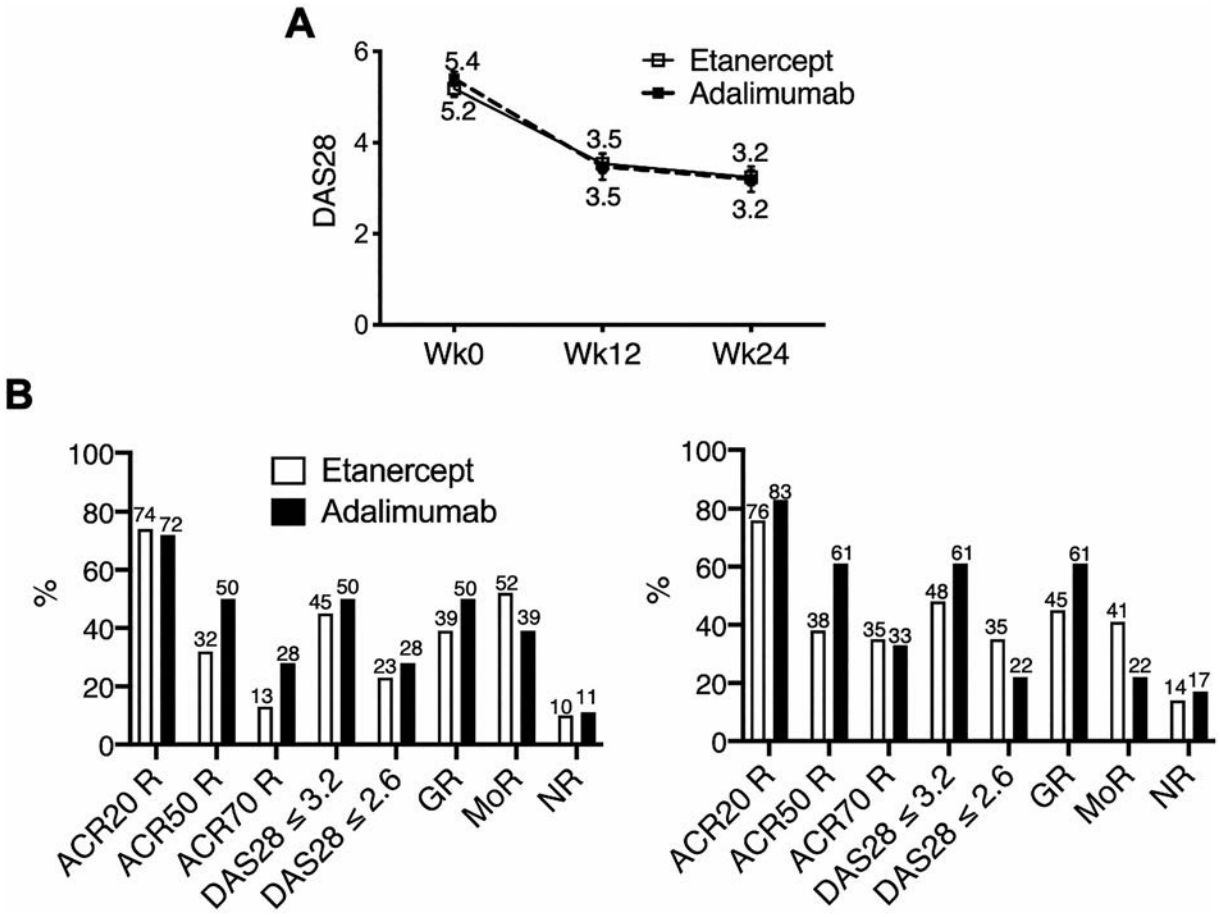

Figure 2. Clinical response at week 12 and week 24 in study participants with rheumatoid arthritis receiving etanercept or adalimumab. **A**, Disease Activity Score in 28 joints (DAS28) at baseline (week 0), week 12, and week 24 by treatment group. Only participants in the per-protocol population were included (for etanercept, n = 29 at weeks 0 and 24 and n = 31 at week 12; for adalimumab, n = 17 at week 0 and n = 18 at weeks 12 and 24). Boxes and error bars show the mean ± SEM. Values are the mean. **B**, Percentages of participants in each treatment group achieving responses according to the indicated criteria at week 12 (left) and week 24 (right) (for etanercept, n = 31 at week 12 and n = 26 at week 24; for adalimumab, n = 18 at weeks 12 and 24). ACR20 R = response according to the American College of Rheumatology criteria for 20% improvement; GR = good response; MoR = moderate response; NR = no response.

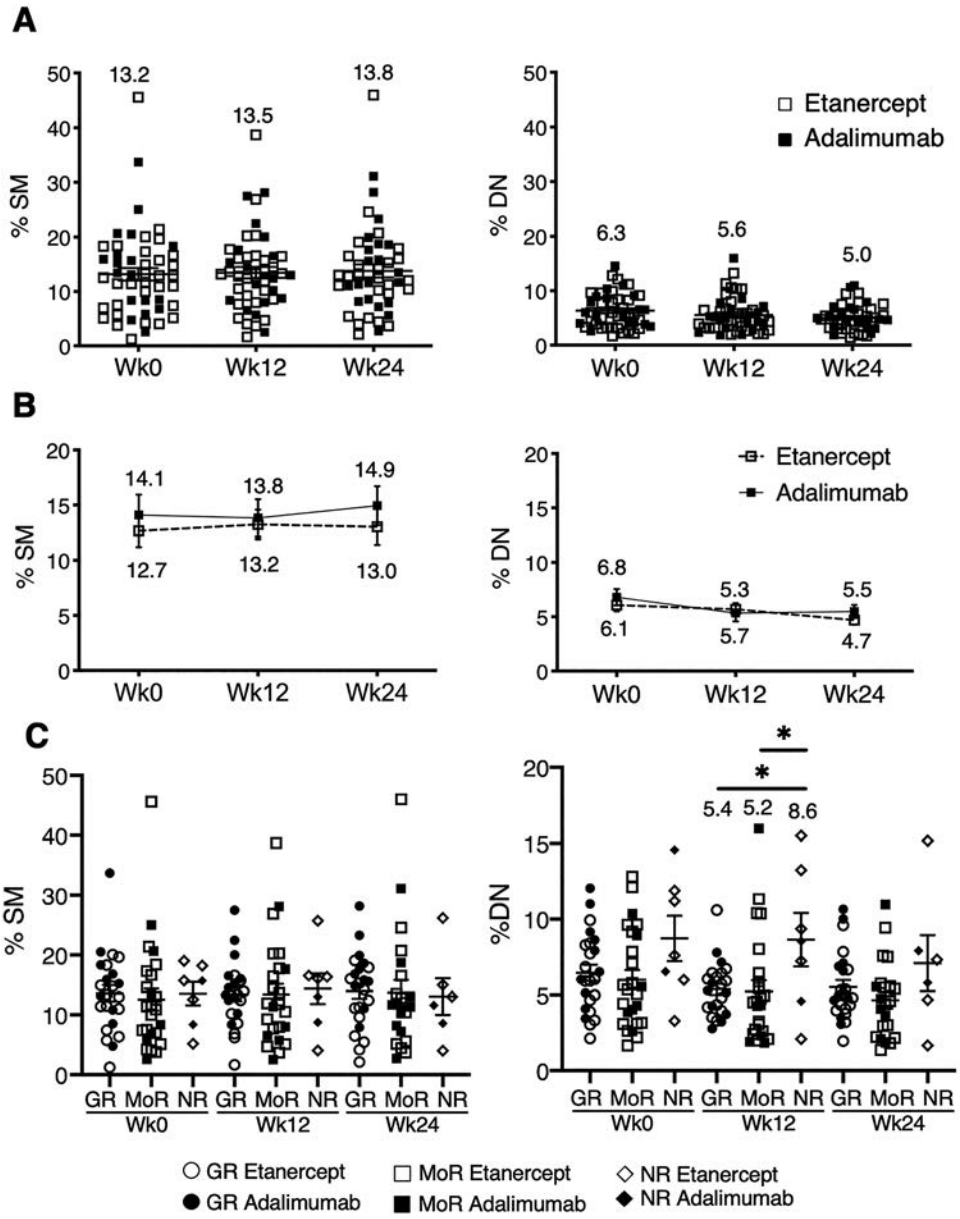

Figure 3. Frequencies of core B cell subsets over time in study participants with rheumatoid arthritis treated with etanercept or adalimumab. **A**, Frequencies of switched memory (SM) and double-negative (DN) B cells among total CD19+ B cells over time. Squares represent individual participants (n = 49 at each time point); horizontal lines and error bars show the mean ± SEM. Values are the mean. **B**, Frequencies of switched memory and double-negative B cells over time in the etanercept group (n = 31) and adalimumab group (n = 18). Boxes and error bars show the mean ± SEM. Values are the mean. **C**, Frequencies of switched memory and double-negative B cells over time in good responders (GR; n = 24 at weeks 0 and 24 and n = 23 at week 12), moderate responders (MoR; n = 25 at week 0, n = 24 at week 12, and n = 22 at week 24), and nonresponders (NR; n = 7 at weeks 0 and 12 and n = 6 at week 24). Squares represent individual participants; horizontal lines and error bars show the mean ± SEM. Values are the mean. * = $P < 0.05$.

and week 12 compared to good and moderate responders (Figure 3C).

Given the putative differences in drug mechanism of action, we also analyzed the B cell populations by responder status within each treatment arm. An analysis comparing responder status within the adalimumab arm over the course of the study did not reveal significant differences in the frequency of switched memory ($P = 0.876$), unswitched memory ($P = 0.318$), double-negative ($P = 0.251$), or naive ($P = 0.686$) B cells. Within the etanercept group, the frequency of double-negative cells was significantly different between the nonresponder and responder groups (higher in the nonresponder group) ($P = 0.0082$ by ANOVA). In contrast, there was no difference in switched memory ($P = 0.952$), unswitched memory ($P = 0.913$), or naive ($P = 0.851$) B cell frequencies between

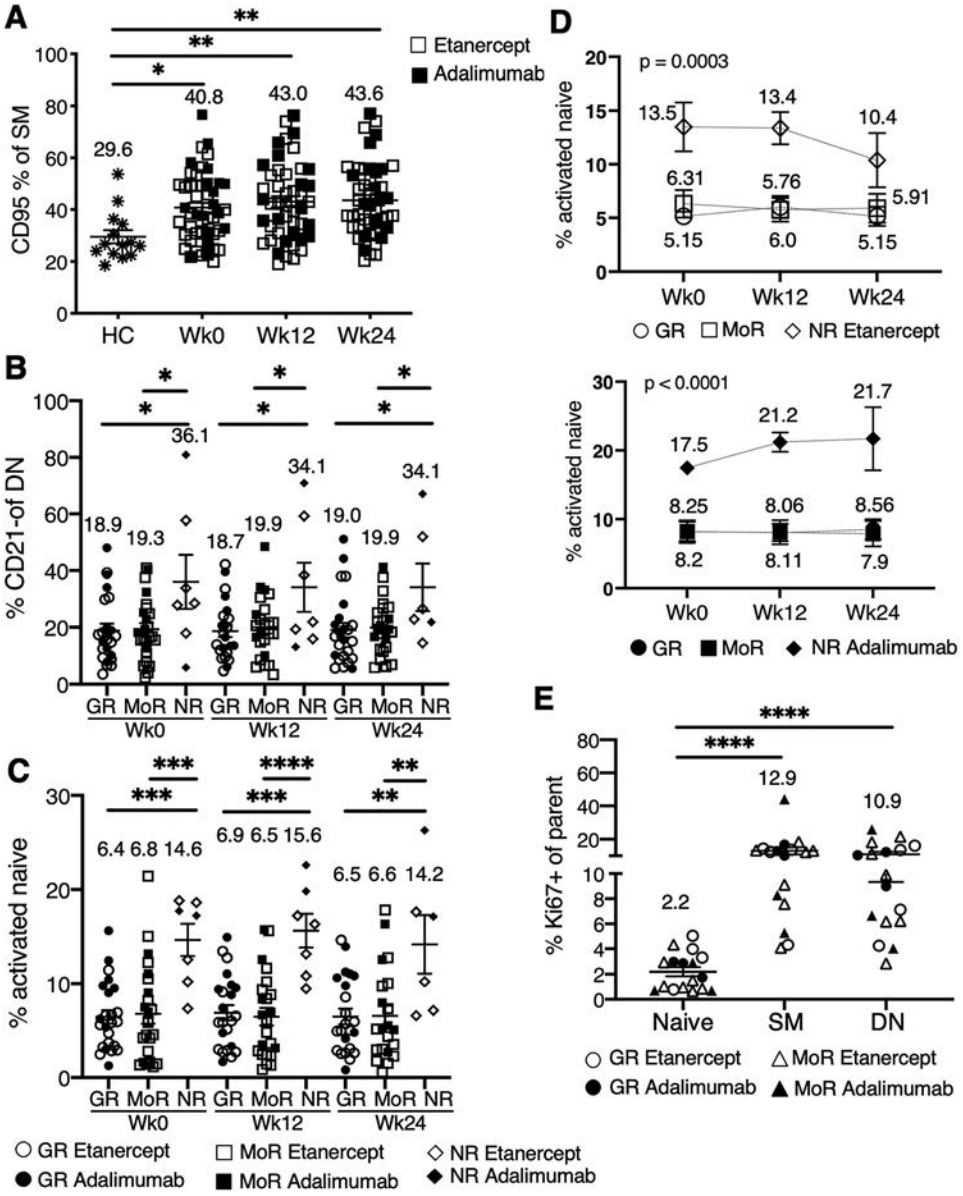

Figure 4. Lower frequencies of activated memory B cells and higher frequencies of proliferating B cells in responders to anti–tumor necrosis factor treatment compared to nonresponders. **A**, Frequencies of CD95+ switched memory (SM) cells at baseline (week 0; n = 49), 12 weeks (n = 48), and 24 weeks (n = 46) in participants with rheumatoid arthritis compared to healthy controls (HC; n = 14). * = $P < 0.05$; ** = $P < 0.01$. **B**, Frequencies of CD21– double-negative (DN) cells at the indicated time points in good responders (GR; n = 24 at weeks 0 and 24 and n = 23 at week 12), moderate responders (MoR; n = 25 at week 0 and n = 24 at weeks 12 and 24), and nonresponders (NR; n = 7 at weeks 0 and 12 and n = 6 at week 24). * = $P < 0.05$. **C**, Frequencies of activated naive B cells in good responders (n = 24 at week 0 and n = 23 at weeks 12 and 24), moderate responders (n = 24 at week 0, n = 23 at week 12, and n = 21 at week 24), and nonresponders (n = 7 at weeks 0 and 12 and n = 6 at week 24). ** = $P < 0.01$;*** = $P < 0.001$; **** = $P < 0.0001$, by Tukey's multiple comparisons test. **D**, Frequencies of activated naive B cells over time in the etanercept group (top) (n = 14 good responders, n = 18 moderate responders, and n = 5 nonresponders) and adalimumab group (bottom) (n = 10 good responders, n = 7 moderate responders, and n = 2 nonresponders). **E**, Frequencies of Ki-67+ cells among naive, switched memory, and double-negative B cells from good responders (n = 7) and moderate responders (n = 10) at week 0. No samples from nonresponders were available for analysis. **** = $P < 0.0001$. In **A**, **B**, **C**, and **E**, symbols represent individual participants; horizontal lines and error bars show the mean ± SEM. In **D**, boxes and error bars show the mean ± SEM. Values are the mean.

nonresponders and responders within the etanercept arm. We also examined the frequency of plasmablasts in both treatment groups over time, but this did not change significantly regardless of treatment arm (Supplementary Figures 2B and C) or responder status (Supplementary Table 3 and Supplementary Figure 2D).

Elevated frequencies of activated B cells in nonresponders. When participants with RA pretreatment were compared to age-matched healthy controls, the total naive (IgD+ CD27−) B cell subset (which includes transitional B cells), the unswitched memory (IgD+CD27+) B cell subset, the CD27+

switched memory (IgD−CD27+) B cell subset (which includes plasmablasts), and the CD27− double-negative memory (IgD−CD27−) B cell subset were similar (data not shown). However, notably, there were more activated B cell populations in participants with RA, as evidenced by up-regulation of CD95 in both the switched memory and double-negative memory subsets (Figure 4A and Supplementary Figures 3A–C). The baseline expansion in activated B cell populations persisted after anti-TNF treatment (Figures 4A and B and Supplementary Figure 3B). Additionally, activated CD21− double-negative memory B cell percentages were higher at baseline and follow-up time points in the nonresponder group (Figure 4B). We also observed significant differences in the percentage of activated CD21− double-negative memory cells between responders and nonresponders within the etanercept group ($P = 0.0023$ by ANOVA) but not within the adalimumab group ($P = 0.116$).

We also examined a recently identified population of activated naive B cells characterized as IgD+CD27−MTG+CD38+CD24− (29). Activated naive B cell percentages were significantly higher in the nonresponders and remained elevated throughout the course of treatment (Figure 4C) but did not change with treatment. The significant differences between responders and nonresponders in the percentage of activated naive cells were also observed when each treatment group was analyzed separately (for adalimumab, $P < 0.0001$ by ANOVA; for etanercept, $P = 0.0003$ by ANOVA) (Figure 4D).

Impact of anti-TNF on distinct class-switched memory or recently activated B cell subsets. The lack of change in global memory B cell populations after anti-TNF treatment was surprising but may be explained if the majority of peripheral blood memory B cells are a relatively long-lived and stable cell pool.

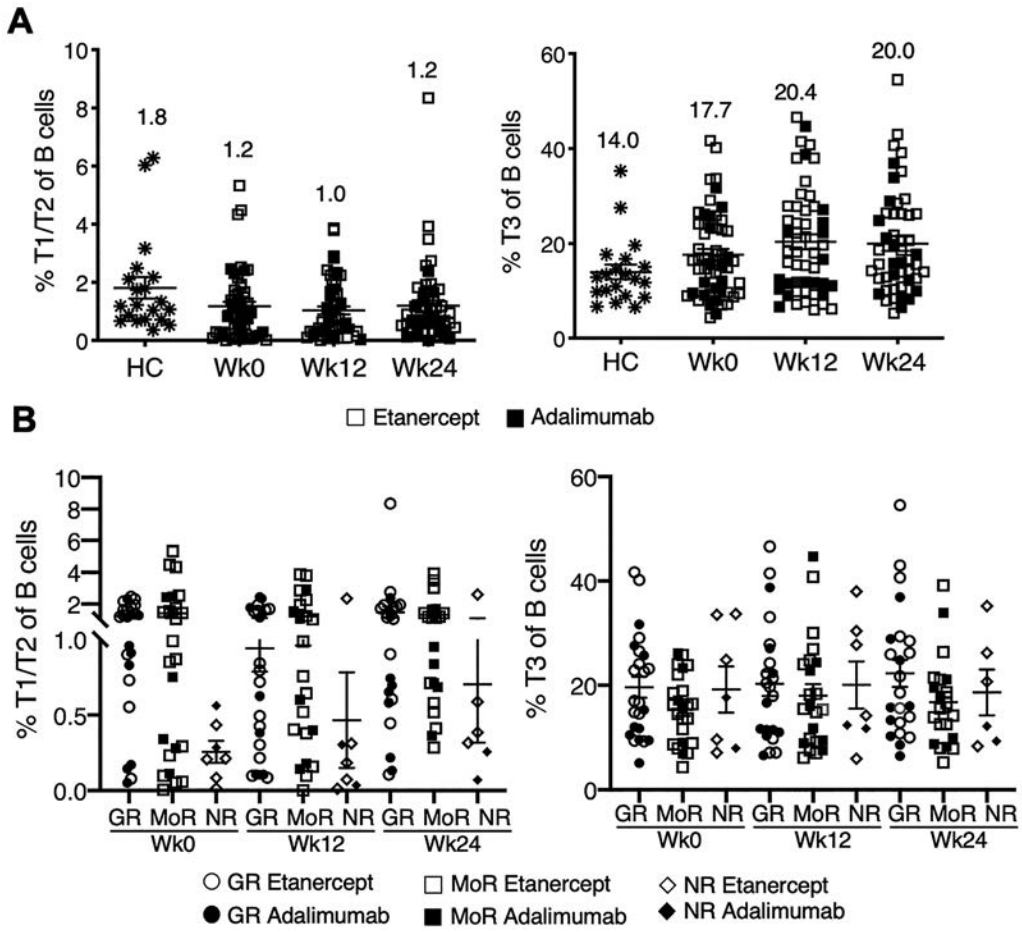

Figure 5. Higher frequencies of transitional type 1/type 2 (T1/T2) B cells in responders to treatment at all time points. **A**, Frequencies of T1/T2 B cells over time in all participants regardless of treatment (n = 56 at week 0, n = 54 at week 12, and n = 52 at week 24) and frequencies of T3 B cells over time in all participants regardless of treatment (n = 49 at week 0, n = 48 at week 12, and n = 46 at week 24) compared to healthy controls (HCs; n = 20). **B**, Frequencies of T1/T2 B cells over time in good responders (GR; n = 24 at weeks 0 and 12 and n = 23 at week 24), moderate responders (MoR; n = 24 at week 0, n = 23 at week 12, and n = 21 at week 24), and nonresponders (NR; n = 7 at weeks 0 and 12 and n = 6 at week 24) and frequencies of T3 B cells over time in good responders (n = 24 at week 0 and n = 23 at weeks 12 and 24), moderate responders (n = 24 at week 0, n = 23 at week 12, and n = 21 at week 24), and nonresponders (n = 7 at weeks 0 and 12 and n = 6 at week 24). Symbols represent individual participants; horizontal lines and error bars show the mean ± SEM. Values are the mean.

Previous work has demonstrated that there are multiple memory B cell subsets originating from distinct GC-dependent and -independent immune pathways that can be distinguished based on class-switch profile (isotype) (30). We reasoned that anti-TNF may have a greater impact on certain memory B cell populations, depending on the immune pathway of origin. In a subset of participants for whom samples were available (n = 7 good responders and n = 10 moderate responders [no nonresponder samples available]), we performed additional flow cytometric analysis to address this possibility. However, none of the class-switched memory B cells examined (IgM, IgG, or IgA) decreased with anti-TNF treatment, including the CD27− IgA+ memory B cell fraction, which is proposed to originate from GC-independent reactions, possibly of mucosal origin (30) (data not shown).

Ki-67 is a proliferation antigen that may mark B cells recently activated in ongoing immune reactions. There were interesting differences in Ki-67 expression depending on the B cell subset examined, with higher proliferation in the memory B cell compartment, particularly activated memory (CD21−CD95+ CD86+) B cells (Figure 4E and Supplementary Figure 3D). We also examined the expression of Ki-67 longitudinally after anti-TNF initiation. Although there were changes in individual patients, overall Ki-67 B cell percentages did not change with anti-TNF treatment (Supplementary Figure 3E; data not shown for CD95+ and CD86+).

Varying transitional B cell percentages depending on responder status. We examined changes in transitional B cell percentages. The naive/transitional subset is composed of type 1 (T1), T2, T3, and mature naive B cells (31). The frequency of early transitional T1/T2 cells, a putative regulatory subset (32,33), was higher in the RA responder group compared to the nonresponder group (Figure 5). However, the frequency of transitional B cells did not change over the 24 weeks of treatment with anti-TNF regardless of treatment response. In a small number of participants (n = 8), cytokine production by B cells was examined after short-term stimulation for 4 hours, but no differences were observed in IL-10, TNF, or IFNγ production (data not shown).

Effects of TNF blockade on T cells. We also examined T cell subsets, including Th1, Th2, Tfh, and Treg cells. They did not change over the course of the study (data not shown for Th1 and Th2; Supplementary Figures 4A and B, available on the *Arthritis & Rheumatology* website at http://onlinelibrary.wiley.com/doi/10.1002/art.41941/abstract), though Treg cells were noted to be higher in the good and moderate responders at week 12 compared to the nonresponders (Supplementary Figure 4C).

DISCUSSION

In this study of active RA, we found no difference between the effects of dual blockade of TNF and LT with etanercept and single blockade of TNF with adalimumab on peripheral blood B cell subsets. Surprisingly, peripheral blood B cell subsets remained remarkably stable after initiation of anti-TNF treatment. We suggest that, once generated, the bulk of memory B cells may be long-lived and not altered by TNF blockade, whereas ongoing generation of memory B cells in lymphoid tissue or ectopic locations may be more amenable to interruption. Although most B cell subsets did not change with treatment, we did observe differences depending on treatment response, with higher frequencies of activated memory and activated naive B cells in nonresponders at baseline and follow-up time points. In contrast, frequencies of transitional B cells, a putative regulatory subset, as well as Treg cells were lower in nonresponders. Overall, these findings suggest an imbalance in the B cell compartment in RA that is heterogeneous and predictive of anti-TNF response. However, these results should be interpreted with caution since there were few nonresponders in the present study.

Our results also suggest that agents that block both TNF and LT are not necessarily more efficacious than those that block TNF alone. This is consistent with clinical trial data suggesting that TNF blockade is the dominant clinical effect. Thus, a monospecific anti-LTα antibody, pateclizumab, failed to show efficacy in a head-to-head phase II randomized controlled study (34).

Our results confirm prior findings that peripheral blood B cells are abnormal in RA. However, results in the literature have not been entirely consistent, perhaps because of variability in disease phenotypes, duration, activity, and therapy. For example, we have previously reported that in contrast to patients with systemic lupus erythematosus (SLE), a disease that is characterized by profound alterations in peripheral blood B cells, RA patients have similar core peripheral blood B cell subsets as that in healthy controls (based on CD27 and IgD expression). However, RA patients were shown to have a significant expansion of activated memory B cell populations expressing high levels of CD95 and low levels of CD21 in the peripheral blood (23); these results were recapitulated in the present study. In addition, we observed an increased frequency of IgD−CD27− double-negative memory B cells in nonresponders compared to responders, a result consistent with data indicating increased frequencies of double-negative B cells in early and established RA.

In contrast to our data, others have described the double-negative expansion restored by anti-TNF therapy (35). Souto-Carneiro and colleagues described an increased frequency of post-switched CD27+IgD− peripheral blood memory B cells in RA patients with longer disease duration compared to patients with a shorter disease duration or normal controls (36), results which were reproduced in another study (37,38). They also noted an increase in the frequency of preswitched memory B cells in the peripheral blood of RA patients after anti-TNF treatment. Those studies differed from ours in that the disease duration was significantly longer (12–13 years), suggesting that global peripheral blood B cell abnormalities may accumulate over time related to

ongoing activation in target tissue. Consistent with this hypothesis, another study demonstrated an expansion of autoreactive B cell and plasma cell clones in the synovium in early RA (disease duration <6 months) and established RA (disease duration >20 months) that was absent from the peripheral blood (39). This finding suggests that the inflamed synovium forms a niche where class-switched activated memory B cells and plasma cells accumulate, consistent with our own published data showing that CD27+ memory B cells dominate in the RA synovium (40).

Although total peripheral blood memory B cells did not decrease with TNF blockade over the time course of the study, the majority of peripheral blood memory B cells are likely long-lived (30,41,42) and may not be altered over a short period of treatment. In a smaller subset of subjects, we examined more discrete memory B cell populations, including IgA and IgG memory and Ki-67–expressing cells. Although we did not observe clear changes with anti-TNF, future studies with a larger sample size may be more informative. For example, CD27−IgA+ memory B cells may be a particularly interesting population to further examine, as it has been proposed to be generated in T cell–independent mucosal immune reactions (30) but may also develop in GC reactions including in ectopic locations (43,44). Additionally highlighting the importance of IgA immune reactions, there are recent reports of IgA plasmablast dominance in CCP+ individuals at risk of developing RA (45).

We previously reported that RA patients receiving anti-TNF treatment (etanercept, a TNFR-Ig p75 decoy that binds both TNF and LTα) display a paucity of FDC networks and GC structures in lymphoid tissue, accompanied by a peripheral blood memory B cell lymphopenia (17). Treatment with either etanercept or anti-TNF monoclonal antibodies (adalimumab or infliximab) has also been associated with a decrease in ectopic lymphoid structures in the RA synovium that correlated with good clinical response (46). It is likely that global peripheral blood B cells do not adequately reflect the effects of TNF blockade on immune reactions in synovium or lymphoid tissue, as suggested by the finding of impaired generation of influenza vaccine–specific antibody-secreting and memory B cells in RA patients receiving anti-TNF treatment (47).

Several candidate markers to predict response to anti-TNF therapy have been investigated, including genetic and protein markers, but their predictive power has been poor (48,49). A recent study combined high-throughput RNA sequencing, DNA genotyping, and proteomics measurements in 185 RA patients, including 59 starting anti-TNF therapy, and found 2 proteins, 2 single-nucleotide polymorphisms, and 8 messenger RNA biomarkers that could be replicated from the literature and in combination explained 51% of the variation in DAS28 response (50). There is also now interest in RNA sequencing biomarkers within discrete cell populations, as has recently been described for neutrophils (51). It has also been suggested that analysis of immune cells in target tissue may provide critical additional information (44,52), as has been demonstrated by a myeloid phenotype predicting the most robust response to TNF blockade (53).

In this study we observed several peripheral B cell flow cytometry–based biomarkers that associate with inadequate response to TNF blockade, including CD21− double-negative and switched memory B cells and activated naive B cells. The CD21− B cell population is particularly interesting, given the recent description of age- or autoimmunity-associated B cells, which encompass this phenotype. This B cell population, which is dependent on T-bet for generation and expresses CD11c, was first reported in aging mice (54); subsequently, it was seen to be expanded in mice with autoimmune disease and SLE patient peripheral blood and enriched for autoreactive specificities (55). We have also recently reported the presence of age- or autoimmunity-associated B cells in the RA synovium correlating with disease activity (44). Results from the present study overall suggest that an activated B cell compartment in RA is associated with inadequate response to TNF blockade. However, it is important to note that these biomarkers are likely not specific to anti-TNF therapy, given that they are also predictive of an inadequate response to B cell depletion (23). Although there are abnormalities in the RA B cell compartment detectable in peripheral blood and associated with response to anti-TNF, we suggest that analysis of cells in joint target tissue, likely by a multiple -omics data approach, has the greatest potential to reveal new biomarkers of treatment response and elucidate disease pathogenesis.

ACKNOWLEDGMENT

Rho Federal Systems Division worked with the investigators to prepare the statistical analysis plan and performed an independent statistical analysis to verify the results presented in this article. We thank the URMC Flow Cytometry Core for their assistance.

AUTHOR CONTRIBUTIONS

All authors were involved in drafting the article or revising it critically for important intellectual content, and all authors approved the final version to be published. Dr. Anolik had full access to all of the data in the study and takes responsibility for the integrity of the data and the accuracy of the data analysis.

Study conception and design. Boyle, Keyes-Elstein, Welch, Goldmuntz, Anolik.

Acquisition of data. Meednu, Barnard, Callahan, Coca, Marston, Thiele, Tabechian, Bolster, Curtis, Mackay, Graf, Keating, Smith, Boyle, Keyes-Elstein, Welch, Goldmuntz, Anolik.

Analysis and interpretation of data. Meednu, Barnard, Boyle, Keyes-Elstein, Welch, Goldmuntz, Anolik.

ADDITIONAL DISCLOSURES

Authors Boyle and Keyes-Elstein are employees of Rho Federal Systems Division.

REFERENCES

1. Myasoedova E, Crowson CS, Kremers HM, Therneau TM, Gabriel SE. Is the incidence of rheumatoid arthritis rising? Results from Olmsted County, Minnesota, 1955–2007. Arthritis Rheum 2010;62:1576–82.
2. Machold KP, Stamm TA, Nell VP, Pflugbeil S, Aletaha D, Steiner G, et al. Very recent onset rheumatoid arthritis: clinical and serological patient characteristics associated with radiographic progression over the first years of disease. Rheumatology (Oxford) 2007;46:342–9.
3. Nielen MM, van Schaardenburg D, Reesink HW, van de Stadt RJ, van der Horst-Bruinsma IE, de Koning MH, et al. Specific autoantibodies precede the symptoms of rheumatoid arthritis: a study of serial measurements in blood donors. Arthritis Rheum 2004;50:380–6.
4. Rantapää-Dahlqvist S, de Jong BA, Berglin E, Hallmans G, Wadell G, Stenlund H, et al. Antibodies against cyclic citrullinated peptide and IgA rheumatoid factor predict the development of rheumatoid arthritis. Arthritis Rheum 2003;48:2741–9.
5. Anolik J, Barnard J, Cappione A, Pugh-Bernard A, Felgar R, Looney J, et al. Rituximab improves peripheral B cell abnormalities in human systemic lupus erythematosus. Arthritis Rheum 2004;50:3580–90.
6. Edwards JC, Cambridge G. Sustained improvement in rheumatoid arthritis following a protocol designed to deplete B lymphocytes. Rheumatology (Oxford) 2001;40:205–11.
7. Edwards JC, Szczepanski L, Szechinski J, Filipowicz-Sosnowska A, Emery P, Close DR, et al. Efficacy of B-cell–targeted therapy with rituximab in patients with rheumatoid arthritis. N Engl J Med 2004; 350:2572–81.
8. Takemura S, Klimiuk PA, Braun A, Goronzy JJ, Weyand CM. T cell activation in rheumatoid synovium is B cell dependent. J Immunol 2001;167:4710–8.
9. Manzo A, Bombardieri M, Humby F, Pitzalis C. Secondary and ectopic lymphoid tissue responses in rheumatoid arthritis: from inflammation to autoimmunity and tissue damage/remodeling [review]. Immunol Rev 2010;233:267–85.
10. Firestein GS. Evolving concepts of rheumatoid arthritis [review]. Nature 2003;423:356–61.
11. Humby F, Bombardieri M, Manzo A, Kelly S, Blades MC, Kirkham B, et al. Ectopic lymphoid structures support ongoing production of class-switched autoantibodies in rheumatoid synovium. PLoS Med 2009;6:e1.
12. Takemura S, Braun A, Crowson C, Kurtin PJ, Cofield RH, O'Fallon WM, et al. Lymphoid neogenesis in rheumatoid synovitis. J Immunol 2001;167:1072–80.
13. O'Rourke KP, O'Donoghue G, Adams C, Mulcahy H, Molloy C, Silke C, et al. High levels of Lymphotoxin-β (LT-β) gene expression in rheumatoid arthritis synovium: clinical and cytokine correlations. Rheumatol Int 2008;28:979–86.
14. Fu YX, Huang G, Wang Y, Chaplin DD. B lymphocytes induce the formation of follicular dendritic cell clusters in a lymphotoxin α-dependent fashion. J Exp Med 1998;187:1009–18.
15. Matsumoto M, Fu YX, Molina H, Chaplin DD. Lymphotoxin-α-deficient and TNF receptor-I-deficient mice define developmental and functional characteristics of germinal centers [review]. Immunol Rev 1997;156:137–44.
16. Pasparakis M, Alexopoulou L, Episkopou V, Kollias G. Immune and inflammatory responses in TNFα-deficient mice: a critical requirement for TNFα in the formation of primary B cell follicles, follicular dendritic cell networks and germinal centers, and in the maturation of the humoral immune response. J Exp Med 1996;184:1397–411.
17. Anolik JH, Ravikumar R, Barnard J, Owen T, Almudevar A, Milner EC, et al. Cutting edge: anti-tumor necrosis factor therapy in rheumatoid arthritis inhibits memory B lymphocytes via effects on lymphoid germinal centers and follicular dendritic cell networks. J Immunol 2008;180: 688–92.
18. Pala O, Diaz A, Blomberg BB, Frasca D. B lymphocytes in rheumatoid arthritis and the effects of anti-TNF-α agents on B lymphocytes: a review of the literature. Clin Ther 2018;40:1034–45.
19. Arnett FC, Edworthy SM, Bloch DA, McShane DJ, Fries JF, Cooper NS, et al. The American Rheumatism Association 1987 revised criteria for the classification of rheumatoid arthritis. Arthritis Rheum 1988;31:315–24.
20. Felson DT, Anderson JJ, Boers M, Bombardier C, Chernoff M, Fried B, et al. The American College of Rheumatology preliminary core set of disease activity measures for rheumatoid arthritis clinical trials. Arthritis Rheum 1993;36:729–40.
21. Van Gestel AM, Prevoo ML, van't Hof MA, van Rijswijk MH, van de Putte LB, van Riel PL. Development and validation of the European League Against Rheumatism response criteria for rheumatoid arthritis: comparison with the preliminary American College of Rheumatology and the World Health Organization/International League Against Rheumatism criteria. Arthritis Rheum 1996;39:34–40.
22. Wei C, Jung J, Sanz I. OMIP-003: phenotypic analysis of human memory B cells. Cytometry A 2011;79:894–6.
23. Adlowitz DG, Barnard J, Biear JN, Cistrone C, Owen T, Wang W, et al. Expansion of activated peripheral blood memory B cells in rheumatoid arthritis, impact of B cell depletion therapy, and biomarkers of response. PLoS One 2015;10:e0128269.
24. Wirth S, Lanzavecchia A. ABCB1 transporter discriminates human resting naive B cells from cycling transitional and memory B cells. Eur J Immunol 2005;35:3433–41.
25. Acosta-Rodriguez EV, Rivino L, Geginat J, Jarrossay D, Gattorno M, Lanzavecchia A, et al. Surface phenotype and antigenic specificity of human interleukin 17-producing T helper memory cells. Nat Immunol 2007;8:639–46.
26. Rivino L, Messi M, Jarrossay D, Lanzavecchia A, Sallusto F, Geginat J. Chemokine receptor expression identifies Pre–T helper (Th)1, Pre–Th2, and nonpolarized cells among human CD4+ central memory T cells. J Exp Med 2004;200:725–35.
27. Schmitt N, Bentebibel SE, Ueno H. Phenotype and functions of memory Tfh cells in human blood [review]. Trends Immunol 2014;35: 436–42.
28. Yu N, Li X, Song W, Li D, Yu D, Zeng X, et al. $CD4^+CD25^+CD127^{low/-}$ T cells: a more specific Treg population in human peripheral blood. Inflammation 2012;35:1773–80.
29. Tipton CM, Fucile CF, Darce J, Chida A, Ichikawa T, Gregoretti I, et al. Diversity, cellular origin and autoreactivity of antibody-secreting cell population expansions in acute systemic lupus erythematosus. Nat Immunol 2015;16:755–65.
30. Berkowska MA, Driessen GJ, Bikos V, Grosserichter-Wagener C, Stamatopoulos K, Cerutti A, et al. Human memory B cells originate from three distinct germinal center-dependent and -independent maturation pathways. Blood 2011;118:2150–8.
31. Palanichamy A, Barnard J, Zheng B, Owen T, Quach T, Wei C, et al. Novel human transitional B cell populations revealed by B cell depletion therapy. J Immunol 2009;182:5982–93.
32. Blair PA, Norena LY, Flores-Borja F, Rawlings DJ, Isenberg DA, Ehrenstein MR, et al. $CD19^+CD24^{hi}CD38^{hi}$ B cells exhibit regulatory capacity in healthy individuals but are functionally impaired in systemic lupus erythematosus patients. Immunity 2010;32:129–40.
33. Flores-Borja F, Bosma A, Ng D, Reddy V, Ehrenstein MR, Isenberg DA, et al. $CD19^+CD24^{hi}CD38^{hi}$ B cells maintain regulatory T cells while limiting T_H1 and T_H17 differentiation. Sci Transl Med 2013;5:173ra23.
34. Kennedy WP, Simon JA, Offutt C, Horn P, Herman A, Townsend MJ, et al. Efficacy and safety of pateclizumab (anti-lymphotoxin-α) compared to adalimumab in rheumatoid arthritis: a head-to-head phase 2 randomized controlled study (The ALTARA Study). Arthritis Res Ther 2014;16:467.

35. Moura RA, Quaresma C, Vieira AR, Goncalves MJ, Polido-Pereira J, Romao VC, et al. B-cell phenotype and IgD−CD27− memory B cells are affected by TNF-inhibitors and tocilizumab treatment in rheumatoid arthritis. PLoS One 2017;12:e0182927.
36. Souto-Carneiro MM, Mahadevan V, Takada K, Fritsch-Stork R, Nanki T, Brown M, et al. Alterations in peripheral blood memory B cells in patients with active rheumatoid arthritis are dependent on the action of tumour necrosis factor. Arthritis Res Ther 2009;11:R84.
37. Fekete A, Soos L, Szekanecz Z, Szabo Z, Szodoray P, Barath S, et al. Disturbances in B- and T-cell homeostasis in rheumatoid arthritis: suggested relationships with antigen-driven immune responses. J Autoimmun 2007;29:154–63.
38. Fedele AL, Tolusso B, Gremese E, Bosello SL, Carbonella A, Canestri S, et al. Memory B cell subsets and plasmablasts are lower in early than in long-standing rheumatoid arthritis. BMC Immunol 2014;15:28.
39. Doorenspleet ME, Klarenbeek PL, de Hair MJ, van Schaik BD, Esveldt RE, van Kampen AH, et al. Rheumatoid arthritis synovial tissue harbours dominant B-cell and plasma-cell clones associated with autoreactivity. Ann Rheum Dis 2014;73:756–62.
40. Meednu N, Zhang H, Owen T, Sun W, Wang V, Cistrone C, et al. Production of RANKL by memory B cells: a link between B cells and bone erosion in rheumatoid arthritis. Arthritis Rheumatol 2016;68:805–16.
41. Macallan DC, Wallace DL, Zhang Y, Ghattas H, Asquith B, de Lara C, et al. B-cell kinetics in humans: rapid turnover of peripheral blood memory cells. Blood 2005;105:3633–40.
42. Van Zelm MC, Szczepanski T, van der Burg M, van Dongen JJ. Replication history of B lymphocytes reveals homeostatic proliferation and extensive antigen-induced B cell expansion. J Exp Med 2007; 204:645–55.
43. Berkowska MA, Schickel JN, Grosserichter-Wagener C, de Ridder D, Ng YS, van Dongen JJ, et al. Circulating human $CD27^{-}IgA^{+}$ memory B cells recognize bacteria with polyreactive Igs. J Immunol 2015;195: 1417–26.
44. Zhang F, Wei K, Slowikowski K, Fonseka CY, Rao DA, Kelly S, et al. Defining inflammatory cell states in rheumatoid arthritis joint synovial tissues by integrating single-cell transcriptomics and mass cytometry. Nat Immunol 2019;20:928–42.
45. Kinslow JD, Blum LK, Deane KD, Demoruelle MK, Okamoto Y, Parish MC, et al. Elevated IgA plasmablast levels in subjects at risk of developing rheumatoid arthritis. Arthritis Rheumatol 2016;68: 2372–83.
46. Cañete JD, Celis R, Moll C, Izquierdo E, Marsal S, Sanmartí R, et al. Clinical significance of synovial lymphoid neogenesis and its reversal after anti-tumour necrosis factor α therapy in rheumatoid arthritis. Ann Rheum Dis 2009;68:751–6.
47. Kobie JJ, Zheng B, Bryk P, Barnes M, Ritchlin CT, Tabechian DA, et al. Decreased influenza-specific B cell responses in rheumatoid arthritis patients treated with anti-tumor necrosis factor. Arthritis Res Ther 2011;13:R209.
48. Hueber W, Tomooka BH, Batliwalla F, Li W, Monach PA, Tibshirani RJ, et al. Blood autoantibody and cytokine profiles predict response to anti-tumor necrosis factor therapy in rheumatoid arthritis. Arthritis Res Ther 2009;11:R76.
49. Liu C, Batliwalla F, Li W, Lee A, Roubenoff R, Beckman E, et al. Genome-wide association scan identifies candidate polymorphisms associated with differential response to anti-TNF treatment in rheumatoid arthritis. Mol Med 2008;14:575–81.
50. Folkersen L, Brynedal B, Diaz-Gallo LM, Ramskold D, Shchetynsky K, Westerlind H, et al. Integration of known DNA, RNA and protein biomarkers provides prediction of anti-TNF response in rheumatoid arthritis: results from the COMBINE study. Mol Med 2016;22: 322–8.
51. Wright HL, Cox T, Moots RJ, Edwards SW. Neutrophil biomarkers predict response to therapy with tumor necrosis factor inhibitors in rheumatoid arthritis. J Leukoc Biol 2017;101:785–95.
52. Donlin LT, Rao DA, Wei K, Slowikowski K, McGeachy MJ, Turner JD, et al. Methods for high-dimensonal analysis of cells dissociated from cyropreserved synovial tissue. Arthritis Res Ther 2018;20:139.
53. Dennis G Jr, Holweg CT, Kummerfeld SK, Choy DF, Setiadi AF, Hackney JA, et al. Synovial phenotypes in rheumatoid arthritis correlate with response to biologic therapeutics. Arthritis Res Ther 2014; 16:R90.
54. Rubtsova K, Rubtsov AV, Cancro MP, Marrack P. Age-associated B cells: a T-bet–dependent effector with roles in protective and pathogenic immunity [review]. J Immunol 2015;195:1933–7.
55. Jenks SA, Cashman KS, Zumaquero E, Marigorta UM, Patel AV, Wang X, et al. Distinct effector B cells induced by unregulated toll-like receptor 7 contribute to pathogenic responses in systemic lupus erythematosus. Immunity 2018;49:725–39.

Arthritis & Rheumatology
Vol. 74, No. 2, February 2022, pp 212–222
DOI 10.1002/art.41950

American College of Rheumatology
Empowering Rheumatology Professionals

Activation of Hypothalamic AMP-Activated Protein Kinase Ameliorates Metabolic Complications of Experimental Arthritis

Patricia Seoane-Collazo,[1] Eva Rial-Pensado,[1] Ánxela Estévez-Salguero,[1] Edward Milbank,[1] Lucía García-Caballero,[2] Marcos Ríos,[1] Laura Liñares-Pose,[1] Morena Scotece,[3] Rosalía Gallego,[2] José Manuel Fernández-Real,[4] Rubén Nogueiras,[1] Carlos Diéguez,[1] Oreste Gualillo,[3] and Miguel López[1]

Objective. To investigate whether thermogenesis and the hypothalamus may be involved in the physiopathology of experimental arthritis (EA).

Methods. EA was induced in male Lewis rats by intradermal injection of Freund's complete adjuvant (CFA). Food intake, body weight, plasma cytokines, thermographic analysis, gene and protein expression of thermogenic markers in brown adipose tissue (BAT) and white adipose tissue (WAT), and hypothalamic AMP-activated protein kinase (AMPK) were analyzed. Virogenetic activation of hypothalamic AMPK was performed.

Results. We first demonstrated that EA was associated with increased BAT thermogenesis and browning of subcutaneous WAT leading to elevated energy expenditure. Moreover, rats experiencing EA showed inhibition of hypothalamic AMPK, a canonical energy sensor modulating energy homeostasis at the central level. Notably, specific genetic activation of AMPK in the ventromedial nucleus of the hypothalamus (a key site modulating energy metabolism) reversed the effect of EA on energy balance, brown fat, and browning, as well as promoting amelioration of synovial inflammation in experimental arthritis.

Conclusion. Overall, these data indicate that EA promotes a central catabolic state that can be targeted and reversed by the activation of hypothalamic AMPK. This might provide new therapeutic alternatives to treat rheumatoid arthritis (RA)–associated metabolic comorbidities, improving the overall prognosis in patients with RA.

INTRODUCTION

Rheumatoid arthritis (RA) is an autoimmune and chronic inflammatory disease that mainly affects the synovium but also induces systemic manifestations causing pain, swelling, stiffness, unsteadiness, and deformity. Of note, RA is frequently associated with fatigue, weakness, fever, and weight loss (1–3). The mechanisms underlying metabolic complications in RA are not well

The Centro Singular de Investigación en Medicina Molecular y Enfermedades Crónicas (CiMUS) is supported by the Xunta de Galicia (2016-2019, ED431G/05). The Centro de Investigación Biomédica en Red Fisiopatología de la Obesidad y Nutrición (CIBERobn) is an initiative of the Instituto de Salud Carlos III. Supported by the Xunta de Galicia (grants 2016-PG057 to Dr. Nogueiras, GPC IN607B2019/10 to Dr. Gualillo, and 2016-PG068 to Dr. López), the Ministerio de Economía y Competitividad (MINECO) co-funded by the FEDER Program of the European Union (grants BFU2017-90578-REDT/Adipoplast to Drs. Fernández-Real and López, RTI2018-099413-B-I00 to Dr. Nogueiras, BFU2017-87721-P to Dr. Diéguez, and RTI2018-101840-B-I00 to Dr. López), the Instituto de Salud Carlos III (grants PI15–01934 and PI18/0102224 to Dr. Fernández-Real and PI17/00409, PI20/00902, RD21/0002/0025, and RD16/0012/0014 to Dr. Gualillo), "la Caixa" Foundation (ID 100010434) (grant LCF/PR/HR19/52160022 to Dr. López), and the European Research Council (synergy grant-2019-WATCH- 810331 to Dr. Nogueiras). Dr. Seoane-Collazo's work was supported by the Xunta de Galicia (fellowship ED481B 2018/050) and the Horizon 2020 Research and Innovation Program of the European Union under the Marie Sklodowska-Curie actions. Drs. Nogueiras and López's work was supported in part by the Atresmedia Corporación. Dr. Nogueiras's work was supported in part by Fundación BBVA and the European Foundation for the Study of Diabetes. Dr. Gualillo's work was supported in part by the Horizon 2020 Research and Innovation Program of the European Union under the Marie Sklodowska-Curie actions (project no. 734899) and by the Xunta de Galicia through a research staff contract (ISCIII/SERGAS).

[1]Patricia Seoane-Collazo, PhD, Eva Rial-Pensado, PhD, Ánxela Estévez-Salguero, PhD, Edward Milbank, PhD, Marcos Ríos, PhD, Laura Liñares-Pose, PhD, Rubén Nogueiras, PhD, Carlos Diéguez, MD, PhD, Miguel López, PhD: Centro Singular de Investigación en Medicina Molecular y Enfermedades Crónicas, Universidade de Santiago de Compostela, Instituto de Investigación Sanitaria, and CIBERobn, Santiago de Compostela, Spain; [2]Lucía García-Caballero, DDS, PhD, Rosalía Gallego, MD, PhD: Universidade de Santiago de Compostela, Santiago de Compostela, Spain; [3]Morena Scotece, PhD, Oreste Gualillo, PharmD, PhD: SERGAS, Instituto de Investigación Sanitaria de Santiago, NEIRID Lab, and Santiago University Clinical Hospital, Santiago de Compostela, Spain; [4]José Manuel Fernández-Real, MD, PhD: CIBERobn, Santiago de Compostela, Spain, and Institut d'Investigació Biomèdica de Girona and Hospital Universitari de Girona Doctor Josep Trueta, Girona, Spain.

Drs. Seoane-Collazo, Rial-Pensado, and Estévez-Salguero contributed equally to this work.

Author disclosures are available at https://onlinelibrary.wiley.com/action/downloadSupplement?doi=10.1002%2Fart.41950&file=art41950-sup-0001-Disclosureform.pdf.

Address correspondence to Oreste Gualillo, PhD, SERGAS, Instituto de Investigación Sanitaria de Santiago, NEIRID Lab, Santiago University Clinical Hospital, Research Area, Laboratory no. 9, Building C, Level 2, Trav. Choupana sn, Santiago de Compostela 15706, Spain (email: oreste.gualillo@sergas.es), or to Miguel López, PhD, CiMUS, Santiago de Compostela, Galicia 15782, Spain (email: m.lopez@usc.es).

Submitted for publication October 26, 2020; accepted in revised form August 10, 2021.

understood, but a serious catabolic status, driven predominantly by proinflammatory cytokines, might be responsible for body cell mass loss, a common feature of RA (4,5). In fact, there is increasing evidence about the contribution of the dysregulation of adipose tissue to RA, in particular dysregulated secretion of adipokines (4–7).

Obesity can play a dual role in RA, both by exacerbating its development and as a result of the disease progression, in part due to the patient's inability to carry out physical exercise and thereby inducing weight gain, something that may also be boosted by certain drugs used in the management of the illness (1,8–10). There is a general consensus that obesity prevention is important in patients with RA since it improves pain perception and metabolic and cardiovascular risk, as well as favoring a better response to treatments, such as anti–tumor necrosis factor (TNF) (11) and anti–interleukin-6 (anti–IL-6) receptor antibody (12).

A link between RA and altered levels of energy balance modulators acting at the central level, such as ghrelin, leptin, and other adipokines, has also been described (1,6,7,13). Moreover, a substantial amount of data highlighted a close relationship between alterations in different neuronal populations, some of them hypothalamic, and experimental arthritis (EA) (14–18). However, whether a dysregulation of these hypothalamic mechanisms is a cause or a consequence of the disease or, more importantly, whether targeting these hypothalamic nuclei may have a positive impact on the development of EA, remains unclear. Here, we aimed to investigate whether the hypothalamus may be involved in the physiopathology of EA. We focused on AMP-activated protein kinase (AMPK) in a specific set of neurons located in the ventromedial nucleus of the hypothalamus (VMH), which recently emerged as a critical canonical mechanism controlling energy homeostasis (19,20). In this sense, current evidence has shown that inhibition of AMPK in steroidogenic factor 1 cells of the VMH leads to sympathetic nervous system–mediated activation of the brown adipose tissue (BAT) thermogenesis, leading to increased energy expenditure and feeding-independent weight loss (19–24). Notably, this mechanism mediates the actions of key thermogenic factors, such as thyroid hormones, bone morphogenetic protein 8B, estradiol, liraglutide receptor agonism, and nicotine (19–24).

Therefore, our aim was to investigate whether this central pathway might be involved in the metabolic alterations induced in an experimental model of arthritis. We used a model of EA induced by intradermal injection of Freund's complete adjuvant (CFA), which does not reflect every aspect of human RA but is a routinely used model and resembles some of the articular and extraarticular features of the disease (13,15,16).

MATERIALS AND METHODS

Animals and experimental protocols. Male Lewis rats (*Lew/OrlRj*, 200 gm, 6–7 weeks old; Janvier Labs) were used. Animals were housed under controlled light (12-hour light/dark cycle), temperature, and humidity conditions. The animals were allowed to freely drink water and were given a standard diet (SD) (Scientific Animal Food & Engineering: 3% fat, 60% carbohydrates, and 16% protein; Amersfoort) or a high-fat diet (HFD) (D12451: 45% fat, 35% carbohydrates, 20% protein; Research Diets, Inc.) for 3 weeks before the initiation of CFA-induced EA. All experiments and procedures were performed in agreement with International Law on Animal Experimentation and the USC Ethical Committee (project ID 15010/14/006 and 15012/2020/010).

CFA-induced EA. EA was induced by intradermal injection of CFA (0.1 ml suspension of *Mycobacterium tuberculosis* [13,15,16] [1 mg/ml] in sterile mineral oil; Sigma-Aldrich) into the dorsal side of the tail base; sham-treated animals were injected with the same volume of mineral oil. The evaluation of clinical arthritis was performed by the following methods: 1) histopathologic analysis of tibiotarsal sections on day 14, 2) measurement of the paw volume using a hydroplethysmometer (Ugo Basile), and 3) measurement of the edema volume change. Edema volume change was calculated using the difference of means in paw volume from SD-fed rats with CFA-induced EA versus SD-fed sham-treated rats or HFD-fed rats with CFA-induced EA versus HFD-fed sham-treated rats, respectively.

Stereotaxic microinjection of adenoviral expression vectors. Adenoviral vectors with green fluorescent protein (GFP) or constitutively active AMPKα1 (AMPKα1-CA) (ViraQuest) were delivered as previously described (21–23).

Indirect calorimetry. Animals were analyzed for energy expenditure, respiratory quotient, and locomotor activity using a calorimetric system (LabMaster; TSE Systems) as previously described (22–24). Rearing locomotor activity was analyzed by the number of bean break counts on the z-axis.

Temperature measurements. Skin temperature surrounding BAT and paw temperature were recorded with an infrared camera (B335: Compact Infrared Thermal Imaging Camera; FLIR) and analyzed with a specific software package (FLIR Tools Software), as previously described (22–24).

Blood biochemistry. Levels of TNF, IL-1, IL-6, IL-10, IL-17, and interferon-γ (IFNγ) were measured using Bio-Plex rat cytokine assays (Bio-Rad).

Real-time polymerase chain reaction (PCR). Real-time PCR (TaqMan; Applied Biosystems) was performed as previously described (21–23), using either of the following: 1) specific sets of primers/probes for peroxisome proliferator–activated receptor γ coactivator 1α (PGC-1α) (*Ppargc1a*; 5′-CGATCACCATATTC CAGGTCAAG-3′ [forward], 5′-CGATGTGTGCGGTGTCTGTAGT-3′ [reverse]; FAM-5′-AGGTCCCCAGGCAGTAGATCCTCT

TCAAGA-3′-TAMRA [probe]), or 2) commercially available and prevalidated TaqMan primer/probe sets for PGC-1β (*Ppargc1b*; assay no. Rn00598552_m1). Gene expression values were expressed in relation to the levels of hypoxanthine guanine phosphoribosyltransferase (5′-AGCCGACCGGTTCT GTCAT-3 ′ [forward], 5′-GGTCATAACCTGGTTCATCATCAC-3′ [reverse], FAM-5′-CGACCCTCAGTCCCAGCGTCGTGAT-3′-TAMRA [probe]).

Histology. Histologic samples were fixed in 10% neutral buffered formalin for 24 hours. For decalcification, the samples were immersed in a 10% formic solution in water (volume/volume; Sharlan) for 10 days at room temperature and subsequently embedded in paraffin routinely. Sections that were 4-μm thick were stained with hematoxylin and eosin (H&E) and imaged at 4× the original magnification using a slide scanner for digital pathology (PathScan Excilone).

Immunohistochemistry. Detection of uncoupling protein 1 (UCP-1) in white adipose tissue (WAT) was performed using an anti–UCP-1 antibody (1:500 dilution) (no. ab10983; Abcam) (22,24). Digital images were quantified using ImageJ version 1.44 (National Institutes of Health), as previously shown (22,24).

Western blotting. Protein lysates from the hypothalamus and BAT were subjected to sodium dodecyl sulfate–polyacrylamide gel electrophoresis, electrotransferred, and probed with antibodies against UCP-1 (1:10,000 dilution) (no. ab10983; Abcam), β-actin (1:5,000 dilution) (no. A5316; Sigma), α-tubulin (1:5,000 dilution) (no. T5168; Sigma), AMPKα1 (1:1,000 dilution) (no. 07-350; Merck Millipore), AMPKα2 (1:1,000 dilution) (no. 07-363; Merck Millipore), phosphorylated AMPKα (pAMPKα; threonine^{172}) (1:1,000 dilution) (no. 2535S; Cell Signaling), phosphorylated acetyl-coenzyme A carboxylase α (p-ACCα; Serine^{79}) (1:1,000 dilution) (no. 3661; Cell Signaling), ACCα (1:1,000 dilution) (no. 04-322; Merck Millipore), and fatty acid synthase (FAS; 1:1,000 dilution) (no. 610962; BD). Band signals were quantified by densitometry using ImageJ version 1.44 (21–23). Values were expressed in relation to β-actin (hypothalamus) or α-tubulin (BAT). In all figures showing images of gels, the bands for each picture were obtained from the same gel, although they may have been spliced for clarity.

Statistical analysis. Data are expressed as the mean ± SEM. Statistical significance was determined by Student's *t*-test (2 groups) or analysis of variance (≥2 groups) followed by a post hoc Tukey test. *P* values less than 0.05 were considered significant. The correlation between parameters was evaluated with Pearson's correlation coefficient.

Data availability. All data generated and analyzed in this study are available upon reasonable request. Access to data generated in this study is available upon request from the corresponding authors.

RESULTS

Occurrence of CFA-induced EA independent of body weight. First, Lewis rats were fed an a SD or HFD for 3 weeks. Animals with diet-induced obesity showed a significant increase in body weight (mean ± SEM 277.30 ± 4.023 gm for SD-fed rats versus 301.30 ± 3.2 gm for HFD-fed rats;

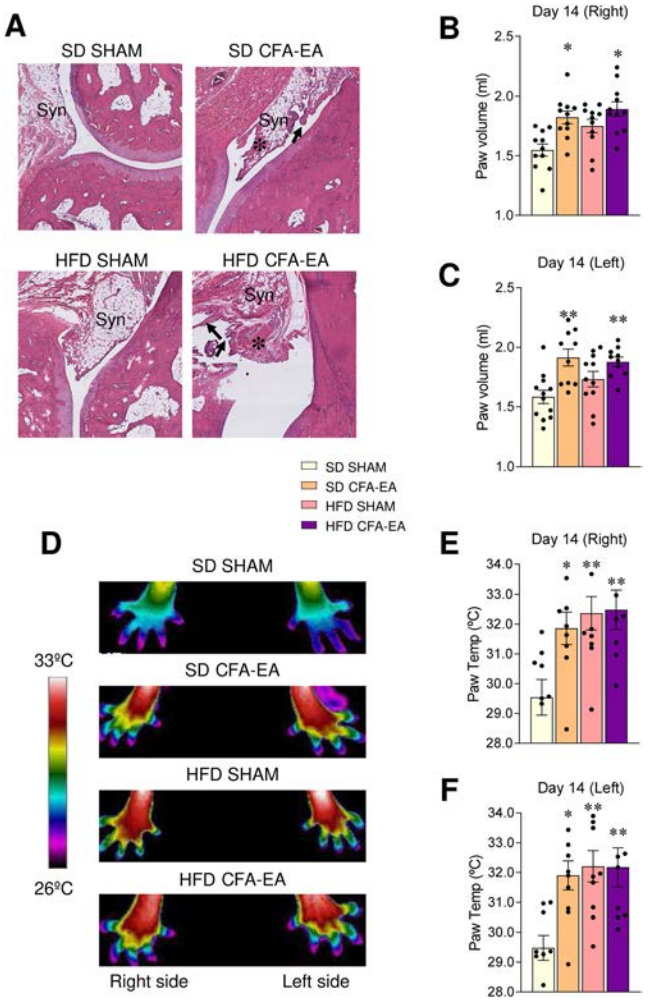

Figure 1. Experimental arthritis (EA) induction with Freund's complete adjuvant (CFA) in rats fed a standard diet (SD) or high-fat diet (HFD). **A,** Representative sections of the tibiotarsal joints of SD-fed or HFD-fed rats intradermally treated with mineral oil or CFA. In the joints of rats with CFA-induced EA, synovia (Syn) show hyperplasia, with papillary projections (**arrows**) and fibrosis (**asterisks**) (hematoxylin and eosin staining at 4× original magnification). **B–F**, Paw volume in right (**B**) and left (**C**) posterior paws, and representative thermal images (**D**) and paw temperature in right (**E**) and left (**F**) posterior paws of SD-fed or HFD-fed rats intradermally treated with mineral oil or CFA. Symbols represent individual rats (n = 7–12 rats per group). Bars show the mean ± SEM. * = $P < 0.05$; ** = $P < 0.01$ versus SD-fed sham-treated animals, by analysis of variance.

$P < 0.001$). Next, CFA was inoculated into the dorsal side of the tail base. Our data show that both SD-fed rats with CFA-induced EA and HFD-fed rats with CFA-induced EA developed signs of inflammation, as demonstrated by histologic analysis showing normal cartilage and bone structures in the H&E–stained tibiotarsal sections of sham-treated animals fed an SD or HFD (Figure 1A). In addition, we observed synovial hyperplasia, narrowing of joint space, and cartilage and bone destruction in the arthritic tibiotarsal joints of SD-fed rats with CFA-induced EA and HFD-fed rats with CFA-induced EA (Figure 1A). Consistent with this, the rats displayed an increase in the right and left posterior paw volume 7 days after the adjuvant injection, reaching maximum levels on day 14 (peak phase) and improving on day 28 (recovery phase) (Figures 1B and C and Supplementary Figures 1A–D, available on the *Arthritis & Rheumatology* website at http://onlinelibrary.wiley.com/doi/10.1002/art.41950/abstract). The analysis of edema volume confirmed those data, showing that maximal volume changes mainly occurred on days 7–14 (Supplementary Figures 1E and F) in SD-fed and HFD-fed rats.

Rats with CFA-induced EA also showed an incapacity to bend the ankle and developed nodules at the base of the tail and ears (data not shown). To add more insight to the inflammatory status of the animals, we analyzed the temperature of the paws using infrared thermography. Our data showed that both an HFD feeding regimen and inoculation with CFA induced an increase of both right and left paw temperature (Figures 1D–F), which is suggestive of inflammation.

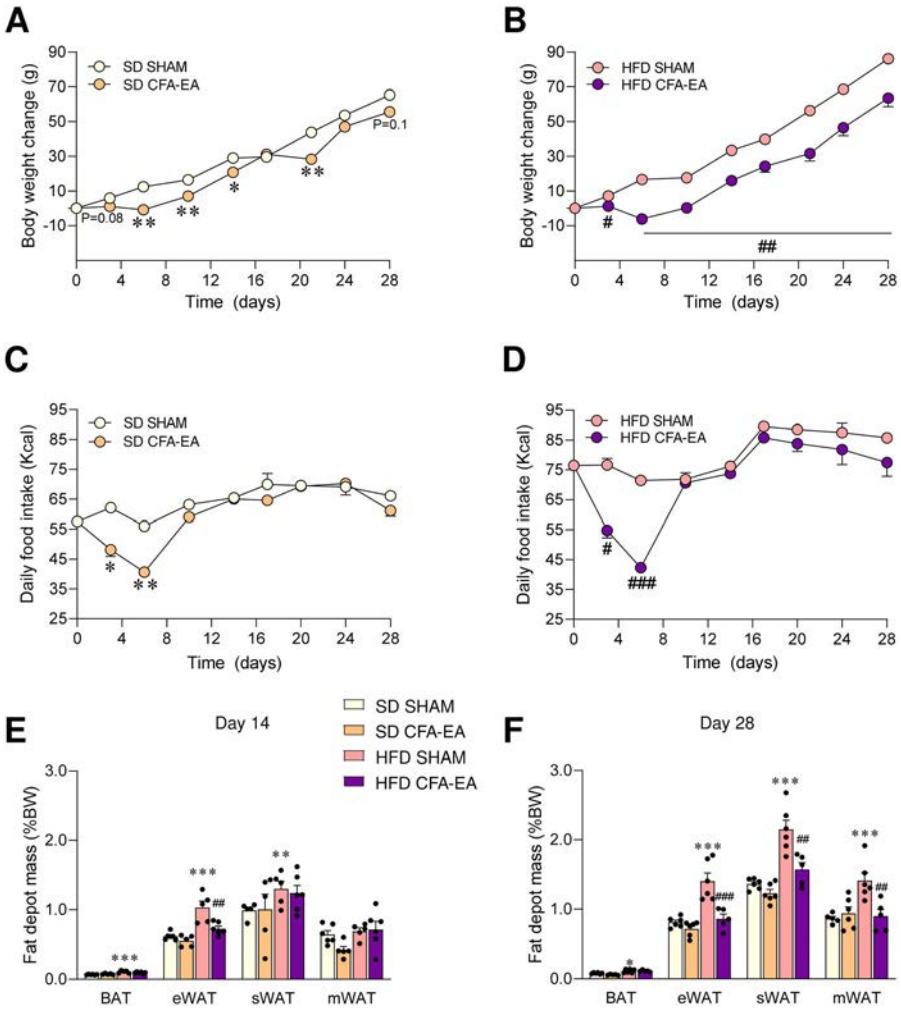

Figure 2. Effect of CFA-induced EA on energy balance in SD-fed or HFD-fed rats. Body weight change (**A** and **B**), daily food intake (**C** and **D**), and fat depot masses at 14 days (**E**) and 28 days (**F**) after intradermal treatment with mineral oil or CFA in SD-fed or HFD-fed rats. Symbols represent individual rats (n = 5–12 rats per group at 14 days and 5–6 rats per group at 28 days). Bars show the mean ± SEM. In **A–D**, *P* values were determined using Student's *t*-test, and in **E** and **F**, analysis of variance was used. * = $P < 0.05$; ** = $P < 0.01$; *** = $P < 0.001$ versus SD-fed sham-treated animals. # = $P < 0.05$; ## = $P < 0.01$; ### = $P < 0.001$ versus HFD-fed sham-treated animals. %BW = percentage body weight; BAT = brown adipose tissue; eWAT = epididymal white adipose tissue; mWAT = mesenteric WAT; sWAT = subcutaneous WAT (see Figure 1 for other definitions). Color figure can be viewed in the online issue, which is available at http://onlinelibrary.wiley.com/doi/10.1002/art.41950/abstract.

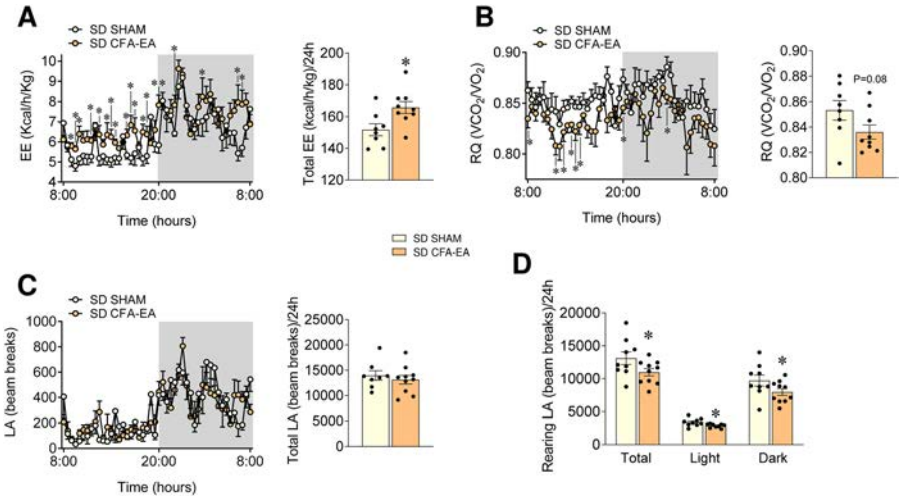

Figure 3. Effect of CFA-induced EA on energy expenditure (EE), respiratory quotient (RQ), and locomotor activity (LA) in SD-fed rats. EE and total EE (**A**), RQ and average RQ (**B**), LA and total LA (**C**), and rearing LA (**D**) in SD-fed rats intradermally treated with mineral oil or CFA. Symbols represent individual rats (n = 8–10 rats per group). Bars show the mean ± SEM. * = $P < 0.05$; ** = $P < 0.01$ versus sham-treated animals, by Student's *t*-test. See Figure 1 for other definitions. Color figure can be viewed in the online issue, which is available at http://onlinelibrary.wiley.com/doi/10.1002/art.41950/abstract.

Negative energy balance state resulting from CFA-induced EA. Analysis of body weight changes demonstrated that both SD-fed and HFD-fed rats with CFA-induced EA showed a negative energy balance, as revealed by weight loss, which was more evident in the HFD group (Figures 2A and B), as well as hypophagia during the first week (Figures 2C and D). This was associated with decreased adiposity, and we observed reduced epididymal WAT (on days 14 and 28), subcutaneous WAT (from the inguinal area, on day 28), and mesenteric WAT (on day 28) pad masses in HFD-fed rats but not in SD-fed rats (Figures 2E and F). Notably, during the peak phase (day 14), no correlation was found between initial body weight and body weight loss in the animals with CFA-induced EA (Supplementary Figure 2A, http://onlinelibrary.wiley.com/doi/10.1002/art.41950/abstract), although there was a nonsignificant trend in the recovery phase (day 28) (Supplementary Figure 2B). Overall, these data indicate that a higher body weight prior to CFA-induced EA does not have any beneficial effect either during the peak of the illness or in the recovery phase and that CFA-induced EA is very similar in both diet-induced obese (HFD) and lean (SD) rodents. On the contrary, according to the obtained data, HFD might worsen the energy balance outcome in the EA model.

Increased energy expenditure in CFA-induced EA. Considering the changes observed in body weight, which could not be simply explained by changes in food intake, we decided to assess energy expenditure–related mechanisms. Therefore, we performed an indirect calorimetry analysis of sham-treated and CFA-induced EA groups fed with SD or HFD. Our data showed that SD-fed rats and HFD-fed rats with CFA-induced EA had a higher energy expenditure and lower respiratory quotient (indicative of higher lipid mobilization) than their respective sham-treated controls (Figures 3A and B and Supplementary Figures 3A and B, http://onlinelibrary.wiley.com/doi/10.1002/art.41950/abstract), while no changes in total locomotor activity were detected (Figures 3C and Supplementary Figure 3C). Of note, rearing locomotor activity was decreased in experimental animals, indicative of difficulties in standing over the hind legs (Figure 3D and Supplementary Figure 3D).

BAT thermogenesis and WAT browning in CFA-induced EA. Next, we analyzed the BAT in rats with CFA-induced EA. Our data showed a significant increase in the protein levels of UCP-1 (a mitochondrial carrier protein located in BAT that generates heat by non-shivering thermogenesis) in the BAT of rats with CFA-induced EA, on days 14 and 28 independently of diet (Figure 4A and Supplementary Figures 4A–C, http://onlinelibrary.wiley.com/doi/10.1002/art.41950/abstract). Further BAT analysis showed that the levels of messenger RNA for *Ppargc1a* (the gene for PGC-1α and a key transcription factor regulating *Ucp1* gene expression), but not *Ppargc1b*, were also increased on day 14 in SD-fed rats with CFA-induced EA (Figure 4B). In accordance with these data, thermographic analysis proved that SD-fed rats with CFA-induced EA displayed an increased BAT temperature, which was indicative of augmented brown fat thermogenesis (Figure 4C). Activation of beige/brite ("brown-in-white") adipocytes in the WAT, a process known as browning, is responsible for a significant increase in total energy expenditure (25,26). However, to date, no data have linked RA to the browning of WAT. Our histologic analysis of subcutaneous WAT showed that SD-fed rats with CFA-induced EA exhibited increased UCP-1 immunostaining (Figures 4D and E) and

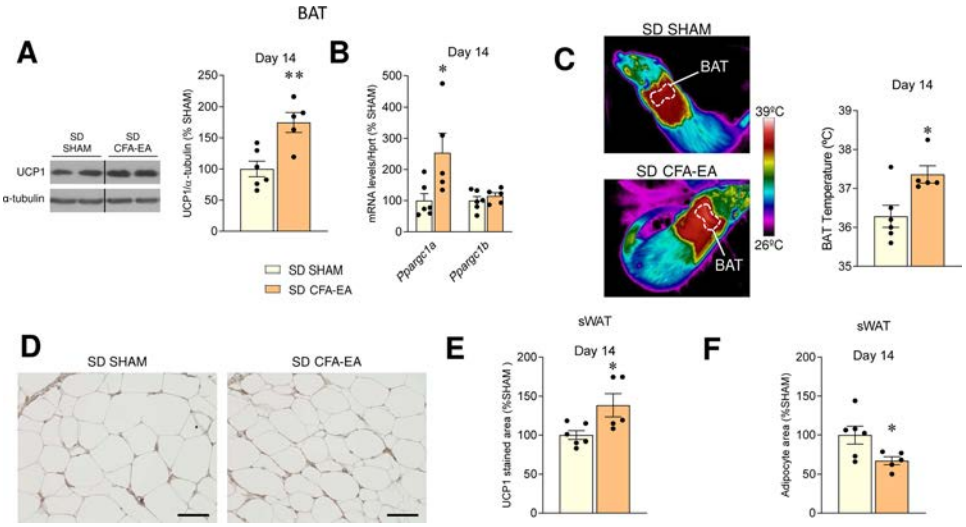

Figure 4. Effect of CFA-induced EA on brown adipose tissue (BAT) and subcutaneous white adipose tissue (sWAT). Representative Western blot images and levels of BAT uncoupling protein 1 (UCP-1) (**A**), BAT levels of mRNA for *Ppargc1a* and *Ppargc1b* (**B**), representative thermal images and levels of BAT temperature (**C**), representative immunohistochemical staining with an anti–UCP-1 antibody (bars = 100 μm) (**D**), UCP-1–stained area (**E**), and adipocyte area (**F**) on day 14 posttreatment in SD-fed rats intradermally treated with mineral oil or CFA. For the Western blot analysis, representative images for all proteins are shown; all bands for each picture were obtained from the same gel, but they may be spliced for clarity, which is indicated by vertical lines. Symbols represent individual rats (n = 5–6 rats per group). Bars show the mean ± SEM. * = $P < 0.05$; ** = $P < 0.01$ versus SD-fed sham-treated animals, by Student's *t*-test. See Figure 1 for other definitions. Color figure can be viewed in the online issue, which is available at http://onlinelibrary.wiley.com/doi/10.1002/art.41950/abstract.

decreased adipocyte area (Figures 4D and F), which are indicative of browning.

Central effects of CFA-induced EA on energy balance dependent on AMPK in the VMH. Rats with CFA-induced EA showed decreased AMPK activity, as demonstrated by reduced levels of pAMPKα and its downstream target p-ACCα in the hypothalamus (Figure 5A and Supplementary Figures 5A–C, http://onlinelibrary.wiley.com/doi/10.1002/art.41950/abstract). Consistent with those findings, protein levels of FAS, which is negatively regulated by AMPK (27), were elevated in the hypothalamus of animals with CFA-induced EA (Figure 5A and Supplementary Figures 5A–C). Notably, as it has been described in other models of hypothalamic AMPK inhibition (21–23), decreased pAMPK was associated with reduced levels (or a trend toward reduction) of the AMPKα1, but not AMPKα2, subunit (Figure 5A and Supplementary Figures 5A–C).

We hypothesized that the negative energy balance that characterized EA-induced weight loss might be mediated by the specific inhibition of AMPK in the VMH, a key mechanism regulating thermogenesis (19–24). To evaluate this, adenoviruses encoding either for an AMPKα1-CA or a GFP control vector were injected stereotaxically into the VMH in rats with CFA-induced EA. First, we induced EA using CFA as indicated above and checked the progression of the illness on day 8 (body weight change mean ± SEM 12.57 ± 3.36 gm for sham-treated controls versus −2.21 ± 2.27 gm for rats with CFA-induced EA; $P < 0.001$). On day 9, we injected the adenovirus to pair the effect of the adenovirus with the peak of EA. The AMPKα1-CA adenovirus was previously validated (21–23) and induced a significant increase in p-ACCα protein levels within the VMH (mean ± SEM 100 ± 18.3 for GFP-injected rats with CFA-induced EA versus 170.7 ± 25.7 for AMPKα1-CA–injected rats with CFA-induced EA; $P < 0.05$). Overexpression of AMPKα1-CA in the VMH, confirmed by GFP immunofluorescence (21–23) (data not shown), promoted an overall improvement in the inflammatory state of the rats, as demonstrated by reduced tissue swelling and ankylosis in the paws and tail as well as fur aspect in comparison with the GFP-injected control rats (Figure 5B). AMPKα1-CA also blunted the weight loss caused by CFA injection and displayed an increased food intake (Figures 5C and D). Notably, this effect was associated with reversal of the CFA-induced thermogenesis (Figures 6A) and browning of subcutaneous WAT, as demonstrated by decreased UCP-1 staining (Figures 6B and C) and enhanced adipocyte area (Figures 6B and D) in CFA-treated rats receiving AMPKα1-CA adenoviruses in the VMH for 6 days, compared to CFA-treated rats treated with control GFP adenoviruses. AMPKα1-CA adenoviruses did not impact any of the aforementioned parameters when administrated in sham-treated rats (data not shown).

Reversal of CFA-induced EA–associated inflammatory phenotype via activation of AMPK in the VMH. Finally, we investigated whether, besides energy balance, the AMPKα1-CA adenovirus injected into the VMH could reverse the overall inflammatory state that characterizes CFA-induced

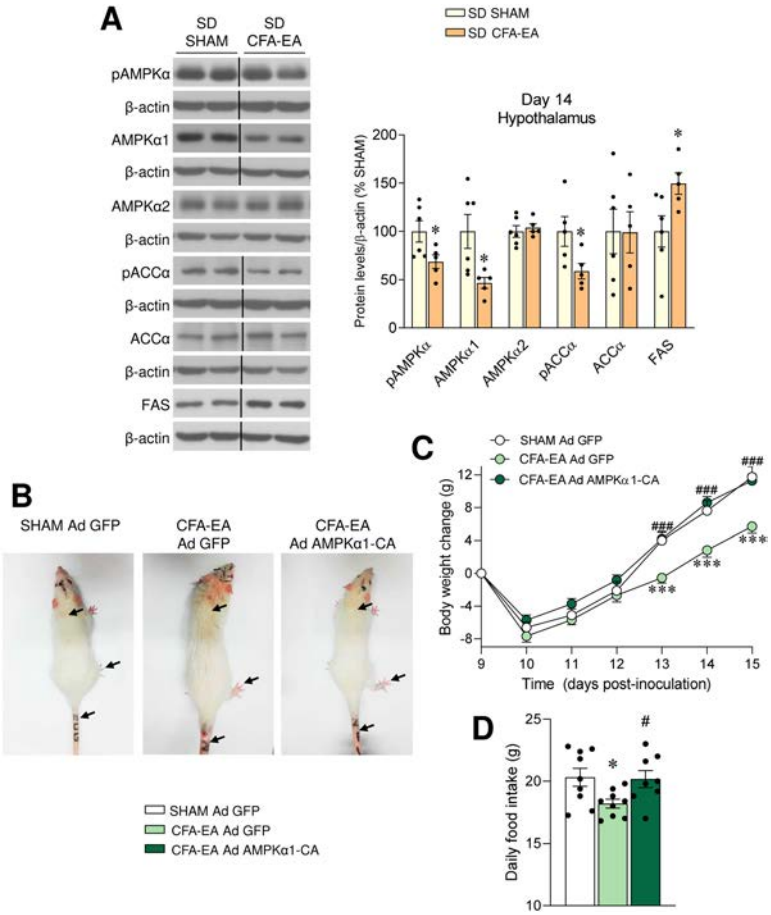

Figure 5. Effect of adenoviral constitutively active AMP-activated protein kinase α1 (AMPKα1-CA) overexpression in the ventromedial nucleus of the hypothalamus (VMH) on energy balance in rats with CFA-induced EA. **A**, Representative Western blot images and hypothalamic protein levels of the AMPK pathway on day 14 posttreatment in SD-fed rats intradermally treated with mineral oil or CFA. **B–D**, Photographs of a representative rat in each group (**B**), body weight change (**C**), and daily food intake (**D**) in SD-fed rats intradermally treated with mineral oil or CFA and stereotaxically injected with green fluorescent protein (GFP) or AMPKα1-CA adenovirus (Ad) in the VMH. Experiments including the sham-treated animals injected with AMPKα1 were performed, but they have been excluded in the graphs for simplification. In **B, arrows** show tissue swelling in the paws and tail as well as fur aspect. For the Western blot analysis, representative images for all proteins are shown; all bands for each picture were obtained from the same gel, but they may be spliced for clarity, which is indicated by vertical lines. Symbols represent individual rats (n = 5–6 rats per group in **A** and 8–10 rats per group in **B–D**). Bars show the mean ± SEM. In **A**, *P* values were determined using Student's *t*-test, and in **C** and **D**, analysis of variance was used. * = $P < 0.05$; *** = $P < 0.001$ versus sham-treated animals with or without GFP injection. # = $P < 0.05$; ### = $P < 0.001$ versus rats with CFA-induced EA injected with GFP. p-ACCα = phosphorylated acetyl-coenzyme A carboxylase α; FAS = fatty acid synthase (see Figure 1 for other definitions). Color figure can be viewed in the online issue, which is available at http://onlinelibrary.wiley.com/doi/10.1002/art.41950/abstract.

EA. Our data showed that, in rats with CFA-induced EA, the circulating levels of inflammatory cytokines, namely TNF, IL-1β, IL-6, IFNγ, and IL-17, were higher, while levels of antiinflammatory cytokine IL-10 were lower (Figure 6E). Notably, when treatment with AMPKα1-CA was administered into the VMH, the inflammatory status observed in rats with CFA-induced EA was improved. AMPKα1-CA adenoviruses did not impact the aforementioned parameters when administrated to sham-treated rats (data not shown). Correlation analyses of those effects also demonstrated that circulating levels of TNF, IL-1, and IL-6 were negatively associated with changes in body weight and/or food intake (Supplementary Table 1, http://onlinelibrary.wiley.com/doi/10.1002/art.41950/abstract).

DISCUSSION

The relationship between obesity and several inflammatory and autoimmune diseases, such as RA, has been broadly studied over the last decades. However, the underlying mechanism is still under debate. There is a general consensus that both diseases are associated with an imbalance between proinflammatory and antiinflammatory cytokines contributing to the onset and progression of RA and obesity (4,5). Therefore, in this study we aimed to clarify whether obesity could influence RA and to uncover the molecular mechanism responsible for RA-induced altered energy balance. With this in mind, we induced EA by CFA inoculation (13,15,16) in a rat model (those fed a control diet [SD] versus

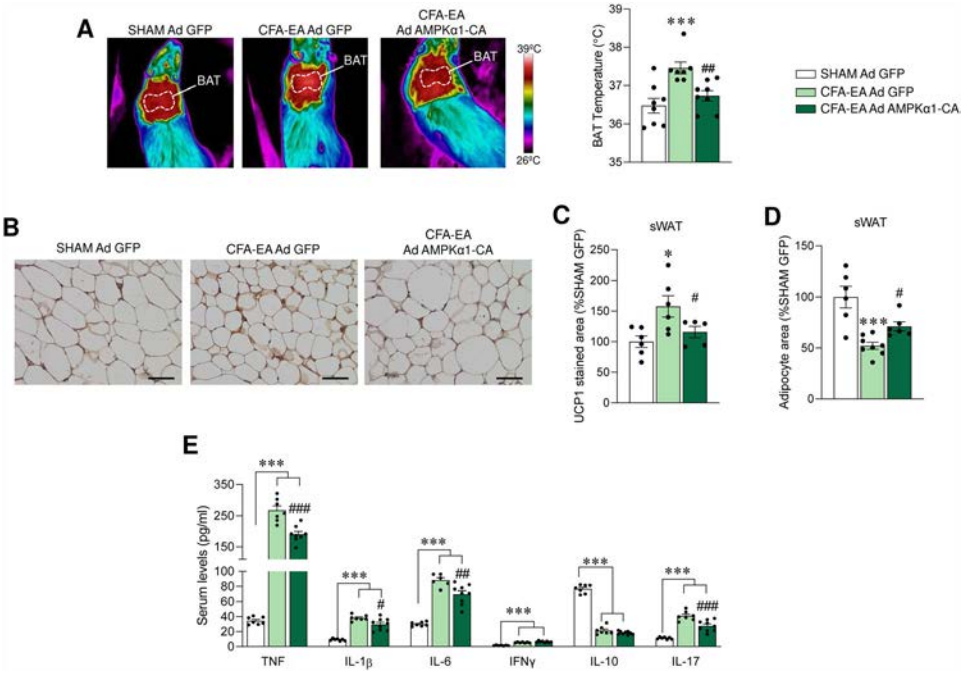

Figure 6. Effect of adenoviral constitutively active AMP-activated protein kinase α1 (AMPKα1-CA) overexpression in the ventromedial nucleus of the hypothalamus (VMH) in rats with CFA-induced EA on energy balance and inflammatory state. Shown are representative thermal images and brown adipose tissue (BAT) temperature (**A**), representative immunohistochemical images of subcutaneous white adipose tissue stained with anti–uncoupling protein 1 (anti–UCP-1) antibody (bars = 100 μm) (**B**), UCP-1–stained area (**C**), adipocyte area (**D**), and circulating levels of tumor necrosis factor (TNF), interleukin-1 (IL-1), IL-6, interferon-γ (IFNγ), IL-10, and IL-17 (**E**) in SD-fed rats intradermally treated with mineral oil or CFA and stereotaxically injected with green fluorescent protein (GFP) or AMPKα1-CA adenovirus (Ad) in the VMH. Experiments including the sham-treated animals injected with AMPKα1 were performed, but they have been excluded in the graphs for simplification. Symbols represent individual rats (n = 6–9 rats per group). Bars show the mean ± SEM. * = $P < 0.05$; *** = $P < 0.001$ versus sham-treated animals with GFP injection, by analysis of variance (ANOVA). # = $P < 0.05$; ## = $P < 0.01$; ### = $P < 0.001$ versus rats with CFA-induced EA injected with GFP, by ANOVA. See Figure 1 for other definitions.

those fed an HFD) and also assessed its impact on peripheral and central mechanisms regulating energy balance. We focused specifically on BAT thermogenesis, since it is known that induction of EA by CFA is characterized, in some cases, by increased energy expenditure (28,29). Furthermore, it is known that RA is characterized by weight loss and wasting, a state known as rheumatoid cachexia (RC), but the mechanism by which some RA patients lose weight is not well defined and may be multifactorial (1–3). A similar situation is present in cancer-induced cachexia, where activation of brown fat thermogenesis has been described (30–33).

The phenotype observed in our preclinical model is consistent with the definition of pre-cachexia, since it fulfils the features required to be present in patients with an underlying disease: chronic and systemic inflammation, hypophagia, and weight loss (34). However, it should be acknowledged that there are some clear differences between cachexia induced by other diseases, such as cancer, and RC. In classic cachexia, loss of body weight, due to muscle and fat loss, is a common feature. These outcomes are consistent with data showing increased resting energy expenditure induced by BAT activation (30–33) or WAT browning (35–37), in both rodent models of cachexia and in patients with cachexia. In contrast, in RC, for which a consensus diagnostic criterion does not exist, the loss of body weight and adiposity rarely occurs (38,39).

Our data showed that both lean and obese rats displayed a similar increase in paw volume after EA induction. No correlation was found between body weight and body weight loss. Remarkably, although both SD-fed and HFD-fed animals with CFA-induced EA displayed initial hypophagia, they restored their food intake after the peak of the illness; however, while SD-fed rats with CFA-induced EA were able to show a progressive body weight recovery, HFD-fed rats with CFA-induced EA failed to recuperate their body weight and continued to lose body weight and fat masses. To further improve our understanding of EA-induced alterations in energy balance, we assessed the effect of CFA-induced EA on BAT thermogenesis. We found a marked activation of BAT in all the stages of EA, in both SD-fed and HFD-fed animals, as shown by increased BAT temperature and/or increased levels of UCP-1 in brown fat, as well as browning of WAT.

Several mechanisms could explain this increased thermogenic tone in our experimental EA model, acting centrally or

directly on brown and white adipocytes. For example, it is known that cancer cachexia–induced browning is dependent on IL-6 (35). However, considering that the proinflammatory milieu represses the thermogenic activity of brown and beige fat via cytokines that inhibit noradrenergic signaling (25), central effects might be more important than direct peripheral actions on adipose cells. Given that AMPK in different hypothalamic neuronal populations regulates whole-body energy homeostasis, from feeding to BAT thermogenesis and browning of WAT (19,20,23,40), we next investigated the effect of EA in this pathway. Our data revealed that VMH AMPK is decreased in EA. Next, we investigated whether this effect was mechanistically associated with EA-induced actions on energy balance. Thus, we targeted AMPKα1 in the VMH, a nucleus where this catalytic subunit has been involved in both the modulation of feeding and BAT thermogenesis (19,20,27).

Our data showed that specific VMH AMPK activation using virogenetic strategies was enough to ameliorate the negative energy balance included by CFA-induced EA. Remarkably, besides body weight gain, restored feeding, and diminished BAT and browning tones, AMPKα1 activation in the VMH decreased the circulating levels of inflammatory cytokines, as well as improving the physical appearance of the animals. These later effects are quite relevant since it is assumed that proinflammatory cytokines are at the root of some of the most serious consequences of RA (4,5). In this sense, the mechanisms underlying metabolic complications in RA are unclear, although proinflammatory cytokines might also be responsible for the loss of body cell mass (4,5). In addition, the link between the hypothalamic AMPK axis and the inflammatory status raises very interesting pathophysiologic as well as physiologic questions. It is known that inflammation of tissues is under neural control, involving the neuroendocrine, sympathetic, and central nervous systems (18,41). Data from the 1990s had already demonstrated an association between sympathetic ganglia and the pathogenesis of EA (42,43). Of note, CFA-induced EA in Lewis rats has been linked to changes in the sympathetic nerves in the spleen and is also responsible for the activation of immune cells in the red pulp of that organ (44,45).

Remarkably, the spinal BAT sympathetic preganglionic neurons in the intermediolateral nucleus of the thoracolumbar spinal cord are in the same area as those innervating the spleen (46,47). Thus, activation of the same centers may promote both BAT thermogenesis and immune activation in the spleen. This connection is functionally supported by our data and a recent report showing that propranolol (a nonselective beta blocker) promotes, in addition to antiarrhythmic effects, a systemic antiinflammatory action in a model of collagen-induced arthritis in Lewis rats (48). Overall, this evidence seems to indicate that reduced sympathetic tone ameliorates EA symptoms, offering a possible alternative mechanism to the antiinflammatory effect of AMPKα1 adenoviral treatment in the VMH.

To our knowledge, this is the first study linking the canonical hypothalamic AMPK–BAT/WAT axis to the development of the symptoms of a systemic disease, such as RA. This is relevant because targeting hypothalamic AMPK, which has been proposed as a potential therapy for obesity (19), may also be a possible strategy to ameliorate the negative energy balance and to improve the inflammatory state associated with RA. In this sense, recent and profuse evidence has shown that metformin, a drug administered for the treatment of type 2 diabetes mellitus that activates AMPK, promotes metabolic improvement in RA patients and in animal models of pharmacologically induced and autoimmune arthritis (49,50).

In summary, our data show that negative energy balance caused by CFA-induced EA is independent of initial body weight, and it is associated with VMH AMPK–mediated activation of BAT thermogenesis and browning. Notably, activation of AMPK in the VMH not only ameliorates the metabolic outcome in CFA-induced EA but also improves the inflammatory status of the animals. Taken together, these findings provide new mechanistic insight into the pathophysiology of RA and suggest new therapeutic strategies for its possible clinical management and treatment.

AUTHOR CONTRIBUTIONS

All authors were involved in drafting the article or revising it critically for important intellectual content, and all authors approved the final version to be published. Dr. López, who is the lead author, had full access to all of the data in the study and takes responsibility for the integrity of the data and the accuracy of the data analysis.

Study conception and design. Seoane-Collazo, Rial-Pensado, Estévez-Salguero, Nogueiras, Diéguez, Gualillo, López.

Acquisition of data. Seoane-Collazo, Rial-Pensado, Estévez-Salguero, Milbank, García-Caballero, Ríos, Liñares-Pose, Scotece, Gallego, Gualillo, López.

Analysis and interpretation of data. Seoane-Collazo, Rial-Pensado, Estévez-Salguero, Milbank, Ríos, Fernández-Real, Nogueiras, Diéguez, Gualillo, López.

REFERENCES

1. Kerekes G, Nurmohamed MT, Gonzalez-Gay MA, Seres I, Paragh G, Kardos Z, et al. Rheumatoid arthritis and metabolic syndrome [review]. Nat Rev Rheumatol 2014;10:691–6.
2. Abella V, Scotece M, Conde J, Pino J, Gonzalez-Gay MA, Gomez-Reino JJ, et al. Leptin in the interplay of inflammation, metabolism and immune system disorders [review]. Nat Rev Rheumatol 2017;13:100–9.
3. Chen Z, Bozec A, Ramming A, Schett G. Anti-inflammatory and immune-regulatory cytokines in rheumatoid arthritis [review]. Nat Rev Rheumatol 2019;15:9–17.
4. Arshad A, Rashid R, Benjamin K. The effect of disease activity on fat-free mass and resting energy expenditure in patients with rheumatoid arthritis versus noninflammatory arthropathies/soft tissue rheumatism. Mod Rheumatol 2007;17:470–5.
5. Conde J, Scotece M, Lopez V, Gomez R, Lago F, Pino J, et al. Adipokines: novel players in rheumatic diseases [review]. Discov Med 2013; 15:73–83.
6. Procaccini C, Pucino V, Mantzoros CS, Matarese G. Leptin in autoimmune diseases [review]. Metabolism 2015;64:92–104.

7. La Cava A. Leptin in inflammation and autoimmunity [review]. Cytokine 2017;98:51–8.
8. Sattar N, McInnes IB. Rheumatoid arthritis: debunking the obesity-mortality paradox in RA. Nat Rev Rheumatol 2015;11:445–6.
9. George MD, Baker JF. The obesity epidemic and consequences for rheumatoid arthritis care [review]. Curr Rheumatol Rep 2016;18:6.
10. Procaccini C, Carbone F, Galgani M, La Rocca C, De Rosa V, Cassano S, et al. Obesity and susceptibility to autoimmune diseases [review]. Expert Rev Clin Immunol 2011;7:287–94.
11. Thomson TM, Lescarbeau RM, Drubin DA, Laifenfeld D, de Graaf D, Fryburg DA, et al. Blood-based identification of non-responders to anti-TNF therapy in rheumatoid arthritis. BMC Med Genomics 2015; 8:26.
12. Tournadre A, Pereira B, Dutheil F, Giraud C, Courteix D, Sapin V, et al. Changes in body composition and metabolic profile during interleukin 6 inhibition in rheumatoid arthritis. J Cachexia Sarcopenia Muscle 2017;8:639–46.
13. Otero M, Nogueiras R, Lago F, Dieguez C, Gomez-Reino JJ, Gualillo O. Chronic inflammation modulates ghrelin levels in humans and rats. Rheumatology (Oxford) 2004;43:306–10.
14. Cutolo M, Foppiani L, Minuto F. Hypothalamic-pituitary-adrenal axis impairment in the pathogenesis of rheumatoid arthritis and polymyalgia rheumatica. J Endocrinol Invest 2002;25 l:19–23.
15. Stofkova A, Haluzik M, Zelezna B, Kiss A, Skurlova M, Lacinova Z, et al. Enhanced expressions of mRNA for neuropeptide Y and interleukin 1 β in hypothalamic arcuate nuclei during adjuvant arthritis-induced anorexia in Lewis rats. Neuroimmunomodulation 2009;16: 377–84.
16. Skurlova M, Stofkova A, Kiss A, Belacek J, Pecha O, Deykun K, et al. Transient anorexia, hyper-nociception and cognitive impairment in early adjuvant arthritis in rats. Endocr Regul 2010;44:165–73.
17. Chikanza IC, Petrou P, Chrousos G. Perturbations of arginine vasopressin secretion during inflammatory stress: pathophysiologic implications [review]. Ann N Y Acad Sci 2000;917:825–34.
18. Bassi GS, Dias DP, Franchin M, Talbot J, Reis DG, Menezes GB, et al. Modulation of experimental arthritis by vagal sensory and central brain stimulation. Brain Behav Immun 2017;64:330–43.
19. López M, Nogueiras R, Tena-Sempere M, Diéguez C. Hypothalamic AMPK: a canonical regulator of whole-body energy balance [review]. Nat Rev Endocrinol 2016;12:421–32.
20. López M. AMPK wars: the VMH strikes back, return of the PVH. Trends Endocrinol Metab 2018;29:135–7.
21. López M, Varela L, Vázquez MJ, Rodríguez-Cuenca S, González CR, Velagapudi VR, et al. Hypothalamic AMPK and fatty acid metabolism mediate thyroid regulation of energy balance. Nat Med 2010;16: 1001–8.
22. Martins L, Seoane-Collazo P, Contreras C, González-García I, Martínez-Sánchez N, González F, et al. A functional link between AMPK and orexin mediates the effect of BMP8B on energy balance. Cell Rep 2016;16:2231–42.
23. Martínez-Sánchez N, Seoane-Collazo P, Contreras C, Varela L, Villarroya J, Rial-Pensado E, et al. Hypothalamic AMPK-ER stress-JNK1 axis mediates the central actions of thyroid hormones on energy balance. Cell Metab 2017;26:212–29.
24. Seoane-Collazo P, Roa J, Rial-Pensado E, Liñares-Pose L, Beiroa D, Ruíz-Pino F, et al. SF1-Specific AMPKα1 deletion protects against diet-induced obesity. Diabetes 2018;67:2213–26.
25. Villarroya F, Cereijo R, Villarroya J, Gavaldà-Navarro A, Giralt M. Toward an understanding of how immune cells control brown and beige adipobiology [review]. Cell Metab 2018;27:954–61.
26. Shabalina IG, Petrovic N, de Jong JM, Kalinovich AV, Cannon B, Nedergaard J. UCP1 in brite/beige adipose tissue mitochondria is functionally thermogenic. Cell Rep 2013;5:1196–203.
27. López M, Lage R, Saha AK, Pérez-Tilve D, Vázquez MJ, Varela L, et al. Hypothalamic fatty acid metabolism mediates the orexigenic action of ghrelin. Cell Metab 2008;7:389–99.
28. Metsios GS, Stavropoulos-Kalinoglou A, Douglas KM, Koutedakis Y, Nevill AM, Panoulas VF, et al. Blockade of tumour necrosis factor-α in rheumatoid arthritis: effects on components of rheumatoid cachexia. Rheumatology (Oxford) 2007;46:1824–7.
29. Binymin K, Herrick A, Carlson G, Hopkins S. The effect of disease activity on body composition and resting energy expenditure in patients with rheumatoid arthritis. J Inflamm Res 2011;4: 61–6.
30. Brooks SL, Neville AM, Rothwell NJ, Stock MJ, Wilson S. Sympathetic activation of brown-adipose-tissue thermogenesis in cachexia. Biosci Rep 1981;1:509–17.
31. Shellock FG, Riedinger MS, Fishbein MC. Brown adipose tissue in cancer patients: possible cause of cancer-induced cachexia. J Cancer Res Clin Oncol 1986;111:82–5.
32. Bing C, Brown M, King P, Collins P, Tisdale MJ, Williams G. Increased gene expression of brown fat uncoupling protein (UCP)1 and skeletal muscle UCP2 and UCP3 in MAC16-induced cancer cachexia. Cancer Res 2000;60:2405–10.
33. Tsoli M, Moore M, Burg D, Painter A, Taylor R, Lockie SH, et al. Activation of thermogenesis in brown adipose tissue and dysregulated lipid metabolism associated with cancer cachexia in mice. Cancer Res 2012;72:4372–82.
34. Muscaritoli M, Anker SD, Argiles J, Aversa Z, Bauer JM, Biolo G, et al. Consensus definition of sarcopenia, cachexia and pre-cachexia: joint document elaborated by Special Interest Groups (SIG) "cachexia-anorexia in chronic wasting diseases" and "nutrition in geriatrics." Clin Nutr 2010;29:154–9.
35. Petruzzelli M, Schweiger M, Schreiber R, Campos-Olivas R, Tsoli M, Allen J, et al. A switch from white to brown fat increases energy expenditure in cancer-associated cachexia. Cell Metab 2014;20:433–47.
36. McCarthy N. Cachexia: running on empty [review]. Nat Rev Cancer 2014;14:576.
37. Argilés JM, Stemmler B, López-Soriano FJ, Busquets S. Inter-tissue communication in cancer cachexia [review]. Nat Rev Endocrinol 2018;15:9–20.
38. Masuko K. Rheumatoid cachexia revisited: a metabolic co-morbidity in rheumatoid arthritis [review]. Front Nutr 2014;1:20.
39. Santo RC, Fernandes KZ, Lora PS, Filippin LI, Xavier RM. Prevalence of rheumatoid cachexia in rheumatoid arthritis: a systematic review and meta-analysis. J Cachexia Sarcopenia Muscle 2018;9:816–25.
40. Claret M, Smith MA, Batterham RL, Selman C, Choudhury AI, Fryer LG, et al. AMPK is essential for energy homeostasis regulation and glucose sensing by POMC and AgRP neurons. J Clin Invest 2007;117:2325–36.
41. Janig W, Green PG. Acute inflammation in the joint: its control by the sympathetic nervous system and by neuroendocrine systems [review]. Auton Neurosci 2014;182:42–54.
42. Wiberg M, Widenfalk B. Involvement of connections between the brainstem and the sympathetic ganglia in the pathogenesis of rheumatoid arthritis: an anatomical study in rats. Scand J Plast Reconstr Surg Hand Surg 1993;27:269–76.
43. Tanaka H, Ueta Y, Yamashita U, Kannan H, Yamashita H. Biphasic changes in behavioral, endocrine, and sympathetic systems in adjuvant arthritis in Lewis rats. Brain Res Bull 1996;39:33–7.
44. Lorton D, Lubahn C, Lindquist CA, Schaller J, Washington C, Bellinger DL. Changes in the density and distribution of sympathetic nerves in spleens from Lewis rats with adjuvant-induced arthritis suggest that an injury and sprouting response occurs. J Comp Neurol 2005;489:260–73.

45. Lorton D, Lubahn C, Sweeney S, Major A, Lindquist CA, Schaller J, et al. Differences in the injury/sprouting response of splenic noradrenergic nerves in Lewis rats with adjuvant-induced arthritis compared with rats treated with 6-hydroxydopamine. Brain Behav Immun 2009;23:276–85.
46. Cano G, Passerin AM, Schiltz JC, Card JP, Morrison SF, Sved AF. Anatomical substrates for the central control of sympathetic outflow to interscapular adipose tissue during cold exposure. J Comp Neurol 2003;460:303–26.
47. Morrison SF, Madden CJ, Tupone D. Central neural regulation of brown adipose tissue thermogenesis and energy expenditure [review]. Cell Metab 2014;19:741–56.
48. Lin TT, Sung YL, Syu JY, Lin KY, Hsu HJ, Liao MT, et al. Anti-inflammatory and antiarrhythmic effects of beta-blocker in a rat model of rheumatoid arthritis. J Am Heart Assoc 2020;9: e016084.
49. Kang KY, Kim YK, Yi H, Kim J, Jung HR, Kim IJ, et al. Metformin downregulates Th17 cells differentiation and attenuates murine autoimmune arthritis. Int Immunopharmacol 2013;16:85–92.
50. Son HJ, Lee J, Lee SY, Kim EK, Park MJ, Kim KW, et al. Metformin attenuates experimental autoimmune arthritis through reciprocal regulation of Th17/Treg balance and osteoclastogenesis. Mediators Inflamm 2014;2014:973986.

DOI 10.1002/art.41932

Clinical Images: The appearance of scurvy on magnetic resonance imaging

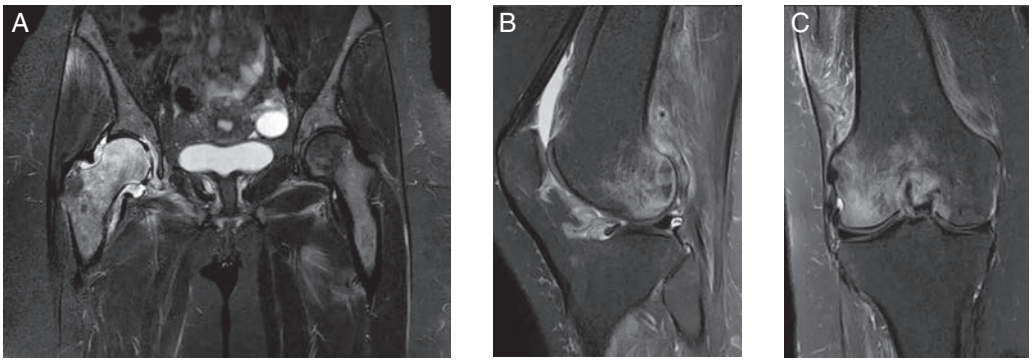

The patient, a 40-year-old woman who had been previously healthy, presented to our rheumatology department with a suspected diagnosis of arthritis based on the presence of bilateral lower limb pain, swollen knee joints, and a 6-month history of difficulty with walking. Physical examination revealed multiple subcutaneous hematomas, gingival hyperplasia, bilateral knee effusion, muscle weakness of the lower extremities, and limited movement of the right hip joint. Laboratory results were remarkable only for iron and folate deficiency with normocytic anemia (hemoglobin 9 mg/dl). A coronal STIR sequence of the hips on magnetic resonance imaging (MRI) revealed bone marrow edema in the right proximal femur (femoral head, femoral neck, intertrochanteric, and subtrochanteric regions), effusion of the right hip joint, edema of the right gluteus and bilateral proximal thigh muscles, and bilateral perifascial edema around the external obturator muscles (**A**). Similar changes were demonstrated on coronal and sagittal T2-weighted fat-saturated MRI of the right knee (**B** and **C**). Vitamin C was not detected in the patient's blood, and a diagnosis of scurvy was made. After treatment with vitamin C and multivitamins, the symptoms of scurvy resolved. Subsequently, it was found that the patient had a selective eating disorder and had restricted her diet to rice and unfortified yogurt. These MRI findings are not specific to scurvy. The appearance of the bone marrow on MRI may represent focal areas of hemorrhage or small infarcts (1). The appearance of the muscle likely represents perivascular edema and hemorrhage into the muscles and soft tissues, and effusion of the hip and knee joints may represent hemarthrosis. These clinical features and MRI findings can also be present in the setting of other, more common conditions, such as osteomyelitis, hematologic diseases, arthritis, inflammatory muscle disease, and other rheumatic and autoimmune diseases (1–3); therefore, such a symptom profile as was seen in our patient should be approached with a high index of clinical suspicion in the diagnosis and management of the disease.

Author disclosures are available at https://onlinelibrary.wiley.com/action/downloadSupplement?doi=10.1002%2Fart.41932&file=art41932-sup-0001-Disclosureform.pdf.

1. Karthiga S, Dubey S, Garber S, Watts R. Scurvy: MRI appearances. Rheumatology (Oxford) 2008;47:1109
2. Choi SW, Park SW, Kwon YS, OH IS, Lim MK, Kim WH, et al. MR imaging in a child with scurvy: a case report. Korean J Radiol 2007;8:443–7.
3. Ferrari C, Possemato N, Pipitone N, Manger B, Salvarani C. Rheumatic manifestations of scurvy [review]. Curr Rheumatol Rep 2015;17:26.

Sami Giryes, MD
Daniela Militianu, MD
Yolanda Braun-Moscovici, MD
Rambam Health Care Campus and Technion-Israel Institute of Technology Haifa, Israel

Arthritis & Rheumatology
Vol. 74, No. 2, February 2022, pp 223–226
DOI 10.1002/art.42031

American College of Rheumatology
Empowering Rheumatology Professionals

BRIEF REPORT

Progression of Knee Osteoarthritis With Use of Intraarticular Glucocorticoids Versus Hyaluronic Acid

Justin Bucci,[1] Xiaoyang Chen,[1] Michael LaValley,[1] Michael Nevitt,[2] James Torner,[3] Cora E. Lewis,[4] and David T. Felson[5]

Objective. To determine whether intraarticular glucocorticoid (GC) injections are associated with increased knee osteoarthritis (OA) progression compared to hyaluronic acid (HA) injections, which have been reported to delay OA progression and knee replacement.

Methods. We identified participants from 2 large cohort studies, the Osteoarthritis Initiative (OAI) and the Multicenter Osteoarthritis Study. Study visits were performed at regular intervals and included questionnaires about intraarticular GC or HA injection use in the previous 6 months and incident total knee replacement (TKR). Knee radiographs were obtained at each study visit and interpreted in a similar manner. Outcome measures were radiographic progression based on Kellgren/Lawrence (K/L) grade and joint space narrowing (JSN) for both cohorts and based on medial joint space width for OAI participants, and incident TKR. We compared preinjection and postinjection radiographs to generate rate ratios of progression comparing GC injection with HA injection. A Cox proportional hazards model was used to estimate the rate of TKR for both groups.

Results. We studied 791 participants (980 knees) with knee OA, of whom 629 reported GC injection use and 162 HA injection use. Rate ratios of progression were similar between those receiving GCs and those receiving HA for JSN (1.00 [95% confidence interval (95% CI) 0.83–1.21]), K/L grade (1.03 [95% CI 0.83–1.29]), and medial joint space width (1.03 [95% CI 0.72–1.48]). Hazard of TKR was slightly lower for those receiving intraarticular GC compared to those receiving HA (hazard ratio 0.75 [95% CI 0.51–1.09]).

Conclusion. Intraarticular GC injections are not associated with an increased risk of knee OA progression compared to HA.

INTRODUCTION

Knee osteoarthritis (OA) affects 1 in 8 Americans over the age of 50 (1) and is associated with reduced quality of life and increased mortality (2). Intraarticular glucocorticoid (GC) injections and hyaluronic acid (HA) injections are popular treatments for this disease.

Recent studies have raised the concern that knees treated with GC injections are at high risk of OA progression. A randomized controlled trial showed a small but statistically significant increase in cartilage loss in knees treated with GC injections (3), and a large cohort study demonstrated a 3-fold increased risk of knee OA progression in patients who received repeated GC injections compared to those who received none (4). A limitation of observational studies is that subjects receiving GC injections are not compared to those receiving comparable treatment. Patients receiving GC injections have more advanced knee OA, itself a risk factor for disease progression (5).

This article was prepared using an Osteoarthritis Initiative (OAI) public-use data set, and its contents do not necessarily reflect the opinions or views of the NIH or the private funding partners of the OAI. The OAI is a public–private partnership between the NIH (contracts N01-AR-2-2258, N01-AR-2-2259, N01-AR-2-2260, N01-AR-2-2261, and N01-AR-2-2262) and private funding partners (Merck Research Laboratories, Novartis Pharmaceuticals, GlaxoSmithKline, and Pfizer, Inc.) and is conducted by the OAI Study Investigators. Private sector funding for the OAI is managed by the Foundation for the NIH.

Supported by the NIH (grants U01-AG-018820, U01-AG-18832, U01-AG-18947, U01-AG-19069, and P30-AR-072571) and the NIHR Manchester Biomedical Research Centre.

[1]Justin Bucci, MD, Xiaoyang Chen, MS, Michael LaValley, PhD: Boston University, Boston, Massachusetts; [2]Michael Nevitt, PhD: University of California at San Francisco; [3]James Torner, PhD: University of Iowa, Iowa City; [4]Cora E. Lewis, MD: University of Alabama at Birmingham; [5]David T. Felson, MD: Boston University, Boston, Massachusetts, University of Manchester and the NIHR Manchester Musculoskeletal Biomedical Research Centre, and Manchester University Hospitals NHS Foundation Trust, Manchester, UK.

Author disclosures are available at https://onlinelibrary.wiley.com/action/downloadSupplement?doi=10.1002%2Fart.42031&file=art42031-sup-0001-Disclosureform.pdf.

Address correspondence to David T. Felson, MD, Suite 200, 650 Albany Street, Boston, MA 02118. Email: dfelson@bu.edu.

Submitted for publication July 8, 2021; accepted in revised form November 18, 2021.

A natural comparator for knees receiving GC injections are those receiving HA injections. Both injections are used in similar patients, and HA injections have not been associated with increased radiographic progression (6) and may even delay knee replacement (7,8). The purpose of this study was to compare radiographic knee OA progression and knee replacement risk in patients receiving GC injections and those receiving HA injections.

PATIENTS AND METHODS

Study population. We utilized 2 observational prospective cohort studies that collected data on treatments and outcomes in persons with or at risk of knee OA. In the Osteoarthritis Initiative (OAI) (for details, see https://nda.nih.gov/oai/), study visits took place every 12 months; we used data from baseline through the 8th annual visit. In the Multicenter Osteoarthritis Study (MOST) (for details, see https://most.ucsf.edu/), study visits take place approximately every 30 months, and we used data from baseline through the year-8 visit.

Assessment of GC injection and HA injection use. At baseline and each follow-up visit in both the MOST and the OAI, participants were asked whether they had received GC injections or HA injections in their knees in the preceding 6 months and, if yes, which knee had received injections.

Assessment of radiographic progression and total knee replacement (TKR). In both studies, knee radiographs were obtained at baseline and follow-up visits using similar acquisition and reading protocols. The same readers read radiographs from both studies. Kellgren/Lawrence (K/L) grades for the knee (on a scale of 0–4) (9) and joint space narrowing (JSN) scores (on a scale of 0–3) were determined separately in the medial and lateral tibiofemoral compartments (10). We used partial grades when JSN progression did not reach a full grade of narrowing (e.g., 1 to 1.5) and considered any increase in JSN score in either the medial or lateral joint as progression (11). Disagreements were resolved by a 3-reader adjudication panel. In the OAI, per recommendations (12), the joint space width at site 250 (referring to the distance along the frontal plane from the edge of the knee) (JSW250) in the medial joint was used for analysis of progression, which provided a continuous quantitative measure for progression assessment.

The presence of TKR was evaluated by history and radiographs at each visit for both studies. Incident TKR was reported by participants at the time of occurrence and confirmed on radiographs.

Statistical analysis. For radiographic progression, we excluded knees with a baseline K/L grade of 4 and those with GC injections or HA injections reported at the baseline visit, since we could not evaluate progression from before to after treatment. Knees from participants reporting GC injections and HA injections at the same examination were also excluded. We compared radiographs from the visit before the first reported injection to radiographs from the visit after the last reported injection (see Figure 1 for an example of the analysis for a participant reporting an injection at a single examination; note that all radiographic follow-up took place ≥1 year after injection). If multiple injections were reported at nonconsecutive examinations, we analyzed only the first postinjection visit. For participants reporting one treatment at one examination and the other treatment later, we examined progression from the first treatment, censoring them when they reported the second. If a knee had undergone a TKR, we assigned it a K/L grade of 4 and JSN score of 3 at the first visit after TKR and, because radiographs showing knee replacement do not permit assessment of joint space loss, JSW250 was not calculated. Because participants with prior injections may be closer to needing TKRs, we also carried out a secondary analysis that was limited to knees for which participants had not reported prior injections of the comparator drug.

Negative binomial regression was used to estimate progression rates based on the number of examinations with progression, with an offset to account for the duration of time under observation. In the OAI, where joint space was quantitatively assessed at each examination, we calculated an annualized rate of change in JSW250. We also carried out a sensitivity analysis excluding knees with lateral JSN at the preinjection examination. Because some participants had both knees injected, we used generalized estimating equations to adjust for the correlation between knees.

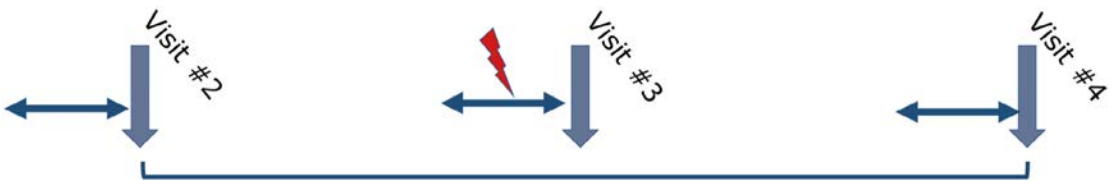

Figure 1. Example analysis for a participant with knee osteoarthritis reporting a single injection (red) of either glucocorticoids or hyaluronic acid into the knee on the visit 3 questionnaire. Questionnaires were administered (horizontal arrows) and radiographs were obtained (vertical arrows) at each study visit. Radiographic progression from the examination before the reported injection (visit 2) to the examination after the reported injection (visit 4) was evaluated.

Table 1. Preinjection clinical and radiographic characteristics of the participants with knee OA*

	Single GC injection	Single HA injection	Consecutive GC injections	Consecutive HA injections
MOST and OAI				
No. of participants	553	142	76	20
Age, mean ± SD years	66.3 ± 9.0	64.8 ± 8.3	66.2 ± 9.1	62.6 ± 7.3
Sex, % female	69	55	58	65
BMI, mean ± SD	30.6 ± 5.3	31.4 ± 6.2	29.2 ± 4.6	31.8 ± 7.4
No. of knees	651	178	122	29
WOMAC pain score, mean ± SD	4.3 ± 3.3	5.0 ± 3.8	4.7 ± 3.7	5.5 ± 2.6
JSN score, mean ± SD (scale 0–3)	1.0 ± 0.9	1.3 ± 0.9	1.0 ± 0.88	1.3 ± 1.0
K/L grade, mean ± SD (scale 0–4)	1.9 ± 1.1	2.1 ± 1.1	1.9 ± 1.03	2.0 ± 1.1
OAI only				
No. of knees	476	111	110	18
JSW250, mean ± SD mm	5.2 ± 1.8	4.7 ± 1.6	5.2 ± 1.9	5.3 ± 2.1

* OA = osteoarthritis; GC = glucocorticoid; HA = hyaluronic acid; MOST = Multicenter Osteoarthritis Study; OAI = Osteoarthritis Initiative; BMI = body mass index; WOMAC = Western Ontario and McMaster Universities Osteoarthritis Index; JSN = joint space narrowing; K/L = Kellgren/Lawrence; JSW250 = joint space width at site 250.

For incident TKR analysis, we included all knees from the progression analysis in addition to knees of participants reporting treatment with GC injection or HA injection at the baseline visit and knees with a baseline K/L grade of ≤4. Starting with the preinjection visit, we carried out Cox proportional hazards modeling with injections as time-dependent covariates. For knees with repeated consecutive injections, we increased the covariate value from 1 to 2 to examine whether repeated injections increase risk. We censored events occurring after 7 years from baseline. All regression analyses were adjusted for age, sex, body mass index (BMI), study of origin, and baseline knee K/L grade, using SAS version 9.4.

RESULTS

For radiographic progression, we assessed 980 knees in 791 participants (65.61% female; mean age 66.2 years) with a mean BMI of 30.7 kg/m^2 and mean baseline K/L grade of 1.91 (Table 1). Of these 980 knees, 773 were treated with GC injections and 207 with HA injections. Rates of radiographic progression were similar for knees treated with GC injections and those treated with HA injections (Table 2). For GC injections compared to HA injections, the rate ratio was 1.00 for JSN (95% confidence interval [95% CI] 0.83–1.21), 1.03 for K/L grade progression (95% CI 0.83–1.29), and 1.03 for JSW250 progression (95% CI 0.72–1.48).

Table 2. Risk of radiographic progression of OA in knees treated with GC injections versus knees treated with HA injections*

	Rate ratio (95% CI)†
Joint space narrowing	1.00 (0.83–1.21)
Kellgren/Lawrence grade	1.03 (0.83–1.29)
Medial joint space width‡	1.03 (0.72–1.48)

* 95% CI = 95% confidence interval.
† Difference in rates of osteoarthritis (OA) progression in knees treated with glucocorticoid (GC) injections versus knees treated with hyaluronic acid (HA) injections. A value >1 indicates higher progression with GC injections. Analyses were adjusted for age, sex, body mass index, study of origin (Osteoarthritis Initiative or Multicenter Osteoarthritis Study), and baseline Kellgren/Lawrence grade.
‡ Medial joint space width (determined by measuring the joint space width 250) was calculated using only Osteoarthritis Initiative data. Progression was defined as a difference of >0.5 mm.

For incident TKR, we assessed 1,513 knees in a group of participants who were 63% female and had a mean age of 63.1 years and mean BMI of 30.8 kg/m^2. Of these 1,513 knees, 1,235 were treated with GC injections and 278 with HA injections. Knees treated with GC injections showed a slightly lower risk of later TKR than knees treated with HA injections (hazard ratio 0.75 [95% CI 0.51–1.09]). In a secondary analysis of knees in which prior injections of the comparator drug were not reported (775 knees treated with GC injections and 244 knees treated with HA injections), we found that the risk of TKR for those receiving GC injections was 0.74 (95% CI 0.37–1.47).

DISCUSSION

Our findings suggest similar rates of disease progression and TKR in those receiving GC injections and those receiving HA injections. HA injection has been proposed as a treatment that may delay time to TKR. Delbarre et al found that knees treated with HA injections had a prolonged TKR-free survival time compared to knees that received no HA injections (7). While this finding has not been demonstrated consistently (8), no studies have suggested that HA injection accelerates disease progression. While we found that knees receiving GC injections had a slightly lower rate of subsequent TKR than those treated with HA, this difference was modest, not statistically significant, and of uncertain meaning.

Using data from the OAI, Zeng et al reported that those receiving GC injections had a greater risk of radiographic progression and TKR than untreated participants (4). Patients often receive GC injections in an attempt to delay surgery. Our findings suggest there may be fundamental differences between patients who receive injections and those who do not, which are not eliminated by statistical adjustments.

While current insurance coverage for HA injections requires that OA has previously failed to respond to GC injections, that was not true when our study was being conducted. For Medicare, insurance coverage policy changed in October 2015, and the baseline examinations in our study took place in 2004 and 2005.

Our study has some limitations. In both cohorts, participants only reported injections received 6 months prior to the study visit, and earlier injections were not recorded. Participants may also not have correctly recalled the type of injection received.

In conclusion, in 2 large prospective cohorts, the rate of disease progression among knees receiving GC injections was not different from the rate of progression among those receiving HA injections. Our data should provide reassurance to clinicians and patients. The risk of OA progression attributed to GC injections in earlier studies may reflect more advanced disease in those receiving GC injections.

AUTHOR CONTRIBUTIONS

All authors were involved in drafting the article or revising it critically for important intellectual content, and all authors approved the final version to be published. Dr. Felson had full access to all of the data in the study and takes responsibility for the integrity of the data and the accuracy of the data analysis.

Study conception and design. Bucci, Felson.
Acquisition of data. Nevitt, Torner, Lewis.
Analysis and interpretation of data. Chen, LaValley.

REFERENCES

1. Wallace IJ, Worthington S, Felson DT, Jurmain RD, Wren KT, Maijanen H, et al. Knee osteoarthritis has doubled in prevalence since the mid-20th century. Proc Natl Acad Sci USA 2017;114:9332–6.
2. Wang Y, Nguyen UD, Lane NE, Lu N, Wei J, Lei G, et al. Knee osteoarthritis, potential mediators, and risk of all-cause mortality: data from the Osteoarthritis Initiative. Arthritis Care Res (Hoboken) 2021;73:566–73.
3. McAlindon TE, LaValley MP, Harvey WF, Price LL, Driban JB, Zhang M, et al. Effect of intra-articular triamcinolone vs saline on knee cartilage volume and pain in patients with knee osteoarthritis: a randomized clinical trial. JAMA 2017;317:1967–75.
4. Zeng C, Lane NE, Hunter DJ, Wei J, Choi HK, McAlindon TE, et al. Intra-articular corticosteroids and the risk of knee osteoarthritis progression: results from the Osteoarthritis Initiative. Osteoarthritis Cartilage 2019;27:855–62.
5. Bastick AN, Runhaar J, Belo JN, Bierma-Zeinstra SM. Prognostic factors for progression of clinical osteoarthritis of the knee: a systematic review of observational studies. Arthritis Res Ther 2015;17:152.
6. Jubb RW, Piva S, Beinat L, Dacre J, Gishen P. A one-year, randomised, placebo (saline) controlled clinical trial of 500-730 kDa sodium hyaluronate (Hyalgan) on the radiological change in osteoarthritis of the knee. Int J Clin Pract 2003;57:467–74.
7. Delbarre A, Amor B, Bardoulat I, Tetafort A, Pelletier-Fleury N. Do intra-articular hyaluronic acid injections delay total knee replacement in patients with osteoarthritis - a Cox model analysis. PLoS One 2017;12:e0187227.
8. Shewale AR, Barnes CL, Fischbach LA, Ounpraseuth ST, Painter JT, Martin BC. Comparative effectiveness of intra-articular hyaluronic acid and corticosteroid injections on the time to surgical knee procedures. J Arthroplasty 2017;32:3591–7.
9. Kellgren JH, Lawrence JS. Radiological assessment of osteo-arthrosis. Ann Rheum Dis 1957;16:494–502.
10. Altman RD, Gold GE. Atlas of individual radiographic features in osteoarthritis, revised. Osteoarthritis Cartilage 2007;15 Suppl:A1–56.
11. Cranney A, Tugwell P, Cummings S, Sambrook P, Adachi J, Silman AJ, et al. Osteoporosis clinical trials endpoints: candidate variables and clinimetric properties. J Rheumatol 1997;24:1222–9.
12. Neumann G, Hunter D, Nevitt M, Chibnik LB, Kwoh K, Chen H, et al. Location specific radiographic joint space width for osteoarthritis progression. Osteoarthritis Cartilage 2009;17:761–5.

Arthritis & Rheumatology
Vol. 74, No. 2, February 2022, pp 227–236
DOI 10.1002/art.41955

American College of Rheumatology
Empowering Rheumatology Professionals

Association of Increased Serum Lipopolysaccharide, But Not Microbial Dysbiosis, With Obesity-Related Osteoarthritis

Richard F. Loeser,[1] Liubov Arbeeva,[1] Kathryn Kelley,[1] Anthony A. Fodor,[2] Shan Sun,[2] Veronica Ulici,[1] Lara Longobardi,[1] Yang Cui,[1] Delisha A. Stewart,[3] Susan J. Sumner,[3] M. Andrea Azcarate-Peril,[1] R. Balfour Sartor,[1] Ian M. Carroll,[3] Jordan B. Renner,[1] Joanne M. Jordan,[1] and Amanda E. Nelson[1]

Objective. To test the hypothesis that an altered gut microbiota (dysbiosis) plays a role in obesity-associated osteoarthritis (OA).

Methods. Stool and blood samples were collected from 92 participants with a body mass index (BMI) ≥30 kg/m^2, recruited from the Johnston County Osteoarthritis Project. OA patients (n = 50) had hand and knee OA (Kellgren/Lawrence [K/L] grade ≥2 or arthroplasty). Controls (n = 42) had no hand OA and a K/L grade of 0–1 for the knees. Compositional analysis of stool samples was carried out by 16S ribosomal RNA amplicon sequencing. Alpha- and beta-diversity and differences in taxa relative abundances were determined. Blood samples were used for multiplex cytokine analysis and measures of lipopolysaccharide (LPS) and LPS binding protein. Germ-free mice were gavaged with patient- or control-pooled fecal samples and fed a 40% fat, high-sucrose diet for 40 weeks. Knee OA was evaluated histologically.

Results. On average, OA patients were slightly older than the controls, consisted of more women, and had a higher mean BMI, higher mean Western Ontario and McMaster Universities Osteoarthritis Index pain score, and higher mean K/L grade. There were no significant differences in α- or β-diversity or genus level composition between patients and controls. Patients had higher plasma levels of osteopontin ($P = 0.01$) and serum LPS ($P < 0.0001$) compared to controls. Mice transplanted with patient or control microbiota exhibited a significant difference in α-diversity ($P = 0.02$) and β-diversity, but no differences in OA severity were observed.

Conclusion. The lack of differences in the gut microbiota, but increased serum LPS levels, suggest the possibility that increased intestinal permeability allowing for greater absorption of LPS, rather than a dysbiotic microbiota, may contribute to the development of OA associated with obesity.

INTRODUCTION

Major risk factors for osteoarthritis (OA) include age, obesity, genetics, and prior joint injury (1). Obesity is a risk factor not only for knee and hip OA, but also hand OA, suggesting that factors associated with obesity, in addition to increased joint loads, have a role in OA, including altered metabolism and low-grade systemic inflammation (2,3). A number of studies have shown that the composition of the gut microbiota plays a central role in mediating the effects of what we eat on the development of obesity and obesity-related conditions (4–7). Very few studies to date have examined the role of the gut microbiota in human OA, and none have focused on OA associated with obesity.

Supported by the Arthritis Foundation, the National Center for Advancing Translational Sciences, NIH (grant UL1-TR-002489), and the National Institute of Arthritis and Musculoskeletal and Skin Diseases, NIH (grant P30-AR-072580). The Johnston County Osteoarthritis Project is supported by the Centers for Disease Control and Prevention (grant U01-DP-006266). The UNC Microbiome and Gnotobiotic Cores are supported by the National Institute of Diabetes and Digestive and Kidney Diseases, NIH (grants P30-DK-034987 and P30-DK-056350) and the Office of the Director, NIH (grant P40-OD-010995). The cytokine analysis was supported by the Nutrition Obesity Resource Core of the National Institute of Diabetes and Digestive and Kidney Diseases, NIH (grant P30-DK-056350).

[1]Richard F. Loeser, MD, Liubov Arbeeva, MS, Kathryn L. Kelley, BS, Veronica Ulici, MD, PhD, Lara Longobardi, PhD, Yang Cui, PhD, M. Andrea Azcarate-Peril, PhD, R. Balfour Sartor, MD, Jordan B. Renner, MD, Joanne M. Jordan MD, MPH, Amanda E. Nelson, MD, MSCR: University of North Carolina School of Medicine, Chapel Hill; [2]Anthony A. Fodor, PhD, Shan Sun, PhD: University of North Carolina, Charlotte; [3]Delisha A. Stewart, PhD, Susan Summer, PhD, Ian M Carroll, PhD: University of North Carolina, Chapel Hill.

Author disclosures are available at https://onlinelibrary.wiley.com/action/downloadSupplement?doi=10.1002%2Fart.41955&file=art41955-sup-0001-Disclosureform.pdf.

Address correspondence to Richard F. Loeser, MD, Division of Rheumatology, Allergy and Immunology and the Thurston Arthritis Research Center, 3300 Thurston Building, Campus Box 7280, University of North Carolina School of Medicine, Chapel Hill, NC 27599. Email: richard_loeser@med.unc.edu.

Submitted for publication December 22, 2020; accepted in revised form August 19, 2021.

Two forms of arthritis that are mechanistically distinct from each other in etiology, ankylosing spondylitis (8) and rheumatoid arthritis (RA) (9), have been linked to altered composition of the gut microbiota. Theoretically, development of OA could also be promoted by gut microbial factors, not only because of the strong links of OA to diet and obesity, but also due to findings in older adults (the group at highest risk of OA) which show that the composition of the gut microbiota and the presence of dysbiosis correlate with measures of physical function, systemic markers of inflammation, and the number of comorbidities (10). Intestinal dysbiosis is a state of microbial imbalance that results from "a change in the structural and/or functional configuration of the microbiota that disrupts homeostasis between the host and the microbial community" (11). Dysbiosis can result in altered metabolism, obesity, malnutrition, and increased intestinal permeability resulting in increased systemic levels of lipopolysaccharide (LPS) and other inflammatory microbial products (4–7,11).

A potential connection between obesity-associated OA and the microbiome was suggested by a metabolomics analysis performed using urine samples from overweight and obese adults with knee OA who were participants in the Intensive Diet and Exercise for Arthritis trial. Participants who exhibited radiographic progression of their knee OA over the course of the 18-month trial had increased levels of several metabolites that included hippurate (12). Hippurate is a mammalian–microbial "co-metabolite" well known to be affected by the composition of the gut microbiota (5), suggesting that the gut microbiota could be influencing OA progression in overweight and obese adults.

The purpose of the present study was to determine whether an altered gut microbiota plays a causal role in obesity-associated OA, by analyzing the microbial composition of fecal samples from OA patients and controls as well as plasma levels of cytokines and serum levels of the microbial product LPS, also known as endotoxin. To enrich the study population with individuals more likely to have obesity-associated OA and its associated systemic metabolic changes, we recruited participants who were obese (body mass index [BMI] ≥30 kg/m^2) and exhibited both hand and knee OA. In order to test for causality and microbial functional changes not detected by DNA sequence analysis, we measured knee OA severity after transplanting pooled human fecal microbiota from OA patients and controls to germ-free mice and then inducing obesity-associated OA by placing the mice on a high-fat and high-sucrose ("Western") diet for 40 weeks.

PATIENTS AND METHODS

Study participants. Blood and fecal samples were collected from selected patients and controls recruited from the Johnston County Osteoarthritis (JoCo OA) Project, which is a longitudinal, population-based, prospective study designed to investigate prevalence, incidence, and progression of OA and its risk factors. A detailed description of the study can be found elsewhere (13). Briefly, at the baseline visit (referred to as time 0 [T0]; 1991–1997), 3,187 adults were enrolled into the original cohort. Participants completed 4 follow-up visits ~5 years apart (T1–T4). An enrichment cohort (T1*) entered the study in 2003–2004, and therefore, T1* enrollees have a shorter follow-up period (only T2–T4). For the present microbiome study, participants were recruited at the time of the most recent follow-up evaluation (T4; 2016–2018).

Ninety-two individuals were enrolled (50 patients and 42 controls) who fulfilled the following conditions: 1) agreed to participate through T4 and to be contacted about future studies, 2) met eligibility criteria and consented to participate in this substudy (University of North Carolina [UNC] Institutional Review Board no. 15-1834), and 3) provided stool samples and completed a diet questionnaire in addition to the standard JoCo OA Project measures. To be eligible for recruitment as an OA patient, the participant needed to be obese (BMI ≥30 kg/m^2) and have clinical and/or radiographic hand OA defined as involvement of ≥3 joints across both hands (14), as well as Kellgren/Lawrence (K/L) (15) grade 2–4 knee OA or knee arthroplasty for OA. Controls were also obese but did not have evidence of hand OA and had a K/L grade of 0–1 for knees based on a reading by one of the study investigators (RFL) of the radiographs obtained at the time of recruitment during the T4 visit. Radiographs were reread by the study radiologist (JBR) and were paired with prior knee radiographs after all participants had been enrolled in the study. Participants were older than 45 years of age, and there was an attempt to recruit controls to the study who were age- and sex-matched to the patients. Exclusion criteria included the following: recent (in the past 6 weeks) antibiotic and/or probiotic use, bowel surgery, a history of inflammatory bowel disease and/or celiac disease, or a history of fecal microbiota transplantation (all self-reported). All individuals who met eligibility criteria provided consent and had a stool sample collection kit (EasySampler; Alpco Diagnostics) delivered to their home along with instructions on how to collect and store the samples.

Sample collection. Details of the fecal and blood sample collection are provided in the Supplementary Methods (available on the *Arthritis & Rheumatology* website at https://onlinelibrary.wiley.com/doi/10.1002/art.41955).

Demographic and clinical measurements. Data collected on participants as part of the JoCo OA Project T4 follow-up and used in the present study included demographic information and evaluation of knee pain using the Knee Injury and Osteoarthritis Outcome Score subscale for pain for the left and right knees separately, as previously described (16). The Australian Canadian Osteoarthritis Hand Index (AUSCAN) (17) subscales were used to assess hand symptoms. For the present study, we also added a validated dietary questionnaire to evaluate the fat content of the diet at the time of stool collection (18).

Nonsteroidal antiinflammatory drug (NSAID) use and nutraceutical use (e.g., glucosamine, chondroitin sulfate) were also recorded.

Fecal microbiome analysis. Isolation of total DNA from stool samples and analysis by Illumina MiSeq 16S ribosomal RNA (rRNA) amplicon sequencing was performed in the UNC Microbiome Core, as previously described (19,20). Details are provided in the Supplementary Methods.

Cytokine and LPS measures. Cytokine analysis was performed using G5 series arrays to profile 80 markers in the plasma samples (n = 73) according to the instructions of the manufacturer (RayBiotech Life). Details are provided in the Supplementary Methods, and results for all cytokines are shown in Supplementary Table 1 (https://onlinelibrary.wiley.com/doi/10.1002/art.41955). Serum samples (n = 78) were used to measure LPS using an EndoZyme Recombinant Factor C Endotoxin Detection Assay (no. 890030; Hyglos) and LPS binding protein (LBP) using an enzyme-linked immunosorbent assay kit for human LBP (Hycult Biotech), as previously described (21).

Fecal transplant to germ-free mice and subsequent diet. The use of mice for this study was approved by the UNC Animal Care and Use Committee (no. 16-294). Fecal samples from 5 OA patients and 5 controls (Supplementary Table 2, https://onlinelibrary.wiley.com/doi/10.1002/art.41955) were randomly selected to be used for fecal transplant to germ-free mice. Pooled fecal samples from each group of 5 were used to reduce heterogeneity within groups. Thirty-one 10–13-week-old male germ-free C57BL/6 mice were obtained from the UNC National Gnotobiotic Rodent Resource Center. Mice were randomly assigned to be gavaged with fecal pools from either patients (n = 16 mice) or controls (n = 15 mice). The number of mice per group was based on prior studies using the same mouse strain for histologic OA studies in which articular cartilage structure (ACS) score was the primary outcome measure. Previous studies have shown that 15 animals per group is sufficient to provide ≥90% power when $\alpha = 0.05$ to detect a biologically meaningful difference of 50% between 2 groups (22,23). Details of the fecal transplantation are provided in the Supplementary Methods, https://onlinelibrary.wiley.com/doi/10.1002/art.41955/abstract. For the first 2 weeks after fecal transplant, recipient mice were fed standard chow ad libitum, to allow sufficient time for complete colonization ("humanization"). Next, all mice were switched to sterilized Western diet chow (no. D12079B; Research Diets), which is a 40% fat and high-sucrose diet, and were maintained on the diet until the end of the study (40 weeks on diet).

The fecal gavage was repeated every 4 weeks to help maintain the humanized microbiome. Mice were weighed every other week. Stool pellets were collected from individual mice 2 weeks after each gavage and stored at −80°C until the end of the mouse study period when they were submitted to the UNC Microbiome Core facility for analysis, along with samples from the original OA patient and control pools that had been used for transplant. Microbiome analysis was performed as described above. After mice were fed this diet for 40 weeks, body composition was measured by magnetic resonance imaging in the UNC Nutrition Obesity Research Center Animal Metabolism Phenotyping Core, and mice were then euthanized.

Histologic evaluation. Mouse stifle (knee) joints were collected, fixed, and processed for histology as previously described (22,24). Details of the grading are presented in the Supplementary Methods.

Statistical analysis. *Primary analysis using 16S rRNA amplicon sequencing data.* We used QIIME version 1.9.0 to generate measures of microbial diversity (25). Alpha (within-sample)–diversity measures, including the Shannon diversity index (26), Chao1 (27), phylogenetic diversity (whole tree), and observed species number metrics, were estimated at a rarefaction depth of 1,000 sequences per sample. Associations of α-diversity (Shannon Index) with OA status, sex, age, and BMI were examined by univariate and multivariable linear regression models. Beta (between-sample)–diversity estimates were calculated using weighted and unweighted UniFrac distances between samples at a subsampling depth of 1,000 (28,29). Principal coordinate analysis (PCoA) was used to summarize these results. Permutation multivariate analysis of variance (PERMANOVA) was used to test the null hypothesis that patient and control microbial communities share the same distribution. The associations with OA status were examined for all participants and stratified by sex.

Further, comparisons between the 2 groups were performed individually for each taxon, as follows. Taxa were summarized based at their taxonomic levels with QIIME's summarize_taxa.py, and the analysis was focused on genera. The operational taxonomic unit (OTU) table for genus level was normalized and transformed to the table format with taxa as columns and individuals as rows using Python. We applied an arbitrary threshold and removed taxa that were absent in >75% of samples. To identify the individual OTU identifiers that were significantly different between the patient and control groups and between women and men, we applied the nonparametric Wilcoxon test following Benjamini and Hochberg adjustment for *P* values in multiple comparisons (30), with a significance level of 0.05 implemented in *r. adjust* R function. The effect size was calculated as the Z statistic divided by the square root of the sample size as previously described (31). The interpretation of effect size coincides with the one for Pearson's correlation coefficient.

To ensure that the results were not a consequence of the QIIME algorithm, we repeated these steps using the "vegan" R package. The "adonis" function in the vegan package was used to test differences of the Bray–Curtis dissimilarity between obese OA patients and obese non-OA participants. Multidimensional scaling ordination was performed using the "capscale" function with Bray–Curtis dissimilarity.

Pain and microbial community composition. We performed exploratory analysis (as detailed in the Supplementary Methods, https://onlinelibrary.wiley.com/doi/10.1002/art.41955/abstract) to evaluate whether the gut microbiota were associated with knee and/or hand pain. In addition, we attempted to replicate findings from a recent study that showed an association between the composition of the gut microbiota and Western Ontario and McMaster Universities Arthritis Index (WOMAC) (32) knee pain score in the Rotterdam study (33). In that study, the abundance of the *Streptococcus* genus (in the order *Lactobacillales* and class *Bacilli*) was found to be significant. We considered these taxa to replicate if they reached a nominal significance of $P = 0.05$ in our data.

Methods for analysis of LPS/LBP results, cytokine levels, and the mouse data are provided in the Supplementary Methods.

RESULTS

Demographic and clinical characteristics of the study participants. A total of 92 individuals were recruited for this project (50 obese patients with both hand and knee OA, and 42 obese controls). The patient group was slightly older, included more women, and had a higher mean BMI compared to the controls (Table 1). As expected, the patients had higher WOMAC knee pain scores and AUSCAN hand pain scores. There were no differences between groups in the proportion of African Americans, dietary fat intake, glucosamine use, or NSAID use. The patient group had a predominance of severe knee OA, with 70% of the participants having a K/L grade of 4 in the knee (42%) or prior knee arthroplasty (28%). In the majority of controls, the K/L grade in the knees was grade 1 (76%), but 9 individuals (21%) showed K/L grade 2 when the radiographs were graded by the study radiologist. These had all been read as K/L grade 1 at the time of screening for recruitment.

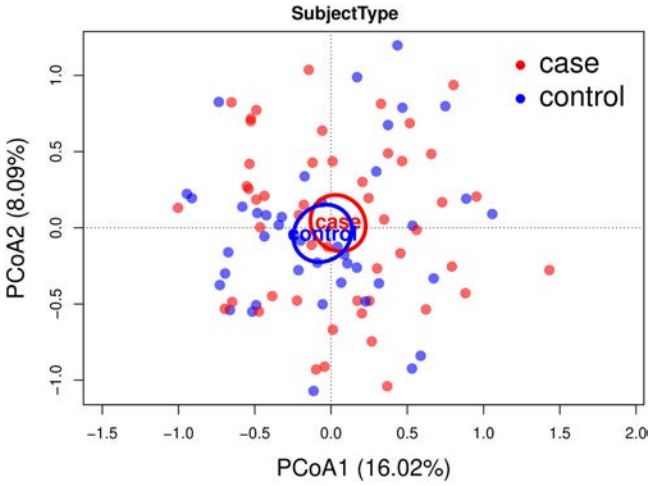

Figure 1. Microbial similarity biplot for study participants with knee and hand osteoarthritis (OA) (red) and those without OA (blue). Principal coordinate analysis (PCoA) is shown. Numbers in parentheses indicate the percent variation explained by the corresponding axis. Each symbol represents an individual sample. The distance between 2 points shows how compositionally different the samples are. Ellipsoids illustrate the 95% confidence interval for the mean location of each group.

Microbiome analysis. In univariate analyses, α-diversity was inversely associated with BMI and was not associated with OA status, sex, or age. In a multivariable linear regression model, none of these variables were significantly associated with the Shannon diversity index (Supplementary Table 3, https://onlinelibrary.wiley.com/doi/10.1002/art.41955). There was also no difference in β-diversity ($P = 0.73$ by PERMANOVA), and a

Table 1. Demographic and clinical characteristics of the osteoarthritis patients and controls*

Characteristic	Patients (n = 50)	Controls (n = 42)	*P*
Age, mean ± SD years	73.7 ± 6.9	70.8 ± 6.4	0.04
Female	43 (86)	26 (62)	0.01
African American	17 (34)	18 (43)	0.39
BMI, mean ± SD kg/m^2	36.3 ± 4.4	33.4 ± 3.1	0.001
WOMAC left knee pain score (range 0–20), mean ± SD	5.2 ± 5.1	2.2 ± 3.7	0.002
WOMAC right knee pain score (range 0–20), mean ± SD	5.3 ± 4.9	1.8 ± 3.3	0.0001
AUSCAN hand pain score, mean ± SD	5.3 ± 6.1	2.4 ± 3.9	0.01
Percent calories from fat, mean ± SD	33.1 ± 2.6	34.2 ± 4.7	0.20
Glucosamine use	2 (4)	2 (5)†	0.53
NSAID use	33 (66)	27 (66)	0.99
Maximum K/L grade			
0	0	1 (2.4)	–
1	0	32 (76.2)	–
2	2 (4.0)	9 (21.4)	–
3	13 (26.0)	0	–
4	21 (42.0)	0	–
Total knee replacement	14 (28.0)	0	–

* Except where indicated otherwise, values are the number (%) of subjects. BMI = body mass index; WOMAC = Western Ontario and McMaster Universities Arthritis Index; AUSCAN = Australian Canadian Osteoarthritis Hand Index; NSAID = nonsteroidal antiinflammatory drug; K/L = Kellgren/ Lawrence.
† Missing data on glucosamine use (n = 1).

Table 2. Relative abundance of genera in Johnston County Osteoarthritis Project participants with knee and hand OA (patients) and those without (controls)

QIIME taxon name	Relative abundance, mean ± SD			Effect size (*P**)	Q†
	All participants	Patients	Controls		
k__Bacteria.p__Cyanobacteria.c__4C0d.2.o__YS2.f__.g__	$2.64 \times 10^{-3} \pm 1.24 \times 10^{-2}$	$5.17 \times 10^{-4} \pm 1.96 \times 10^{-3}$	$5.17 \times 10^{-3} \pm 1.80 \times 10^{-2}$	0.33 (0.001)	0.13
k__Bacteria.p__Firmicutes.c__Clostridia.o__Clostridiales. f__Christensenellaceae.g__Christensenella	$3.00 \times 10^{-5} \pm 6.21 \times 10^{-5}$	$1.71 \times 10^{-5} \pm 4.83 \times 10^{-5}$	$4.53 \times 10^{-5} \pm 7.30 \times 10^{-5}$	0.26 (0.01)	0.56
k__Bacteria.p__Lentisphaerae.c__.Lentisphaeria.o__Victivallales. f__Victivallaceae.g__	$9.57 \times 10^{-4} \pm 4.86 \times 10^{-3}$	$4.84 \times 10^{-4} \pm 1.70 \times 10^{-3}$	$1.52 \times 10^{-3} \pm 6.96 \times 10^{-3}$	0.23 (0.03)	0.68
k__Bacteria.p__Firmicutes.c__Clostridia.o__Clostridiales. f__Eubacteriaceae.g__Anaerofustis	$3.01 \times 10^{-5} \pm 6.74 \times 10^{-5}$	$2.52 \times 10^{-5} \pm 5.85 \times 10^{-5}$	$3.58 \times 10^{-5} \pm 7.70 \times 10^{-5}$	0.20 (0.06)	0.68
k__Bacteria.p__Synergistetes.c__Synergistia.o__Synergistales. f__Dethiosulfovibrionaceae.g__Pyramidobacter	$1.24 \times 10^{-3} \pm 8.19 \times 10^{-3}$	$1.43 \times 10^{-3} \pm 9.99 \times 10^{-3}$	$1.02 \times 10^{-3} \pm 5.42 \times 10^{-3}$	0.20 (0.06)	0.68
k__Bacteria.p__Proteobacteria.c__Gammaproteobacteria. o__Enterobacteriales.f__Enterobacteriaceae.Other	$1.12 \times 10^{-4} \pm 2.74 \times 10^{-4}$	$6.81 \times 10^{-5} \pm 1.48 \times 10^{-4}$	$1.64 \times 10^{-4} \pm 3.68 \times 10^{-4}$	0.19 (0.07)	0.68
k__Bacteria.p__Firmicutes.c__Clostridia.o__Clostridiales. f__Peptococcaceae.g__rc4.4	$1.74 \times 10^{-4} \pm 6.22 \times 10^{-4}$	$5.04 \times 10^{-5} \pm 1.34 \times 10^{-4}$	$3.20 \times 10^{-4} \pm 8.92 \times 10^{-4}$	0.19 (0.07)	0.68
k__Bacteria.p__Proteobacteria.c__Gammaproteobacteria. o__Pasteurellales.f__Pasteurellaceae.g__Haemophilus	$1.08 \times 10^{-3} \pm 3.98 \times 10^{-3}$	$1.28 \times 10^{-3} \pm 4.93 \times 10^{-3}$	$8.50 \times 10^{-4} \pm 2.44 \times 10^{-3}$	0.19 (0.07)	0.68
k__Bacteria.p__Firmicutes.c__Clostridia.o__Clostridiales. f__Lachnospiraceae.g__Roseburia	$1.30 \times 10^{-3} \pm 1.51 \times 10^{-3}$	$1.09 \times 10^{-3} \pm 1.39 \times 10^{-3}$	$1.54 \times 10^{-3} \pm 1.63 \times 10^{-3}$	0.18 (0.08)	0.68
k__Bacteria.p__Firmicutes.c__Clostridia.o__Clostridiales. f__Lachnospiraceae.g__Dorea	$5.78 \times 10^{-3} \pm 7.71 \times 10^{-3}$	$5.55 \times 10^{-3} \pm 8.36 \times 10^{-3}$	$6.06 \times 10^{-3} \pm 6.94 \times 10^{-3}$	0.18 (0.08)	0.68

* By nonparametic Wilcoxon test.
† False discovery rate–adjusted *P* values.

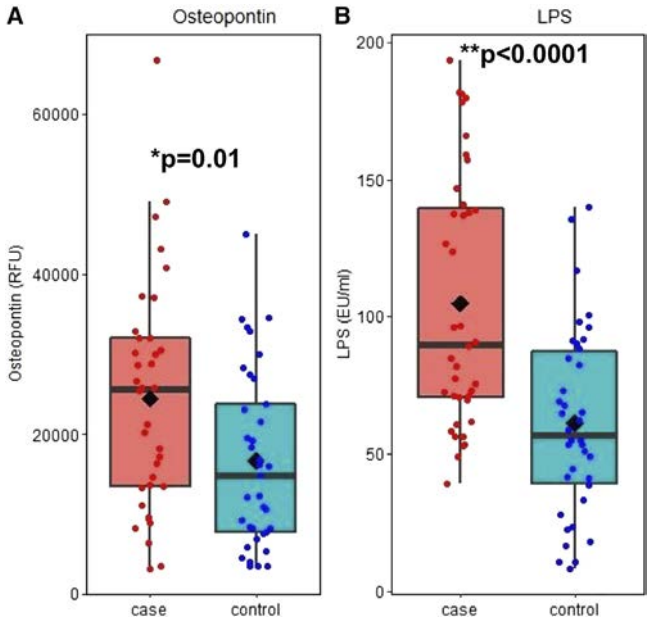

Figure 2. Osteopontin and lipopolysaccharide (LPS) levels in blood samples from osteoarthritis patients (cases) and controls. Osteopontin was measured in plasma samples using a cytokine array, and LPS was measured in serum using an endotoxin assay, as detailed in Patients and Methods. Data were analyzed using Student's 2-sided *t*-test. Data are shown as box plots. Each box represents the upper and lower interquartile range (IQR). Lines inside the boxes represent the median. Whiskers represent 1.5 times the upper and lower IQRs. Circles indicate individual data points. Diamonds represent the mean. RFU = relative fluorescence units; EU = endotoxin units.

PCoA based on weighted UniFrac distance between samples showed no differences between the patient and control groups (Figure 1). All results were consistent in the analysis using the vegan R package with Bray–Curtis dissimilarity (data not shown). We found that 3 taxa had nominally significant ($P < 0.05$) associations with OA status (effect size range 0.23–0.33), but none of the associations remained significant after Benjamini and Hochberg adjustment (Table 2). There were no overall significant taxonomic differences between men and women, and no significant differences were found in the relative abundance of specific genera (Supplementary Table 4, https://onlinelibrary.wiley.com/doi/10.1002/art.41955). No differences in α- and β-diversity were seen when stratifying by sex. A sensitivity analysis was performed to account for the 9 participants in the control group with K/L grade 2, but the results were not meaningfully different (data not shown).

Association of gut microbiota composition and pain. We conducted a secondary analysis to examine the association between the gut microbiota and WOMAC knee pain scores as well as AUSCAN hand pain scores in the patients and controls, but we did not find any significant differences after adjusting for multiple comparisons (Supplementary Tables 5 and 6, https://onlinelibrary.wiley.com/doi/10.1002/art.41955). In addition, the associations of *Lactobacillales* or *Streptococcus* with WOMAC pain scores reported in the Rotterdam study (33) were not replicated in our study ($P = 0.44$ and $P = 0.64$, respectively).

Differences in cytokines and LPS. Plasma samples from patients (n = 36) and controls (n = 37) were analyzed for differences in 80 cytokines (Supplementary Table 1, https://onlinelibrary.wiley.com/doi/10.1002/art.41955/abstract), which included 55 that were characterized as proinflammatory, 15 antiinflammatory, and 10 with pleotropic activity. Levels of osteopontin, a proinflammatory cytokine (34,35), were noted to be significantly higher in the patients (mean ± SD 24,380.6 ± 14,315.9 relative fluorescence units [RFUs]) than in controls (mean ± SD 16,620.2 ± 10,997.53 RFUs; $P = 0.01$) (Figure 2A). None of the other cytokines differed between the 2 groups. However, there were differences in several cytokines, within each group, between men and women or between African American and White participants (Supplementary Table 1). Serum LPS levels measured in 40 patients (mean ± SD 104.9 ± 45.8 endotoxin units [EU]/ml) were significantly higher than those in 38 controls (mean ± SD 61.3 ± 33.9 EU/ml; $P < 0.0001$) (Figure 2B). There was no difference in serum LBP between patients (mean ± SD 11.3 ± 5.0 μg/ml) and controls (mean ± SD 13.3 ± 6.0 μg/ml). The osteopontin and LPS results remained significant when reanalyzed with the 9 participants in the control group with K/L grade 2 treated as patients (data not shown). No correlation between osteopontin, LPS, or LBP levels and knee or hand pain was noted (data not shown).

Severity of OA in mice after fecal transplant and Western diet consumption. All 31 mice that received the fecal transplants and were fed the high-fat and high-sucrose Western diet for 40 weeks completed the study. There were no differences in weight gain over the course of the study or in percent body fat at time of euthanization between mice that received the patient fecal pool compared to those that received the control fecal pool (Figures 3A and B). There were significant differences in the Shannon (α) diversity index between fecal microbiota in the 2 groups at baseline ($P = 0.02$), which remained over the course of the study (Figure 3C). A PCoA emperor plot for β-diversity revealed that 1 case mouse clustered with the control mice at baseline (T0), which was 2 weeks after transplant when the diet was started, but at the subsequent time points, the case and control mice clustered in their respective groups (Figure 3D). Individual clade analysis revealed 15 taxa that were different between groups at baseline (false discovery rate–adjusted $P < 0.05$) (Supplementary Table 8, https://onlinelibrary.wiley.com/doi/10.1002/art.41955).

The Western diet induced histologic OA changes, including cartilage degradation and matrix loss, which were measured using the ACS and Safranin O scores, as well as osteophyte

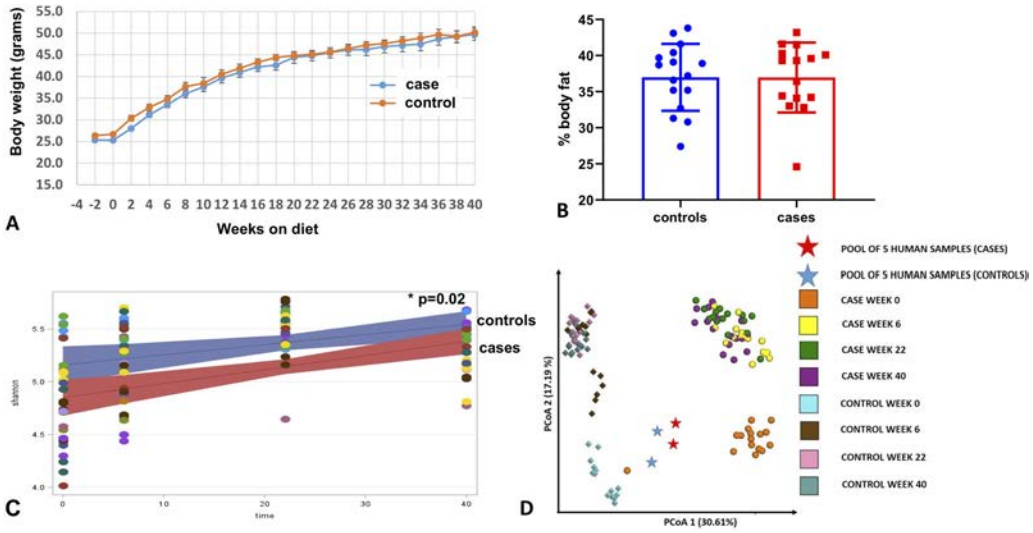

Figure 3. Effects of a high-fat, high-sucrose diet after transfer of human osteoarthritis (OA) case and control fecal samples to germ-free mice. **A**, Body weight of mice starting at the time of fecal transplant (−2 weeks) and then biweekly while being fed a high-fat, high-sucrose diet for 40 weeks. **B**, Percentage of body fat measured by magnetic resonance imaging after 40 weeks on diet. Each symbol represents an individual mouse. Bars show the mean ± SD. **C**, Linear mixed-effects model regression of Shannon diversity index from fecal samples collected at the start of the diet (time 0; 2 weeks after fecal transplant) and after 6, 22, and 40 weeks on diet. Lines represent linear mixed-effects regression (and 95% confidence interval) of Shannon diversity index over time. Each symbol represents a mouse, and those with the same color indicate that they were caged together. **D**, Principal coordinate analysis (PCoA) emperor plot based on Bray-Curtis β-diversity metric. Each point represents a sample from the 2 groups: OA cases (circles) and controls (diamonds). Time points are color-coded as indicated on the graph. Stars indicate duplicate samples of the pooled human feces analyzed prior to transplant to mice. Numbers in parentheses indicate the percent variation explained by the corresponding axis. The distance between 2 points shows how compositionally different the samples are.

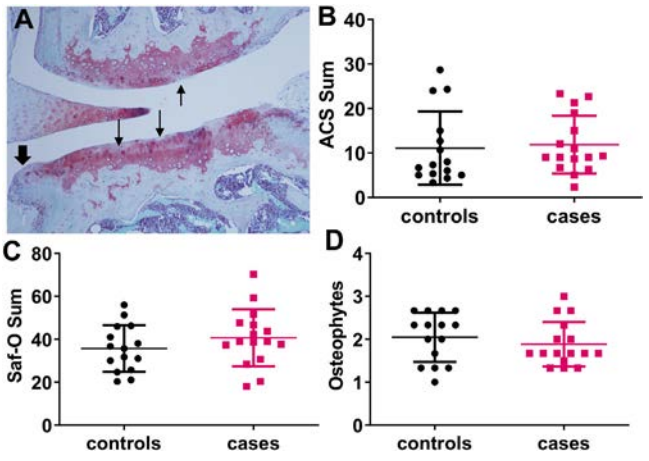

Figure 4. Results of histologic analysis of knee joints from mice transplanted with osteoarthritis (OA) patient (case) or control fecal pools and fed a high-fat, high-sucrose diet for 40 weeks. **A**, Representative images demonstrating histologic findings of OA, including cartilage degradation with loss of matrix staining (**long arrows**) and osteophyte formation (**short arrow**). **B–D,** Results of histologic measures of OA including articular cartilage structure (ACS) scores (**B**), Safranin O (Saf-O) scores (**C**), and osteophyte scores (**D**). Each symbol represents an individual mouse. Bars show the mean ± SD. None of the measures were significantly different between cases and controls, by Mann-Whitney test.

formation (Figure 4), but minimal synovitis was observed (data not shown). There were no differences in any of the histologic measures between mice that received the fecal transplants from patients compared to controls.

DISCUSSION

The present study did not demonstrate a difference in the fecal microbial communities between obese adults with hand OA and advanced knee OA compared to obese controls without hand and knee OA. However, we did find serum LPS levels to be significantly elevated in the OA patients relative to controls. Since LPS is produced by enteric gram-negative bacteria, including those in the gut, elevated serum levels suggest the presence of increased intestinal mucosal permeability, sometimes referred to as a "leaky gut." This is consistent with a previous report of increased LPS in the serum and synovial fluid of adults with knee OA, where the levels of serum LPS were associated with activated macrophages in the knee (21). Huang and Kraus proposed that LPS uptake from the gut due to an altered microbiome contributes to a low-grade inflammatory state that promotes the development of OA as a "second hit" when other OA risk factors, such as obesity or joint injury, are present (36). In further work,

they demonstrated an association of plasma LBP with radiographic progression of knee OA (37), but we were unable to show a difference in LBP between the patients and controls in the present study.

We also noted a significant increase in the proinflammatory mediator osteopontin in the OA patients. Although originally described as a bone matrix protein, subsequent studies have shown that osteopontin is a proinflammatory mediator and can serve as a Th1 cytokine (for review, see ref. 35). Osteoblasts from OA subchondral bone have increased expression of osteopontin (38) as do OA chondrocytes (39,40) and, as we found with combined hand and knee OA, systemic levels of osteopontin have been shown to be increased in association with knee OA (41).

Similar to our results in 92 JoCo OA Project participants, a study of ~1,400 participants from the Rotterdam Study did not demonstrate an association between the fecal microbiome and the presence of radiographic knee OA (33). However, researchers did find an association of *Streptococcus* species with WOMAC pain scores, which they replicated in a second Dutch cohort of 867 individuals. We could not replicate this result and our sample size of 92 individuals may have been too small, although not even a trend was observed. Published studies on the association between the gut microbiota and OA in humans were lacking when we designed our study. We based our recruitment of 92 participants on prior work in RA, in which highly significant microbial associations were observed in 44 patients with new-onset RA compared to 28 healthy controls, with multiple taxa displaying robust effect sizes (>2) (9). We attempted to enrich our OA patient population with a phenotype expected to have a systemic component to their OA, potentially related to the gut microbiome, by recruiting obese individuals who exhibited both hand and knee OA. Our findings suggest that the fecal microbial communities found in obese adults with combined hand and knee OA do not have as strong of an effect on the risk for OA as those seen in RA. Since our participants had advanced knee OA, with the majority exhibiting K/L grade 4 or prior knee arthroplasty, our findings do not rule out the possibility that a dysbiosis was present earlier in the disease course.

Rodent studies have suggested a role of the gut microbiota in OA. A study of diet-induced obesity in rats demonstrated a link between the severity of cartilage damage and fat mass, serum LPS concentrations, and the increased presence of *Methanobrevibacter* species in fecal samples, while the presence of *Lactobacillus* was negatively associated with cartilage damage (42). Treatment of rats (43) and mice (44) on a high-fat diet with the prebiotic fiber oligofructose restored the fecal microbiota to that seen with a normal chow diet. This restoration was associated with reduced serum LPS levels and, in the mouse study, less cartilage damage after OA was surgically induced. In a previous study, we noted less cartilage damage and fewer osteophytes in germ-free mice with surgically induced OA compared to mice housed in a standard facility, and the severity of cartilage damage correlated with serum LBP levels (45).

In the present study, we transplanted germ-free mice with pools of fecal samples from human OA patients and controls and then placed the mice on a Western diet. Although there were no differences between the human patient gut microbiome and control gut microbiome according to 16S rRNA sequencing in the entire group of 92 participants, this method does not allow for the full taxonomic identification down to the species level, such that strain-level differences or functional alterations could still be present. Therefore, a lack of differences in composition according to 16S rRNA sequencing does not necessarily translate into a lack of differences in microbial metabolic activities or metagenomic differences that could contribute to the development of OA. Importantly, clade analysis did identify differences in the mouse fecal samples after transfer of human patient and control fecal pools (Supplementary Table 8, https://onlinelibrary.wiley.com/doi/10.1002/art.41955/abstract). This included higher levels of *Eubacterium* in the group of controls who were obese and did not have OA. Huang et al reported that the presence of *Eubacterium* correlated with lower Osteoarthritis Research Society International scores of histologically evaluated OA in mice that had OA induced by meniscal injury after receiving human fecal transplants (46).

Higher levels of *Akkemansia* were noted in the group of patients who were obese and had OA. In a rat study of diet-induced obesity by Rios et al, *Akkemansia* was positively correlated with severity of joint damage (43). We also found 3 taxa from the *Ruminococcaceae* family that were different between controls and OA samples, with *Ruminnococcus* more abundant in the non-OA group and *Anaerotruncus and Oscillospira* more abundant in the OA group. *Ruminococcaceae* are butyrate producers, and butyrate is proposed to be a beneficial metabolite; a decreased abundance of *Ruminococcaceae* was associated with more severe OA in the study by Huang et al (46).

Despite a difference in the microbiota between the 2 groups of mice after fecal transfer of human patient and control fecal samples that included taxa potentially expected to influence the development of OA, there was no difference in the severity of histologic OA after 40 weeks of being fed a Western diet. Although human fecal transfer to germ-free mice has been used to establish causality in other conditions including obesity (7), a limitation to this technique is that selective colonization of microbial community members during transfer from humans to germ-free mice can occur, such that potential causative organisms may not be in the same abundance in the recipient mice as in the human donors (47).

Our findings, combined with those of the published studies noted above, indicate that future studies are needed to further evaluate increased intestinal mucosal permeability as a potential contributing factor to the development of OA and to elucidate the underlying mechanisms. Although NSAIDs can cause increased intestinal permeability in some individuals, we did not find an association with LPS levels and NSAID use; both patients and controls reported similar usage. Increased intestinal

permeability, resulting in higher levels of systemic LPS, can occur independent of differences in the microbiome or from differences in just a few taxa that may not have been detected given the sample size available for this study. Causes of increased LPS also include impaired clearance by the liver, high fat intake, alterations in the endocannabinoid system, deceased intestinal motility, and decreased physical activity (for review, see ref. 36). In addition to LPS, other factors produced by gut microbes that could enter the circulation through a leaky gut may be discovered to have the ability to promote OA. Intriguingly, recent reports that microbial DNA, including that from typical gut microbes, was present in OA cartilage (48) and synovial tissue (49) suggest that increased intestinal permeability could allow gut microbes access to joint tissues. Although there was no evidence that the microbial DNA was from viable bacteria or associated with joint infections, taken together, findings from these studies indicate that in OA, microbial products or microbes from the gut that enter the circulation may have a local effect on joints.

ACKNOWLEDGMENTS

The authors would like to thank the staff and participants in the Johnston County Osteoarthritis Project, without whom this work would not be possible.

AUTHOR CONTRIBUTIONS

All authors were involved in drafting the article or revising it critically for important intellectual content, and all authors approved the final version to be published. Dr. Loeser had full access to all of the data in the study and takes responsibility for the integrity of the data and the accuracy of the data analysis.

Study conception and design. Loeser, Kelley, Ulici, Sartor, Carrol, Jordan, Nelson.

Acquisition of data. Loeser, Kelley, Ulici, Longobardi, Cui, Stewart, Sumner, Azcarate-Peril, Renner, Nelson.

Analysis and interpretation of data. Loeser, Arbeeva, Kelley, Fodor, Sun, Stewart, Sumner, Azcarate-Peril, Sartor, Carroll, Renner, Jordan, Nelson.

REFERENCES

1. Johnson VL, Hunter DJ. The epidemiology of osteoarthritis [review]. Best Pract Res Clin Rheumatol 2014;28:5–15.
2. Sellam J, Berenbaum F. Is osteoarthritis a metabolic disease? Joint Bone Spine 2013;80:568–73.
3. Visser AW, Ioan-Facsinay A, de Mutsert R, Widya RL, Loef M, de Roos A, et al. Adiposity and hand osteoarthritis: the Netherlands Epidemiology of Obesity study. Arthritis Res Ther 2014;16:R19.
4. Kau AL, Ahern PP, Griffin NW, Goodman AL, Gordon JI. Human nutrition, the gut microbiome and the immune system [review]. Nature 2011;474:327–36.
5. Nicholson JK, Holmes E, Kinross J, Burcelin R, Gibson G, Jia W, et al. Host-gut microbiota metabolic interactions [review]. Science 2012; 336:1262–7.
6. Lozupone CA, Stombaugh JI, Gordon JI, Jansson JK, Knight R. Diversity, stability and resilience of the human gut microbiota [review]. Nature 2012;489:220–30.
7. Ridaura VK, Faith JJ, Rey FE, Cheng J, Duncan AE, Kau AL, et al. Gut microbiota from twins discordant for obesity modulate metabolism in mice. Science 2013;341:1241214.
8. Costello ME, Elewaut D, Kenna TJ, Brown MA. Microbes, the gut and ankylosing spondylitis [review]. Arthritis Res Ther 2013;15:214.
9. Scher JU, Sczesnak A, Longman RS, Segata N, Ubeda C, Bielski C, et al. Expansion of intestinal Prevotella copri correlates with enhanced susceptibility to arthritis. Elife 2013;2:e01202.
10. Claesson MJ, Jeffery IB, Conde S, Power SE, O'Connor EM, Cusack S, et al. Gut microbiota composition correlates with diet and health in the elderly. Nature 2012;488:178–84.
11. Gordon JI. Honor thy gut symbionts redux. Science 2012;336:1251–3.
12. Loeser RF, Pathmasiri W, Sumner SJ, McRitchie S, Beavers D, Saxena P, et al. Association of urinary metabolites with radiographic progression of knee osteoarthritis in overweight and obese adults: an exploratory study. Osteoarthritis Cartilage 2016;24:1479–86.
13. Jordan JM, Linder GF, Renner JB, Fryer JG. The impact of arthritis in rural populations [review]. Arthritis Care Res 1995;8:242–50.
14. Scherzer ZA, Alvarez C, Renner JB, Murphy LB, Schwartz TA, Jordan JM, et al. Effects of comorbid cardiovascular disease and diabetes on hand osteoarthritis, pain, and functional state transitions: the Johnston County Osteoarthritis Project. J Rheumatol 2020;47: 1541–9.
15. Kellgren JH, Lawrence JS. Radiological assessment of osteo-arthrosis. Ann Rheum Dis 1957;16:494–502.
16. Roos H, Laurén M, Adalberth T, Roos EM, Jonsson K, Lohmander LS. Knee osteoarthritis after meniscectomy: prevalence of radiographic changes after twenty-one years, compared with matched controls. Arthritis Rheum 1998;41:687–93.
17. Bellamy N, Campbell J, Haraoui B, Gerecz-Simon E, Buchbinder R, Hobby K, et al. Clinimetric properties of the AUSCAN Osteoarthritis Hand Index: an evaluation of reliability, validity and responsiveness. Osteoarthritis Cartilage 2002;10:863–9.
18. Thompson FE, Midthune D, Williams GC, Yaroch AL, Hurley TG, Resnicow K, et al. Evaluation of a short dietary assessment instrument for percentage energy from fat in an intervention study. J Nutr 2008; 138:193S–9S.
19. Allali I, Arnold JW, Roach J, Cadenas MB, Butz N, Hassan HM, et al. A comparison of sequencing platforms and bioinformatics pipelines for compositional analysis of the gut microbiome. BMC Microbiol 2017; 17:194.
20. Azcarate-Peril MA, Butz N, Cadenas MB, Koci M, Ballou A, Mendoza M, et al. An attenuated Salmonella enterica serovar typhimurium strain and galacto-oligosaccharides accelerate clearance of Salmonella infections in poultry through modifications to the gut microbiome. Appl Environ Microbiol 2018;84:e02526-17.
21. Huang Z, Stabler T, Pei F, Kraus VB. Both systemic and local lipopolysaccharide (LPS) burden are associated with knee OA severity and inflammation. Osteoarthritis Cartilage 2016;24:1769–75.
22. Loeser RF, Olex A, McNulty MA, Carlson CS, Callahan M, Ferguson C, et al. Microarray analysis reveals age-related differences in gene expression during the development of osteoarthritis in mice. Arthritis Rheum 2012;64:705–17.
23. Loeser RF, Kelley KL, Armstrong A, Collins JA, Diekman BO, Carlson CS. Deletion of JNK enhances senescence in joint tissues and increases the severity of age-related osteoarthritis in mice. Arthritis Rheumatol 2020;72:1679–88.
24. Rowe MA, Harper LR, McNulty MA, Lau AG, Carlson CS, Leng L, et al. Deletion of macrophage migration inhibitory factor reduces severity of osteoarthritis in aged mice. Arthritis Rheumatol 2017;69:352–61.
25. Caporaso JG, Kuczynski J, Stombaugh J, Bittinger K, Bushman FD, Costello EK, et al. QIIME allows analysis of high-throughput community sequencing data. Nat Methods 2010;7:335–6.

26. Shannon CE. The mathematical theory of communication. 1963. MD Comput 1997;14:306–17.
27. Chao A. Nonparametric-estimation of the number of classes in a population. Scand J Statist 1984;11:265–70.
28. Lozupone C, Hamady M, Knight R. UniFrac: an online tool for comparing microbial community diversity in a phylogenetic context. BMC Bioinformatics 2006;7:371.
29. Lozupone C, Knight R. UniFrac: a new phylogenetic method for comparing microbial communities. Appl Environ Microbiol 2005;71: 8228–35.
30. Benjamini Y, Hochberg Y. Controlling the false discovery rate: a practical and powerful approach to multiple testing. J R Stat Soc Series B (Methodol) 1995;57:289–300.
31. Fritz CO, Morris PE, Richler JJ. Effect size estimates: current use, calculations, and interpretation. J Exp Psychol Gen 2012;141:2–18.
32. Bellamy N, Buchanan WW, Goldsmith CH, Campbell J, Stitt LW. Validation study of WOMAC: a health status instrument for measuring clinically important patient relevant outcomes to antirheumatic drug therapy in patients with osteoarthritis of the hip or knee. J Rheumatol 1988;15:1833–40.
33. Boer CG, Radjabzadeh D, Medina-Gomez C, Garmaeva S, Schiphof D, Arp P, et al. Intestinal microbiome composition and its relation to joint pain and inflammation. Nature Commun 2019;10:4881.
34. Sennels H, Sorensen S, Ostergaard M, Knudsen L, Hansen M, Skjodt H, et al. Circulating levels of osteopontin, osteoprotegerin, total soluble receptor activator of nuclear factor-κ B ligand, and high-sensitivity C-reactive protein in patients with active rheumatoid arthritis randomized to etanercept alone or in combination with methotrexate. Scand J Rheumatol 2008;37:241–7.
35. Lund SA, Giachelli CM, Scatena M. The role of osteopontin in inflammatory processes. J Cell Commun Signal 2009;3:311–22.
36. Huang Z, Kraus VB. Does lipopolysaccharide-mediated inflammation have a role in OA? [review]. Nat Rev Rheumatol 2016;12:123–9.
37. Huang ZY, Perry E, Huebner JL, Katz B, Li YJ, Kraus VB. Biomarkers of inflammation– LBP and TLR— predict progression of knee osteoarthritis in the DOXY clinical trial. Osteoarthritis Cartilage 2018;26: 1658–65.
38. Sanchez C, Deberg MA, Bellahcène A, Castronovo V, Msika P, Delcour JP, et al. Phenotypic characterization of osteoblasts from the sclerotic zones of osteoarthritic subchondral bone. Arthritis Rheum 2008;58:442–55.
39. Pullig O, Weseloh G, Gauer S, Swoboda B. Osteopontin is expressed by adult human osteoarthritic chondrocytes: protein and mRNA analysis of normal and osteoarthritic cartilage. Matrix Biol 2000;19: 245–55.
40. Li Y, Xiao W, Sun M, Deng Z, Zeng C, Li H, et al. The expression of osteopontin and Wnt5a in articular cartilage of patients with knee osteoarthritis and its correlation with disease severity. Biomed Res Int 2016;2016:9561058.
41. Min S, Shi T, Han X, Chen D, Xu Z, Shi D, et al. Serum levels of leptin, osteopontin, and sclerostin in patients with and without knee osteoarthritis. Clin Rheumatol 2021:40:287–94.
42. Collins KH, Paul HA, Reimer RA, Seerattan RA, Hart DA, Herzog W. Relationship between inflammation, the gut microbiota, and metabolic osteoarthritis development: studies in a rat model. Osteoarthritis Cartilage 2015;23:1989–98.
43. Rios JL, Bomhof MR, Reimer RA, Hart DA, Collins KH, Herzog W. Protective effect of prebiotic and exercise intervention on knee health in a rat model of diet-induced obesity. Sci Rep 2019;9:3893.
44. Schott EM, Farnsworth CW, Grier A, Lillis JA, Soniwala S, Dadourian GH, et al. Targeting the gut microbiome to treat the osteoarthritis of obesity. JCI Insight 2018;3:e95997.
45. Ulici V, Kelley KL, Azcarate-Peril MA, Cleveland RJ, Sartor RB, Schwartz TA, et al. Osteoarthritis induced by destabilization of the medial meniscus is reduced in germ-free mice. Osteoarthritis Cartilage 2018;26:1098–109.
46. Huang Z, Chen J, Li B, Zeng B, Chou CH, Zheng X, et al. Faecal microbiota transplantation from metabolically compromised human donors accelerates osteoarthritis in mice. Ann Rheum Dis 2020;79: 646–56.
47. Fouladi F, Glenny EM, Bulik-Sullivan EC, Tsilimigras MC, Sioda M, Thomas SA, et al. Sequence variant analysis reveals poor correlations in microbial taxonomic abundance between humans and mice after gnotobiotic transfer. ISME J 2020;14:1809–20.
48. Dunn CM, Velasco C, Rivas A, Andrews M, Garman C, Jacob PB, et al. Identification of cartilage microbial DNA signatures and associations with knee and hip osteoarthritis. Arthritis Rheumatol 2020;72: 1111–22.
49. Zhao Y, Chen B, Li S, Yang L, Zhu D, Wang Y, et al. Detection and characterization of bacterial nucleic acids in culture-negative synovial tissue and fluid samples from rheumatoid arthritis or osteoarthritis patients. Sci Rep 2018;8:14305.

Arthritis & Rheumatology
Vol. 74, No. 2, February 2022, pp 237–243
DOI 10.1002/art.41946

American College of Rheumatology
Empowering Rheumatology Professionals

Incidence of Psoriatic Arthritis Among Patients Receiving Biologic Treatments for Psoriasis: A Nested Case–Control Study

Yael Shalev Rosenthal,[1] Naama Schwartz,[2] Iftach Sagy,[3] and Lev Pavlovsky[4]

Objective. To investigate the effect of biologic treatments for psoriasis on the incidence of psoriatic arthritis (PsA).

Methods. This retrospective cohort study was conducted using electronic medical records from a large health maintenance organization. Patients who received biologic treatment for psoriasis and were not diagnosed as having PsA before or at the time of biologic treatment initiation were included. Control psoriasis patients who did not receive biologic treatment were matched by age at time of diagnosis, sex, time from psoriasis diagnosis until treatment initiation, maximum body mass index, and smoking status. The groups were different in most characteristics. Therefore, propensity score matching was implemented. Log rank test and multivariable Cox proportional hazards regression were used to compare the groups.

Results. Overall, 1,326 patients were included, of whom 663 had received biologic treatment and 663 had not. The Kaplan-Meier curve for the propensity score–matched groups reflected a statistically significant increased risk for PsA among the control group compared to the biologic treatment group. The results of the multivariable Cox regression showed that the control group had a significantly higher risk for PsA compared to the biologic treatment group within 10 years of follow-up (adjusted hazard ratio 1.39 [95% confidence interval 1.03–1.87]).

Conclusion. Our findings show a statistically and clinically significant decreased risk for developing PsA among patients with psoriasis who receive biologic treatments. The results suggest that biologic medications should be considered for patients who present with significant risk factors for PsA at an earlier stage of treatment.

INTRODUCTION

Psoriasis is a common inflammatory skin disorder affecting ~2.5% of the population (1). Its manifestations are multisystemic, with skin and joint predominance. Approximately 30% of patients with psoriasis eventually develop psoriatic arthritis (PsA), with a mean time from skin disease diagnosis to PsA development of 10 years (1). Psoriasis has a significant psychological and emotional burden, with a substantial effect on quality of life (2–5) that is further worsened by PsA (6,7).

The pathogenesis of PsA remains unclear. However, many findings suggest that a dysregulated immune response plays an important role. For example, numerous studies indicate the involvement of tumor necrosis factor (TNF) and interleukin-23 (IL-23) and IL-17 in PsA pathogenesis (8). Moreover, patients with PsA have been found to have high levels of osteoclast precursors, which play an important role in the pathogenesis of PsA, and whose levels decrease with TNF antagonist therapy (9). Other studies have demonstrated inflammatory properties in the synovial fluid of patients with PsA (10). All of these contribute to an understanding of the role of biologic medications in the treatment of PsA.

Despite their modest efficacy for skin disease and questionable disease-modifying effect in various clinical types of PsA, conventional disease-modifying antirheumatic drugs (DMARDs) are still recommended as first-line therapies (11–13). Biologic medications, biologically manufactured proteins that modulate the immune system, were first used for the treatment of psoriasis in ~2005. Several biologic agents have been shown to be superior to DMARDs in treating PsA symptoms and have also shown effectiveness in slowing articular damage (14,15). However, they are not used as a first-line therapy in moderate-to-severe psoriasis, largely due to their high cost.

[1]Yael Shalev Rosenthal, MPH: Tel Aviv University, Tel Aviv, Israel; [2]Naama Schwartz, PhD: University of Haifa, Haifa, Israel; [3]Iftach Sagy, MD, MPA, PhD: Soroka University Medical Center and Ben-Gurion University of the Negev, Beer Sheva, Israel; [4]Lev Pavlovsky, MD, PhD: Tel Aviv University, Tel Aviv, Israel, and Rabin Medical Center, Petah Tikva, Israel.

Author disclosures are available at https://onlinelibrary.wiley.com/action/downloadSupplement?doi=10.1002%2Fart.41946&file=art41946-sup-0001-Disclosureform.pdf.

Address correspondence to Lev Pavlovsky, MD, PhD, Division of Dermatology, Rabin Medical Center, Petah Tikva, Israel. Email: levp@clalit.org.il.

Submitted for publication March 31, 2021; accepted in revised form August 3, 2021.

The influence of biologic treatment for psoriasis on the incidence and timing of PsA onset is unknown. Since biologic agents were shown to slow the progression of PsA (14,15), it is reasonable to assume that their use in subjects diagnosed as having psoriasis with no evidence of PsA at the time of treatment initiation will prevent or delay the onset of PsA.

The fact that up to 30% of patients with psoriasis will eventually develop PsA in a mean time of 10 years provides a unique opportunity for early intervention. This is especially relevant in patients who are at increased risk for developing PsA. Our study was designed to investigate the effect of biologic treatments for psoriasis on the incidence of PsA.

PATIENTS AND METHODS

Study setting. Maccabi Healthcare Services (MHS) is the second largest health maintenance organization in Israel, insuring >2 million members. In accordance with the Israeli National Health Insurance Law, MHS is prohibited from denying any citizen who wishes to be insured. Therefore, MHS ensures every section of the population and its data are representative of the Israeli population (16). In the early 1990s, MHS established an electronic medical record system where all medical data are collected, including diagnoses, medication prescriptions, and medication purchases. In accordance with the Israeli regulatory guidelines for the treatment of psoriasis and MHS internal guidelines, patients are eligible to receive biologic agents or apremilast treatment if they fulfill the following criteria: body surface area affected by psoriasis >50%, Psoriasis Area and Severity Index score >50 (17), or involvement of sensitive areas (defined as genitalia, palms, and face, etc.) and have previously been treated unsuccessfully with at least 2 standard systemic therapies, including phototherapy. Before these medications are purchased, MHS members are required to obtain authorization from the MHS drug authorization center to ensure they comply with the guidelines.

Study population and statistical methods. To examine the potential association between biologic agents and the incidence of PsA, data were collected for patients who had received biologic treatment (i.e., adalimumab, etanercept, infliximab, ustekinumab, secukinumab, ixekizumab, or guselkumab) for psoriasis (International Classification of Diseases, Ninth Revision [ICD-9] codes 696 and 696.1) but were not diagnosed as having PsA before receiving biologic treatment or at the time of biologic treatment initiation. Although the association between disease severity and PsA is controversial, to avoid the potential confounding effect of disease severity, the control group was defined as patients who were diagnosed as having psoriasis by a dermatologist and had received at least 2 systemic medications or 1 systemic medication plus phototherapy, but had not received biologic treatment. These

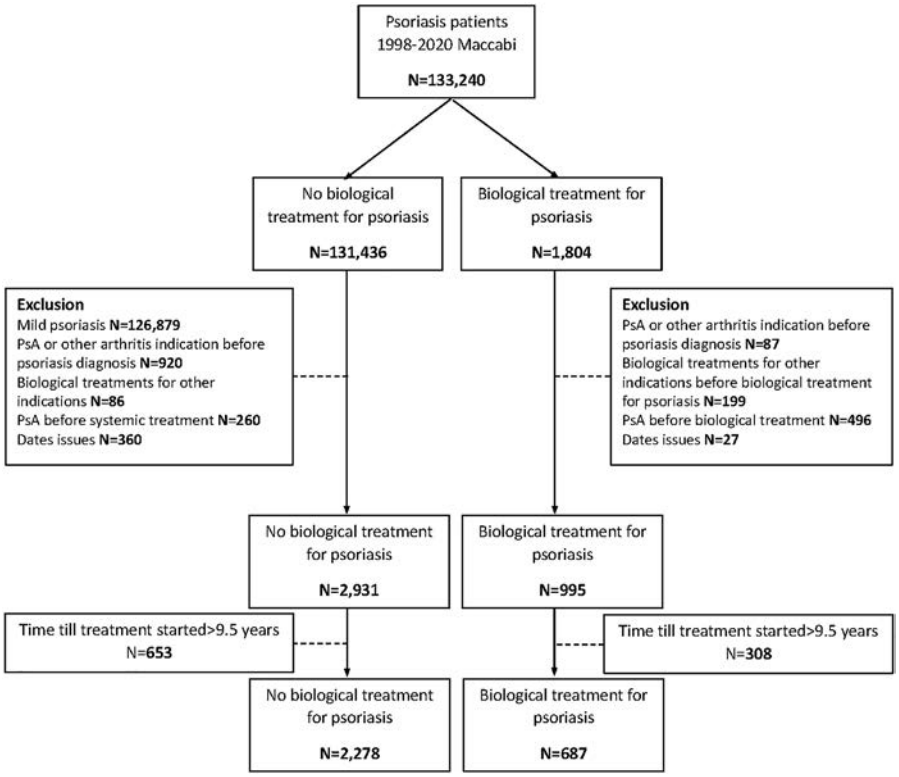

Figure 1. Flow chart of the patients with psoriasis who received biologic treatment and the patients who did not receive biologic treatment. PsA = psoriatic arthritis.

patients were assumed to be in a relatively similar disease severity state as those who had received biologic medications. In both groups, the maximum follow-up time was set at 10 years. This was based on the assumption that patients with longer follow-up time have a greater risk for developing PsA, especially due to the fact that biologic agents were only available since 2005, making the follow-up time of the control group longer by definition.

Patients were excluded if they had received biologic treatment for a different indication, were diagnosed as having PsA before the time of biologic or systemic treatment initiation, were diagnosed as having arthritis prior to the time of psoriasis diagnosis, or if the time from psoriasis diagnosis to treatment initiation was >10 years (Figure 1). Arthritis was defined as the presence of a diagnosis of PsA or nonrheumatoid, noninfectious, and not otherwise specified arthritis (ICD-9 codes 696.0, 714.9, 726.90, 721.3, 716.9, 726.4, 720.0, 716.6, 716.5, 716.96, 716.98, and 716.99). In <9% of the eligible cases, patients with data containing illogical timelines were identified and were therefore excluded (e.g., if a patient received treatment for psoriasis [i.e., medication or phototherapy] prior to the date of diagnosis). The primary outcome measure was the incidence of PsA during 10 years of follow-up. Psoriasis and arthritis diagnoses were extracted from patient medical records in accordance with the ICD-9 codes. This study was approved by the MHS ethical committee.

Statistical analysis. The study groups were initially compared by chi-square test (or Fisher's exact test) for categorical

Table 1. Comparison of demographic and clinical characteristics between the study groups*

	No biologic treatment (n = 2,278)	Biologic treatment (n = 687)	*P*
Age at time of psoriasis diagnosis, years			<0.0001
Mean ± SD	46.72 ± 15.74	35.25 ± 15.09	
Median (IQR)	48.1 (1.74–88.83)	33.3 (0.97–86.68)	
Age, years			<0.0001
0–18	104 (4.57)	80 (11.64)	
>18–25	127 (5.58)	101 (14.7)	
>25–35	294 (12.91)	202 (29.4)	
>35–45	438 (19.23)	120 (17.47)	
>45–55	596 (26.16)	107 (15.57)	
>55–65	442 (19.4)	57 (8.3)	
>65–75	218 (9.57)	16 (2.33)	
>75	59 (2.59)	4 (0.58)	
Female	837 (36.74)	244 (35.52)	0.5584
No. of BMI measures during study period†			<0.0001
Mean ± SD	10.7 ± 10.8	8.9 ± 9.5	
Median (IQR)	8 (1–135)	6 (1–72)	
Maximum BMI, kg/m^2†			0.0032
Mean ± SD	30.25 ± 6.4	29.5 ± 6.78	
Median (IQR)	29.3 (14.3–60)	28.7 (13.9–58.2)	
Mean BMI, kg/m^2†			0.0038
Mean ± SD	28 ± 5.3	27.4 ± 5.8	
Median (IQR)	27.4 (14.3–49.4)	27 (12.9–47)	
BMI ≥30 kg/m^2†	976 (44.94)	277 (41.04)	0.0747
Smoking status†			0.0845
Current or past	1,206 (53.79)	335 (50)	
Never	1,036 (46.21)	335 (50)	
Time between diagnosis and treatment initiation, years			<0.0001
Mean ± SD	2.7 ± 2.8	3.8 ± 3	
Median (IQR)	1.6 (0–9.5)	3.4 (0–9.5)	
Time between diagnosis and treatment initiation, years			<0.0001
0–1	941 (41.31)	174 (25.33)	
>1–3	499 (21.91)	145 (21.11)	
>3–6	448 (19.67)	169 (24.6)	
>6	390 (17.12)	199 (28.97)	
Year of diagnosis			0.0001
1998–2004	917 (40.25)	218 (31.73)	
2005–2011	708 (31.08)	227 (33.04)	
2012–2020	653 (28.67)	242 (35.23)	
Follow-up time, years			0.4292
Mean ± SD	7.6 ± 3.1	7.8 ± 3	
Median (IQR)	10 (0–10)	10 (0–10)	
PsA in 10 years	374 (16.4)	76 (11.1)	0.0006

* Except where indicated otherwise, values are the number (%). IQR = interquartile range; PsA = psoriatic arthritis.
† Data on smoking status were missing for 53 patients (1.8%), and data on body mass index (BMI) were missing for 118 patients (4%).

variables and *t*-test (or Wilcoxon's 2-sample rank sum test) for continuous variables. Time-to-event analysis was performed using Kaplan-Meier curves. Several potential confounders (i.e., age at time of diagnosis, maximum body mass index [BMI], time from psoriasis diagnosis until treatment initiation) differed between the study groups; therefore, a propensity score 1:1 matching was performed using the greedy matching method. In general, propensity score matching attempts to reduce the treatment assignment bias by creating a sample of patients who received biologic agents that is comparable to all or most variables in the control group. Controls were matched by age at time of diagnosis, sex, time from psoriasis diagnosis until treatment initiation, maximum BMI, and smoking status. There were 24 patients in the study group who did not have any controls available according to the above combinations (24 of 687 = ~3%). Those patients were eliminated from the analysis. Multivariable Cox proportional hazards regression analysis and log rank test were performed, and adjusted hazard ratios (HRs) with 95% confidence intervals (95% CIs) were calculated.

The statistical analysis and data management were performed using SAS 9.4 software. *P* values less than 0.05 were considered significant.

RESULTS

Overall, 687 patients who had received biologic treatment and 2,278 patients who had not received biologic treatment (controls) were considered in the analysis (Figure 1). Patients in the

Table 2. Comparison of characteristics between propensity score–matched study groups*

	No biologic treatment (n = 663)	Biologic treatment (n = 663)	*P*
Age at time of psoriasis diagnosis, years			0.8965
Mean ± SD	36 ± 15.4	35.7 ± 14.9	
Median (IQR)	34.1 (3.7–81)	33.8 (3.5–86.7)	
Age, years			0.3269
0–18	86 (12.97)	68 (10.26)	
>18–25	95 (14.33)	98 (14.78)	
>25–35	160 (24.13)	199 (30.02)	
>35–45	126 (19)	115 (17.35)	
>45–55	108 (16.29)	106 (15.99)	
>55–65	62 (9.35)	57 (8.6)	
>65–75	22 (3.32)	16 (2.41)	
>75	4 (0.6)	4 (0.6)	
Female	194 (29.26)	234 (35.29)	0.0188
No. of BMI measures during study period			0.5411
Mean ± SD	8.9 ± 10.3	9 ± 9.5	
Median (IQR)	6 (1–135)	6 (1–72)	
Maximum BMI, kg/m^2			0.7101
Mean ± SD	29.6 ± 6.9	29.7 ± 6.7	
Median (IQR)	28.7 (14.3–56.9)	28.7 (13.9–58.2)	
Mean BMI, kg/m^2			0.7944
Mean ± SD	27.5 ± 5.6	27.6 ± 5.6	
Median (IQR)	26.9 (14.3–49.3)	27 (12.9–47)	
BMI ≥30 kg/m^2	269 (40.57)	276 (41.63)	0.6960
Smoking status			0.5827
Current or past	345 (52.04)	335 (50.53)	
Never	318 (47.96)	328 (49.47)	
Time between diagnosis and treatment initiation, years			0.3343
Mean ± SD	4 ± 3	3.9 ± 3	
Median (IQR)	3.9 (0–9.5)	3.4 (0–9.5)	
Time between diagnosis and treatment initiation, years			0.8422
0–1	158 (23.83)	162 (24.43)	
>1–3	128 (19.31)	139 (20.97)	
>3–6	176 (26.55)	167 (25.19)	
>6	201 (30.32)	195 (29.41)	
Year of diagnosis			<0.0001
1998–2004	277 (41.78)	216 (32.58)	
2005–2011	230 (34.69)	223 (33.63)	
2012–2020	156 (23.53)	224 (33.79)	
Follow-up time, years			
Mean ± SD	8.2 ± 2.7	7.9 (2.9)	
Median (IQR)	10 (0.1–10)	10 (0–10)	
PsA in 10 years	109 (16.44)	75 (11.31)	0.0069

* Except where indicated otherwise, values are the number (%). IQR = interquartile range; BMI = body mass index; PsA = psoriatic arthritis.

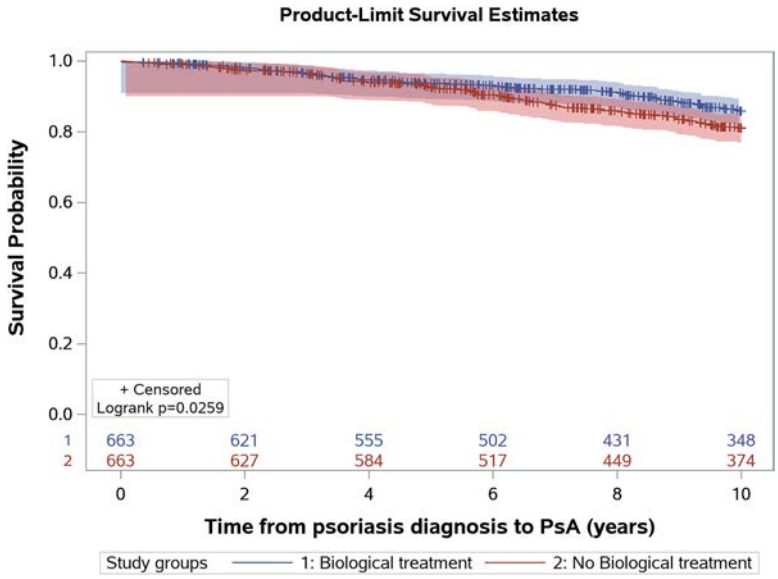

Figure 2. Kaplan-Meier curves comparing incidence of psoriatic arthritis (PsA) within 10 years among propensity score–matched patients with psoriasis who received biologic treatment and those who did not receive biologic treatment.

control group were significantly older at the time of psoriasis diagnosis compared to patients in the biologic treatment group (mean ± SD age 46.7 ± 15.7 years versus 35.3 ± 15.1 years; $P < 0.0001$). Moreover, patients in the control group compared to patients in the biologic treatment group had a higher mean BMI (mean 28 kg/m^2 versus 27.4 kg/m^2; $P = 0.0038$), and a shorter median time from diagnosis until treatment initiation (2.7 years versus 3.8 years; $P < 0.0001$) (Table 1). However, the follow-up time was similar between the study groups, and the log rank test demonstrated a significantly increased risk for PsA within 10 years following treatment with nonbiologic agents compared to that within 10 years following treatment with biologic agents ($P = 0.0006$).

As seen in Table 1, the study groups were significantly different in most of the demographic characteristics and other potential PsA predictors. Thus, propensity score matching was implemented, resulting in a comparable or similar control group (Table 2). Overall, 1,326 patients were included (663 patients who had received biologic treatment and 663 who had not received biologic treatment). Aside from sex, all of the predictors and potential confounders were similar between the study groups ($P > 0.05$ for each variable). The Kaplan-Meier curve for the matched groups reflected a statistically significant increased risk for PsA among the control group compared to the biologic treatment group ($P = 0.026$ by log rank test) (Figure 2). Although propensity score matching balanced the study groups, the groups were still unbalanced regarding sex and the year of diagnosis. Therefore, we adjusted for these factors and other PsA predictors such as age at time of diagnosis and time until treatment initiation using a multivariable Cox regression. After adjustment for all of the factors and confounders described above, the control group still had a significantly higher risk for PsA compared to the biologic treatment group (adjusted HR 1.39 [95% CI 1.03–1.87]). Finally, according to our data, women were at higher risk for developing PsA (adjusted HR 1.8 [95% CI 1.34–2.42]).

DISCUSSION

The results of our study demonstrate a statistically significant decreased risk for developing PsA among patients with psoriasis who were treated with biologic medications for their skin disease. This result was consistently shown in both the original and propensity score–matched data sets, using multivariable and univariable Cox proportional hazards regression, respectively (Figure 2). To our knowledge, this is the first study to demonstrate this effect of biologic treatment on psoriasis.

Since a considerable number of patients eventually develop PsA, in addition to its heavy burden on quality of life (2–7), the prevention of PsA should be considered as a factor in favor of initiating biologic treatment for psoriasis. Biologic agents have been used for the treatment of psoriasis for <2 decades. Cost plays an important role in the allocation of these medications in the treatment algorithm. Numerous studies have shown the effectiveness of various biologic agents in the treatment of psoriasis and PsA (18–23). Some studies have demonstrated a decrease in radiographic damage (14,15). Eventually, the concept of treat-to-target was developed (24). The results of this study suggest that biologic treatments may delay the risk of PsA development.

We compared the prevalence rates of PsA recorded in our data to those reported in other studies. The prevalence of PsA in the literature varies from 5–40% (25–31). Since our data present a point prevalence among patients with up to 10 years of follow-up,

in addition to the fact that the mean time of PsA onset is 10 years, it is safe to say that our results lie within the range reported in other studies.

In the present study, women appeared to be at higher risk for developing PsA (adjusted HR 1.8 [95% CI 1.34–2.42]). There is no consensus about the difference in prevalence between men and women. To our knowledge, most studies have shown no significant differences between the sexes (32). However, some studies have demonstrated greater prevalence of PsA in men (33), whereas others showed greater prevalence in women (30).

As noted above, the association between disease severity and the onset of arthritis among patients with psoriasis is controversial. However, many studies have shown a positive association between the severity of psoriasis and PsA onset (34,35). Therefore, assuming that patients with more advanced disease are treated with biologic medications, we would expect to see a higher incidence of PsA among patients in this group. The results indicate the opposite, which strengthens the link between treatment with biologic medications and lower incidence of PsA.

Many risk factors for PsA have been suggested. These include clinical features such as nail dystrophy, scalp and intergluteal lesions, genetic factors (e.g., HLA–B27), and biomarkers (e.g., C-reactive protein). These may all help to identify patients with the highest need for secondary prevention for PsA.

Our study has several strengths and limitations. A major strength is the large population-based, real-life cohort, which made it possible to obtain clinically meaningful results. Moreover, our study demonstrated prevalence rates similar to those found in other studies, corroborating the reliability of our data.

A potential weakness of our study is that we did not have information about clinical features of the disease, such as the extent of skin involvement and nail involvement. This is mainly due to the fact that this is a retrospective study based on computerized data rather than clinical data. Such information might have helped identify patients at particularly high risk for developing PsA and therefore would have potentially helped clarify the role of biologic treatments in these patients. In addition, the historical data from years prior to the availability of biologic treatment were scarce. Had this information been available, it would have allowed comparison to more similar patients who did not have the option to be treated with biologic agents at the time. In this study, we used propensity score matching in order to compare the biologic treatment group to the control group. Propensity score matching is a popular analytic method used to estimate the effects of treatments when using observational data, but this method is not as robust as the fully blocked randomized experiment. However, we used a multivariable model on the propensity score–matched group in order to account for possible residual biases. Finally, we do not know whether discontinuation of treatment was due to intolerance or inefficacy.

Further studies are needed to understand in depth the relationship between biologic medications and PsA onset. However, the results of our study show a statistically and clinically significant decreased risk for developing PsA among patients receiving biologic medications for psoriasis. These results may support the initiation of treatment with biologic medications at an earlier stage in patients who present with significant risk factors for PsA.

AUTHOR CONTRIBUTIONS

All authors were involved in drafting the article or revising it critically for important intellectual content, and all authors approved the final version to be published. Ms. Rosenthal had full access to all of the data in the study and takes responsibility for the integrity of the data and the accuracy of the data analysis.

Study conception and design. Rosenthal, Pavlovsky.
Acquisition of data. Rosenthal, Pavlovsky.
Analysis and interpretation of data. Schwartz, Sagy, Pavlovsky.

REFERENCES

1. Ritchlin CT, Colbert RA, Gladman DD. Psoriatic arthritis [review]. N Engl J Med 2017;376:2095–6.
2. Gelfand JM, Feldman SR, Stern RS, Thomas J, Rolstad T, Margolis DJ. Determinants of quality of life in patients with psoriasis: a study from the US population. J Am Acad Dermatol 2004;51:704–8.
3. De Korte J, Sprangers MA, Mombers FM, Bos JD. Quality of life in patients with psoriasis: a systematic literature review. J Investig Dermatol Symp Proc 2004;9:140–7.
4. Russo PA, Ilchef R, Cooper AJ. Psychiatric morbidity in psoriasis: a review. Australas J Dermatol 2004;45:155–9.
5. Esposito M, Saraceno R, Giunta A, Maccarone M, Chimenti S. An Italian study on psoriasis and depression. Dermatology 2006;212:123–7.
6. Mease PJ, Menter MA. Quality-of-life issues in psoriasis and psoriatic arthritis: outcome measures and therapies from a dermatological perspective [review]. J Am Acad Dermatol 2006;54:685–704.
7. Lundberg L, Johannesson M, Silverdahl M, Hermansson C, Lindberg M. Health-related quality of life in patients with psoriasis and atopic dermatitis measured with SF-36, DLQI and a subjective measure of disease activity. Acta Derm Venereol 2000;80:430–4.
8. Bravo A, Kavanaugh A. Bedside to bench: defining the immunopathogenesis of psoriatic arthritis [review]. Nat Rev Rheumatol 2019;15:645–56.
9. Ritchlin CT, Haas-Smith SA, Li P, Hicks DG, Schwarz EM. Mechanisms of TNF-α– and RANKL-mediated osteoclastogenesis and bone resorption in psoriatic arthritis. J Clin Invest 2003;111:821–31.
10. McGonagle DG, McInnes IB, Kirkham BW, Sherlock J, Moots R. The role of IL-17A in axial spondyloarthritis and psoriatic arthritis: recent advances and controversies [review]. Ann Rheum Dis 2019;78:1167–78.
11. Gossec L, Smolen JS, Ramiro S, de Wit M, Cutolo M, Dougados M, et al. European League Against Rheumatism (EULAR) recommendations for the management of psoriatic arthritis with pharmacological therapies: 2015 update. Ann Rheum Dis 2016;75:499–510.
12. Coates LC, Kavanaugh A, Mease PJ, Soriano ER, Acosta-Felquer ML, Armstrong AW, et al. Group for research and assessment of psoriasis and psoriatic arthritis 2015 treatment recommendations for psoriatic arthritis. Arthritis Rheumatol 2016;68:1060–71.
13. Gladman DD. Should methotrexate remain the first-line drug for psoriasis? Lancet 2017;389:482–3.
14. Van der Heijde D, Kavanaugh A, Gladman DD, Antoni C, Krueger GG, Guzzo C, et al. Infliximab inhibits progression of radiographic damage in patients with active psoriatic arthritis through one year of treatment:

results from the induction and maintenance psoriatic arthritis clinical trial 2. Arthritis Rheum 2007;56:2698–707.

15. Antoni C, Krueger GG, de Vlam K, Birbara C, Beutler A, Guzzo C, et al. Infliximab improves signs and symptoms of psoriatic arthritis: results of the IMPACT 2 trial. Ann Rheum Dis 2005;64:1150–7.
16. Shalev V, Chodick G, Goren I, Silber H, Kokia E, Heymann AD. The use of an automated patient registry to manage and monitor cardiovascular conditions and related outcomes in a large health organization. Int J Cardiol 2011;152:345–9.
17. Fredriksson T, Pettersson U. Severe psoriasis—oral therapy with a new retinoid. Dermatologica 1978;157:238–44.
18. Reich K, Nestle FO, Papp K, Ortonne JP, Evans R, Guzzo C, et al. Infliximab induction and maintenance therapy for moderate-to-severe psoriasis: a phase III, multicentre, double-blind trial. Lancet 2005;366:1367–74.
19. Menter A, Feldman SR, Weinstein GD, Papp K, Evans R, Guzzo C, et al. A randomized comparison of continuous vs. intermittent infliximab maintenance regimens over 1 year in the treatment of moderate-to-severe plaque psoriasis. J Am Acad Dermatol 2007;56:31.e1–15.
20. McInnes IB, Kavanaugh A, Gottlieb AB, Puig L, Rahman P, Ritchlin C, et al. Efficacy and safety of ustekinumab in patients with active psoriatic arthritis: 1 year results of the phase 3, multicentre, double-blind, placebo-controlled PSUMMIT 1 trial. Lancet 2013;382:780–9.
21. Gladman DD, Mease PJ, Ritchlin CT, Choy EH, Sharp JT, Ory PA, et al. Adalimumab for long-term treatment of psoriatic arthritis: forty-eight week data from the adalimumab effectiveness in psoriatic arthritis trial. Arthritis Rheum 2007;56:476–88.
22. Mease P, Genovese MC, Gladstein G, Kivitz AJ, Ritchlin C, Tak PP, et al. Abatacept in the treatment of patients with psoriatic arthritis: results of a six-month, multicenter, randomized, double-blind, placebo-controlled, phase II trial. Arthritis Rheum 2011;63:939–48.
23. Wu JJ. Brodalumab, an anti-IL17RA monoclonal antibody, for psoriasis and psoriatic arthritis. J Psoriasis Psoriatic Arthritis 2016;1:91.
24. Singh JA, Guyatt G, Ogdie A, Gladman DD, Deal C, Deodhar A, et al. 2018 American College of Rheumatology/National Psoriasis Foundation guideline for the treatment of psoriatic arthritis. Arthritis Care Res (Hoboken) 2019;71:2–29.
25. Ibrahim G, Waxman R, Helliwell PS. The prevalence of psoriatic arthritis in people with psoriasis. Arthritis Rheum 2009;61:1373–8.
26. Henes JC, Ziupa E, Eisfelder M, Adamczyk A, Knaudt B, Jacobs F, et al. High prevalence of psoriatic arthritis in dermatological patients with psoriasis: a cross-sectional study. Rheumatol Int 2014;34:227–34.
27. Carneiro JN, de Paula AP, Martins GA. Psoriatic arthritis in patients with psoriasis: evaluation of clinical and epidemiological features in 133 patients followed at the University Hospital of Brasília. An Bras Dermatol 2012;87:539–44.
28. Li R, Sun J, Ren LM, Wang HY, Liu WH, Zhang XW, et al. Epidemiology of eight common rheumatic diseases in China: a large-scale cross-sectional survey in Beijing. Rheumatology (Oxford) 2012;51:721–9.
29. Jamshidi F, Bouzari N, Seirafi H, Farnaghi F, Firooz A. The prevalence of psoriatic arthritis in psoriatic patients in Tehran, Iran. Arch Iran Med 2008;11:162–5.
30. Love TJ, Gudbjornsson B, Gudjonsson JE, Valdimarsson H. Psoriatic arthritis in Reykjavik, Iceland: prevalence, demographics, and disease course. J Rheumatol 2007;34:2082–8.
31. Khraishi M, Chouela E, Bejar M, Landells I, Hewhook T, Rampakakis E, et al. High prevalence of psoriatic arthritis in a cohort of patients with psoriasis seen in a dermatology practice. J Cutan Med Surg 2012;16:122–7.
32. Alamanos Y, Papadopoulos NG, Voulgari PV, Siozos C, Psychos DN, Tympanidou M, et al. Epidemiology of psoriatic arthritis in northwest Greece, 1982–2001. J Rheumatol 2003;30:2641–4.
33. Chandran V, Raychaudhuri SP. Geoepidemiology and environmental factors of psoriasis and psoriatic arthritis [review]. J Autoimmun 2010;34:J314–21.
34. Eder L, Haddad A, Rosen CF, Lee KA, Chandran V, Cook R, et al. The incidence and risk factors for psoriatic arthritis in patients with psoriasis: a prospective cohort study. Arthritis Rheumatol 2016;68:915–23.
35. Ogdie A, Langan S, Love T, Haynes K, Shin D, Seminara N, et al. Prevalence and treatment patterns of psoriatic arthritis in the UK. Rheumatology (Oxford). 2013;52:568–75.

American College of Rheumatology
Empowering Rheumatology Professionals

Arthritis & Rheumatology
Vol. 74, No. 2, February 2022, pp 244–252
DOI 10.1002/art.41923

Risk of Inflammatory Bowel Disease in Patients With Psoriasis and Psoriatic Arthritis/Ankylosing Spondylitis Initiating Interleukin-17 Inhibitors: A Nationwide Population-Based Study Using the French National Health Data System

Laetitia Penso,[1] Christina Bergqvist,[2] Antoine Meyer,[3] Philippe Herlemont,[4] Alain Weill,[4] Mahmoud Zureik,[5] Rosemary Dray-Spira,[4] and Emilie Sbidian[6]

Objective. To investigate whether the initiation of treatment with an interleukin-17 inhibitor (IL-17i) in real life is associated with a higher risk of inflammatory bowel disease (IBD) in patients who had both psoriasis (PsO) and psoriatic arthritis (PsA)/ankylosing spondylitis (AS).

Methods. This nationwide cohort study was conducted using the French National Health Data System database. All adult patients with PsO and PsA/AS who were identified as having newly initiated treatment with an IL-17i during 2016–2019 were included. As controls, patients with PsO and PsA/AS who had newly initiated either 1) apremilast or 2) etanercept (ETN) during this period but had not received IL-17i were included. The follow-up end date was September 30, 2019. The primary end point was the risk of occurrence of IBD associated with exposure to an IL-17i compared to exposure to the other treatments, as determined in a time-to-event analysis with propensity score–weighted Cox and Fine-Gray proportional hazards models.

Results. The study included a total of 16,793 new IL-17i users (mean ± SD age 48.4 ± 13 years, 45% men), 20,556 new apremilast users (age 52.6 ± 15 years, 54% men), and 10,294 new ETN users (age 46.3 ± 15 years, 44% men). New IL-17i users and new ETN users had received more biologics for their underlying disease compared to new apremilast users. IBD occurred in 132 patients: 72 new IL-17i users (0.43%), 11 new apremilast users (0.05%), and 49 new ETN users (0.48%). Most IBD cases occurred after 6 months of exposure (82%, 55%, and 76%, respectively). After propensity score weighting, the risk of IBD was significantly greater among patients initiating an IL-17i compared to those initiating apremilast (weighted hazard ratio [HR] 3.8 [95% confidence interval (95% CI) 2.1–6.8]). No difference in the risk of IBD between new IL-17i users and new ETN users was observed (weighted HR 0.8 [95% CI 0.5–1.2]).

Conclusion. Patients with PsO and PsA/AS who initiate treatment with an IL-17i do not have a higher risk of developing IBD when compared to patients initiating ETN who display the same severity of underlying disease. These results need to be confirmed in other large studies of patients with PsO and PsA/AS.

INTRODUCTION

Psoriasis (PsO) and inflammatory arthritis, including psoriatic arthritis (PsA) and ankylosing spondylitis (AS), are chronic immune-mediated inflammatory disorders that can significantly alter an individual's quality of life (1). Although there is no cure for these conditions, insights about their pathogenesis have led to the development of cytokine-based therapies that have revolutionized disease management. Since the interleukin-23 (IL-23)/Th17 immune axis plays a crucial role in the pathogenesis of both

[1]Laetitia Penso, MSc: EPI-PHARE and Université Paris Est Créteil, Paris, France; [2]Christina Bergqvist, MD: EPI-PHARE and Henri Mondor Hôpital, AP-HP, Paris, France; [3]Antoine Meyer, MD, MSc: EPI-PHARE, Hôpital Bicêtre, AP-HP, and Université Paris Sud, Paris, France; [4]Philippe Herlemont, MSc, Alain Weill, MD, Rosemary Dray-Spira, MD, PhD: EPI-PHARE, Paris, France; [5]Mahmoud Zureik, MD, PhD: EPI-PHARE, Université Paris-Saclay, Université de Versailles Saint-Quentin-en-Yvelines, Université Paris-Sud, INSERM, and Centre d'Etude des Supports de Publicité, Paris, France; [6]Emilie Sbidian, MD, PhD: EPI-PHARE, Université Paris Est Créteil, Centre d'Investigation Clinique 1430, and Henri Mondor Hôpital, AP-HP, INSERM, Paris, France.

Ms. Penso and Dr. Bergqvist contributed equally to this work.

Author disclosures are available at https://onlinelibrary.wiley.com/action/downloadSupplement?doi=10.1002%2Fart.41923&file=art41923-sup-0001-Disclosureform.pdf.

Address correspondence to Emilie Sbidian, MD, PhD, Department of Dermatology, Henri Mondor Hospital, 51 Avenue du Maréchal de Lattre de Tassigny, Paris Cedex 94010, France. Email: emilie.sbidian@aphp.fr.

Submitted for publication January 21, 2021; accepted in revised form July 8, 2021.

PsO and PsA/AS, there has been interest in targeting this pathway for treatment (2–5). Indeed, commercial IL-17 inhibitors (IL-17i), namely secukinumab (SEC), ixekizumab, and brodalumab, have emerged as some of the most efficacious biologics for moderate-to-severe PsO and PsA/AS (6–12). Both SEC and ixekizumab work by inhibiting IL-17A, while brodalumab blocks the IL-17 receptor, thereby blocking all IL-17 isoforms.

Epidemiology studies have established strong associations between PsO/PsA/AS and inflammatory bowel disease (IBD), with an increased risk of Crohn's disease (CD) and ulcerative colitis (UC) in patients with PsO and PsA/AS, and an increased risk of PsO and PsA/AS in patients with CD or UC (13–15). IBD occurs in 1% of patients with PsO, which is ~4 times more frequent than in the general population, with the highest risk occurring in patients with PsA/AS (13,16). PsO and PsA/AS share common genetic susceptibility loci and pathologic mechanisms with IBD, including several immune-signaling and cytokine pathways (17). Therefore, many drugs have been approved to manage both PsO/PsA/AS and IBD (18). These include anti–tumor necrosis factor (anti-TNF) therapy and anti–IL-12/IL-23 antibody therapy (19,20). The immune pathways of PsO and IBD also share the IL-23/Th17 axis (21). However, IL-17i treatments have been reported to exacerbate or trigger new-onset IBD in patients with PsO (6–8). Additionally, clinical trials of IL-17i in IBD were unsuccessful and were terminated early due to worse clinical outcomes with IL-17i than with placebo (22,23).

Information regarding the risk of new-onset IBD among patients with PsO exposed to IL-17i is primarily based on a limited number of observations in trials and case reports, and very few observational studies have evaluated the risk of IBD among patients with PsO who are exposed to IL-17i (24–26). Thus, future large studies are needed to quantify the comparative risk of IBD associated with IL-17i in patients with PsO and PsA/AS outside the restricted scope of randomized controlled trials (RCTs).

The purpose of this study was to investigate whether IL-17i initiation is associated with a higher risk of IBD in a large and comprehensive French general population of patients with PsO and patients with PsA/AS, as compared to patients with PsO and PsA/AS who initiated treatment with apremilast or etanercept (ETN).

PATIENTS AND METHODS

Data source and study design. This French nationwide cohort study used administrative health data obtained from the French National Health Data System (Système National des Données de Santé [SNDS]), which covers ~99% of the French population (~67 million individuals) and includes comprehensive data on ambulatory care and hospitalizations since 2006, as previously described (27,28). This large database has been used in several pharmacoepidemiology studies (28–31). The SNDS contains the following information on each individual patient: sociodemographic characteristics (age, sex); vital status; attribution of long-term disease status allowing full coverage of all relevant medical costs for a renewable 5-year period; outpatient care, including the number of units and date of reimbursement for drug dispensation, date and nature of medical and paramedical interventions, and date of laboratory tests; and any hospitalization in a public or private French hospital (admission date, stay duration, discharge diagnoses according to International Statistical Classification of Diseases and Related Health Problems, Tenth Revision [ICD-10] codes for the main, related, or accompanying diagnoses and medical procedures).

The French public institution in which this study was conducted has permanent access to the SNDS database in accordance with the provisions of the French Public Health Code (article R. 1461-12 et seq.) and with approval from the French data protection authority (approval no. CNIL-2016-316). Therefore, no informed consent was required.

Study population and follow-up. All adult patients age ≥18 years for whom an IL1-7i, apremilast, or ETN was newly prescribed for treatment of PsO or PsA/AS at least once between July 1, 2016 and May 31, 2019 were eligible for study inclusion. We selected patients who had not filled a prescription for an IL-17i, apremilast, or ETN within 2 years before the study start (i.e., those previously naive to treatment [new users]). Among these patients, the index date was established as the date of first reimbursement for an IL-17i, apremilast, or ETN during the study period. Patients were followed up to the date of occurrence of the IBD event, occurrence of death from any cause, switch to a different systemic treatment, loss to follow-up (defined as no reimbursement for 12 consecutive months), or September 30, 2019, whichever came first.

In identifying the study population, we excluded patients with rheumatoid arthritis (RA) who were diagnosed within 5 years before the index date, with the diagnosis defined according to whether they had at least 1 hospital discharge or long-term disease diagnosis code relevant to RA (ICD-10 codes M05, M06, M08, or M09). In addition, we excluded patients with CD or UC who were diagnosed within 5 years prior to the index date. These patients were identified based on having least 1 hospital discharge or long-term disease diagnosis code relevant to CD or UC (ICD-10 codes K50 or K51) and having filled a prescription for 1 of the following drugs within the 5 years preceding the index date: aminosalicylic acid (product no. A07EC), mesalamine (ATC code A07EC02), olsalazine (product no. A07EC03), enteral budesonide (ATC code A07A06), azathioprine (ATC code L04AX01), mercaptopurine (ATC code L01BB02), or vedolizumab (ATC code L04AA33).

Underlying diseases in the study population. For the criteria used to classify patients according to underlying diseases (PsO, PsO/PsA, or PsA/AS), see Supplementary Table 1 (available on the *Arthritis & Rheumatology* website at http://onlinelibrary.

wiley.com/doi/10.1002/art.41923/abstract). Classification of patients was based on the specialty of the prescriber, the attribution of long-term disease status, and specific drugs.

Definition of the unexposed population. As stated above, patients with PsO and patients with PsA/AS are at an increased risk of developing IBD. This increased risk is all the more important as the underlying condition is severe (13). Therefore, we defined the unexposed populations (i.e., patients not initiating treatment with an IL-17i) according to the following 2 important criteria: 1) the severity of PsO and PsA/AS had to be comparable to that in exposed patients (i.e., patients receiving systemic treatment with an IL-17i), and 2) any systemic therapy being initiated should not be indicated for the treatment of IBD, and therefore patients receiving ustekinumab or anti–tumor necrosis factor (anti-TNF) agents (except ETN) were excluded. Indeed, an effective treatment for IBD prescribed for another indication could mask gastrointestinal symptoms and delay the diagnosis of IBD. Both ETN and apremilast were considered to be good candidate systemic therapies because they are frequently indicated for the treatment of moderate-to-severe PsO/PsA/AS and PsO/PsA, respectively.

As the first unexposed population, we chose patients who were started on treatment with apremilast, since apremilast was marketed for PsO/PsA and was commercialized in France during the same time period as IL-17i therapies; this allowed us to minimize selection bias. It is important to note that apremilast is not associated with a higher risk of IBD among patients with chronic inflammatory diseases (24). In addition, for a post hoc analysis, we chose a second unexposed population, comprising patients with PsO and patients with PsA/AS who were started on treatment with ETN, since patients who initiated ETN as a first-line biologic treatment had a level of disease severity at baseline that was comparable to that seen in patients who initiated other anti-TNF agents (32,33). Therefore, the underlying disease in patients taking ETN should be similar in severity to that in patients taking an IL-17i.

Definition of exposure. For the exposed population (i.e., those who were started on IL-17i therapy), the IL-17i treatments included SEC, ixekizumab, and brodalumab. Each of these drugs was identified according to the World Health Organization Anatomical Therapeutic Chemical classification codes.

The duration of exposure to the IL17i or to any other systemic treatment was considered to be from the time of treatment initiation to the time of discontinuation. We defined discontinuation of treatment as 1) a period of >90 days without dispensation of the same treatment after the time period covered by the previous reimbursement (34) or 2) a patient switching to a different systemic treatment. The time period covered by a prescription was 30 days for all systemic treatments. The discontinuation date was defined as the end of the 90-day period, and the switch date was defined as the date on which another systemic treatment was first reimbursed. Only the first therapeutic sequence of IL-17i, apremilast, or ETN was considered in this analysis.

Definition of the outcome. The primary end point was the occurrence of an IBD, either CD or UC. Events were identified by either 2 hospital discharge diagnoses of CD or UC (ICD-10 codes K50 and K51, respectively), by attribution of a long-term IBD disease status after the index date, or 1 hospital discharge diagnosis and a prescription filled for 1 of the following drugs: aminosalicylic acid, mesalamine, olsalazine, enteral budesonide, azathioprine, mercaptopurine, or vedolizumab.

Covariates. Covariates at baseline included age, sex, and comorbidities (diabetes, hypertension, dyslipidemia, chronic obstructive pulmonary disease, acute myocardial infarction, ischemic stroke, chronic renal failure, cancer, hepatic insufficiency/cirrhosis, and hepatitis B, hepatitis C, and HIV infections). We also considered the number of gastrointestinal medications taken by the patients in the year preceding the index date, excluding the month preceding the index date, the number of colonoscopies and other imaging of the gastrointestinal tract in the year preceding the index date, and the number of hospital admissions in the 6 months preceding the index date, as well as the number and type of other PsO and PsA treatments (cyclosporine, methotrexate, anti-TNF agents, anti–IL-12/IL-23, nonsteroidal antiinflammatory drugs [NSAIDs], topical treatments, and systemic glucocorticoids) in the 2 years preceding the index date. For definitions of covariates, see Supplementary Table 2 (available on the *Arthritis & Rheumatology* website at http://onlinelibrary.wiley.com/doi/10.1002/art.41923/abstract).

Statistical analysis. For descriptions of the study population, categorical data are reported as the number and percentage of patients. Quantitative data are reported as the median and interquartile range (IQR) or the mean ± SD.

For the primary analysis, we calculated cause-specific Cox proportional hazards regression models to estimate the hazard ratio (HR) and 95% confidence interval (95% CI) for the occurrence and risk of IBD associated with exposure to an IL-17i, with apremilast or ETN used as the reference group. The proportional hazards model assumption was formally tested by using Schoenfeld residuals. To control for confounding by baseline covariates, weighted HR values were adjusted by using inverse probability of treatment weighting (IPTW). Weights were based on the propensity score, which was estimated using a multinomial logistic regression analysis including the covariates collected at the index date. Stabilized weights were calculated to preserve the sample size of the original data and produce an appropriate estimation of the main effect variance (35). The balance in baseline covariates was compared to standardized differences before and after weighting of the data. Age, sex, use of biologic agents, nonbiologic systemic glucocorticoids, and systemic glucocorticoids in the

2 years preceding the index date, number of comorbidities among those listed above (none, 1, or ≥2), and undergoing a colonoscopy in the 5 years preceding the index date were included in the propensity score. We performed prespecified subgroup analyses in patients who had not received a biologic agent in the 2 years preceding the index date and other subgroup analyses in patients with a diagnosis of exclusively either PsO, PsO/PsA, or PsA/AS.

To assess the sensitivity of the estimated weighted HR with respect to several possible models, we performed the following additional analyses: 1) a Fine-Gray competing risks analysis in which we determined the IPTW subhazard ratios to account for the competing risks between all-cause death and hospitalization for IBD; 2) a conventional multivariate Cox model in which we adjusted the HRs for the presence of covariates, including adjusted HRs for sex, comorbidities, colonoscopy, nonbiologic systemic treatment, systemic glucocorticoid treatments, and biologic treatments (i.e., the same covariates included in the propensity score); 3) modification of the outcome definition in which we applied a broader definition of IBD, i.e., either 1 pertinent hospital discharge diagnosis code for an IBD or as an attribution of a long-term IBD disease status after the index date; and 4) a model in which we defined treatment discontinuation as >60 days or >120 days without filling a prescription for the same

Table 1. Demographic and clinical characteristics of the patients with PsO and PsA/AS included in the 3 cohorts of newly treated patients*

	IL-17i (n = 16,793)	Apremilast (n = 20,556)	ETN (n = 10,294)
Follow-up, median (IQR) days	323 (199–605)	212 (129–390)	276 (171–536)
Sociodemographic characteristics			
Age, mean ± SD years	48.4 ± 13	52.6 ± 15	46.3 ± 15
Sex, male	7,612 (45)	11,009 (54)	4,534 (44)
Previous drug exposure†			
None	688 (4)	2,249 (11)	841 (8)
No biologic treatments	4,394 (26)	19,533 (95)	7,464 (72.5)
Cyclosporine	417 (2)	309 (2)	86 (1)
MTX	5,844 (35)	5,305 (26)	2,741 (27)
Infliximab	1,911 (11)	116 (1)	296 (3)
ADA	5,551 (33)	437 (2)	1,900 (18)
ETN	4,416 (26)	355 (2)	–
GOL	2,605 (16)	94 (1)	572 (6)
Certolizumab	2,085 (12)	70 (1)	374 (4)
UST	2,360 (14)	266 (1)	90 (1)
Topical treatments	5,040 (30)	13,935 (68)	1,181 (11)
NSAIDs	13,392 (80)	12,959 (63)	8,569 (83)
Systemic steroids	9,255 (55)	8,591 (42)	5,823 (57)
No. of GI medications, mean ± SD‡	3.8 ± 4.7	3.1 ± 4.1	1.7 ± 3.5
No. of hospital admissions, mean ± SD§	4.2 ± 6.1	2.9 ± 7.8	1.4 ± 1.0
Comorbidities			
Hepatic insufficiency/cirrhosis	69 (0.4)	94 (0.5)	21 (0.2)
Hepatitis B or C infection	43 (0.3)	80 (0.4)	31 (0.3)
HIV infection	25 (0.1)	58 (0.3)	38 (0.4)
COPD	90 (0.5)	169 (0.8)	47 (0.5)
Chronic renal failure	40 (0.2)	85 (0.4)	66 (0.6)
Hypertension	2,145 (13)	2,785 (14)	1,461 (14)
Acute myocardial infarction or ischemic stroke	526 (3)	976 (5)	263 (3)
Cancer	442 (3)	1,473 (7)	318 (3)
Diabetes	1,327 (8)	2,242 (11)	700 (7)
Dyslipidemia	1,529 (9)	3,107 (15)	1,019 (10)
Underlying diseases			
PsO exclusively	2,135 (13)	12,284 (60)	466 (5)
PsA/AS	8,668 (52)	1,880 (9)	6,033 (59)
Both PsO and PsA	5,990 (36)	6,392 (31)	3,795 (37)

* Except where indicated otherwise, values are the number (%) of patients. PsO = psoriasis; PsA = psoriatic arthritis; AS = ankylosing spondylitis; IL-17i = interleukin-17 inhibitor; ETN = etanercept; IQR = interquartile range; MTX = methotrexate; ADA = adalimumab; GOL = golimumab; UST = ustekinumab; NSAIDs = nonsteroidal antiinflammatory drugs; COPD = chronic obstructive pulmonary disease.
† Exposure during the 2 years before the index date.
‡ Number of gastrointestinal (GI) medications delivered in the year preceding the index date, excluding the month preceding the index date.
§ Hospital admissions during the 6 months preceding the index date.

treatment after the time period covered by the previous prescription.

P values less than 0.05 were considered significant. All analyses were performed using the SAS Enterprise Guide version 7.1.

Data availability. Access to data generated in this study is available upon request from the corresponding author.

RESULTS

Description of the cohort population. A total of 47,643 PsO patients and PsA/AS patients (mean ± SD age 49.7 ± 14.7 years, 49% men) were identified. After excluding patients with IBD, there were 16,793 new IL-17i users (age 48.4 ± 13 years, 45% men; median follow-up 323 days [IQR 199–605]), including 15,162 patients (90%) initiating SEC, 1,477 patients (9%) initiating ixekizumab, and 154 patients (1%) initiating brodalumab. For the other treatment groups, there were 20,556 new apremilast users (age 52.6 ± 15 years, 54% men; median follow-up 212 days [IQR 129–390]), and 10,294 new ETN users (age 46.3 ± 15 years, 44% men; median follow-up 276 days [IQR 171–536]) (Table 1 and Figure 1).

The demographic and clinical characteristics of the patients in the IL-17i, ETN, and apremilast cohorts are shown in Table 1. Patients initiating IL-17i or ETN were younger and were mostly women, were mostly diagnosed as having PsA/AS, and had fewer comorbidities than new apremilast users. The majority of new IL-17i users (71%) received a biologic treatment during the 2 years preceding the index date, compared to 7% of new apremilast users and 27% of new ETN users. Among new IL-17i users, 80% received NSAIDs, 55% received systemic steroids, 35% received methotrexate, 30% received topical treatments, and 2% received cyclosporine during the 2 years preceding the index date. The proportions of new apremilast users and new ETN users receiving NSAIDs, systemic steroids, methotrexate, topical treatments, and cyclosporine in this same time period were 63%, 42%, 26%, 68%, and 2%, respectively, and 83%, 57%, 27%, 11%, and 1%, respectively.

Association of treatment exposure and IBD. During follow-up, we identified 72 new cases of IBD in new IL-17i users (0.43%), 11 new cases of IBD in new apremilast users (0.05%) (crude HR 6.3 [95% CI 3.3–11.9] relative to new IL-17i users), and 49 new cases of IBD in new ETN users (0.48%) (crude HR 0.8 [95% CI 0.5–1.2] relative to new IL-17i users). Among all 3 treatment groups, most of the IBD cases occurred after 6 months of exposure (new IL-17i users, 59 IBD cases [82%]); new apremilast users, 6 IBD cases [55%]; new ETN users, 37 IBD cases [76%]). The incidence rates for the development of IBD were 3.68 cases per 1,000 person-years (95% CI 2.83–4.53) in new IL-17i users, 0.64 cases per 1,000 person-years (95% CI 0.26–1.02) in new apremilast users, and 2.81 cases per 1,000 person-years (95% CI 2.02–3.60) in new ETN users.

Stabilized propensity scores were applied to the treatment groups to adjust for baseline covariates. With propensity score weighting, we obtained pseudo-cohorts in which the distribution of variables was similar, as indicated by a standardized difference of <0.1 in new IL-17i users compared to new apremilast users or

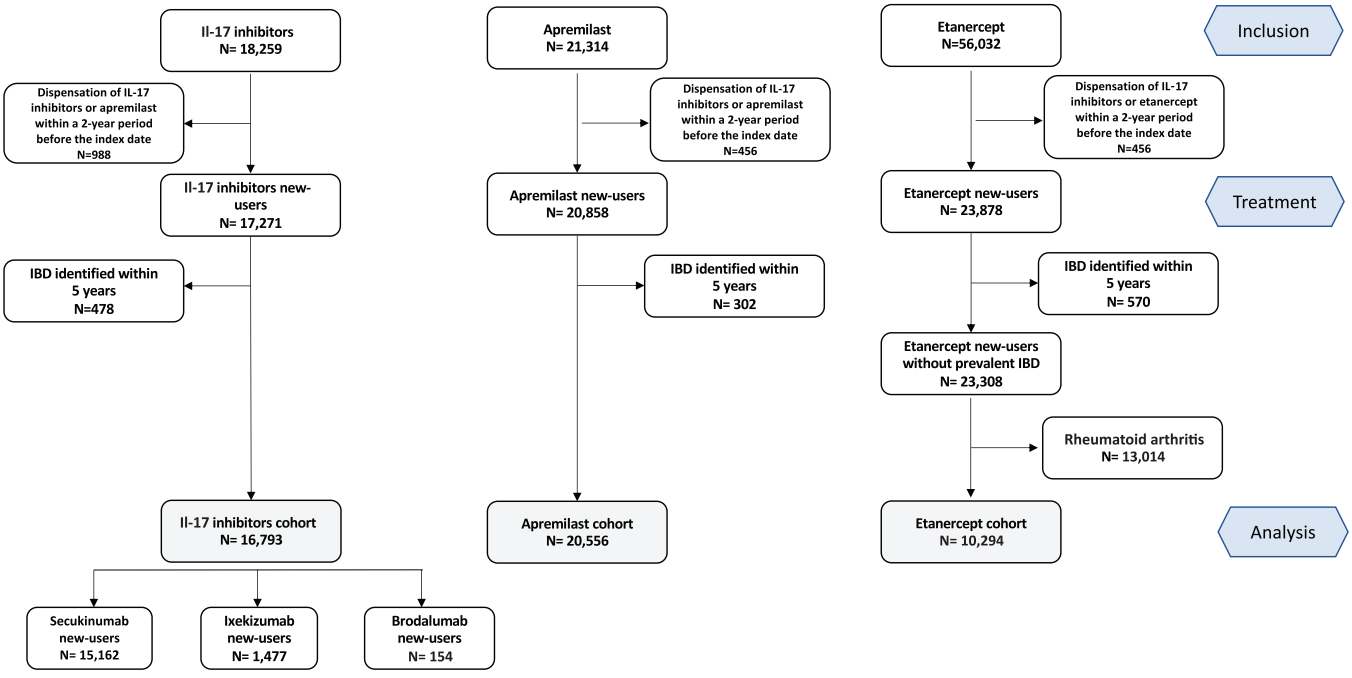

Figure 1. Flow chart showing the number of patients with psoriasis and psoriatic arthritis/ankylosing spondylitis assigned to receive either an interleukin-17 inhibitor (IL-17i), apremilast, or etanercept. IBD = inflammatory bowel disease.

Table 2. Incidence and risk of IBD in patients with psoriasis and psoriatic arthritis/ankylosing spondylitis who were unexposed or newly exposed to an IL-17i and had not received treatment with either apremilast or ETN

	Unexposed to apremilast		Unexposed to ETN	
	Incidence or risk of IBD	*P*	Incidence or risk of IBD	*P*
No. of IBD events/no. of individuals at risk				
IL-17i exposed	72/16,793	–	47/12,377*	–
Unexposed to IL-17i	11/20,556	–	49/10,294	–
Risk of IBD with IL-17i exposure				
Crude analysis, RR (95% CI)†	6.3 (3.3–11.9)	<0.0001	0.8 (0.5–1.2)	0.26
Propensity score analyses with inverse probability weighting, HR (95% CI)‡	3.8 (2.1–6.8)	<0.0001	0.8 (0.5–1.2)	0.30
Fine-Gray analysis, subhazard ratio (95% CI)§	3.8 (2.1–6.8)	<0.0001	0.8 (0.5–1.2)	0.30
Conventional multivariate Cox analysis, HR (95% CI)¶	3.9 (2.0–7.4)	<0.0001	0.7 (0.5–1.1)	0.14

* New interleukin-17 inhibitor (IL-17i) users with a previous 2-year exposure to etanercept (ETN) were removed from this analysis of the incidence and risk of inflammatory bowel disease (IBD).
† Crude analysis used cause-specific Cox proportional hazards regression models to estimate the relative risk (RR) with 95% confidence interval (95% CI) for the risk of IBD associated with exposure to an IL-17i.
‡ Propensity score–adjusted analyses were used to calculate the hazard ratio (HR) with 95% CIs for the risk of IBD associated with new exposure to an IL-17i from the multivariable Cox proportional hazards model with inverse probability weighting according to the propensity score (including the following covariables: sex, comorbidities, colonoscopy, use of nonbiologic systemic treatment, use of systemic glucocorticoids, and use of biologic treatments).
§ The Fine-Gray model was used to calculate the subhazard ratio with 95% CI for the risk of IBD associated with new exposure to an IL-17i from the multivariable conditional Fine-Gray regression model with inverse probability weighting according to the propensity score–adjusted analysis.
¶ A conventional multivariate Cox regression model was used to calculate the HR with 95% CI for the risk of IBD associated with new exposure to an IL-17i, with the same covariates included in the propensity score.

new ETN users (see Supplementary Figures 1 and 2, available on *Arthritis & Rheumatology* website at http://onlinelibrary.wiley.com/doi/10.1002/art.41923/abstract).

The results of the main analysis are shown in Table 2. The risk of IBD was significantly higher (overall $P < 0.0001$) with exposure to IL-17i compared to exposure to apremilast (weighted HR 3.8 [95% CI 2.1–6.8]). New IL-17i users were 4 times more likely to develop CD than new apremilast users (weighted HR 4.0 [95% CI 2.0–8.1], $P < 0.0001$) and were 2 times more likely to develop UC (weighted HR 2.0 [95% CI 1.0–4.3]; $P = 0.0583$), although the latter result was not statistically significant. No differences in the risk of IBD between new IL-17i users and new ETN users were observed (weighted HR 0.8 [95% CI 0.5–1.2]; $P = 0.30$).

Subgroup analyses. In subgroup analyses restricted to patients with a single diagnosis or restricted to patients who were naive to treatment with biologic agents, some differences in the risk of IBD were observed. Among patients with PsO, new IL-17i users were 8 times more likely to develop IBD than new apremilast users (weighted HR 8.3 [95% CI 2.8–25.0]). Among patients with PsA/AS, no differences in the risk of IBD were observed between new IL-17i users and new apremilast users (weighted HR 1.3 [95% CI 0.5–3.5]) (Table 3). No differences between new IL-17i users and new ETN users were observed, regardless of the underlying disease (Table 4).

Sensitivity analyses. Using the broader definition of IBD, a total of 173 new cases of IBD were identified: 97 in new IL-17i users, 17 in new apremilast users, and 59 in new ETN users. Results of the sensitivity analysis using the broader definition of IBD, as well as results of the additional sensitivity analyses, were consistent with those of the main analysis with regard to the risk of IBD associated with new exposure to an IL-17i (Table 5).

Table 3. Association between new exposure to an IL-17i, as compared with new exposure to apremilast, and occurrence and risk of IBD, by diagnosis or biologic-naive status*

	PsO exclusively	PsA or AS exclusively	PsO or PsA	Biologic-naive
No. of IBD events/no. of individuals at risk				
New IL-17i user	8/2,131	38/8,668	26/5,990	13/4,394
New apremilast user	5/12,284	2/1,880	4/6,393	11/19,533
Risk of IBD in new IL-17i users, weighted HR (95% CI)†	8.3 (2.8–25)	1.3 (0.5–3.5)	3.5 (1.3–9.7)	3.0 (1.3–7.0)

* PsO = psoriasis; PsA = psoriatic arthritis; AS = ankylosing spondylitis.
† The weighted hazard ratio (HR) with 95% confidence interval (95% CI) for the risk of inflammatory bowel disease (IBD) in new interleukin-17 inhibitor (IL-17i) users compared with new apremilast users was calculated from the multivariable Cox proportional hazards model with inverse probability weighting according to the propensity score (including the following covariables: sex, comorbidities, colonoscopy, use of nonbiologic systemic treatment, systemic glucocorticoids, and biologic treatments).

Table 4. Association between new exposure to an IL-17i, as compared with new exposure to ETN, and occurrence and risk of IBD, by diagnosis and biologic-naive status*

	PsO exclusively	PsA or AS exclusively	PsO or PsA	Biologic-naive
No. of IBD events/no. of individuals at risk				
New IL-17i user†	7/1,658	21/4,835	19/5,884	13/4,394
New ETN user	0/466	31/6,033	18/3,795	37/7,464
Risk of IBD in new IL-17i users, weighted HR (95% CI)‡	4.1 (0.2–89.5)	0.8 (0.5–1.5)	0.7 (0.3–1.3)	0.6 (0.3–1.1)

* PsO = psoriasis; PsA = psoriatic arthritis; AS = ankylosing spondylitis.
† New interleukin-17 inhibitor (IL-17i) users with a previous 2-year exposure to etanercept (ETN) were removed from this analysis.
‡ The weighted hazard ratio (HR) with 95% confidence interval (95% CI) for the risk of inflammatory bowel disease (IBD) in new IL-17i users compared with new ETN users was calculated from the multivariable Cox proportional hazards model with inverse probability weighting according to the propensity score (including the following covariables: sex, comorbidities, colonoscopy, use of nonbiologic systemic treatment, systemic glucocorticoids, and biologic treatments).

DISCUSSION

In this nationwide PsO and PsA/AS cohort study involving 16,793 new IL-17i users, 20,556 new apremilast users, and 10,294 new ETN users with no history of IBD, the overall risk of IBD, after controlling for available confounding factors, was 4 times greater among new IL-17i users compared to new apremilast users. However, no difference between new IL-17i users and new ETN users was observed.

IBD pathogenesis involves an uncontrolled and excessive immune response against normal microbiota through the activation of CD4+ T helper cells (36). Th17 cells and related cytokines have recently been identified as fundamental mediators in both diseases (37). The implication of the IL-23/IL-17 axis in the pathogenesis of IBD prompted the clinical investigation of IL-17i treatments (brodalumab and SEC) in CD. Both trials demonstrated worsening CD at week 6 in patients receiving an IL-17i compared to patients receiving placebo, and therefore these trials were prematurely terminated (22,23). A possible explanation for this unexpected worsening disease could be attributed to the essential functions of IL-17 in the immune response against extracellular pathogens in the gut (38–40). Indeed, inhibiting IL-17 hinders its gut-protective function and interferes with its role in tissue homeostasis repair, thereby impairing intestinal wall integrity and exacerbating disease (41).

Table 5. Risk of IBD in new IL-17i users, as determined in sensitivity analyses using a Cox logistic regression model with IPTW*

	Time since treatment discontinuation		Broader definition of IBD
	60-day gap	120-day gap	
New IL-17i users, vs. new apremilast users			
HR	5.0	5.0	3.5
95% CI	2.8–9.0	2.8–9.0	2.1–5.7
P	0.0001	0.0001	0.0001
New IL-17i users, vs. new ETN users			
HR	0.8	0.8	0.9
95% CI	0.5–1.2	0.5–1.3	0.6–1.2
P	0.31	0.40	0.40

* Values are the hazard ratio (HR) with 95% confidence interval (95% CI) for the risk of inflammatory bowel disease (IBD) in new interleukin-17 inhibitor (IL-17i) users versus the other 2 treatment groups, as determined in separate sensitivity analyses adjusted by inverse probability treatment weighting (IPTW) for sex, comorbidities, colonoscopy, and use of nonbiologic systemic treatment, systemic glucocorticoids, and biologic treatments. ETN = etanercept.

In our study, we demonstrated that treatment with IL-17i was not associated with a higher risk of IBD when ETN was used as a comparator, whereas the risk of IBD was significantly greater with IL-17i than with apremilast. The severity of the underlying disease could explain such a difference between the 2 comparators. The demographic and clinical characteristics of the IL-17i population were more similar to those of the ETN population compared to those of the apremilast population, especially regarding the previous biologic treatments prescribed. Patients included in the IL-17i group or the ETN group most likely presented with more severe disease compared to patients taking apremilast. Thus, they were at a higher risk of developing an IBD (15,42).

A systematic review and meta-analysis of 38 RCTs evaluated the risk of new-onset IBD with the use of IL-17i in patients with PsO, PsA, AS, or RA. A total of 12 new IBD events (5 cases of CD and 7 cases of UC) were identified during the 60-week follow-up in 16,690 patients treated with IL-17i (43). This analysis did not identify a difference in the risk of developing new-onset IBD between patients taking IL-17i compared to those taking a placebo.

Another study pooled 21 RCTs including 7,355 patients treated with SEC. Fourteen cases of new-onset IBD were identified among 5,181 patients with PsO and 7 cases of new-onset IBD were identified among 1,380 patients with PsA, suggesting an overall low rate of IBD events in these patients. In the per-year analysis, the exposure-adjusted incidence rates did not increase over time with SEC treatment (44). Placebo was used as the comparator in these meta-analyses, but patients in the placebo group fulfilled the same inclusion criteria, including disease severity. However, a major limitation of these estimates of incidence rates across these trials is that they are based on a very limited number of cases of IBD.

To date, only 3 observational studies have investigated the risk of new-onset IBD in patients exposed to an IL-17i, some of which had serious limitations (24–26). In a case series from a single center in the US, incidence rates of CD and UC were explored among

patiens exposed to SEC and those exposed to ixekizumab (25). No UC or CD cases were identified in 80 ixekizumab-exposed patients, and only 1 new case of UC was identified among 142 SEC-exposed patients. The very small sample size and the lack of a control group were major limitations of this study. A claims-based study evaluated the incidence rates of IBD after IL-17i exposure among patients with PsO, PsA, RA, or AS (24). IL-17i treatment was associated with a nearly 3-fold higher risk of IBD. However, the comparator was apremilast, with the same limitations we highlighted regarding the severity of the disease. Another claims-based study of 1,821 patients with PsO exposed to IL-17i treatments demonstrated no significant difference in the odds of developing IBD at 6 months and 1 year between patients with PsO who were exposed to an IL-17i and patients with PsO who were unexposed (26). Most of these studies (both RCTs and observational studies) were limited by small sample sizes and/or a very limited number of outcome events.

Our cohort included a large number of patients from a national, comprehensive database, with quality control of coding, and with information captured during routine medical care. This framework minimizes selection bias. We identified a large number of outcome events. IBD diagnoses were identified using comprehensive data from the National Hospital Discharge database, in which outcomes were previously validated (45,46). Moreover, we used a new-user design (47) and applied a propensity score method to more accurately estimate the risk of IBD.

This study has several limitations. First, we defined drug exposure according to health care reimbursement data, which are not necessarily equivalent to days of use. However, in patients with PsO, adherence rates for biologic treatments are generally higher than those for other treatment categories (48). Second, although we applied a propensity score to reduce confounding bias, it was not completely neutralized. Indeed, our analyses are limited by the availability of data on PsO and PsA/AS activity, certain individual risk factors, and family history of IBD, as well as by the inability to account for over-the-counter NSAID use.

We have demonstrated in this study that treatment with an IL-17i is not associated with a higher risk of IBD in patients with PsO, PsA, or AS when taking into account the severity of the underlying disease, i.e., when using ETN as a comparator. However, these results need to be confirmed in studies using patient data from other large databases.

AUTHOR CONTRIBUTIONS

All authors were involved in drafting the article or revising it critically for important intellectual content, and all authors approved the final version to be published. Dr. Sbidian had full access to all of the data in the study and takes responsibility for the integrity of the data and the accuracy of the data analysis.

Study conception and design. Meyer, Weill, Zureik, Dray-Spira, Sbidian.
Acquisition of data. Penso, Herlemont, Sbidian.
Analysis and interpretation of data. Bergqvist, Meyer, Weill, Zureik, Dray-Spira, Sbidian.

REFERENCES

1. Dubertret L, Mrowietz U, Ranki A, van de Kerkhof PC, Chimenti S, Lotti T, et al. European patient perspectives on the impact of psoriasis: the EUROPSO patient membership survey. Br J Dermatol 2006;155: 729–36.
2. Veale DJ, Fearon U. The pathogenesis of psoriatic arthritis. Lancet 2018;391:2273–84.
3. Greb JE, Goldminz AM, Elder JT, Lebwohl MG, Gladman DD, Wu JJ, et al. Psoriasis [review]. Nat Rev Dis Primers 2016;2:16082.
4. Girolomoni G, Strohal R, Puig L, Bachelez H, Barker J, Boehncke WH, et al. The role of IL-23 and the IL-23/T_H 17 immune axis in the pathogenesis and treatment of psoriasis [review]. J Eur Acad Dermatol Venereol 2017;31:1616–26.
5. Feld J, Chandran V, Haroon N, Inman R, Gladman D. Axial disease in psoriatic arthritis and ankylosing spondylitis: a critical comparison [review]. Nat Rev Rheumatol 2018;14:363–71.
6. Langley RG, Elewski BE, Lebwohl M, Reich K, Griffiths CE, Papp K, et al. Secukinumab in plaque psoriasis: results of two phase 3 trials. N Engl J Med 2014;371:326–38.
7. Gordon KB, Blauvelt A, Papp KA, Langley RG, Luger T, Ohtsuki M, et al. Phase 3 trials of ixekizumab in moderate-to-severe plaque psoriasis. N Engl J Med 2016;375:345–56.
8. Lebwohl M, Strober B, Menter A, Gordon K, Weglowska J, Puig L, et al. Phase 3 studies comparing brodalumab with ustekinumab in psoriasis. N Engl J Med 2015;373:1318–28.
9. Mease PJ, van der Heijde D, Ritchlin CT, Okada M, Cuchacovich RS, Shuler CL, et al. Ixekizumab, an interleukin-17A specific monoclonal antibody, for the treatment of biologic-naive patients with active psoriatic arthritis: results from the 24-week randomised, double-blind, placebo-controlled and active (adalimumab)-controlled period of the phase III trial SPIRIT-P1. Ann Rheum Dis 2017;76:79–87.
10. Baeten D, Sieper J, Braun J, Baraliakos X, Dougados M, Emery P, et al. Secukinumab, an interleukin-17A inhibitor, in ankylosing spondylitis. N Engl J Med 2015;373:2534–48.
11. Van der Heijde D, Cheng-Chung WJ, Dougados M, Mease P, Deodhar A, Maksymowych WP, et al. Ixekizumab, an interleukin-17A antagonist in the treatment of ankylosing spondylitis or radiographic axial spondyloarthritis in patients previously untreated with biological disease-modifying anti-rheumatic drugs (COAST-V): 16 week results of a phase 3 randomised, double-blind, active-controlled and placebo-controlled trial. Lancet 2018;392: 2441–51.
12. Mease PJ, McInnes IB, Kirkham B, Kavanaugh A, Rahman P, van der Heijde D, et al. Secukinumab inhibition of interleukin-17A in patients with psoriatic arthritis. N Engl J Med 2015;373:1329–39.
13. Egeberg A, Jemec GB, Kimball AB, Bachelez H, Gislason GH, Thyssen JP, et al. Prevalence and risk of inflammatory bowel disease in patients with hidradenitis suppurativa. J Invest Dermatol 2017;137:1060–4.
14. Stolwijk C, Boonen A, van Tubergen A, Reveille JD. Epidemiology of spondyloarthritis [review]. Rheum Dis Clin North Am 2012;38:441–76.
15. Charlton R, Green A, Shaddick G, Snowball J, Nightingale A, Tillett W, et al. Risk of uveitis and inflammatory bowel disease in people with psoriatic arthritis: a population-based cohort study. Ann Rheum Dis 2018;77:277–80.
16. Eppinga H, Poortinga S, Thio HB, Nijsten TE, Nuij VJ, van der Woude CJ, et al. Prevalence and phenotype of concurrent psoriasis and inflammatory bowel disease. Inflamm Bowel Dis 2017;23:1783–9.
17. Fiorino G, Omodei PD. Psoriasis and inflammatory bowel disease: two sides of the same coin? [editorial]. J Crohns Colitis 2015;9:697–8.
18. Whitlock SM, Enos CW, Armstrong AW, Gottlieb A, Langley RG, Lebwohl M, et al. Management of psoriasis in patients with inflammatory bowel disease: from the medical board of the National Psoriasis Foundation [review]. J Am Acad Dermatol 2018;78:383–94.

19. Colombel JF, Sandborn WJ, Rutgeerts P, Enns R, Hanauer SB, Panaccione R, et al. Adalimumab for maintenance of clinical response and remission in patients with Crohn's disease: the CHARM trial. Gastroenterology 2007;132:52–65.
20. Feagan BG, Sandborn WJ, Gasink C, Jacobstein D, Lang Y, Friedman JR, et al. Ustekinumab as induction and maintenance therapy for Crohn's disease. N Engl J Med 2016;375:1946–60.
21. Gooderham MJ, Papp KA, Lynde CW. Shifting the focus - the primary role of IL-23 in psoriasis and other inflammatory disorders [review]. J Eur Acad Dermatol Venereol 2018;32:1111–9.
22. Targan SR, Feagan B, Vermeire S, Panaccione R, Melmed GY, Landers C, et al. A randomized, double-blind, placebo-controlled phase 2 study of brodalumab in patients with moderate-to-severe Crohn's disease. Am J Gastroenterol 2016;111:1599–607.
23. Hueber W, Sands BE, Lewitzky S, Vandemeulebroecke M, Reinisch W, Higgins PD, et al. Secukinumab, a human anti-IL-17A monoclonal antibody, for moderate to severe Crohn's disease: unexpected results of a randomised, double-blind placebo-controlled trial. Gut 2012;61:1693–700.
24. Emond B, Ellis LA, Chakravarty SD, Ladouceur M, Lefebvre P. Real-world incidence of inflammatory bowel disease among patients with other chronic inflammatory diseases treated with interleukin-17a or phosphodiesterase 4 inhibitors. Curr Med Res Opin 2019;35:1751–9.
25. Orrell KA, Murphrey M, Kelm RC, Lee HH, Pease DR, Laumann AE, et al. Inflammatory bowel disease events after exposure to interleukin 17 inhibitors secukinumab and ixekizumab: postmarketing analysis from the RADAR ("Research on Adverse Drug events And Reports") program. J Am Acad Dermatol 2018;79:777–8.
26. Wright S, Alloo A, Strunk A, Garg A. Real-world risk of new-onset inflammatory bowel disease among patients with psoriasis exposed to interleukin 17 inhibitors. J Am Acad Dermatol 2020;83:382–7.
27. Tuppin P, Rudant J, Constantinou P, Gastaldi-Ménager C, Rachas A, de Roquefeuil L, et al. Value of a national administrative database to guide public decisions: from the système national d'information interrégimes de l'Assurance Maladie (SNIIRAM) to the système national des données de santé (SNDS) in France. Rev Epidemiol Sante Publique 2017;65 Suppl 4:149–67.
28. Pina Vegas L, Sbidian E, Penso L, Claudepierre P. Epidemiologic study of patients with psoriatic arthritis in a real-world analysis: a cohort study of the French health insurance database. Rheumatology (Oxford) 2021;60:1243–51.
29. Lemaitre M, Kirchgesner J, Rudnichi A, Carrat F, Zureik M, Carbonnel F, et al. Association between use of thiopurines or tumor necrosis factor antagonists alone or in combination and risk of lymphoma in patients with inflammatory bowel disease. JAMA 2017;318:1679–86.
30. Weill A, Dalichampt M, Raguideau F, Ricordeau P, Blotière PO, Rudant J, et al. Low dose oestrogen combined oral contraception and risk of pulmonary embolism, stroke, and myocardial infarction in five million French women: cohort study. BMJ 2016 10;353:i2002.
31. Meyer A, Rudant J, Drouin J, Weill A, Carbonnel F, Coste J. Effectiveness and safety of reference infliximab and biosimilar in Crohn disease: a French equivalence study. Ann Intern Med 2019;170:99–107.
32. Lindström U, Glintborg B, Di Giuseppe D, Jørgensen TS, Gudbjornsson B, Grøn KL, et al. Comparison of treatment retention and response to secukinumab versus tumour necrosis factor inhibitors in psoriatic arthritis. Rheumatology (Oxford) 2021;60:3635–45.
33. Sbidian E, Giboin C, Bachelez H, Paul C, Beylot-Barry M, Dupuy A, et al. Factors associated with the choice of the first biologic in psoriasis: real-life analysis from the Psobioteq cohort. J Eur Acad Dermatol Venereol 2017;31:2046–54.
34. Warren RB, Smith CH, Yiu ZZ, Ashcroft DM, Barker JN, Burden AD, et al. Differential drug survival of biologic therapies for the treatment of psoriasis: a prospective observational cohort study from the British Association of Dermatologists Biologic Interventions Register (BADBIR). J Invest Dermatol 2015;135:2632–40.
35. Xu S, Ross C, Raebel MA, Shetterly S, Blanchette C, Smith D. Use of stabilized inverse propensity scores as weights to directly estimate relative risk and its confidence intervals. Value Health 2010;13:273–7.
36. Bouma G, Strober W. The immunological and genetic basis of inflammatory bowel disease [review]. Nat Rev Immunol 2003;3:521–33.
37. Gálvez J. Role of Th17 cells in the pathogenesis of human IBD [review]. ISRN Inflamm 2014;2014:928461.
38. Belkaid Y, Hand TW. Role of the microbiota in immunity and inflammation [review]. Cell 2014;157:121–41.
39. Ohnmacht C, Marques R, Presley L, Sawa S, Lochner M, Eberl G. Intestinal microbiota, evolution of the immune system and the bad reputation of pro-inflammatory immunity [review]. Cell Microbiol 201113:653–9.
40. Maxwell JR, Zhang Y, Brown WA, Smith CL, Byrne FR, Fiorino M, et al. Differential roles for interleukin-23 and interleukin-17 in intestinal immunoregulation. Immunity 2015;43:739–50.
41. Whibley N, Gaffen SL. Gut-busters: IL-17 ain't afraid of no IL-23. Immunity 2015;43:620–2.
42. Egeberg A, Thyssen JP, Burisch J, Colombel JF. Incidence and risk of inflammatory bowel disease in patients with psoriasis: a nationwide 20-year cohort study. J Invest Dermatol 2019;139:316–23.
43. Yamada A, Wang J, Komaki Y, Komaki F, Micic D, Sakuraba A. Systematic review with meta-analysis: risk of new onset IBD with the use of anti-interleukin-17 agents. Aliment Pharmacol Ther 2019;50:373–85.
44. Schreiber S, Colombel JF, Feagan BG, Reich K, Deodhar AA, McInnes IB, et al. Incidence rates of inflammatory bowel disease in patients with psoriasis, psoriatic arthritis and ankylosing spondylitis treated with secukinumab: a retrospective analysis of pooled data from 21 clinical trials. Ann Rheum Dis 2019;78:473–9.
45. Giroud M, Hommel M, Benzenine E, Fauconnier J, Béjot Y, Quantin C, et al. Positive predictive value of French hospitalization discharge codes for stroke and transient ischemic attack. Eur Neurol 2015;74:92–9.
46. Bezin J, Girodet PO, Rambelomanana S, Touya M, Ferreira P, Gilleron V, et al. Choice of ICD-10 codes for the identification of acute coronary syndrome in the French hospitalization database. Fundam Clin Pharmacol 2015;29:586–91.
47. Ray WA. Evaluating medication effects outside of clinical trials: new-user designs. Am J Epidemiol 2003;158:915–20.
48. Aleshaki JS, Cardwell LA, Muse ME, Feldman SR. Adherence and resource use among psoriasis patients treated with biologics [review]. Expert Rev Pharmacoecon Outcomes Res 2018;18:609–17.

Arthritis & Rheumatology
Vol. 74, No. 2, February 2022, pp 253–262
DOI 10.1002/art.41239

American College of Rheumatology
Empowering Rheumatology Professionals

Association of Structural Entheseal Lesions With an Increased Risk of Progression From Psoriasis to Psoriatic Arthritis

David Simon,[1] Koray Tascilar,[1] Arnd Kleyer,[1] Sara Bayat,[1] Eleni Kampylafka,[1] Maria V. Sokolova,[1] Ana Zekovic,[2] Axel J. Hueber,[3] Jürgen Rech,[1] Louis Schuster,[1] Klaus Engel,[4] Michael Sticherling,[5] and Georg Schett[1]

Objective. To test whether the presence of structural entheseal lesions in psoriasis patients influences the risk of progression to psoriatic arthritis (PsA).

Methods. We conducted a prospective cohort study of psoriasis patients without clinical evidence of musculoskeletal involvement who underwent baseline assessment of structural entheseal lesions and volumetric bone mineral density (vBMD) at entheseal and intraarticular sites by high-resolution peripheral quantitative computed tomography. Adjusted relative risks of developing PsA associated with baseline vBMD and the presence of structural entheseal lesions were calculated using multivariable Cox regression models.

Results. The cohort included 114 psoriasis patients (72 men and 42 women) with a mean ± SD follow-up duration of 28.2 ± 17.7 months, during which 24 patients developed PsA (9.7 per 100 patient-years [95% confidence interval (95% CI) 6.2–14.5]). Patients with structural entheseal lesions were at higher risk of developing PsA compared to patients without such lesions (21.4 per 100 patient-years [95% CI 12.5–34.3]; hazard ratio [HR] 5.10 [95% CI 1.53–16.99], $P = 0.008$). With respect to vBMD, a 1-SD increase in entheseal, but not intraarticular, vBMD was associated with an ~30% reduced risk of progression to PsA. Especially, higher cortical vBMD at entheseal segments was associated with a lower risk of developing PsA (HR 0.32 per 1 SD [95% CI 0.14–0.71]), and the association remained robust after multiple imputation of missing data (HR 0.64 [95% CI 0.42–0.98]).

Conclusion. The presence of structural entheseal lesions as well as low cortical vBMD at entheseal segments are associated with an increased risk of developing PsA in patients with psoriasis.

INTRODUCTION

Psoriatic disease is a chronic inflammatory condition affecting the skin, the entheses, and the joints (1). The disease has a robust genetic basis linked to HLA class I alleles and the interleukin-23 (IL-23) receptor and is associated with the development of a specific immune pathology characterized by innate immune cell and T cell activation (1). Clinical studies have shown that, in addition to tumor necrosis factor, IL-17 and IL-23 are pivotally involved in the pathogenesis of psoriatic disease (2,3). Experimental (4,5) as well as clinical studies (6,7) suggest that environmental factors such as mechanical load essentially contribute to the pathology of psoriatic disease ("mechanoinflammation"). Hence, psoriatic skin disease usually develops at mechanically exposed areas of the skin, and psoriatic plaque formation based on physical irritation of the skin (Koebner

Supported by the Deutsche Forschungsgemeinschaft (DFG FOR 2886 PANDORA and the CRC1181 Checkpoints for Resolution of Inflammation), the BMBF (project MASCARA), the ERC Synergy grant 4D Nanoscope, the Innovative Medicines Initiative (project HIPPOCRATES), the Emerging Fields Initiative MIRACLE of the Friedrich–Alexander University Erlangen–Nuremberg, the Else Kröner Memorial Scholarship of the Else Kröner-Fresenius Foundation (to Dr. Simon), and the Partner Fellowship Program (grant to Dr. Zekovic).

[1]David Simon, MD, Koray Tascilar, MD, Arnd Kleyer, MD, Sara Bayat, MD, Eleni Kampylafka, MD, Maria V. Sokolova, MD, Jürgen Rech, MD, Louis Schuster, PhD, Georg Schett, MD: Department of Internal Medicine 3 - Rheumatology and Immunology, Friedrich Alexander University Erlangen–Nuremberg and Universitätsklinikum Erlangen, Erlangen, Germany, Deutsches Zentrum Immuntherapie, Friedrich Alexander University Erlangen–Nuremberg and Universitätsklinikum Erlangen, Erlangen, Germany; [2]Ana Zekovic, MD: Department of Rheumatology, University of Belgrade, Belgrade, Serbia; [3]Axel J. Hueber, MD, PhD: Sozialstiftung Bamberg, Bamberg, Germany; [4]Klaus Engel, PhD: Siemens Healthineers, Erlangen, Germany; [5]Michael Sticherling, MD: Deutsches Zentrum Immuntherapie, Friedrich Alexander University Erlangen–Nuremberg and Universitätsklinikum Erlangen, Erlangen, Germany, Department of Dermatology, Friedrich Alexander University Erlangen–Nuremberg and Universitätsklinikum Erlangen, Erlangen, Germany.

No potential conflicts of interest relevant to this article were reported.

Address correspondence to Georg Schett, MD, Department of Internal Medicine 3–Rheumatology and Immunology, Friedrich–Alexander University (FAU) Erlangen–Nuremberg and Universitätsklinikum Erlangen, Ulmenweg 18, 91054 Erlangen, Germany. Email: georg.schett@uk-erlangen.de.

Submitted for publication October 3, 2019; accepted in revised form February 20, 2020.

phenomenon) has been described (8). Similarly, entheseal sites, which typically become inflamed in psoriatic disease, are highly mechanically exposed tissues that are essential for the transduction of physical forces (9–12).

It is well-known that clinical manifestations of psoriatic skin disease usually precede joint disease. While this concept appears correct when considering clinically visible disease, it also has some shortcomings, since psoriatic skin is much easier to detect than joint disease. Given these considerations, skin and joint disease may indeed arise from the same underlying process (e.g., mechanoinflammation) at the same time, with patients developing similar inflammatory lesions in the skin and entheses, while the speed of detection of these lesions is different and allows skin changes to be detected earlier. Independent from this, stable monomorphic psoriatic disease manifestations exist, in which skin disease indeed remains the only manifestation of the disease (most frequent), or isolated joint, or even entheseal, disease can occur. Conceptually, however, skin and entheseal manifestations of psoriatic disease may arise simultaneously, at least in a subset of patients, but may be recognized at different times.

In support of this concept, several studies have suggested that subclinical inflammatory lesions can be detected in the joints and the entheses of a subset of psoriasis patients without signs of clinical arthritis (13–16). Notably, discrete structural entheseal lesions, sometimes also referred to as "deep Koebner" phenomenon, are a key finding in the joints of patients with psoriasis, suggesting that similar mechanoinflammation-induced tissue responses can be found in the skin and the joints in psoriasis patients (17). Structural entheseal lesions emerge from resident tissue responses, are similar to psoriatic plaques at entheseal sites, and are characterized by periosteal proliferation and new bone formation (18).

While structural entheseal lesions in patients with psoriasis may represent the first sign of musculoskeletal involvement of psoriatic disease, it is unclear whether patients with such lesions face a higher risk of developing psoriatic arthritis (PsA). To test whether structural entheseal lesions are an indicator of the later development of PsA, we assessed a cohort of patients with psoriasis for the presence or absence of structural entheseal lesions and other signs of bone changes in the hand joints and prospectively followed up this cohort for later development of PsA. We hypothesized that the risk of developing PsA is higher in patients who exhibit structural entheseal lesions, indicating that the clinical manifestation of psoriatic disease is already determined early on in the disease process, i.e., before the development of clinical joint disease.

PATIENTS AND METHODS

Psoriasis patients. Between January 2011 and July 2018, psoriasis patients attending the Dermatology Department of the University of Erlangen–Nuremberg were screened for recruitment into this cohort study using the German Psoriasis Arthritis Diagnostic (GEPARD) questionnaire (19).

Only patients who answered yes to at least one of the GEPARD questions were subsequently referred to the Rheumatology Department for clinical and imaging assessment. Patients who answered no to every single question were not referred. Patients who were referred to the Rheumatology Department had a mean ± SD number of positive answers on the questionnaire of 4.9 ± 3.2. In the Rheumatology Department an experienced rheumatologist (SB) examined the referred patients for clinical signs of musculoskeletal involvement. In detail, the clinical examination included a tender joint count (68 joints assessed), swollen joint count (66 joints assessed), and clinical assessment of 29 entheseal sites used in the Spondyloarthritis Research Consortium of Canada enthesitis scoring system (20), Leeds Enthesitis Index (21), and Maastricht Ankylosing Spondylitis Enthesitis Score (22). In addition, the presence of dactylitis and of clinical symptoms of inflammatory back pain was recorded.

Patients who showed joint swelling, dactylitis, clinical signs of enthesitis or inflammatory back pain, and those who fulfilled the Classification of Psoriatic Arthritis (CASPAR) criteria for PsA (23) were not allowed to participate in the study. To exclude past musculoskeletal involvement, all patient records were also carefully reviewed. Identification of a history of synovitis, enthesitis, dactylitis, and/or inflammatory back pain in past records or evidence of meeting the CASPAR criteria at any time also led to exclusion (Supplementary Figure 1, available on the *Arthritis & Rheumatology* website at http://onlinelibrary.wiley.com/doi/10.1002/art.41239/abstract).

For psoriasis patients who met the requirements described above, additional demographic data, such as age, sex, height, body weight, body mass index (BMI), and smoking status were collected, and disease-specific characteristics, such as psoriasis disease severity (Psoriasis Area and Severity Index [PASI]) (24), disease duration, and psoriasis subtype, including nail and scalp involvement, were also recorded. Quality of life was assessed using the Dermatology Life Quality Index (25). C-reactive protein levels (mg/liter) were measured, and the presence of rheumatoid factor (RF) and anti–citrullinated protein antibodies was determined. Current treatments, including topical and systemic drugs for psoriasis, were recorded for all patients. Patients were evaluated at regular 1-year follow-up visits, during which the detailed examination by the rheumatologist was repeated and disease-specific parameters were recorded. Such investigations were also done whenever new musculoskeletal symptoms occurred.

Patients were followed up until study end or a clinical diagnosis of PsA was made. PsA was defined as the presence of inflammatory musculoskeletal involvement (arthritis as defined by joint swelling, enthesitis as defined by entheseal pain plus power Doppler ultrasound signal, dactylitis as determined by clinical examination, or axial involvement as determined by inflammatory back pain and radiographic/magnetic resonance imaging [MRI] evidence of sacroiliitis or spondylitis) assessed by an experienced rheumatologist (SB) and a score of ≥3 points on the CASPAR

criteria. The study was conducted upon approval of the local ethics committee of the University of Erlangen. Each patient provided informed consent.

High-resolution peripheral quantitative computed tomography (QCT) measurement and data analysis. All psoriasis patients underwent high-resolution peripheral QCT of the second and third metacarpophalangeal (MCP) joints of the dominant hand (XtremeCT I; Scanco Medical). Correct positioning of the hand was ensured by the use of a custom holder to reduce movement artifacts. Resolution was 82 μm isotropic voxels. The reference line was set on the joint space of the third MCP joint. Scanning of the MCP region was 322 slices, with a scanning time of 8.4 minutes.

After image reconstruction, the measurement was converted into a Digital Imaging and Communication in Medicine (DICOM) file. Imaging analysis was performed using the DICOM viewer OsiriX v.4.1 MD v.8.0.1. The definition of the region of interest (ROI) allowed the visualization of the portions of the metacarpal head and the phalangeal base adjacent to the insertion of the joint capsule resembling entheseal sites. Sites of new bone formation within the limits of the ROI defined above were referred to as structural entheseal lesions when found at the insertion sites of tendons, ligaments, or capsule, or at the locations of functional entheses. The extent of structural entheseal lesions was graded on a scale of 1–3, where 1 = maximum height ≤1 mm, 2 = maximum height >1 mm, and 3 = diffuse osteoproliferation (26). These evaluations were done once by 2 independent readers who were blinded with regard to clinical data (DS and EK). The kappa coefficient for interobserver agreement was 0.80 for structural entheseal lesions.

Only the MCP2 head was used to determine intraarticular and entheseal bone mineral density (BMD). Intraarticular BMD was assessed using an established method (27,28), while the assessment of entheseal BMD took into account the exact and individually different anatomy of the entheseal region (Figure 1 and Supplementary Video 1, available on the *Arthritis & Rheumatology* website at http://onlinelibrary.wiley.com/doi/10.1002/art.41239/abstract). Contouring was started at the distal part of the entheseal site where the bone has a triangular shape and where the joint capsule inserts; contouring was stopped proximally where the shape of the bone becomes squared. We have previously shown that this segmentation method accurately reflects the insertion site of the joint capsule to the MCP2 head (27). After contouring, a graphical object (Geoworks Object) was generated and evaluated using the automated standard evaluation protocol provided by the manufacturer. The following density parameters for entheseal and intraarticular bone were determined: total volumetric BMD (vBMD), trabecular vBMD, and cortical vBMD in milligrams of hydroxyapatite per cubic centimeter (mg HA/cm^3). Images with a motion grade of IV or V were excluded from analyses of vBMD.

Statistical analysis. We constructed tables summarizing appropriate descriptive analyses of continuous and categorical variables to characterize the cohort, overall and stratified by the development of PsA. We calculated the incidence of PsA as the number of events divided by person-time at risk, and calculated 95% confidence intervals (95% CIs) based on the Poisson distribution for the overall cohort, and by variables of interest. We also performed survival analysis using the Kaplan–Meier method, with weeks of follow-up after the date of baseline high-resolution peripheral QCT assessment as the time scale to demonstrate the development of PsA over time in cohort subgroups. Curves were compared using the log rank test, or a log rank test for trend when more than 2 groups were analyzed (29,30).

In order to model the risk of PsA as a function of structural bone changes, we conducted 14 separate Cox regression analyses for the time to the clinical diagnosis of PsA using each baseline high-resolution peripheral QCT measurement of interest, namely, 1) the presence of structural entheseal lesions, 2) total vBMD, 3) cortical vBMD, and 4) trabecular vBMD. Separate models were fitted using the vBMD measurements for entheseal and intraarticular segments. Overall, 7 unadjusted and 7 adjusted hazard ratios (HRs) and their respective 95% CIs were calculated. Adjustments were based on causal models (Supplementary Figures 2 and 3, available on the *Arthritis & Rheumatology* website at http://onlinelibrary.wiley.com/doi/10.1002/art.41239/abstract).

We performed a sensitivity analysis to test the robustness of our findings from the 12 vBMD models to missing volumetric BMD measurements and covariates. We used the multiple imputation by chained equations method with predictive mean matching to generate 25 complete data sets with 100 iterations each. Regression analyses for the vBMD models were repeated on each complete data set and pooled using Rubin's rules (31,32). Further details and justification for the adjustments and sensitivity analyses are explained in the Supplementary Methods, available on the *Arthritis & Rheumatology* website at http://onlinelibrary.wiley.com/doi/10.1002/art.41239/abstract. *P* values less than 0.05 (2-tailed) or 95% CIs for the HR that did not include a null effect were considered significant. Data were analyzed using open-source R software (33).

RESULTS

Demographic and clinical features of the psoriasis patients at baseline. A total of 114 psoriasis patients (42 women and 72 men) were included (Supplementary Figure 1). At baseline, the patients had a mean ± SD age of 45.3 ± 13.9 years, duration of psoriasis of 15.8 ± 14.8 years, and PASI score of 7.3 ± 6.5. Thirty-five percent of the patients showed nail disease, while 43% had scalp involvement. A total of 47 patients (41%) reported arthralgia with overall low intensity (mean ± SD pain score 18.8 ± 25.2 on a 100-mm visual analog scale;

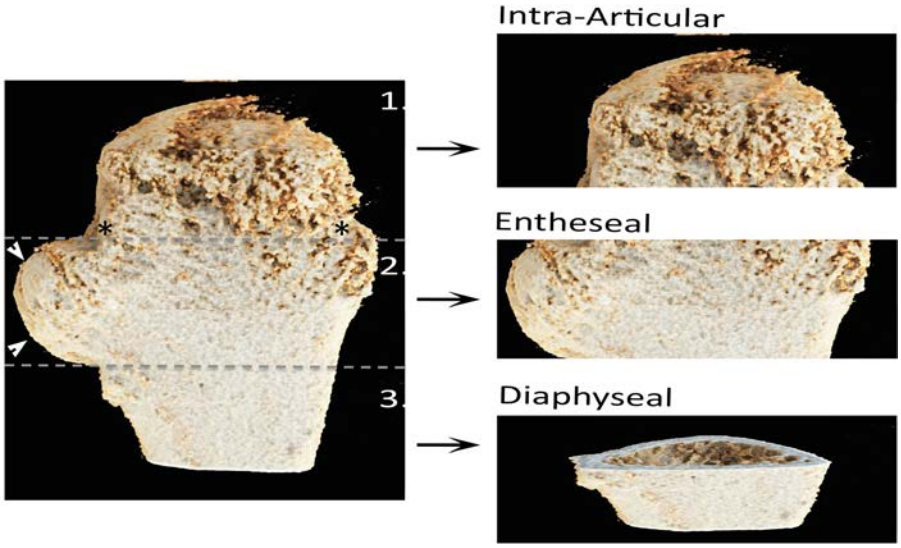

Figure 1. Anatomic orientation of the metacarpophalangeal joint for high-resolution peripheral quantitative computed tomography. An image of the metacarpal head with 1) the intraarticular region distal to the capsule insertion site (**asterisks**), 2) the entheseal region immediately proximal to the capsule insertion site showing a structural entheseal lesion (**arrowheads**), and 3) the further proximal diaphyseal site is shown. Volumetric bone mineral density was measured at the intraarticular region and the entheseal region.

mean ± SD number of tender joints 0.8 ± 2.4). At the time of cohort entry, 24 patients (21%) were not receiving any treatment, 54 (47%) were receiving topical therapy, 7 (6%) were receiving fumaric acid, 13 (11%) were receiving conventional disease-modifying antirheumatic drugs (DMARDs), and 20 (18%) were receiving targeted synthetic or biologic DMARDs. Further characteristics of the cohort are summarized in Table 1.

Incidence of new-onset PsA. The mean ± SD follow-up duration was 28.2 ± 17.7 months, corresponding to 246.8 patient-years. During the observation period 24 patients developed PsA after a mean ± SD duration of 17.5 ± 10.0 months. Of these 24 patients classified as having PsA according to the CASPAR criteria, 5 patients developed ultrasound-proven enthesitis (21%), 1 patient developed clinical dactylitis (4%), 1 patient developed axial involvement (inflammatory back pain plus positive sacroiliac MRI scan) (4%), and the remaining 17 patients (71%) developed clinical arthritis. The corresponding incidence of PsA was 9.7 per 100 patient-years (95% CI 6.2–14.5). The incidence of PsA according to baseline characteristics is summarized in Table 2. The only incidence value for which point estimates were mutually outside 95% CIs with overall cohort incidence was the presence of structural entheseal lesions. The probability of PsA-free survival based on the presence or absence of structural entheseal lesions is illustrated in Figure 2A.

Structural entheseal lesions and the development of PsA. At baseline, 41 patients (36%) had ≥1 structural entheseal lesion at the MCP joints, with a mean ± SD grade of 0.73 ± 1.37 (Table 1). A higher percentage of patients who developed PsA than those who did not develop PsA during follow-up had structural entheseal lesions (70.8% versus 26.7%), with a higher grade of structural changes (mean ± SD 1.58 ± 1.69 versus 0.50 ± 1.18). The incidence of PsA was 4.2 per 100 patient-years among patients who did not have structural entheseal lesions at cohort entry (95% CI 1.7–8.6) compared to 21.4 per 100 patient-years among patients who had structural entheseal lesions (95% CI 12.5–34.3) (Table 2). These data corresponded to an unadjusted HR of 4.91 (95% CI 2.03–11.89) ($P < 0.001$). Adjustment for covariates based on causal models (Supplementary Figure 2) did not change the point estimate (HR 5.10 [95% CI 1.53–16.99], $P = 0.008$) (Supplementary Table 1, available on the *Arthritis & Rheumatology* website at http://onlinelibrary.wiley.com/doi/10.1002/art.41239/abstract).

Volumetric BMD and the development of PsA. We also assessed vBMD at the entheseal and intraarticular bone segments (Table 1). The mean ± SD overall total vBMD was 278 ± 36 mg HA/cm^3 at the entheseal insertion segment. Patients progressing to PsA had a lower baseline total vBMD at entheseal segments (265.5 ± 34.5 mg HA/cm^3) than patients not progressing to PsA (281.2 ± 35.4 mg HA/cm^3). Differences between the 2 groups were also found for cortical vBMD (633.4 ± 50.4 versus 652.4 ± 50.1 mg HA/cm^3) and trabecular vBMD (173.6 ± 26.0 versus 185.4 ± 27.0 mg HA/cm^3), providing evidence of trabecular and cortical bone loss in psoriasis patients progressing to PsA. Similar trends for bone loss in patients progressing from psoriasis to PsA were observed at the intraarticular regions, albeit the differences were smaller (Table 1).

In unadjusted Cox regression models, a 1-SD increase in baseline vBMD at entheseal segments was associated with an

Table 1. Baseline cohort characteristics*

	Overall (n = 114)	No psoriatic arthritis at follow-up (n = 90)	Psoriatic arthritis at follow-up (n = 24)
Demographic characteristics			
Sex, no. male/female	72/42	59/31	13/11
Age, years	45.3 ± 13.9	45.0 ± 14.1	46.4 ± 13.5
Duration of follow up, months	28.2 ± 17.7	31.0 ± 18.3	17.5 ± 10.0
Body mass index	28.1 ± 6.4	27.3 ± 5.3	30.7 ± 8.7
Smoker, no. (%)	37 (33)	32 (36)	5 (21)
Disease-specific characteristics			
Duration of PsO, years	15.8 ± 14.8	15.5 ± 14.9	16.9 ± 14.7
Nail involvement, no. (%)	40 (35)	36 (40)	4 (17)
Scalp involvement, no. (%)	49 (43)	38 (42)	11 (46)
PASI	7.3 ± 6.5	7.5 ± 6.4	5.9 ± 7.0
DLQI	11.1 ± 9.8	10.9 ± 9.8	12.3 ± 10.5
Arthralgia, no. (%)	47 (41)	36 (40)	11 (46)
Pain score (100-mm VAS)	18.8 ± 25.2	16.9 ± 25.4	25.2 ± 24.1
Patient global assessment of disease activity (100-mm VAS)	16.7 ± 24.3	15.6 ± 24.1	21.5 ± 25.4
TJC (78 joints assessed)	0.8 ± 2.4	0.7 ± 1.7	1.3 ± 4.3
Other clinical characteristics			
Positive low-titer ACPA, no. (%)†	0 (0)	0 (0)	0 (0)
Positive low-titer RF, no. (%)‡	5 (4)	2 (2)	3 (13)
C-reactive protein, mg/liter§	4.1 ± 4.6	3.7 ± 4.4	5.4 ± 5.5
Treatment, no. (%)			
No current treatment	24 (21)	17 (19)	7 (29)
Topical therapies	54 (47)	43 (48)	11 (46)
Fumarates	7 (6)	7 (8)	0 (0)
csDMARDs	13 (11)	9 (10)	4 (17)
bDMARDs/tsDMARDs	20 (18)	17 (19)	3 (13)
Bone imaging			
Any structural lesion, no. (%)	41 (36)	24 (26.7)	17 (70.8)
Structural lesion grade			
Mean ± SD	0.73 ± 1.37	0.50 ± 1.18	1.58 ± 1.69
Median (IQR)	0 (0–1)	0 (0–1)	1 (0–2)
Volumetric density			
Entheseal segment, mg HA/cm^3			
Total vBMD	278.01 ± 35.62	281.18 ± 35.42	265.47 ± 34.52
Trabecular vBMD	183.01 ± 27.11	185.40 ± 27.04	173.61 ± 26.01
Cortical vBMD	648.53 ± 50.47	652.36 ± 50.12	633.43 ± 50.39
Intraarticular segment, mg HA/cm^3			
Total vBMD	288.90 ± 37.00	289.65 ± 35.70	285.66 ± 43.38
Trabecular vBMD	194.36 ± 27.74	194.53 ± 26.72	193.64 ± 32.79
Cortical vBMD	641.91 ± 72.78	645.24 ± 70.76	627.33 ± 81.86

* Except where indicated otherwise, values are the mean ± SD. PsO = psoriasis; PASI = Psoriasis Area and Severity Index; DLQI = Dermatology Life Quality Index; VAS = visual analog scale; TJC = tender joint count; ACPA = anti–citrullinated protein antibody; RF = rheumatoid factor; csDMARDs = conventional synthetic disease-modifying antirheumatic drugs; bDMARDs = biologic DMARDs; tsDMARDs = targeted synthetic DMARDs; IQR = interquartile range; HA = hydroxyapatite; vBMD = volumetric bone mineral density.
† <20 units/ml.
‡ >50 IU/ml.
§ Normal value <5 mg/liter.

~30% reduction in the risk of progression to PsA (Table 3), whereas the HRs for total and trabecular vBMD at intraarticular segments showed no association. All unadjusted 95% CIs spanned unity and therefore were not considered significant. In the adjusted analyses (Supplementary Figure 2), all point estimates showed an association of increased vBMD with 50–65% reduced risk of PsA. Confidence intervals for the HRs for total and cortical vBMD values at entheseal segments did not include the null and were considered significant. Hence, 1-SD increases in the total and cortical vBMD at entheseal segments were associated with a significant reduction in the risk of developing PsA, whereas the estimates for intraarticular vBMD do not rule out a null effect with good certainty (Table 3). Full model summaries for the risk for progression to PsA for total, trabecular, and cortical vBMD are shown in Supplementary Table 2, available on the *Arthritis & Rheumatology* website at http://onlinelibrary.wiley.com/doi/10.1002/art.41239/abstract.

Results remained robust after the imputation of missing exposure and covariate data. The numeric differences between adjusted and unadjusted HRs for entheseal vBMD measurements

Table 2. Incidence of PsA according to baseline cohort characteristics*

	No. of events	Patient-years	Incidence (95%CI)†
Overall	24	246.8	9.7 (6.2–14.5)
Sex			
Male	13	166.7	7.8 (4.2–13.3)
Female	11	80.2	13.7 (6.8–24.5)
Arthralgia‡			
No	7	117.9	5.9 (2.4–12.2)
Yes	11	88.0	12.5 (6.2–22.4)
Structural entheseal lesions			
Absent	7	167.4	4.2 (1.7–8.6)
Present	17	79.4	21.4 (12.5–34.3)
Nail involvement‡			
Absent	18	131.4	13.7 (8.1–21.6)
Present	4	96.2	4.2 (1.1–10.7)
Scalp involvement‡			
Absent	11	123.3	8.9 (4.45–16.0)
Present	11	104.7	10.5 (5.2–18.8)
csDMARD/bDMARD/tsDMARD use			
No	18	184.3	9.8 (5.8–15.4)
Yes	6	62.5	9.6 (3.5–20.9)

* PsA = psoriatic arthritis; 95% CI = 95% confidence interval; csDMARD = conventional synthetic disease-modifying antirheumatic drug; bDMARD = biologic DMARD; tsDMARD = targeted synthetic DMARD.
† Per 100 patient-years.
‡ Events/patient-time excluded due to missing data.

were smaller, the adjusted HR for total vBMD at the entheseal segment was no longer significant (HR 0.71 [95% CI 0.42–1.19]), and the HR for cortical vBMD at the entheseal segment remained significant (Table 3). Full model summaries after multiple imputation for the risk of progression to PsA for total, trabecular, and cortical vBMD are shown in Supplementary Table 3, available

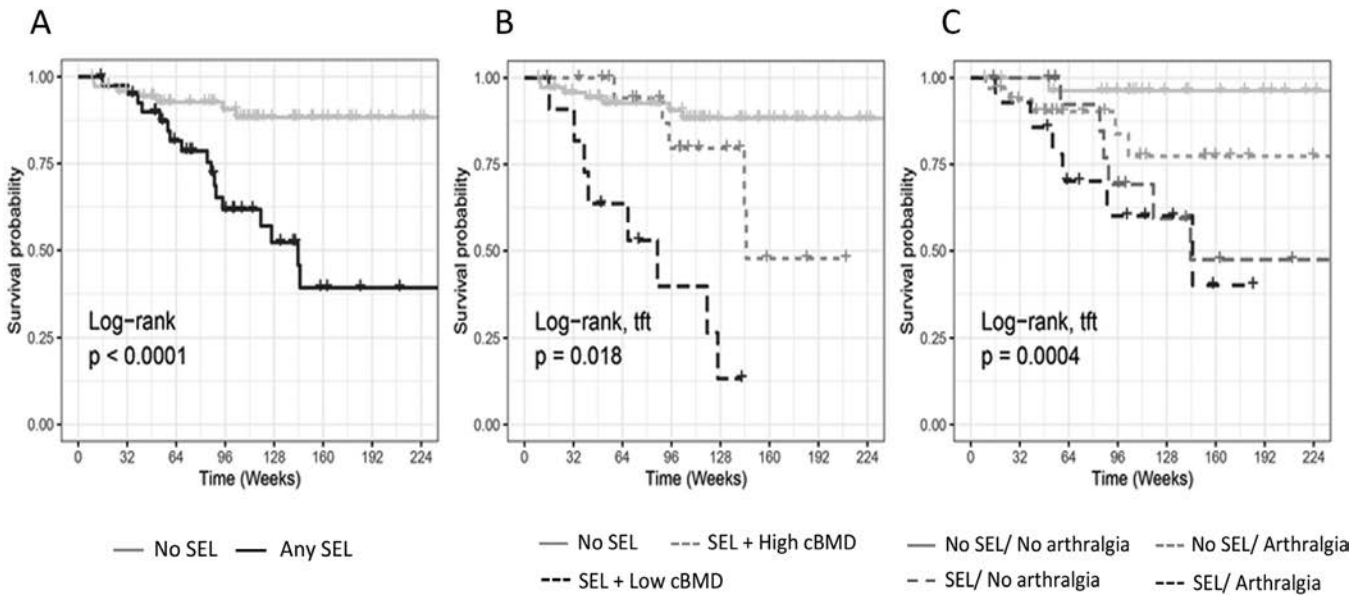

Figure 2. Survival curves for progression to psoriatic arthritis (PsA). **A**, Kaplan–Meier plots of PsA-free survival according to the presence or absence of structural entheseal lesions (SEL) at baseline. **B**, Kaplan–Meier plots of PsA-free survival in 3 groups: patients without structural entheseal lesions, patients with structural entheseal lesions and entheseal cortical volumetric bone mineral density (cBMD) greater than the cohort mean, and patients with structural entheseal lesions and cortical volumetric BMD less than the cohort mean. Nine patients, including 4 who developed PsA, were excluded due to missing cortical volumetric BMD data. **C**, Kaplan–Meier plots of PsA-free survival in 4 groups: patients without arthralgia or structural entheseal lesions, patients with arthralgia but no structural entheseal lesions, patients with structural entheseal lesions but no arthralgia, and patients with both arthralgia and structural entheseal lesions at baseline. Tft = test for trend. See Supplementary Figure 4, available on the *Arthritis & Rheumatology* website at http://onlinelibrary.wiley.com/doi/10.1002/art.41239/abstract, for the numbers of patients at risk and the numbers of events.

Table 3. Adjusted and unadjusted HRs for the risk of developing PsA according to vBMD measurements, with and without multiple imputation*

	Unadjusted HR (95% CI)	Adjusted HR (95% CI)
Complete case analysis		
Total vBMD		
Intraarticular	1.00 (0.61–1.63)	0.46 (0.20–1.10)
Entheseal	0.69 (0.44–1.11)	0.33 (0.13–0.83)
Cortical vBMD		
Intraarticular	0.80 (0.50–1.28)	0.51 (0.21–1.24)
Entheseal	0.72 (0.46–1.12)	0.32 (0.14–0.71)
Trabecular vBMD		
Intraarticular	1.07 (0.66–1.75)	0.42 (0.15–1.17)
Entheseal	0.72 (0.45–1.15)	0.35 (0.12–1.00)
Multiple imputation		
Total vBMD		
Intraarticular	0.97 (0.60–1.57)	0.78 (0.36–1.69)
Entheseal	0.86 (0.53–1.40)	0.71 (0.42–1.19)
Cortical vBMD		
Intraarticular	0.91 (0.55–1.49)	0.87 (0.49–1.55)
Entheseal	0.75 (0.48–1.18)	0.64 (0.42–0.98)
Trabecular vBMD		
Intra-articular	1.12 (0.66–1.89)	0.91 (0.36–2.28)
Entheseal	0.97 (0.64–1.45)	0.87 (0.53–1.42)

* Models were adjusted for age, sex, body mass index, duration of psoriasis, presence of structural entheseal lesions, and arthralgia. HRs = hazard ratios; PsA = psoriatic arthritis; vBMD = volumetric bone mineral density; 95% CI = 95% confidence interval.

on the *Arthritis & Rheumatology* website at http://onlinelibrary.wiley.com/doi/10.1002/art.41239/abstract.

Combination of structural entheseal lesions and cortical vBMD in progression to PsA. In a further analysis, we aimed to explore whether the risk of development of PsA in patients with structural entheseal lesions could be further stratified by cortical vBMD at entheseal segments. Survival curves were plotted for 3 groups: 1) patients with structural entheseal lesions plus cortical vBMD greater than the cohort mean, 2) patients with structural entheseal lesions plus cortical vBMD less than the cohort mean, and 3) patients without structural entheseal lesions. Among 73 patients with no structural entheseal lesions, 7 patients developed PsA (9.6%), while 5 (23.8%) of 21 patients with structural entheseal lesions plus high cortical vBMD developed PsA, and 8 (72.7%) of 11 patients with structural entheseal lesions plus low cortical vBMD developed PsA (Figure 2B). Hence, cortical vBMD at entheseal segments could further stratify the risk of PsA in patients with psoriasis and structural entheseal lesions ($P = 0.02$ by log rank test for trend).

Combination of structural entheseal lesions and arthralgia in progression to PsA. Finally, we explored the impact of arthralgia on the risk of development of PsA in patients with and those without structural entheseal lesions (Figure 2C). While patients without arthralgia or structural entheseal lesions showed a very low rate of progression to PsA (1 [3.4%] of 29), patients with arthralgia without structural entheseal lesions showed a higher progression rate (5 [15.2%] of 33), which was consistent with previous observations (15). The presence of structural entheseal lesions further enhanced the risk of progression to PsA both in the absence of arthralgia (6 [37.5%] of 16) and in the presence of arthralgia (6 [42.8%] of 14), with the highest progression rate observed in those subjects who had both arthralgia and structural entheseal lesions ($P < 0.001$ by log rank test for trend).

DISCUSSION

Our data show that the presence of structural entheseal lesions in patients with psoriasis represents a robust and independent marker for the later development of PsA. These findings support the concept of mechanoinflammation in the development of PsA, with the initial development of entheseal lesions in the disease process (5). Structural entheseal lesions are highly typical of psoriatic joint disease and part of the CASPAR criteria for the classification of PsA (23). They are anatomically different from bony spurs observed in osteoarthritis (26) and progressively increase during the course of PsA (34). Even more importantly, such lesions can already be observed in a subset of psoriasis patients without PsA, suggesting that the initial insult to joints in patients with psoriatic disease may be enthesitis associated with localized tissue responses (17). As such, these lesions appear to represent a very early feature of joint involvement in psoriatic disease and are thus found to be associated with the later development of signs and symptoms of PsA.

The observation of localized reduction in bone mass at the entheseal region of the joints in patients with psoriasis progressing to PsA is another notable finding of this study. This link between BMD and progression to PsA is specific to the entheseal region and is not apparent in the intraarticular region of the joint. After multiple imputation, the association of decreased cortical vBMD with progression to PsA remained a robust finding. Furthermore, the concomitant presence of structural entheseal lesions and low cortical vBMD substantially increased the risk of developing PsA, suggesting a state of imminent PsA. These results provide evidence of early localized cortical bone changes in psoriasis patients who progress to PsA and translate preclinical observations showing that inflammatory cytokines involved in psoriatic disease induce a negative net balance of bone homeostasis (35,36).

Entheses insert into the cortical bone, which is strongly vascularized (37) with a multitude of bone channels ("transcortical vessels") shuttling immune cells in and out of the bone marrow and harboring bone-resorbing osteoclasts (38,39). Inflammation along these transcortical vessels may activate osteoclasts and thereby trigger bone loss. This concept is supported by 1) the

observation of subclinical inflammatory changes in the joints of patients with psoriasis (15), 2) IL-17 dependency of such preclinical inflammatory changes predominantly affecting entheseal segments (40), and 3) the presence of localized periarticular bone loss already in psoriasis, while systemic bone loss is confined to patients with PsA (41).

By observing structural changes in the joints of psoriasis patients that are associated with later development of PsA, this study highlights the early phase of musculoskeletal involvement in a subset of patients with psoriatic disease. These data support the importance of the concept of early disease interception (42) to prevent damage, disability, and poor outcomes in patients with PsA (43,44). Since structural joint changes occur very early in a subgroup of psoriasis patients, the benefit of systemic treatment may be based on the prevention of progression to more severe and clinically overt joint disease. It is particularly important to consider that the progression to PsA in an unselected psoriasis population is rather limited, and hence the identification of an at-risk population is of importance (45).

One intriguing finding of our study was the lack of a positive association between PsA and nail involvement. Nail dystrophy is among the CASPAR criteria (18) for the classification of PsA and was associated with CASPAR-defined PsA in previous prospective studies (45,46). This association, however, is necessitated by design, such that when any 2 individuals with a given clinical finding suggesting PsA are compared, one that has nail dystrophy is more likely to be classified as having PsA by the CASPAR criteria, compared to one that does not. Interestingly, in one of those observational studies, the nail dystrophy association did not persist when psoriasis severity was included in a multivariable model (46), suggesting that nail dystrophy is likely a correlate of psoriasis severity, which could be considered an intermediate along the causal pathway from psoriasis to PsA. Including psoriasis severity as such an intermediate in our causal models did not necessitate any further adjustment to our estimates. We consider the lack of this association, which we had also previously observed, to be a result of sampling variation (15).

A limitation of the study is the rather small number of patients who did develop PsA during the observation period relative to the number of adjustment variables. This might impact the precision of our effect estimates. Another limitation is the potential overestimation of the risk of PsA explained by exposure. It is therefore necessary that our observations are confirmed by others using similar methods. In addition, there was some data loss due to the meticulous quality standards required to reliably measure volumetric bone densities using high-resolution peripheral QCT. We tried to address this issue using multiple imputation to test the robustness of our findings to such missing data and thereby verified the association between PsA risk and cortical vBMD at entheseal segments. Finally, our study sample consisted of patients conditionally selected among a psoriasis population attending a tertiary dermatology center, and as can be inferred from the high incidence of PsA, does not necessarily reflect an overall psoriasis population. Since our analyses are causal inference oriented, the generalizability and predictive potential of our results for daily practice should be considered limited. Our findings, however, can be considered among potential predictors in a PsA risk prediction exercise.

In summary, our findings show that specific structural features of the joints in psoriasis patients, namely, structural entheseal lesions as well as cortical bone loss at entheseal segments, are associated with the later development of PsA. These findings not only substantiate the concept of mechanoinflammation in the pathogenesis of psoriatic disease but also show that the presence of entheseal lesions predicts the onset of clinical joint disease. Based on these data, interventions with high efficacy in controlling entheseal inflammation appear to be a particularly valuable strategy for interfering with the onset of PsA in patients with psoriatic disease.

ACKNOWLEDGMENT

We thank the staff of Siemens Healthineers for creating images with Cinematic Rendering (Figure 1 and Supplementary Video 1).

AUTHOR CONTRIBUTIONS

All authors were involved in drafting the article or revising it critically for important intellectual content, and all authors approved the final version to be published. Dr. Schett had full access to all of the data in the study and takes responsibility for the integrity of the data and the accuracy of the data analysis.

Study conception and design. Simon, Tascilar, Kleyer, Rech, Sticherling, Schett.

Acquisition of data. Simon, Kleyer, Bayat, Kampylafka, Sokolova, Zekovic, Hueber, Rech, Schuster, Sticherling.

Analysis and interpretation of data. Simon, Tascilar, Kleyer, Bayat, Hueber, Rech, Engel, Sticherling, Schett.

ADDITIONAL DISCLOSURES

Author Engel is an employee of Siemens Healthineers.

REFERENCES

1. Ritchlin CT, Colbert RA, Gladman DD. Psoriatic arthritis. N Engl J Med 2017;376:2095–6.
2. Nash P. Psoriatic arthritis: novel targets add to a therapeutic renaissance. Lancet 2018;391:2187–9.
3. McGonagle DG, McInnes IB, Kirkham BW, Sherlock J, Moots R. The role of IL-17A in axial spondyloarthritis and psoriatic arthritis: recent advances and controversies. Ann Rheum Dis 2019;78:1167–78.
4. Jacques P, Lambrecht S, Verheugen E, Pauwels E, Kollias G, Armaka M, et al. Proof of concept: enthesitis and new bone formation in spondyloarthritis are driven by mechanical strain and stromal cells. Ann Rheum Dis 2014;73:437–45.
5. Cambre I, Gaublomme D, Burssens A, Jacques P, Schryvers N, De Muynck A, et al. Mechanical strain determines the site-specific

localization of inflammation and tissue damage in arthritis. Nat Commun 2018;9:4613.
6. Thorarensen SM, Lu N, Ogdie A, Gelfand JM, Choi HK, Love TJ. Physical trauma recorded in primary care is associated with the onset of psoriatic arthritis among patients with psoriasis. Ann Rheum Dis 2017;76:521–5.
7. Zhou W, Chandran V, Cook R, Gladman DD, Eder L. The association between occupational-related mechanical stress and radiographic damage in psoriatic arthritis. Semin Arthritis Rheum 2019;48:638–43.
8. Köbner H. Zur Aetiologie der Psoriasis. 1877 Vjschr Dermatol 9:204–7.
9. McGonagle D, Lories RJ, Tan AL, Benjamin M. The concept of a "synovio-entheseal complex" and its implications for understanding joint inflammation and damage in psoriatic arthritis and beyond [review]. Arthritis Rheum 2007;56:2482–91.
10. Schett G, Lories RJ, D'Agostino MA, Elewaut D, Kirkham B, Soriano ER, et al. Enthesitis: from pathophysiology to treatment. Nat Rev Rheumatol 2017;13:731–41.
11. Cuthbert RJ, Fragkakis EM, Dunsmuir R, Li Z, Coles M, Marzo-Ortega H, et al. Group 3 innate lymphoid cells in human enthesis. Arthritis Rheumatol 2017;69:1816–22.
12. Watad A, Cuthbert RJ, Amital H, McGonagle D. Enthesitis: much more than focal insertion point inflammation. Curr Rheumatol Rep 2018;20:41.
13. Naredo E, Moller I, de Miguel E, Batlle-Gualda E, Acebes C, Brito E, et al. High prevalence of ultrasonographic synovitis and enthesopathy in patients with psoriasis without psoriatic arthritis: a prospective case-control study. Rheumatology (Oxford) 2011;50:1838–48.
14. Tinazzi I, McGonagle D, Biasi D, Confente S, Caimmi C, Girolomoni G, et al. Preliminary evidence that subclinical enthesopathy may predict psoriatic arthritis in patients with psoriasis. J Rheumatol 2011;38:2691–2.
15. Faustini F, Simon D, Oliveira I, Kleyer A, Haschka J, Englbrecht M, et al. Subclinical joint inflammation in patients with psoriasis without concomitant psoriatic arthritis: a cross-sectional and longitudinal analysis. Ann Rheum Dis 2016;75:2068–74.
16. Savage L, Goodfield M, Horton L, Watad A, Hensor E, Emery P, et al. Regression of peripheral subclinical enthesopathy in therapy-naive patients treated with ustekinumab for moderate-to-severe chronic plaque psoriasis: a fifty-two–week, prospective, open-label feasibility study. Arthritis Rheumatol 2019;71:626–31.
17. Simon D, Faustini F, Kleyer A, Haschka J, Englbrecht M, Kraus S, et al. Analysis of periarticular bone changes in patients with cutaneous psoriasis without associated psoriatic arthritis. Ann Rheum Dis 2016;75:660–6.
18. Lories RJ, McInnes IB. Primed for inflammation: enthesis-resident T cells. Nat Med 2012;18:1018–9.
19. Harle P, Hartung W, Lehmann P, Ehrenstein B, Schneider N, Muller H, et al. Detection of psoriasis arthritis with the GEPARD patient questionnaire in a dermatologic outpatient setting. Z Rheumatol 2010;69:157–160, 162–153. In German.
20. Maksymowych WP, Mallon C, Morrow S, Shojania K, Olszynski WP, Wong RL, et al. Development and validation of the Spondyloarthritis Research Consortium of Canada (SPARCC) Enthesitis Index. Ann Rheum Dis 2009;68:948–53.
21. Healy PJ, Helliwell PS. Measuring clinical enthesitis in psoriatic arthritis: assessment of existing measures and development of an instrument specific to psoriatic arthritis. Arthritis Rheum 2008;59:686–91.
22. Heuft-Dorenbosch L, Spoorenberg A, van Tubergen A, Landewé R, van ver Tempel H, Mielants H, et al. Assessment of enthesitis in ankylosing spondylitis. Ann Rheum Dis 2003;62:127–32.
23. Taylor W, Gladman D, Helliwell P, Marchesoni A, Mease P, Mielants H. Classification criteria for psoriatic arthritis: development of new criteria from a large international study. Arthritis Rheum 2006;54:2665–73.
24. Fredriksson T, Pettersson U. Severe psoriasis—oral therapy with a new retinoid. Dermatologica 1978;157:238–44.
25. Finlay AY, Khan GK. Dermatology Life Quality Index (DLQI)-a simple practical measure for routine clinical use. Clin Exp Dermatol 1994;19:210–6.
26. Finzel S, Sahinbegovic E, Kocijan R, Engelke K, Englbrecht M, Schett G. Inflammatory bone spur formation in psoriatic arthritis is different from bone spur formation in hand osteoarthritis. Arthritis Rheumatol 2014;66:2968–75.
27. Simon D, Kleyer A, Stemmler F, Simon C, Berlin A, Hueber AJ, et al. Age- and sex-dependent changes of intra-articular cortical and trabecular bone structure and the effects of rheumatoid arthritis. J Bone Miner Res 2017;32:722–30.
28. Simon D, Kleyer A, Englbrecht M, Stemmler F, Simon C, Berlin A, et al. A comparative analysis of articular bone in large cohort of patients with chronic inflammatory diseases of the joints, the gut and the skin. Bone 2018;116:87–93.
29. Therneau TM, Grambsch PM. Modeling survival data: extending the Cox model. New York: Springer; 2000.
30. Kassambara A, Kosinski M. survminer: drawing survival curves using 'ggplot2'. 2019. URL: https://CRAN.R-project.org/package=survminer.
31. Buuren SV, Groothuis-Oudshoorn K. MICE: multivariate imputation by chained equations in R. J Stat Softw 2011;45:1–67.
32. Heymans M. psfmi: prediction model selection and performance evaluation in multiple imputed datasets. 2019. URL: https://CRAN.R-project.org/package=psfmi.
33. R. Core Team. R: a language and environment for statistical computing. Vienna, Austria: R Foundation for Statistical Computing; 2019.
34. Simon D, Kleyer A, Faustini F, Englbrecht M, Haschka J, Berlin A, et al. Simultaneous quantification of bone erosions and enthesiophytes in the joints of patients with psoriasis or psoriatic arthritis - effects of age and disease duration. Arthritis Res Ther 2018;20:203.
35. Adamopoulos IE, Chao CC, Geissler R, Laface D, Blumenschein W, Iwakura Y, et al. Interleukin-17A upregulates receptor activator of NF-κB on osteoclast precursors. Arthritis Res Ther 2010;12:R29.
36. Gravallese EM, Schett G. Effects of the IL-23-IL-17 pathway on bone in spondyloarthritis. Nat Rev Rheumatol 2018;14:631–40.
37. D'Agostino MA, Said-Nahal R, Hacquard-Bouder C, Brasseur JL, Dougados M, Breban M. Assessment of peripheral enthesitis in the spondylarthropathies by ultrasonography combined with power Doppler: a cross-sectional study. Arthritis Rheum 2003;48:523–33.
38. Grüneboom A, Hawwari I, Weidner D, Culemann S, Müller S, Henneberg S, et al. A network of trans-cortical capillaries as mainstay for blood circulation in long bones. Nat Metab 2019;1:236–50.
39. Ritchlin C, Adamopoulos IE. Go with the flow—hidden vascular passages in bone. Nat Metab 2019;1:173–4.
40. Kampylafka E, Simon D, d'Oliveira I, Linz C, Lerchen V, Englbrecht M, et al. Disease interception with interleukin-17 inhibition in high-risk psoriasis patients with subclinical joint inflammation-data from the prospective IVEPSA study. Arthritis Res Ther 2019;21:178.
41. Uluckan O, Jimenez M, Karbach S, Jeschke A, Grana O, Keller J, et al. Chronic skin inflammation leads to bone loss by IL-17-mediated inhibition of Wnt signaling in osteoblasts. Sci Transl Med 2016;8:330ra337.
42. Scher JU, Ogdie A, Merola JF, Ritchlin C. Preventing psoriatic arthritis: focusing on patients with psoriasis at increased risk of transition. Nat Rev Rheumatol 2019;15:153–66.
43. Kirkham B, de Vlam K, Li W, Boggs R, Mallbris L, Nab HW, et al. Early treatment of psoriatic arthritis is associated with improved patient-reported outcomes: findings from the etanercept PRESTA trial. Clin Exp Rheumatol 2015;33:11–9.

44. Haroon M, Gallagher P, FitzGerald O. Diagnostic delay of more than 6 months contributes to poor radiographic and functional outcome in psoriatic arthritis. Ann Rheum Dis 2015;74:1045–50.
45. Wilson FC, Icen M, Crowson CS, McEvoy MT, Gabriel SE, Kremers HM. Incidence and clinical predictors of psoriatic arthritis in patients with psoriasis: a population-based study. Arthritis Rheum 2009;61:233–9.
46. Eder L, Haddad A, Rosen CF, Lee KA, Chandran V, Cook R, et al. The incidence and risk factors for psoriatic arthritis in patients with psoriasis: a prospective cohort study. Arthritis Rheumatol 2016;68:915–23.

DOI 10.1002/art.41921

Clinical Images: Diffuse systemic sclerosis, skin bleaching, and telangiectasia

The patient, a 31-year-old African Caribbean woman, was diagnosed as having diffuse systemic sclerosis in 2004 at age 15 years when she presented with Raynaud's phenomenon, sclerodactyly, and diffuse sclerodermatous skin with pigmentary changes. At the time of diagnosis, focal areas of depigmentation at the inner corner of both eyes and patchy hyperpigmentation of the upper eyelids were observed (**A**), as well as hyperpigmentation with loss of wrinkling of the skin of the neck (**B**). The patient declined all medical therapy over the next 16 years and had no cardiopulmonary, gastrointestinal, or renal disease. It was documented that she developed digital pits and telangiectasias on the face and palms. At age 31 years, she began liberal application of over-the-counter hydroquinone bleaching creams to her face and entire body to inhibit melanogenesis. As a result, telangiectasias on the face (**C**), neck, and anterior chest wall (**D**) became more clearly visible in her depigmented skin, and the skin lesions appeared to be extensively distributed and large (>5 mm). Patients of African origin have a differing systemic sclerosis disease phenotype compared to White patients, with earlier onset, predominantly diffuse disease, and risk of more severe complications. Telangiectasias are dilated postcapillary venules located in the papillary and superficial reticular dermis; they increase with disease duration and have an important potential correlation with overall vascular disease, including pulmonary hypertension (1). The frequency of documentation of telangiectasias in patients of African origin varies from as high as 50% in the Genome Research in African American Scleroderma Patients study (2) to as low as 13% in case series (3), and it is likely that these lesions sometimes escape detection. This patient, through a potentially harmful practice of medically unsupervised cosmetic skin bleaching, removed the veil of pigment to demonstrate how profuse telangiectasias can be in the skin of patients of African origin, thereby encouraging a more careful clinical examination for these lesions in other patients.

Author disclosures are available at https://onlinelibrary.wiley.com/action/downloadSupplement?doi=10.1002%2Fart41921&file=art41921-sup-0001-Disclosureform.pdf.

1. Shah AA, Wigley FM, Hummers LH. Telangiectasia in scleroderma: a potential clinical marker of pulmonary arterial hypertension. J Rheumatol 2010;37:98–104.
2. Morgan ND, Shah AA, Mayes MD, Domsic RT, Medsger TA Jr, Steen VD, et al. Clinical and serological features of systemic sclerosis in a multicenter African American cohort: analysis of the genome research in African American scleroderma patients clinical database. Medicine (Baltimore) 2017;96:e8980.
3. Erzer JN, Jaeger VK, Tikly M, Walker UA. Systemic sclerosis in sub-Saharan Africa: a systematic review. Pan Afr Med J 2020;37:176.

Cindy Flower, MBBS, DM, FACP
University of the West Indies Cave Hill Campus
Wanstead, Barbados

Arthritis & Rheumatology
Vol. 74, No. 2, February 2022, pp 263–273
DOI 10.1002/art.41930

American College of Rheumatology
Empowering Rheumatology Professionals

International Consensus for the Dosing of Corticosteroids in Childhood-Onset Systemic Lupus Erythematosus With Proliferative Lupus Nephritis

Nathalie E. Chalhoub,[1] Scott E. Wenderfer,[2] Deborah M. Levy,[3] Kelly Rouster-Stevens,[4] Amita Aggarwal,[5] Sonia I. Savani,[6] Natasha M. Ruth,[6] Thaschawee Arkachaisri,[7] Tingting Qiu,[8] Angela Merritt,[8] Karen Onel,[9] Beatrice Goilav,[10] Raju P. Khubchandani,[11] Jianghong Deng,[12] Adriana R. Fonseca,[13] Stacy P. Ardoin,[14] Coziana Ciurtin,[15] Ozgur Kasapcopur,[16] Marija Jelusic,[17] Adam M. Huber,[18] Seza Ozen,[19] Marisa S. Klein-Gitelman,[20] Simone Appenzeller,[21] André Cavalcanti,[22] Lampros Fotis,[23] Sern Chin Lim,[24] Rodrigo M. Silva,[13] Julia Ramírez- Miramontes,[25] Natalie L. Rosenwasser,[26] Claudia Saad-Magalhaes,[27] Dieneke Schonenberg-Meinema,[28] Christiaan Scott,[29] Clovis A. Silva,[30] Sandra Enciso,[31] Maria T. Terreri,[32] Alfonso-Ragnar Torres-Jimenez,[33] Maria Trachana,[34] Sulaiman M. Al-Mayouf,[35] Prasad Devarajan,[36] Bin Huang,[36] and Hermine I. Brunner[36]

Objective. To develop a standardized steroid dosing regimen (SSR) for physicians treating childhood-onset systemic lupus erythematosus (SLE) complicated by lupus nephritis (LN), using consensus formation methodology.

Methods. Parameters influencing corticosteroid (CS) dosing were identified (step 1). Data from children with proliferative LN were used to generate patient profiles (step 2). Physicians rated changes in renal and extrarenal childhood-onset SLE activity between 2 consecutive visits and proposed CS dosing (step 3). The SSR was developed using patient profile ratings (step 4), with refinements achieved in a physician focus group (step 5). A second type of patient profile describing the course of childhood-onset SLE for ≥4 months since kidney biopsy was rated to validate the SSR-recommended oral and intravenous (IV) CS dosages (step 6). Patient profile adjudication was based on majority ratings for both renal and extrarenal disease courses, and consensus level was set at 80%.

Results. Degree of proteinuria, estimated glomerular filtration rate, changes in renal and extrarenal disease activity, and time since kidney biopsy influenced CS dosing (steps 1 and 2). Considering these parameters in 5,056 patient profile ratings from 103 raters, and renal and extrarenal course definitions, CS dosing rules of the SSR were developed (steps 3–5). Validation of the SSR for up to 6 months post–kidney biopsy was achieved with 1,838 patient profile ratings from 60 raters who achieved consensus for oral and IV CS dosage in accordance with the SSR (step 6).

Conclusion. The SSR represents an international consensus on CS dosing for use in patients with childhood-onset SLE and proliferative LN. The SSR is anticipated to be used for clinical care and to standardize CS dosage during clinical trials.

The content is solely the responsibility of the authors and does not necessarily represent the official views of the NIH.

Supported by Pediatric Musculoskeletal & Rheumatology Innovation Core center (PORTICO) (National Institute of Arthritis and Musculoskeletal and Skin Diseases [NIAMS] award P30-AR-076316, NIAMS award R34-AR-071651, an Institutional Clinical and Translational Science Award, and the National Center for Advancing Translational Sciences, NIH grant 8UL1-TR-000077). REDCap is supported by the NIH (grant UL1-TR-000445). Dr. Chalhoub's work was supported by the National Center for Advancing Translational Sciences (grant 2UL1-TR-001425) and the Internal Medicine Scholars Training for Academic Research (IM STAR) program. Dr. Savani's work was supported by NIH training grant T32-AR-050958. Dr. Deng's work was supported by a Beijing Municipal Bureau of Foreign Affairs Training award. Dr. Ciurtin's work was supported by the Centre for Adolescent Rheumatology Versus Arthritis (grant 21593) and NIHR University College London Hospitals Biomedical Research Centre (grant BRC 525 III/CC). Dr. Silva's work was supported by the Conselho Nacional de Desenvolvimento Científico e Tecnológico (grant CNPq 303422/2015-7), Fundação de Amparo à Pesquisa do Estado de São Paulo (grant FAPESP 2015/03756-4), and the Núcleo de Apoio à Pesquisa "Saúde da Criança e do Adolescente" da USP (NAP-CriAd). Dr. Devarajan's work was supported by the National Institute of Diabetes and Digestive and Kidney Diseases, NIH (grant P50-DK-096418). The Childhood Arthritis and Rheumatology Research Alliance is supported in part by the Arthritis Foundation.

[1]Nathalie E. Chalhoub, MD, MSc: University of Cincinnati College of Medicine, Cincinnati, Ohio; [2]Scott E. Wenderfer, MD, PhD: Baylor College of Medicine, Houston, Texas; [3]Deborah M. Levy, MD, MS: The Hospital for Sick Children and The University of Toronto, Toronto, Ontario, Canada; [4]Kelly Rouster-Stevens, MD, MSc: Emory University and Children's Healthcare of Atlanta, Atlanta, Georgia; [5]Amita Aggarwal, MD, DM: Sanjay Gandhi

INTRODUCTION

Corticosteroids (CS) remain one of the mainstays of therapy in childhood-onset systemic lupus erythematosus (SLE), especially with major organ involvement such as lupus nephritis (LN). Due to lack of strong medical evidence, dosing of CS for childhood-onset SLE treatment remains mainly provider-dependent (1). Delphi surveys and expert opinion were previously employed to propose standards for CS use (2,3), including for proliferative LN in children as part of the consensus treatment plans for pediatric LN (4). However, when tested in real-life settings, providers were following the CS dosing recommended by the consensus treatment plans for pediatric LN in only 68% of patients by 3 months of induction therapy for LN and in just 37% of patients by 6 months of induction therapy for LN (5).

In this study, our goal was to use consensus formation methods in conjunction with real-life patient data to 1) delineate determinants that influence CS dosage in childhood-onset SLE with proliferative LN, 2) develop the standardized steroid dosing regimen (SSR), and 3) initially validate the SSR.

PATIENTS AND METHODS

Study overview. Figure 1 sketches the experimental design (steps 1–6). Building on the experience from the consensus treatment plans for pediatric LN (4), we focused on patients with childhood-onset SLE who had biopsy-proven, new-onset class III or IV LN with or without class V overlap, in accordance with the International Society for Nephrology/Renal Pathology Society guidelines (6). Consensus formation methodology was combined with statistical modeling of patient profile ratings that were derived from a contemporary childhood-onset SLE cohort. We invited an international group of physicians experienced in the care of pediatric LN to participate in this study. These study collaborators are listed in Supplementary Material – Study Collaborators, on the *Arthritis & Rheumatology* website at http://onlinelibrary.wiley.com/doi/10.1002/art.41930/abstract.

Details of the experimental design. *Step 1.* A review of the literature was conducted, revealing only limited high-quality evidence regarding CS dosing in patients with childhood-onset SLE (7). In April 2018, after literature review followed by a Delphi survey, consensus was achieved with regard to candidate determinants of oral CS use and intravenous (IV) CS use (CS determinants) at an in-person meeting held in Denver, CO, using a modified nominal group technique (8). Demographic, laboratory, and clinical parameters were identified as candidate CS determinants. Fifty-one members of the Childhood Arthritis and Rheumatology Research Alliance (CARRA) LN Work Group participated in the consensus meeting.

Step 2. The medical records of 143 LN patients followed up at 8 pediatric tertiary care centers were retrospectively reviewed for up to 24 months, starting from the time patients received a kidney biopsy from which they were newly diagnosed as having proliferative LN (6). Table 1 summarizes principal eligibility criteria in patients whose data were abstracted for patient profile generation.

Patient profile formats previously developed to adjudicate the overall disease course of childhood-onset SLE (9) were adapted and piloted among 20 physicians. Profiles included information regarding demographic characteristics (e.g., age, sex, race, and ethnicity), organ involvement with SLE in accordance with the 1997 American College of Rheumatology (ACR) classification criteria (10), kidney biopsy results (e.g., LN class [6], activity score,

Postgraduate Institute of Medical Sciences, Lucknow, India; [6]Sonia I. Savani, MD, Natasha M. Ruth, MD, MS: Medical University of South Carolina, Charleston; [7]Thaschawee Arkachaisri, MD: KK Women's and Children's Hospital, Singapore; [8]Tingting Qiu, MPH, Angela Merritt, BA: Cincinnati Children's Hospital Medical Center, Cincinnati, Ohio; [9]Karen Onel, MD: Hospital for Special Surgery, New York, New York; [10]Beatrice Goilav, MD: Albert Einstein College of Medicine, New York, New York; [11]Raju P Khubchandani, MD: SRCC Children's Hospital, Mumbai, India; [12]Jianghong Deng, MD, PhD: Capital Medical University and National Center for Children's Health, Beijing, China; [13]Adriana R. Fonseca, MD, MSc, PhD, Rodrigo M. Silva, MD: Universidade Federal do Rio de Janeiro, Rio de Janeiro, Brazil; [14]Stacy P. Ardoin, MD, MS: Nationwide Children's Hospital, Columbus, Ohio; [15]Coziana Ciurtin, MD, PhD, FRCP: University College London, London, UK; [16]Ozgur Kasapcopur, MD: Cerrahpasa Medical School, Istanbul University-Cerrahpasa, Istanbul, Turkey; [17]Marija Jelusic, MD, PhD: University of Zagreb School of Medicine, Zagreb, Croatia; [18]Adam M. Huber, MD, MSc: IWK Health Centre and Dalhousie University, Halifax, Nova Scotia, Canada; [19]Seza Ozen, MD: Hacettepe University, Ankara, Turkey; [20]Marisa S. Klein-Gitelman, MD, MPH: Northwestern University Feinberg School of Medicine and Ann & Robert H. Lurie Children's Hospital of Chicago, Chicago, Illinois; [21]Simone Appenzeller, MD, PhD: University of Campinas, Campinas, Brazil; [22]André Cavalcanti, MD: Hospital das Clínicas da Universidade Federal de Pernambuco, Recife, Brazil; [23]Lampros Fotis, MD, PhD: National and Kapodistian University of Athens, Athens, Greece; [24]Sern Chin Lim, MD, FRCPCH: University Teknologi MARA, Sungaig Buloh, Malaysia; [25]Julia Ramírez-Miramontes, MD: Instituto Mexicano del Seguro Social, Monterrey, Mexico; [26]Natalie L. Rosenwasser, MD: University of Washington and Seattle Children's Hospital, Seattle, Washington; [27]Claudia Saad-Magalhaes, MD, PhD: São Paulo State University, Botucatu, Brazil; [28]Dieneke Schonenberg-Meinema, MD: Amsterdam University Medical Center, Amsterdam, The Netherlands; [29]Christiaan Scott, MBChB: Red Cross War Memorial Children's Hospital and University of Cape Town, Cape Town, South Africa; [30]Clovis A. Silva, MD, PhD: Universidade de São Paulo, Sao Paulo, Brazil; [31]Sandra Enciso, MD: Hospital de la Beneficencia Española, Mexico City, Mexico; [32]Maria T. Terreri, MD: Universidade Federal de São Paulo, Sao Paulo, Brazil; [33]Alfonso-Ragnar Torres-Jimenez, MD: National Medical Center La Raza, Mexico City, Mexico; [34]Maria Trachana, MD: Aristotle University of Thessaloniki, Thessaloniki, Greece; [35]Sulaiman M. Al-Mayouf, MD: King Faisal Specialist Hospital and Research Center and Alfaisal University, Riyadh, Saudi Arabia; [36]Prasad Devarajan, MD, Bin Huang, PhD, Hermine I. Brunner, MD, MSc, MBA: University of Cincinnati College of Medicine and Cincinnati Children's Hospital Medical Center, Cincinnati, Ohio.

Author disclosures are available at https://onlinelibrary.wiley.com/action/downloadSupplement?doi=10.1002%2Fart.41930&file=art41930-sup-0001-Disclosureform.pdf.

Address correspondence to Hermine I. Brunner, MD, MSc, MBA, Cincinnati Children's Hospital Medical Center, 3333 Burnet Avenue, MLC 4010, Cincinnati, OH 45229-3039. Email: Hermine.Brunner@cchmc.org

Submitted for publication March 14, 2021; accepted in revised form July 15, 2021.

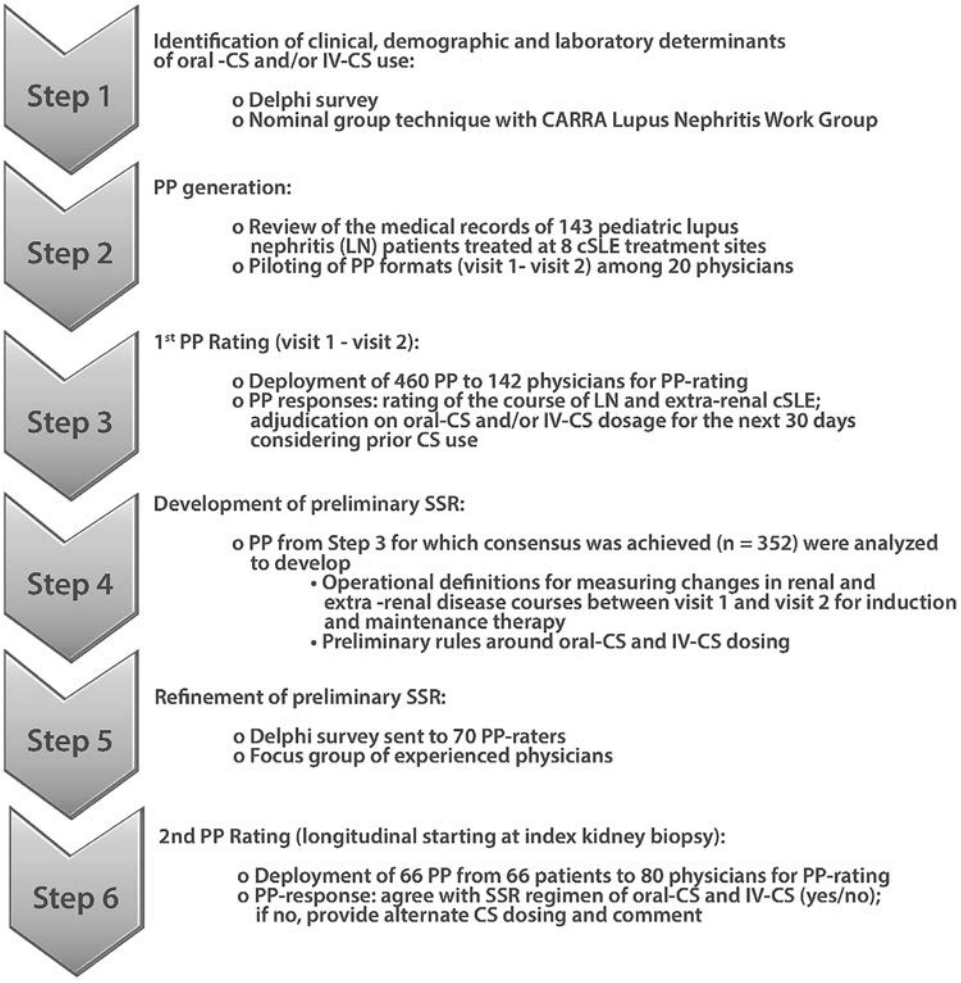

Figure 1. Development of the standardized steroid dosing regimen (SSR) for patients with childhood-onset systemic lupus erythematosus (cSLE). The experimental design used can be summarized in steps 1–6, and consists of various consensus formation methods, statistical analyses, and the use of real-life data from pediatric patients with lupus nephritis (LN) in patient profile (PP) ratings. Data were collected using Research Electronic Data Capture software (https://projectredcap.org/software). CS = corticosteroid; IV = intravenous; CARRA = Childhood Arthritis and Rheumatology Research Alliance.

and chronicity score [11,12]), vital signs (e.g., body surface area, height, body weight, and blood pressure), and laboratory findings (e.g., complete blood cell count, erythrocyte sedimentation rate [ESR], C3, C4, and anti–double-stranded DNA antibodies). Profiles also included the response variables for pediatric LN (4), namely proteinuria (spot urine protein-to-creatinine ratio or 24-hour timed proteinuria), renal function (estimated glomerular filtration rate [eGFR] and serum creatinine), and urine sediment (white blood cells [WBCs]/high-power field [hpf], red blood cells [RBCs]/hpf, and heme-granular or RBC casts); Systemic Lupus International Collaborating Clinics/ACR Damage Index (13) and SLE Disease Activity Index 2000 (SLEDAI-2K) scores (14); parent/patient global assessment of overall well-being; physician global assessment of overall disease activity; and use of oral CS and IV CS (e.g., dose, route, and frequency), immunosuppressants (e.g., mycophenolate mofetil or cyclophosphamide with dose and frequency), and angiotensin system blockers (yes/no). Each patient profile provided this information for 2 consecutive patient assessments (visit 1 and visit 2) to describe the course of childhood-onset SLE over a 4-week period.

Step 3. Of 2,215 patient profiles generated, 460 with complete patient information were selected for rating by 142 physicians (patient profile raters) who were members of the CARRA LN Work Group, the Pediatric Rheumatology European Society Lupus Working Party, or the Pediatric Nephrology Research Consortium. Patient profile selection for the development data set focused on capturing all permutations of combined renal and extrarenal disease courses between visit 1 and visit 2. Raters adjudicated the renal and extrarenal disease courses as follows: active–stable, active–improved, active–worse, inactive, or not enough information. Patient profile raters were also asked to suggest oral CS and IV CS dosages for the 30 days following visit 2 at stable, increasing, or tapering dosages. Raters were randomized to rate 66 patient profiles each (Supplementary Figure 1, available

Table 1. Principal eligibility criteria for patients used for patient profile generation*

Inclusion criteria	Exclusion criteria
Men and women fulfilling 1997 ACR classification criteria for SLE	Use of rituximab within 6 months of diagnosis of proliferative LN
Age ≤18 years at the time of index kidney biopsy†	Chronic medical conditions, other than SLE, that necessitate prolonged CS use
Time of index kidney biopsy between January 2008 and June 2018	Renal replacement therapy requirement within 6 months of index kidney biopsy
Index kidney biopsy consistent with new diagnosis of class III, III/V, class IV, or class IV/V LN, per the ISN/RPS classification criteria for LN	History of kidney transplant
Induction therapy with cyclophosphamide or mycophenolate mofetil	Follow-up for LN at the center for <6 months after index kidney biopsy
	Lack of biopsy report for index kidney biopsy in patient's medical record

* ACR = American College of Rheumatology; SLE = systemic lupus erythematosus; CS = corticosteroid; ISN = International Society for Nephrology; RPS = Renal Pathology Society.
† Patient could have had other renal biopsies indicating the presence of other classes of lupus nephritis (LN).

on the *Arthritis & Rheumatology* website at http://onlinelibrary.wiley.com/doi/10.1002/art.41930/abstract).

Step 4. Only patient profiles for which consensus regarding the course of childhood-onset SLE between visits was achieved were included in the data set that was used to develop the SSR. As done in the past (9), adjudication of the renal and extrarenal disease courses described in a given patient profile was based on majority vote among raters, i.e., ≥50% of raters agreed on one specific combination of renal disease and extrarenal disease courses between visit 1 and visit 2. SSR-recommended CS dosage was the median daily dose for which consensus was achieved by patient profile raters.

Step 5. Following statistical analysis (detailed below), an additional Delphi questionnaire was sent to a randomly selected subset of patient profile raters (n = 70). The aim of this questionnaire was to clarify maximum daily oral CS dosages, use of divided daily oral CS doses, IV CS use at time of initiation of induction therapy, and IV and/or oral CS dosages prescribed for flares (LN and/or extrarenal childhood-onset SLE). This was followed by a physician focus group (KO, DML, SW, and MKG) to clarify CS use for children <40 kg and the importance of the type of immunosuppressant prescribed (cyclophosphamide or mycophenolate mofetil) for the use of IV CS. Information from step 5 information was used to refine the preliminary SSR (from step 4) (4,5).

Step 6. Among available patients with ≥4 months of follow-up, 66 patients (or patient profiles) were selected to serve as the validation set. The profile format used in step 6 was similar to those used in step 3. However, in addition to renal and extrarenal disease course information, the SSR-recommended dosages of oral and/or IV CS for up to 6 months since kidney biopsy were shown (Supplementary Figure 2, http://onlinelibrary.wiley.com/doi/10.1002/art.41930/abstract). These 66 patient profiles were sent to 80 raters randomly selected from the pool of available raters (step 3); each rater was asked to rate 33 patient profiles. Specifically, raters were asked whether the SSR-recommended CS dosage at each time point was acceptable for treating the vast majority of patients (>80%) with similar clinical presentations and comparable renal and extrarenal disease courses.

Ethics approval. The study was approved by the ethics committees and institutional review boards of the participating centers.

Data management and statistical analysis. Following patient profile ratings (step 3), the frequencies and percentage agreement were calculated for each profile for the renal, extrarenal, and overall (renal plus extrarenal) disease courses. At the analysis unit, each profile was reviewed and rated by multiple pediatric rheumatologists and nephrologists, and their responses were summarized and analyzed to evaluate the level of consensus for oral and IV CS dosage as recommended by the SSR. Only profiles with majority ratings (≥50%) for a given disease course were considered in these statistical analyses. Logistic regression analyses identified CS determinants relevant to renal, extrarenal, and overall disease courses (step 3). Descriptive statistics (mean ± SD, median, interquartile range) for the percentage agreement among raters for oral and IV CS dosing were computed, followed by distribution and probability plots (step 4). CS dosing regimens for each disease course were summarized and synthesized to develop the preliminary SSR (step 4). Step 5 considered consensus among survey respondents. The validation of the SSR (step 6) used statistics similar to those used in step 4. Research Electronic Data Capture software (https://projectredcap.org/software) was used for data capture, storage, surveys, and profile ratings. Data were analyzed using SAS, version 9.4.

RESULTS

Proposed determinants that influence CS use in childhood-onset SLE with LN. For step 1, 25 of 51 physicians of the CARRA LN Work Group responded to the Delphi questionnaire (49% response rate). The questionnaire was aimed at confirming the response variables for pediatric LN and identifying additional CS determinants. There was consensus (>80%) that complement levels (C3 and C4) and the urine protein-to-creatinine ratio were important determinants of CS dosage. Structured discussions and voting as part of a nominal group

Table 2. Baseline characteristics of the patients with childhood-onset SLE used for patient profile development*

	Patients for step 3 (n = 120)	Patients for step 6 (n = 66)
Age at LN onset, mean ± SD years	13.47 ± 3.06	13.50 ± 2.89
Female	96 (80)	55 (83)
Race		
White	59 (49)	35 (53)
Black or African American	45 (37.5)	25 (38)
Other	13 (11)	5 (8)
Unknown	3 (2.5)	1 (1)
Ethnicity		
Hispanic	35 (29)	19 (29)
Non-Hispanic	84 (70)	47 (71)
Unknown	1 (1)	0 (0)
Laboratory testing, mean ± SD		
Urine protein-to-creatinine ratio, mg/mg	3.04 ± 3.85	2.77 ± 2.46
Serum creatinine, mg/dl	0.90 ± 0.70	0.98 ± 0.89
SDI total score at LN onset, mean ± SD†	0.19 ± 0.58	0.15 ± 0.47
SLEDAI-2K feature present‡		
Seizure	2 (2)	1 (2)
Organic brain syndrome	3 (3)	1 (2)
Visual disturbances	2 (2)	0 (0)
Cranial nerve disorder	1 (1)	1 (2)
Lupus headache	1 (1)	1 (2)
CVA	1 (1)	0 (0)
Vasculitis	10 (10)	8 (14)
Arthritis	45 (43)	28 (49)
Myositis	7 (7)	5 (9)
Urinary casts	36 (35)	17 (30)
Hematuria	80 (77)	47 (82)
Proteinuria	92 (88)	53 (93)
Pyuria	60 (58)	36 (63)
Rash	58 (56)	34 (60)
Alopecia	7 (7)	4 (7)
Mucosal ulcers	13 (12.5)	8 (14)
Pleurisy	7 (7)	1 (2)
Pericarditis	12 (12)	5 (9)
Low complement	96 (92)	53 (93)
Increased DNA binding	93 (89)	53 (93)
Fever	21 (20)	12 (21)
Thrombocytopenia	15 (14)	9 (16)
Leukopenia	19 (18)	12 (21)
SLEDAI-2K total score, mean ± SD	19.88 ± 7.43	20.86 ± 6.78
Oral prednisone equivalent dose, mg/day§		
<7.5	11 (9)	6 (9)
7.5–16	7 (6)	1 (2)
>16–45	51 (42.5)	28 (42)
>45	51 (42.5)	31 (47)
Other medications at visit 1		
IV methylprednisolone	3 (2.5)	1 (2)
Mycophenolate mofetil	3 (2.5)	1 (2)
Cyclophosphamide	33 (27.5)	26 (39)
Angiotensin system blockers	51 (42.5)	24 (36)

* Except where indicated otherwise, values are the number (%). LN = lupus nephritis; SDI = Systemic Lupus International Collaborating Clinics/American College of Rheumatology Damage Index; SLEDAI-2K = Systemic Lupus Erythematosus Disease Activity Index 2000; CVA = cerebrovascular accident; IV = intravenous.
† For item definitions, see ref. 13.
‡ For item definitions, see ref. 14.
§ Other corticosteroid doses were converted to prednisone equivalent doses.

exercise at a subsequent face-to-face meeting provided confirmation of these candidate CS determinants. These included time since index kidney biopsy, kidney histologic features, status of and change in the response variables for pediatric LN since prior assessment, and extrarenal disease activity as measured by the scores from the respective domains of the SLEDAI-2K, ESR, physician global assessment of disease activity, and parent/patient global assessment of overall well-being. Presented case examples highlighted the extent of variation in CS prescribing among group members (n = 15) when treating proliferative LN, hence supporting the rationale for developing the SSR.

Determinants influencing patient profile rater adjudication of status and changes in renal and extrarenal disease used in the SSR. In step 3, 103 physicians (of 142 [response rate 73%]) reviewed 460 patient profiles producing 5,080 ratings. Of the 5,080 patient profile ratings, 24 were excluded due to data quality issues, resulting in the analysis of 5,056 ratings. These 460 profiles represented 120 of the 143 LN patients with available data. Table 2 summarizes the baseline characteristics of these 120 patients with childhood-onset SLE represented by the patient profile. Of the 460 profiles, 352 (77%) achieved majority ratings for the renal disease course and extrarenal disease course between visit 1 and visit 2, hence qualifying for inclusion in the subsequent steps of the SSR development.

Among the proposed CS determinants included in step 3, the renal course was best predicted by the eGFR, urine protein-to-creatinine ratio, and urinary RBCs. Pyuria was common (Table 2); however, it was not associated with LN disease course (active–stable, active–improved, active–worse, or inactive) (odds ratio [OR] 1.03, $P = 0.97$). Disease course of extrarenal disease from patient profile ratings was closely associated with a change in extrarenal SLEDAI-2K score (OR 0.91, $P = 0.004$). Thus, the following CS determinants were considered in the preliminary SSR: patient actual body weight, time since index kidney biopsy, extrarenal SLEDAI-2K score, urine protein-to-creatinine ratio,

Renal courses		Extrarenal course [$]
Induction therapy (weeks 1–26)	*Maintenance therapy (after week 27)*	
LN active–worse [#]***:*** Worsening of ≥1 LN-RV[†]	***LN flare after PRR or CRR:*** Worsening (persistent[¥] & substantial) of ≥1 LN-RV	***Active–much worse:*** Δ SLEDAI-2K score: ≥ +8
LN active–stable: Neither *active–worse* nor *active–improved*	***LN worse*** [#] ***after PRR or CRR:*** Worsening of ≥1 LN-RV	***Active–mild/moderate worse:*** Δ SLEDAI-2K score: +4 to +7
LN active–improved: Improvement of ≥1 LN-RV with the remaining LN-RV(s) not being worse	***PRR stable:*** PRR with changes of LN-RVs not qualifying for being worse or improved	***Active–stable:*** Δ SLEDAI-2K score: ± 3
PRR [‡]***:*** Clinically relevant improvement of ≥2 LN-RVs with the remaining LN-RV not being worse	***PRR improved:*** PPR with improvement of ≥1 LN-RV with the remaining LN-RV(s) not being worse	***Active–improved:*** Δ SLEDAI-2K score: ≤-4
LN inactive: All LN-RVs are within normal range	***CRR:*** All LN-RVs are within normal range	***Inactive:*** Absolute SLEDAI-2K score: ≤2

Figure 2. Categorization of renal and extrarenal disease courses between visits 1 and 2 as used in the SSR. # All "worsening" is considered to be due to LN. † LN response variables (LN-RVs), i.e., urine protein-to-creatinine ratio (UPCR), hematuria, and estimated glomerular filtration rate (eGFR). Normal values in LN-RVs are always considered as "improved" for the purpose of the course definitions (see Figure 3 for details). ‡ Partial renal remission (PRR) assesses the change in LN-RVs between baseline and week 26 and can only be measured starting at week 26 of induction therapy. ¥ Worsening of ≥1 LN-RV at >2 subsequent time points >1 week apart, as follows: newly abnormal eGFR or abnormal eGFR that decreased by >10%, persistent increase of UPCR to >0.5 after complete renal remission (CRR), persistent doubling of UPCR with values >1.0 after partial renal remission, and newly active or worsening by 2 categories of urinary red blood cells. $ Based on changes in the Systemic Lupus Erythematosus Disease Activity Index 2000 (SLEDAI-2K) score (for item definitions, see ref. 14). See Figure 1 for other definitions.

urinary RBCs, and eGFR. We used a conservative estimate for normal eGFR of ≥95 ml/minute/1.73 m^2 (15,16).

Summary and overarching principles of the SSR. According to the SSR, the oral CS of choice is prednisone, and the IV CS of choice is methylprednisolone. It is understood that patients are treated with an additional immunosuppressant during induction therapy and maintenance therapy for LN. Building on the consensus treatment plans for pediatric LN (4), the SSR considers time since the index kidney biopsy in determining oral and IV CS use. The SSR assumes that potential CS dose adjustments will potentially occur every 4 weeks. More frequent adjustments may occur during the initial 4 weeks of induction therapy and in cases of severe renal or extrarenal flares. In the following sections, we assume that patients have body weights of ≥40 kg and that the maximum daily oral CS dosage is 60 mg. In patients with childhood-onset SLE with a body weight of <40 kg, the equivalent maximum dose is 1.5 mg/kg/day (step 5). Lower dosages of oral CS (prednisone) for patients who weigh <40 kg can be calculated as follows: daily SSR dosage for patients ≥40 kg × body weight × 0.025. We anticipate that the SSR can be used for the vast majority of children (>80%), as indicated by the patient profile rater responses regarding oral and IV CS dosing (step 6).

Categorization of disease course between assessments. The SSR categorizes changes in extrarenal activity between assessment as a–d, as follows: (a) active–much worse; (b) active–mild/moderate worse; (c) active–stable or active–improved; or (d) inactive. For induction therapy, changes in renal activity between assessments are categorized as A–D,

as follows: (A) active–worse; (B) active–stable; (C) active–improved or inactive prior to week 12; or (D) inactive starting week 12. Changes in renal activity categories (i–iv) used during maintenance therapy are as follows: (i) LN flare after partial renal remission or complete renal remission; (ii) worse after partial renal remission or complete renal remission; (iii) partial renal remission stable; or (iv) complete renal remission or partial renal remission improved. Figure 2 summarizes the definitions of the changes in renal and extrarenal disease courses between visits that govern SSR-recommended CS dosages. Additional details pertaining to the interpretation of the changes in the response variables for pediatric LN are provided in Figure 3. Logistic regression analysis identified variable thresholds that were used in the proposed definitions to classify renal disease courses and extrarenal disease courses. Using these definitions allowed us to model renal and extrarenal courses (per the patient profile raters) with >90% accuracy based on area under the curve from receiver operating characteristic curve analysis (Supplementary Figure 3, http://onlinelibrary.wiley.com/doi/10.1002/art.41930/abstract).

SSR-recommended CS dosage during the initial 4 weeks post–index kidney biopsy. The SSR allows for up to 3 infusions of high-dose methylprednisolone (30 mg/kg/dose; maximum 1 gram) following a diagnosis of proliferative LN. The maximum starting dosage of daily oral CS is 60 mg, which may be given in divided doses. Depending on extrarenal disease

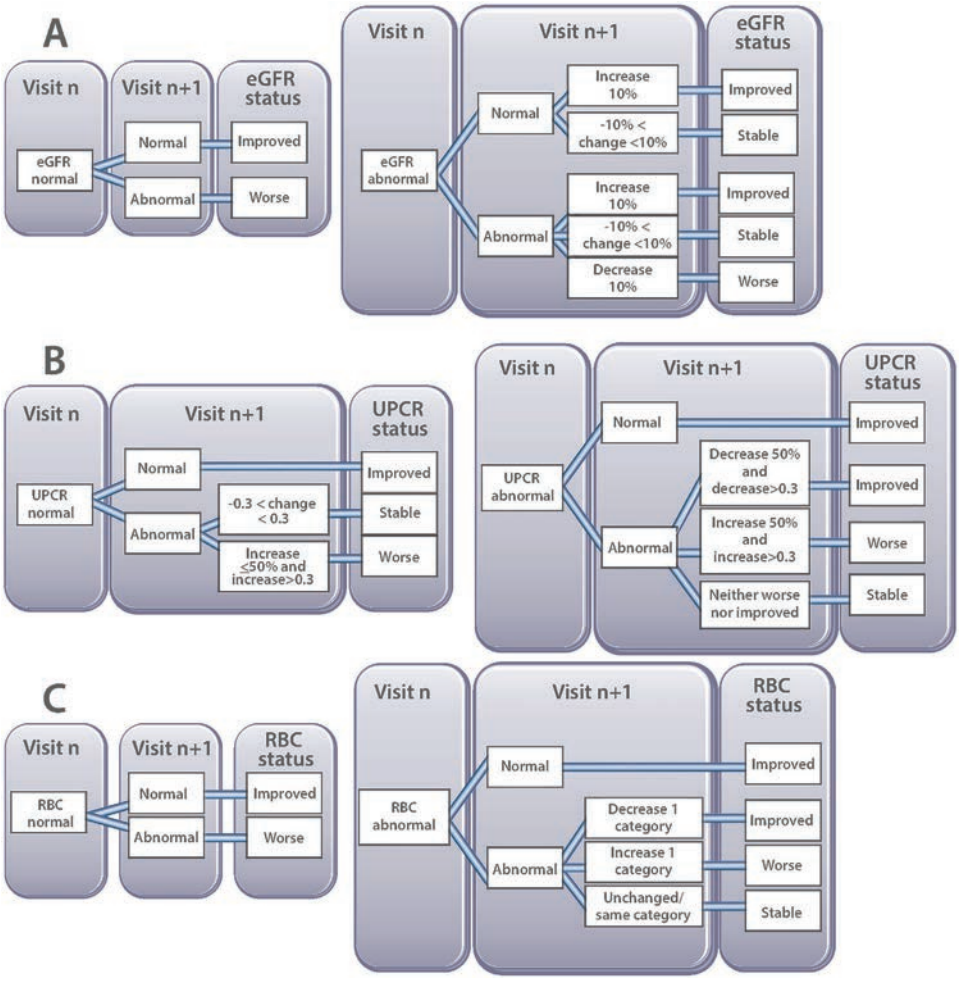

Figure 3. Operational definitions for changes in the LN response variables for use in the SSR. **A**, Estimated glomerular filtration rate (eGFR) of ≥95 ml/minute/1.73 m^2 was considered to be normal, and eGFR of <95 ml/minute/1.73 m^2 was considered to be abnormal, regardless of patient age. **B**, Urine protein-to-creatinine ratio (UPCR) of ≤0.2 mg/mg in a random urine sample was considered normal, and UPCR of >0.2 mg/mg was considered abnormal. Increases or decreases of <0.3 mg/mg in the UPCR were deemed to represent stable proteinuria. Examples of changes in the UPCR between visit 1 and visit 2 and assessment of UPCR status are as follows: 0.5 → 0.25 (decrease of 50%, but decrease is <0.3, so UPCR is stable); 0.5 → 0.2 (UPCR is normal); 0.5 → 0.8 (increase of >50% and increase by 0.3, so UPCR is worse); 0.5 → 0.75 (increase of 50%, but increase is <0.3, so UPCR is stable). **C**, Only glomerular hematuria was considered when assessing urine microscopy, whereas pyuria and cellular casts were excluded. Five categories of glomerular hematuria measures were defined as follows: normal (0–5 red blood cells [RBCs]/high-power field [hpf]), mild (6–10 RBCs/hpf), moderate (11–25 RBCs/hpf), severe (26–50 RBCs/hpf), and gross (>50 RBCs/hpf). See Figure 1 for other definitions.

activity and response of LN to therapy, the oral CS dosage may be decreased weekly, resulting in a minimum daily oral CS dosage of 40 mg (maximum 60 mg) at week 4 of induction therapy.

SSR-recommended CS dosage during induction therapy (weeks 5–26). The SSR is adjusted in at least monthly intervals in weeks 5 to 26 of induction therapy (minimum oral CS dosage 10 mg at week 26). Considering the pathology of LN, even if all response variables for pediatric LN have normalized, CS dosage reduction is more conservative prior to week 12 than thereafter. Given the known toxicity of CS, small decreases in oral CS dosage occur even with stable renal activity and/or extrarenal activity. Figure 4A provides an example of the SSR-recommended CS dosage adjustment for patients who experience major worsening of extrarenal disease activity in the setting of improving renal disease during the first 12 weeks post–index kidney biopsy.

SSR-recommended CS dosage during maintenance therapy (starting week 27). The determination of partial renal remission and complete renal remission occurs upon completion of induction therapy at week 26. Based on focus group feedback, the SSR assumes that nonresponders to induction therapy are likely to undergo repeat kidney biopsy, with CS dosage then chosen according to repeat biopsy findings. For all other patients, CS dosage will depend on categories of both renal activity courses and extrarenal activity courses. As during induction therapy, provided there is well-controlled extrarenal disease, the SSR allows for CS tapering even in the setting of active–stable renal disease. Likewise, with moderate worsening of extrarenal disease in the setting of improving renal disease, the CS dosage is kept stable. In patients who receive maintenance therapy during complete renal remission and who are taking 10 mg of oral CS, oral CS will be tapered by 1–2 mg monthly, provided extrarenal disease is not worsening. An example of the SSR-recommended CS dosage for a patient receiving 30 mg of oral CS at the time of an LN flare during maintenance therapy is shown in Figure 4B.

Major worsening of extrarenal disease. Exploratory analyses suggested that daily oral CS dosages of ≥40 mg should be guided by the renal disease course, except in the setting of major extrarenal flares with potential organ damage. In the SSR, major increases in extrarenal disease activity will prompt an increase in the oral CS dosage by 60–70% with stable renal disease courses and by 30–40% with renal improvement or with the use of oral CS doses of ≥40 mg at the time of the extrarenal exacerbation. If major extrarenal deterioration fails to respond to increased oral CS dosages within 10–14 days as adjudicated by the physician, then the SSR recommends the potential use of IV CS.

SSR validation. The complete SSR is shown in Supplementary Table 1 (http://onlinelibrary.wiley.com/doi/10.1002/art.41930/abstract). In step 6, a total of 66 patient profiles describing

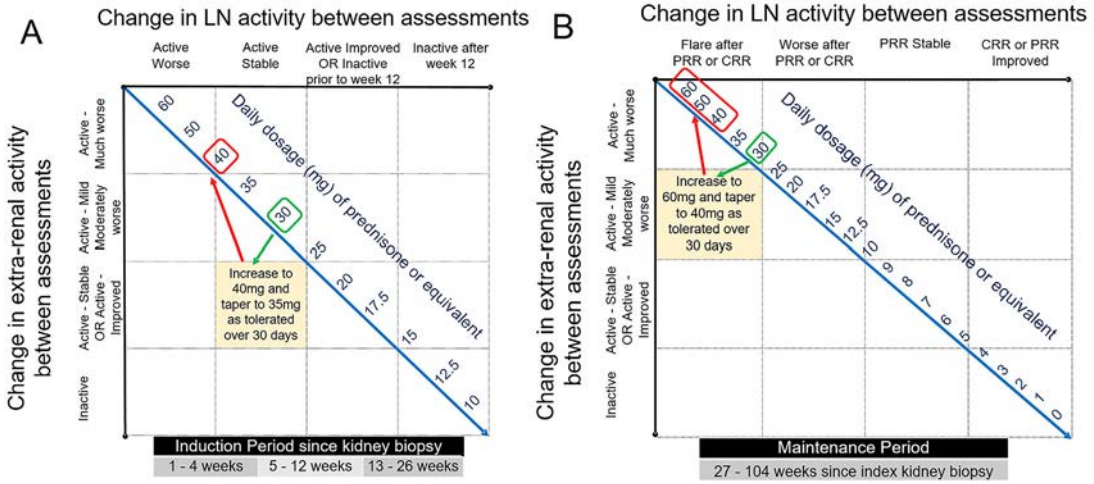

Figure 4. Examples of SSR-recommended changes in prednisone dosage (or equivalent dose of another CS). **A**, Recommended prednisone dose adjustment in a patient with childhood-onset SLE weighing ≥40 kg whose kidney biopsy showed proliferative LN within the preceding 12 weeks. Upon reassessment, the patient was taking prednisone 30 mg daily, his renal disease course was "active–improved," and his extrarenal disease course was "active–much worse." The SSR recommends increasing the daily prednisone dose to 40 mg. If tolerated, tapering of oral CS during the subsequent 4 weeks post-assessment to 35 mg/day is recommended. **B**, Recommended prednisone dose adjustment in a patient with childhood-onset SLE (≥40 kg) who completed induction therapy for LN and achieved at least partial renal remission at week 26. Upon reassessment, the patient was taking prednisone 30 mg daily and experienced an "LN flare after partial renal remission (PRR)." The SSR recommends increasing the daily prednisone dose to 60 mg, regardless of the extrarenal course. If renal response is improved with higher oral CS doses, then oral CS tapering can be initiated on day 10. The minimum allowable daily prednisone dose on day 30 following an LN flare is 40 mg. If the patient has not improved by day 10, then IV pulse methylprednisolone (1–3 doses) should be considered. CRR = complete renal remission (see Figure 1 for other definitions).

the disease course of childhood-onset SLE for 4–6 months post–index kidney biopsy were rated by 60 physicians (of 80 raters invited [response rate 75%]), which provided a total of 1,838 ratings. Table 2 shows the baseline characteristics of the patients represented by the patient profiles used in step 6. Raters achieved agreement (95%) on all SSR-recommended oral and/or IV CS dosages. Patient profile raters stated that in >80% of their patients with similar features of childhood-onset SLE, with regard to both renal disease course and extrarenal disease course, the SSR-recommended oral and/or IV CS dosage was appropriate for clinical care.

DISCUSSION

In this study, an international group of pediatric rheumatologists and nephrologists collaborated to develop the SSR, a novel algorithm that standardizes oral CS and IV CS dosing decisions in patients with childhood-onset SLE with proliferative LN. As part of this research, determinants that influence medical decisions pertaining to CS dosage were identified. This allowed us to model CS dosage based on the renal and extrarenal disease courses with high accuracy.

Practice patterns are strongly variable among physicians (1,3,17,18) and indicate that physician attributes may be more important than patient characteristics when prescribing CS (1,3). While crucial in the treatment of childhood-onset SLE, CS use is associated with damage accrual (19–21), and the severity of CS side effects makes dosage a constant focus for the treating physician. This emphasizes the importance of the developed SSR as an innovative tool to standardize CS dosage among physicians and centers treating patients with childhood-onset SLE.

A review of the literature has confirmed the lack of strong medical evidence to guide CS dosing in childhood-onset SLE and LN (7). Our overall approach to this project was based on a stringent methodologic framework using consensus formation techniques that were successfully used in previous pediatric rheumatology studies to develop the criteria for childhood-onset SLE flare (9,22), childhood-onset SLE inactive disease and remission (23), previous consensus treatment plans for pediatric LN (4), and classification criteria for macrophage activation syndrome (24,25). Our methodology was aligned with the recommendations of the Classification and Response Criteria Subcommittee of the ACR Committee on Quality Measures (26).

A strength of the SSR is that it has been derived from real-life patient data and was developed based on the consensus of a large number of experienced physicians who regularly treat patients with childhood-onset SLE and LN. The preliminary SSR developed in steps 4 and 5 was further validated among a group of experts in the management of childhood-onset SLE and LN using longitudinal data for the initial 6 months of induction therapy (step 6). Our study validation achieved majority agreement (95%) among patient profile raters for the use of the SSR-recommended oral CS and IV CS dosages, which they considered acceptable in the vast majority (>80%) of their patients with childhood-onset SLE during induction therapy for LN. Although not specifically tested, we hypothesize that the SSR-recommended dosing for maintenance therapy can also be used in the treatment of patients with childhood-onset SLE that is not complicated by renal disease.

The SSR builds on the consensus treatment plans for pediatric LN which offer guidance for CS use in the treatment of active proliferative LN, under the assumption of complete LN response at week 24 and CS use governed solely by LN (4). Unfortunately, such childhood-onset SLE courses are rare based on the findings of a pilot study analyzing the consensus treatment plans for pediatric LN (5). Unlike in the development of the consensus treatment plans for pediatric LN (4), the current study used real-life data from patients to deduce common CS use with childhood-onset SLE. Disease courses considered in the SSR include variable courses of proliferative LN, extrarenal involvement with childhood-onset SLE over time, multiorgan involvement with childhood-onset SLE, renal and extrarenal flares, and inactive disease. Findings from our validation exercise (step 6) provide evidence that the SSR is highly acceptable among physicians who treat patients with childhood-onset SLE, supporting its future relevance for the clinical care and research of childhood-onset SLE.

By design, the SSR is expected to support CS dosing decisions in the treatment of most patients with childhood-onset SLE. However, the limitations of this study are related to the known marked phenotypic variation with childhood-onset SLE, which may prohibit SSR use in patients with extreme phenotypes, such as children with life-threatening acute manifestations of childhood-onset SLE. Notably, patients with childhood-onset SLE requiring renal replacement therapy were not reflected in our patient profiles. Thus, additional validation is needed to evaluate the usefulness of the SSR in such situations.

Long-term use of CS, especially in high doses, is a major risk factor for the development of infections, which is a leading cause of death in SLE (7). Due to their CS-sparing properties, concurrent use of immunosuppressive medications is recommended during induction therapy for LN and was considered in the development of the SSR. In exploratory analysis, use of mycophenolate mofetil as opposed to cyclophosphamide did not influence CS dosing by the patient profile raters.

A shortcoming of the SSR is that it assumes patients are adherent to their medications, including CS. Nonadherence to the prescribed CS regimen could be associated with lack of improvement in childhood-onset SLE and LN, or even disease flares. The uncontrolled childhood-onset SLE disease course would in turn be reflected in an inability to taper CS, per the SSR, and would likely prompt clinicians to consider a patient's difficulty with adherence to a treatment plan.

Personalized CS dosing that takes into account the pharmacogenetic and pharmacodynamic makeup of patients

with childhood-onset SLE is a highly active area of research (27,28). We consider the SSR to be a long-needed tool to advance such research into the association between CS use, CS pharmacology, and control of inflammation or development of damage with childhood-onset SLE.

We are cognizant that the development of the SSR is a dynamic process, especially with new progress in biomarker studies. In our opinion, this process will require validation in large longitudinal data sets that capture the differential accrual of disease damage with specific CS uses. Indeed, additional insights in the biologic factors that modulate response to and damage from CS should be used in future research to enhance the SSR. In this context, the SSR provides a new template to which other CS dosing regimens can be compared. Potentially, the use of biologic agents with marked steroid-sparing effects may support more rapid CS tapering. Such a steroid-sparing effect could be quantified using the SSR and, subsequently, may necessitate updates to the SSR for patients treated with such medications.

In clinical trials, variability of CS dosing introduces bias and threatens the validity of study findings (17). By standardizing CS use, the SSR can counterbalance such bias and possibly increase the willingness of physicians to refer patients for studies. The SSR may also support CS use in clinical care, especially by health care providers with less experience in the treatment of patients with childhood-onset SLE and pediatric LN. Finally, we would like to point out that to enhance the widespread use of the SSR, a web-based calculator is in development.

ACKNOWLEDGMENTS

We thank the Pediatric Nephrology Research Consortium for their contributions, and Drs. Emily von Scheven and Jennifer Cooper for providing access to background information about their unpublished research on CS dosing for pediatric LN. We also thank the Coordinating Center of the Pediatric Rheumatology Collaborative Study Group for their assistance with this project.

AUTHOR CONTRIBUTIONS

All authors were involved in drafting the article or revising it critically for important intellectual content, and all authors approved the final version to be published. Dr. Chalhoub had full access to all of the data in the study and takes responsibility for the integrity of the data and the accuracy of the data analysis.

Study conception and design. Chalhoub, Wenderfer, Levy, Klein-Gitelman, Devarajan, Huang, Brunner.

Acquisition of data. Chalhoub, Wenderfer, Levy, Rouster-Stevens, Aggarwal, Savani, Ruth, Arkachaisri, Merritt, Onel, Goilav, Khubchandani, Deng, Fonseca, Ardoin, Ciurtin, Kasapcopur, Jelusic, Huber, Ozen, Klein-Gitelman, Appenzeller, Cavalcanti, Fotis, Lim, R Silva, Ramirez-Miramontes, Rosenwasser, Saad-Magalhaes, Schonenberg-Meinema, Scott, C Silva, Enciso, Terreri, Torres-Jimenez, Trachana, Al-Mayouf, Devarajan, Huang, Brunner.

Analysis and interpretation of data. Chalhoub, Wenderfer, Levy, Rouster-Stevens, Aggarwal, Savani, Ruth, Arkachaisri, Qiu, Merritt, Onel, Goilav, Khubchandani, Deng, Fonseca, Ardoin, Ciurtin, Kasapcopur, Jelusic, Huber, Ozen, Klein-Gitelman, Appenzeller, Cavalcanti, Fotis, Lim, R Silva, Ramirez-Miramontes, Rosenwasser, Saad-Magalhaes, Schonenberg-Meinema, Scott, C Silva, Enciso, Terreri, Torres-Jimenez, Trachana, Al-Mayouf, Devarajan, Huang, Brunner.

REFERENCES

1. Brunner HI, Klein-Gitelman MS, Ying J, Tucker LB, Silverman ED. CS use in childhood-onset systemic lupus erythematosus-practice patterns at four pediatric rheumatology centers. Clin Exp Rheumatol 2009;27:155–62.
2. Ilowite NT, Sandborg CI, Feldman BM, Grom A, Schanberg LE, Giannini EH, et al. Algorithm development for CS management in systemic juvenile idiopathic arthritis trial using consensus methodology. Pediatr Rheumatol Online J 2012;10:31.
3. Ad Hoc Working Group on Steroid-Sparing Criteria in Lupus. Criteria for steroid-sparing ability of interventions in systemic lupus erythematosus: report of a consensus meeting. Arthritis Rheum 2004;50:3427–31.
4. Mina R, von Scheven E, Ardoin SP, Eberhard BA, Punaro M, Ilowite N, et al. Consensus treatment plans for induction therapy of newly diagnosed proliferative lupus nephritis in juvenile systemic lupus erythematosus. Arthritis Care Res (Hoboken) 2012;64:375–83.
5. Cooper JC, Rouster-Stevens K, Wright TB, Hsu JJ, Klein-Gitelman MS, Ardoin SP, et al. Pilot study comparing the childhood arthritis and rheumatology research alliance consensus treatment plans for induction therapy of juvenile proliferative lupus nephritis. Pediatr Rheumatol Online J 2018;16:65.
6. Weening JJ, D'Agati VD, Schwartz MM, Seshan SV, Alpers CE, Appel GB, et al. The classification of glomerulonephritis in systemic lupus erythematosus revisited [review]. J Am Soc Nephrol 2004;15:241–50.
7. Deng J, Chalhoub NE, Sherwin CM, Li C, Brunner HI. Glucocorticoids pharmacology and their application in the treatment of childhood-onset systemic lupus erythematosus [review]. Sem Arthritis Rheum 2019;49:251–9.
8. Delbecq AL, Van de Ven AH, Gustafson DH. Group techniques for program planning: a guide to nominal group and Delphi processes. Glenview (IL): Scott, Foresman; 1975.
9. Brunner HI, Mina R, Pilkington C, Beresford MW, Reiff A, Levy DM, et al. Preliminary criteria for global flares in childhood-onset systemic lupus erythematosus. Arthritis Care Res (Hoboken) 2011;63:1213–23.
10. Hochberg MC. Updating the American College of Rheumatology revised criteria for the classification of systemic lupus erythematosus. Arthritis Rheum 1997;40:1725.
11. Austin HA III, Boumpas DT, Vaughan EM, Balow JE. Predicting renal outcomes in severe lupus nephritis: contributions of clinical and histologic data. Kidney Int 1994;45:544–50.
12. Austin HA III, Muenz LR, Joyce KM, Antonovych TT, Balow JE. Diffuse proliferative lupus nephritis: identification of specific pathologic features affecting renal outcome. Kidney Int 1984;25:689–95.
13. Gladman D, Ginzler E, Goldsmith C, Fortin P, Liang M, Urowitz M, et al. The development and initial validation of the Systemic Lupus International Collaborating Clinics/American College of Rheumatology damage index for systemic lupus erythematosus [review]. Arthritis Rheum 1996;39:363–9.
14. Gladman DD, Ibañez D, Urowitz MB. Systemic lupus erythematosus disease activity index 2000. J Rheumatol 2002;29:288–91.
15. Pierrat A, Gravier E, Saunders C, Caira MV, Aït-Djafer Z, Legras B, et al. Predicting GFR in children and adults: a comparison of the Cockcroft-Gault, Schwartz, and Modification of Diet in Renal Disease formulas. Kidney Int 2003;64:1425–36.

16. Schwartz GJ, Muñoz A, Schneider MF, Mak RH, Kaskel F, Warady BA, et al. New equations to estimate GFR in children with CKD. J Am Soc Nephrol 2009;20:629–37.
17. Corzillius M, Bae SC. Methodological issues of CS use in SLE clinical trials [review]. Lupus 1999;8:692–7.
18. Walsh M, Jayne D, Moist L, Tonelli M, Pannu N, Manns B. Practice pattern variation in oral glucocorticoid therapy after the induction of response in proliferative lupus nephritis. Lupus 2010;19:628–33.
19. Brunner HI, Silverman ED, To T, Bombardier C, Feldman BM. Risk factors for damage in childhood-onset systemic lupus erythematosus: cumulative disease activity and medication use predict disease damage. Arthritis Rheum 2002;46:436–44.
20. Gutiérrez-Suárez R, Ruperto N, Gastaldi R, Pistorio A, Felici E, Burgos-Vargas R, et al. A proposal for a pediatric version of the Systemic Lupus International Collaborating Clinics/American College of Rheumatology Damage Index based on the analysis of 1,015 patients with juvenile-onset systemic lupus erythematosus. Arthritis Rheum 2006;54:2989–96.
21. Heshin-Bekenstein M, Trupin L, Yelin E, von Scheven E, Yazdany J, Lawson EF. Longitudinal disease- and steroid-related damage among adults with childhood-onset systemic lupus erythematosus. Semin Arthritis Rheum 2019;49:267–72.
22. Brunner HI, Holland M, Beresford MW, Ardoin SP, Appenzeller S, Silva CA, et al. American College of Rheumatology provisional criteria for global flares in childhood-onset systemic lupus erythematosus. Arthritis Care Res (Hoboken) 2018;70:813–22.
23. Mina R, Klein-Gitelman MS, Ravelli A, Beresford MW, Avcin T, Espada G, et al. Inactive disease and remission in childhood-onset systemic lupus erythematosus. Arthritis Care Res (Hoboken) 2012; 64:683–93.
24. Ravelli A, Minoia F, Davì S, Horne A, Bovis F, Pistorio A, et al. 2016 classification criteria for macrophage activation syndrome complicating systemic juvenile idiopathic arthritis: a European League Against Rheumatism/American College of Rheumatology/Paediatric Rheumatology International Trials Organisation collaborative initiative. Arthritis Rheumatol 2016;68:566–76.
25. Ravelli A, Minoia F, Davì S, Horne A, Bovis F, Pistorio A, et al. Expert consensus on dynamics of laboratory tests for diagnosis of macrophage activation syndrome complicating systemic juvenile idiopathic arthritis. RMD Open 2016;2:e000161.
26. Classification and Response Criteria Subcommittee of the American College of Rheumatology Committee on Quality Measures. Development of classification and response criteria for rheumatic diseases. Arthritis Rheum 2006;55:348–52.
27. Ngo D, Beaulieu E, Gu R, Leaney A, Santos L, Fan H, et al. Divergent effects of endogenous and exogenous glucocorticoid-induced leucine zipper in animal models of inflammation and arthritis. Arthritis Rheum 2013;65:1203–12.
28. Northcott M, Gearing LJ, Nim HT, Nataraja C, Hertzog P, Jones SA, et al. Glucocorticoid gene signatures in systemic lupus erythematosus and the effects of type I interferon: a cross-sectional and in-vitro study. Lancet Rheumatol 2021;3:e357–70.

American College of Rheumatology
Empowering Rheumatology Professionals

Arthritis & Rheumatology
Vol. 74, No. 2, February 2022, pp 274–283
DOI 10.1002/art.41935

Association of a Combination of Healthy Lifestyle Behaviors With Reduced Risk of Incident Systemic Lupus Erythematosus

May Y. Choi,[1] Jill Hahn,[2] Susan Malspeis,[2] Emma F. Stevens,[2] Elizabeth W. Karlson,[2] Jeffrey A. Sparks,[2] Kazuki Yoshida,[2] Laura Kubzansky,[3] and Karen H. Costenbader[2]

Objective. While previous studies have demonstrated an association between individual factors related to lifestyle and the risk of systemic lupus erythematosus (SLE), it is unclear how the combination of these factors might affect the risk of incident SLE. This study was undertaken to prospectively evaluate whether a combination of healthy lifestyle factors is associated with a lower risk of incident SLE and its subtypes (anti–double-stranded DNA [anti-dsDNA]–positive and anti-dsDNA–negative SLE).

Methods. The study included 185,962 women from the Nurses' Health Study (NHS) and NHSII cohorts, among whom there were 203 incident cases of SLE (96 with anti-dsDNA–positive SLE, 107 with anti-dsDNA–negative SLE) during 4,649,477 person-years of follow-up. The Healthy Lifestyle Index Score (HLIS) was calculated at baseline and approximately every 2 years during follow-up, with scores assigned for 5 healthy lifestyle factors: alcohol consumption, body mass index, smoking, diet, and exercise. A time-varying Cox proportional hazards regression model was used to estimate the adjusted hazard ratios (HRs) with 95% confidence intervals (95% CIs) for the risk of SLE. In addition, the percentage of partial population attributable risk (PAR%) of SLE development was calculated.

Results. A higher HLIS was associated with a lower risk of SLE overall (HR 0.81 [95% CI 0.71–0.94]) and a lower risk of anti-dsDNA–positive SLE (HR 0.78 [95% CI 0.63–0.95]). Women with ≥4 healthy lifestyle factors had the lowest risk of SLE overall (HR 0.42, 95% CI 0.25–0.70) and lowest risk of anti-dsDNA–positive SLE (HR 0.35, 95% CI 0.17–0.75) as compared to women with only 1 healthy behavior or no healthy behaviors. The PAR% of SLE development was 47.7% (95% CI 23.1–66.6%), assuming that the entire population had adhered to at least 4 healthy lifestyle behaviors.

Conclusion. These results indicate that the risk of developing SLE, a disease in which significant evidence of genetic involvement has been established, might be reduced by nearly 50% with adherence to modifiable healthy lifestyle behaviors.

INTRODUCTION

Systemic lupus erythematosus (SLE) is a chronic, multisystem inflammatory autoimmune disease that remains a leading cause of death among young women (1). It was recently estimated that ~200,000 individuals in the US are currently diagnosed as having SLE based on the American College of Rheumatology (ACR) 1997 updated classification criteria (2), with a prevalence that is 9 times higher among women than among men (3). Although the mortality risk in SLE patients has decreased substantially over the past few decades, many will still experience progressive disease and/or a complicated disease course, underscoring the public health impact of SLE and the importance of research into disease prevention strategies, given that few effective medical therapies are available.

A complex interplay between genetic factors and environmental exposures are thought to ultimately lead to autoimmunity

Supported by NIH grants R01-AR-057327, UM1-CA-186107, U01-CA-176726, U01-HL-145386, and K24-AR-066109. Dr. Choi's work was supported by a Gary S. Gilkeson Career Development award from the Lupus Foundation of America.

[1]May Y. Choi, MD, MPH, FRCPC: Brigham and Women's Hospital, Harvard Medical School, Boston, Massachusetts, and University of Calgary, Calgary, Alberta, Canada; [2]Jill Hahn, DSc, Susan Malspeis, MS, Emma F. Stevens, BA, Elizabeth W. Karlson, MD, MS, Jeffrey A. Sparks, MD, MMSc, Kazuki Yoshida, MD, MPH, ScD, Karen H. Costenbader, MD, MPH: Brigham and Women's Hospital, Harvard Medical School, Boston, Massachusetts; [3]Laura Kubzansky, PhD: Harvard University T.H. Chan School of Public Health, Social and Behavioral Sciences, Boston, Massachusetts.

Author disclosures are available at https://onlinelibrary.wiley.com/action/downloadSupplement?doi=10.1002%2Fart.41935&file=art41935-sup-0001-Disclosureform.pdf.

Address correspondence to May Y. Choi, MD, MPH, FRCPC, Division of Rheumatology, Department of Medicine, Cumming School of Medicine, University of Calgary, 3230 Hospital Drive Northwest, Calgary NW T2N 4Z6, Alberta, Canada. Email: may.choi@ucalgary.ca.

Submitted for publication February 12, 2021; accepted in revised form July 22, 2021.

in SLE. It is estimated that ~5–12% of subjects with a first-degree relative with SLE will develop SLE in their lifetime. Moreover, studies have shown that SLE will develop in up to 90% of individuals with a congenital deficiency of the complement component C4 (4). Environmental exposures, such as ultraviolet light (5), medications (6), infectious agents (7), silica (8), cigarette smoke (9,10), alcohol consumption (10–13), hormonal factors (14), and obesity (15), have been hypothesized as being potential risk factors associated with the development of SLE, although the strength of these associations varies. Potential biologic mechanisms linking environmental exposures to SLE risk include increased severity of systemic inflammation, oxidative stress, up-regulation of the levels of inflammatory cytokines, and epigenetic modifications (16). Observations of a strong association between smoking exposure and risk of SLE development, specifically in individuals who are positive for anti–double-stranded DNA (anti-dsDNA) antibodies (i.e., a more severe subtype of SLE), also support the possibility that a history of smoking may have a direct role in anti-dsDNA antibody production (9).

In previous SLE studies, individual modifiable lifestyle factors were examined within the Nurses' Health Study (NHS) and NHSII cohorts (9,11,15,17,18) and other cohorts (10,12,13,19,20). Individual healthy lifestyle factors have previously been shown to reduce the risk of developing other autoimmune diseases, such as rheumatoid arthritis (RA) (21,22) and multiple sclerosis (23). However, most individuals tend to follow an established pattern of lifestyle behaviors, as these factors are often correlated with each other. Studies have demonstrated that having a relatively high Healthy Lifestyle Index Score (HLIS) (indicative of a favorable combination of meeting recommended guidelines for diet, exercise, smoking, alcohol consumption, and body weight) was associated with reduced risk of developing various diseases, including cardiovascular disease (24), stroke (25), sudden cardiac death (26), diabetes (27), and cancer (28,29), as well as an increased overall life expectancy (30). A high HLIS has also been implicated in a reduced risk of developing autoimmune diseases such as RA (31). The findings from these studies suggest that adopting a healthier lifestyle could attenuate the risk of chronic diseases, including autoimmune diseases; therefore, primary prevention through lifestyle interventions is a strategy that should be promoted.

The joint impact of multiple healthy behaviors and maintaining healthy body weight on the prevention of SLE development has not been assessed. Furthermore, as an association between some risk factors and the presence of anti-dsDNA antibodies has been recognized, studying specific SLE subtypes may provide insight into potential mechanisms of disease pathogenesis. Therefore, in this study, we prospectively evaluated whether a healthy lifestyle, as measured by HLIS scores for the number of healthy lifestyle behaviors in subjects from the NHS and NHSII cohorts, was associated with a lower risk of incident SLE and a lower risk of SLE according to subtype (anti-dsDNA–positive versus anti-dsDNA–negative SLE).

PATIENTS AND METHODS

Study design and population. The NHS and NHSII cohorts were established in 1976 and 1989, respectively (32). A total of 121,700 married female registered nurses, ages 30–55 years from 11 US states, were enrolled in the NHS cohort, while 116,430 married female registered nurses, ages 25–42 years from 14 US states, were enrolled in the NHSII cohort. Although the participants had a slightly higher socioeconomic status compared to the general population, and the cohorts comprised mostly White subjects (97%), the nurses' health knowledge and commitment to the research provided high-quality data. Furthermore, follow-up rates in these longitudinal cohort studies have been high, with only ~5% of person-time lost to follow-up (33). Since the NHSII is a cohort of subjects who were younger than those in the NHS, new information on exposures in adolescence and early adult life was obtained; this new information included more details on oral contraceptive use and other reproductive risk factors.

Subjects were given questionnaires that included assessments of a range of lifestyle factors, health-related behaviors, and newly diagnosed diseases, including SLE, as well as other outcomes. The questionnaires were mailed to and completed by participants at baseline and then biennially in follow-up. A validated comprehensive, self-administered Food Frequency Questionnaire containing >130 items was mailed to participants approximately every 4 years, starting in 1984 in the NHS and 1991 in the NHSII. Past validation studies have demonstrated that lifestyle behaviors, such as dietary patterns and body mass index (BMI), tend to remain stable over time (34–36).

The present study excluded participants who had prevalent SLE or other connective tissue diseases (CTDs) at baseline ($n = 7,177$ in the NHS and $n = 1,371$ in the NHSII). We included 96,240 women from the NHS cohort (followed up from 1986 to 2016) and 105,460 women from the NHSII cohort (followed up from 1991 to 2017). This study was approved by the Partners' HealthCare Institutional Review Board.

Identification of incident SLE. Incident SLE in the NHS cohorts was identified in 2 stages (37). Participants self-reported the presence of any newly diagnosed diseases biennially on their follow-up questionnaires. For any report of a new diagnosis of SLE, the participant was asked to complete a validated CTD screening questionnaire, which included 13 questions concerning symptoms of SLE (37). For those participants whose CTD questionnaire indicated a new diagnosis of SLE, medical records were requested, and the records were independently reviewed by 2 board-certified rheumatologists (KHC and EWK) to confirm whether the diagnosis fulfilled the ACR 1997 updated classification criteria for SLE (2). The methods used for SLE case identification and validation have been described previously (14,37). The

reviewers were blinded with regard to each patient's lifestyle exposure data on the questionnaires.

Participants with prevalent SLE or those with other CTDs at the time of enrollment were excluded. During follow-up, participants were censored from the study if they reported having a non–SLE-related CTD or if the diagnosis of SLE was not confirmed by medical records review. Each patient's anti-dsDNA status at the time of SLE diagnosis was determined by medical records review. Laboratory tests, including testing for anti-dsDNA antibodies, were performed using standard assays at participating sites. In a secondary outcome analysis, SLE patients were assessed according to subtype based on anti-dsDNA status (anti-dsDNA–positive versus anti-dsDNA–negative SLE).

Scoring of healthy behaviors on the HLIS. For assessment of healthy lifestyle behaviors, the HLIS was calculated for each participant at baseline and approximately every 2 years of follow-up. The HLIS was computed as the sum of component scores for healthy lifestyle behaviors on a scale of 0–5, ranging from a score of 0 (least healthy) to a score of 5 (most healthy). The components of the HLIS are based on 5 traditional lifestyle factors, all of which have been identified in prior NHS and NHSII studies utilizing the HLIS (24,27). Following the same HLIS scoring system and definitions as were used in those prior studies, we applied a binary score for each factor, in which participants were assigned 1 point for each of the following low-risk behaviors: never smokers or past smokers (having quit smoking for >4 years), not being overweight or obese (having a baseline BMI of <25 kg/m^2), drinking alcohol in moderation (consuming ≥5 gm/day [considered a healthy behavior] as opposed to low alcohol consumption [considered a high-risk behavior]), having a healthy diet (being in the highest 40th percentile of the Alternative Healthy Eating Index [AHEI] [38]), and performing regular exercise (i.e., completing at least 19 metabolic equivalent [MET] hours of exercise per week, corresponding to at least 30 minutes of brisk walking every day). As with prior studies utilizing the HLIS, subjects who were considered underweight (BMI <18.5 kg/m^2) or those who reported drinking >30 gm of alcohol per day were not excluded from the study. BMI was calculated using updated self-reported height and weight, and was treated as a dichotomous variable (normal weight versus overweight or obese). Self-reported weight ($r = 0.97$) and self-reported alcohol intake ($r = 0.9$) among subjects in the NHS and NHSII cohorts are variables that have been previously validated as highly accurate (35,39).

The HLIS was computed for each participant for whom complete data on the healthy behavior components were available. Several methods, defined a priori, were used for handling missing data. Subjects who had missing items in every questionnaire cycle were excluded. Imputation of individual mean values was used for alcohol consumption and exercise (using the cumulative mean MET hours per week). For missing BMI, the subject's previous BMI value was carried forward twice, and then individual mean imputation was used for further missing values. Data on a healthy diet, obtained using the AHEI, were updated approximately every 4 years; for missing AHEI data, the subject's previous AHEI scores were carried forward once, and then individual mean imputation was used for further missing values. Data on smoking status were carried forward if necessary; subjects for whom data on smoking status were missing in every cycle were excluded.

Time-varying covariates. Demographic and clinical data were updated on biennial questionnaires. Race was treated as binary (White versus non-White). Median household income for each US Census tract, as a marker of socioeconomic status, was categorized by quartiles. As confounders, we also included covariates related to reproductive factors that have been shown to be associated with incident SLE, including oral contraceptive use (never versus ever), age at onset of menarche (≤10 years versus >10 years), menopausal status (premenopausal, postmenopausal/never having received postmenopausal hormone therapy, and postmenopausal/ever having received postmenopausal hormone therapy) (14).

Statistical analysis. Time-varying Cox proportional hazards regression models were used to estimate the multivariable-adjusted hazard ratios (HRs) with 95% confidence intervals (95% CIs) for the risk of incident SLE associated with the number of healthy lifestyle factors reported by participants, both for SLE overall and according to anti-dsDNA SLE subtype, with adjustments for potential confounders. Confounders were chosen a priori based on pertinent factors discussed in the existing literature. We calculated significant differences [*P* for trend] between groups from the continuous HLIS model. *P* values less than 0.05 were considered statistically significant.

Due to the small number of SLE cases on each end of the spectrum of HLIS scores, we created 4 HLIS score categories, in which we collapsed HLIS scores of 0 and 1 into a single category and HLIS scores of 4 and 5 into a single category. In addition, we calculated the percentage of partial population attributable risk (PAR%) (40,41), an estimate of the percentage of incident SLE cases in this population during follow-up that would not have occurred if all participants had adhered to at least 4 healthy lifestyle behaviors, based on the assumption that lack of these healthy behaviors could be causally related to SLE development.

We performed a sensitivity analysis to calculate the risk of SLE associated with healthy lifestyle behaviors on an SLE-specific HLIS, in which 3 a priori–established SLE risk factors were used (11,15), including cigarette smoking status, BMI, and alcohol consumption, but not exercise or dietary quality, as the impact of regular exercise on SLE development has not been examined, and an association between dietary quality and SLE risk has not been demonstrated (17,18). An additional 80 SLE cases were included

in this sensitivity analysis, because these subjects developed SLE during the 8 years prior to the first diet questionnaire. Also in this sensitivity analysis, participants were assigned 1 point for each of the following low-risk behaviors: never smokers or past smokers (having quit smoking for >4 years), normal BMI (ranging 18–24.9 kg/m^2, with exclusion of underweight participants due to insufficient numbers of subjects, as was also seen in prior NHS/NHSII studies [15]), and drinking alcohol in moderation (consuming ≥5 gm/day).

Additional sensitivity analyses were performed, including the following: 1) redefining smoking status as never smokers versus ever smokers; 2) redefining moderate alcohol consumption as drinking ≥5 gm to <30 gm of alcohol per day, to ensure that this association was not driven by outliers; and 3) excluding incident SLE cases diagnosed within 12 months of HLIS assessment (e.g., time lag analysis), to address potential reverse causation whereby underlying disease might affect lifestyle factors.

All statistical analyses were conducted using SAS version 9.4 (SAS Institute).

RESULTS

Characteristics of the study participants. During 4,649,477 person-years of follow-up, there were 203 incident SLE cases (96 with anti-dsDNA–positive SLE, 107 with anti-dsDNA–negative SLE), diagnosed at a median duration of 10.8 years (range 0.3–38.4 years) after cohort enrollment. Table 1 summarizes the baseline demographic and clinical characteristics of all study participants (for the characteristics of the 203 patients with incident SLE, see Supplementary Table 1, available on the *Arthritis & Rheumatology* website at http://onlinelibrary.wiley.com/doi/10.1002/art.41935/abstract). Among all study subjects, the mean ± SD HLIS was 1.4 ± 1.0. The mean ± SD age of the patients at the time of SLE diagnosis was 52.1 ± 11.4 years, and the race of most of the patients was self-reported as White. Serum samples from >98% of patients were positive for antinuclear antibodies (ANAs) and 47.3% were positive for anti-dsDNA antibodies at the time of diagnosis.

Incident SLE risk estimates in relation to traditional HLIS factors. In multivariable models, a higher continuous score for healthy lifestyle behaviors on the traditional HLIS was associated with a lower risk of SLE overall (HR 0.81 [95% CI 0.71–0.94]) and lower risk of anti-dsDNA–positive SLE (HR 0.78 [95% CI 0.63–0.95]) per 1-unit increase in the number of healthy behaviors (Table 2). The risk of anti-dsDNA–negative SLE per 1-unit increase in the number of healthy behaviors was also reduced (HR 0.85 [95% CI 0.70–1.03]), although this was

Table 1. Baseline demographic and clinical characteristics of the study subjects from the NHS and NHSII cohorts, by traditional HLIS score categories*

Characteristic	HLIS category			
	Score 0–1 (n = 40,715)	Score 2 (n = 62,188)	Score 3 (n = 51,110)	Score 4–5 (n = 31,949)
Sociodemographic				
Age, mean ± SD years	44.81 ± 9.71	43.46 ± 10.02	43 ± 10.03	42.67 ± 9.93
White, %	93.13	93.20	92.60	93.61
Census-tract median household income <$60,000 by zip code, %	30.27	25.66	21.30	16.40
Components of the HLIS				
BMI, mean ± SD kg/m^2	28.94 ± 5.72	25.01 ± 5	23.3 ± 3.7	22.06 ± 2.27
Healthy BMI, %	17.30	60.10	79.78	95.01
Alcohol consumption, mean ± SD gm/day	2.07 ± 5.29	3.89 ± 8.04	5.35 ± 8.32	8.13 ± 8.73
Moderate alcohol consumption, %	5.86	18.63	33.70	61.34
Never or past smoker, %	54.25	78.43	86.95	94.45
Regular exercise, %	3.58	17.10	46.43	82.96
Healthy diet, %	5.57	25.74	53.14	85.35
Medications and reproductive factors				
Oral contraceptive use, %	67.65	67.77	68.40	70.59
Age at menarche ≤10 years, %	9.26	6.71	6.15	5.72
Premenopausal, %	66.60	68.02	68.80	69.62
Postmenopausal, %				
Never taken postmenopausal hormones	16.87	14.81	13.50	12.13
Ever taken postmenopausal hormones	13.87	14.66	15.20	15.92

* Subjects (n = 185,962) were identified from the Nurses' Health Study (NHS) cohort (1986–2016) and NHSII cohort (1991–2017). The healthy lifestyle index score (HLIS) is a summed score on a scale of 0–5, ranging from the category score of 0–1 (no healthy behaviors or 1 healthy behavior) to 4–5 (≥4 healthy behaviors). The components of the HLIS are defined as follows: drinking alcohol in moderation (≥5 gm/day), maintaining a healthy body weight (body mass index [BMI] <25 kg/m^2), never or past smoking (having quit >4 years prior to study entry), healthy diet (highest 40th percentile of the Alternative Healthy Eating Index), and regular exercise (performing at least 19 metabolic equivalent hours of exercise per week).

Table 2. Risk of incident SLE among women in the NHS and NHSII cohorts overall and by anti-dsDNA status, according to traditional HLIS score categories and continuous scores*

Group	HLIS score category				Continuous HLIS
	Score 0–1	Score 2	Score 3	Score 4–5	
Overall SLE (n = 203)					
No. of cases/person-years of follow-up	58/1,079,480	67/1,490,963	58/1,220,655	20/858,380	203/4,649,477
Multivariable HR (95% CI)†	1.00 (referent)	0.81 (0.57–1.15)	0.85 (0.59–1.23)	0.42 (0.25–0.70)	0.81 (0.71–0.94)
P for trend	0.004				–
Anti-dsDNA–positive SLE (n = 96)					
No. of cases/person-years of follow-up	30/1,079,160	30/1,490,581	27/1,220,331	9/858,223	96/4,648,294
Multivariable HR (95% CI)†	1.00 (referent)	0.72 (0.43–1.20)	0.78 (0.46–1.32)	0.35 (0.17–0.75)	0.78 (0.63–0.95)
P for trend	0.016				–
Anti-dsDNA–negative SLE (n = 107)					
No. of cases/person-years of follow-up	28/1,079,143	37/1,490,576	31/1,220,310	11/858,229	107/4,648,257
Multivariable HR (95% CI)†	1.00 (referent)	0.92 (0.56–1.51)	0.94 (0.56–1.57)	0.50 (0.24–1.01)	0.85 (0.70–1.03)
P for trend	0.10				–

* Study subjects were identified from the Nurses' Health Study (NHS) cohort (1986–2016) and NHSII cohort (1991–2017) and were assessed according to traditional Healthy Lifestyle Index Score (HLIS) categories (scale 0–5) or continuous HLIS scores (per 1-unit increase in the number of healthy behaviors). The traditional HLIS is a summed score ranging from category score 0–1 (no healthy behaviors or 1 healthy behavior) to 4–5 (≥4 healthy behaviors). The components of the HLIS are defined as follows: drinking alcohol in moderation (≥5 gm/day), maintaining a healthy body weight (body mass index <25 kg/m^2), never or past smoking (having quit >4 years prior to study entry), healthy diet (highest 40th percentile of the Alternative Healthy Eating Index), and regular exercise (performing at least 19 metabolic equivalent hours of exercise per week). Anti-dsDNA = anti–double-stranded DNA.

† Values are the multivariable-adjusted hazard ratios (HRs) with 95% confidence intervals (95% CIs) for the risk of incident systemic lupus erythematosus (SLE) in time-varying Cox proportional hazards models, adjusted for age (months), questionnaire cycle, cohort, non-White race, census-tract median household income (quartiles), ever use of oral contraceptives, age at menarche ≤10 years, and menopausal status (premenopausal status versus postmenopausal status according to never use or ever use of postmenopausal hormone therapy).

not statistically significant. Women in the highest category of the HLIS (having at least 4 healthy behaviors) had the lowest risk of developing SLE overall (HR 0.42 [95% CI 0.25–0.70]) and lowest risk of anti-dsDNA–positive SLE (HR 0.35 [95% CI 0.17–0.75]) compared to women with only 1 healthy behavior or no healthy behaviors. The PAR% of SLE development was 47.7% (95% CI 23.1–66.6%), assuming that the entire population had adhered to at least 4 healthy lifestyle behaviors.

Incident SLE risk estimates in relation to SLE-specific HLIS factors. In analyses using an HLIS based on previously established SLE-specific healthy lifestyle behaviors (alcohol consumption, BMI, and cigarette smoking), 283 incident SLE cases were identified (120 with anti-dsDNA–positive SLE, 163 with anti-dsDNA–negative SLE) over 5,815,211 person-years of follow-up. The characteristics of the study subjects in this SLE-specific HLIS analysis were similar to those of the participants in the primary analysis (see Supplementary Tables 2 and 3, available on the *Arthritis & Rheumatology* website at http://onlinelibrary.wiley.com/doi/10.1002/art.41935/abstract). The incidence rate of SLE overall in this cohort was 4.9 cases per 100,000 person-years, which was similar to that in the primary analysis cohort.

In multivariable models, a higher continuous SLE-specific HLIS score was associated with a lower risk of SLE overall (HR 0.75 [95% CI 0.64–0.88]), as well as a lower risk of anti-dsDNA–positive SLE (HR 0.67 [95% CI 0.53–0.85]) and anti-dsDNA–negative SLE (HR 0.82 [95% CI 0.67–1.00]) per 1-unit increase in score (Table 3). Women in the highest category of SLE-specific HLIS (having 3 healthy behaviors) had a reduced risk of SLE overall (HR 0.45 [95% CI 0.24–0.85]) compared to women with no healthy behaviors. Among participants with anti-dsDNA–positive SLE, those with 2 healthy behaviors (HR 0.46 [95% CI 0.23–0.93]) and those with 3 healthy behaviors (HR 0.39 [95% CI 0.16–0.94]) had a reduced risk of SLE. Unlike the traditional HLIS, when the SLE-specific HLIS was used, a larger reduction in SLE risk could be observed for every 1-unit increase in HLIS category score. The PAR% of SLE development in the analysis using the SLE-specific HLIS was 43.4% (95% CI 17.4–63.8%), assuming that the entire population had adhered to all 3 healthy lifestyle behaviors.

Additional sensitivity analyses. The results regarding SLE risk remained similar to the primary analysis when we changed the classification of cigarette smoking status to never smokers versus ever smokers (see Supplementary Table 4, available on the *Arthritis & Rheumatology* website at http://onlinelibrary.wiley.com/doi/10.1002/art.41935/abstract), where a higher continuous traditional HLIS score was still associated with a lower risk of SLE overall (HR 0.79 [95% CI 0.68–0.92]) and a lower risk of anti-dsDNA–positive SLE (HR 0.74 [95% CI 0.59–0.93]). After participants who reported consuming ≥30 gm/day of alcohol were excluded, a higher continuous traditional HLIS score remained associated with a lower risk of SLE overall (HR 0.76 [95% CI 0.65–0.89]), as well as a lower risk of anti-dsDNA–positive SLE (HR 0.70 [95% CI 0.55–0.89]) and anti-dsDNA–negative SLE (HR 0.81 [95% CI 0.66–0.99])

Table 3. Risk of incident SLE among women in the NHS and NHSII cohorts overall and by anti-dsDNA status, according to SLE-specific HLIS score categories and continuous scores*

Group	SLE-specific HLIS score category				Continuous SLE-specific HLIS
	Score 0	Score 1	Score 2	Score 3	
Overall SLE (n = 283)					
No. of cases/person-years of follow-up	19/269,502	133/2,337,444	110/2,444,354	21/763,911	283/5,815,211
Multivariable HR (95% CI)†	1.00 (referent)	1.00 (0.61–1.62)	0.73 (0.45–1.19)	0.45 (0.24–0.85)	0.75 (0.64–0.88)
P for trend	0.0003				–
Anti-dsDNA–positive SLE (n = 120)					
No. of cases/person-years of follow-up	10/269,391	62/2,336,573	38/2,443,370	10/763,669	120/5,813,003
Multivariable HR (95% CI)†	1.00 (referent)	0.80 (0.41–1.58)	0.46 (0.23–0.93)	0.39 (0.16–0.94)	0.67 (0.53–0.85)
P for trend	0.001				–
Anti-dsDNA–negative SLE (n = 163)					
No. of cases/person-years of follow-up	9/269,379	71/2,336,593	72/2,443,709	11/763,684	163/5,813,366
Multivariable HR (95% CI)†	1.00 (referent)	1.22 (0.60–2.45)	1.05 (0.52–2.12)	0.53 (0.22–1.28)	0.82 (0.67–1.00)
P for trend	0.048				–

* Study subjects were identified from the Nurses' Health Study (NHS) cohort (1986–2016) and NHSII cohort (1991–2017) and were assessed according to systemic lupus erythematosus (SLE)–specific Healthy Lifestyle Index Scores (HLIS) (scale 0–3) or continuous scores (per 1-unit increase in the number of healthy behaviors). The SLE-specific HLIS scores are summed scores ranging from 0 (no healthy behaviors) to 3 (all 3 healthy behaviors). The components of the SLE-specific HLIS include moderate alcohol consumption (drinking ≥5 gm/day alcohol), maintaining a healthy body weight (body mass index <25 kg/m^2), and cigarette smoking status of never smoker or past smoker (having quit >4 years prior to study entry), but do not include dietary quality or exercise components. Anti-dsDNA = anti–double-stranded DNA.

† Values are the multivariable-adjusted hazard ratios (HRs) with 95% confidence intervals (95% CIs) for the risk of incident SLE in time-varying Cox proportional hazards models, adjusted for age (months), questionnaire cycle, cohort, non-White race, census-tract median household income (quartiles), ever use of oral contraceptives, age at menarche ≤10 years, and menopausal status (premenopausal status versus postmenopausal status according to never use or ever use of postmenopausal hormone therapy).

(see Supplementary Table 5, available on the *Arthritis & Rheumatology* website at http://onlinelibrary.wiley.com/doi/10.1002/art.41935/abstract).

In the analysis in which a time lag was added to address potential reverse causation whereby underlying SLE might affect exercise and diet, we identified a total of 178 incident SLE cases (Table 4). However, the results were similar to those in our primary analysis, which did not include the time lag. In this sensitivity analysis, a higher continuous traditional HLIS score was still associated with a lower risk of SLE overall (HR 0.78 [95% CI 0.67–0.91]) and a lower risk of anti-dsDNA–positive SLE (HR 0.75 [95% CI 0.60–0.93]) per 1-unit increase in score. Women in the highest category of HLIS (with at least 4 healthy behaviors) had the lowest risk of developing SLE overall (HR 0.40 [95% CI 0.23–0.69]), as well as the lowest risk of anti-dsDNA–positive SLE (HR 0.34 [95% CI 0.15–0.74]) and anti-dsDNA–negative

Table 4. Risk of incident SLE among the study participants overall and by anti-dsDNA status, in sensitivity analyses accounting for a time lag between exposure to regular exercise or dietary changes and diagnosis of SLE*

Group	HLIS score category				Continuous HLIS
	Score 0–1	Score 2	Score 3	Score 4–5	
Overall SLE (n = 178)					
No. of cases/person-years of follow-up	56/988,626	57/1,365,758	47/1,112,595	18/773,959	178/4,240,937
Multivariable HR (95% CI)†	1.00 (referent)	0.72 (0.50–1.04)	0.72 (0.49–1.07)	0.40 (0.23–0.69)	0.78 (0.67–0.91)
P for trend	0.002				–
Anti-dsDNA–positive SLE (n = 89)					
No. of cases/person-years of follow-up	28/988,374	30/1,365,452	23/1,112,347	8/773,830	89/4,240,003
Multivariable HR (95% CI)†	1.00 (referent)	0.77 (0.46–1.29)	0.70 (0.40–1.24)	0.34 (0.15–0.74)	0.75 (0.60–0.93)
P for trend	0.008				–
Anti-dsDNA–negative SLE (n = 89)					
No. of cases/person-years of follow-up	28/988,345	27/1,365,449	24/1,112,296	10/773,838	89/4,239,927
Multivariable HR (95% CI)†	1.00 (referent)	0.68 (0.40–1.16)	0.74 (0.43–1.30)	0.47 (0.23–0.99)	0.82 (0.66–1.01)
P for trend	0.068				–

* Study participants were assessed according to traditional Healthy Lifestyle Index Score (HLIS) categories (scale 0–5) or continuous HLIS scores (per 1-unit increase in the number of healthy behaviors). Anti-dsDNA = anti–double-stranded DNA.

† Values are the multivariable-adjusted hazard ratios (HRs) with 95% confidence intervals (95% CIs) for the risk of incident systemic lupus erythematosus (SLE) in time-varying Cox proportional hazards models, adjusted for age (months), questionnaire cycle, cohort, non-White race, census-tract median household income (quartiles), ever use of oral contraceptives, age at menarche ≤10 years, and menopausal status (premenopausal status versus postmenopausal status according to never use or ever use of postmenopausal hormone therapy).

SLE (HR 0.47 [95% CI 0.23–0.99]), compared to women with only 1 healthy behavior or no healthy behaviors.

DISCUSSION

To our knowledge, this is the first study to prospectively evaluate the association between an overall healthy lifestyle and SLE risk. In order to evaluate the temporal relationship between a healthy lifestyle and SLE risk, we required a data set that was sufficiently large in scope, with collection of accurate longitudinal data and minimal loss to follow-up in a well-characterized prospective cohort. We believe the NHS and NHSII cohorts are among the only data sources in the US that meet these criteria, notwithstanding limitations regarding the demographic makeup of the cohort recruitment. Therefore, we applied the well-established HLIS to these 2 large, nationwide cohorts of female nurses followed up for up to 40 years, with detailed and updated covariable data obtained from biennial questionnaires and with >5.8 million person-years of follow-up. We found that adherence to multiple healthy behaviors was associated with a lower risk of SLE development overall (19% reduction for each additional healthy behavior) and lower risk of anti-dsDNA–positive SLE (22% reduction for each additional healthy behavior). Those with the highest number of healthy behaviors had the lowest risk of SLE overall and lowest risk of anti-dsDNA–positive SLE, compared to those with the least healthy lifestyle. Strikingly, we found that the risk of SLE in participants who are likely already at risk due to inherited genetic risk factors could potentially be reduced by nearly 50% with adherence to healthy and modifiable lifestyle behaviors.

Prior studies, including those outside of the NHS and NHSII, have evaluated the impact of lifestyle behaviors on the risk of SLE development, but with consideration of each factor individually, yielding findings of variable associations with SLE risk. Cigarette smoking (9,10,19) and obesity (15) have been associated with increased SLE risk, while an inverse association with alcohol consumption was observed (10–13), and no association between SLE risk and various dietary patterns was identified (17,18). In the prior NHS and NHSII studies, current smokers had a higher risk of anti-dsDNA–positive SLE compared to never smokers (HR 1.86 [95% CI 1.14–13.04]) (9), obese women had an 85% higher risk of SLE compared to women with a normal BMI (HR 1.85, 95% CI 1.17–2.91) (15), and moderate alcohol intake (≥5 gm/day or >0.5 drinks/day) was associated with a decreased risk of incident SLE (HR 0.61 [95% CI 0.41–0.89]) (11). However, no association between SLE risk and various diets including the AHEI has been observed (17,18). On the other hand, the role of physical activity in the risk of developing SLE has not been elucidated. The impact of exercise on the immune system, including higher levels of Treg cells and a shift in the Th1/Th2 balance, has been shown to be protective against other autoimmune diseases, such as RA (21), which suggests that it may also influence SLE risk. Despite varying strengths of association with SLE risk, our study showed that in combination, these modifiable risk factors significantly reduce the risk of SLE.

The approach of studying multiple lifestyle factors together rather than individually provides a more pragmatic and holistic understanding of how lifestyle factors can affect risk of disease events. As a standard tool that has been used to recognize whether individuals are meeting recommended guidelines for healthy behaviors across multiple lifestyle factors, the HLIS has also been applied to examine its impact on other chronic diseases (24,25,27–29). For instance, women who adhered to all 5 healthy lifestyle factors had an 80% lower incidence of coronary events (24) and 91% lower incidence of type 2 diabetes (27). Future studies using the HLIS tool should examine how multiple healthy lifestyle behaviors can reduce the risk of other autoimmune diseases, such as psoriatic arthritis. It is also important to recognize that although the evidence thus far points to encouraging patients to adhere to as many healthy behaviors as possible for the greatest benefit, there are many institutional and structural factors that contribute to one's ability to adhere to or achieve a healthy lifestyle. The many social determinants of health, including effects of poverty, pollution, toxins, stress, and institutional and structural racism, have disproportionate impacts on non-White groups in the US, the same groups that have the highest incidence and severity of SLE. These factors likely negatively affect the ability to achieve a healthy lifestyle and were not examined in the current study, but should be explored further.

Therefore, even though these results suggest that SLE may be, to some degree, preventable, the barriers to achieving a healthy lifestyle, and thus modifying a person's risk of developing SLE, are unlikely to be distributed equally in the population. Future studies should examine how to improve adherence to lifestyle interventions, and should also address the factors that prevent or limit a person's ability to meet these healthy goals among populations of individuals from racially/ethnically/culturally diverse backgrounds who are considered to be at risk of SLE.

Recognition of lifestyle behaviors acting in combination to influence the risk of SLE—potentially producing stronger effects when acting together than when acting individually—provides some insights into the pathogenesis of SLE. It is plausible that environmental exposures may work synergistically via common biologic pathways to influence the risk of SLE, with the mechanisms of action including induction of oxidative stress, damage to endogenous proteins and DNA, autoantibody production, and up-regulation of proinflammatory cytokines, leading to epigenetic changes and altered gene expression affecting immune homeostasis. Both exposure to the toxic components of cigarette smoke and the presence of obesity are known to cause oxidative stress, resulting in elevated intracellular levels of reactive oxygen species that can damage DNA-forming immunogenic DNA adducts, which may promote dsDNA antibody production (42,43). This is consistent with the results of our study showing that a healthier

lifestyle is strongly associated with a lower risk of developing anti-dsDNA–positive SLE. This relationship was less clear with regard to the risk of anti-dsDNA–negative SLE. The smoke byproducts themselves could also augment autoreactive B cells in the native immune system repertoire. Moreover, in studies of obese human subjects and in animal models of obesity, production of autoantibodies has been demonstrated (44).

Cigarette smoking has also been shown to induce production of ANAs in the lungs of human subjects, and to increase the expression of the SLE-associated proinflammatory cytokine B-lymphocyte stimulator (BLyS) in the lungs of exposed mice (45). In a recent NHS and NHSII study, elevated BLyS levels and lower levels of interleukin-10 (IL-10) (an antiinflammatory cytokine) were detected in current smokers, particularly among women who were ANA positive (46). Furthermore, smoking has been shown to increase the expression of proinflammatory cytokines, including tumor necrosis factor (TNF) and IL-6 (47), which play important roles in the modulation of insulin resistance. Adipose tissue, in particular visceral fat, secretes proinflammatory adipocyte-derived cytokines. Obese individuals have higher levels of C-reactive protein, soluble TNF receptor type 2, and IL-6 compared to nonobese individuals (48). Alcohol consumption, on the other hand, contains several compounds (e.g., ethanol and antioxidants) that can potentially counteract the changes induced by smoking and obesity, including diminishing cellular responses to immunogens, suppressing synthesis of immunoglobulins, influencing the production of proinflammatory cytokines (TNF, IL-6, IL-8, and interferon-γ), and inhibiting key enzymes in DNA synthesis (49). In vitro studies and animal studies may further elucidate the biologic mechanisms and pathways by which joint risk factors may play a role in the etiology of SLE.

The strengths of our study include using data from well-described cohorts with up to 5.8 million person-years of prospective follow-up. There were detailed data on potential time-varying confounders to reduce the within-subject variation, minimize inaccuracy of exposure data, and decrease the potential for reverse causation and recall biases. The strengths of the HLIS as a tool to assess healthy lifestyle factors include strong face validity and ease of application at the individual level or for public health purposes.

We also recognize some important limitations in this study. The study population was predominantly White, and all participants were female nurses; their lifestyle habits, such as dietary intake, likely differ from that of other ethnic populations. Therefore, it will be important to validate our findings in other, more diverse SLE cohorts. Also, there was a relatively small number of incident SLE cases, limiting the ability to examine more extreme categories. As there may be a long prodromal period in the development SLE, an extra lag period between the exposure and the outcome windows was added to address potential reverse causation. As a result, a large number of cases were not analyzed, thus limiting the statistical power of the study, particularly in the analysis of relationship to exercise. The overall incidence rate of SLE in our study is lower than the recently reported incidence rates of SLE among women in the US, likely as a result of our stringent case definition of SLE (50). This may have been attributable to exclusion of cases of early-onset SLE (i.e., before age 35 years in the NHS and before age 25 years in the NHSII), exclusion of possible SLE cases that later became definite cases, and exclusion of patients who were entered in the cohort prior to administration of the diet questionnaire in the NHS (but not in the NHSII), which was administered ~8 years after cohort inception. Moreover, due to the higher mean age of the subjects in the cohorts and the inclusion of potentially less severe SLE cases, these study findings should also be reexamined in a cohort of younger women and those with more severe disease. Finally, there is a potential for misclassification because self-reported questionnaires were used, and there may be unknown confounders not accounted for in the analysis.

In conclusion, we demonstrated an inverse association between adherence to a combination of healthy lifestyle behaviors and the risk of developing SLE, with our data showing that nearly one-half of the PAR% was attributable to this association. Our findings have implications for the development of SLE prevention strategies and should help support the promotion of multiple healthy lifestyle behaviors of greatest benefit to SLE patients. These findings have also provided further insight into the pathogenesis of SLE, as a greater-than-expected proportion of the SLE risk was attributable to lack of adherence to modifiable healthy lifestyle factors.

ACKNOWLEDGMENT

We would like to acknowledge the nurses for their long-term devotion to the Nurses' Health Studies and the Channing Division of Network Medicine.

AUTHOR CONTRIBUTIONS

All authors were involved in drafting the article or revising it critically for important intellectual content, and all authors approved the final version to be published. Dr. Choi had full access to all of the data in the study and takes responsibility for the integrity of the data and the accuracy of the data analysis.

Study conception and design. Choi, Hahn, Malspeis, Stevens, Karlson, Sparks, Yoshida, Kubzansky, Costenbader.

Acquisition of data. Choi, Hahn, Malspeis, Stevens, Karlson, Sparks, Yoshida, Kubzansky, Costenbader.

Analysis and interpretation of data. Choi, Hahn, Malspeis, Stevens, Karlson, Sparks, Yoshida, Kubzansky, Costenbader.

REFERENCES

1. Yen EY, Singh RR. Lupus—an unrecognized leading cause of death in young females: a population-based study using nationwide death certificates, 2000–2015. Arthritis Rheumatol 2018;70:1251–5.
2. Hochberg MC, for the Diagnostic and Therapeutic Criteria Committee of the American College of Rheumatology. Updating the American College of Rheumatology revised criteria for the classification of systemic lupus erythematosus [letter]. Arthritis Rheum 1997;40:1725.

3. Izmirly PM, Parton H, Wang L, McCune WJ, Lim SS, Drenkard C, et al. Prevalence of systemic lupus erythematosus in the United States: estimates from a meta-analysis of the Centers for Disease Control and Prevention National Lupus Registries. Arthritis Rheumatol 2021; 73:991–6.
4. Walport MJ. Complement and systemic lupus erythematosus [review]. Arthritis Res 2002;4 Suppl 3:S279–93.
5. Barbhaiya M, Costenbader KH. Ultraviolet radiation and systemic lupus erythematosus [review]. Lupus 2014;23:588–95.
6. Montanaro A, Bardana EJ Jr. Dietary amino acid-induced systemic lupus erythematosus [review]. Rheum Dis Clin North Am 1991;17: 323–32.
7. James JA, Kaufman KM, Farris AD, Taylor-Albert E, Lehman TJ, Harley JB. An increased prevalence of Epstein-Barr virus infection in young patients suggests a possible etiology for systemic lupus erythematosus. J Clin Invest 1997;100:3019–26.
8. Parks CG, Cooper GS, Nylander-French LA, Sanderson WT, Dement JM, Cohen PL, et al. Occupational exposure to crystalline silica and risk of systemic lupus erythematosus: a population-based, case-control study in the southeastern United States. Arthritis Rheum 2002;46:1840–50.
9. Barbhaiya M, Tedeschi SK, Lu B, Malspeis S, Kreps D, Sparks JA, et al. Cigarette smoking and the risk of systemic lupus erythematosus, overall and by anti-double stranded DNA antibody subtype, in the Nurses' Health Study cohorts. Ann Rheum Dis 2018;77: 196–202.
10. Cozier YC, Barbhaiya M, Castro-Webb N, Conte C, Tedeschi SK, Leatherwood C, et al. Relationship of cigarette smoking and alcohol consumption to incidence of systemic lupus erythematosus in a prospective cohort study of black women. Arthritis Care Res (Hoboken) 2019;71:671–7.
11. Barbhaiya M, Lu B, Sparks JA, Malspeis S, Chang SC, Karlson EW, et al. Influence of alcohol consumption on the risk of systemic lupus erythematosus among women in the Nurses' Health Study Cohorts. Arthritis Care Res (Hoboken) 2017;69:384–92.
12. Bengtsson AA, Rylander L, Hagmar L, Nived O, Sturfelt G. Risk factors for developing systemic lupus erythematosus: a case–control study in southern Sweden. Rheumatology (Oxford) 2002;41: 563–71.
13. Wang J, Pan HF, Ye DQ, Su H, Li XP. Moderate alcohol drinking might be protective for systemic lupus erythematosus: a systematic review and meta-analysis. Clini Rheumatol 2008;27:1557–63.
14. Costenbader KH, Feskanich D, Stampfer MJ, Karlson EW. Reproductive and menopausal factors and risk of systemic lupus erythematosus in women. Arthritis Rheum 2007;56:1251–62.
15. Tedeschi SK, Barbhaiya M, Malspeis S, Lu B, Sparks JA, Karlson EW, et al. Obesity and the risk of systemic lupus erythematosus among women in the Nurses' Health Studies. Semin Arthritis Rheum 2017; 47:376–83.
16. Barbhaiya M, Costenbader KH. Environmental exposures and the development of systemic lupus erythematosus [review]. Curr Opin Rheumatol 2016;28:497–505.
17. Tedeschi SK, Barbhaiya M, Sparks JA, Karlson EW, Kubzansky LD, Roberts AL, et al. Dietary patterns and risk of systemic lupus erythematosus in women. Lupus 2020;29:67–73.
18. Barbhaiya M, Tedeschi S, Sparks JA, Leatherwood C, Karlson EW, Willett WC, et al. Association of dietary quality with risk of incident systemic lupus erythematosus in the Nurses' Health Study and Nurses' Health Study II. Arthritis Care Res (Hoboken) 2021;73:1250–8.
19. Washio M, Horiuchi T, Kiyohara C, Kodama H, Tada Y, Asami T, et al. Smoking, drinking, sleeping habits, and other lifestyle factors and the risk of systemic lupus erythematosus in Japanese females: findings from the KYSS study. Mod Rheumatol 2006;16:143–50.
20. Cozier YC, Barbhaiya M, Castro-Webb N, Conte C, Tedeschi S, Leatherwood C, et al. A prospective study of obesity and risk of systemic lupus erythematosus (SLE) among Black women. Sem Arthritis Rheum 2019;48:1030–4.
21. Liu X, Tedeschi SK, Lu B, Zaccardelli A, Speyer CB, Costenbader KH, et al. Long-term physical activity and subsequent risk for rheumatoid arthritis among women: a prospective cohort study. Arthritis Rheumatol 2019;71:1460–71.
22. Liu X, Tedeschi SK, Barbhaiya M, Leatherwood CL, Speyer CB, Lu B, et al. Impact and timing of smoking cessation on reducing risk of rheumatoid arthritis among women in the Nurses' Health Studies. Arthritis Care Res (Hoboken) 2019;71:914–24.
23. Marrie RA. Environmental risk factors in multiple sclerosis aetiology [review]. Lancet Neurol 2004;3:709–18.
24. Stampfer MJ, Hu FB, Manson JE, Rimm EB, Willett WC. Primary prevention of coronary heart disease in women through diet and lifestyle. N Engl J Med 2000;343:16–22.
25. Kurth T, Moore SC, Gaziano JM, Kase CS, Stampfer MJ, Berger K, et al. Healthy lifestyle and the risk of stroke in women. Arch Intern Med 2006;166:1403–9.
26. Chiuve SE, Fung TT, Rexrode KM, Spiegelman D, Manson JE, Stampfer MJ, et al. Adherence to a low-risk, healthy lifestyle and risk of sudden cardiac death among women. JAMA 2011; 306:62–9.
27. Hu FB, Manson JE, Stampfer MJ, Colditz G, Liu S, Solomon CG, et al. Diet, lifestyle, and the risk of type 2 diabetes mellitus in women. N Engl J Med 2001;345:790–7.
28. Aleksandrova K, Pischon T, Jenab M, Bueno-de-Mesquita HB, Fedirko V, Norat T, et al. Combined impact of healthy lifestyle factors on colorectal cancer: a large European cohort study. BMC Med 2014;12:168.
29. Arthur R, Kirsh VA, Kreiger N, Rohan T. A healthy lifestyle index and its association with risk of breast, endometrial, and ovarian cancer among Canadian women. Cancer Causes Control 2018;29:485–93.
30. Li Y, Pan A, Wang DD, Liu X, Dhana K, Franco OH, et al. Impact of healthy lifestyle factors on life expectancies in the US population. Circulation 2018;138:345–55.
31. Ye D, Mao Y, Xu Y, Xu X, Xie Z, Wen C. Lifestyle factors associated with incidence of rheumatoid arthritis in US adults: analysis of National Health and Nutrition Examination Survey database and meta-analysis. BMJ Open 2021;11:e038137.
32. Bao Y, Bertoia ML, Lenart EB, Stampfer MJ, Willett WC, Speizer FE, et al. Origin, methods, and evolution of the Three Nurses' Health Studies. Am J Public Health 2016;106:1573–81.
33. Colditz GA, Manson JE, Hankinson SE. The Nurses' Health Study: 20-year contribution to the understanding of health among women. J Womens Health 1997;6:49–62.
34. Frazier AL, Willett WC, Colditz GA. Reproducibility of recall of adolescent diet: Nurses' Health Study (United States). Cancer Causes Control 1995;6:499–506.
35. Rimm EB, Stampfer MJ, Colditz GA, Chute CG, Litin LB, Willett WC. Validity of self-reported waist and hip circumferences in men and women. Epidemiology 1990;1:466–73.
36. Hu FB, Rimm E, Smith-Warner SA, Feskanich D, Stampfer MJ, Ascherio A, et al. Reproducibility and validity of dietary patterns assessed with a food-frequency questionnaire. Am J Clin Nutr 1999;69:243–9.
37. Karlson EW, Sanchez-Guerrero J, Wright EA, Lew RA, Daltroy LH, Katz JN, et al. A connective tissue disease screening questionnaire for population studies. Ann Epidemiol 1995;5:297–302.
38. McCullough ML, Feskanich D, Stampfer MJ, Giovannucci EL, Rimm EB, Hu FB, et al. Diet quality and major chronic disease risk in men and women: moving toward improved dietary guidance. Am J Clin Nutr 2002;76:1261–71.

39. Willett WC, Sampson L, Stampfer MJ, Rosner B, Bain C, Witschi J, et al. Reproducibility and validity of a semiquantitative food frequency questionnaire. Am J Epidemiol 1985;122:51–65.
40. Rothman KJ, Greenland S. Modern epidemiology. 2nd ed. Philadelphia: Lippincott–Raven; 1998.
41. Wacholder S, Benichou J, Heineman EF, Hartge P, Hoover RN. Attributable risk: advantages of a broad definition of exposure. Am J Epidemiol 1994;140:303–9.
42. Włodarczyk M, Nowicka G. Obesity, DNA damage, and development of obesity-related diseases [review]. Int J Mol Sci 2019;20:1146.
43. Mooney LA, Perera FP, Van Bennekum AM, Blaner WS, Karkoszka J, Covey L, et al. Gender differences in autoantibodies to oxidative DNA base damage in cigarette smokers. Cancer Epidemiol Biomarkers Prev 2001;10:641–8.
44. Tsigalou C, Vallianou N, Dalamaga M. Autoantibody production in obesity: is there evidence for a link between obesity and autoimmunity? [review]. Curr Obes Rep 2020;9:245–54.
45. Morissette MC, Gao Y, Shen P, Thayaparan D, Bérubé JC, Paré PD, et al. Role of BAFF in pulmonary autoantibody responses induced by chronic cigarette smoke exposure in mice. Physiol Rep 2016;4:e13057.
46. Hahn J, Leatherwood C, Malspeis S, Liu X, Lu B, Roberts AL, et al. Associations between smoking and systemic lupus erythematosus–related cytokines and chemokines among US female nurses. Arthritis Care Res (Hoboken) 2021;73:1583–9.
47. Bermudez EA, Rifai N, Buring JE, Manson JE, Ridker PM. Relation between markers of systemic vascular inflammation and smoking in women. Am J Cardiol 2002;89:1117–9.
48. Panagiotakos DB, Pitsavos C, Yannakoulia M, Chrysohoou C, Stefanadis C. The implication of obesity and central fat on markers of chronic inflammation: the ATTICA study. Atherosclerosis 2005;183:308–15.
49. Gonzalez-Quintela A, Alende R, Gude F, Campos J, Rey J, Meijide LM, et al. Serum levels of immunoglobulins (IgG, IgA, IgM) in a general adult population and their relationship with alcohol consumption, smoking and common metabolic abnormalities. Clin Exp Immunol 2008;151:42–50.
50. Dall'Era M, Cisternas MG, Snipes K, Herrinton LJ, Gordon C, Helmick CG. The incidence and prevalence of systemic lupus erythematosus in San Francisco County, California: the California Lupus Surveillance Project. Arthritis Rheumatol 2017;69:1996–2005.

American College of Rheumatology
Empowering Rheumatology Professionals

Arthritis & Rheumatology
Vol. 74, No. 2, February 2022, pp 284–294
DOI 10.1002/art.41937

Evaluation of Immune Response and Disease Status in Systemic Lupus Erythematosus Patients Following SARS–CoV-2 Vaccination

Peter M. Izmirly,[1] Mimi Y. Kim,[2] Marie Samanovic,[1] Ruth Fernandez-Ruiz,[1] Sharon Ohana,[1] Kristina K. Deonaraine,[1] Alexis J. Engel,[1] Mala Masson,[1] Xianhong Xie,[2] Amber R. Cornelius,[1] Ramin S. Herati,[1] Rebecca H. Haberman,[1] Jose U. Scher,[1] Allison Guttmann,[1] Rebecca B. Blank,[1] Benjamin Plotz,[1] Mayce Haj-Ali,[1] Brittany Banbury,[1] Sara Stream,[1] Ghadeer Hasan,[1] Gary Ho,[1] Paula Rackoff,[1] Ashira D. Blazer,[1] Chung-E Tseng,[1] H. Michael Belmont,[1] Amit Saxena,[1] Mark J. Mulligan,[1] Robert M. Clancy,[1] and Jill P. Buyon[1]

Objective. To evaluate seroreactivity and disease flares after COVID-19 vaccination in a multiethnic/multiracial cohort of patients with systemic lupus erythematosus (SLE).

Methods. Ninety SLE patients and 20 healthy controls receiving a complete COVID-19 vaccine regimen were included. IgG seroreactivity to the SARS–CoV-2 spike receptor-binding domain (RBD) and SARS–CoV-2 microneutralization were used to evaluate B cell responses; interferon-γ (IFNγ) production was measured by enzyme-linked immunospot (ELISpot) assay in order to assess T cell responses. Disease activity was measured by the hybrid SLE Disease Activity Index (SLEDAI), and flares were identified according to the Safety of Estrogens in Lupus Erythematosus National Assessment–SLEDAI flare index.

Results. Overall, fully vaccinated SLE patients produced significantly lower IgG antibodies against SARS–CoV-2 spike RBD compared to fully vaccinated controls. Twenty-six SLE patients (28.8%) generated an IgG response below that of the lowest control (<100 units/ml). In logistic regression analyses, the use of any immunosuppressant or prednisone and a normal anti–double-stranded DNA antibody level prior to vaccination were associated with decreased vaccine responses. IgG seroreactivity to the SARS–CoV-2 spike RBD strongly correlated with the SARS–CoV-2 microneutralization titers and correlated with antigen-specific IFNγ production determined by ELISpot. In a subset of patients with poor antibody responses, IFNγ production was similarly diminished. Pre- and postvaccination SLEDAI scores were similar in both groups. Postvaccination flares occurred in 11.4% of patients; 1.3% of these were severe.

Conclusion. In a multiethnic/multiracial study of SLE patients, 29% had a low response to the COVID-19 vaccine which was associated with receiving immunosuppressive therapy. Reassuringly, severe disease flares were rare. While minimal protective levels remain unknown, these data suggest that protocol development is needed to assess the efficacy of booster vaccination.

INTRODUCTION

As scientific advances have been applied with unprecedented speed during the COVID-19 pandemic, physicians and their patients have pivoted from treatment of infection and passive immunization to full-scale preventative measures, particularly in high-risk individuals (1,2). Patients with systemic lupus erythematosus (SLE) comprise a unique population with regard to risk for infection and outcomes associated with SARS–CoV-2, given underlying demographics, associated organ damage, and

Supported by the National Institute of Arthritis and Musculoskeletal and Skin Diseases, NIH (grant P50-AR-07059), the National Institute of Allergy and Infectious Diseases, NIH (grant AI-148574), and a Bloomberg Philanthropies COVID-19 Response Initiative grant.

[1]Peter M. Izmirly, MD, Marie Samanovic, PhD, Ruth Fernandez-Ruiz, MD, Sharon Ohana, BS, Kristina K. Deonaraine, MSc, Alexis J. Engel, BS, Mala Masson, BA, Amber R. Cornelius, MS, Ramin S. Herati, MD, Rebecca H. Haberman, MD, Jose U. Scher, MD, Allison Guttmann, MD, Rebecca B. Blank, MD, Benjamin Plotz, MD, Mayce Haj-Ali, MD, Brittany Banbury, MD, Sara Stream, MD, Ghadeer Hasan, MD, Gary Ho, MD, Paula Rackoff, MD, Ashira D. Blazer, MD, Chung-E Tseng, MD, H. Michael Belmont, MD, Amit Saxena, MD, Mark J. Mulligan, MD, Robert M. Clancy, PhD, Jill P. Buyon, MD: New York University Grossman School of Medicine, New York, New York;

[2]Mimi Y. Kim, ScD, Xianhong Xie, PhD: Albert Einstein College of Medicine, New York, New York.

Drs. Izmirly, Kim, Samanovic, and Fernandez-Ruiz contributed equally to this work. Drs. Mulligan, Clancy, and Buyon contributed equally to this work.

Author disclosures are available at https://onlinelibrary.wiley.com/action/downloadSupplement?doi=10.1002%2Fart.41937&file=art41937-sup-0001-Disclosureform.pdf.

Address correspondence to Peter M. Izmirly, MD, NYU Langone Health, 550 First Avenue, Medical Science Building 625, New York, NY 10016. Email: peter.izmirly@nyulangone.org.

Submitted for publication June 4, 2021; accepted in revised form July 29, 2021.

comorbidities. In addition, medications commonly used to treat SLE have been associated with an increased risk of death from COVID-19 (3). Early data provided evidence that patients with SLE have a high risk of hospitalization from COVID-19, with factors including race/ethnicity, comorbidities such as cardiovascular disease and renal insufficiency, and higher body mass index identified as independent predictors of hospitalization (1,4). Further raising concern, infection was reported to be associated with flares of disease (5). In subsequent studies, patients with SLE and confirmed COVID-19 were demonstrated to generate and maintain serologic responses despite the use of a variety of immunosuppressants (6). These data provided reassurance regarding the efficacy and durability of humoral immunity and protection against reinfection with SARS–CoV-2, as well as potential insights into the efficacy of active immunization in SLE patients.

Since the phase III clinical studies of all 3 vaccines excluded patients treated with immunosuppressants or immune-modifying drugs within 6 months of enrollment, data on SLE are virtually absent (7–9). Furthermore, given the potential for disease flares following immunization, it is not surprising that a recent study reported hesitancy for vaccination in patients with rheumatic diseases, including SLE (10). Accordingly, the current study was initiated to address these critical gaps and examine the efficacy of these promising COVID-19 vaccines in patients with SLE. This was accomplished by evaluating a multiethnic/multiracial cohort of SLE patients using assessments of serologic responses which were compared to healthy controls. The assays included antibodies to the spike protein receptor-binding domain (RBD), virus-neutralizing antibodies, and antigen-specific T cell production of interferon-γ (IFNγ), both prior to and after vaccination. Factors associated with the level of responsiveness were sought. In addition, SLE disease activity pre- and postvaccination was measured, as well as the rate of flare postvaccination.

PATIENTS AND METHODS

Study population and inclusion/exclusion criteria. Patients were recruited from the established New York University (NYU) Lupus Cohort, a prospective convenience registry open to enrolling any patient with SLE seen at NYU Langone Health and Bellevue Hospital Center since 2014. All SLE patients in the NYU Lupus Cohort are age 18 or older and fulfill ≥1 of the following criteria: 1) the American College of Rheumatology (ACR) revised classification criteria (11); 2) the Systemic Lupus International Collaborating Clinics classification criteria (12); and/or 3) the European Alliance of Associations for Rheumatology/ACR classification criteria (13). All NYU Lupus Cohort patients and controls provided written informed consent, which was available in English, Spanish, and Mandarin. All adult patients with SLE planning to receive any of the available COVID-19 vaccines were eligible for inclusion. Exclusion criteria included unwillingness to provide blood after the second dose of the vaccine, incomplete vaccination schedule, and speaking a language other than English, Spanish, or Mandarin. Healthy controls were ≥18 years of age, had no known rheumatic diseases and were receiving no immunosuppressive medications. The study protocol and the NYU Lupus Cohort and recruitment of controls were approved by the NYU and Bellevue Hospital Institutional Review Boards.

Study design and data collection. Patients were recruited using convenience sampling, with inclusion and exclusion criteria as stated above. For most patients, blood samples were available pre- and postvaccination. Disease activity measures and laboratory data prior to vaccination were available as part of the NYU Lupus Cohort but were limited to patients seen within 4 months of their first vaccine dose. Postvaccination follow-ups were scheduled ~2 weeks after the second dose of the messenger RNA (mRNA) vaccines (i.e., BNT162b2 [Pfizer/BioNTech] or mRNA-1273 [Moderna]) or after 1 dose of Ad26.COV2.S (Johnson & Johnson) to collect postvaccination blood samples and assess for any change in SLE activity. Disease activity was measured by the hybrid Safety of Estrogens in Lupus Erythematosus National Assessment (SELENA)–SLE Disease Activity Index (SLEDAI) (urine protein:creatinine ratios >0.5 were always counted), and flares were assessed by the SELENA–SLEDAI flare index (14–16). In addition, the use and doses of immunosuppressive medications were recorded at each visit, including, among others, glucocorticoids, hydroxychloroquine (HCQ), azathioprine, mycophenolate mofetil (MMF), methotrexate (MTX), belimumab, and tacrolimus. Any cyclophosphamide, obinutuzumab, or rituximab administered within 6 months of the patient's visit was also recorded. Considering that our patients were largely enrolled before the ACR updated their guidelines to temporarily hold MMF used to treat more severe manifestations such as nephritis, that medication was not held. We did advise patients to hold MTX and adjusted other medications as recommended per this guidance (17).

Enzyme-linked immunosorbent assay (ELISA) for recombinant SARS–CoV-2 spike protein. Ninety-six–well plates were coated with 1 μg/ml recombinant SARS–CoV-2 spike RBD (no. BT10500; R&D Systems), diluted in phosphate buffered saline (PBS) and incubated overnight at 4°C. Plates were blocked with 0.1% gelatin in PBS. Plasma (spun 10,000 rpm for 1 minute) were diluted 1:200–1:100,000 and added to the plate for 1 hour at room temperature. Samples were run in triplicate. With each run, 2 positive controls were included in the 96-well plate: plasma from control (non-SLE) participants postvaccination, with high and low IgG titers, each diluted 1:500 to ensure that measurements were captured across the assay range. Detection relies on an enzyme-labeled secondary antibody, alkaline phosphatase–conjugated rabbit anti-human IgG (γ-chain–

Table 1. Characteristics of the vaccinated SLE patients and healthy controls*

	Controls (n = 20)	SLE patients (n = 90)
Age, mean ± SD years	45.3 ± 14.2	45.5 ± 14.2
Sex†		
Female	12 (60.0)	79 (87.8)
Male	8 (40.0)	11 (12.2)
Race		
White	13 (65.0)	43 (47.8)
Black	2 (10.0)	16 (17.8)
Asian	4 (20.0)	17 (18.9)
Other	1 (5.0%)	14 (15.5)
Ethnicity		
Hispanic/Latino	1 (5.0)	34 (37.8)
COVID-19 vaccine		
BNT162b2 (Pfizer)	17 (85.0)	61 (67.8)
mRNA-1273 (Moderna)	3 (15.0)	24 (26.7)
Ad26.COV2.S (Johnson & Johnson)	0 (0)	5 (5.5)
Days between 2nd vaccine dose and postvaccine blood draw, mean (range)	23 (14–31)	24 (5–69)
Prior history of COVID-19 (PCR or IgG)	2 (10.0)	11 (12.2)
SLE risk factors		
History of LN	N/A	40 (44.4)
Kidney transplant recipient	N/A	5 (5.6)
APS	N/A	9 (10.0)
Medication(s)		
HCQ	–	71 (79)
Dose, mean ± SD mg	–	321.0 ± 89.7
Chloroquine	–	1 (1)
Dose, mg	–	250.0
Prednisone	–	26 (29)
Dose, mean ± SD mg	–	7.2 ± 7.6
Immunosuppressants	–	38 (42)
AZA	–	5 (6)
Dose, mean ± SD mg	–	130.0 ± 27.4
MMF	–	19 (21)
Dose, mean ± SD mg	–	1,967.1 ± 731.1
Mycophenolic acid	–	2 (2)
Dose, mean ± SD mg	–	900.0 ± 254.6
Tacrolimus	–	5 (6)
Dose, mean ± SD mg	–	4.0 ± 2.3
MTX	–	8 (9)
Dose, mean ± SD mg‡	–	14.6 ± 6.0
Belimumab	–	10 (11)
Cyclophosphamide	–	0 (0)
Rituximab	–	3 (3)
Leflunomide	–	1 (1)
Abatacept	–	1 (1)
Adalimumab	–	1 (1)
Obinutuzumab	–	1 (1)
Eculizumab	–	1 (1)
Apremilast	–	1 (1)
SLE clinical trial	–	1 (1)
Prednisone + immunosuppressant	–	22 (24)
Combination immunosuppressants	–	15 (17)

* Except where indicated otherwise, values are the number (%) of subjects. SLE = systemic lupus erythematosus; PCR = polymerase chain reaction; LN = lupus nephritis; APS = antiphospholipid syndrome; N/A = not applicable; HCQ = hydroxychloroquine; AZA = azathioprine; MMF = mycophenolate mofetil.
† $P = 0.007$.
‡ Includes 1 patient with an unknown dose of methotrexate (MTX), prescribed at an outside institution.

specific) (Sigma) diluted 1:2,000. After developing with the addition of phosphatase substrate, the optical density (OD) was measured at 405 nm, and the reaction was evaluated when the low positive control reached an OD of 1. The OD measured for a tested sample was multiplied by the dilution factor, which gave an OD in the range of 0.3–0.8.

SARS–CoV-2 microneutralization assay. Viral neutralization activity of plasma was measured in an immunofluorescence-based microneutralization assay by detecting the neutralization of infectious virus in cultured Vero E6 cells (no. CRL-1586, African green monkey kidney cells; ATCC). Cells were maintained according to standard ATCC protocols. Briefly, Vero E6 cells were grown in minimum essential medium (MEM) supplemented with 10% heat-inactivated fetal bovine serum (FBS), 2 m*M* L-glutamine, and 1% of MEM Nonessential Amino Acid Solution (no. MT25025CI; Fisher). Cell cultures were grown in 75 or 150 cm^2 flasks at 37°C with 5% CO_2 and passaged 2–3 times per week using trypsin–EDTA. Cell cultures used for virus testing were prepared as subconfluent monolayers. All incubations containing cells were performed at 37°C with 5% CO_2. All SARS–CoV-2 infection assays were performed in the Centers for Disease Control and Prevention (CDC)/US Department of Agriculture–approved biosafety level 3 facility in compliance with NYU Grossman School of Medicine guidelines for biosafety level 3. SARS–CoV-2 isolate USA-WA1/2020, deposited by the CDC, was obtained through BEI Resources, National Institute of Allergy and Infectious Diseases, National Institutes of Health (NR-52281, GenBank accession no. MT233526). Serial dilutions of heat-inactivated plasma (56°C for 1 hour) were incubated with USA-WA1/2020 stock (at fixed 1×10^6 plaque-forming units/ml) for 1 hour at 37°C. One hundred microliters of the plasma–virus mix was then added to the cells and incubated at 37°C with 5% CO_2. Twenty-four hours postinfection, cells were fixed with 10% formalin solution (4% active formaldehyde) for 1 hour, stained with an anti-SARS–CoV-2 nucleocapsid antibody (no 10-605; ProSci), and a goat anti-mouse IgG Alexa Fluor 647 secondary antibody along with DAPI and visualized by microscopy with the CellInsight CX7 High-Content Screening Platform (ThermoFisher) and high-content software.

Enzyme-linked immunospot (ELISpot). ELISpot plates (Human IFNγ ELISpot Plus, no. 3420-4HPT-2) were preseeded under sterile conditions following the recommendations of the manufacturer (Mabtech) in duplicates with 250,000 cells per well from cryopreserved peripheral blood mononuclear cells (PBMCs) isolated from each participant. Cells were incubated for 24 hours with SARS–CoV-2 spike protein S1 (1 μg/well) (no. RP-87681; Invitrogen) or vehicle, in the presence of anti-CD28 (1 μg/ml) (Biolegend). Cells were removed by washing the wells with PBS + 1% FBS. Membrane was probed with a 1:1,000 dilution of the detection antibody provided by the manufacturer (1 hour at 22°C). After washing, plates were developed using tetramethylbenzidine substrate solution. Spots were imaged and counted using an ImmunoSpot S6 Analyzer (Cellular Technology Limited). For each sample, the monoclonal antibody CD3-2 was used to capture cytokine production as a positive control.

Statistical analysis. Categorical variables were summarized by computing counts and proportions of patients. Continuous variables are expressed as the mean ± SD or the median and interquartile range (IQR) or range, as appropriate. Two-group comparisons were performed using the chi-square or Fisher's exact test for categorical variables and the 2-sample *t*-test or Mann–Whitney U test for continuous variables. Spearman's rank correlation coefficient was computed for the association between the ELISA and microneutralization assays. An exploratory logistic regression analysis was also conducted to identify potential independent predictors of low postvaccine ELISA antibody response (≤100 units/ml, the lowest value seen in controls). Variable selection in the final model was based on both statistical significance ($P < 0.10$, given limited sample size and power of the study) as

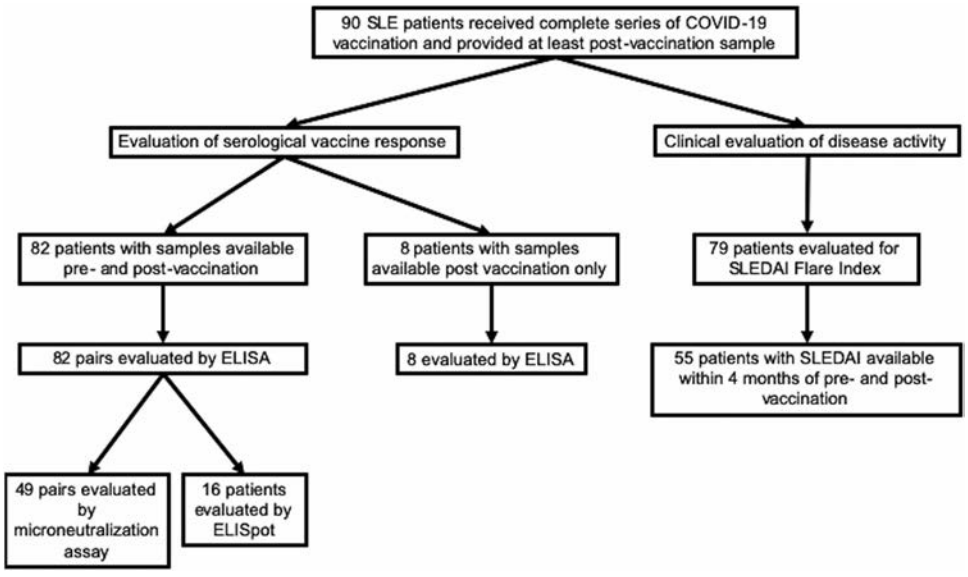

Figure 1. Flow diagram of the systemic lupus erythematosus (SLE) patients included in each analysis. ELISA = enzyme-linked immunosorbent assay; ELISpot = enzyme-linked immunospot; SLEDAI = SLE Disease Activity Index.

well as clinical considerations. All statistical analyses were performed using SAS version 9.4.

RESULTS

Patient population. A total of 90 patients with SLE and 20 controls were included in this study. Table 1 shows the demographics of the patients and controls in addition to SLE-specific information. Cases and controls were relatively well-matched; however, controls were more likely to be male ($P = 0.007$). Whereas controls only received the BNT162b2 and mRNA-1273 vaccines, SLE patients received all 3 vaccines currently available in the US, including Ad26.COV2.S. In addition, 12% of the SLE patients had a history of prior COVID-19 infection compared to 10% of controls. Forty-four percent of patients had a history of lupus nephritis (LN), 10% had secondary antiphospholipid syndrome (APS), and 5.6% had received a kidney transplant. The majority of SLE patients (79%) were receiving HCQ, and 29% were receiving systemic glucocorticoids (mean dose of 7 mg prednisone). Forty-two percent were receiving ≥1 immunosuppressant, with MMF being the most common (21%), followed by belimumab (11%). In addition, 17% of patients were receiving a combination of immunosuppressants. Figure 1 shows the number of SLE patients included in each subsequent analysis.

Decreased COVID-19 antibody responses in SLE patients compared to controls. Ninety SLE patients (82 with data from pre- and postvaccination analyses) and 20 healthy controls (all with data from pre- and postvaccination analyses) were evaluated for IgG antibody levels against the RBD of SARS–CoV-2 spike protein (anti-RBD) (Figures 2A–D). Overall, prevaccine levels in patients with SLE were significantly lower (median 9.1 [IQR 2.8–23.9]) than in controls (median 34.5 [IQR 11.2–74.0]; $P = 0.001$), as were the postvaccine levels (median 235.2 [IQR 75.9–531.4] versus median 435.7 [IQR 269.0–768.6], respectively; $P = 0.01$). Postvaccine antibody levels in 26 SLE patients (28.8%) fell below the lowest level of the controls (≤100 units/ml), which is shown in Figure 2D.

To address the functionality of the antibody responses assessed by ELISA, pre- and postvaccine samples from 49 SLE patients and 18 controls were also evaluated by the SARS–CoV-2 live microneutralization assay. As shown in Figure 2E, there was a strong correlation between the 2 assays (R = 0.76, $P < 0.0001$), suggesting that the ELISA is a good end point assay to evaluate the immune response to the vaccines. Similar to what we observed with the ELISA results, postvaccine microneutralization titers were significantly lower in SLE patients compared to controls ($P = 0.0075$) (Figure 2F).

A comparison of clinical and laboratory factors in the 64 SLE patients who generated responses to COVID-19 vaccine that were compatible with controls and the 26 patients with low responses who had ELISA results ≤100 units/ml is shown in Table 2. In unadjusted analyses, subjects with low responses were more likely to be receiving prednisone, MMF or mycophenolic acid, a combination of prednisone and ≥1 immunosuppressant, or ≥2 immunosuppressants, while those with high responses were more likely to only be receiving antimalarials or receiving no medication. In addition, low responders were

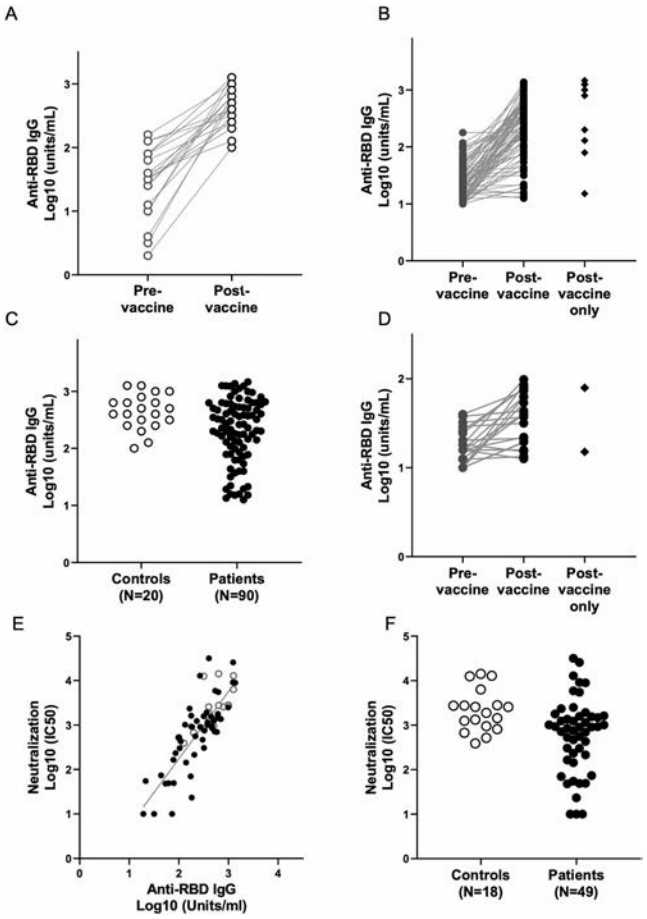

Figure 2. Antibody response to COVID-19 vaccine in SLE patients. Throughout, open circles represent controls, and solid circles represent SLE patients. Serum IgG titers against the SARS–CoV-2 spike protein receptor-binding domain (RBD) were obtained by direct ELISA. Binding of human IgG to recombinant SARS–CoV-2 RBD was performed as described in Patients and Methods. **A**, IgG titers of 20 controls pre- and postvaccination. **B**, IgG titers of 81 SLE patients pre- and postvaccination and 9 SLE patients with only postvaccination data available. **C**, Comparison of IgG titers postvaccination between the 2 groups, with controls showing significantly higher titers than SLE patients. **D**, IgG titers of a subgroup of patients (n = 24) from **B** with anti-RBD IgG ≤100 units/ml (the lowest response in controls). **E**, Correlation of SARS–CoV-2 virus neutralization titers in the sera of vaccinated subjects with IgG titers. Each dot represents the serum evaluation of a participant with binding of human IgG to recombinant SARS–CoV-2 RBD (x-axis) versus live virus neutralization at 50% inhibition concentration (IC_{50}; y-axis). There is a strong correlation between spike RBD IgG and live virus neutralization (R = 0.76, $P < 0.0001$). **F**, Log_{10} postvaccination neutralization titers for controls compared to SLE patients. See Figure 1 for other definitions.

Table 2. Bivariate analysis of predictors for poor postvaccine ELISA antibody response (≤100 units/ml) among the SLE patients*

	Postvaccine ELISA antibody response		
	≤100 units/ml (n = 26)	>100 units/ml (n = 64)	*P*
Age, mean ± SD years	47.7 ± 13.3	44.6 ± 14.5	0.36
Sex			0.29
Female	21 (80.8)	58 (90.6)	
Male	5 (19.2)	6 (9.4)	
Race			0.46
White	11 (42.3)	32 (50.0)	
Black	3 (11.5)	13 (20.3)	
Asian	7 (26.9)	10 (15.6)	
Other	5 (19.2)	9 (14.1)	
Ethnicity			0.93
Hispanic	10 (38.5)	24 (37.5)	
Non-Hispanic	16 (61.5)	40 (62.5)	
Days between 2nd vaccine dose and postvaccine blood draw, median (IQR)	19.5 (14.0–44.0)	17.0 (12.0–26.0)	0.11
Vaccine type			0.039
BNT162b2	15 (57.7)	46 (71.9)	
mRNA-1273	7 (26.9)	17 (26.6)	
Ad26.COV2.S	4 (15.4)	1 (1.6)	
Prior history of COVID-19 (PCR or IgG)	4 (18.2)	7 (13.7)	0.72
History of LN	15 (57.7)	25 (39.7)	0.12
Kidney transplant recipient	3 (11.5)	2 (3.1)	0.14
APS	0 (0)	9 (14.1)	0.055
Prednisone + ≥1 immunosuppressant	10 (38.5)	12 (18.8)	0.049
Combination immunosuppressants	9 (34.6)	6 (9.4)	0.01
Only antimalarials (HCQ + chloroquine) among those receiving medication	3 (12.0)	33 (56.9)	0.0002
Any MMF (MMF + mycophenolic acid)	12 (46.2)	9 (14.1)	0.001
Any prednisone	12 (46.2)	14 (21.9)	0.021
Any belimumab	4 (15.4)	6 (9.4)	0.47
No immunosuppressants	1 (3.8)	6 (9.4)	0.67
Only HCQ or no medications	4 (15.4)	39 (60.9)	<0.0001
Prevaccine anti-dsDNA antibody level†			0.023
Normal	14 (87.5)	28 (56.0)	
High	2 (12.5)	22 (44.0)	
C3 level			0.35
Low	3 (18.8)	17 (34.0)	
Normal	13 (81.3)	33 (66.0)	
C4 level			1.00
Low	4 (25.0)	12 (24.0)	
Normal	12 (75.0)	38 (76.0)	
SLEDAI score, mean ± SD†	2.00 ± 2.34	3.46 ± 4.16	0.085
Platelet count, mean ± SD × 10^3/μl†	202.81 ± 78.37	243.74 ± 85.60	0.095
Urine protein:creatinine ratio, mean ± SD†	0.17 ± 0.18	0.28 ± 0.58	0.26
Lymphocyte count, mean ± SD × 10^3/μl†	1.19 ± 0.65	1.36 ± 0.97	0.43

* Except where indicated otherwise, values are the number (%) of subjects. ELISA = enzyme-linked immunosorbent assay; SLE = systemic lupus erythematosus; IQR = interquartile range; PCR = polymerase chain reaction; LN = lupus nephritis; APS = antiphospholipid syndrome; HCQ = hydroxychloroquine; MMF = mycophenolate mofetil; anti-dsDNA = anti–double-stranded DNA (see Table 1 for other definitions).
† Laboratory measures and SLE Disease Activity Index (SLEDAI) scores were based on patients with prevaccine data available within 4 months of vaccine (n = 66).

more likely to have received Ad26.COV2.S, although sample sizes were limited, and to have had a normal anti–double-stranded DNA (anti-dsDNA) antibody level prior to vaccination (Table 2). Logistic regression analysis yielded a final model that included the following 4 independent predictors of low ELISA response among SLE patients: receiving any immunosuppressive therapy other than antimalarials (adjusted odds ratio [OR] 15.14 [95% CI 2.80–82.03] compared to antimalarials/no medications; $P = 0.002$), normal anti-dsDNA antibody level prior to vaccination (OR 14.50 [95% CI 2.20–95.66] compared to abnormal anti-dsDNA antibody level; $P = 0.006$), lower platelet count (OR 1.55 [95% CI 0.96–2.51] per 50 × 10^9 cells/liter decrease; $P = 0.07$), and normal C3 level (OR 4.95 [95% CI 0.91–26.0] compared to low C3 level; $P = 0.06$). A separate subgroup analysis including only those patients who were receiving any immunosuppressants confirmed the association of a normal anti-dsDNA

Table 3. Demographic information and medications of the SLE patients with lower vaccine responses (n = 26)*

Patient	Age	Sex	Vaccine type	Medication(s)
1	39	Male	BNT162b2	HCQ, MMF, obinutuzumab
2	71	Female	BNT162b2	MTX, abatacept
3	57	Female	BNT162b2	HCQ, belimumab
4	57	Female	BNT162b2	Prednisone (4 mg), HCQ, MTX, adalimumab
5	61	Female	BNT162b2	HCQ, MMF
6	42	Female	BNT162b2	HCQ, tacrolimus, rituximab
7	38	Female	BNT162b2	Prednisone (5 mg), mycophenolic acid, tacrolimus
8	59	Female	BNT162b2	Prednisone (5 mg), HCQ
9	62	Male	BNT162b2	HCQ, belimumab
10	54	Female	BNT162b2	HCQ
11	49	Female	BNT162b2	Prednisone (3 mg), MMF, belimumab
12	53	Female	BNT162b2	MMF
13	47	Female	BNT162b2	Prednisone (10 mg), HCQ, MMF
14	40	Male	BNT162b2	Prednisone (5 mg), HCQ, MMF
15	29	Female	BNT162b2	Prednisone (2.5 mg), HCQ, MMF
16	39	Male	mRNA-1273	HCQ, rituximab
17	46	Female	mRNA-1273	Prednisone (5 mg), HCQ, MMF
18	35	Female	mRNA-1273	HCQ, AZA, belimumab
19	66	Female	mRNA-1273	Prednisone (5 mg)
20	28	Female	mRNA-1273	HCQ
21	44	Female	mRNA-1273	HCQ
22	41	Female	mRNA-1273	Prednisone (20 mg), MMF
23	55	Female	Ad26.COV2.S	Prednisone (5 mg), HCQ, mycophenolic acid
24	72	Female	Ad26.COV2.S	None
25	27	Female	Ad26.COV2.S	HCQ, MMF
26	28	Male	Ad26.COV2.S	Prednisone (10 mg), MTX

* SLE = systemic lupus erythematosus; HCQ = hydroxychloroquine; MMF = mycophenolate mofetil; MTX = methotrexate; AZA = azathioprine.

antibody level with poor antibody response (OR 8.98 [95%CI 1.89–42.6]; $P = 0.006$ after adjustment for platelet and C3). Further details about the patients with lower responses are provided in Table 3.

Evaluation of IFNγ secretion in response to SARS–CoV-2 spike protein S1. Sixteen SLE patients (of whom 4 had pre- and postvaccine data available) and 2 controls (both with pre- and postvaccine data available) were further evaluated addressing T cell reactivity, which was operationally reported by the release of IFNγ in response to challenge of PBMCs in the absence and presence of the full-length S1 protein (COVID-19 antigen), as described in Patients and Methods. Individuals were chosen to represent a range of responses to the SARS–CoV-2 spike protein and SARS–CoV-2 microneutralization assay but with a particular focus on the patients with low seroreactivity on both assays. As shown in Supplementary Figure 1 (available on the *Arthritis & Rheumatology* website at http://onlinelibrary.wiley.com/doi/10.1002/art.41937/abstract), there was a correlation between the postvaccine ELISpot number and ELISA evaluations ($R = 0.57$, $P = 0.0135$). In a subset of patients with poor antibody responses, IFNγ production was likewise diminished (Supplementary Figure 1).

Stable disease activity in the majority of SLE patients after COVID-19 vaccination. Of the 90 patients evaluated, 55 patients had completed a SLEDAI assessment within 4 months of their first vaccine dose, which was then compared to their postvaccine SLEDAI assessment that was completed an average of 23.6 days (range 5–70) after the final vaccine dose (Supplementary Table 1, http://onlinelibrary.wiley.com/doi/10.1002/art.41937/abstract). Overall, there was no meaningful difference in SLEDAI score between pre- and postvaccine visits (3.2 versus 2.9). There were no changes in the percentages of patients with abnormal anti-dsDNA antibodies and/or abnormal complement levels; likewise, the levels of C3 and C4 were similar pre- and postvaccination (Supplementary Table 1). Nine of the 79 patients (11.4%) experienced a postvaccination flare, with all but 1 considered to be mild/moderate (2 in new organ systems: arthritis with no treatment and pericarditis treated with naproxen). The severe flare was characterized by arthritis and treated with MTX; the patient had discontinued HCQ due to maculopathy several years prior to vaccination. Further details of the flares are provided in Table 4.

DISCUSSION

To our knowledge, this is the first reported study focused on patients with SLE who received full regimens of a COVID-19 vaccine, and overall IgG antibody responses against the SARS–CoV-2 spike protein RBD were significantly decreased compared to vaccinated controls, with 28.8% of patients generating responses falling below the lowest level observed in the healthy

Table 4. SLE flares postvaccination*

Flare severity	Flare type	Flare details	Timing of flare	Vaccine type	Treatment
Mild/moderate	Pleuritis	Recurrent mild pleuritis	After 1st dose	BNT162b2	No treatment
Mild/moderate	Arthritis	Recurrent mild joint pain and swelling	After 2nd dose	BNT162b2	No treatment
Mild/moderate	Renal	Recurrent proteinuria; urine protein:creatinine ratio increased from 0.8 to 1.4	After 2nd dose	BNT162b2	Rituximab/tacrolimus changed to voclosporin
Mild/moderate	Oral ulcers	Recurrent oral ulcers; patient had been off of belimumab for 3 months	After 2nd dose	mRNA-1273	No treatment
Mild/moderate	Pericarditis	New presumed pericarditis, EKG negative; resolved with naproxen	After 2nd dose (2 weeks)	BNT162b2	Naproxen
Severe	Arthritis	Recurrent arthritis	After 2nd dose	mRNA-1273	Methotrexate
Mild/moderate	Thrombocytopenia	Recurrent thrombocytopenia within patient's range	After 2nd dose	BNT162b2	No treatment
Mild/moderate	Arthritis	New mild joint pain and swelling	After 2nd dose	BNT162b2	No treatment
Mild/moderate†	Thrombocytopenia	Recurrent thrombocytopenia	After 2nd dose	BNT162b2	No treatment
Non–SLE-related event	COPD/asthma flare		After 2nd dose	BNT162b2	Treated in emergency room with steroids, then released

* EKG = electrocardiogram; COPD = chronic obstructive pulmonary disease.
† A patient with systemic lupus erythematosus (SLE), antiphospholipid syndrome, and end-stage renal disease was admitted 13 days after the second vaccine dose. The patient had anticoagulation therapy temporarily withheld for a procedure, presented with shortness of breath, and was found to have superior vena cava syndrome. The patient had a prolonged hospital course, complicated by bleeding and sepsis, and was transitioned to hospice care and died 50 days after the second dose.

controls. Receiving any immunosuppressive agent other than antimalarials and having a normal anti-dsDNA antibody level prior to vaccination were identified as independent predictors for poor response to the COVID-19 vaccine. Seroreactivity to the SARS–CoV-2 spike RBD strongly correlated with the functional SARS–CoV-2 microneutralization assay and correlated with the ELISpot assay. Overall, there was no change in SLEDAI score pre- and postvaccination, with 11.4% of patients having a flare and 1.3% of those flares being severe, supporting the relative safety of the vaccination in SLE patients.

The finding of anti-dsDNA antibodies positively correlating with higher responses to COVID-19 vaccination was initially unexpected, especially given that this finding persisted even after controlling for medication use. Moreover, disease activity per se was not associated with more effective seroreactivity. It could be hypothesized that the presence of anti-dsDNA antibodies is a proxy of elevated type I IFN activity in these patients. Indeed, studies have shown that high IFNα activity in patients with SLE is associated with the presence of disease-specific autoantibodies, such as anti-dsDNA (18). These autoantibodies can form immune complexes, further stimulating type I IFN production (19). Besides their potent antiviral properties, type I IFNs induce the maturation and activation of myeloid dendritic cells, and promote B cell survival and differentiation into antibody-producing cells (20,21). These considerations support the hypothesis that those with stronger responses to the COVID-19 vaccines could have higher baseline type I IFN activity, due to its potential to enhance antibody responses to foreign antigens. Thus, patients with anti-dsDNA antibodies, despite receiving immunosuppressive therapy, may be more likely to develop a strong humoral response to the COVID-19 vaccines. Alternatively, these analyses did not account for patient adherence to medication or the possibility that elevated dsDNA antibodies reflects inefficacy of immunosuppression, which might account for these findings. These potential insights merit further investigation.

Given the exclusion of patients receiving immunosuppressants from the regulatory vaccine studies, several groups have already explored the influence of immunosuppressive medications on the response to vaccination. Boyarsky et al evaluated patients with organ transplants and reported that antimetabolite maintenance immunosuppression was associated with an absent or reduced anti-RBD spike response after the first dose of the vaccine (22). A follow-up study from the same group in 658 transplant recipients who received the second dose of the SARS–CoV-2 mRNA vaccine showed an increase in seroreactivity in response to the second dose; however, poor responses were associated with antimetabolite immunosuppressive treatment (23).

Concordant with our results, several studies have shown decreased vaccine-induced seroreactivity in patients with rheumatic diseases. In 123 such patients, including 24 with SLE, those receiving MMF or rituximab were less likely to develop an antibody response to the spike protein after the first dose of the SARS–CoV-2 mRNA vaccine; these findings were confirmed in a larger study of 404 patients, including 87 with SLE, after the second dose (24,25). In an analysis of 26 patients with chronic

inflammatory diseases (CIDs) that included 2 patients with SLE who were receiving HCQ, SARS–CoV-2 antibodies were significantly lower in patients, compared to controls, after both doses of BNT162b2 or mRNA-1273. No patients experienced a disease flare after both doses of the vaccine (26). A large study of 133 patients with CIDs, including 15 patients with SLE, who received an mRNA vaccine showed that patients with CIDs had a 3-fold reduction in anti–spike protein IgG response with B cell depletion, glucocorticoids, and antimetabolites (27). A subsequent analysis of 89 patients that included 10 patients with SLE showed that rituximab was associated with impaired serologic response to the SARS–CoV-2 vaccine (28). Haberman et al demonstrated that MTX adversely affected both the humoral and cellular immune responses to COVID-19 mRNA vaccines in patients with immune-mediated inflammatory diseases (29). A large study from Furer et al that included 101 patients with SLE showed that older age and treatment with glucocorticoids, rituximab, MMF, and abatacept were associated with reduced immunogenicity as measured by serum IgG antibody levels against SARS–CoV-2 spike S1/S2 proteins 2–6 weeks after vaccination (30). Our study showed that receiving any non-antimalarial immunosuppressive therapy was independently associated with decreased response to COVID-19 vaccines in patients with SLE.

In addition to concerns regarding inefficient immune responses to COVID vaccination, it may be the case that vaccination induces increased autoantibody production and disease activity. As speculated by Tang et al, delivery of mRNA encoding S protein via the vaccine, likely degraded by normal cellular processes, could interact with a number of cytoplasmic RNA-binding proteins involved in the posttranscriptional regulation of inflammation and result in worsening SLE (5). Similarly, RNA vaccines may trigger Toll-like receptors, generating further production of type I IFN, already well-recognized to be elevated in most SLE patients (19). It has been reported that influenza vaccines triggered a transient increase in several autoantibody specificities in 72 SLE patients, with a flare rate of 19.4% within 6 weeks postvaccination; 10 (13.9%) were mild/moderate and 4 (5.6%) were severe (31). In a study evaluating SLE flares after immunization against poliomyelitis, only 4 of 73 patients (5%) experienced flares (32). In aggregate, despite apprehensions, the data presented herein did not support significantly increased anti-dsDNA antibody production or flares postvaccination. These results are consistent with a recent study which showed that the majority of vaccinated SLE patients had no change or decrease in disease activity after COVID-19 vaccination as measured by the SLEDAI (30).

Our study has several limitations. Similar to other studies evaluating potential surrogate markers for vaccine efficacy, it is premature to assign a threshold level of protection based on either the IgG response to the anti-RBD of SARS–CoV-2 spike protein or the microneutralization assay given the number of controls. There was vaccine hesitancy among patients in the NYU Lupus Cohort, in large part due to concern regarding the potential effect on lupus activity, and thus the patients in this study may not be fully representative of the patients seen in our cohort. While known prior COVID-19 infection was accounted for in all patients, it remains possible that asymptomatic or mild infection occurred between prevaccine blood draw and vaccination, which could influence subsequent seroreactivity. While this study included 90 patients with SLE, the number of patients receiving individual medications was too small to draw any definitive conclusions about their effects on vaccine response in SLE patients, and in our analyses, receiving any non-antimalarial immunosuppressive agent was ultimately the strongest predictor of a poor antibody response to the COVID-19 vaccines. Another limitation of the work is the absence of a direct comparator of SLE flare rates over the same time period. It also remains possible that a perceived SLE flare could have been a vaccine side effect.

This study has several strengths. In contrast to previous reports, the focus was limited to patients with SLE and assessed the COVID-19 vaccines' effects on lupus-specific disease activity with availability of a validated disease index pre- and postvaccination in the majority of patients. Flares were rare, with only 1.3% being severe. These data are reassuring and support the notion that vaccines do not exacerbate disease activity, a finding that should hopefully alleviate vaccine hesitancy. Our study assessed 2 surrogate markers for B cell reactivity and a surrogate for T cell–mediated responses. Although the latter was limited to fewer patients, it was particularly applied to evaluate those with lower humoral responses and reinforced the concern about vaccine efficacy in a subset of these individuals.

In summary, in a multiracial/multiethnic study of SLE patients receiving a complete COVID-19 vaccine regimen, nearly 30% had a low response. Having a normal anti-dsDNA antibody level and taking any immunosuppressive medication other than antimalarials were independently associated with a decreased vaccine response. While minimal protective antibody levels remain unknown, these results, supported by other studies, raise concerns for our lupus patients, many of whom rely on medications to maintain low disease activity. Accordingly, the next phase of scientific inquiry and advance should focus on protocols addressing additional vaccination. Reassuringly, severe disease flares are infrequent, which should encourage patients to consider vaccination.

ACKNOWLEDGMENTS

The authors would like to thank the patients who participated in the study. They would also like to acknowledge Ranit Shriky and Rebecca Cohen for their assistance with regulatory matters and Benjamin Wainwright for his contributions to the manuscript.

AUTHOR CONTRIBUTIONS

All authors were involved in drafting the article or revising it critically for important intellectual content, and all authors approved the final version to be published. Dr. Izmirly had full access to all of the data in the study and takes responsibility for the integrity of the data and the accuracy of the data analysis.

Study conception and design. Izmirly, Kim, Samanovic, Fernandez-Ruiz, Haberman, Scher, Mulligan, Clancy, Buyon.
Acquisition of data. Izmirly, Samanovic, Fernandez-Ruiz, Ohana, Deonaraine, Engel, Masson, Cornelius, Herati, Guttmann, Blank, Plotz, Haj-Ali, Banbury, Stream, Hasan, Ho, Rackoff, Blazer, Tseng, Belmont, Saxena, Mulligan, Clancy, Buyon.
Analysis and interpretation of data. Izmirly, Kim, Samanovic, Fernandez-Ruiz, Xie, Belmont, Saxena, Mulligan, Clancy, Buyon.

REFERENCES

1. Fernandez-Ruiz R, Masson M, Kim MY, Myers B, Haberman RH, Castillo R, et al. Leveraging the United States epicenter to provide insights on COVID-19 in patients with systemic lupus erythematosus. Arthritis Rheumatol 2020;72:1971–80.
2. Fernandez-Ruiz R, Paredes JL, Niewold TB. COVID-19 in patients with systemic lupus erythematosus: lessons learned from the inflammatory disease [review]. Transl Res 2021;232:13–36.
3. Strangfeld A, Schäfer M, Gianfrancesco MA, Lawson-Tovey S, Liew JW, Ljung L, et al. Factors associated with COVID-19-related death in people with rheumatic diseases: results from the COVID-19 Global Rheumatology Alliance physician-reported registry. Ann Rheum Dis 2021;80:930–42.
4. Gianfrancesco M, Hyrich KL, Al-Adely S, Carmona L, Danila MI, Gossec L, et al. Characteristics associated with hospitalisation for COVID-19 in people with rheumatic disease: data from the COVID-19 Global Rheumatology Alliance physician-reported registry. Ann Rheum Dis 2020;79:859–66.
5. Tang W, Askanase AD, Khalili L, Merrill JT. SARS–CoV-2 vaccines in patients with SLE. Lupus Sci Med 2021;8:e000479.
6. Saxena A, Guttmann A, Masson M, Kim MY, Haberman RH, Castillo R, et al. Evaluation of SARS–CoV-2 IgG antibody reactivity in patients with systemic lupus erythematosus: analysis of a multi-racial and multi-ethnic cohort. Lancet Rheumatol 2021;3:e585–94.
7. Polack FP, Thomas SJ, Kitchin N, Absalon J, Gurtman A, Lockhart S, et al. Safety and efficacy of the BNT162b2 mRNA Covid-19 vaccine. New Engl J Med 2020;383:2603–15.
8. Baden LR, El Sahly HM, Essink B, Kotloff K, Frey S, Novak R, et al. Efficacy and safety of the mRNA-1273 SARS–CoV-2 vaccine. New Engl J Med 2020;384:403–16.
9. Sadoff J, Gray G, Vandebosch A, Cárdenas V, Shukarev G, Grinsztejn B, et al. Safety and efficacy of single-dose Ad26.COV2.S vaccine against Covid-19. New Engl J Med 2021;384:2187–201.
10. Boekel L, Hooijberg F, van Kempen ZL, Vogelzang EH, Tas SW, Killestein J, et al. Perspective of patients with autoimmune diseases on COVID-19 vaccination. Lancet Rheumatol 2021;3:e241–3.
11. Hochberg MC. Updating the American College of Rheumatology revised criteria for the classification of systemic lupus erythematosus. Arthritis Rheum 1997;40:1725–34.
12. Petri M, Orbai AM, Alarcón GS, Gordon C, Merrill JT, Fortin PR, et al. Derivation and validation of the Systemic Lupus International Collaborating Clinics classification criteria for systemic lupus erythematosus. Arthritis Rheum 2012;64:2677–86.
13. Aringer M, Costenbader K, Daikh D, Brinks R, Mosca M, Ramsey-Goldman R, et al. 2019 European League Against Rheumatism/American College of Rheumatology classification criteria for systemic lupus erythematosus. Arthritis Rheumatol 2019;71:1400–12.
14. Gladman DD, Ibanez D, Urowitz MB. Systemic lupus erythematosus disease activity index 2000. J Rheumatol 2002;29:288–91.
15. Buyon JP, Petri MA, Kim MY, Kalunian KC, Grossman J, Hahn BH, et al. The effect of combined estrogen and progesterone hormone replacement therapy on disease activity in systemic lupus erythematosus: a randomized trial. Ann Intern Med 2005;142:953–62.
16. Touma Z, Gladman DD, Ibanez D, Urowitz MB. Development and initial validation of the systemic lupus erythematosus disease activity index 2000 responder index 50. J Rheumatol 2011;38:275–84.
17. Curtis JR, Johnson SR, Anthony DD, Arasaratnam RJ, Baden LR, Bass AR, et al. American College of Rheumatology guidance for COVID-19 vaccination in patients with rheumatic and musculoskeletal diseases: version 2. Arthritis Rheumatol 2021;73:e30–45.
18. Niewold TB, Hua J, Lehman TJ, Harley JB, Crow MK. High serum IFN-α activity is a heritable risk factor for systemic lupus erythematosus. Genes Immun 2007;8:492–502.
19. Postal M, Vivaldo JF, Fernandez-Ruiz R, Paredes JL, Appenzeller S, Niewold TB. Type I interferon in the pathogenesis of systemic lupus erythematosus [review]. Curr Opin Immunol 2020;67:87–94.
20. López P, Rodríguez-Carrio J, Caminal-Montero L, Mozo L, Suárez A. A pathogenic IFNα, BLyS and IL-17 axis in systemic lupus erythematosus patients. Sci Rep 2016;6:20651.
21. Psarras A, Emery P, Vital EM. Type I interferon-mediated autoimmune diseases: pathogenesis, diagnosis and targeted therapy [review]. Rheumatology (Oxford) 2017;56:1662–75.
22. Boyarsky BJ, Werbel WA, Avery RK, Tobian AA, Massie AB, Segev DL, et al. Immunogenicity of a single dose of SARS–CoV-2 messenger RNA vaccine in solid organ transplant recipients. JAMA 2021;325:1784–6.
23. Boyarsky BJ, Werbel WA, Avery RK, Tobian AA, Massie AB, Segev DL, et al. Antibody response to 2-Dose SARS–CoV-2 mRNA vaccine series in solid organ transplant recipients. JAMA 2021;21:2204–6.
24. Boyarsky BJ, Ruddy JA, Connolly CM, Ou MT, Werbel WA, Garonzik-Wang JM, et al. Antibody response to a single dose of SARS–CoV-2 mRNA vaccine in patients with rheumatic and musculoskeletal diseases. Ann Rheum Dis 2021. doi: 10.1136/annrheumdis-2021-220289. E-pub ahead of print.
25. Ruddy JA, Connolly CM, Boyarsky BJ, Werbel WA, Christopher-Stine L, Garonzik-Wang J, et al. High antibody response to two-dose SARS–CoV-2 messenger RNA vaccination in patients with rheumatic and musculoskeletal diseases. Ann Rheum Dis 2021. doi: 0.1136/annrheumdis-2021-220656. E-pub ahead of print.
26. Geisen UM, Berner DK, Tran F, Sümbül M, Vullriede L, Ciripoi M, et al. Immunogenicity and safety of anti-SARS–CoV-2 mRNA vaccines in patients with chronic inflammatory conditions and immunosuppressive therapy in a monocentric cohort. Ann Rheum Dis 2021. doi: 10.1136/annrheumdis-2021-220272. E-pub ahead of print.
27. Deepak P, Kim W, Paley MA, Yang M, Carvidi AB, El-Qunni AA, et al. Glucocorticoids and B Cell depleting agents substantially impair immunogenicity of mRNA vaccines to SARS–CoV-2 [preprint]. medRxiv 2021. doi: 10.1101/2021.04.05.21254656. E-pub ahead of print.
28. Spiera R, Jinich S, Jannat-Khah D. Rituximab, but not other antirheumatic therapies, is associated with impaired serological response to SARS- CoV-2 vaccination in patients with rheumatic diseases. Ann Rheum Dis 2021. doi: 10.1136/annrheumdis-2021-220604. E-pub ahead of print.
29. Haberman RH, Herati R, Simon D, Samanovic M, Blank RB, Tuen M, et al. Methotrexate hampers immunogenicity to BNT162b2 mRNA COVID-19 vaccine in immune-mediated inflammatory disease. Ann Rheum Dis 2021. doi: 10.1101/2021.05.11.21256917. E-pub ahead of print.
30. Furer V, Eviatar T, Zisman D, Peleg H, Paran D, Levartovsky D, et al. Immunogenicity and safety of the BNT162b2 mRNA COVID-19 vaccine in adult patients with autoimmune inflammatory rheumatic

diseases and in the general population: a multicentre study. Ann Rheum Dis 2021. doi: 10.1136/annrheumdis-2021-220647. E-pub ahead of print.

31. Crowe SR, Merrill JT, Vista ES, Dedeke AB, Thompson DM, Stewart S, et al. Influenza vaccination responses in human systemic lupus erythematosus: impact of clinical and demographic features. Arthritis Rheum 2011;63:2396–406.
32. Schattner A, Ben-Chetrit E, Schmilovitz H. Poliovaccines and the course of systemic lupus erythematosus—a retrospective study of 73 patients. Vaccine 1992;10:98–100.

Arthritis & Rheumatology
Vol. 74, No. 2, February 2022, pp 295–306
DOI 10.1002/art.41943

American College of Rheumatology
Empowering Rheumatology Professionals

Mepolizumab for Eosinophilic Granulomatosis With Polyangiitis: A European Multicenter Observational Study

Alessandra Bettiol,[1] Maria Letizia Urban,[1] Lorenzo Dagna,[2] Vincent Cottin,[3] Franco Franceschini,[4] Stefano Del Giacco,[5] Franco Schiavon,[6] Thomas Neumann,[7] Giuseppe Lopalco,[8] Pavel Novikov,[9] Chiara Baldini,[10] Carlo Lombardi,[11] Alvise Berti,[12] Federico Alberici,[13] Marco Folci,[14] Simone Negrini,[15] Renato Alberto Sinico,[16] Luca Quartuccio,[17] Claudio Lunardi,[18] Paola Parronchi,[1] Frank Moosig,[19] Georgina Espígol-Frigolé,[20] Jan Schroeder,[21] Anna Luise Kernder,[22] Sara Monti,[23] Ettore Silvagni,[24] Claudia Crimi,[25] Francesco Cinetto,[26] Paolo Fraticelli,[27] Dario Roccatello,[28] Angelo Vacca,[29] Aladdin J. Mohammad,[30] Bernhard Hellmich,[31] Maxime Samson,[32] Elena Bargagli,[33] Jan Willem Cohen Tervaert,[34] Camillo Ribi,[35] Davide Fiori,[1] Federica Bello,[1] Filippo Fagni,[1] Luca Moroni,[2] Giuseppe Alvise Ramirez,[2] Mouhamad Nasser,[3] Chiara Marvisi,[36] Paola Toniati,[37] Davide Firinu,[5] Roberto Padoan,[6] Allyson Egan,[38] Benjamin Seeliger,[39] Florenzo Iannone,[8] Carlo Salvarani,[36] David Jayne,[38] Domenico Prisco,[1] Augusto Vaglio,[40] and Giacomo Emmi,[1] on behalf of the European EGPA Study Group

Objective. Mepolizumab proved to be an efficacious treatment for eosinophilic granulomatosis with polyangiitis (EGPA) at a dose of 300 mg every 4 weeks in the randomized, controlled MIRRA trial. In a few recently reported studies, successful real-life experiences with the approved dose for treating severe eosinophilic asthma (100 mg every 4 weeks) were observed. We undertook this study to assess the effectiveness and safety of mepolizumab 100 mg every 4 weeks and 300 mg every 4 weeks in a large European EGPA cohort.

Methods. We included all patients with EGPA treated with mepolizumab at the recruiting centers in 2015–2020. Treatment response was evaluated from 3 months to 24 months after initiation of mepolizumab. Complete response to treatment was defined as no disease activity (Birmingham Vasculitis Activity Score [BVAS] = 0) and a prednisolone or prednisone dose (or equivalent) of ≤4 mg/day. Respiratory outcomes included asthma and ear, nose, and throat (ENT) exacerbations.

Results. Two hundred three patients, of whom 191 received a stable dose of mepolizumab (158 received 100 mg every 4 weeks and 33 received 300 mg every 4 weeks) were included. Twenty-five patients (12.3%) had a complete response to treatment at 3 months. Complete response rates increased to 30.4% and 35.7% at 12 months and 24 months, respectively, and rates were comparable between mepolizumab 100 mg every 4 weeks and 300 mg every 4 weeks. Mepolizumab led to a significant reduction in BVAS score, prednisone dose, and eosinophil counts from 3 months to 24 months, with no significant differences observed between 100 mg every 4 weeks and 300 mg every 4 weeks. Eighty-two patients (40.4%) experienced asthma exacerbations (57 of 158 [36%] who received 100 mg every 4 weeks; 17 of 33 [52%] who received 300 mg every 4 weeks), and 31 patients (15.3%) experienced ENT exacerbations. Forty-four patients (21.7%) experienced adverse events (AEs), most of which were nonserious AEs (38 of 44).

Conclusion. Mepolizumab at both 100 mg every 4 weeks and 300 mg every 4 weeks is effective for the treatment of EGPA. The 2 doses should be compared in the setting of a controlled trial.

Presented in part at the 2020 European Alliance of Associations for Rheumatology e-Congress, June 2020.

[1]Alessandra Bettiol, PhD, Maria Letizia Urban, MD, Paola Parronchi, PhD, Davide Fiori, MD, Federica Bello, MD, Filippo Fagni, MD, Domenico Prisco, MD, Giacomo Emmi, MD, PhD: University of Florence, Florence, Italy; [2]Lorenzo Dagna, MD, Luca Moroni, MD, Giuseppe Alvise Ramirez, MD: San Raffaele Hospital, IRCCS, Vita-Salute San Raffaele University, Milan, Italy; [3]Vincent Cottin, PhD, Mouhamad Nasser, MD: Hospices Civils de Lyon and University of Lyon, Lyon, France; [4]Franco Franceschini, MD: ASST Spedali Civili of Brescia and University of Brescia, Brescia, Italy; [5]Stefano Del Giacco, MD, Davide Firinu, MD: University of Cagliari, Cagliari, Italy; [6]Franco Schiavon, MD, Roberto Padoan, MD: Azienda Ospedaliera-Universitaria di Padova, Padova, Italy; [7]Thomas Neumann, MD: Cantonal Hospital St. Gallen, St. Gallen, Switzerland, and Jena University Hospital, Jena, Germany; [8]Giuseppe Lopalco, MD, Florenzo Iannone, MD: Polyclinic Hospital, University of Bari, Bari, Italy; [9]Pavel Novikov, MD: Tareev Clinic of Internal Diseases, Sechenov First Moscow State Medical

INTRODUCTION

Eosinophilic granulomatosis with polyangiitis (EGPA) is an antineutrophil cytoplasmic antibody (ANCA)–associated vasculitis characterized by asthma, ear, nose, and throat (ENT) involvement, blood and tissue eosinophilia, and systemic vasculitis manifestations (1,2). Treatment mainly relies on systemic glucocorticoids and inhaled therapies for respiratory symptoms (3). EGPA usually follows a chronic relapsing course; thus, patients are at risk of permanent tissue or organ damage, which can also be due to glucocorticoid-related toxicity. Therefore, immunosuppressive treatments are often required and are also used as glucocorticoid-sparing agents (3,4).

Among novel therapeutic options, mepolizumab is a monoclonal antibody targeting interleukin-5 (IL-5), a cytokine involved in eosinophil maturation, differentiation, and survival. Increased serum levels of IL-5 are observed in eosinophilic disorders, including EGPA (5), and a genome-wide association study identified the *IL5* region as one of the main EGPA-associated loci (6).

Mepolizumab is approved for the treatment of severe eosinophilic asthma at 100 mg every 4 weeks subcutaneously (7) and for the treatment of hypereosinophilic syndrome (HES) at 300 mg every 4 weeks (8). After encouraging results from previous studies (9,10), the phase III MIRRA trial proved the efficacy of mepolizumab 300 mg every 4 weeks subcutaneously for relapsing or refractory EGPA (11,12), leading to its approval by the US Food and Drug Administration (FDA), while in Europe it is currently used off-label.

Recent smaller studies showed the successful use of mepolizumab 100 mg every 4 weeks for the treatment of EGPA, especially for the control of respiratory manifestations (13–15). However, the benefits and side effects of mepolizumab 100 mg every 4 weeks versus 300 mg every 4 weeks for systemic and respiratory EGPA involvement have never been compared. Therefore, its optimal dose is still debated (16). This study aimed to investigate the effectiveness and safety of mepolizumab 100 mg versus 300 mg every 4 weeks in a large European cohort of patients with EGPA.

PATIENTS AND METHODS

Study design and setting. This multicenter, retrospective study was conducted on a cohort of patients with EGPA treated with mepolizumab between May 2015 and February 2020 at 38 EGPA referral centers in 8 European countries (Italy, France, Germany, the UK, Russia, Spain, Switzerland, and Sweden; see Appendix A for members of the European EGPA Study Group). The study received approval from the University of Florence Ethics Committee (reference no. 16821_OSS).

Study population and treatment. The cohort included adult patients who met the American College of Rheumatology classification criteria for EGPA (17) or the criteria proposed in the MIRRA trial (11), who received mepolizumab 100 mg every 4 weeks or 300 mg every 4 weeks, in accordance with local practice. Patients with a follow-up of <3 months after the first mepolizumab dose or those enrolled in clinical trials were excluded.

Data collection and outcome assessment. Demographic, clinical, laboratory, and treatment-related data were retrospectively collected from medical records at the time of mepolizumab initiation (time 0) and at 3 months, 6 months, 12 months, and 24 months of follow-up. The effectiveness of mepolizumab in controlling systemic disease activity was assessed using the Birmingham Vasculitis Activity Score (BVAS) (18). Complete response to treatment was defined as no disease activity (BVAS = 0) and a prednisolone or

University, Moscow, Russia; [10]Chiara Baldini, MD: University of Pisa, Pisa, Italy; [11]Carlo Lombardi, MD: Fondazione Poliambulanza Istituto Ospedaliero, Brescia, Italy; [12]Alvise Berti, MD: Santa Chiara Hospital and University of Trento, Trento, Italy; [13]Federico Alberici, PhD: University of Brescia and Spedali Civili Hospital, ASST Spedali Civili di Brescia, Brescia, Italy; [14]Marco Folci, MD: Humanitas Clinical and Research Center, IRCCS and Humanitas University, IRCCS, Milan, Italy; [15]Simone Negrini, MD: IRCCS Ospedale Policlinico San Martino and University of Genoa, Genoa, Italy; [16]Renato Alberto Sinico, MD: University of Milano Bicocca, Monza, Italy; [17]Luca Quartuccio, MD: University of Udine, Azienda sanitaria universitaria Friuli Centrale Udine, Udine, Italy; [18]Claudio Lunardi, MD: University of Verona, Italy; [19]Frank Moosig, MD: Rheumazentrum Schleswig-Holstein Mitte, Neumünster, Germany; [20]Georgina Espígol-Frigolé, MD: Hospital Clínic, University of Barcelona and Institut d'investigacions Biomèdiques August Pi I Sunyer (IDIBAPS), Barcelona, Spain; [21]Jan Schroeder, MD: ASST Grande Ospedale Metropolitano Niguarda, Milan, Italy; [22]Anna Luise Kernder, MD: Heinrich Heine University Düsseldorf, Düsseldorf, Germany; [23]Sara Monti, PhD: Policlinico S. Matteo Fondazione, IRCCS, University of Pavia, Pavia, Italy; [24]Ettore Silvagni, MD: University of Ferrara, Ferrara, Italy; [25]Claudia Crimi, PhD: Policlinico-Vittorio Emanuele San Marco University Hospital, Catania, Italy; [26]Francesco Cinetto, MD: University of Padova, Padova, Italy; [27]Paolo Fraticelli, MD: University Hospital Ospedali Riuniti, Ancona, Italy; [28]Dario Roccatello, MD: San Giovanni Bosco Hospital and University of Turin, Turin, Italy; [29]Angelo Vacca, MD: Aldo Moro University of Bari, Bari, Italy; [30]Aladdin J. Mohammad, MD: Lund University, Skåne University Hospital, Lund, Sweden, and University of Cambridge, Cambridge, UK; [31]Bernhard Hellmich, MD: Medius Kliniken, University of Tübingen, Kirchheim unter Teck, Germany; [32]Maxime Samson, PhD: Dijon University Hospital, Dijon, France; [33]Elena Bargagli, MD: University of Siena, Siena, Italy; [34]Jan Willem Cohen Tervaert, PhD: University of Alberta, Edmonton, Alberta, Canada, and Maastricht University, Maastricht, The Netherlands; [35]Camillo Ribi, MD: University Hospital Center of Lausanne, Lausanne, Switzerland; [36]Chiara Marvisi, MD, Carlo Salvarani, MD: Azienda USL-IRCCS di Reggio Emilia, IRCCS, and Università di Modena e Reggio Emilia, Reggio Emilia, Italy; [37]Paola Toniati, MD: ASST Spedali Civili of Brescia, Brescia, Italy; [38]Allyson Egan, MD, David Jayne, MD: University of Cambridge, Cambridge, UK; [39]Benjamin Seeliger, MD: Hannover Medical School, Hannover, Germany; [40]Augusto Vaglio, PhD: University of Florence and Meyer Children's Hospital, Florence, Italy.

Drs. Prisco, Vaglio, and Emmi contributed equally to this work.

Author disclosures are available at https://onlinelibrary.wiley.com/action/downloadSupplement?doi=10.1002%2Fart.41943&file=art41943-sup-0001-Disclosureform.pdf.

Address correspondence to Giacomo Emmi, MD, PhD, Department of Experimental and Clinical Medicine, University of Florence, Florence, Italy. Email: giacomo.emmi@unifi.it.

Submitted for publication May 4, 2021; accepted in revised form July 29, 2021.

prednisone dose (or equivalent) of ≤4.0 mg/day, as defined by the MIRRA trial (11). Partial response to treatment was defined as no disease activity and a prednisolone or prednisone dose of >4.0 mg/day.

Relapse was assessed only in patients in whom complete response to treatment had been achieved and was defined, as in the MIRRA trial, by at least 1 of the following criteria: 1) active vasculitis (defined as BVAS >0) and/or 2) worsening asthma and/or ENT manifestations leading to an increase in prednisolone or prednisone dose to >4.0 mg/day, initiation of a new immunosuppressive therapy, or hospitalization (11).

With regard to respiratory outcomes, we assessed asthma exacerbations, defined as any of the following events: asthma attack needing an increase in oral prednisone dose, asthma-related emergency department admission, and/or use of acute oral glucocorticoids, antibiotics, or short-acting beta agonists. In addition, the effect of mepolizumab on lung function was monitored by the variation in pre-bronchodilator forced expiratory volume in 1 second (FEV_1). ENT relapse was defined as the reappearance of ENT symptoms, following symptoms having been under complete control at the previous time point.

Additional outcomes assessed included changes in organ manifestations (assessed separately from BVAS items), glucocorticoid-sparing and disease-modifying antirheumatic drug (DMARD)–sparing effect, variation in the proportion of ANCA-positive patients, and reduction in eosinophil count.

During follow-up, variations in monthly mepolizumab dose or treatment discontinuation were recorded. All adverse events (AEs) occurring during treatment were also recorded, and their seriousness was assessed in accordance with the World Health Organization criteria (19). All study outcome measures were analyzed in the entire cohort and compared between patients receiving stable treatment with mepolizumab 100 mg every 4 weeks and those treated with 300 mg every 4 weeks. Stable treatment was defined as no change in the monthly mepolizumab dose during the entire follow-up period.

Statistical analysis. Data are presented as the median and interquartile range (IQR) for continuous variables, and as the absolute number and percentage for qualitative variables. Continuous end points at 3–24 months were compared with time 0 (baseline) using the Wilcoxon signed rank test, whereas qualitative variables were compared using McNemar's test. Nonparametric tests were used since the distribution of the data was not normal. Complete response and partial response rates and AE rates were compared between patients receiving stable treatment with mepolizumab 100 mg every 4 weeks and those receiving 300 mg every 4 weeks using Fisher's exact test. Cox proportional hazards regression models were fitted to derive Kaplan–Meier curves and to estimate hazard ratios (HRs) and 95% confidence intervals (95% CIs) for the occurrence of asthma and ENT exacerbations over time.

If a patient was still receiving mepolizumab treatment at a given follow-up time point but had missing data regarding EGPA manifestations, BVAS score, and/or daily glucocorticoid dose, the data were imputed using the last observation carried forward method, as these parameters were necessary to assess the primary outcome measure of this study. For all other clinical and laboratory parameters, the analyses were conducted only on subjects with available data at the given time point.

Statistical analyses were performed using Stata, version 14. *P* values less than 0.05 were considered significant.

Data availability. Deidentified individual participant data will be made available upon reasonable request to the corresponding author.

RESULTS

We included 203 patients, of whom 57.1% were women (Table 1). The median age at the time of mepolizumab initiation was 55.1 years (IQR 46.7–62.5), and the median disease duration was 4.8 years (IQR 4.9–9.2). At the time of EGPA diagnosis, 70 patients (34.5%) were positive for ANCAs, most of whom had either perinuclear ANCAs or myeloperoxidase ANCAs (84.3%). Before mepolizumab treatment was initiated, 150 of 203 patients (73.9%) had received traditional DMARDs, 51 (25.1%) received biologic DMARDs, and 18 (9.0%) received intravenous immunoglobulin. Disease remission, according to clinical judgment, was achieved in 120 patients after induction therapy. At the time of mepolizumab initiation (baseline), 92.1% of the patients had active disease, with a median BVAS score of 4 (IQR 2–8). The most common manifestations were pulmonary (89.7%), ENT (71.4%), constitutional (27.6%), and peripheral neurologic (22.7%). Ten patients had cardiac involvement at baseline, including 1 case of pericarditis, 1 case of myocarditis, and 8 cases of cardiomyopathy with cardiac failure. Of 190 patients with available ANCA test results, 38 (20.0%) were ANCA positive at the time mepolizumab was initiated, most of whom had perinuclear ANCAs or myeloperoxidase-ANCAs (89.5%). At baseline, almost all patients (95.6%) had received stable glucocorticoid treatment in the previous 3 months, at a median prednisone dose of 10 mg/day (IQR 5–20). Additional therapies included conventional DMARDs, mostly methotrexate (18.7%), azathioprine (11.3%), rituximab (11.3%), or intravenous immunoglobulin (5.9%). One hundred ninety-two patients (95%) were receiving inhaled therapy for asthma.

One hundred sixty-eight patients initially received mepolizumab at 100 mg every 4 weeks, and 35 at 300 mg every 4 weeks. During follow-up, 10 patients switched from 100 mg to 300 mg every 4 weeks due to inefficacy. Another 2 patients switched from 300 mg to 100 mg every 4 weeks due to personal reasons (Supplementary Figure 1, available on the *Arthritis & Rheumatology* website at http://onlinelibrary.wiley.com/doi/10.1002/art.

Table 1. Characteristics of the patients with EGPA at the time of mepolizumab initiation*

	Overall (n = 203)	Mepolizumab 100 mg/4 weeks (n = 158)	Mepolizumab 300 mg/4 weeks (n = 33)	*P*
Female	116 (57.1)	88 (55.7)	22 (66.7)	0.333
Smoking status				
Former	44 (21.7)	36 (22.8)	5 (15.2)	0.640
Current	3 (1.5)	3 (1.9)	0	
Age at diagnosis, median (IQR) years	49.1 (37.7–57.1)	48.7 (37.9–57.5)	49.2 (39.8–53.4)	0.380
Age at mepolizumab initiation, median (IQR) years	55.1 (46.7–62.5)	55.1 (46.7–62.8)	53.0 (47.3–59.3)	0.426
Disease duration at mepolizumab initiation, median (IQR) years	4.8 (4.9–9.2)	4.9 (1.6–8.9)	3.9 (1.1–14.1)	0.921
Active organ involvement at mepolizumab initiation				
Constitutional	56 (27.6)	50 (31.7)	3 (9.1)	0.009
Purpura	15 (7.4)	11 (7.0)	2 (6.1)	1.000
ENT	145 (71.4)	121 (76.6)	17 (51.5)	0.005
Pulmonary	182 (89.7)	141 (89.2)	29 (87.9)	0.765
Cardiac	10 (4.9)	8 (5.1)	1 (3.0)	1.000
Gastrointestinal	9 (4.4)	8 (5.1)	1 (3.0)	1.000
Renal	5 (2.5)	5 (3.2)	0	NA
Peripheral neurologic	46 (22.7)	36 (22.8)	6 (18.2)	0.650
Active disease at mepolizumab initiation (BVAS >0)	187 (92.1)	144 (91.1)	31 (93.9)	0.792
BVAS score at mepolizumab initiation, median (IQR)	4 (2–8)	4 (2–8)	4 (2–7)	0.163
Laboratory parameters at mepolizumab initiation†				
ANCA positive	38 (20.0)	28 (18.9)	9 (27.3)	0.339
Perinuclear ANCA	34 (17.9)	26 (17.6)	8 (24.2)	
Cytoplasmic ANCA	4 (2.1)	2 (1.4)	1 (3.0)	
MPO ANCA	34 (17.9)	27 (18.2)	8 (24.2)	
PR3 ANCA	4 (2.1)	2 (1.4)	1 (3.0)	
Eosinophil count, median (IQR)‡	610 (200–1,040)	700 (200–1,080)	440 (200–910)	0.328
Pharmacologic therapies administered before mepolizumab initiation				
Oral glucocorticoids	201 (99.0)	156 (98.7)	33 (100.0)	NA
Azathioprine	91 (44.8)	69 (43.7)	17 (51.5)	0.446
Methotrexate	78 (38.4)	56 (35.4)	18 (54.6)	0.050
Cyclophosphamide	57 (28.1)	44 (27.9)	11 (33.3)	0.531
Mycophenolate	39 (19.2)	29 (18.4)	6 (18.2)	1.000
Cyclosporine	21 (10.3)	18 (11.4)	1 (3.0)	0.206
Rituximab	39 (19.2)	36 (22.8)	3 (9.1)	0.097
IV immunoglobulin	18 (8.9)	17 (10.8)	1 (3.0)	0.321
Omalizumab	17 (8.4)	13 (8.2)	2 (6.1)	1.000
Other immunosuppressants	16 (7.9)	13 (8.2)	1 (3.0)	0.471
Pharmacologic therapies at mepolizumab initiation				
Prednisone equivalent daily dose in the previous 3 months, median (IQR)§	10 (5–20)	10 (IQR 5-20)	10 (IQR 5-22.5)	0.854
Oral glucocorticoids	194 (95.6)	149 (94.3)	33 (100.0)	NA
Prednisone equivalent daily dose, median (IQR)	10 (5–20)	10 (5–20)	10 (5–25)	0.511
Methotrexate	38 (18.7)	29 (18.4)	9 (27.3)	0.240
Azathioprine	23 (11.3)	19 (12.0)	3 (9.1)	0.772
Mycophenolate	18 (8.9)	12 (7.6)	4 (12.1)	0.486
Cyclosporine	2 (1.0)	1 (0.6)	0	NA
Rituximab	23 (11.3)	20 (12.7)	3 (9.1)	0.771
IV immunoglobulin	12 (5.9)	11 (7.0)	1 (3.0)	0.695
Other immunosuppressants	5 (2.5)	3 (1.9)	1 (3.0)	0.535
Inhaled therapy for asthma	192 (95.0)	150 (94.9)	30 (90.9)	0.407

* Except where indicated otherwise, values are the number (%). EGPA = eosinophilic granulomatosis with polyangiitis; IQR = interquartile range; ENT = ear, nose, and throat; NA = not applicable; BVAS = Birmingham Vasculitis Activity Score; ANCA = antineutrophil cytoplasmic antibody; MPO = myeloperoxidase; PR3 = proteinase 3; IV = intravenous.
† Data were available for 190 patients overall, 148 patients receiving mepolizumab 100 mg/4 weeks, and 33 patients receiving mepolizumab 300 mg/4 weeks.
‡ Data were available for 194 patients overall, 152 patients receiving mepolizumab 100 mg/4 weeks, and 32 patients receiving mepolizumab 300 mg/4 weeks.
§ Data were available for 195 patients overall, 151 patients receiving mepolizumab 100 mg/4 weeks, and 32 patients receiving mepolizumab 300 mg/4 weeks.

41943). Conversely, in 158 patients (77.8%) and 33 patients (16.3%), stable treatment with mepolizumab of 100 mg every 4 weeks and 300 mg every 4 weeks, respectively, was maintained over the entire follow-up period.

Baseline demographic and clinical characteristics were comparable between these 2 groups, with the exception of constitutional and ENT manifestations, which were more frequent among patients receiving mepolizumab 100 mg every 4 weeks than those receiving 300 mg every 4 weeks (31.7% versus 9.1% [$P = 0.009$] and 76.6% versus 51.5% [$P = 0.005$], respectively) (Table 1).

Effectiveness of mepolizumab on systemic disease activity. At 3 months, complete response to treatment had already been achieved in 25 of 203 patients (12.3%), whereas partial response to treatment had been achieved in 64 patients (31.5%) (Supplementary Table 1, available on the *Arthritis & Rheumatology* website at http://onlinelibrary.wiley.com/doi/10.1002/art.41943). Complete response rates increased to 23.6% at 6 months, 30.4% at 12 months, and 35.7% at 24 months. Response rates were similar between patients receiving mepolizumab 100 mg every 4 weeks and those receiving 300 mg every 4 weeks (Figure 1). In particular, complete response to treatment had been achieved in 12.0% and 18.2% of patients receiving 100 mg every 4 weeks and 300 mg every 4 weeks, respectively, at 3 months, whereas partial response to treatment had been achieved in 32.9% and 36.4% of patients receiving 100 mg every 4 weeks and 300 mg every 4 weeks, respectively, at 3 months ($P = 0.474$). Complete response rates further increased during follow-up for both treatment groups ($P = 0.204$ and $P = 0.809$ for mepolizumab 100 mg versus 300 mg every 4 weeks at 6 months and 12 months, respectively). At 24 months, only 39 patients receiving mepolizumab 100 mg every 4 weeks and 12 patients receiving 300 mg every 4 weeks had available follow-up data. A greater proportion of patients receiving mepolizumab 300 mg every 4 weeks had complete response to treatment (58.3% versus 33.3%) or partial response to treatment

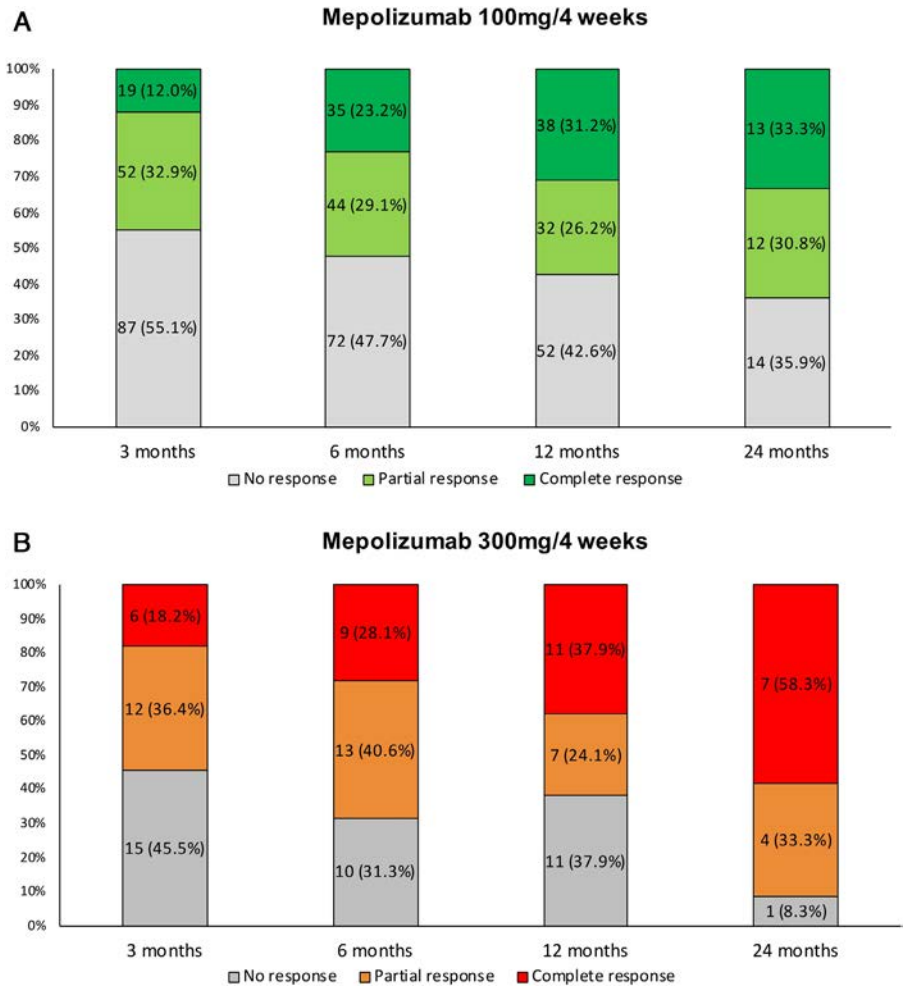

Figure 1. Complete and partial response rates in patients with eosinophilic granulomatosis with polyangiitis who received stable treatment with mepolizumab 100 mg every 4 weeks (**A**) and 300 mg every 4 weeks (**B**). Complete response was defined as no disease activity (Birmingham Vasculitis Activity Score [BVAS] = 0) and daily prednisone dose ≤4 mg/day. Partial response was defined as no disease activity (BVAS = 0) and daily prednisone dose >4 mg/day. No response was defined as active disease (BVAS >0).

Table 2. Organ involvement among the patients with EGPA receiving stable treatment with mepolizumab 100 mg or 300 mg every 4 weeks*

	Mepolizumab initiation (baseline) (n = 158/33)	3 months (n = 158/33)	*P*, 3 months vs. baseline	6 months (n = 151/32)	*P*, 6 months vs. baseline	12 months (n = 122/29)	*P*, 12 months vs. baseline	24 months (n = 39/12)	*P*, 24 months vs. baseline
Constitutional symptoms									
100 mg/4 weeks	50 (31.7)	25 (15.8)	<0.001	23 (15.2)	<0.001	15 (12.3)	<0.001	6 (15.4)	0.035
300 mg/4 weeks	3 (9.1)	0	NA	2 (6.3)	0.564	2 (6.9)	1.564	0	NA
Purpura									
100 mg/4 weeks	11 (7.0)	6 (3.8)	0.025	4 (2.7)	0.014	3 (2.5)	0.008	0	NA
300 mg/4 weeks	2 (6.1)	1 (3.0)	0.317	1 (3.1)	0.317	2 (6.9)	1.000	0	NA
ENT									
100 mg/4 weeks	121 (76.6)	64 (40.5)	<0.001	55 (36.4)	<0.001	34 (27.9)	<0.001	8 (20.5)	<0.001
300 mg/4 weeks	17 (51.5)	12 (36.4)	0.025	7 (21.9)	0.003	8 (27.6)	0.034	0	NA
Pulmonary									
100 mg/4 weeks	141 (89.2)	61 (38.6)	<0.001	46 (30.5)	<0.001	37 (30.3)	<0.001	7 (18.0)	<0.001
300 mg/4 weeks	29 (87.9)	10 (30.3)	<0.001	5 (15.6)	<0.001	9 (31.0)	<0.001	1 (8.3)	0.005
Cardiac									
100 mg/4 weeks	8 (5.1)	4 (2.5)	0.046	4 (2.7)	0.046	3 (2.5)	0.046	1 (2.6)	0.317
300 mg/4 weeks	1 (3.0)	0	NA	0	NA	0	NA	0	NA
Gastrointestinal									
100 mg/4 weeks	8 (5.1)	0	0.005	5 (3.3)	0.257	4 (3.3)	0.257	0	0.083
300 mg/4 weeks	1 (3.0)	1 (3.0)	NA	0	NA	0	NA	0	NA
Renal									
100 mg/4 weeks	5 (3.2)	1 (0.6)	0.046	0	NA	1 (0.8)	0.180	0	0.317
300 mg/4 weeks	0	2 (6.1)	0.157	0	NA	1 (3.5)	0.317	0	NA
Peripheral neurologic									
100 mg/4 weeks	36 (22.8)	23 (14.6)	0.005	21 (13.9)	0.001	15 (12.3)	0.001	2 (5.1)	0.005
300 mg/4 weeks	6 (18.2)	6 (18.2)	NA	3 (9.4)	0.157	2 (6.9)	0.157	0	NA

* Except where indicated otherwise, values are the number (%); n values are the number of patients receiving mepolizumab 100 mg every 4 weeks/number of patients receiving mepolizumab 300 mg every 4 weeks. EGPA = eosinophilic granulomatosis with polyangiitis; NA = not applicable; ENT = ears, nose, and throat.

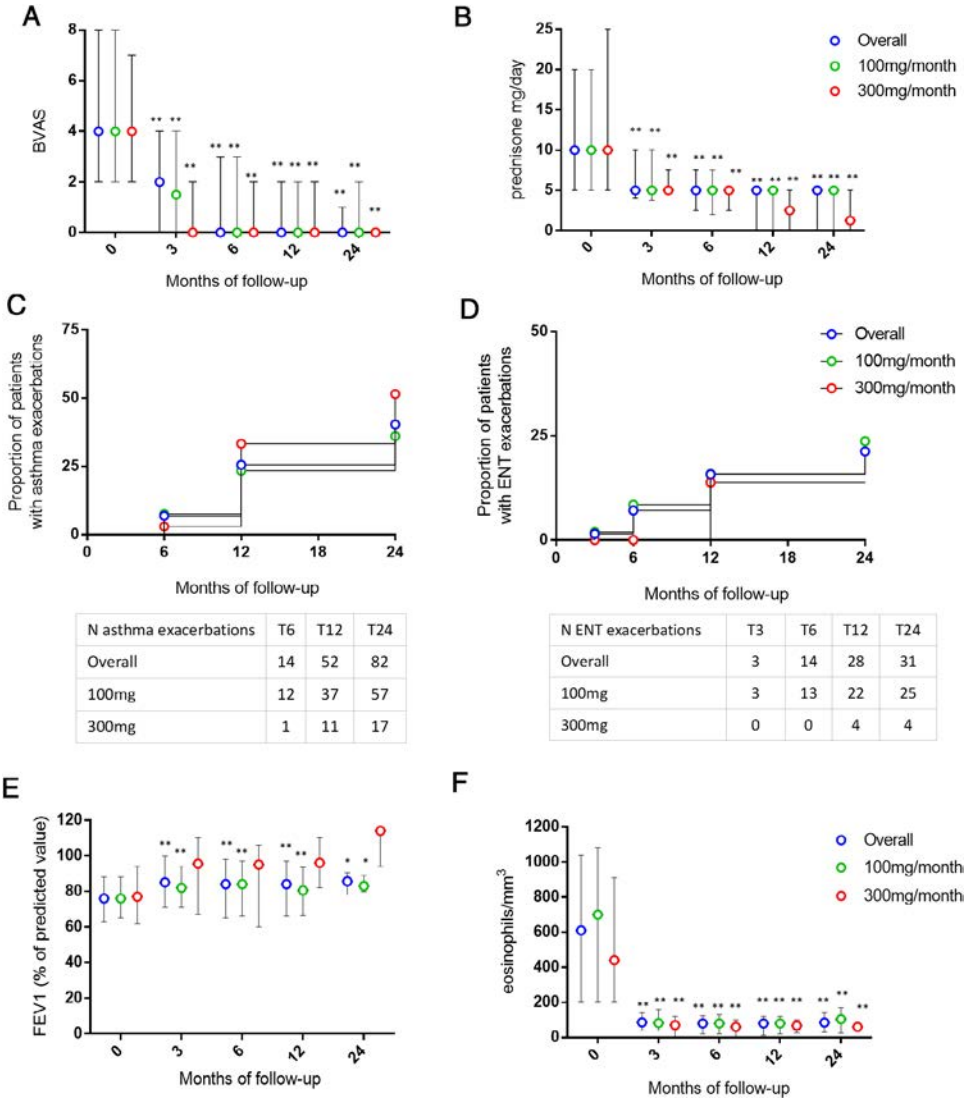

Figure 2. **A** and **B,** Variation in disease activity using the Birmingham Vasculitis Activity Score (BVAS) (**A**) and daily dose of prednisone equivalents (**B**) among patients with eosinophilic granulomatosis with polyangiitis receiving mepolizumab 100 mg every 4 weeks and those receiving mepolizumab 300 mg every 4 weeks. **C** and **D,** Respiratory outcomes in patients during mepolizumab treatment. Kaplan–Meier curves show the occurrence of asthma exacerbations (**C**) and ear, nose, and throat (ENT) exacerbations (**D**). **E** and **F**, Variation in the forced expiratory volume in 1 second (FEV_1) (**E**) and eosinophil count (**F**). Values in **A**, **B**, **E**, and **F** are the median and interquartile range.* = $P < 0.05$; ** = $P < 0.01$, versus baseline.

(33.3% versus 30.8%), but these differences were not statistically significant ($P = 0.168$). Notably, the small number of patients at the different follow-up time points, particularly those receiving mepolizumab 300 mg every 4 weeks, did not allow sufficient power to detect significant differences in the proportion of complete responses between the 2 doses at the different time points (Supplementary Table 2, available on the *Arthritis & Rheumatology* website at http://onlinelibrary.wiley.com/doi/10.1002/art.41943).

Of 71 patients in whom complete response to treatment had been achieved, 22 (31.0%) experienced a relapse after a median time of 6 months (IQR 6–9). At all time points, relapse rates were comparable between both treatment groups ($P = 1.000$ at 6 months and 12 months; $P = 0.642$ at 24 months), the overall relapse rates being 32.1% (17 of 53) and 25.0% (4 of 16) for mepolizumab 100 versus 300 mg every 4 weeks, respectively. The median time to relapse was 6 months (IQR 3–9) and 10 months (IQR 9–12) in the mepolizumab 100 mg every 4 weeks group compared to the 300 mg every 4 weeks group, respectively ($P = 0.081$). Response rates were higher among ANCA-negative patients, especially at 24 months, but the differences were not statistically significant (Supplementary Table 3, available on the *Arthritis & Rheumatology* website at http://onlinelibrary.wiley.com/doi/10.1002/art.41943).

The efficacy outcomes in the 10 patients who switched from mepolizumab 100 mg every 4 weeks to 300 mg every 4 weeks are summarized in Supplementary Figure 2 (http://onlinelibrary.wiley.com/doi/10.1002/art.41943). Follow-up data suggested

Table 3. AEs in the patients with EGPA during mepolizumab treatment*

	0–3 months	4–6 months	7–12 months	13–24 months
At least 1 AE experienced, no. of patients/total no. of patients (%)	21/203 (10.3)	20/195 (10.3)	16/161 (9.9)	9/56 (16.1)
Receiving stable treatment with mepolizumab 100 mg/4 weeks	10/158 (6.3)	13/151 (8.6)	6/122 (4.9)	3/39 (7.7)
Receiving stable treatment with mepolizumab 300 mg/4 weeks	9/33 (27.3)	5/32 (15.6)	10/29 (34.5)	6/12 (50.5)
P	<0.001	0.322	<0.001	0.003
No. of patients with AEs requiring hospitalization	0	2	2	2
Receiving stable treatment with mepolizumab 100 mg/4 weeks	0	1	2	1
Receiving stable treatment with mepolizumab 300 mg/4 weeks	0	1	0	1
AEs requiring treatment discontinuation	2	3	1	0
Receiving stable treatment with mepolizumab 100 mg/4 weeks	2	3	1	0
Receiving stable treatment with mepolizumab 300 mg/4 weeks	0	0	0	0
Type of AE and no. of cases				
Infections and infestations				
Lower respiratory tract infections	4	3†	7†	2
Upper respiratory tract infections	2	–	–	1
Other infections	–	2†	1	1
Musculoskeletal and connective tissue disorders				
Myalgia/arthralgia	3	1	1	–
Osteoporosis/fractures	1	1	1	1
Epicondylitis	–	1	–	–
Nervous system disorders				
Dizziness	1	–	1	–
Headache	2	1	–	–
Transient color vision disorder	–	1	–	–
Skin and subcutaneous tissue disorders				
Eczema/urticaria	2	1	–	–
Papillary edema	–	–	1	–
General disorders and administration site conditions				
Malaise	2	–	–	–
Swelling at injection site	1	–	–	–
Endocrine disorders				
Secondary adrenal insufficiency	–	–	–	1†
Blood and lymphatic system disorders				
Sialoadenitis	–	1	–	–
Cardiac disorders				
Myocarditis	–	–	–	1†
Hepatobiliary disorders				
Acute hepatitis	–	–	1	–
Renal and urinary disorders				
Renal colic	–	1	–	–
Respiratory, thoracic, and mediastinal disorders				
Lung consolidation	–	–	1	–
Vascular disorders				
TIA	–	–	1†	–

* AEs = adverse events; EGPA = eosinophilic granulomatosis with polyangiitis; TIA = transient ischemic attack.
† Hospitalization required in 1 patient.

no clear benefit in terms of EGPA control following the increase in monthly mepolizumab dose.

The impact of mepolizumab on the different disease manifestations is summarized in Table 2 and in Supplementary Table 4 (available on the *Arthritis & Rheumatology* website at http://onlinelibrary.wiley.com/doi/10.1002/art.41943). A significant reduction in all active manifestations was already observed at 3 months in patients receiving stable mepolizumab 100 mg every 4 weeks. Control of constitutional, pulmonary, ENT, and peripheral neurologic manifestations was maintained during follow-up. With mepolizumab 300 mg every 4 weeks, a significant reduction in the proportion of patients with pulmonary and ENT manifestations was observed at all time points, whereas no clear effect was observed on nonrespiratory manifestations.

Systemic disease activity also decreased during follow-up for both treatment groups, with the median BVAS score of the entire

cohort decreasing from 4 (IQR 2–8) at baseline to 2 (IQR 0–4) at 3 months ($P < 0.001$). The median BVAS score decreased further to 0 at the subsequent time points ($P < 0.001$ for both treatment groups at 6 months, 12 months, and 24 months) (Figure 2A). Similarly, both mepolizumab doses were associated with a significant reduction in the daily glucocorticoid dose (Figure 2B), with a significant proportion of patients able to discontinue glucocorticoid use (29.2% and 41.7% at 24 months in the 100 mg mepolizumab group and the 300 mg mepolizumab group, respectively) (Supplementary Table 5, available on the *Arthritis & Rheumatology* website at http://onlinelibrary.wiley.com/doi/10.1002/art.41943). Concomitantly, a DMARD-sparing effect was observed in both treatment groups, though statistical significance was only achieved for mepolizumab 100 mg every 4 weeks (Supplementary Table 5).

Effectiveness of mepolizumab on respiratory outcomes. Respiratory outcomes are reported in Figures 2C–F and in Supplementary Table 6 (http://onlinelibrary.wiley.com/doi/10.1002/art.41943). Overall, 82 patients (40.4%) experienced asthma exacerbations after a median time of 12 months (IQR 12–24). Asthma exacerbations occurred in 36.1% of patients receiving stable mepolizumab 100 mg every 4 weeks and in 51.5% receiving mepolizumab 300 mg every 4 weeks ($P = 0.139$) (Figure 2C). ENT relapses occurred after a median time of 12 months (IQR 6–12) in 25 patients receiving mepolizumab 100 mg every 4 weeks (15.8%), 4 receiving 300 mg every 4 weeks (12.2%), and 2 who switched mepolizumab dose (unadjusted HR 0.67 [95% CI 0.23–1.91] for mepolizumab 300 mg every 4 weeks versus 100 mg every 4 weeks, $P = 0.450$) (Figure 2D).

With regard to lung function, a significant improvement in FEV_1 was already observed 3 months after the initiation of mepolizumab 100 mg every 4 weeks (Figure 2E). FEV_1 also improved in patients receiving mepolizumab 300 mg every 4 weeks, though statistical significance was not reached.

Additional outcomes. Both mepolizumab regimens were already associated with a dramatic reduction in eosinophil count at 3 months. This was maintained during the entire follow-up period (Figure 2F). Although ANCA testing was available for only a small subgroup of patients during follow-up, a significant reduction in the proportion of ANCA-positive patients was observed among those receiving stable mepolizumab 100 mg every 4 weeks and those receiving 300 mg every 4 weeks (Supplementary Figure 3, available on the *Arthritis & Rheumatology* website at http://onlinelibrary.wiley.com/doi/10.1002/art.41943).

Treatment persistence and safety. Twenty-three patients discontinued mepolizumab. Sixteen of these patients were receiving mepolizumab 100 mg every 4 weeks; reasons for discontinuation were AEs in 6 cases (malaise in 2 patients, arthralgia in 1, reactivation of herpes zoster in 1, and not reported in 2) and inefficacy in 3 cases. In the remaining 7 patients, the reason for treatment discontinuation was unknown. Seven patients discontinued mepolizumab 300 mg every 4 weeks due to inefficacy (4 patients) and unknown reasons (3 patients).

Forty-four patients (21.7%) experienced AEs, mostly related to lower respiratory tract infections or to myalgias or arthralgias. At all time points, AEs were more frequent among patients receiving mepolizumab 300 mg every 4 weeks (Table 3). Overall, 6 AEs required hospitalization, of which 4 occurred in patients receiving mepolizumab 100 mg every 4 weeks (lower respiratory tract infection, secondary adrenal insufficiency, transient ischemic attack, and infection of the central venous catheter). The other 2 AEs occurred in patients receiving mepolizumab 300 mg every 4 weeks (lower respiratory tract infection and myocarditis).

DISCUSSION

In this study, conducted on the largest series of mepolizumab-treated patients with EGPA reported so far to our knowledge, we observed that mepolizumab at either 100 mg every 4 weeks or 300 mg every 4 weeks is effective and safe in controlling systemic and respiratory disease manifestations. The use of mepolizumab in EGPA has solid evidence. Indeed, the randomized controlled MIRRA trial proved the superiority of mepolizumab 300 mg every 4 weeks compared to placebo for relapsing and/or refractory EGPA (11,12), leading to the FDA approval of mepolizumab 300 mg every 4 weeks.

Despite this, our data show that, in real practice, most patients with EGPA received mepolizumab 100 mg every 4 weeks, the dose approved for severe eosinophilic asthma, rather than 300 mg every 4 weeks. This prescription was probably based on the rationale that mepolizumab 100 mg every 4 weeks effectively controls severe eosinophilic asthma, which is an invariable feature of EGPA, and was also driven by regulatory reasons, since mepolizumab 300 mg every 4 weeks is not currently approved in Europe.

In the MIRRA trial, the dose choice was based on the phase IIb/III dose range–finding study of mepolizumab in severe eosinophilic asthma (7), and in a trial of HES (20,21). This choice was also supported by the concept that EGPA, similarly to HES, is a more aggressive condition compared to eosinophilic asthma (14). After the FDA approval of mepolizumab 300 mg every 4 weeks for EGPA, a growing body of literature from real clinical practice suggested that mepolizumab 100 mg every 4 weeks might also be used for EGPA (13–15,22). Notably, in all patients included in these studies, disease was in remission (13,15) or disease activity was low (14) at treatment initiation, with mepolizumab being initiated mainly for the control of asthma.

Our results indicate that mepolizumab at both 100 mg every 4 weeks and 300 mg every 4 weeks was associated with effective control of respiratory EGPA manifestations and an improvement in systemic disease activity. Both also allowed glucocorticoid-sparing.

Also, the proportion of ANCA-positive patients significantly decreased unexpectedly; nevertheless, given the small number of patients with ANCA (re)testing, this finding should be interpreted with caution. Though the exact mechanisms of ANCA positivity-to-negativity switch are unknown, this may be accounted for by anti–IL-5–mediated eosinophil depletion. Eosinophils have been shown to promote B cell survival, T-independent and T-dependent B cell activation and proliferation, and immunoglobulin secretion (23). B cells and their progeny produce and release ANCAs; thus, eosinophil depletion following mepolizumab treatment may account for the reduction in antigen presentation and plasma cell survival, with a consequent reduction in ANCA titers.

The proportion of complete responses steadily increased throughout follow-up, reaching 31.2% and 37.9% at 12 months and 33.3% and 58.3% at 24 months for mepolizumab 100 mg every 4 weeks and 300 mg every 4 weeks, respectively, with only a small proportion of patients experiencing disease relapse. However, response rates at 24 months must be interpreted with caution, as only 39 patients receiving mepolizumab 100 mg every 4 weeks and 12 patients receiving 300 mg every 4 weeks had available follow-up data. Notably, complete response rates observed with both doses were similar to that reported in the MIRRA trial for mepolizumab 300 mg every 4 weeks, where complete response to treatment was achieved in 32% of patients at both weeks 36 and 48 (11). The response rates in our study were lower than those in the observational study by Canzian et al (14) in a small EGPA cohort (76% and 82% complete responses at 12 months for mepolizumab 100 mg every 4 weeks and 300 mg every 4 weeks, respectively, as defined by BVAS = 0 and a prednisone dose ≤5 mg/day) (14).

In our study, complete response rates appeared to be higher among ANCA-negative patients, though the subgroups were too small to draw conclusions. We speculate that these findings reflect the different nature of ANCA-positive EGPA and ANCA-negative EGPA, the latter being traditionally associated with a more prominent eosinophilic phenotype (24–26).

Control of systemic disease activity was paralleled by the improvement in asthma and lung function with both mepolizumab regimens. Interestingly, the lower mepolizumab dose was not associated with an increased risk of asthma re-exacerbation during follow-up. Additionally, both mepolizumab doses were associated with good control of ENT manifestations, according to recent data (27). Moreover, we also observed a remarkable reduction in peripheral neuropathy during treatment with mepolizumab. In EGPA, neuropathy seems to have not only a vasculitic etiology but also a neurotoxic etiology, mainly due to eosinophil products (28,29). Thus, eosinophil depletion via mepolizumab could effectively counteract this pathogenetic mechanism. To date, the possible role of mepolizumab in the control of EGPA neurologic manifestations was reported only in a retrospective study of 6 patients (30). Our results, however, must be taken with caution, as other factors may contribute to the improvement of neuropathy, including progressive nerve function recovery or delayed effects of previous and concomitant therapies.

In our study, mepolizumab was generally well-tolerated. Approximately one-fifth of patients experienced AEs, and the 100 mg every 4 weeks dose appeared to be associated with a lower rate of AEs. Most AEs were related to infections or to myalgias/arthralgias, as observed in the MIRRA trial (11). Only a few AEs required treatment discontinuation or hospitalization. However, as is the case in all retrospective studies, underreporting of AEs cannot be excluded.

Our study has other limitations, mostly related to its retrospective nature. First, as data were retrospectively captured from medical records, some data were missing, and the assessment of clinical parameters was not systematic. Second, heterogeneity in clinical management among centers cannot be excluded. Third, consistent with the MIRRA trial, the BVAS calculation was used to retrospectively assess disease activity and treatment outcomes, as no standard assessment tool is validated specifically for EGPA. Nevertheless, it cannot be excluded that items related to chronic or persistent damage were erroneously counted in the BVAS score. Fourth, the disparity in sample size between the 100 mg every 4 weeks group and 300 mg every 4 weeks group did not allow us to draw definite conclusions. Finally, given the small sample size, the effect of mepolizumab dose escalation in patients with inappropriate response to 100 mg every 4 weeks could not be ascertained. Despite these limitations, this study also had several strengths, including a long follow-up period, large sample size representative of the European clinical setting, and availability of detailed longitudinal clinical data.

In conclusion, this large European real-world study shows that mepolizumab is associated with effective control of respiratory EGPA manifestations, with a good safety profile. Our results further suggest a role of mepolizumab in the treatment of systemic manifestations, though the retrospective assessment of systemic disease activity requires cautious interpretation of these findings.

Our data also suggest that mepolizumab 100 mg every 4 weeks could be an acceptable dose for patients with EGPA and a valid alternative to the dose approved for this therapeutic indication (300 mg every 4 weeks). Nevertheless, caution is needed, as some reports suggest a risk of systemic disease flare in patients receiving anti–IL-5 treatments at the dose for asthma control (31,32). Randomized clinical trials are advocated to compare the efficacy and safety of these 2 EGPA treatment regimens and assess whether dose escalation from 100 mg to 300 mg every 4 weeks can be effective in case of unsatisfactory clinical responses, as well as to compare the efficacy of mepolizumab as an alternative to or sequential treatment with other biologic therapies for EGPA.

ACKNOWLEDGMENT

The authors would like to dedicate this manuscript to the memory of Professor Claus Kroegel. Open Access Funding provided by Universita degli Studi di Firenze within the CRUI-CARE Agreement. [Correction added on 23 May 2022, after first online publication: CRUI funding statement has been added.]

AUTHOR CONTRIBUTIONS

All authors were involved in drafting the article or revising it critically for important intellectual content, and all authors approved the final version to be published. Dr. Bettiol had full access to all of the data in the study and takes responsibility for the integrity of the data and the accuracy of the data analysis.

Study conception and design. Bettiol, Urban, Prisco, Vaglio, Emmi.

Acquisition of data. Dagna, Cottin, Franceschini, Del Giacco, Schiavon, Neumann, Lopalco, Novikov, Baldini, Lombardi, Berti, Alberici, Folci, Negrini, Sinico, Quartuccio, Lunardi, Parronchi, Moosig, Espígol-Frigolé, Schroeder, Kernder, Monti, Silvagni, Crimi, Cinetto, Fraticelli, Roccatello, Vacca, Mohammad, Hellmich, Samson, Bargagli, Cohen Tervaert, Ribi, Fiori, Bello, Fagni, Moroni, Ramirez, Nasser, Marvisi, Toniati, Firinu, Padoan, Egan, Seeliger, Iannone, Salvarani, Jayne.

Analysis and interpretation of data. Bettiol, Urban, Salvarani, Jayne, Prisco, Vaglio, Emmi.

REFERENCES

1. Trivioli G, Terrier B, Vaglio A. Eosinophilic granulomatosis with polyangiitis: understanding the disease and its management [review] Rheumatology (Oxford) 2020;59:iii84–94.
2. Bettiol A, Sinico RA, Schiavon F, Monti S, Bozzolo EP, Franceschini F, et al. Risk of acute arterial and venous thromboembolic events in eosinophilic granulomatosis with polyangiitis (Churg-Strauss syndrome). Eur Respir J 2021;57:2004158.
3. Groh M, Pagnoux C, Baldini C, Bel E, Bottero P, Cottin V, et al. Eosinophilic granulomatosis with polyangiitis (Churg–Strauss) (EGPA) Consensus Task Force recommendations for evaluation and management. Eur J Intern Med 2015;26:545–53.
4. Emmi G, Rossi GM, Urban ML, Silvestri E, Prisco D, Goldoni M, et al. Scheduled rituximab maintenance reduces relapse rate in eosinophilic granulomatosis with polyangiitis. Ann Rheum Dis 2017;77:952–4.
5. Fagni F, Bello F, Emmi G. Eosinophilic granulomatosis with polyangiitis: dissecting the pathophysiology [review]. Front Med 2021;8:267776.
6. Lyons PA, Peters JE, Alberici F, Liley J, Coulson RM, Astle W, et al. Genome-wide association study of eosinophilic granulomatosis with polyangiitis reveals genomic loci stratified by ANCA status. Nat Commun 2019;10:5120.
7. Pavord ID, Korn S, Howarth P, Bleecker ER, Buhl R, Keene ON, et al. Mepolizumab for severe eosinophilic asthma (DREAM): a multicentre, double-blind, placebo-controlled trial. Lancet 2012;380:651–9.
8. Roufosse F, Kahn JE, Rothenberg ME, Wardlaw AJ, Klion AD, Kirby SY, et al. Efficacy and safety of mepolizumab in hypereosinophilic syndrome: a phase III, randomized, placebo-controlled trial. J Allergy Clin Immunol 2020;146:1397–405.
9. Herrmann K, Gross WL, Moosig F. Extended follow-up after stopping mepolizumab in relapsing/refractory Churg-Strauss syndrome. Clin Exp Rheumatol 2012;30:S62–5.
10. Moosig F, Gross WL, Herrmann K, Bremer JP, Hellmich B. Targeting interleukin-5 in refractory and relapsing Churg-Strauss syndrome. Ann Intern Med 2011;155:341.
11. Wechsler ME, Akuthota P, Jayne D, Khoury P, Klion A, Langford CA, et al. Mepolizumab or placebo for eosinophilic granulomatosis with polyangiitis. N Engl J Med 2017;376:1921–32.
12. Steinfeld J, Bradford ES, Brown J, Mallett S, Yancey SW, Akuthota P, et al. Evaluation of clinical benefit from treatment with mepolizumab for patients with eosinophilic granulomatosis with polyangiitis. J Allergy Clin Immunol 2019;143:2170–7.
13. Vultaggio A, Nencini F, Bormioli S, Vivarelli E, Dies L, Rossi O, et al. Low-dose mepolizumab effectiveness in patients suffering from eosinophilic granulomatosis with polyangiitis. Allergy Asthma Immunol Res 2020;12:885–93.
14. Canzian A, Venhoff N, Urban ML, Sartorelli S, Ruppert A, Groh M, et al. Use of biologics to treat relapsing and/or refractory eosinophilic granulomatosis with polyangiitis: data from a European collaborative study. Arthritis Rheumatol 2020;73:498–503.
15. Caminati M, Crisafulli E, Lunardi C, Micheletto C, Festi G, Maule M, et al. Mepolizumab 100 mg in severe asthmatic patients with EGPA in remission phase. J Allergy Clin Immunol Pract 2020;9:1386–8.
16. Faverio P, Bonaiti G, Bini F, Vaghi A, Pesci A. Mepolizumab as the first targeted treatment for eosinophilic granulomatosis with polyangiitis: a review of current evidence and potential place in therapy. Ther Clin Risk Manag 2018;14:2385–96.
17. Masi AT, Hunder GG, Lie JT, Michel BA, Bloch DA, Arend WP, et al. The American College of Rheumatology 1990 criteria for the classification of Churg-Strauss syndrome (allergic granulomatosis and angiitis). Arthritis Rheum 1990;33:1094–100.
18. Mukhtyar C, Lee R, Brown D, Carruthers D, Dasgupta B, Dubey S, et al. Modification and validation of the Birmingham Vasculitis Activity Score (version 3). Ann Rheum Dis 2009;68:1827–32.
19. European Medicines Agency. ICH Topic E 2 A. Clinical safety data management: definitions and standards for expedited reporting. 1995. URL: https://www.ema.europa.eu/en/documents/scientific-guideline/international-conference-harmonisation-technical-requirements-registration-pharmaceuticals-human-use_en-15.pdf.
20. Moiseev S, Zagvozdkina E, Kazarina V, Bulanov N, Novikov P. Mepolizumab in patients with eosinophilic granulomatosis with polyangiitis. J Allergy Clin Immunol 2019;144:621.
21. Roufosse FE, Kahn JE, Gleich GJ, Schwartz LB, Singh AD, Rosenwasser LJ, et al. Long-term safety of mepolizumab for the treatment of hypereosinophilic syndromes. J Allergy Clin Immunol 2013;131:461–7.
22. Thompson G, Vasilevski N, Ryan M, Baltic S, Thompson P. Low-dose mepolizumab effectively treats chronic relapsing eosinophilic granulomatosis with polyangiitis [abstract]. Australia and New Zealand Society of Respiratory Science and The Thoracic Society of Australia and New Zealand: Abstracts from the Annual Scientific Meeting in Adelaide, Australia, 23-27 March 2018. URL: https://www.cochranelibrary.com/central/doi/10.1002/central/CN-01607187/full.
23. Wong TW, Doyle AD, Lee JJ, Jelinek DF. Eosinophils regulate peripheral B cell numbers in both mice and humans. J Immunol 2014;192:3548–58.
24. Sablé-Fourtassou R, Cohen P, Mahr A, Pagnoux C, Mouthon L, Jayne D, et al. Antineutrophil cytoplasmic antibodies and the Churg-Strauss syndrome. Ann Intern Med 2005;143:632–8.
25. Papo M, Sinico RA, Teixeira V, Venhoff N, Urban ML, Iudici M, et al. Significance of PR3-ANCA positivity in eosinophilic granulomatosis with polyangiitis (Churg-Strauss). Rheumatology (Oxford) 2021;60:4355–60.
26. Comarmond C, Pagnoux C, Khellaf M, Cordier JF, Hamidou M, Viallard JF, et al. Eosinophilic granulomatosis with polyangiitis (Churg-Strauss): clinical characteristics and long-term followup of the 383 patients enrolled in the French Vasculitis Study Group cohort. Arthritis Rheum 2013;65:270–81.
27. Han JK, Bachert C, Fokkens W, Desrosiers M, Wagenmann M, Lee SE, et al. Mepolizumab for chronic rhinosinusitis with nasal polyps

(SYNAPSE): a randomised, double-blind, placebo-controlled, phase 3 trial. Lancet Respir Med 2021;9:1141–53.
28. Khoury P, Grayson PC, Klion AD. Eosinophils in vasculitis: characteristics and roles in pathogenesis [review]. Nat Rev Rheumatol 2014; 10:474–83.
29. Kingham PJ, McLean WG, Walsh MT, Fryer AD, Gleich GJ, Costello RW. Effects of eosinophils on nerve cell morphology and development: the role of reactive oxygen species and p38 MAP kinase. Am J Physiol Lung Cell Mol Physiol 2003;285:L915–24.
30. Kitamura N, Hamaguchi M, Nishihara M, Ikumi N, Sugiyama K, Nagasawa Y, et al. The effects of mepolizumab on peripheral circulation and neurological symptoms in eosinophilic granulomatosis with polyangiitis (EGPA) patients. Allergol Int 2021;70:148–9.
31. Mukherjee M, Lim HF, Thomas S, Miller D, Kjarsgaard M, Tan B, et al. Airway autoimmune responses in severe eosinophilic asthma following low-dose Mepolizumab therapy. Allergy Asthma Clin Immunol 2017;13:2.
32. Caminati M, Menzella F, Guidolin L, Senna G. Targeting eosinophils: severe asthma and beyond [review]. Drugs Context 2019;8:212587.

APPENDIX A: EUROPEAN EGPA STUDY GROUP

Members of the EGPA Study Group are as follows: Kais Ahmad (Hospices Civils de Lyon, Lyon, France), Mirko Beccalli (IRCCS Ospedale Policlinico San Martino, Genoa, Italy), Bernard Bonnotte (Dijon University Hospital, Dijon, France), Roberto Bortolotti (Santa Chiara Hospital, Trento, Italy), Adriana Cariddi (IRCCS San Raffaele Hospital, Vita-Salute San Raffaele University, Milan, Italy), Marco Caminati (University of Verona, Italy), Maria C Cid (University of Barcelona; Institut d'investigacions Biomèdiques August Pi I Sunyer (IDIBAPS), Barcelona, Spain), Margherita Deidda (University of Cagliari, Cagliari, Italy), Paolo Delvino (IRCCS Policlinico S. Matteo Fondazione, University of Pavia, Pavia, Italy), Gerardo Di Scala (University of Florence, Florence, Italy), Mara Felicetti (Azienda Ospedaliera-Universitaria di Padova, Padova, Italy), Francesco Ferro (University of Pisa, Pisa, Italy), Federica Furini (University of Ferrara, Ferrara, Italy), Elena Gelain (Meyer Children's University Hospital, Florence, Italy), Giulia Ghirelli (University Hospital "Ospedali Riuniti," Ancona, Foggia, Italy), Julia Holle (Rheumazentrum Schleswig-Holstein Mitte, Neumünster, Germany), Laura Michelina Losappio (ASST GOM Niguarda, Milan, Italy), Alfred Mahr (Cantonal Hospital St. Gallen, St. Gallen, Switzerland), Danilo Malandrino (University of Florence, Florence, Italy), Juliane Marhhold (Medius Kliniken, Kirchheim-Teck, Germany), Irene Mattioli (University of Florence, Florence, Italy), Laura Moi (University Hospital Center of Lausanne, Lausanne, Switzerland), Sergey Moiseev (Sechenov First Moscow State Medical University, Moscow, Russia), Francesco Muratore (Azienda USL-IRCCS di Reggio Emilia, Reggio Emilia, Italy), Santi Nolasco (University of Catania, Catania, Italy), Bianca Olivieri (University of Verona, Verona, Italy), Adalgisa Palermo (University of Florence, Florence, Italy), Francesca Regola (University of Brescia, Brescia, Italy), Oliver Sander (Heinrich-Heine-University Düsseldorf, Düsseldorf, Germany), Riccardo Scarpa (University of Padova, Padova, Italy), Savino Sciascia (San Giovanni Bosco Hospital and University of Turin, Turin, Italy), Elena Silvestri (University of Florence, Florence, Italy), Nicola Susca (University of Brescia, Brescia, Italy), Benjamin Terrier (University of Paris, Assistance Publique-Hôpitaux de Paris, Cochin Hospital, Paris, France), Elena Treppo (University of Udine, Udine, Italy), Barbara Trezzi (University of Milano Bicocca, Monza, Italy), Martina Uzzo (ASST Santi Paolo e Carlo, Milan, Italy; University of Milano, Milan, Italy), Gianfranco Vitiello (University of Florence, Florence, Italy), and Elaine Yacyshyn (University of Alberta, Edmonton, Alberta, Canada; Maastricht University, Maastricht, The Netherlands).

Arthritis & Rheumatology
Vol. 74, No. 2, February 2022, pp 307–317
DOI 10.1002/art.41927

American College of Rheumatology
Empowering Rheumatology Professionals

Defective Early B Cell Tolerance Checkpoints in Patients With Systemic Sclerosis Allow the Production of Self Antigen–Specific Clones

Salome Glauzy, Brennan Olson, Christopher K. May, Daniele Parisi, Christopher Massad, James E. Hansen, Changwan Ryu, Erica L. Herzog, and Eric Meffre

Objective. Early selection steps preventing autoreactive naive B cell production are often impaired in patients with autoimmune diseases, but central and peripheral B cell tolerance checkpoints have not been assessed in patients with systemic sclerosis (SSc). This study was undertaken to characterize early B cell tolerance checkpoints in patients with SSc.

Methods. Using an in vitro polymerase chain reaction–based approach that allows the expression of recombinant antibodies cloned from single B cells, we tested the reactivity of antibodies expressed by 212 CD19+CD21^{low}CD10+IgM^{high}CD27− new emigrant/transitional B cells and 190 CD19+CD21+CD10−IgM+CD27− mature naive B cells from 10 patients with SSc.

Results. Compared to serum from healthy donors, serum from patients with SSc displayed elevated proportions of polyreactive and antinuclear-reactive new emigrant/transitional B cells that recognize topoisomerase I, suggesting that defective central B cell tolerance contributes to the production of serum autoantibodies characteristic of the disease. Frequencies of autoreactive mature naive B cells were also significantly increased in SSc patients compared to healthy donors, thus indicating that a peripheral B cell tolerance checkpoint may be impaired in SSc.

Conclusion. Defective counterselection of developing autoreactive naive B cells in SSc leads to the production of self antigen–specific B cells that may secrete autoantibodies and allow the formation of immune complexes, which promote fibrosis in SSc.

INTRODUCTION

Scleroderma, or systemic sclerosis (SSc), is an autoimmune disease characterized by vascular abnormalities, fibroblast activation leading to extracellular matrix synthesis and fibrosis of the skin and internal organs, and dysregulated immunity (1,2). Patients with SSc are classified into 2 main groups—diffuse cutaneous SSc (dcSSc) and limited cutaneous SSc (lcSSc). The dcSSc subtype is characterized by skin fibrosis proximal to the elbows and knees and internal organ damage, especially to the lungs, resulting in pulmonary fibrosis, a major cause of disease-associated morbidity and mortality (1,2). In contrast, patients with lcSSc usually have skin alterations restricted to the hands and face and are less commonly affected by visceral fibrosis.

These 2 subgroups of patients with SSc are also characterized by the production of specific autoantibodies. Anti–topoisomerase I/anti–Scl-70, anti–RNA polymerase III, and anti–U3 RNP are usually found in patients with dcSSc, whereas anticentromere, anti-PM/Scl, anti-Th/To, and anti–U1 RNP are often associated with lcSSc (1,2). All of these autoantibodies that target nucleic acid–containing self antigens demonstrate a break in B cell tolerance in SSc; however, the origin of the autoreactive B cells secreting these serum autoantibodies remains unknown.

Analysis of patients with various autoimmune diseases, including rheumatoid arthritis (RA), systemic lupus erythematosus (SLE), Sjögren's syndrome (SS), type 1 diabetes mellitus (DM), myasthenia gravis, neuromyelitis optica spectrum disorder (NMOSD), and multiple sclerosis (MS), revealed an impaired

Supported by the NIH (grants AI-061093, AI-071087, and AI-082713 from the National Institute of Allergy and Infectious Diseases), the Scleroderma Research Foundation (grant to Dr. Meffre), and Patrys Ltd. (grant to Dr. Hansen).

Salome Glauzy, PhD, Brennan Olson, PhD, Christopher K. May, PhD, Daniele Parisi, PhD, Christopher Massad, MPH, James E. Hansen, MD, Changwan Ryu, MD, MPH, Erica L. Herzog, MD, PhD, Eric Meffre, PhD: Yale University School of Medicine, New Haven, Connecticut.

Author disclosures are available at https://onlinelibrary.wiley.com/action/downloadSupplement?doi=10.1002%2Fart.41927&file=art41927-sup-0001-Disclosureform.pdf.

Address correspondence to Eric Meffre, PhD, Yale University School of Medicine, 300 George Street, Room 353F, New Haven, CT 06511. Email: eric.meffre@yale.edu.

Submitted for publication February 18, 2021; accepted in revised form July 13, 2021.

selection of developing autoreactive B cells in either (or both) the bone marrow and the periphery, resulting in the accumulation of large numbers of circulating autoreactive naive B cells (3).

We report herein that both dcSSc patients and lcSSc patients display defective central and peripheral B cell tolerance checkpoints, leading to the production of autoreactive naive B cell clones expressing unmutated antibodies with self antigen specificity characteristic of the disease. These autoreactive antibodies have recently been shown to promote fibrosis in SSc through the formation of immune complexes (4), thereby revealing that failed B cell tolerance mechansims play an essential role in disease pathophysiology.

PATIENTS AND METHODS

Patient characteristics. Patients with SSc according to current criteria were enrolled from the Yale ILD Center of Excellence and the Yale Scleroderma Center (Supplementary Table 1, available on the *Arthritis & Rheumatology* website at http://onlinelibrary.wiley.com/doi/10.1002/art.41927/abstract). Most patients were naive to any medication, and all met diagnostic criteria for SSc (1). The characteristics of the patients with SSc, their autoantibody profiles, and the presence of the 1858T PTPN22 polymorphism associated with the disease and leading to impaired early B cell tolerance checkpoints are summarized in Supplementary Table 1 (5–9). The study protocol was approved by the Institutional Review Board at Yale (HIC#1307012431, HIC#0906005336), and informed consent was obtained from all patients before participation.

Cell staining and sorting. Mononuclear cells from healthy donors and patients with SSc were enriched for B cells by magnetic separation with anti-CD20 microbeads (Miltenyi Biotec) and stained with Pacific Blue–conjugated anti-human CD19, PerCP–Cy5.5–conjugated anti-human CD27, phycoerythrin (PE)–Cy7–conjugated anti-human CD10, allophycocyanin (APC)–conjugated anti-human CD21, and fluorescein isothiocyanate–conjugated anti-human IgM (all from BioLegend). Single $CD19+CD21^{low}CD10+IgM^{high}CD27-$ new emigrant/transitional and $CD19+CD21+CD10-IgM+CD27-$ mature naive B cells were sorted on a FACSAria system (BD Biosciences) into 96-well polymerase chain reaction (PCR) plates and immediately frozen on dry ice.

The following antibodies were used for T cell phenotyping: APC–Cy7–conjugated anti-CD4, PE–Cy7–conjugated anti-CD25, PerCP–Cy5.5–conjugated anti-CD127 (all from BioLegend), and eFluor 605NC–conjugated anti-CD3 (eBioscience). Intracellular staining with Alexa Fluor 488–conjugated anti-FoxP3 (clone PCH101; eBioscience) was performed using a FoxP3/Transcription Factor Staining Buffer Set in accordance with instructions of the manufacturer (eBioscience).

Complementary DNA (cDNA) synthesis, Ig gene amplification, antibody production, and purification. Complementary DNA synthesis, reverse transcriptase–PCRs, primer sequences, cloning strategy, expression vectors, in vitro recombinant antibody production, and purification were performed as previously described (10). Briefly, cDNA was synthesized in the original 96-well PCR plate in which single B cells were sorted. RNA from single cells was reverse-transcribed in a 14 μl volume at 37°C for 55 minutes; 3.5 μl of cDNA or first PCR product was used to amplify IgH, Igκ, or Igλ transcripts by 2 rounds of PCR in 40-μl reactions containing 20 p*M* primers and 1.2U HotstarTaq DNA polymerase (Qiagen). PCR products were then purified (QIAquick; Qiagen), sequenced, and analyzed by IgBLAST comparison with GenBank.

Since gene restriction sites were introduced by second PCRs, digested IgH, Igκ, and Igλ PCR products were purified (QIAquick; Qiagen) and cloned into expression vectors containing human IgG1, Igκ, or Igλ constant regions (10); 12.5 μg of IgH and IgL chain encoding plasmid DNA was co*transfected* with polyethyleneimine in 293A human embryonic kidney fibroblasts washed with serum-free Dulbecco's modified Eagle's medium (DMEM) and thereafter cultured in DMEM supplemented with 1% Nutridoma SP (Roche). Supernatants were collected and titrated after 8–10 days of culture. HEp-2 reactivity enzyme-linked immunosorbent assays (ELISAs) and immunofluorescence assays (IFAs) were performed using antibodies purified on protein G–Sepharose (Amersham Pharmacia Biosciences).

Repertoire analysis. Immunoglobulin sequences and mutation status were determined using IgBLAST comparison with GenBank using the NCBI IgBLAST server (http://www.ncbi.nlm.nih.gov/igblast/). Heavy-chain complementarity-determining region 3 (CDR3) was defined as the interval between amino acid at position 94 in the V_H framework 3 and the conserved tryptophan at position 103 in J_H segments. Antibody sequences and reactivity are shown in Supplementary Tables 2 and 3, available on the *Arthritis & Rheumatology* website at http://onlinelibrary.wiley.com/doi/10.1002/art.41927/abstract.

ELISAs and IFAs. Recombinant antibody reactivity was assessed as previously reported using the highly polyreactive ED38 recombinant antibody as a positive control for HEp-2 reactivity and polyreactivity assays (10). Antibodies were considered polyreactive when they recognized all 3 distinct antigens: double-stranded DNA (dsDNA), insulin, and lipopolysaccharide (LPS). For indirect IFAs, HEp-2 cell–coated slides (Bion Enterprises) were incubated in a moist chamber at room temperature with purified recombinant antibodies at 50–100 μg/ml according to the manufacturer's instructions.

Immunoprecipitation and Western blotting. DLD1 cells grown to confluence in a T-25 flask (2–3 × 10^6 cells) were lysed in M-PER (catalog no. 78501; ThermoFisher) for 5 minutes on ice with 1× Halt Protease Inhibitor (catalog no. 87786; ThermoFisher). The lysate was clarified by centrifugation for 10 minutes

at 10,000 rpm at 4°C. Two hundred microliters of lysate was added to Protein A/G beads with 2 μg κ24 or the equivalent volume of phosphate buffered saline for a 1-hour rotation at 4°C. Beads were washed 3 times in Gentle Ag/Ab Binding Buffer, pH 8.0, and eluted by the addition of 2× Laemmli buffer. Western blot of κ24 input, DLD1 total lysate, and elutions from control and κ24 beads was probed with primary monoclonal anti–topoisomerase I (catalog no. sc-271285; Santa Cruz Biotechnology) and secondary HRP-linked anti-mouse IgG antibody (catalog no.7076S; Cell Signaling Technology), with signal detection by enhanced chemiluminescence (ThermoFisher).

In vitro Treg cell suppression assay. CD4+ T cells were enriched using an EasySep human CD4+ T cell enrichment kit (StemCell Technologies). CD4+CD25^{high}CD127$^{low/-}$ Treg cells and CD3+CD4+CD25− T responder cells were sorted by flow cytometry. T responder cells were then labeled with CellTrace CFSE (InvivoGen) at 5 μ*M*. Treg cells and T responder cells were cocultured at a 1:1 ratio in the presence of beads loaded with anti-CD2, anti-CD3, and anti-CD28 (Treg Suppression Inspector [human]; Miltenyi Biotec) at a 1:1 ratio of beads to cells (11). On days 3.5–4.5, cocultures were stained for viability with a Live/Dead kit (Invitrogen), and the proliferation of viable T responder cells was assessed following carboxyfluorescein succinimidyl ester dilution.

Statistical analysis. Statistical analysis was performed using GraphPad Prism software version 5.0. Differences between subject groups were tested for statistical significance by nonparametric Mann-Whitney U tests or unpaired Z tests. *P* values less than or equal to 0.05 were considered significant.

RESULTS

Impaired central B cell tolerance in patients with SSc. Central B cell tolerance mediates the removal of developing polyreactive and antinuclear-reactive immature B cells in the bone marrow (3,10). To determine whether this early B cell selection step is altered in SSc, we enrolled patients with SSc, many of whom were naive for treatment (Table 1 and Supplementary Table 1). We cloned 212 recombinant antibodies expressed by single CD19+CD21^{low}CD10+IgM^{high}CD27− transitional B cells that recently emigrated from the bone marrow and were isolated from 10 of these patients (5 with dcSSc and 5 with lcSSc) and tested the reactivity of these antibodies by ELISA. Of note, flow cytometry revealed that transitional B cell subsets including early T1 and more mature T2 B cells were found at similar frequencies in healthy donors and patients with SSc (Supplementary Figure 1, available on the *Arthritis & Rheumatology* website at http://onlinelibrary.wiley.com/doi/10.1002/art.41927/abstract). In contrast, SSc patients displayed significantly increased proportions of CD19+CD21+CD10−IgM+CD27− mature naive B cells that differentiate from transitional B cells, but decreased frequencies of CD19+CD21+CD10−CD27+ conventional memory B cells compared to controls (Supplementary Figure 1).

Table 1. Characteristics of the patients with SSc*

	Patients with dcSSc (n = 5)	Patients with lcSSc (n = 5)
Age, mean ± SD years	45.4 ± 15.6	51.6 ± 9.8
Sex, female	5 (100)	5 (100)
Race, White	5 (100)	5 (100)
Anti–Scl-70 antibody status		
Positive	4 (80)	1 (20)
Negative	1 (20)	4 (80)
Anticentromere antibody status		
Positive	1 (20)	2 (40)
Negative	4 (80)	3 (60)
Treatment naive	3 (60)	4 (80)
Clinically significant ILD	5 (100)	3 (60)
Group I PAH	0 (0)	0 (0)
GERD	5 (100)	5 (100)
MRSS, mean	15	5

* Except where indicated otherwise, values are the number (%) of patients. SSc = systemic sclerosis; dcSSc = diffuse cutaneous SSc; lcSSc = limited cutaneous SSc; ILD = interstitial lung disease; PAH = pulmonary arterial hypertension; GERD = gastroesophageal reflux disease; MRSS = modified Rodnan skin thickness score.

The first evidence suggesting that central B cell tolerance was not properly established in SSc came from the Ig repertoire analysis of SSc new emigrant/transitional B cells (Supplementary Figure 2 and Supplementary Table 2, available on the *Arthritis & Rheumatology* website at http://onlinelibrary.wiley.com/doi/10.1002/art.41927/abstract). Pooled heavy-chain gene (IgH) sequences from SSc new emigrant/transitional B cells revealed a significantly higher frequency of long IgH CDR3, a feature that favors antibody self-reactivity (10,12), in SSc patients, whereas the density of positive charges in IgH CDR3 was similar between healthy donors and SSc patients (Supplementary Figure 2).

The reactivities of antibodies expressed by new emigrant/transitional B cells from 10 patients with SSc were then compared to those in 13 previously studied healthy donors (3) (Figures 1A–C). We found that the frequencies of new emigrant/transitional B cells expressing polyreactive antibodies in both patients with dcSSc and those with lcSSc were significantly increased and averaged 22.1% and 26.9%, respectively, compared to only 7.1% in healthy controls, revealing that central B cell tolerance is impaired in SSc ($P < 0.0001$) (Figures 1A and B; Supplementary Figure 3, and Supplementary Table 2, available on the *Arthritis & Rheumatology* website at http://onlinelibrary.wiley.com/doi/10.1002/art.41927/abstract). The proportion of antinuclear-reactive clones in new emigrant/transitional B cells from SSc patients was also significantly increased compared to that in healthy donors, further demonstrating the impaired removal of developing autoreactive B cells in the bone marrow of these patients

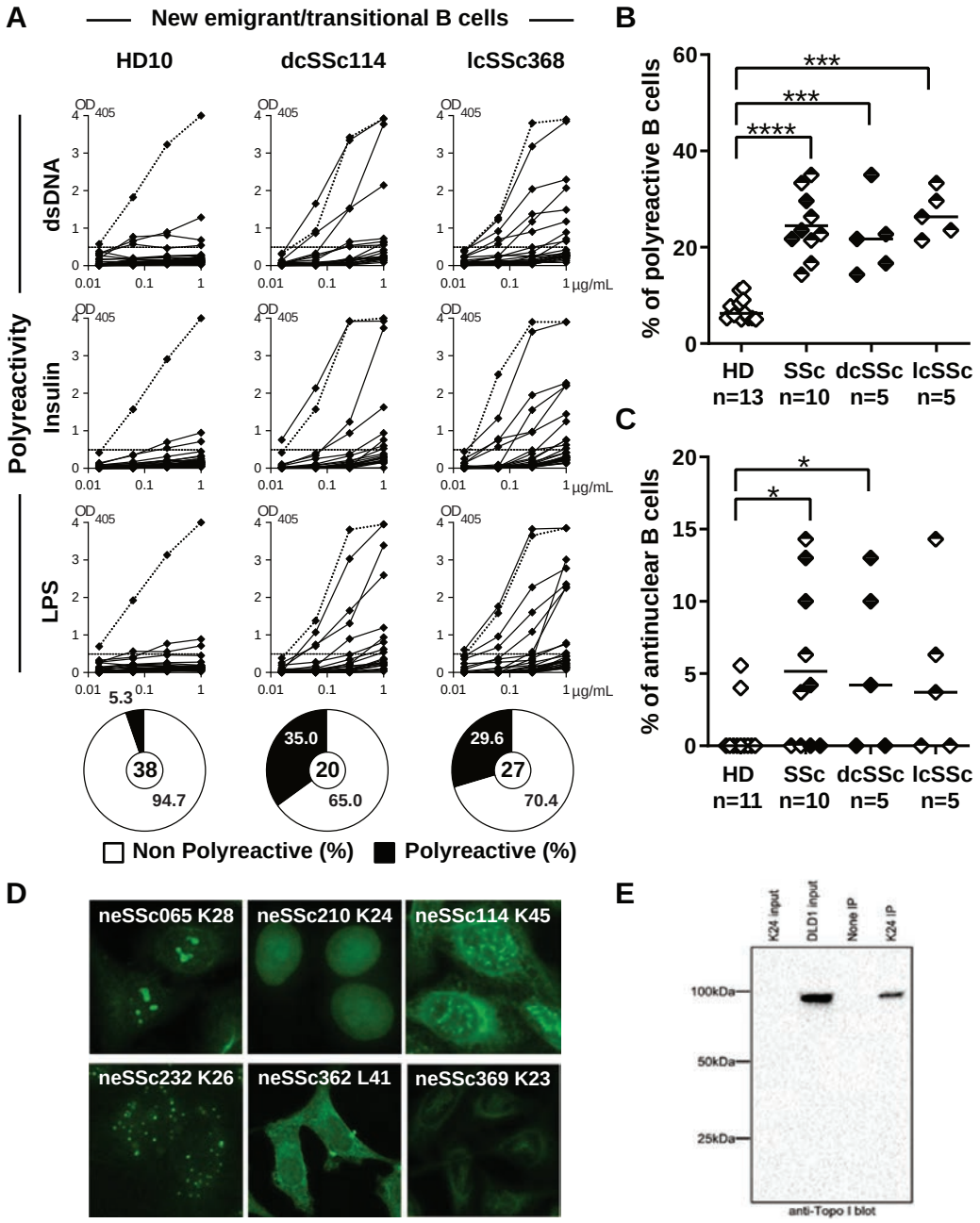

Figure 1. Defective central B cell tolerance in patients with systemic sclerosis (SSc). **A**, Antibodies cloned from single new emigrant/transitional B cells from a representative healthy donor (HD10), a patient with diffuse cutaneous SSc (dcSSc114), and a patient with limited cutaneous SSc (lcSSc368) were tested by enzyme-linked immunosorbent assay for reactivity against different concentrations of double-stranded DNA (dsDNA), insulin, and lipopolysaccharide (LPS). Dotted lines show the ED38-positive control. Horizontal lines show the cutoff for positive reactivity at OD_{405}. Pie charts show the frequencies of nonpolyreactive and polyreactive clones. Values in the center are the number of antibodies tested. **B** and **C**, Frequencies of polyreactive (**B**) and antinuclear-reactive (**C**) new emigrant B cells were compared between healthy donors and patients with SSc (subdivided into dcSSc and lcSSc). Open diamonds represent healthy donors, solid diamonds represent patients with dcSSc, and half-solid/half-open diamonds represent patients with lcSSc; horizontal lines show the median. * = $P < 0.05$; *** = $P < 0.001$; **** = $P < 0.0001$, by Mann-Whitney U test. **D**, Antinuclear antibodies in B cells from SSc patients show various patterns of HEp-2 staining. Original magnification × 40. **E**, Immunoprecipitation (IP) experiments were performed using recombinant antibody κ24 cloned from a new emigrant/transitional B cell from SSc patient 210 (neSSc210 κ24). A topoisomerase I Western blot for κ24 input supernatant and DLD1 total lysate is shown, with either no antibody or neSSc210 κ24 included for IP. The recombinant antibody neSSc210 κ24 bound topoisomerase I. Results are representative of 3 experiments.

($P = 0.036$) (Figures 1C and D). Antinuclear-reactive new emigrant/transitional B cells from patients with SSc recognized diverse structures in the nucleus, as illustrated by the different antinuclear staining patterns shown for recombinant antibody κ28 cloned from a new emigrant/transitional B cell from SSc patient 65 (neSSc065 κ28), neSSc210 κ24, and neSSc114 κ45 (Figure 1D).

Both polyreactive and antinuclear-reactive new emigrant B cells from patients with SSc were enriched in clones that displayed positively charged amino acids in their IgH CDR3, whereas long IgH CDR3 favored polyreactivity but not antinuclear reactivity (Supplementary Figure 2). Of note, similar autoreactive B cell frequencies were observed in patients with SSc whether or not they harbored the PTPN22 risk allele, which is associated with this disease and results in impaired early B cell tolerance checkpoints (5–9) (Supplementary Figure 4, *Arthritis & Rheumatology* website at http://onlinelibrary.wiley.com/doi/10.1002/art.41927/abstract). Hence, other polymorphisms or factors may result in altered autoreactive B cell counterselection in these patients. Taken together, our data show that central B cell tolerance is defective in both dcSSc patients and lcSSc patients.

Identification of an anti–topoisomerase I/Scl-70–reactive clone in a patient with dcSSc. Clone neSSc210 κ24 was of particular interest due to its strong, compact fine

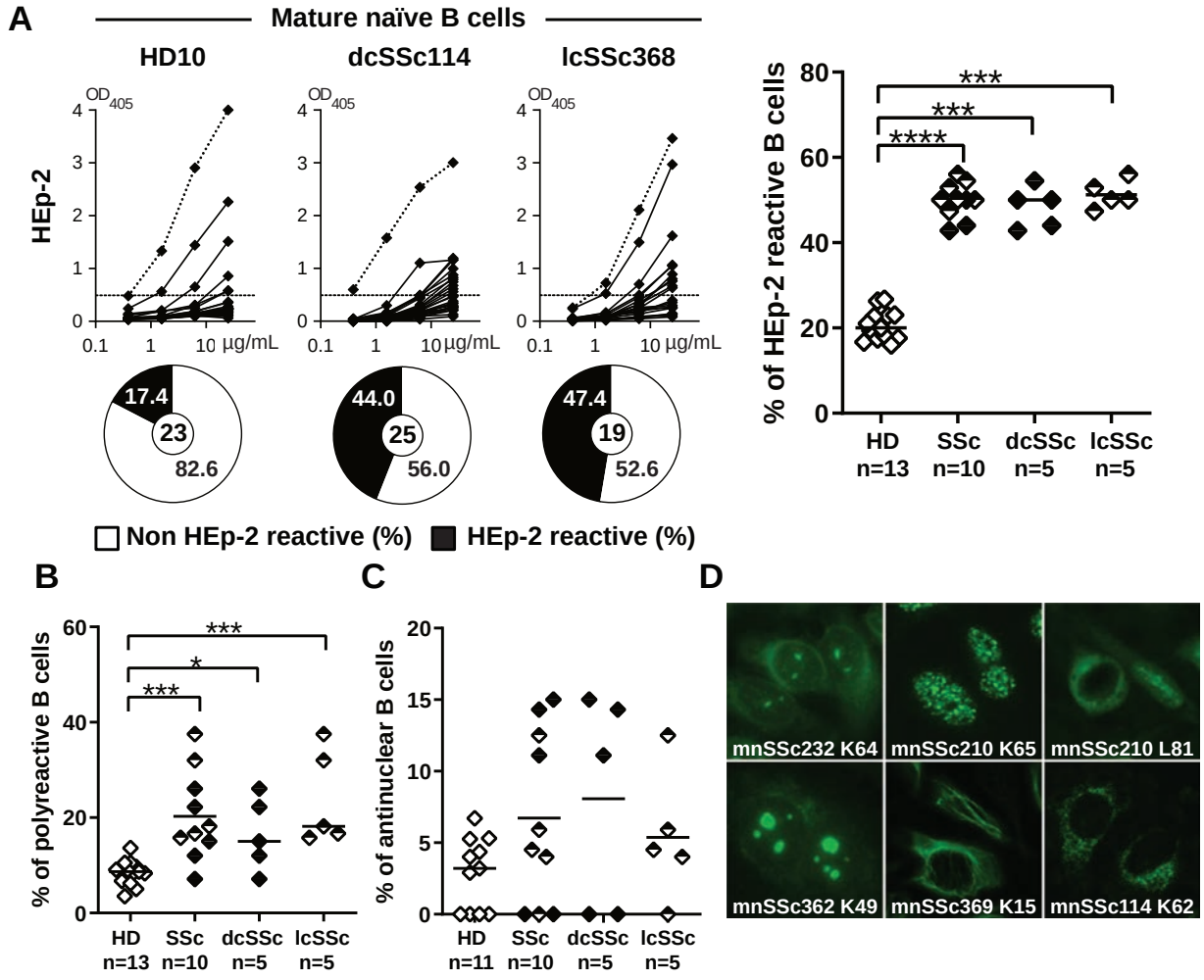

Figure 2. Defective peripheral B cell tolerance checkpoint in patients with SSc. **A**, Left, Antibodies cloned from single mature naive B cells from a representative healthy donor (HD10), a patient with dcSSc (dcSSc114), and a patient with lcSSc (lcSSc368) were tested at different concentrations by enzyme-linked immunosorbent assay for reactivity against HEp-2 cell lysate. Dotted lines show the ED38-positive control. Horizontal lines show the cutoff for positive reactivity at OD_{405}. Pie charts show the frequencies of non–HEp-2–reactive clones and HEp-2–reactive clones. Values in the center are the number of antibodies tested. Right, Frequencies of HEp-2-reactive clones in mature naive B cells were compared between healthy donors and patients with SSc (subdivided into dcSSc and lcSSc). **B** and **C**, Frequencies of clones that were polyreactive against dsDNA, insulin, and LPS (**B**), and of antinuclear-reactive clones (**C**) in mature naive B cells were compared between healthy donors and patients with SSc (subdivided into dcSSc and lcSSc). In the right panel of **A** and in **B** and **C**, open diamonds represent healthy donors, solid diamonds represent patients with dcSSc, and half-solid/half-open diamonds represent patients with lcSSc; horizontal lines show the median. * = $P < 0.05$; *** = $P < 0.001$; **** = $P < 0.0001$, by Mann-Whitney U test. **D**, Examples of mature naive B cells from patients with SSc that expressed antibodies recognizing either cytoplasmic structures (mature naive B cells from SSc patient 210 [mnSSc210] λ81, mnSSc369 κ15, and mnSSc114 κ62) or nuclear structures (mnSSc232 κ64, mnSSc210 κ65, and mnSSc362 κ49) are shown. Original magnification × 40. See Figure 1 for other definitions.

speckled pattern, which resembled staining characteristic of anti–topoisomerase I/Scl-70, suggesting that this clone may recognize this self antigen targeted in dcSSc (Figure 1D) (13). To determine whether neSSc210 κ24 is an anti–topoisomerase I–reactive antibody, we performed immunoprecipitation experiments with this recombinant antibody using the DLD1 cell line. Indeed, the presence of topoisomerase I was revealed using a monoclonal anti-human topoisomerase I antibody (Figure 1E). We found that neSSc210 κ24 bound topoisomerase I, the major self antigen in dcSSc, in the absence of somatic hypermutation, which normally improves antibody affinity (Figure 1E). Thus, defects in central B cell tolerance in patients with SSc may result in the production of autoreactive clones that recognize self antigen specifically targeted in this disease.

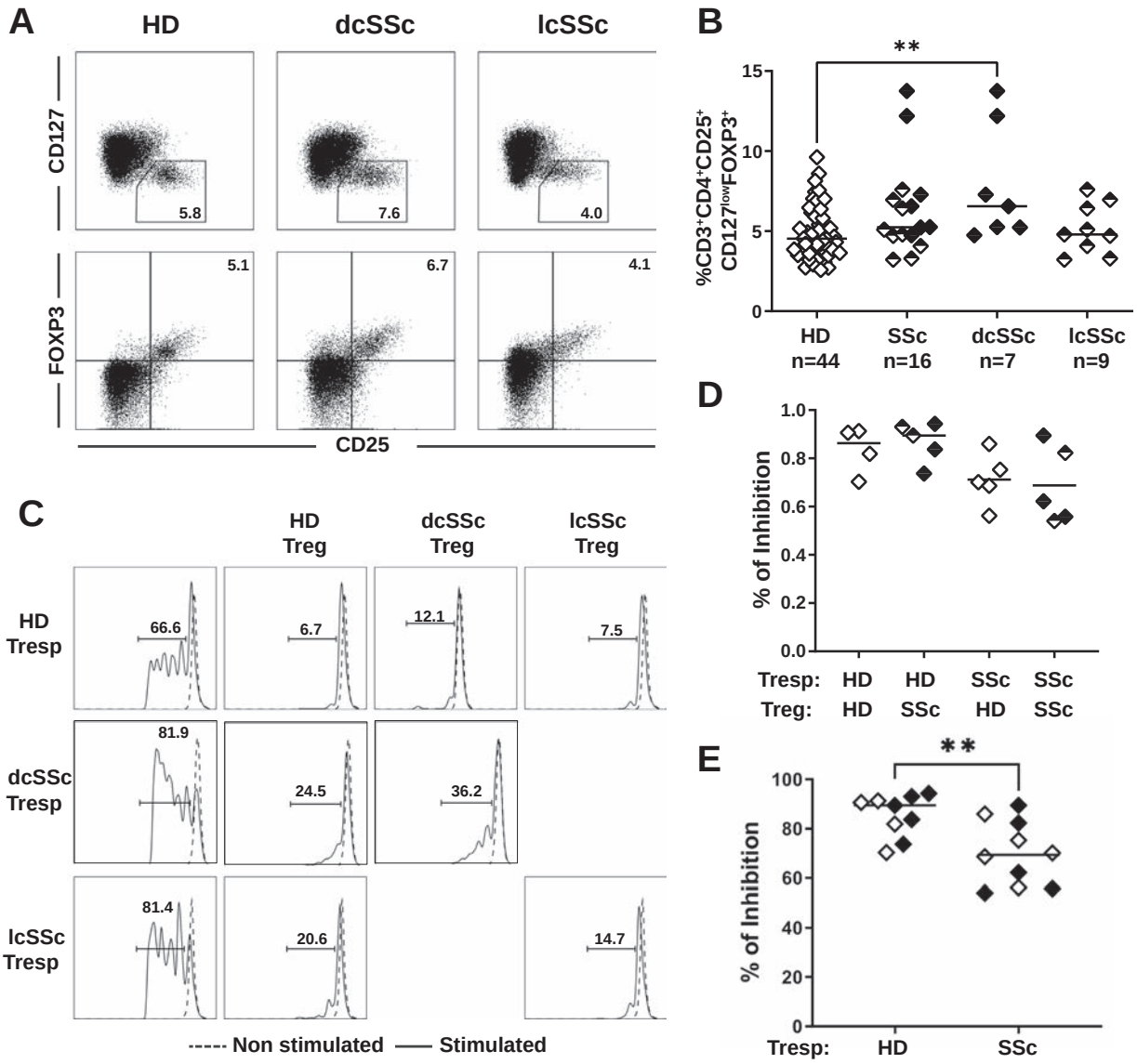

Figure 3. Identification of T cells refractory to in vitro Treg cell suppression in SSc. **A**, CD3+CD4+ T cells from a representative healthy donor, a patient with dcSSc, and a patient with lcSSc were stained for CD25 versus CD127 or CD25 versus intracellular FoxP3. **B**, CD3+CD4+ $CD25^{high}CD127^{low}$FoxP3+ Treg cell frequencies were compared between healthy donors and patients with SSc (subdivided into dcSSc and lcSSc). ** = $P < 0.01$, by Mann-Whitney U test. **C**, Representative histograms show Treg cell–mediated suppression of autologous and heterologous 5,6-carboxyfluorescein succinimidyl ester (CFSE)–labeled T responder (Tresp) cells on day 3.5 from a patient with dcSSc and a patient with lcSSc compared to a healthy donor. **D**, The autologous and heterologous suppressive abilities of Treg cells were compared between 4 healthy donors and 5 SSc patients (dcSSc210, dcSSc366, lcSSc368, lcSSc369, and dcSSc370). **E**, Combined Treg cell suppression data for T responder cells was compared between healthy donors and patients with SSc. In **B** and **D**, open diamonds represent healthy donors, solid diamonds represent patients with dcSSc, and half-solid/half-open diamonds represent patients with lcSSc; horizontal lines show the median. In **E**, open diamonds represent healthy donors, and solid diamonds represent patients with SSc; horizontal lines show the median. ** = $P < 0.01$, by Mann-Whitney U test. See Figure 1 for other definitions.

Impaired peripheral B cell tolerance checkpoint in patients with SSc. Autoreactive B cells that recognize peripheral self antigens are normally eliminated at a second B cell tolerance checkpoint before entering the long-lived mature naive B cell compartment (3,10). As a consequence, mature naive B cells from both healthy donors and patients with SSc displayed shorter and less positively charged IgH CDR3 than their new emigrant/transitional B cell counterparts (Supplementary Figures 2 and 5, available on the *Arthritis & Rheumatology* website at http://onlinelibrary.wiley.com/doi/10.1002/art.41927/abstract). However, mature naive B cells from patients with SSc were significantly enriched in clones with longer IgH CDR3 compared to their counterparts in healthy donors, suggesting that the peripheral B cell tolerance checkpoint may not be properly regulated in SSc (Supplementary Figure 5A).

We therefore investigated this peripheral B cell selection step by testing the self-reactivity of antibodies expressed by 190 mature naive B cells from the same 10 patients with SSc using various ELISAs and indirect immunofluorescence (10). We found that the frequencies of mature naive B cells expressing antibodies reactive to HEp-2 cell lysate, a commonly used ELISA for the detection of autoreactive immunoglobulins (10), were significantly increased in both dcSSc patients and lcSSc patients (42.9–56.5%) compared with healthy donors (16.0–26.3%) ($P < 0.0001$) (Figure 2A; Supplementary Figure 6 and Supplementary Table 3, available on the *Arthritis & Rheumatology* website at http://onlinelibrary.wiley.com/doi/10.1002/art.41927/abstract). Peripheral B cell tolerance checkpoint defects in patients with SSc were further evidenced by the increased frequency of mature naive B cells expressing polyreactive antibodies in SSc patients compared with healthy donors ($P = 0.0004$), whether or not they carried the PTPN22 risk allele (Figure 2B and Supplementary Figures 4 and 7, available on the *Arthritis & Rheumatology* website at http://onlinelibrary.wiley.com/doi/10.1002/art.41927/abstract).

The proportion of antinuclear-reactive clones in mature naive B cells from patients with SSc was also increased compared to healthy donors, but differences failed to reach significance (Figures 2C and D). Antinuclear-reactive clones showed nucleolar staining patterns (recombinant antibody κ64 cloned from a mature naive B cell from SSc patient 232 [mnSSc232 κ64] and mnSSc362 κ49) or speckled staining patterns (mnSSc210 κ65) (Figure 2D). Notably, the serum of SSc patient 232 displayed antinuclear autoantibodies (Supplementary Table 1), suggesting that the impaired peripheral B cell tolerance checkpoint in SSc may also contribute to the break in B cell tolerance and autoantibody secretion in this disease. Analysis of heavy-chain sequences from mature naive B cells revealed that long IgH CDR3 favored polyreactivity, whereas the presence of positively charged amino acids was associated with HEp-2 reactivity, polyreactivity, and antinuclear reactivity (Supplementary Figure 5).

Since the regulation of the peripheral B cell tolerance checkpoint involves T cells and potentially Treg cells (14–17), we assessed Treg cell frequency and suppressive function in patients with SSc (Figure 3). We found that the proportion of Treg cells in the blood of 16 patients with SSc was globally similar and potentially increased in patients with dcSSc compared to healthy

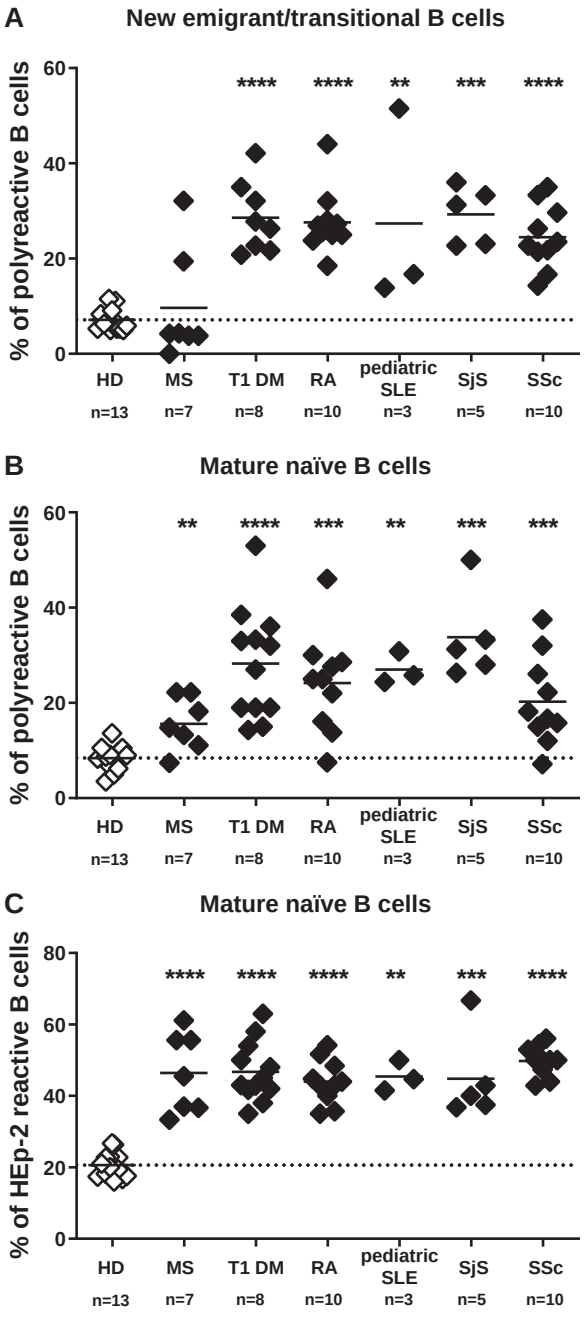

Figure 4. Defective central and peripheral B cell tolerance checkpoints in many autoimmune diseases. The frequencies of polyreactive new emigrant/transitional B cells (**A**), polyreactive mature naive B cells (**B**), and HEp-2–reactive mature naive B cells (**C**) were compared between healthy donors, patients with multiple sclerosis (MS), patients with type 1 diabetes mellitus (T1 DM), patients with rheumatoid arthritis (RA), pediatric patients with systemic lupus erythematosus (SLE), patients with primary Sjögren's syndrome (SjS), and patients with systemic sclerosis (SSc). Open diamonds represent healthy donors, and solid diamonds represent patients with autoimmune disease; horizontal lines show the median. Dotted lines show the median in healthy donors. ** = $P < 0.01$; *** = $P < 0.001$; **** = $P < 0.0001$, by Mann-Whitney U test.

donors, as previously reported (18,19) (Figures 3A and B). Healthy donor and SSc patient Treg cells similarly suppressed in vitro the induced proliferation of CD4+CD127+ T responder cells isolated from either healthy donors or patients with SSc (Figures 3C and D). In contrast, we observed that T responder cells from patients with SSc, which included dcSSc patient 210, dcSSc patient 366, lcSSc patient 368, and lcSSc patient 369, who displayed defective autoreactive B cell selection, were refractory to suppression by either autologous Treg cells isolated from the same patients or heterologous Treg cells isolated from healthy donors (Figures 3D and E). Hence, altered T cell responses in patients with SSc correlate with the impaired selection of autoreactive B cells in the periphery.

BAFF is a molecule that controls the number of peripheral B cells and may interfere with peripheral B cell tolerance (20). We found that patients with SSc displayed serum BAFF concentrations similar to those in healthy donors, suggesting that BAFF is not responsible for peripheral B cell selection defects in SSc (Supplementary Figure 8, available on the *Arthritis & Rheumatology* website at http://onlinelibrary.wiley.com/doi/10.1002/art.41927/abstract). We conclude that patients with SSc have a dysfunctional peripheral B cell tolerance checkpoint.

Failure of early B cell tolerance checkpoints in most autoimmune diseases. We compared the frequencies of polyreactive and HEp-2–reactive clones in the new emigrant/transitional and mature naive B cell compartments of patients with SSc to those in patients with other autoimmune diseases that we previously tested (3). We found that the elevated frequencies of polyreactive new emigrant/transitional B cells observed in patients with SSc differed from those in healthy donors and patients with MS but were similar to those in patients with type 1 DM, RA, pediatric SLE, or SS, revealing that central B cell tolerance defects are a common feature of these autoimmune diseases—excluding MS (3) (Figure 4A). In contrast, patients with these autoimmune diseases, including MS, displayed an impaired peripheral B cell tolerance checkpoint, resulting in the accumulation of both polyreactive and HEp-2–reactive B cells in their blood (Figures 4B and C). Hence, the dysregulated removal of developing autoreactive naive B cells continuously produced throughout life correlates with autoimmunity.

DISCUSSION

We report herein that patients with SSc display impaired central and peripheral B cell tolerance checkpoints, which results in the increased production of autoreactive naive B cells. In addition, we showed that V(D)J recombination of germline Ig gene segments can produce immature B cells that recognize SSc-specific self antigens (i.e., topoisomerase I) in the absence of somatic hypermutation or affinity maturation. Consistent with this observation, it was recently reported that the activation of transitional B cells isolated from patients with SSc could lead to the detection of anti–topoisomerase I antibody secretion (21). Reversion experiments that consisted of removing somatic hypermutation in self-antigen–specific mutated antibodies previously suggested that circulating pathogenic autoantibodies targeting the aquaporin 4 water channel in patients with NMOSD can originate from autoreactive naive B cells, which escape early B cell tolerance checkpoints (22).

Our data further support the notion of a direct contribution of impaired central and peripheral B cell tolerance checkpoints in promoting autoimmune diseases through the production of self antigen–specific naive B cells that may not only present self antigens to T cells and initiate autoimmune responses, but also be the precursors of the plasma cells secreting autoantibodies involved in the formation of immune complexes. Defective autoreactive B cell selection likely plays an important role in SSc pathophysiology since it was recently reported that the secretion of autoantibodies and the formation of immune complexes in patients with SSc promote fibrosis through the activation of fibroblasts via interleukin-6 (IL-6)– and macrophage colony-stimulating factor–induced osteopontin secretion by macrophages (4).

It remains to be determined if autoantibodies in SSc may originate from the activation of autoreactive new emigrant/transitional or mature naive B cells. The identification of anti–topoisomerase I–reactive clones in the new emigrant/transitional B cell compartment of patients with SSc, in this study and previously (21), further supports a direct involvement of transitional B cells in autoantibody secretion in autoimmune diseases. Several studies have suggested that antinuclear autoantibodies in SLE may be secreted upon transitional B cell activation via Toll-like receptor 7 (TLR-7) and interferon-α (IFNα) (23–25). Since a type I IFN–induced gene signature typically associated with SLE is also present in about half of SSc patients, it is plausible that the latter scenario may also promote autoantibody production in SSc (26,27). In addition, secretion of IFNα by plasmacytoid dendritic cells is enhanced in SSc due to dysregulated and enhanced TLR function (28,29).

Transitional B cells can also be stimulated by TLR-9 ligands, which induce cell proliferation, somatic hypermutation, and antibody secretion (30). However, B cell receptor (BCR)/TLR-9 cotriggering normally prevents the production of autoreactive antibodies targeting DNA-containing self antigens by inducing B cell death (31). Thus, anti–topoisomerase I–reactive transitional B cells from patients with SSc may develop in antibody-secreting cells if TLR-9 tolerogenic function is impaired. While TLR-9 function is defective in naive B cells from patients with SLE who also secrete autoantibodies targeting DNA-containing antigens such as anti-dsDNA and antihistones (32), Taher et al suggested that TLR-9 responses in total B cells from patients with SSc may also be decreased compared to their healthy donor counterparts (21). Hence, impaired TLR-9 function following the cocrosslinking of autoreactive BCRs with TLR-9 by DNA-containing

self antigens may allow for the survival of anti–topoisomerase I–reactive transitional B cells in patients with dcSSc and anticentromere-reactive clones in patients with lcSSc, and may lead to the secretion of autoreactive antibodies in the serum of these patients.

We cannot rule out the possibility that autoantibodies may also emerge from the activation of mature naive B cells, which also contained antinuclear-reactive clones in patients with SSc or other autoimmune diseases. Impaired early B cell tolerance checkpoints and the production of autoreactive B cells may also favor autoimmunity via the secretion of proinflammatory cytokines such as granulocyte–macrophage colony-stimulating factor in SSc and MS (33,34) or IL-6 in SSc and RA (21,35). B cell production of lymphotoxin β may also favor tertiary lymphoid organ formation (36). Regardless, rituximab, which eliminates B cells, has shown therapeutic efficacy in SSc, further solidifying the importance of B cells in SSc pathophysiology (37,38). Alternatively, restoring central B cell tolerance may represent a novel alternative therapeutic strategy to prevent autoantibody secretion and the formation of immune complexes, which may slow down or stop fibrotic processes in SSc (9).

What are the origins of defective central and peripheral B cell tolerance checkpoints in SSc? The analysis of early B cell tolerance checkpoints in patients with primary immunodeficiency with rare genetic mutations has revealed that decreased signaling from receptors that recognize self antigens at the immature B cell stage, i.e., the BCR and potentially TLRs, resulted in an impaired central B cell tolerance, whereas decreased Treg cell numbers, defective Treg cell suppressive function, or T cells refractory to Treg cell suppression were associated with an increase in autoreactive clones in the mature naive B cell compartment (3,14–17).

Consistent with these observations, the 1858T polymorphism in the PTPN22 gene identified by genome-wide association studies (GWAS) is associated with type 1 DM, RA, SLE, and SSc (5–7), decreases BCR and TCR signaling in human cells, and interferes with developing autoreactive B cell counterselection (8,9,39,40). Three of the 10 patients with SSc enrolled in this study harbored the 1858T PTPN22 variant, which likely accounts for their defective early B cell tolerance checkpoints (8,9). Other gene variants associated with SSc, SLE, and other autoimmune diseases encoding B cell–specific scaffold protein with ankyrin repeats 1 and B lymphocyte kinase, both of which regulate BCR and TLR signaling, may also contribute to the alteration of central B cell tolerance in SSc (41–44).

In contrast to central B cell tolerance, the peripheral B cell tolerance checkpoint relies on B cell extrinsic factors such as T cells. Indeed, the absence of T cells in CD3-deficient patients or defective Treg cell function in FoxP3-deficient patients, or in other patients with primary immunodeficiencies, resulted in an impaired peripheral B cell tolerance checkpoint (14–17). T cells may also provide survival signals to autoreactive B cells and favor the accumulation of autoreactive B cells. For instance, defective thymocyte selection in autoimmune regulator deficiency, which favors the accumulation of autoreactive T cells in the conventional CD4+ rather than in the Treg cell compartment, results in the expansion of anti-insulin mature naive B cells that are not detected in the absence of T cells in patients with CD3D or CD3E deficiency (14,45). While Treg cell numbers and suppression function in SSc appeared unaffected, we found that T responder cells from patients with SSc were refractory to Treg cell suppression in vitro. Similarly, patients with either type 1 DM or X-linked lymphoproliferative disease caused by signaling lymphocytic activation molecule–associated protein deficiency also displayed T responder cells that are refractory to Treg cell suppression in vitro, a feature that correlated with a defective peripheral B cell tolerance checkpoint (11,46).

The increased production of various cytokines in SSc, especially IL-4 and IL-6, may alter Treg cell suppression in vitro and favor the fibrotic process (11,47). In addition to rendering T responder cells refractory to Treg cells and perhaps directly affecting Treg cell suppressive function, Th2/Tfh cytokines in SSc, including IL-4, IL-6, IL-10, and IL-21, favor B cell activation, class-switch recombination, plasma cell development, and the production of anti–topoisomerase I autoantibodies (48–50). Moreover, and consistent with the type I IFN signature common in SSc, polymorphisms identified by GWAS in several IFN regulatory factor genes are associated with SSc and may also favor autoantibody secretion (51).

In conclusion, our study demonstrates that patients with SSc display multiple defective B cell tolerance mechanisms, ultimately resulting in the production of autoreactive naive B cells and secretion of autoantibodies that target specific self antigen. Impaired early B cell tolerance checkpoints in SSc may be caused by polymorphisms or rare genetic mutations, as is frequently the case in other autoimmune diseases and primary immunodeficiencies. Alternatively, it is conceivable that cytokines or chemokines, both of which are routinely found at elevated concentrations in the serum of patients with autoimmune diseases, may also interfere with the counterselection of autoreactive B cells either in the bone marrow or periphery. Indeed, SSc is associated with a common type I IFN signature and aberrant cytokine and/or chemokine profiles that may influence B cell selection and disease progression. Additional investigations are therefore warranted to explore such hypotheses.

ACKNOWLEDGMENTS

We thank Dr. L. Devine and C. Wang for cell sorting.

AUTHOR CONTRIBUTIONS

All authors were involved in drafting the article or revising it critically for important intellectual content, and all authors approved the final version to be published. Dr. Meffre had full access to all of the data in the study and takes responsibility for the integrity of the data and the accuracy of the data analysis.

Study conception and design. Hansen, Ryu, Herzog, Meffre.
Acquisition of data. Glauzy, Olson, May, Parisi, Massad.
Analysis and interpretation of data. Glauzy, Olson, May, Parisi, Massad.

REFERENCES

1. LeRoy EC, Black C, Fleischmajer R, Jablonska S, Krieg T, Medsger TA Jr, et al. Scleroderma (systemic sclerosis): classification, subsets and pathogenesis. J Rheumatol 1988;15:202–5.
2. Gabrielli A, Avvedimento EV, Krieg T. Scleroderma. N Engl J Med 2009;360:1989–2003.
3. Meffre E, O'Connor KC. Impaired B-cell tolerance checkpoints promote the development of autoimmune diseases and pathogenic autoantibodies. Immunol Rev 2019;292:90–101.
4. Gao X, Jia G, Guttman A, DePianto DJ, Morshead KB, Sun KH, et al. Osteopontin links myeloid activation and disease progression in systemic sclerosis. Cell Rep Med 2020;1:100140.
5. Cho JH, Gregersen PK. Genomics and the multifactorial nature of human autoimmune disease. New Engl J Med 2011;365:1612–23.
6. Gourh P, Tan FK, Assassi S, Ahn CW, McNearney TA, Fischbach M, et al. Association of the PTPN22 R620W polymorphism with anti–topoisomerase I– and anticentromere antibody–positive systemic sclerosis. Arthritis Rheum 2006;54:3945–53.
7. Dieudé P, Guedj M, Wipff J, Avouac J, Hachulla E, Diot E, et al. The PTPN22 620W allele confers susceptibility to systemic sclerosis: findings of a large case–control study of European Caucasians and a meta-analysis. Arthritis Rheum 2008;58:2183–8.
8. Menard L, Saadoun D, Isnardi I, Ng YS, Meyers G, Massad C, et al. The PTPN22 allele encoding an R620W variant interferes with the removal of developing autoreactive B cells in humans. J Clin Invest 2011;121:3635–44.
9. Schickel JN, Kuhny M, Baldo A, Bannock JM, Massad C, Wang H, et al. PTPN22 inhibition resets defective human central B cell tolerance. Sci Immunol 2016;1: aaf7153.
10. Wardemann H, Yurasov S, Schaefer A, Young JW, Meffre E, Nussenzweig MC. Predominant autoantibody production by early human B cell precursors. Science 2003;301:1374–7.
11. Menard L, Cantaert T, Chamberlain N, Tangye SG, Riminton S, Church JA, et al. Signaling lymphocytic activation molecule (SLAM)/SLAM-associated protein pathway regulates human B-cell tolerance. J Allergy Clin Immunol 2014;133:1149–61.
12. Klonowski KD, Primiano LL, Monestier M. Atypical VH-D-JH rearrangements in newborn autoimmune MRL mice. J Immunol 1999;162: 1566–72.
13. Dellavance A, Gallindo C, Soares MG, da Silva NP, Mortara RA, Andrade LE. Redefining the Scl-70 indirect immunofluorescence pattern: autoantibodies to DNA topoisomerase I yield a specific compound immunofluorescence pattern. Rheumatology (Oxford) 2009; 48:632–7.
14. Sng J, Ayoglu B, Chen JW, Schickel JN, Ferre EM, Glauzy S, et al. AIRE expression controls the peripheral selection of autoreactive B cells. Sci Immunol 2019;4: eaav6778.
15. Kinnunen T, Chamberlain N, Morbach H, Choi J, Kim S, Craft J, et al. Accumulation of peripheral autoreactive B cells in the absence of functional human regulatory T cells. Blood 2013;121: 1595–603.
16. Hervé M, Isnardi I, Ng YS, Bussel JB, Ochs HD, Cunningham-Rundles C, et al. CD40 ligand and MHC class II expression are essential for human peripheral B cell tolerance. J Exp Med 2007;204: 1583–93.
17. Cantaert T, Schickel JN, Bannock JM, Ng YS, Massad C, Delmotte FR, et al. Decreased somatic hypermutation induces an impaired peripheral B cell tolerance checkpoint. J Clin Invest 2016; 126:4289–302.
18. Slobodin G, Ahmad MS, Rosner I, Peri R, Rozenbaum M, Kessel A, et al. Regulatory T cells (CD4(+)CD25(bright)FoxP3(+)) expansion in systemic sclerosis correlates with disease activity and severity. Cell Immunol 2010;261:77–80.
19. Radstake TR, van Bon L, Broen J, Wenink M, Santegoets K, Deng Y, et al. Increased frequency and compromised function of T regulatory cells in systemic sclerosis (SSc) is related to a diminished CD69 and TGFβ expression. PLoS One 2009;4:e5981.
20. Mackay F, Schneider P. Cracking the BAFF code. Nat Rev Immunol 2009;9:491–502.
21. Taher TE, Ong VH, Bystrom J, Hillion S, Simon Q, Denton CP, et al. Association of defective regulation of autoreactive interleukin-6–producing transitional B lymphocytes with disease in patients with systemic sclerosis. Arthritis Rheumatol 2018;70:450–61.
22. Cotzomi E, Stathopoulos P, Lee CS, Ritchie AM, Soltys JN, Delmotte FR, et al. Early B cell tolerance defects in neuromyelitis optica favour anti-AQP4 autoantibody production. Brain 2019;142: 1598–615.
23. Giltiay NV, Chappell CP, Sun X, Kolhatkar N, Teal TH, Wiedeman AE, et al. Overexpression of TLR7 promotes cell-intrinsic expansion and autoantibody production by transitional T1 B cells. J Exp Med 2013; 210:2773–89.
24. Menon M, Blair PA, Isenberg DA, Mauri C. A Regulatory feedback between plasmacytoid dendritic cells and regulatory B cells is aberrant in systemic lupus erythematosus. Immunity 2016;44: 683–97.
25. Piper CJ, Wilkinson MG, Deakin CT, Otto GW, Dowle S, Duurland CL, et al. $CD19^{+}CD24^{hi}CD38^{hi}$ B cells are expanded in juvenile dermatomyositis and exhibit a pro-inflammatory phenotype after activation through Toll-like receptor 7 and interferon-α. Front Immunol 2018;9: 1372.
26. Kim D, Peck A, Santer D, Patole P, Schwartz SM, Molitor JA, et al. Induction of interferon-α by scleroderma sera containing autoantibodies to topoisomerase I: association of higher interferon-α activity with lung fibrosis. Arthritis Rheum 2008;58:2163–73.
27. Wu M, Assassi S. The role of type 1 interferon in systemic sclerosis. Front Immunol 2013;4:266.
28. Ah Kioon MD, Tripodo C, Fernandez D, Kirou KA, Spiera RF, Crow MK, et al. Plasmacytoid dendritic cells promote systemic sclerosis with a key role for TLR8. Sci Transl Med 2018;10: eaam8458.
29. Van Bon L, Affandi AJ, Broen J, Christmann RB, Marijnissen RJ, Stawski L, et al. Proteome-wide analysis and CXCL4 as a biomarker in systemic sclerosis. N Engl J Med 2014;370:433–43.
30. Aranburu A, Ceccarelli S, Giorda E, Lasorella R, Ballatore G, Carsetti R. TLR ligation triggers somatic hypermutation in transitional B cells inducing the generation of IgM memory B cells. J Immunol 2010;185:7293–301.
31. Sindhava VJ, Oropallo MA, Moody K, Naradikian M, Higdon LE, Zhou L, et al. A TLR9-dependent checkpoint governs B cell responses to DNA-containing antigens. J Clin Invest 2017;127: 1651–63.
32. Gies V, Schickel JN, Jung S, Joublin A, Glauzy S, Knapp AM, et al. Impaired TLR9 responses in B cells from patients with systemic lupus erythematosus. JCI Insight 2018;3:e96795.
33. Higashioka K, Kikushige Y, Ayano M, Kimoto Y, Mitoma H, Kikukawa M, et al. Generation of a novel CD30+ B cell subset producing GM-CSF and its possible link to the pathogenesis of systemic sclerosis. Clin Exp Immunol 2020;201:233–43.
34. Li R, Rezk A, Miyazaki Y, Hilgenberg E, Touil H, Shen P, et al. Proinflammatory GM-CSF-producing B cells in multiple sclerosis and B cell depletion therapy. Sci Transl Med 2015;7:310ra166.
35. Mensah KA, Chen JW, Schickel JN, Isnardi I, Yamakawa N, Vega-Loza A, et al. Impaired ATM activation in B cells is associated with bone resorption in rheumatoid arthritis. Sci Transl Med 2019;11: eaaw4626.
36. Alsughayyir J, Pettigrew GJ, Motallebzadeh R. Spoiling for a fight: B lymphocytes as initiator and effector populations within tertiary

lymphoid organs in autoimmunity and transplantation. Front Immunol 2017;8:1639.

37. Bosello SL, De Luca G, Rucco M, Berardi G, Falcione M, Danza FM, et al. Long-term efficacy of B cell depletion therapy on lung and skin involvement in diffuse systemic sclerosis. Semin Arthritis Rheum 2015;44:428–36.
38. Ebata S, Yoshizaki A, Fukasawa T, Miura S, Takahashi T, Sumida H, et al. Rituximab therapy is more effective than cyclophosphamide therapy for Japanese patients with anti-topoisomerase I-positive systemic sclerosis-associated interstitial lung disease. J Dermatol 2019; 46:1006–13.
39. Arechiga AF, Habib T, He Y, Zhang X, Zhang ZY, Funk A, et al. Cutting edge: the PTPN22 allelic variant associated with autoimmunity impairs B cell signaling. J Immunol 2009;182:3343–7.
40. Rieck M, Arechiga A, Onengut-Gumuscu S, Greenbaum C, Concannon P, Buckner JH. Genetic variation in PTPN22 corresponds to altered function of T and B lymphocytes. J Immunol 2007;179: 4704–10.
41. Dieudé P, Wipff J, Guedj M, Ruiz B, Melchers I, Hachulla E, et al. BANK1 is a genetic risk factor for diffuse cutaneous systemic sclerosis and has additive effects with IRF5 and STAT4. Arthritis Rheum 2009; 60:3447–54.
42. Ito I, Kawaguchi Y, Kawasaki A, Hasegawa M, Ohashi J, Kawamoto M, et al. Association of the FAM167A-BLK region with systemic sclerosis. Arthritis Rheum 2010;62:890–5.
43. Coustet B, Dieudé P, Guedj M, Bouaziz M, Avouac J, Ruiz B, et al. C8orf13-BLK is a genetic risk locus for systemic sclerosis and has additive effects with BANK1: results from a large French cohort and meta-analysis. Arthritis Rheum 2011;63:2091–6.
44. Wu YY, Kumar R, Iida R, Bagavant H, Alarcon-Riquelme ME. BANK1 regulates IgG production in a lupus model by controlling TLR7-dependent STAT1 activation. PLoS One 2016;11:e0156302.
45. Malchow S, Leventhal DS, Lee V, Nishi S, Socci ND, Savage PA. Aire enforces immune tolerance by directing autoreactive T cells into the regulatory T cell lineage. Immunity 2016;44:1102–13.
46. Schneider A, Rieck M, Sanda S, Pihoker C, Greenbaum C, Buckner JH. The effector T cells of diabetic subjects are resistant to regulation via CD4+ FOXP3+ regulatory T cells. J Immunol 2008; 181:7350–5.
47. O'Reilly S, Hugle T, van Laar JM. T cells in systemic sclerosis: a reappraisal. Rheumatology (Oxford) 2012;51:1540–9.
48. Fairfax KA, Kallies A, Nutt SL, Tarlinton DM. Plasma cell development: from B-cell subsets to long-term survival niches. Semin Immunol 2008;20:49–58.
49. Arpin C, Dechanet J, Van Kooten C, Merville P, Grouard G, Briere F, et al. Generation of memory B cells and plasma cells in vitro. Science 1995;268:720–2.
50. McGaha T, Saito S, Phelps RG, Gordon R, Noben-Trauth N, Paul WE, et al. Lack of skin fibrosis in tight skin (TSK) mice with targeted mutation in the interleukin-4R α and transforming growth factor-β genes. J Invest Dermatol 2001;116:136–43.
51. Broen JC, Radstake TR, Rossato M. The role of genetics and epigenetics in the pathogenesis of systemic sclerosis. Nat Rev Rheumatol 2014;10:671–81.

American College of Rheumatology
Empowering Rheumatology Professionals

Arthritis & Rheumatology
Vol. 74, No. 2, February 2022, pp 318–328
DOI 10.1002/art.41926

Platelet Phagocytosis via P-selectin Glycoprotein Ligand 1 and Accumulation of Microparticles in Systemic Sclerosis

Angelo A. Manfredi,[1] Giuseppe A. Ramirez,[1] Cosmo Godino,[1] Annalisa Capobianco,[1] Antonella Monno,[1] Stefano Franchini,[1] Enrico Tombetti,[1] Sara Corradetti,[1] Jörg H. W. Distler,[2] Marco E. Bianchi,[1] Patrizia Rovere-Querini,[1] and Norma Maugeri[1]

Objective. It is unclear why activated platelets and platelet-derived microparticles (MPs) accumulate in the blood of patients with systemic sclerosis (SSc). This study was undertaken to investigate whether defective phagocytosis might contribute to MP accumulation in the blood of patients with SSc.

Methods. Blood samples were obtained from a total of 81 subjects, including 25 patients with SSc and 26 patients with stable coronary artery disease (CAD). Thirty sex- and age-matched healthy volunteers served as controls. Studies were also conducted in NSG mice, in which the tail vein of the mice was injected with MPs, and samples of the lung parenchyma were obtained for analysis of the pulmonary microvasculature. Tissue samples from human subjects and from mice were assessed by flow cytometry and immunochemical analyses for determination of platelet–neutrophil interactions, phagocytosis, levels and distribution of P-selectin, P-selectin glycoprotein ligand 1 (PSGL-1), and HMGB1 on platelets and MPs, and concentration of byproducts of neutrophil extracellular trap (NET) generation/catabolism.

Results. Activated P-selectin+ platelets and platelet-derived HMGB1+ MPs accumulated in the blood of SSc patients but not in the blood of healthy controls. Patients with CAD, a vasculopathy independent of systemic inflammation, had fewer P-selectin+ platelets and a negligible number of MPs. The expression of the receptor for P-selectin, PSGL-1, in neutrophils from SSc patients was significantly decreased, raising the possibility that phagocytes in SSc do not recognize activated platelets, leading to a failure of phagocytosis and continued neutrophil release of MPs. As evidence of this process, activated platelets were not detected in the neutrophils from SSc patients, whereas they were consistently present in the neutrophils from patients with CAD. HMGB1+ MPs elicited generation of NETs, which were only detected in the plasma of SSc patients. In mice, P-selectin–PSGL-1 interaction resulted in platelet phagocytosis in vitro and influenced the ability of MPs to elicit NETs, endothelial activation, and migration of leukocytes through the pulmonary microvasculature.

Conclusion. The clearance of activated platelets via PSGL-1 limits the undesirable effects of MP-elicited neutrophil activation. This balance is disrupted in patients with SSc. Its reconstitution might curb vascular inflammation and prevent fibrosis.

INTRODUCTION

Systemic sclerosis (SSc) is a rare disease with a high unmet medical need and few effective therapies (1,2). Early events in SSc include activation and death of endothelial cells, loss of capillaries, and exposure of subendothelial tissue. The microvascular damage results in thickening of the medial layer, hyperplasia of the intima, and obliteration of the lumen (2). Findings from a recent comprehensive whole blood transcriptome analysis highlighted the importance of platelet activation and degranulation among pathways replicated in different cohorts of patients (3), an observation consistent with the notion that platelets undergo activation in SSc (4,5). Neutrophils have also attracted attention as major players in SSc vascular damage and organ

Supported by the Gruppo Italiano per la Lotta alla Sclerodermia and the Associazione Italiana Ricerca sul Cancro (grant 20351).

[1]Angelo A. Manfredi, MD, Giuseppe A. Ramirez, MD, Cosmo Godino, MD, Annalisa Capobianco, PhD, Antonella Monno, BSc, Stefano Franchini, MD, Enrico Tombetti, MD, PhD, Sara Corradetti, MD, Marco E. Bianchi, PhD, Patrizia Rovere-Querini, MD, PhD, Norma Maugeri, PhD: Università Vita-Salute San Raffaele and IRCCS San Raffaele Scientific Institute, Milan, Italy; [2]Jörg H. W. Distler, MD, PhD: Friedrich-Alexander-University (FAU) Erlangen-Nürnberg and Universitätsklinikum Erlangen, Erlangen, Germany.

Dr. Bianchi is the founder and co-owner of HMGBiotech. No other disclosures relevant to this article were reported.

Address correspondence to Norma Maugeri, PhD, via Olgettina 58, Milan, Italy. Email: maugeri.norma@hsr.it.

Submitted for publication November 10, 2020; accepted in revised form July 8, 2021.

damage. They are the major determinant of gene expression in the blood of patients with SSc (3).

Microparticles (MPs), membrane-bound structures that are released from activated or dying cells, shuttle bioactive molecules to influence homeostasis at a distance and might contribute to microvascular disease in SSc (6). These structures are derived from endothelial cells and platelets, and they accumulate in the blood of patients with SSc (7–11). MPs perform potentially important functions, including transporting various inflammatory signals, known as damage-associated molecular patterns (DAMPs), such as the prototypical signal HMGB1 (11) and mitochondrial DNA. Furthermore, when MPs derived from SSc patients are injected into immunocompromised mice, many features of human SSc are reproduced, such as microvascular alterations and tissue fibrosis (11).

Activated neutrophils and platelets carry out antimicrobial and hemostatic actions in inflamed tissue. Their interaction contributes to leukocytes extravasation and migration to the inflamed tissue and increases the production of neutrophil extracellular traps (NETs) (12,13), an event dependent on HMGB1 presentation to neutrophils (10,13–16).

Phagocytosis eliminates activated platelets from the bloodstream, removing a procoagulant template and a source of signals that damage the microvasculature (17–19). Phagocytes comprise endothelial cells and macrophages (18,19). Neutrophils also recognize P-selectin on tethered activated platelets via the P-selectin glycoprotein 1 (PSGL-1) receptor and internalize them via a phosphatidylserine-dependent pathway (20,21). Of note, PSGL-1 alterations have been described in SSc, while PSGL-1–deficient mice develop scleroderma features, including activation and dysfunction of the pulmonary endothelial cells (22–24).

The accumulation of activated platelets and platelet-derived MPs in SSc is well established (5), but we do not have mechanistic information on the underlying causes and processes. We reasoned that defective phagocytosis of activated platelets could account for their accumulation. In turn, activated platelets that have escaped clearance could generate MPs that reach distant sites through the circulatory system (25,26), perpetuating injury and remodeling the microvasculature (11,27,28) possibly via the activation of neutrophils and the generation of NETs (11,29). Using an approach that combines in vitro and in vivo studies and clinical investigation, we have discovered that clearance of activated platelets by vascular neutrophils prevents the accumulation of bioactive platelet-derived MPs, thus protecting the microvasculature. This pathway requires integrity of the P-selectin–PSGL-1 axis, which is defective in patients with SSc.

PATIENTS AND METHODS

Patients. The study group consisted of 25 patients classified as having SSc according to the 2013 American College of Rheumatology/European Alliance of Associations for Rheumatology criteria for SSc (30). Patients with other systemic autoimmune disorders or overlap syndromes were excluded. Thirty age-matched healthy donors (median age 52 years [range 25–74 years] years; 36 women, 17 men) and 26 patients with coronary artery disease (CAD), confirmed using coronary angiography, were enrolled as controls. The demographic and clinical characteristics of patients with SSc and healthy controls are summarized in Table 1. Written informed consent was obtained from all subjects. The institutional review board at the San Raffaele Scientific Institute approved the study protocol.

Reagents and monoclonal antibodies (mAb). Monoclonal antibodies against CD15 (clone 80H5), CD42 (clone SZ1), CD45 (clone J33), CD61 (clone SZ21), CD66b (clone 80H3), CD62P (clone Thromb-6), PSGL-1 (clone PL-1), relevant IgG isotype controls mAb for flow cytometry, ThromboFix, and Flow-Count Fluorospheres were obtained from Beckman Coulter. Monoclonal IgG1 isotype control (clone W3/25) was obtained from Acris Antibodies. Reagent mAb against HMGB1 (clone HAP-46.5), PGE1, Cell Death Detection Kit, glycated albumin, Thrombin Receptor Agonist Peptide-6 (TRAP-6), and Hoechst were obtained from Sigma. Fix & Perm Kit was from Caltag. Recombinant human interleukin-8 (IL-8) was from R&D. Enzyme-linked immunosorbent assay (ELISA) kit for E-selectin was obtained from Cabru. Zenon Alexa Fluor mouse IgG1 Labeling kits (488 or 546) were obtained from Invitrogen. Rabbit polyclonal anti-H4 histone (citrulline R3, polyclonal antibody ab81797) was obtained from Abcam. Reagent mAb anti-human MPO used for the determination of DNA–MPO complexes was from ABD Serotec, and mAb against activated Mac-1 (clone CBRM1/5) was obtained from BioLegend. BoxA and recombinant HMGB1 were obtained from HMGBiotech.

Blood sampling. Venous blood was drawn using a 19-gauge butterfly needle. After discarding the first 3–5 ml, blood was carefully collected in tubes containing EDTA, to purify MPs, platelets, and neutrophils and to assess the concentration of NET byproducts. Other blood samples were collected in tubes containing sodium citrate and antiproteases, to be analyzed by flow cytometry (10,11,13,20,21).

Flow cytometry. All blood samples were analyzed using a daily aligned Navios flow cytometer (Beckman Coulter). Whole blood samples were immediately fixed with equal volumes of ThromboFix, stored at 4°C, and analyzed within 6–24 hours. The extent of platelet and leukocyte activation and platelet phagocytosis by neutrophils was assessed using multiparametric flow cytometry, as previously described (20,21,31). Quantification of MPs in platelet-free plasma or in the supernatant of purified platelets stimulated in the presence or the absence of autologous neutrophils was performed as described (10) (see Supplementary Figures 1–4 for the gating strategy used for each experimental

Table 1. Demographic and clinical characteristics of the SSc patients, CAD patients, and healthy controls*

	Healthy controls (n = 30)	SSc patients (n = 25)	CAD patients (n = 26)
Sex, female/male	–	23/2	3/23
Age, median (range) years	59 (46–74)	57 (33–79)	60 (46–78)
History of CVD	0	5	26
History of neoplasm	0	0	0
Disease duration, median (range) years	–	3 (1–22)	–
Diffuse SSc/limited SSc	–	8/17	–
Sicca syndrome	–	5	–
MRSS, median (range)	–	5 (0–26)	–
NVC (scleroderma pattern/unspecific findings)	–	16/9	–
Fingertip ulcers	–	10	–
Pulmonary involvement			
ILD	–	7	–
Arterial PH	–	1	–
Autoantibody positivity			
ANA	–	20	–
Anti–topo I	–	6	–
ACA	–	11	–
Treatment			
Aspirin	3	6	21
Thienopyridine	0	2	7
HCQ	0	1	0
Prednisone	0	2	0
Dose, median (range) mg/day	–	6.25 (0–7.5)	–
Immunosuppressive drugs	–	1	–
Bosentan	–	2	–

* Except where indicated otherwise, values are the number of patients. SSc = systemic sclerosis; CAD = coronary artery disease; CVD = cardiovascular disease; MRSS = modified Rodnan skin thickness score; NVC = nailfold videocapillaroscopy; ILD = interstitial lung disease; PH = pulmonary hypertension; ANA = antinuclear antibody; anti–topo I = anti– topoisomerase I; ACA = anticentromere antibody; HCQ = hydroxychloroquine.

approach, available on the *Arthritis & Rheumatology* website at https://onlinelibrary.wiley.com/doi/10.1002/art.41926).

Human cells and preparation of MPs. Platelets and neutrophils were purified from samples of human peripheral blood and analyzed in a manner as previously described (10,11,13,21). To obtain platelet-derived MPs, purified platelets (10–100 $\times$ 10^5/μl, as indicated) were stimulated with TRAP-6 (25 μ*M*) for 5–60 minutes at 37°C in static conditions, placed in chilled water for 2 minutes, and centrifuged (2,000*g* for 15 minutes at 4°C). Supernatants were retrieved, centrifuged again (100,000*g* for 1 minute at 4°C), aliquoted, and frozen.

Assessment of platelet–neutrophil interaction. Platelets (1 $\times$ 10^5/μl) were stimulated with TRAP-6 (25 μ*M*) in the presence or the absence of autologous neutrophils (5 $\times$ 10^3/μl). At different time points (15–60 minutes), aliquots were fixed as detailed above and were stored at 4°C until the flow cytometry analysis was conducted. For the quantification and characterization of MPs, platelets were stimulated with TRAP-6 (25 μ*M*) in the presence or the absence of autologous neutrophils (5 $\times$ 10^3 μl). At different time points (15–60 minutes), samples were centrifuged (100,000*g* for 1 minute at 4°C), and supernatants were analyzed using flow cytometry (see Supplementary Figure 2, available on the *Arthritis & Rheumatology* website at https://onlinelibrary.wiley.com/doi/10.1002/art.41926). When indicated, platelets or platelet-derived MPs were pretreated with P-selectin–blocking mAb (10 μg/ml) before coincubation with neutrophils, or neutrophils were pretreated with anti–PSGL-1 mAb (10 μg/ml) before incubation with platelets and platelet-derived MPs (20). An irrelevant IgG1 isotype mAb (10 μg/ml) was used as a control.

Quantification of platelet phagocytosis by neutrophils was carried out as described (20,21). Briefly, fixed samples were permeabilized with Fix & Perm (according to the manufacturer's instructions), and intracellular platelets were identified by labeling with anti-CD61 mAb (Supplementary Figure 4, available on the *Arthritis & Rheumatology* website at https://onlinelibrary.wiley.com/doi/10.1002/art.41926).

Assessment of human NETs generating in vitro. NETs were generated as previously described (11,13). Briefly, neutrophils (5 $\times$ 10^6/ml) were placed on poly-L-lysine–coated slides for 20 minutes at 37°C and were either left unchallenged

or challenged with MPs derived from resting platelets, activated platelets, or platelets activated in the presence of autologous neutrophils (platelet-derived MPs generated in the presence of neutrophils) with or without blocking antibodies. When indicated, MPs were pretreated with the HMGB1 inhibitor BoxA (10 μg/ml) and with anti–P-selectin mAb (10 μg/ml), while neutrophils were pretreated with anti–PSGL-1 mAb (10 μg/ml). As positive controls for the analysis of NET formation, neutrophils were stimulated with recombinant IL-8 (100 ng/ml) or HMGB1 (10 μg/ml). After 20 minutes of incubation, plates were centrifuged (1,000*g* for 5 minutes at 4°C) and supernatants were retrieved, further cleared by centrifugation (100,000*g* for 5 minutes at 4°C), and frozen. Cell-free soluble DNA–MPO complexes were assessed in the culture supernatant or in the plasma using ELISA (see below). Slides were fixed with ThromboFix and then stored at 4°C for 18–48 hours until analyzed by confocal microscopy.

Mice. Ten-to-twelve–week-old male NOD.Cg-Prkdc<scid> Il2rg < tm1Wjl>/SzJ (NSG) mice were kindly provided by Monica Casucci (San Raffaele Scientific Institute). Mouse experiments were performed in accordance with national and institutional guidelines, and all experiments were approved by the Institutional Animal Care and Use Committee of the San Raffaele Scientific Institute.

Analysis of the in vivo effects of MPs in mice. Platelet-derived MPs released from resting platelets or activated platelets derived from human blood or MPs generated by platelets activated in the presence of autologous human neutrophils were injected into the tail vein of NSG mice (11). Sham-treated mice were injected with HEPES Tyrode's buffer (1 m*M* $CaCl_2$). After 18 hours, blood was obtained from the mouse orbital vein, and the concentrations of soluble E-selectin and of citrullinated histone 4 were assessed using ELISA (11). Lungs were isolated, fixed, and analyzed to assess inflammatory cell infiltration, tissue damage, and fibrosis.

NET quantification. MPO–DNA complexes, as well as the proportions of citrullinated histone 4, were identified using capture ELISA, as previously described (11,13,32).

Histochemical analyses of mouse lung tissue. Lungs were isolated and immediately fixed in 4% paraformaldehyde at 4°C for 6 hours. For better cryopreservation, the lung tissue was incubated with glucose at increasing concentrations (10%, 20%, and 30%; 24 hours of incubation at each concentration), and thereafter the tissue was embedded in OCT compound and stored at –80°C. Subsequently, 10-μm–thick lung slices were prepared for histochemical analyses.

Statistical analysis. Results were reported as the mean ± SEM, unless otherwise indicated. The normal distribution of each continuous variable was assessed using the Kolmogorov–Smirnov test. All patient data sets were found to be normally distributed. Statistical analyses were performed using one-way analysis of variance, followed by Bonferroni adjustment for multiple comparisons or Student's *t*-test for comparisons between 2 different groups. All tests were 2-sided, and *P* values lower than 0.05 were considered statistically significant. All analyses were performed using GraphPad Prism software version 5.

RESULTS

Failure of platelet phagocytosis in the blood of patients with SSc. In the blood of patients with SSc—and not that of sex- and age-matched healthy controls—there was accumulation of activated platelets, which were marked by expression of P-selectin (Figure 1A). Moreover, platelet-derived MPs accumulated in the blood of patients with SSc. Most platelet-derived MPs expressed the prototypical DAMP, HMGB1 (Figure 1B and Supplementary Table 1, https://onlinelibrary.wiley.com/doi/10.1002/art.41926). In contrast, only a small proportion of platelet-derived MPs expressed P-selectin (Supplementary Table 1), as expected (33).

P-selectin+ platelets were detected at significantly lower levels in the blood of patients with CAD, a condition in which vessel remodeling occurs in a manner independent of systemic inflammation. This observation may be consistent with the notion of reduced phagocyte removal of P-selectin+ platelets. As evidence of this, the blood of patients with SSc had significantly fewer neutrophils containing platelets compared to the blood of patients with CAD (Figure 1C).

Blood neutrophils from SSc patients expressed significantly lower levels of the P-selectin counterreceptors PSGL-1 and CD15s than neutrophils from healthy controls or those from patients with CAD (Figure 1D and Supplementary Table 2, available on the *Arthritis & Rheumatology* website at https://onlinelibrary.wiley.com/doi/10.1002/art.41926). This suggests that neutrophils in patients with SSc are less effective at recognizing activated platelets, the source of HMGB1+ platelet-derived MPs. To confirm this, platelets from the blood of healthy subjects and patients with CAD were activated with the selective agonist TRAP-6, which resulted in rapid and effective phagocytosis of the platelets by neutrophils. In contrast, the extent of phagocytosis was substantially less pronounced in the blood of SSc patients (Supplementary Table 3, available on the *Arthritis & Rheumatology* website at https://onlinelibrary.wiley.com/doi/10.1002/art.41926).

This failure of phagocytosis of platelets by neutrophils could explain the accumulation of HMGB1+ MPs in the blood of patients with SSc, known to trigger the generation of NETs. Indeed, byproducts of NETs were abundant in the blood of SSc patients, but not in sex- and age-matched healthy controls or CAD patients (Figure 1E). Platelet phagocytosis by

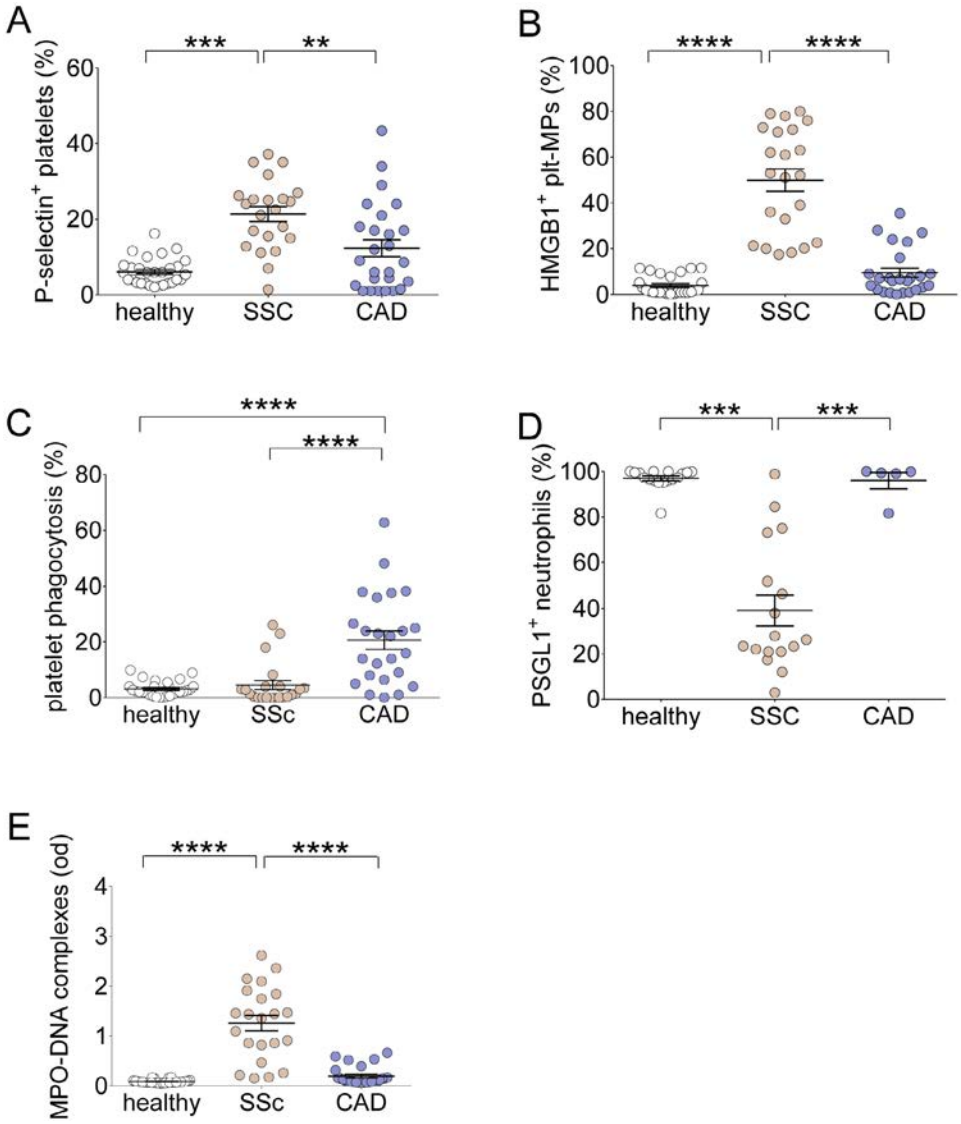

Figure 1. Biomarkers of platelet and neutrophil interaction. The percentages of P-selectin+ platelets (**A**), HMGB1+ platelet-derived microparticles (plt-MPs) (**B**), neutrophils incorporating intracellular platelets during phagocytosis (**C**), and P-selectin glycoprotein ligand 1–positive (PSGL-1+) neutrophils (**D**) as well as the concentration of myeloperoxidase (MPO)–DNA complexes in the blood (measured as optical density [od]) (**E**) were assessed in samples from patients with systemic sclerosis (SSc), patients with coronary artery disease (CAD), and healthy controls. Symbols represent individual samples; bars show the mean ± SEM. ** = $P < 0.01$; *** = $P < 0.001$; **** = $P < 0.0001$. Color figure can be viewed in the online issue, which is available at http://onlinelibrary.wiley.com/doi/10.1002/art.41926/abstract.

neutrophils, down-regulation of PSGL-1 expression by neutrophils, and accumulation of HMGB1+ MPs were all significantly more evident in SSc patients with interstitial lung disease (Supplementary Table 4, available on the *Arthritis & Rheumatology* website at https://onlinelibrary.wiley.com/doi/10.1002/art.41926). In contrast, no statistically significant differences were observed between patients with limited cutaneous SSc and those with the diffuse cutaneous SSc, or between patients who were positive for antitopoisomerase antibodies and patients who were positive for anticentromere antibodies (Supplementary Table 4).

Neutrophils hindering the release of MPs from activated platelets. We set up an in vitro system to verify cause-and-effect links between the phagocytic clearance of platelets and the accumulation of MPs. Platelets were purified from human blood and activated with TRAP-6, an agonist of the thrombin receptor, in the presence or the absence of autologous neutrophils. TRAP-6 is a selective platelet agonist and does not detectably influence neutrophils (20).

MPs accumulated in the supernatant of activated platelets. Conversely, we observed a reduction in the numbers of activated

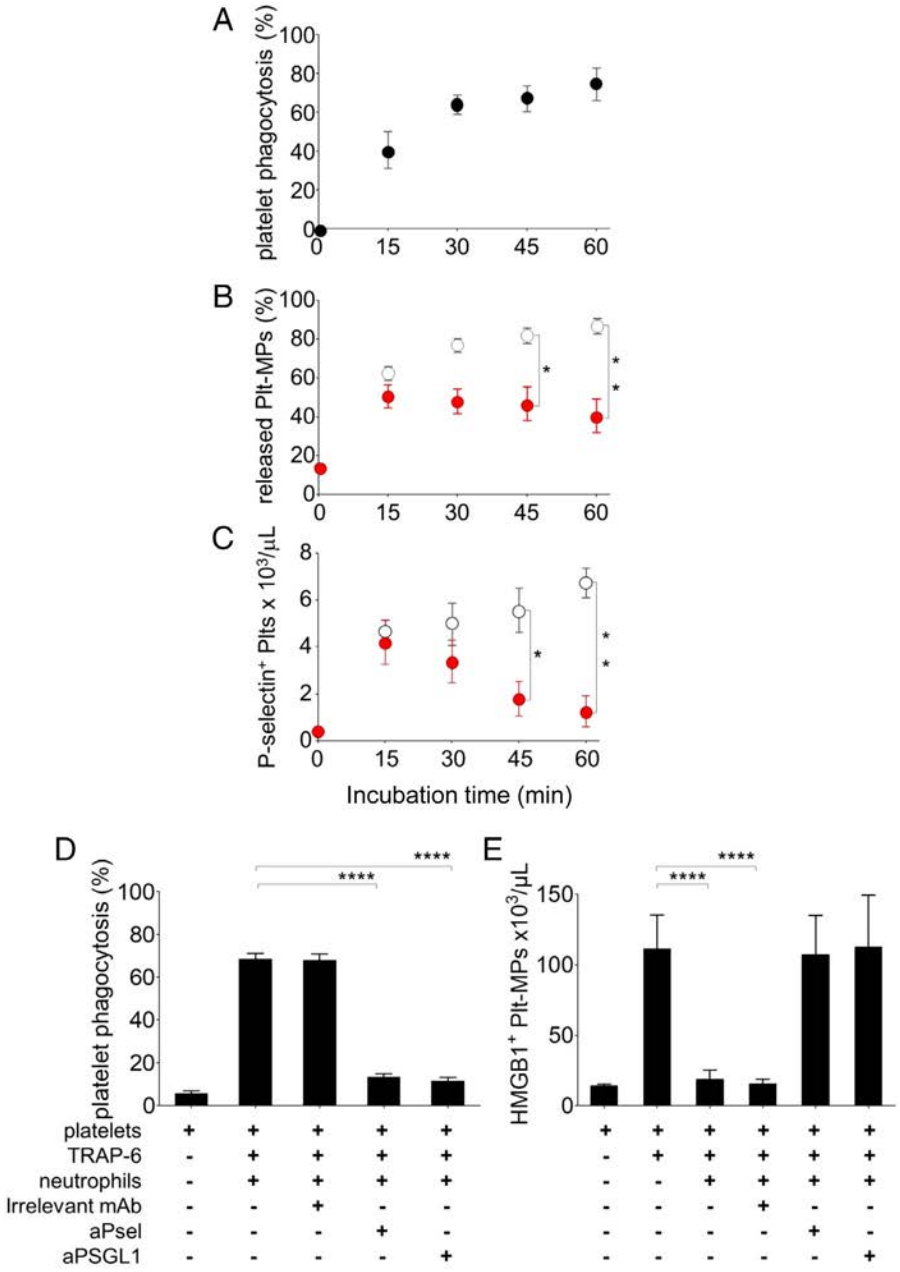

Figure 2. Phagocytosis quenches the release of platelet-derived MPs and depends on the P-selectin–PSGL-1 axis. Platelets were left unstimulated or stimulated with thrombin receptor agonist peptide 6 (TRAP-6) and cultured in the absence or presence of autologous neutrophils. **A**–**C**, The proportions of neutrophils with phagocytosed platelets, proportion of released MPs (platelet MPs [Plt-MPs]), and proportion of platelets expressing P-selectin in the supernatants were determined by flow cytometry at incubation intervals of 15 minutes. Red circles represent results obtained with platelets in the presence of neutrophils, and open circles represent results obtained with platelets alone. * = $P < 0.01$; ** = $P < 0.001$. **D** and **E**, The effects of antibodies blocking P-selectin (aPsel) or antibodies blocking PSGL-1 (aPSGL1) were examined in the supernatants. Phagocytosis of activated platelets abated in the presence of anti–P-selectin and anti–PSGL-1 antibodies (**D**), and the proportion of HMGB1+ platelet-derived MPs increased when phagocytosis was blocked with either of these antibodies (**E**). Bars show the mean ± SEM of 5–7 experiments. **** = $P < 0.0001$. See Figure 1 for other definitions. Color figure can be viewed in the online issue, which is available at http://onlinelibrary.wiley.com/doi/10.1002/art.41926/abstract.

platelets that were generating MPs (Figure 2 and Supplementary Figure 5, available on the *Arthritis & Rheumatology* website at https://onlinelibrary.wiley.com/doi/10.1002/art.41926). MP accumulation abated when platelets were activated in the presence of neutrophils (Figures 2B and E), possibly because of phagocytosis of platelets by neutrophils (Figure 2D and Table 2). We observed that activated platelets were being removed from the environment based on the results showing a reduced number of P-selectin+ platelets in the presence of neutrophils (Figure 2C).

Table 2. Extent of adhesion and phagocytosis of neutrophils alone or neutrophils interacting with activated platelets or platelet-derived MPs*

	Adhesion	Phagocytosis
Neutrophils alone	1.5 ± 0.6	1.8 ± 0.5
Neutrophils plus activated platelets		
Irrelevant IgG1 mAb	30.8 ± 4.0	66.5 ± 3.9
mAb against P-selectin	3.5 ± 0.6	4.3 ± 0.5
mAb against PSGL-1	5.0 ± 0.7	5.0 ± 0.9
Neutrophils plus platelet-derived MPs		
Irrelevant IgG1 mAb	85.4 ± 4.0	3.5 ± 0.5
mAb against P-selectin	86.9 ± 4.3	3.2 ± 0.9
mAb against PSGL-1	85.5 ± 5.7	3.0 ± 0.7

* Purified human neutrophils were left alone or incubated with activated platelets or platelet-derived microparticles (MPs) in the presence of irrelevant monoclonal antibodies (mAb) or blocking mAb against P-selectin or P-selectin glycoprotein ligand 1 (PSGL-1). Values are the mean ± SEM percentage of cells.

When antibodies specific to P-selectin or to PSGL-1 (being a counterreceptor to P-selectin on neutrophils) were added to the supernatants to block phagocytosis, the ability of activated platelets to release MPs was restored (Figure 2E). This indicates that neutrophils prevented the accumulation of MPs by phagocytosing platelets that generate them. Platelets were indeed the source of most MPs under these experimental conditions, with MP-generating platelets being derived from neutrophils that were consistently fewer than 3% of the total cell population in the blood (data not shown). Purified platelet-derived MPs effectively adhered to neutrophils (Table 2). Antibodies specific to P-selectin or PSGL-1 did not interfere with adhesion, a result which is consistent with the small proportion of MPs expressing P-selectin (Table 2 and Supplementary Table 1 available on the *Arthritis & Rheumatology* website at https://onlinelibrary.wiley.com/doi/10.1002/art.41926). The phagocytosis of MPs by neutrophils was limited and was also not influenced by the presence of antibodies specific to P-selectin or PSGL-1 (Table 2).

Neutrophils hindering the biologic action of platelet MPs. MPs formed after platelet activation in the presence of neutrophils did not elicit the generation of NETs, as assessed using immunofluorescence microscopy or by measuring the concentrations of complexes of low molecular weight DNA with the neutrophil enzyme MPO (Figures 3A and B). Interference with platelet P-selectin or neutrophil PSGL-1 during MP generation reconstituted their bioactivity (Figure 3B). Platelets induce the generation of NETs via the release of HMGB1 (13–16). Accordingly, phagocytosing neutrophils prevented the release of HMGB1+ MPs, an event that requires integrity of the P-selectin–PSGL-1 axis (Figure 3C).

We compared the effects of injecting total MPs and injecting neutrophil-purged MPs in NSG mice, which have systemically defective adaptive immunity and are receptive to cell/tissue grafting. Total platelet-derived MPs activated murine neutrophils

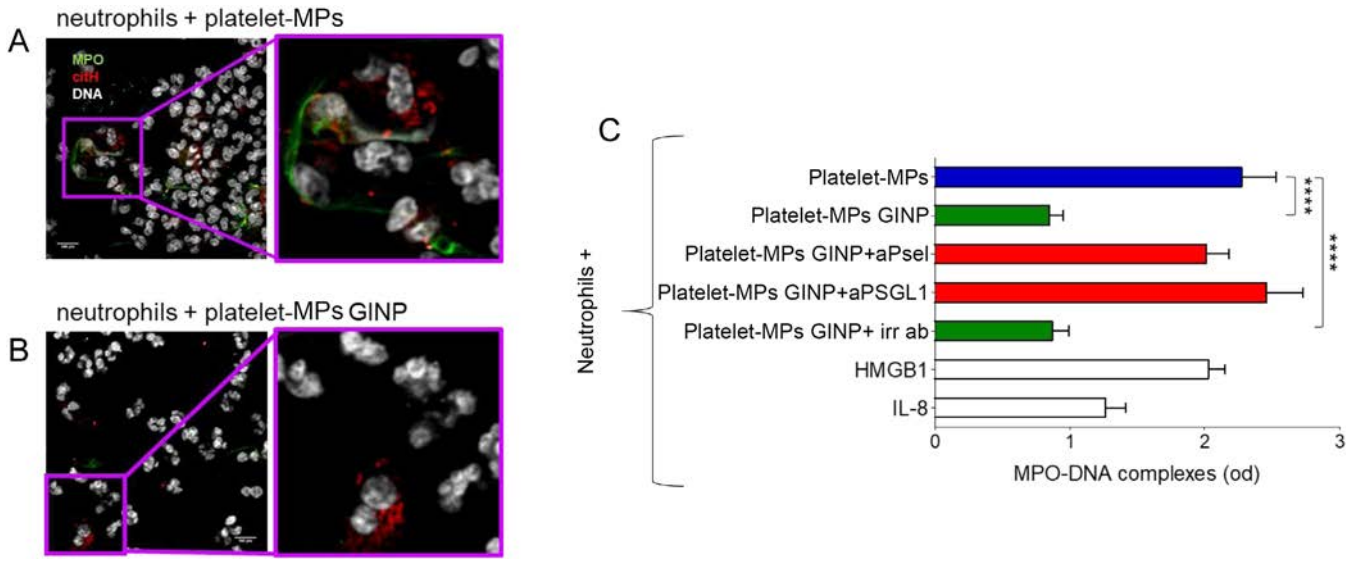

Figure 3. Neutrohil extracellular trap (NET) formation depends on the number of HMGB1+ platelet MPs. **A** and **B**, Representative confocal images of NET formation elicited by neutrophils stimulated with platelet MPs alone (**A**) or with platelet MPs generated in the presence of neutrophils (GINP) (**B**). NETs were identified as lattices of DNA (white fluorescence) with green fluorescence indicating positivity for MPO and red fluorescence indicating positivity for citrullinated histone H4 (CitH). Images on the right are higher-magnification views of the boxed areas on the left. Original magnification × 63 on left; × 163.8 on right. **C**, Quantification of NETs elicited by neutrophils stimulated with platelet-derived MPs or platelet-derived MPs generated in the presence of neutrophils, in the absence or presence of anti–P-selectin or anti–PSGL-1 mAb or an irrelevant control isotype-matched mAb (irr ab). Formation of NETs was measured as the optical density of DNA–MPO complexes, as assessed by enzyme-linked immunosorbant assay. Bars show the mean ± SEM of 4–9 experiments. Recombinant HMGB1 or interleukin-8 (IL-8) were used as positive controls for analysis of NET induction. **** = $P < 0.0001$. See Figure 1 for other definitions. Color figure can be viewed in the online issue, which is available at http://onlinelibrary.wiley.com/doi/10.1002/art.41926/abstract.

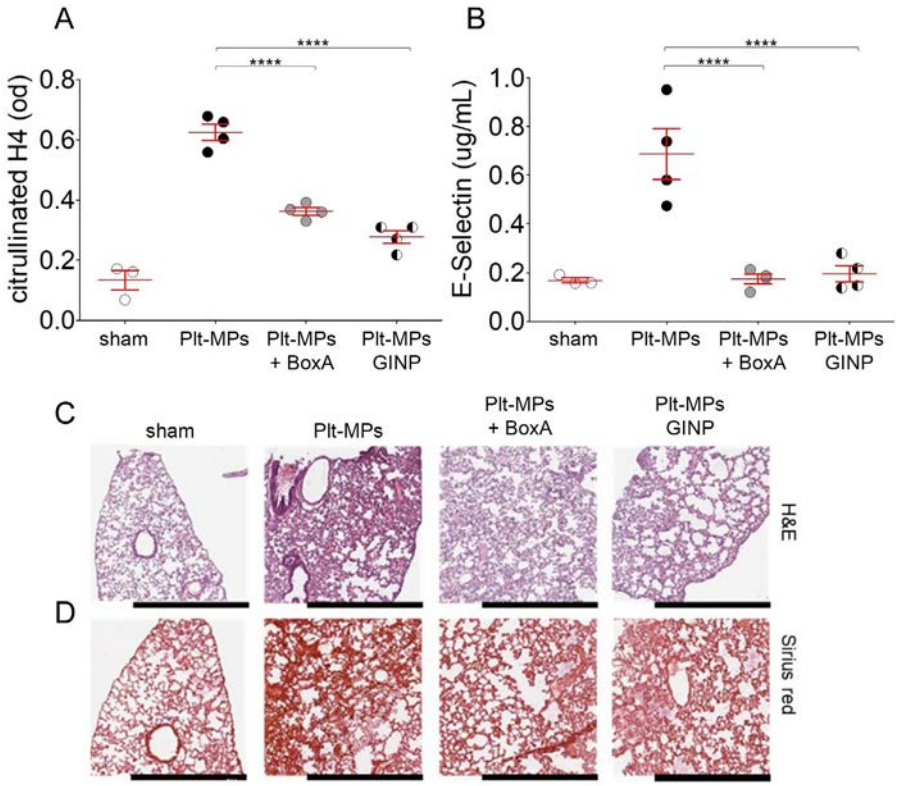

Figure 4. Neutrophil extracellular trap (NET) formation and vascular damage depend on platelet-derived MPs. MPs released from platelets activated alone (platelet MPs [Plt-MPs]) or platelet MPs generated in the presence of neutrophils (GINP) were injected into the tail vein of NSG mice. At 18 hours after injection, tissue samples were collected. **A** and **B**, Plasma concentrations of citrullinated histone H4 (**A**) and E-selectin (**B**) were determined under each condition. When indicated, platelet MPs were infused together with the HMGB1 inhibitor BoxA. Symbols represent individual samples; bars show the mean ± SEM. **C** and **D**, The histologic architecture of lung sections from representative mice under each condition was assessed using hematoxylin and eosin (H&E) and sirius red staining. **** = $P < 0.0001$. See Figure 1 for other definitions. Color figure can be viewed in the online issue, which is available at http://onlinelibrary.wiley.com/doi/10.1002/art.41926/abstract.

in vivo, thereby inducing the generation of NETs, as assessed according to the accumulation of citrullinated histone H4 in cell-free plasma. In contrast, neutrophil-purged MPs did not elicit NETs (Figure 4A). Total MPs also activated endothelial cells in vivo, as evidenced by the fact that levels of soluble E-selectin were increased in the blood of NSG mice (Figure 4B). In addition, MPs induced the recruitment of neutrophils in the lung parenchyma, within the pulmonary vasculature of mice (Figure 4C). Neutrophil purging of platelet-derived MPs quenched the ability of the MPs to exacerbate vascular inflammation in vivo (Figures 4B and C). Neutrophil purging of platelet-derived MPs was as effective as blockade of HMGB1 action in vivo using the competitive inhibitor BoxA (Figures 4A and B).

DISCUSSION

Previous studies have demonstrated that MPs accumulate in the blood of patients with SSc and are mostly derived from platelets (7,34). MPs purified from the blood of SSc patients are biologically active (11,35) and have been shown to cause microvascular inflammation and pulmonary fibrosis in mice (11), indicating potential involvement in the pathogenesis of the disease. The cause of the accumulation of platelet MPs in the blood of patients with SSc remains to be determined. The current study is the first to demonstrate that defective clearance of activated platelets might contribute to MP accumulation in SSc blood. We found that, in normal conditions, neutrophils prevent the release of MPs from activated platelets, thereby quenching the bioactivity of activated platelets. Beneficial effects included reduced activation of endothelial cells and leukocytes, suppression of microvascular lung inflammation, and decreased production of NETs in vivo.

One likely mechanism was demonstrated by our in vitro results, which indicated that the MPs released from activated platelets expressed the prototypical DAMP, HMGB1 (9,13) (Figures 2 and 3). HMGB1 promotes regeneration of injured and infected tissue (36). When harmful agents cannot be eliminated, HMGB1 persistently accumulates in the tissue, thus leading to tissue remodeling and the development of fibrosis (36–40). Platelet HMGB1 coordinates the actions of monocytes and neutrophils (15) and contributes to lung inflammation (41), sustaining vasculopathy associated with SSc (9–11). Confirming this, the actions of

HMGB1 on neutrophil activation and NET generation abated in the presence of its competitive antagonist, BoxA (13).

We show that, in normal conditions, neutrophils sequester activated platelets, preventing the release of HMGB1+ MPs in the environment. Given the role of platelets as guardians of the integrity of the vascular system (42,43), platelets undergo frequent activation in vivo. This could result in MP accumulation in the blood. MPs are able to activate leukocytes and endothelial cells, spreading inflammation to sites far from the site of the initial platelet involvement. Homeostatic mechanisms are likely to prevent the systemic diffusion of vascular inflammation after platelet activation.

Taken together, these results reveal that phagocytosis suppresses the inflammatory potential of activated platelets. Platelets are continuously activated in patients with SSc. By interacting with lymphocytes, fibroblasts, and endothelial cells, activated platelets represent a likely candidate factor that is able to sustain the sterile tissue damage leading to capillary dropout and tissue fibrosis, which are hallmarks of the disease (5). Moreover, evidence in experimental models supports the hypothesis that platelet activation plays a direct role in the natural history of SSc (5). We speculated whether a defect in the homeostatic system could be involved in maintaining platelet activation in patients with SSc.

Previous studies have shown that removal of platelets in physiologic conditions requires recognition of P-selectin (18,20,21,44). The best-characterized receptor for P-selectin is PSGL-1, a highly conserved moiety (45) that mediates the adhesion of activated platelets to neutrophils and is required for phagocytosis (20). Previous studies have demonstrated PSGL-1 defects in the blood cells of patients with SSc and in experimental models of the disease. Conversely, in mice, PSGL-1 genetic deletion causes an experimental disease that strongly resembles SSc (22–24,46). These studies highlight the importance of leukocyte–endothelium interactions for maintaining vessel homeostasis and show that this defect of leukocyte PSGL-1, which interacts with P-selectin and E-selectin on the surface of the activated endothelium and platelets, has various biologic consequences, affecting regulatory T cell accumulation in the lung, levels of angiopoietin 2 in the lung, and endothelial cell nitric oxide synthase phosphorylation (28–30). Furthermore, the P-selectin–PSGL-1 axis controls signaling events downstream of Toll-like receptor 4 activation in dendritic cells in conditions of hypercholesterolemia and inflammation, directly influencing vascular remodeling associated with the progression of atherosclerosis (47). Our findings imply that a failure in the recognition and clearance of P-selectin–expressing platelets also contributes to typical SSc vasculopathy.

Unlike with activated platelets, limited expression of P-selectin characterizes platelet MPs, which is consistent with previous studies (33,48). Different levels of expression of P-selectin in activated platelets and MPs could be dependent on the rapid shedding of the molecule (49,50). Given the fact that the MPs poorly express P-selectin, and since the P-selectin–PSGL-1 interaction is crucial for internalization (20,21), this could explain why the MPs are poorly phagocytosed (see Table 2).

More patients with CAD than those with SSc were treated with aspirin at the time of blood collection (81% versus 24%) (see Table 1). We found no detectable differences associated with aspirin in either patient group for the parameters we examined. However, we cannot exclude the possibility that this may represent a confounding factor.

In conclusion, our results presented here indicate a new, direct role of the phagocytosis of activated platelets in limiting the release of MPs and the reactivity of leukocytes in the blood, thus preventing unwanted systemic spread of local intravascular platelet activation. This homeostatic mechanism is dependent on the interaction of P-selectin with its counterreceptor, PSGL-1 and is compromised in patients with SSc, in which a cycle comprising platelet activation, accumulation of HMGB1+ MPs, systemic endothelial damage, and generation of NETs culminates in vasculopathy and fibrosis. Strategies aimed at breaking this cycle could present valuable tools for molecular interventions in SSc, answering an unmet medical need.

ACKNOWLEDGMENTS

We would like to thank M. Casucci for providing NSG mice, C. Covino for conducting confocal microscopy, and A. Fiocchi for conducting histochemical analyses of the lung samples. Confocal microscopy was conducted in the Advanced Light and Electron Microscopy BioImaging Center, an advanced microscopy laboratory established by the San Raffaele Scientific Institute and the Vita-Salute San Raffaele University. We also thank the patients who have provided the blood for the experiments described in this study.

AUTHOR CONTRIBUTIONS

All authors were involved in drafting the article or revising it critically for important intellectual content, and all authors approved the final version to be published. Dr. Maugeri had full access to all of the data in the study and takes responsibility for the integrity of the data and the accuracy of the data analysis.

Study conception and design. Manfredi, Maugeri.

Acquisition of data. Ramirez, Godino, Capobianco, Monno, Franchini, Tombetti, Corradetti, Maugeri.

Analysis and interpretation of data. Manfredi, Distler, Bianchi, Rovere-Querini, Maugeri.

REFERENCES

1. Gabrielli A, Avvedimento EV, Krieg T. Scleroderma [review]. N Engl J Med 2009;360:1989–2003.
2. Allanore Y, Distler O, Matucci-Cerinic M, Denton CP. Defining a unified vascular phenotype in systemic sclerosis [review]. Arthritis Rheumatol 2018;70:162–70.
3. Beretta L, Barturen G, Vigone B, Bellocchi C, Hunzelmann N, De Langhe E, et al. Genome-wide whole blood transcriptome profiling in a large European cohort of systemic sclerosis patients. Ann Rheum Dis 2020;79:1218–26.

4. Scherlinger M, Guillotin V, Truchetet ME, Contin-Bordes C, Sisirak V, Duffau P, et al. Systemic lupus erythematosus and systemic sclerosis: all roads lead to platelets [review]. Autoimmun Rev 2018;17:625–35.
5. Ntelis K, Bogdanos D, Dimitroulas T, Sakkas L, Daoussis D. Platelets in systemic sclerosis: the missing link connecting vasculopathy, autoimmunity, and fibrosis? [review]. Curr Rheumatol Rep 2019;21:15.
6. Distler JH, Distler O. Inflammation: microparticles and their roles in inflammatory arthritides [review]. Nat Rev Rheumatol 2010;6:385–6.
7. Guiducci S, Distler JH, Jungel A, Huscher D, Huber LC, Michel BA, et al. The relationship between plasma microparticles and disease manifestations in patients with systemic sclerosis. Arthritis Rheum 2008;58:2845–53.
8. Distler JH, Akhmetshina A, Dees C, Jungel A, Stürzl M, Gay S, et al. Induction of apoptosis in circulating angiogenic cells by microparticles. Arthritis Rheum 2011;63:2067–77.
9. Maugeri N, Franchini S, Campana L, Baldini M, Ramirez GA, Sabbadini MG, et al. Circulating platelets as a source of the damage-associated molecular pattern HMGB1 in patients with systemic sclerosis. Autoimmunity 2012;45:584–7.
10. Maugeri N, Rovere-Querini P, Baldini M, Baldissera E, Sabbadini MG, Bianchi ME, et al. Oxidative stress elicits platelet/leukocyte inflammatory interactions via HMGB1: a candidate for microvessel injury in sytemic sclerosis. Antioxid Redox Signal 2014;20:1060–74.
11. Maugeri N, Capobianco A, Rovere-Querini P, Ramirez GA, Tombetti E, Valle PD, et al. Platelet microparticles sustain autophagy-associated activation of neutrophils in systemic sclerosis. Science Transl Med 2018;10:eaao3089.
12. Clark SR, Ma AC, Tavener SA, McDonald B, Goodarzi Z, Kelly MM, et al. Platelet TLR4 activates neutrophil extracellular traps to ensnare bacteria in septic blood. Nat Med 2007;13:463–9.
13. Maugeri N, Campana L, Gavina M, Covino C, De Metrio M, Panciroli C, et al. Activated platelets present high mobility group box 1 to neutrophils, inducing autophagy and promoting the extrusion of neutrophil extracellular traps. J Thromb Haemost 2014;12:2074–88.
14. Vogel S, Bodenstein R, Chen Q, Feil S, Feil R, Rheinlaender J, et al. Platelet-derived HMGB1 is a critical mediator of thrombosis. J Clin Invest 2015;125:4638–54.
15. Stark K, Philippi V, Stockhausen S, Busse J, Antonelli A, Miller M, et al. Disulfide HMGB1 derived from platelets coordinates venous thrombosis in mice. Blood 2016;128:2435–49.
16. Zhou H, Deng M, Liu Y, Yang C, Hoffman R, Zhou J, et al. Platelet HMGB1 is required for efficient bacterial clearance in intra-abdominal bacterial sepsis in mice. Blood Adv 2018;2:638–48.
17. Manfredi AA, Rovere-Querini P, Maugeri N. Dangerous connections: neutrophils and the phagocytic clearance of activated platelets [review]. Curr Opin Hematol 2010;17:3–8.
18. Ji S, Dong W, Qi Y, Gao H, Zhao D, Xu M, et al. Phagocytosis by endothelial cells inhibits procoagulant activity of platelets of essential thrombocythemia in vitro. J Thromb Haemost 2020;18:222–33.
19. Deppermann C, Kratofil RM, Peiseler M, David BA, Zindel J, Castanheira F, et al. Macrophage galactose lectin is critical for Kupffer cells to clear aged platelets. J Exp Med 2020;217:e20190723.
20. Maugeri N, Rovere-Querini P, Evangelista V, Covino C, Capobianco A, Bertilaccio MT, et al. Neutrophils phagocytose activated platelets in vivo: a phosphatidylserine, P-selectin, and β2 integrin-dependent cell clearance program. Blood 2009;113:5254–65.
21. Maugeri N, Malato S, Femia EA, Pugliano M, Campana L, Lunghi F, et al. Clearance of circulating activated platelets in polycythemia vera and essential thrombocythemia. Blood 2011;118:3359–66.
22. Pérez-Frías A, González-Tajuelo R, Núñez-Andrade N, Tejedor R, García-Blanco MJ, Vicente-Rabaneda E, et al. Development of an autoimmune syndrome affecting the skin and internal organs in P-selectin glycoprotein ligand 1 leukocyte receptor–deficient mice. Arthritis Rheumatol 2014;66:3178–89.
23. Silván J, González-Tajuelo R, Vicente-Rabaneda E, Pérez-Frías A, Espartero-Santos M, Muñoz-Callejas A, et al. Deregulated PSGL-1 expression in B cells and dendritic cells may be implicated in human systemic sclerosis development. J Invest Dermatol 2018;138:2123–32.
24. González-Tajuelo R, de la Fuente-Fernández M, Morales-Cano D, Muñoz-Callejas A, González-Sánchez E, Silván J, et al. Spontaneous pulmonary hypertension associated with systemic sclerosis in P-selectin glycoprotein ligand 1–deficient mice. Arthritis Rheumatol 2020;72:477–87.
25. Boudreau LH, Duchez AC, Cloutier N, Soulet D, Martin N, Bollinger J, et al. Platelets release mitochondria serving as substrate for bactericidal group IIA-secreted phospholipase A2 to promote inflammation. Blood 2014;124:2173–83.
26. Zhao Z, Wang M, Tian Y, Hilton T, Salsbery B, Zhou EZ, et al. Cardiolipin-mediated procoagulant activity of mitochondria contributes to traumatic brain injury–associated coagulopathy in mice. Blood 2016;127:2763–72.
27. Linge P, Fortin PR, Lood C, Bengtsson AA, Boilard E. The non-haemostatic role of platelets in systemic lupus erythematosus [review]. Nat Rev Rheumatol 2018;14:195–213.
28. Mobarrez F, Fuzzi E, Gunnarsson I, Larsson A, Eketjall S, Pisetsky DS, et al. Microparticles in the blood of patients with SLE: size, content of mitochondria and role in circulating immune complexes. J Autoimmun 2019;102:142–9.
29. Didier K, Giusti D, Le Jan S, Terryn C, Muller C, Pham BN, et al. Neutrophil extracellular traps generation relates with early stage and vascular complications in systemic sclerosis. J Clin Med 2020;9:2136.
30. Van den Hoogen F, Khanna D, Fransen J, Johnson SR, Baron M, Tyndall A, et al. 2013 classification criteria for systemic sclerosis: an American College of Rheumatology/European League Against Rheumatism collaborative initiative. Arthritis Rheum 2013;65:2737–47.
31. Manfredi AA, Baldini M, Camera M, Baldissera E, Brambilla M, Peretti G, et al. Anti-TNFα agents curb platelet activation in patients with rheumatoid arthritis. Ann Rheum Dis 2016;75:1511–20.
32. D'Abbondanza M, Martorelli EE, Ricci MA, De Vuono S, Migliola EN, Godino C, et al. Increased plasmatic NETs by-products in patients in severe obesity. Sci Rep 2019;9:14678.
33. Roka-Moiia Y, Miller-Gutierrez S, Palomares DE, Italiano JE, Sheriff J, Bluestein D, et al. Platelet dysfunction during mechanical circulatory support: elevated shear stress promotes downregulation of $\alpha_{IIb}\beta_3$ and GPIb via microparticle shedding decreasing platelet aggregability. Arterioscler Thromb Vasc Biol 2021;41:1319–36.
34. Iversen LV, Ullman S, Ostergaard O, Nielsen CT, Halberg P, Karlsmark T, et al. Cross-sectional study of soluble selectins, fractions of circulating microparticles and their relationship to lung and skin involvement in systemic sclerosis. BMC Musculoskelet Disord 2015;16:191.
35. Ryu C, Walia A, Ortiz V, Perry C, Woo S, Reeves BC, et al. Bioactive plasma mitochondrial DNA is associated with disease progression in scleroderma-associated interstitial lung disease. Arthritis Rheumatol 2020;72:1905–15.
36. Bianchi ME, Crippa MP, Manfredi AA, Mezzapelle R, Querini PR, Venereau E. High-mobility group box 1 protein orchestrates responses to tissue damage via inflammation, innate and adaptive immunity, and tissue repair [review]. Immunol Rev 2017;280:74–82.
37. Li LC, Gao J, Li J. Emerging role of HMGB1 in fibrotic diseases [review]. J Cell Mol Med 2015;18:2331–9.
38. Zhang M, Guo Y, Fu H, Hu S, Pan J, Wang Y, et al. Chop deficiency prevents UUO-induced renal fibrosis by attenuating fibrotic signals

originated from Hmgb1/TLR4/NFκB/IL-1β signaling. Cell Death Dis 2015;6:e1847.

39. Zhu Z, Hu X. HMGB1 induced endothelial permeability promotes myocardial fibrosis in diabetic cardiomyopathy. Int J Cardiol 2015; 227:875.
40. Gorgulho CM, Romagnoli GG, Bharthi R, Lotze MT. Johnny on the spot: chronic inflammation is driven by HMGB1 [review]. Front Immunol 2019;10:1561.
41. Liu T, Barrett NA, Kanaoka Y, Buchheit K, Laidlaw TM, Garofalo D, et al. Cysteinyl leukotriene receptor 2 drives lung immunopathology through a platelet and high mobility box 1-dependent mechanism. Mucosal Immunol 2019;12:679–90.
42. Gaertner F, Ahmad Z, Rosenberger G, Fan S, Nicolai L, Busch B, et al. Migrating platelets are mechano-scavengers that collect and bundle bacteria. Cell 2017;171:1368–82.
43. Koupenova M, Clancy L, Corkrey HA, Freedman JE. Circulating platelets as mediators of immunity, inflammation, and thrombosis [review]. Circ Res 2018;122:337–51.
44. Morales-Camacho RM, Serrano-Chacon MD, Prats-Martin C, Vargas MT, Bernal R, Burillo-Sanz S. Platelet phagocytosis by granulopoietic precursors in a myelodysplastic syndrome overexpressing the P-selectin gene. Br J Haematol 2017;177:171.
45. Baisse B, Spertini C, Galisson F, Smirnova T, Spertini O. The function of P-selectin glycoprotein ligand-1 is conserved from ancestral fishes to mammals. J Leukoc Biol 2019;106:1271–83.
46. Yoshizaki A, Yanaba K, Iwata Y, Komura K, Ogawa A, Akiyama Y, et al. Cell adhesion molecules regulate fibrotic process via Th1/-Th2/Th17 cell balance in a bleomycin-induced scleroderma model. J Immunol 2010;185:2502–15.
47. Ye Z, Zhong L, Zhu S, Wang Y, Zheng J, Wang S, et al. The P-selectin and PSGL-1 axis accelerates atherosclerosis via activation of dendritic cells by the TLR4 signaling pathway. Cell Death Dis 2019;10:507.
48. Skeppholm M, Mobarrez F, Malmqvist K, Wallén H. Platelet-derived microparticles during and after acute coronary syndrome. Thromb Haemost 2012;107:1122–9.
49. Michelson AD, Barnard MR, Krueger LA, Valeri CR, Furman MI. Circulating monocyte-platelet aggregates are a more sensitive marker of in vivo platelet activation than platelet surface P-selectin: studies in baboons, human coronary intervention, and human acute myocardial infarction. Circulation 2001;104:1533–7.
50. Gardiner EE, De Luca M, McNally T, Michelson AD, Andrews RK, Berndt MC. Regulation of P-selectin binding to the neutrophil P-selectin counter-receptor P-selectin glycoprotein ligand-1 by neutrophil elastase and cathepsin G. Blood 2001;98:1440–7.

Arthritis & Rheumatology
Vol. 74, No. 2, February 2022, pp 329–341
DOI 10.1002/art.41813

American College of Rheumatology
Empowering Rheumatology Professionals

Expansion of Fcγ Receptor IIIa–Positive Macrophages, Ficolin 1–Positive Monocyte-Derived Dendritic Cells, and Plasmacytoid Dendritic Cells Associated With Severe Skin Disease in Systemic Sclerosis

Dan Xue,[1] Tracy Tabib,[2] Christina Morse,[2] Yi Yang,[3] Robyn T. Domsic,[2] Dinesh Khanna,[4] and Robert Lafyatis[2]

Objective. In this study, we sought a comprehensive understanding of myeloid cell types driving fibrosis in diffuse cutaneous systemic sclerosis (dcSSc) skin.

Methods. We analyzed the transcriptomes of 2,465 myeloid cells from skin biopsy specimens from 12 dcSSc patients and 10 healthy control subjects using single-cell RNA sequencing. Monocyte-derived dendritic cells (mo-DCs) were assessed using immunohistochemical staining and immunofluorescence analyses targeting ficolin-1 (FCN-1).

Results. A t-distributed stochastic neighbor embedding analysis of single-cell transcriptome data revealed 12 myeloid cell clusters, 9 of which paralleled previously described healthy control macrophage/DC clusters, and 3 of which were dcSSc-specific myeloid cell clusters. One SSc-associated macrophage cluster, highly expressing Fcγ receptor IIIA, was suggested on pseudotime analysis to be derived from normal CCR1+ and MARCO+ macrophages. A second SSc-associated myeloid population highly expressed monocyte markers FCN-1, epiregulin, S100A8, and S100A9, but was closely related to type 2 conventional DCs on pseudotime analysis and identified as mo-DCs. Mo-DCs were associated with more severe skin disease. Proliferating macrophages and plasmacytoid DCs were detected almost exclusively in dcSSc skin, the latter clustering with B cells and apparently derived from lymphoid progenitors.

Conclusion. Transcriptional signatures in these and other myeloid populations indicate innate immune system activation, possibly through Toll-like receptors and highly up-regulated chemokines. However, the appearance and activation of myeloid cells varies between patients, indicating potential differences in the underlying pathogenesis and/or temporal disease activity in dcSSc.

INTRODUCTION

Systemic sclerosis (SSc, also known as scleroderma), is a heterogeneous autoimmune disease with an unknown etiology characterized by fibrosis, vasculopathy, and immune dysfunction. Current treatment remains ineffective for controlling many complications, resulting in high morbidity and mortality (1). Diffuse cutaneous SSc (dcSSc) is a subtype of SSc characterized by widespread skin fibrosis. Myeloid cells, including macrophages and dendritic cells (DCs), heterogeneous immune cells in human skin, have been implicated in initiating and perpetuating SSc by releasing or activating profibrotic and proinflammatory factors;

Supported by the National Institute of Arthritis and Musculoskeletal and Skin Diseases, NIH (grant 2P50-AR-060780) and by an unrestricted grant from Pfizer. Dr. Xue's work was supported by the China Scholarship Council (grant 201706370258).

[1]Dan Xue, MD: University of Pittsburgh, Pittsburgh, Pennsylvania, and Xiangya Hospital, Central South University, Changsha, China; [2]Tracy Tabib, MS, Christina Morse, BS, Robyn T. Domsic, MD, MPH, Robert Lafyatis, MD: University of Pittsburgh, Pittsburgh, Pennsylvania; [3]Yi Yang, MD: Xiangya Hospital, Central South University, Changsha, China; [4]Dinesh Khanna, MD: University of Michigan, Ann Arbor.

Dr. Domsic has received consulting fees from Eicos Sciences and Boehringer-Ingelheim (less than $10,000 each). Dr. Khanna has received consulting fees from Actelion, Acceleron, Bristol Myers Squibb, Blade Therapeutics, Bayer, ChemomAB, Cytori, Celgene, Curzion, Corbus Pharmaceuticals, CSL Behring, GlaxoSmithKline, Genentech, Mitsubishi Tanabe Pharma Development America, Sanofi-Aventis, and UCB (less than $10,000 each) and from Eicos Sciences, Horizon, and Boehringer Ingelheim (more than $10,000 each), has received grant support from Bristol Myers Squibb, Pfizer, Bayer, and Horizon, and owns stock or stock options in Eicos Sciences and CiviBio Pharma. Dr. Lafyatis has received consulting fees from Bristol Myers Squibb, Formation, Sanofi, Biocon, Boehringer-Mannheim, Merck, and Genentech/Roche (less than $10,000 each) and research grants from Corbus, Formation, Elpidera, Regeneron, Pfizer, and Kiniksa. No other disclosures relevant to this article were reported.

Address correspondence to Robert Lafyatis, MD, 200 Lothrop, BST S720, Pittsburgh, PA 15260. Email: lafyatis@pitt.edu.

Submitted for publication June 2, 2020; accepted in revised form May 11, 2021.

however, the precise mechanisms that contribute to SSc pathogenesis remain poorly understood (2,3).

Infiltration of macrophages in SSc skin was first described in the 1990s (4,5). More recent studies have shown increased expression of specific macrophage markers in dcSSc skin, including Siglec-1 (CD169), a type I interferon (IFN)–inducible gene, and CD163 and CD204, markers of activated M2 macrophages (6,7). Other studies have implicated several chemokines in SSc pathogenesis: CCL2, CCL5, CCL18, CCL19, CXCL9, and CXCL13 (8). CCL19, in particular, is a strong macrophage chemoattractant (8,9). Further supporting the idea that macrophages play an important role in SSc pathogenesis, expression of macrophage markers CD14, MS4A4A, CD163, and CCL2 correlate with clinical disease severity, as assessed using the modified Rodnan skin score (MRSS), and are prognostic biomarkers of progressive skin disease in dcSSc (10,11). Macrophage and DC genes were also detected by bulk gene expression analysis in a subset of inflamed skin biopsy specimens (12,13).

Recent studies indicate that DCs may also play important roles in the pathophysiology of SSc skin disease (3,14). The role of myeloid or conventional DCs (cDCs) in SSc skin is uncertain, since markers used in previous studies are not specific to these cells (3). On the other hand, several studies have shown increased levels of plasmacytoid dendritic cells (pDCs) in the skin of SSc patients (14–16), and studies have also shown that circulating SSc pDCs secrete CXCL4, as well as IFNα (14,16).

Despite these multiple studies, altered myeloid cell numbers and functions in SSc remain poorly understood, in part due to the complexity of macrophage and DC subsets. Here, we compare recently detailed transcriptomes of macrophage and DC subsets in normal skin (17) to discern alterations in myeloid cell subsets in dcSSc skin.

PATIENTS AND METHODS

Single-cell RNA sequencing (RNA-seq). For single-cell RNA-seq analyses, 3-mm skin punch biopsy specimens from the dorsal mid-forearm were obtained after receiving informed consent under protocols approved by the University of Pittsburgh or University of Michigan institutional review boards. Skin was digested enzymatically, and cells were loaded into the Chromium instrument (10x Genomics), as described (18). Data analysis was performed with the R package Seurat version 2.3.4. Differential gene expression analysis comparing dcSSc cells to healthy control cells for each cluster was performed using the Wilcoxon rank sum test with a cutoff $P < 0.05$, a fold change >1.5, and further requiring the expression of genes from >25% of denoted cells. All single-cell RNA-seq data, including a gene/cell unique molecular identifier matrix and a BAM file containing aligned reads, are available at the GEO (accession no. GSE138669).

Staining of paraffin-embedded skin biopsy specimens. Immunohistochemical (IHC) and immunofluorescence staining using tyramide signal amplification was performed with monoclonal mouse anti–ficolin-1 (anti–FCN-1) on formalin-fixed paraffin-embedded human skin tissue from 38 SSc patients and 16 healthy control subjects.

Microarray analysis. Microarray RNA gene expression data from 64 SSc skin biopsy specimens and 15 healthy control skin biopsy specimens were analyzed using Cluster 3.0 software and were visualized using TreeView 1.1.6 software. Additional methods used in this study are described in detail in the Supplementary Methods (see the *Arthritis & Rheumatology* website at http://onlinelibrary.wiley.com/doi/10.1002/art.41813/abstract).

RESULTS

Single-cell transcriptome profiles of myeloid cells from dcSSc and healthy control skin. Using single-cell RNA-seq analysis, we examined gene expression of all enzymatically digested skin cells obtained from 12 patients with dcSSc and 10 healthy control subjects. All subjects have been included in another analysis of fibroblasts in fibrotic skin (19). Patients with dcSSc and control subjects were balanced across sex and age (Supplementary Table 1, available on the *Arthritis & Rheumatology* website at http://onlinelibrary.wiley.com/doi/10.1002/art.41813/abstract). Transcriptomes of 28,216 cells from healthy control subjects and 36,983 cells from dcSSc patients were grouped and analyzed together. Similar numbers of cells were included from healthy control and dcSSc skin (mean 2,822 cells per biopsy specimen and mean 3,082 cells per biopsy specimen, respectively) (Table 1).

Combined cell/gene count matrices were analyzed by t-distributed stochastic neighbor embedding (t-SNE) dimensional reduction, visualization, and clustering. Twenty-eight distinct clusters were aligned to expected cell types according to the top highly expressed genes in each cluster as described previously (18) (Supplementary Figure 1A and Supplementary Tables 2 and 3, available on the *Arthritis & Rheumatology* website at http://onlinelibrary.wiley.com/doi/10.1002/art.41813/abstract). All clusters included cells from multiple subjects and were unbiased from V1 and V2 chemistries (Supplementary Figures 1B, 2A, and 2B). Cluster 9 was identified as myeloid cells, showing specific LIN(CD3D/CD79A/NKG7)–HLA–DQ+ and expression of myeloid-specific genes (*ITGAM*, *ITGAX*, *CD14*, *CSF1R*, *CD68* and *CD209*); and verified by expression of MS4A4A, CD1C and CLEC9A, markers for macrophage, cDC2 and cDC1, respectively (Supplementary Figures 3A–C, available on the *Arthritis & Rheumatology* website at http://onlinelibrary.wiley.com/doi/10.1002/art.41813/abstract) (17).

Table 1. Proportions of each macrophage/dendritic cell subpopulation in skin samples from SSc patients and healthy controls*

	Total no. of cells	No. of myeloid cells	Macrophages and DCs, % among all cells	No. of MS4A4A+ macrophages	MS4A4A+ macrophages, % among all cells	No. of FCGR3A+ macrophages	FCGR3A+ macrophages, % among myeloid cells	No. of FCN-1+ cells	FCN-1+ cells, % among myeloid cells	No. of proliferating macrophages	Proliferating macrophages, % among myeloid cells
Individual sample											
Healthy control											
SC1nor	1,488	51	3.43	23	1.55	0	0.00	1	1.96	0	0.00
SC4nor	3,887	56	1.44	21	0.54	4	7.14	4	7.14	0	0.00
SC18nor	3,183	154	4.84	68	2.14	1	0.65	8	5.19	1	0.65
SC32nor	1,956	100	5.11	35	1.79	0	0.00	2	2.00	0	0.00
SC33nor	2,156	173	8.02	92	4.27	0	0.00	4	2.31	0	0.00
SC34nor	2,118	24	1.13	6	0.28	2	8.33	1	4.17	0	0.00
SC50nor	3,670	54	1.47	19	0.52	0	0.00	1	1.85	0	0.00
SC68nor	2,116	64	3.02	33	1.56	4	6.25	1	1.56	0	0.00
SC124nor	4,552	99	2.17	36	0.79	3	3.03	0	0.00	0	0.00
SC125nor	3,090	62	2.01	21	0.68	0	0.00	0			
SSc patient									0.00	0	0.00
SC2ssc	1,608	10	0.62	4	0.25	0	0.00	1	10.00	0	0.00
SC5ssc	4,120	158	3.83	100	2.43	2	1.27	11	6.96	1	0.63
SC19ssc	1,920	127	6.61	51	2.66	4	3.15	12	9.45	0	0.00
SC49ssc	3,091	15	0.49	1	0.03	0	0.00	2	13.33	0	0.00
SC60ssc	1,785	38	2.13	10	0.56	0	0.00	10	26.32	0	0.00
SC69ssc	2,407	169	7.02	79	3.28	44	26.04	11	6.51	1	0.59
SC70ssc	2,714	25	0.92	9	0.33	0	0.00	4	16.00	0	0.00
SC86ssc	3,663	88	2.40	31	0.85	1	1.14	2	2.27	0	0.00
SC119ssc	4,696	35	0.75	12	0.26	0	0.00	1	2.86	1	2.86
SC185ssc	3,443	262	7.61	124	3.60	2	0.76	5	1.91	0	0.00
SC188ssc	3,993	219	5.48	88	2.20	2	0.91	59	26.94	13	5.94
SC189ssc	3,543	482	13.60	267	7.54	155	32.16	68	14.11	10	2.07
Combined group, mean											
SSc patients	3,082	136	4.41	65	2.11	18	13.24	16	11.76	2	1.47
Healthy controls	2,822	84	2.98	35	1.24	1	1.19	2	2.38	0	0.00
P†	0.3139	0.3857	0.4614	0.404	0.4106	0.3342	0.416	0.0048	0.001	0.0831	0.0654

* SSc = systemic sclerosis; FCGR3A = Fcγ receptor IIIa; FCN-1+ = ficolin-1–positive.
† By Wilcoxon's rank sum test.

The percentage of myeloid cells of the total cells analyzed for each subject was strikingly variable, ranging from 0.49% of total cells (15 myeloid cells of 3,091 cells for patient SC49ssc) to 13.60% of total cells (482 myeloid cells of 3,543 cells for patient SC189ssc), and the percentage of myeloid cells showed a trend toward an increased percentage of myeloid cells in SSc, ranging from 2.98% in healthy control skin to 4.41% in dcSSc skin (Table 1). The percentage of myeloid cells in SSc patients showed a weak negative correlation with disease duration but was not statistically significant ($R = -0.26$) (Supplementary Figure 3B, available on the *Arthritis & Rheumatology* website at http://onlinelibrary.wiley.com/doi/10.1002/art.41813/abstract). Notably, the shared correlation strength calculated based on gene expression of all cells from each subject in a canonical correlation analysis showed that SC188, SC189, and SC69 patient samples deviated from other samples (Supplementary Figure 4).

All myeloid cell clusters identified in healthy skin were preserved in dcSSc skin. Reanalysis by t-SNE dimensions of 2,465 myeloid cells from dcSSc and healthy control skin showed 12 clusters of macrophage/DCs (Figure 1A). Each cluster was composed of cells from ≥6 subjects (Figure 1C and Supplementary Table 4, available on the *Arthritis & Rheumatology* website at http://onlinelibrary.wiley.com/doi/10.1002/art.41813/abstract). Nine of these 12 clusters paralleled previously described macrophage/DC clusters in healthy human skin (17).

The myeloid cell clusters were highly preserved in dcSSc skin (Figure 1B), identified by the top 50 differentially expressed genes in each subcluster (Supplementary Table 5, available on the *Arthritis & Rheumatology* website at http://onlinelibrary.wiley.com/doi/10.1002/art.41813/abstract). Subclusters 1 and 3 highly expressed CD1c and represented 2 cDC2 populations, each highly expressing either markers mucolipin-2 (MCOLN-2) or

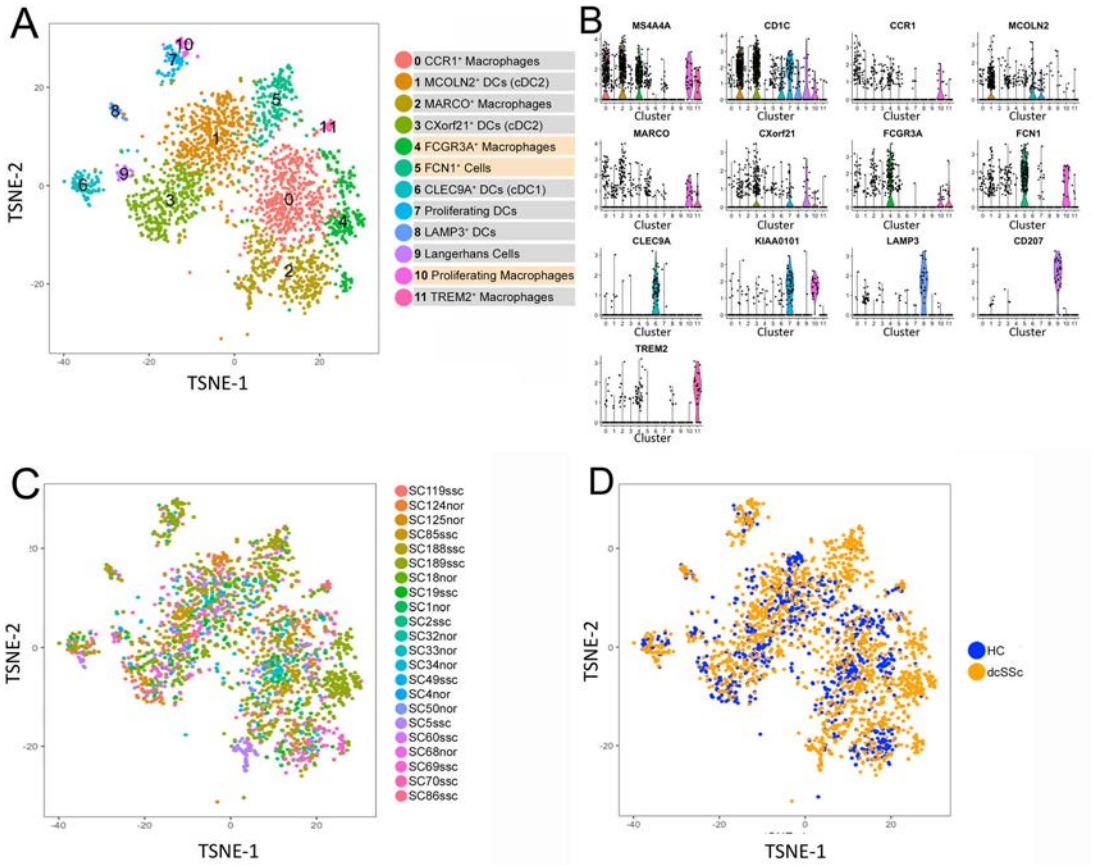

Figure 1. Single-cell RNA sequencing analysis of myeloid cell populations from healthy control subjects (HC) and patients with diffuse cutaneous systemic sclerosis (dcSSc). **A**, The 2-dimensional t-distributed stochastic neighbor embedding (t-SNE) cluster plot shows clustering of myeloid cells from all 22 healthy control and dcSSc patient skin samples, identified by cell type. Each point represents a single cell, with results illustrating the dimensional reduction in cell transcriptomes. Cells were assigned a color in the k-nearest neighbor graph according to the Euclidean distance in a principal components analysis, using a smart local moving algorithm to iteratively group cells. **B**, Violin plots of marker gene expression distinguish each cluster of myeloid cells. Values below the plots represent the cluster numbers shown in **A**. Each point represents a single cell. **C** and **D**, Cells were grouped using t-SNE according to individual sample identity number (**C**) or health status (**D**). MCOLN-2 = mucolipin-2; DCs = dendritic cells; cDC2 = type 2 conventional DCs; MARCO = macrophage receptor with collagenous structure; FCGR3A = Fcγ receptor IIIa; FCN-1 = ficolin-1; CLEC9A = C-type lectin domain containing 9A; LAMP-3 = lysosome-associated membrane protein 3; TREM-2 = triggering receptor expressed on myeloid cells 2. Color figure can be viewed in the online issue, which is available at http://onlinelibrary.wiley.com/doi/10.1002/art.41813/abstract.

CXorf21 (MCOLN2+ DCs and CXorf21+ DCs). These populations correspond closely to the DC2 and DC3 circulating DCs (20) we previously described in healthy skin (17). Cells in subcluster 6 highly expressed CLEC9A and other cDC1 markers and were identified as cDC1 cells, corresponding closely to circulating DC1 cells (17,20). The cells in myeloid cluster 7 highly expressing CD1c and proliferation genes, such as *MKI67*, *KIAA0101*, *TYMS*, and *PTTG1*, were identified as proliferating cDC2. Cells in subcluster 8 highly expressing lysosome-associated membrane protein 3 (LAMP-3), CCL17, and BIRC-3 were identified as a mature subpopulation of cDC (LAMP-3+ DCs), and cells in subcluster 9 highly expressing CD207, FCGBP, and HLA–DQB2 were identified as Langerhans' cells (Figure 1B and Supplementary Figures 5 and 6, available on the *Arthritis & Rheumatology* website at http://onlinelibrary.wiley.com/doi/10.1002/art.41813/abstract). The cells in these myeloid clusters showed no noticeable shift in the phenotype of the clusters between healthy controls and dcSSc (Figure 1D).

Three previously described macrophage clusters in healthy skin, selectively expressing CCR1, macrophage receptor with collagenous structure (MARCO), or triggering receptor expressed on myeloid cells 2 (TREM-2), were also detected (Figures 1A and B and Supplementary Table 5, available on the *Arthritis & Rheumatology* website at http://onlinelibrary.wiley.com/doi/10.1002/art.41813/abstract). The specific expression of *MS4A4A*, as well as other macrophage marker genes, and the absence of DC markers in subclusters 0, 2, 4, 10, and 11, indicated that these are macrophage clusters (Figure 1A and Supplementary Figure 5). The percentage of all macrophage populations increased from 1.24% in healthy control skin to 2.11% in dcSSc skin (Table 1). CCR-1 and MARCO, which we previously described as good markers for 2 major macrophages subsets in healthy control skin (17), were somewhat more highly expressed by cells in clusters 0 and 2, respectively (Figure 1B and Supplementary Figure 5, available on the *Arthritis & Rheumatology* website at http://onlinelibrary.wiley.com/doi/10.1002/art.41813/abstract), but were not observed to be discrete markers in this combined analysis of dcSSc and healthy control skin, apparently because the disease altered expression of these markers. However, comparing the top 15 genes distinguishing clusters in the combined database with healthy control clusters indicated that other markers of these 2 healthy control macrophages were preserved. *HMOX1*, *MMP9*, *MMP19*, *CCL2*, *CEBPB*, *CTSL*, *CREM*, *THBD*, and *EIF4E* were still highly expressed by cells in subcluster 0 (CCR-1+ macrophages) and *SEPP1*, *CCL13*, *FOLR2*, and *C1QA* were still highly expressed by cells in subcluster 2 (MARCO+ macrophages) (Supplementary Table 5 and Supplementary Figure 5B, available on the *Arthritis & Rheumatology* website at http://onlinelibrary.wiley.com/doi/10.1002/art.41813/abstract).

A distinct third macrophage population seen in both healthy control subjects and SSc patients was distinguished by high expression of TREM-2, fatty acid binding protein 4 (FABP-4), and FABP-5, parallel to the TREM-2+ macrophages, which we previously identified in healthy skin (17) (Figure 1B and Supplementary Figure 5, available on the *Arthritis & Rheumatology* website at http://onlinelibrary.wiley.com/doi/10.1002/art.41813/abstract). In contrast to the 9 myeloid populations common to healthy control and dcSSc skin samples, 3 other myeloid populations (clusters 4, 5, and 10) were detected almost exclusively in dcSSc skin (Figures 1A–D).

We reanalyzed the data set using Harmony to correct for potential batch effects (21). Harmony analysis detected the same clusters shown above (Figure 1 and Supplementary Figure 6, available on the *Arthritis & Rheumatology* website at http://onlinelibrary.wiley.com/doi/10.1002/art.41813/abstract), except it failed to identify a discrete cluster for proliferating macrophages (described further below) and indicated an additional population of macrophages (see cluster 4 in Supplementary Figure 6A). Although this additional macrophage cluster included cells from healthy skin (Supplementary Figure 6C), this population was not seen previously when analyzing only healthy skin (17).

Differential gene expression of dcSSc myeloid populations. Mean values for differential gene expression in cells within each myeloid cluster were compared between dcSSc skin and healthy control skin (Supplementary Table 6, available on the *Arthritis & Rheumatology* website at http://onlinelibrary.wiley.com/doi/10.1002/art.41813/abstract). We then analyzed the Gene Ontology (GO) pathways activated in each myeloid population in SSc skin after selecting differentially expressed genes with a fold change >1.5, detectable expression of each gene in >25% of SSc cells in the cluster, and an uncorrected *P* value <0.05 (Supplementary Table 7). CCR-1+ macrophages in dcSSc skin showed several statistically significant up-regulated pathways, including genes associated with the IFNγ pathway, *ICAM1*, *IFIT3*, *CCL13*, and *MT2A* (22), and innate immune response pathways (genes not shown). SSc MARCO+ macrophages showed up-regulated genes in several pathways, including the following: pathways associated with leukocyte chemotaxis (*IL10*, *CXCL1*, *CCL4*, *GPR183*, *CXCL8*, *S100A9*, *IL1B*, and *CCL3*), innate immune response pathways (genes not shown), pathways associated with response to type 1 IFN (*EGR1*, *ISG15*, and *IFITM3*), and pathways associated with response to IFNγ (*CCL3*, *CCL4*, *HLA-DRB5*, and *IFITM3*), as well as other pathways. Both SSc cDC2 subsets showed up-regulation of similar genes, but the only significant GO pathway was associated with immune response genes (*C1QC*, *HLA–DRB5*, *CRIP1*, *IFITM3*, *LTB*, *PKM*, *IFITM2*, *S100B*, and *CST7*). SSc cDC1 showed up-regulated genes in several pathways, including the Fcγ receptor signaling pathway involved in phagocytosis (*ACTR1*, *ACTR2*, *ACTR3*, *ACTB*) and the pathway associated with *CDC42* and response to wounding (*ANXA1*, *TNFAIP3*, *CXCR4*, *GRN*, *ACTG*, and *KLF4*). However,

macrophage-related genes previously detected as highly expressed in dcSSc skin by bulk RNA expression analysis in the skin (23) were not found to be up-regulated in these clusters (Supplementary Figure 6, available on the *Arthritis & Rheumatology* website at http://onlinelibrary.wiley.com/doi/10.1002/art.41813/abstract).

SIGLEC1 (CD169), a marker of IFN in SSc skin and a marker of disease severity (6,11), was expressed only in the macrophage/DC cluster and was up-regulated in this cluster. On subsetting this cluster, SIGLEC1 was found mainly on subclusters 0, 1, 2, 4, and 11 (all macrophage clusters except cluster 1) and was up-regulated in SSc, mainly on clusters 0, 1, 4, and 10 (see Supplementary Table 6, available on the *Arthritis & Rheumatology* website at http://onlinelibrary.wiley.com/doi/10.1002/art.41813/abstract).

Fcγ receptor IIIa–positive (FCGR3A+) macrophages and potential progenitor populations in dcSSc skin. Cells in subcluster 4 (FCG3RA+ macrophages) highly expressed macrophage markers, including MS4A4A and FCGR3A encoding CD16A (Figures 1A and B and Supplementary Figures 5 and 6). These cells also selectively expressed SLC40A1, IFI27, macrophage scavenger receptor 1 (MSR1), RCAN1, and OLR1, suggesting specialized functions of FCGR3A+ macrophages (Figure 2A). Most of the cells in this cluster were from only 2 of the 12 dcSSc subjects: patient SC69ssc (44 cells) and patient SC189ssc (155 cells), whereas the remaining 25 cells were from 5 healthy control subjects (14 cells) and 5 dcSSc patients (11 cells) (Figures 1C and D and Table 1), suggesting that this subpopulation is highly expanded, but only in select dcSSc patients.

The differential gene expression in FCGR3A+ macrophages, determined by assessing gene expression in dcSSc skin relative to healthy control skin, showed only a few genes that were significantly differentially expressed in SSc skin (Supplementary Table 7, available on the *Arthritis & Rheumatology* website at http://onlinelibrary.wiley.com/doi/10.1002/art.41813/abstract). We therefore compared gene expression by cells in this cluster with all the other macrophage/DCs from healthy control clusters (Supplementary Table 8), showing many significantly up-regulated genes. Genes encoding chemokines CCL18, CXCL1,

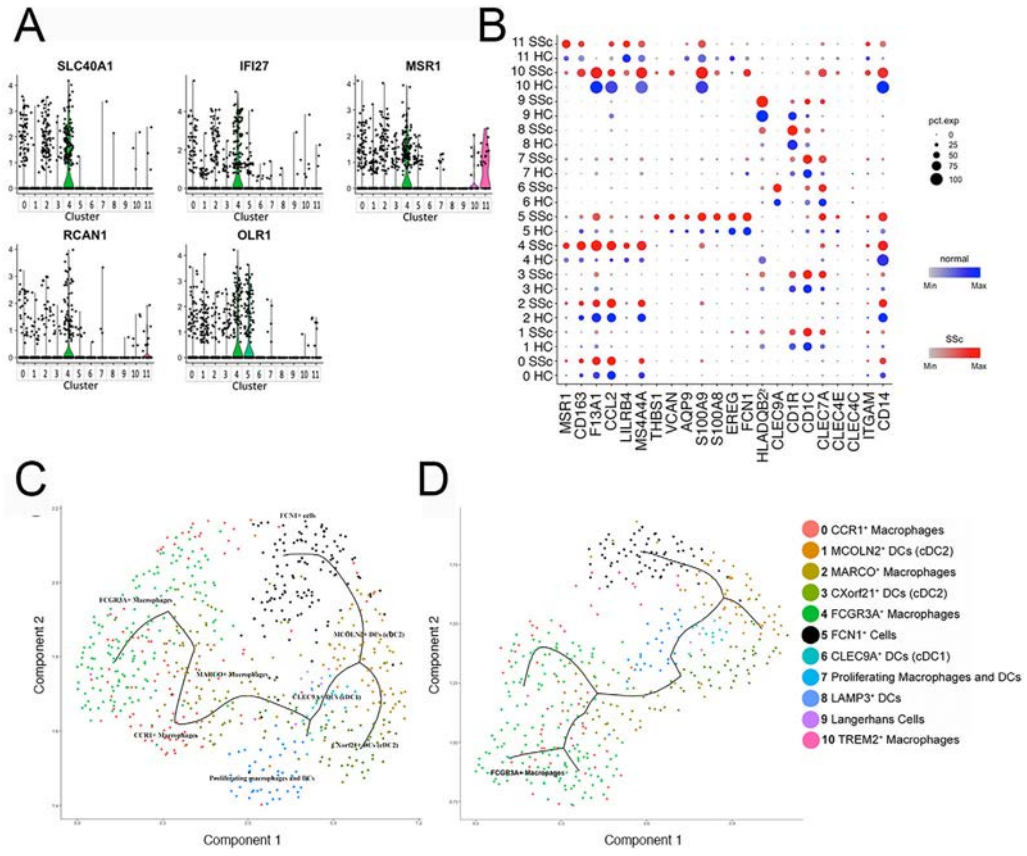

Figure 2. Gene signatures and putative functions of cluster 4 FCGR3A+ macrophages. **A**, Violin plots show marker gene expression in cluster 4. Each point represents a single cell; colors correspond to the cell subtypes defined in **D**. **B**, Dot plots show genes selectively expressed by FCGR3A+ macrophages in the skin of dcSSc patients and healthy controls. **C** and **D,** Pseudotime analysis tracking the relationship between transcriptomes of all myeloid cells from dcSSc and healthy control skin samples (**C**) and myeloid cells from a single dcSSc skin sample (patient SC189) (**D**) showing FCGR3A+ macrophages trajectory from CCR1+ and MARCO+ macrophages, and FCN-1+ monocyte-derived DC trajectory from MCOLN2+ cDC2. Each dot represents an individual cell. pct. exp = percent expressing (see Figure 1 for other definitions). Color figure can be viewed in the online issue, which is available at http://onlinelibrary.wiley.com/doi/10.1002/art.41813/abstract.

CCL8, CCL3, CCL4, CCL2, CCL13, and CXCL2 were highly expressed in this cluster. FCGR3A+ macrophages also showed up-regulated expression of genes correlated with the severity of dcSSc, such as *MSR1*, *CD163*, *F13A1*, *CCL2*, *LILRB4*, and *MS4A4A* (11,23) (Figure 2B). Based on the highly expressed genes of FCGR3A+ macrophages, GO analysis revealed significantly enriched, relatively broad functions such as "immune system process" and "immune response," but also several more specific enriched functions, including multiple pathways involved in chemotaxis, and Toll-like receptor (TLR)/innate immune activation, including "response to lipopolysaccharide (LPS)" and "TLR-6:TLR-2 signaling pathway" (Supplementary Table 9, available on the *Arthritis & Rheumatology* website at http://onlinelibrary.wiley.com/doi/10.1002/art.41813/abstract).

FCGR3A+ macrophages expressed many of the most highly differentially expressed genes of CCR1+ cells (subcluster 0) and MARCO+ macrophages (subcluster 2) at moderate levels, suggesting a close relationship between these macrophage subpopulations (Figure 2B and Supplementary Figure 6, available on the *Arthritis & Rheumatology* website at http://onlinelibrary.wiley.com/doi/10.1002/art.41813/abstract). To further explore the relationship between FCGR3A+, CCR1+, and MARCO+ macrophages, we analyzed the data set trajectory using pseudotime analysis, an algorithm that tracks the relationship between transcriptomes of single cells (24). Pseudotime analysis of myeloid cells from all subjects showed that FCGR3A+ macrophages very closely related to and even admixed with CCR1+ macrophages but were also closely adjacent to MARCO+ macrophages (Figures 2C and D).

Increased numbers of FCN-1+ myeloid cells in dcSSc skin. The number of FCN-1+ myeloid cells was significantly increased in dcSSc skin compared with healthy control skin ($P = 0.001$), indicating that this cluster is specifically expanded in dcSSc (Table 1). These cells were unevenly distributed across different dSSc samples, with many of the cells coming from 2 patients: SC188ssc and SC189ssc (Figure 1 and Table 1). Cells in this cluster (cluster 5, FCN-1+ mo-DCs) selectively showed up-regulated expression of *FCN1*, *EREG*, *S100A8*, *AQP9*, *VCAN*, and *THBS1*, and expressed macrophage markers *CD163*, *F13A1*, and *MS4A4A* at only moderate levels (Figure 2B and 3A and Supplementary Figure 6, available on the *Arthritis & Rheumatology* website at http://onlinelibrary.wiley.com/doi/10.1002/art.41813/abstract). As FCN-1 and EREG are monocyte markers, relative signature scores were calculated for the expression levels of CD14 monocyte and FCGR3A+ monocyte marker genes, previously described by single-cell RNA-seq analyses of human peripheral blood mononuclear cells (PBMCs) (25). FCN-1+ cells showed some similarity to CD14 monocytes, but not FCGR3A+ monocytes (Supplementary Figures 7A and B, available on the *Arthritis & Rheumatology* website at http://onlinelibrary.wiley.com/doi/10.1002/art.41813/abstract). Among the FCN-1+ myeloid cells, the 50 top differentially expressed genes, *FCN1*, *S100A8*, *AQP9*, *VCAN*, *CD300E*, *S100A9*, *FPR1*, *SOD2*, and *C5AR1*, are markers of classic monocytes (Supplementary Table 5); however, other monocyte marker genes, *ITGAM/CD11B*, *ITGB2/CD18*, *TLR2*, and *CLEC7A*, were not enriched in this cluster (Figure 2B).

In SSc skin, FCN-1+ cells maintained expression of CD14, CD13/ANPEP, CD172a/SIRPA, as well as S100A8 and S100A9, all described as markers of mo-DCs (Supplementary Figure 11A, available on the *Arthritis & Rheumatology* website at http://onlinelibrary.wiley.com/doi/10.1002/art.41813/abstract) (26), with only low expression of CD1c, CD1a, and IFN regulatory factor 4 (IRF-4), distinguishing these cells from DCs, and no expression of MS4A4A and CD163, distinguishing these cells from macrophages (Figure 2B). In a pseudotime analysis, FCN-1+ cells were on a trajectory closest to cDC2 (Figures 2C and D), further supporting their designation as mo-DCs (26).

Based on the differentially expressed genes of FCN-1+ mo-DCs, GO pathway analyses revealed significantly enriched, relatively nonspecific terms such as "inflammatory response," "defense response," "response to stress," and "immune response." These and many other terms overlapped with those seen in FCGR3A+ macrophages, including pathways involved in chemotaxis and response to LPS (Supplementary Table 9, available on the *Arthritis & Rheumatology* website at http://onlinelibrary.wiley.com/doi/10.1002/art.41813/abstract).

To verify the associations of FCN-1+ and FCGR3A+ myeloid cells with SSc skin, we compared 15 additional dcSSc biopsy specimens from another cohort to the same 10 healthy control biopsy specimens. FCN-1+ but not FCGR3A+ cells were again identified as a discrete cluster in a t-SNE plot of myeloid cells (subcluster 4) (Supplementary Figures 8 and 9, available on the *Arthritis & Rheumatology* website at http://onlinelibrary.wiley.com/doi/10.1002/art.41813/abstract), were significantly increased in dcSSc skin (Supplementary Table 10), and correlated with the total number of myeloid cells in biopsy specimens (Figure 3B).

Perivascular localization of FCN-1+ myeloid cells in dcSSc skin. IHC analysis of dcSSc skin showed FCN-1+ myeloid cells distributed primarily in perivascular regions in dcSSc skin (Figure 3C). Immunofluorescence staining of FCN-1+ cells in 16 healthy control and 39 dcSSc skin biopsy specimens showed an increased number of FCN-1+ cells in dcSSc patients compared with healthy control subjects ($P = 0.0141$) (Figure 3D, Supplementary Figure 10, and Supplementary Table 11, available on the *Arthritis & Rheumatology* website at http://onlinelibrary.wiley.com/doi/10.1002/art.41813/abstract). More FCN-1+ myeloid cells were seen in dcSSc skin biopsy specimens from patients with a higher MRSS (>20) compared with a lower MRSS (<20) ($P = 0.0005$) (Figure 3E), FCN-1+ myeloid cells were also significantly correlated with the MRSS ($P < 0.05$) (Supplementary

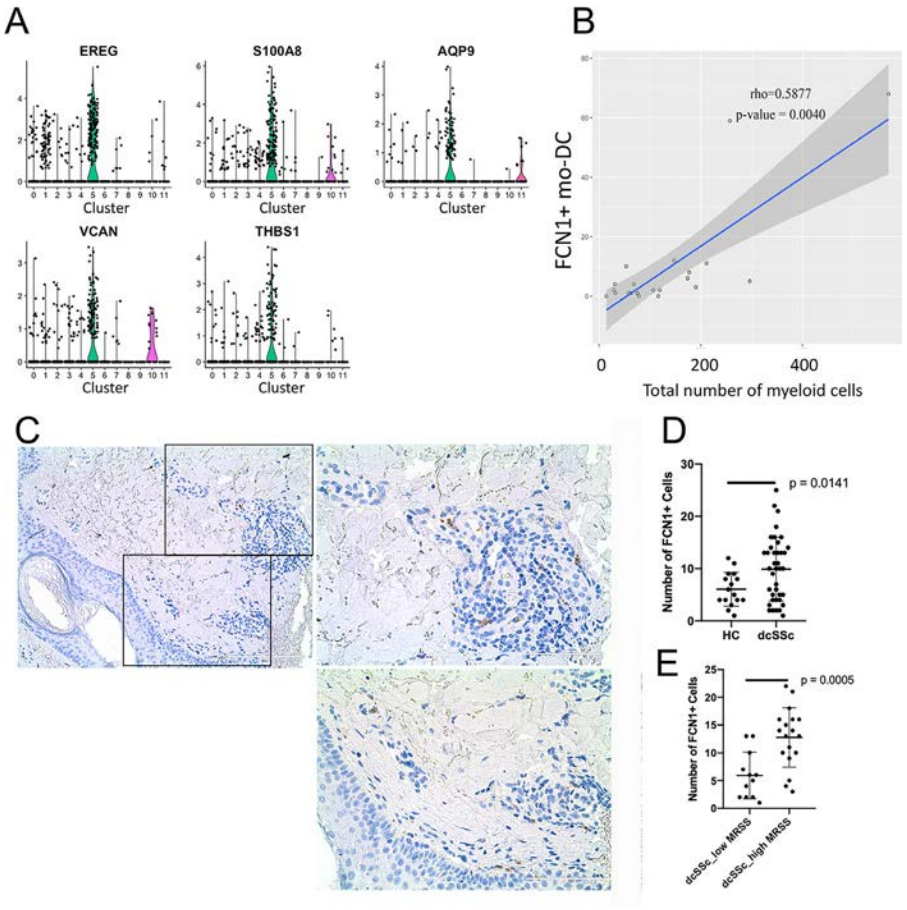

Figure 3. Gene signatures and putative functions of cluster 5 FCN-1+ monocyte-derived DCs (mo-DCs). **A**, Violin plots show marker gene expression in cluster 5 FCN-1+ cells. Each point represents a single cell; colors correspond to the cell subtypes defined in Figure 1A. **B**, The correlation between the total number of myeloid cells and the number of FCN-1+ mo-DCs in dcSSc skin samples was assessed using Spearman's rho. **C** and **D**, Staining shows the perivascular distribution of FCN-1+ cells in a representative skin sample from a patient with dcSSc (**C**) (immunofluorescence is shown in Supplementary Figure 10, http://onlinelibrary.wiley.com/doi/10.1002/art.41813/abstract), with the results revealing more FCN-1+ cells in dcSSc skin compared to healthy control skin (**D**). In **C**, the right panels show higher-magnification views of the boxed areas (original magnification × 10 on left; × 40 on right). **E**, Immunofluorescence staining of skin biopsy specimens from patients with dcSSc shows that the number of FCN-1+ cells differed according to whether the patients had either a low or high modified Rodnan skin thickness score (MRSS) (with high MRSS being defined as >20). *P* values in **D** and **E** were determined by Wilcoxon's rank sum test. Symbols represent individual patients; horizontal lines with bars show the mean ± SD. See Figure 1 for other definitions. Color figure can be viewed in the online issue, which is available at http://onlinelibrary.wiley.com/doi/10.1002/art.41813/abstract.

Figure 10B, available on the *Arthritis & Rheumatology* website at http://onlinelibrary.wiley.com/doi/10.1002/art.41813/abstract).

Identification of FCN-1+ myeloid cell markers in bulk microarray analyses of messenger RNA expression in the skin of patients with dcSSc. To extend our single-cell RNA-seq observations, we examined bulk microarray data from 64 SSc and 15 HC skin biopsy specimens. Several genes, including *LILRA5*, *FCN1*, *SERPINA1*, *FPR1*, *LILRB2*, and *TREM1*, were expressed by myeloid cells (cluster 9 in all cells shown in a t-SNE cluster plot) and were most highly expressed by FCN-1+ myeloid cells (myeloid subcluster 5) (Supplementary Figures 11A and B, available on the *Arthritis & Rheumatology* website at http://onlinelibrary.wiley.com/doi/10.1002/art.41813/abstract) and not by other skin cells or myeloid cell populations (Supplementary Figure 12). The expression of these genes from bulk sequencing analysis confirms the emergence of FCN-1+ mo-DCs in a subset of dcSSc patients (Figure 4A). Most of the genes in these clusters were selectively expressed in FCN-1+ mo-DCs (*FCN1*, *LILRA5*, *SERPINEA1*, *FPR1*, *LILRB2*, and *TREM1*), were selectively expressed in macrophages (*CD14* and *CD163*), or were more broadly expressed by myeloid cells (*AIF1* and *PLEK*) (Figure 4B). Moreover, the MRSS scores for SSc patients expressing markers of FCN-1+ cells were higher than those of dcSSc patients not expressing these markers ($P = 0.0019$) (Figure 4C), consistent with a general increase in macrophage/inflammatory cell infiltration in patients who have FCN-1+ mo-DCs, as shown by histologic findings and by the observed correlation between FCN-1+ mo-DCs and numbers of myeloid cells (Figure 4A).

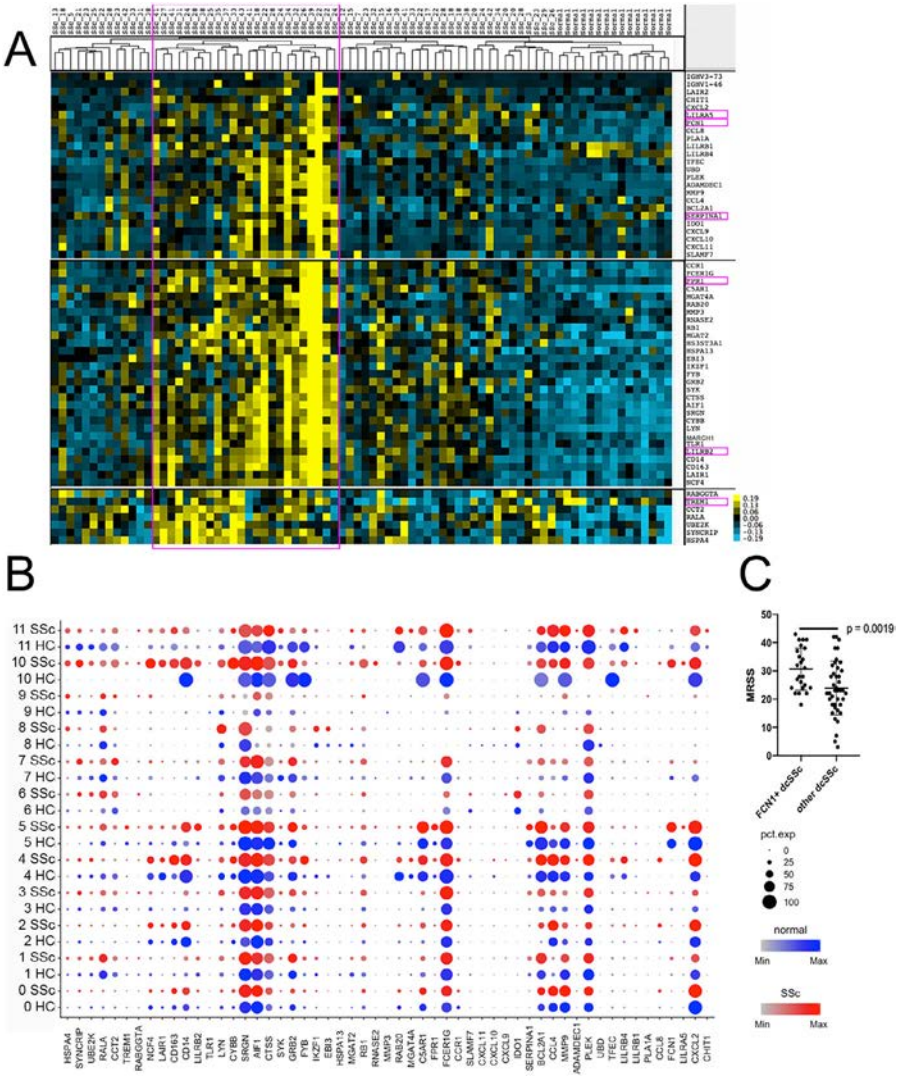

Figure 4. **A**, Heatmaps from hierarchical clustering analyses of bulk sequencing data reveal clusters of genes showing increased expression in myeloid cells, macrophages, and FCN1+ monocyte-derived DCs (mo-DCs) from patients with dcSSc (n = 64) relative to healthy controls (n = 15). The pink boxes highlight those gene markers with increased expression in FCN-1+ cells, which were used to identify cluster 5. **B**, Dot plots show gene expression in each myeloid cell type based on the results of a single-cell RNA sequencing analysis of skin samples from dcSSc patients and healthy controls. **C**, The modified Rodnan skin thickness score (MRSS) was compared between dcSSc patients in gene cluster 5 (high gene expression in FCN-1+ cells) and dcSSc patients having different gene cluster profiles ($P = 0.0019$, by Wilcoxon's rank sum test). Symbols represent individual patients; horizontal lines with bars show the mean ± SD. pct. exp = percent expressing (see Figure 1 for other definitions). Color figure can be viewed in the online issue, which is available at http://onlinelibrary.wiley.com/doi/10.1002/art.41813/abstract.

Proliferating macrophages and DCs in dcSSc skin. Proliferating myeloid cells (subclusters 7 and 10), predicted to be in the G_2/S phase by a cell phase analysis (Supplementary Figure 13A, available on the *Arthritis & Rheumatology* website at http://onlinelibrary.wiley.com/doi/10.1002/art.41813/abstract), were clustered separately by their uniquely high expression of genes associated with active cell proliferation, including *KIAA0101*, *MKI67*, *TYMS*, *PTTG1*, *CDK1*, and *PCNA* (Supplementary Figure 6 and Supplementary Table 5). Cells in the lower corner in subcluster 7 were identified as proliferating cDC2 cells, as we have previously described in healthy skin, expressing both *KIAA0101* and *CD1c* (Supplementary Figure 13B). These were found in similar numbers in dcSSc and healthy control skin (Figure 1D). In addition, we identified a group of proliferating macrophages based on coexpression of cell proliferation genes and MS4A4A (subcluster 10) (see Supplementary Figure 13C, available on the *Arthritis & Rheumatology* website at http://onlinelibrary.wiley.com/doi/10.1002/art.41813/abstract). Cells making up this cluster were mainly from patient SC188ssc (13 of 25 cells) and patient SC189ssc (10 of 25 cells), the same patient samples showing the most FCN-1+ mo-DCs (Supplementary Table 4).

To track which macrophage subpopulations were proliferating, we examined expression of single marker genes in each macrophage cluster and module scores of each cluster based on the

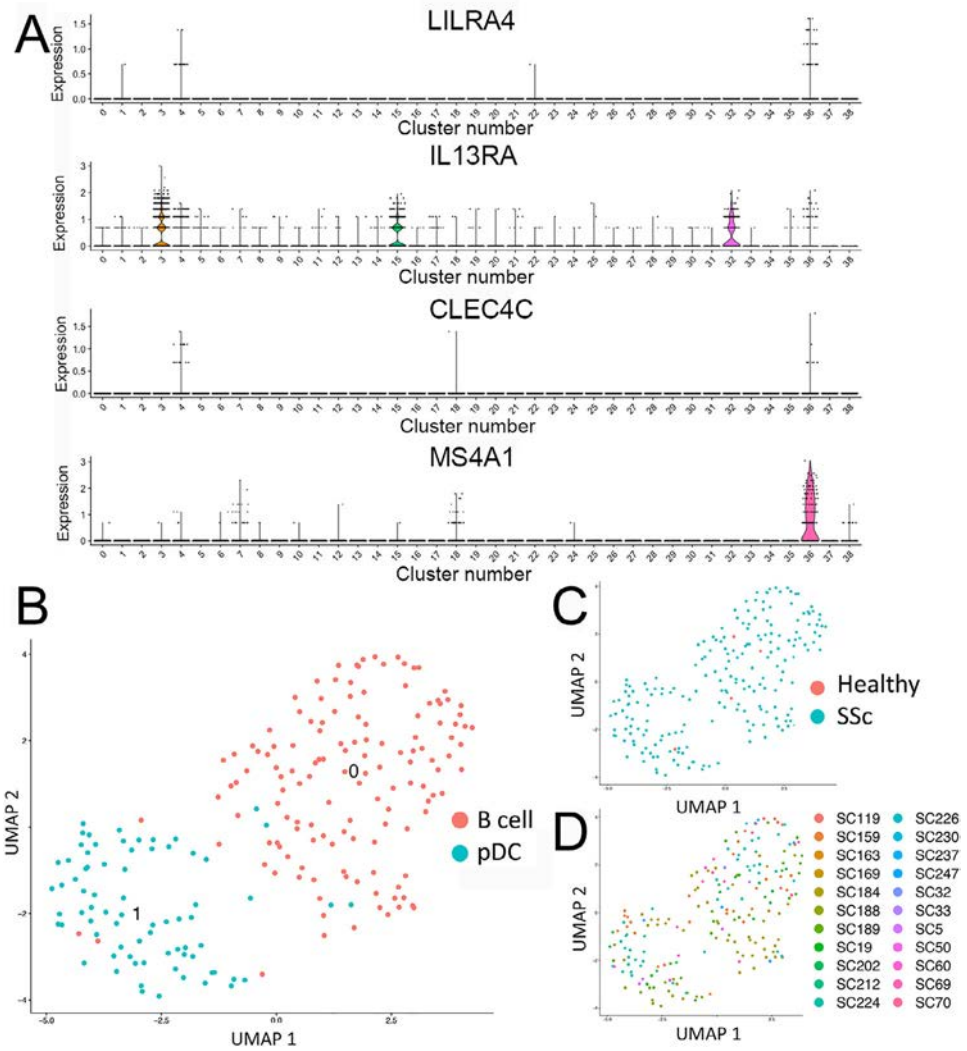

Figure 5. Gene cluster analyses of plasmacytoid DCs (pDCs) in dcSSc and healthy control skin. **A**, Violin plots show expression of pDC markers *LILRA4*, *IL3RA* (*CD123*), and *CLEC4C* (*BDCA2*), as well as B cell marker *MS4A1* (*CD20*) in 27 dcSSc skin samples and 10 healthy control samples in cluster 36. **B**–**D**, Dot plots show reclustered cells in cluster 36 according to the subsets of B cells or pDCs (**B**), health status (**C**), or sample origin (**D**). Each dot represents an individual cell. See Figure 1 for other definitions. Color figure can be viewed in the online issue, which is available at http://onlinelibrary.wiley.com/doi/10.1002/art.41813/abstract.

top 10 most highly expressed genes in each macrophage cluster in the proliferating cell cluster (Supplementary Figure 14, available on the *Arthritis & Rheumatology* website at http://onlinelibrary.wiley.com/doi/10.1002/art.41813/abstract). It appeared that all the macrophage subsets, as well as FCN-1+ mo-DCs, were represented in the proliferating cell cluster.

Clustering of pDCs with B cells and increased pDCs in dcSSc skin. Because we did not find pDCs in our initial clustering, we clustered all 27 dcSSc samples with the 10 normal skin samples (data not shown) and searched again for markers of these cells. *LILRA4*, *IL3RA*, and *CLEC4C* were coexpressed in a cluster comprising mostly B cells (Figure 5). Reclustering these cells resulted in the detection of 2 clusters, 1 prominently expressing B cell markers (*MS4A1A*, *CD79A*, and Ig genes) and the other expressing markers of pDCs (*LILRA4*, *IL3RA*, and *CLEC4C*), described previously as circulating DC6 (17,20). The identified pDCs came nearly exclusively from dcSSc patients (73 cells of 74 total cells versus 1 of 74 total cells from the 10 healthy controls). We detected up-regulated expression of transcription factors that are important in pDC differentiation: IRF-4, IRF-7, IRF-8, and ZEB-2 compared to other skin cells or B cells, but not expression of IFNA1–11 or CXCL4 (Supplementary Figure 15 and Supplementary Table 12, available on the *Arthritis & Rheumatology* website at http://onlinelibrary.wiley.com/doi/10.1002/art.41813/abstract).

DISCUSSION

Using bulk RNA analyses, we have previously implicated markers of macrophages in both the severity and progression of SSc skin disease (11,23,27). Single-cell RNA-seq studies here

provide a comprehensive analysis of myeloid cell populations in dcSSc skin. While all myeloid clusters detected in healthy skin were preserved in dcSSc skin, 4 dcSSc-specific myeloid populations were discovered: FCGR3A+ macrophages, FCN-1+ mo-DCs, pDCs, and proliferating macrophages. The transcriptomes of each of these populations revealed gene signatures and putative altered functions of each cluster. Importantly, FCN-1+ mo-DCs were perivascularly distributed along with other inflammatory cells, were found at a higher frequency in dcSSc, and were associated with the severity of skin disease.

Fibrotic SSc skin preserved all of the myeloid populations that we previously reported in healthy skin, including CCR1+, MARCO+, and TREM2+ macrophages, as well as 6 clusters of DCs: cDC1, 2 cDC2 populations, Langerhans' cells, a mature subpopulation of LAMP-3+ cDCs, and a population of proliferating cDC2 cells (17). Up-regulated genes in these clusters indicated pathways of innate immune and TLR activation and responses to both type I and type II IFNs, consistent with several previous studies (6,10,28,29).

The highly increased frequency of FCN-1+ mo-DCs in dcSSc skin was verified by single-cell RNA-seq, microarray analysis, IHC, and immunofluorescence staining for FCN-1. The expression of monocyte marker genes *FCN1*, *S100A8*, and *S100A9* by these cells indicates that these cells are recruited from circulating monocytes. A trajectory analysis, as well as low-level expression of CD1a and CD1c, indicated that FCN+ cells are most closely related to mo-DCs (30). Cells with very similar gene expression profiles have been identified in blister fluid of saline and house dust mite–stimulated human skin (31). In humans, mo-DCs are one of several myeloid cell types capable of cross-presentation (26). The association of these cells with perivascular inflammation and high expression of multiple chemokines suggests that they may promote the migration of other inflammatory cells.

THBS1 and *FPR1*, which are both pharmacodynamic biomarkers for the extent of skin disease and are prognostic markers for progressive skin disease in dcSSc (11,23), were predominantly expressed by FCN-1+ mo-DCs (Supplementary Figure 15, available on the *Arthritis & Rheumatology* website at http://onlinelibrary.wiley.com/doi/10.1002/art.41813/abstract). FCN-1+ mo-DCs were also shown to be significantly associated with dcSSc severity (MRSS >20), suggesting a key role in disease pathogenesis. In addition, these cells have likely played a prominent role in previous bulk RNA SSc skin expression studies, which have described a subset of patients with dcSSc (12,32), as patients overexpressing FCN-1+ markers also overexpressed both IFN-regulated and Ig genes (Supplementary Figure 16).

FCGR3A+ macrophages expressed most other macrophage markers, though they failed to express monocyte markers, and trajectory analysis suggested that CCR1+ macrophages and/or MARCO+ macrophages are the progenitors of these cells. As CCR1+ and MARCO+ macrophages are present in normal skin and proliferate in SSc skin, it is likely that these are resident cell populations that differentiate the FCGR3A+ macrophages in SSc skin. Enriched GO terms suggest that FCGR3A+ macrophages are activated through TLR signaling. Several recent studies have placed TLR signaling upstream of inflammatory and profibrotic changes in SSc (33–35). Potentially, TLR stimulates FCGR3A+ macrophages that highly express many cytokines and chemokines that attract and activate other immune cells, including CCL18 and interleukin-6 (IL-6). We have previously reported that *CCL18*, the gene shown to have the highest increase in expression (4.4-fold increase), is up-regulated in SSc skin and SSc-related interstitial lung disease (ILD) (8,10). Serum levels of CCL18 were rapidly reduced to normal levels, and CCL18 expression in the skin was blocked upon inhibition of IL-6, suggesting that IL-6 may play a role in the differentiation/activation of FCGR3A+ macrophages in select patients demonstrating infiltration with this macrophage population (36).

We identified proliferating macrophages in dcSSc skin, but not normal skin. It appeared that all macrophage subsets and FCN-1+ mo-DC cells were proliferating in some dcSSc patients. The majority of the proliferating cells were from patient SC188ssc and patient SC189ssc, the same patients who contributed most of cluster 5 of FCN-1+ mo-DCs. We have recently characterized proliferating macrophages in idiopathic pulmonary fibrosis and have seen similar cells in SSc-associated ILD (37,38), suggesting that common cytokine signals may drive macrophage proliferation in both SSc skin and the SSc lung.

Previous studies have detected perivascular pDCs in the affected skin of SSc patients, but not the skin of control subjects, by co-staining of CD123 and in situ *IFNA* expression (15), or by expression of *CLEC4* (BCDA-2) (16). Consistent with these studies, we found that pDCs were very rare in normal skin (1 of 20,073 cells) and were increased in numbers but still rare in dcSSc skin (73 of 74,607 cells). We were unable to detect expression of *IFNA1–IFNA11* or *CXCL4* genes by PDCs or any other cell type in SSc skin, the former classically secreted by these pDCs and the latter described as up-regulated in SSc pDCs (16) and implicated in the coactivation of TLR-9 (14,39). This likely represents the relatively low-level expression of these genes, though we were able to easily detect CXCL4 in platelets in a different data set (Lafyatis R, et al: unpublished observations). Although rare, these pDCs are likely the main source of type I IFNs in SSc skin and the resulting effects on multiple other cell types. The functional importance of these cells in skin fibrosis is supported by markedly ameliorated bleomycin-induced fibrosis in skin upon pDC depletion (14). Our data confirm the expression of IRF-8 in dermal pDCs, previously shown to be up-regulated in pDCs in SSc PBMCs (14), as well as up-regulated expression of IRF-4 and IRF-7 compared to other dermal myeloid cells or their closest transcriptome relative, B cells. The clustering of SSc pDCs with B cells is intriguing in terms of the recent understanding that pDCs can differentiate along a myeloid or lymphoid pathway with a

common B cell and pDC progenitor (40,41). The clustering of these cells with B cells in SSc skin suggests that pDCs differentiate exclusively along the lymphoid pathway from an IL-7R+FLT-3+ lymphoid progenitor.

Not all SSc patients demonstrate dramatic myeloid expansion, so it remains possible that myeloid cells drive pathogenesis in only a subset of patients, consistent with bulk microarray studies (32). As macrophage subsets are also involved in repair, it is also possible that their presence reflects repair processes in the skin (42). The lack of local skin disease score data is a limitation in this study.

In summary, our data reveal several populations of myeloid cells in dcSSc that are likely driving SSc vascular pathology and skin fibrosis. This more profound understanding of differing subsets of patients with inflammatory dcSSc provides new insights into stratifying patients for targeted therapies and can possibly be used for predicting responses to immunosuppressive treatment.

ACKNOWLEDGMENTS

We would like to thank Dr. Weiru Zhang and Dr. Xiaoxia Zu for their support.

AUTHOR CONTRIBUTIONS

All authors were involved in drafting the article or revising it critically for important intellectual content, and all authors approved the final version to be published. Dr. Lafyatis had full access to all of the data in the study and takes responsibility for the integrity of the data and the accuracy of the data analysis.

Study conception and design. Xue, Tabib, Morse, Domsic, Khanna, Lafyatis.

Acquisition of data. Xue, Tabib, Morse, Yang, Domsic, Khanna, Lafyatis.

Analysis and interpretation of data. Xue, Tabib, Morse, Yang, Domsic, Khanna, Lafyatis.

REFERENCES

1. Denton CP, Khanna D. Systemic sclerosis [review]. Lancet 2017;390: 1685–99.
2. Toledo DM, Pioli PA. Macrophages in systemic sclerosis: novel insights and therapeutic implications [review]. Curr Rheumatol Rep 2019;21:31.
3. Affandi AJ, Carvalheiro T, Radstake T, Marut W. Dendritic cells in systemic sclerosis: advances from human and mice studies [review]. Immunol Lett 2018;195:18–29.
4. Ishikawa O, Ishikawa H. Macrophage infiltration in the skin of patients with systemic sclerosis. J Rheumatol 1992;19:1202–6.
5. Kraling BM, Maul GG, Jimenez SA. Mononuclear cellular infiltrates in clinically involved skin from patients with systemic sclerosis of recent onset predominantly consist of monocytes/macrophages. Pathobiology 1995;63:48–56.
6. York MR, Nagai T, Mangini AJ, Lemaire R, van Seventer JM, Lafyatis R. A macrophage marker, Siglec-1, is increased on circulating monocytes in patients with systemic sclerosis and induced by type I interferons and toll-like receptor agonists. Arthritis Rheum 2007;56: 1010–20.
7. Higashi-Kuwata N, Jinnin M, Makino T, Fukushima S, Inoue Y, Muchemwa FC, et al. Characterization of monocyte/macrophage subsets in the skin and peripheral blood derived from patients with systemic sclerosis. Arthritis Res Ther 2010;12:R128.
8. Mathes AL, Christmann RB, Stifano G, Affandi AJ, Radstake TR, Farina GA, et al. Global chemokine expression in systemic sclerosis (SSc): CCL19 expression correlates with vascular inflammation in SSc skin. Ann Rheum Dis 2014;73:1864–72.
9. Xuan W, Qu Q, Zheng B, Xiong S, Fan GH. The chemotaxis of M1 and M2 macrophages is regulated by different chemokines. J Leukoc Biol 2015;97:61–9.
10. Christmann RB, Sampaio-Barros P, Stifano G, Borges CL, de Carvalho CR, Kairalla R, et al. Association of interferon- and transforming growth factor β–regulated genes and macrophage activation with systemic sclerosis–related progressive lung fibrosis. Arthritis Rheumatol 2014;66:714–25.
11. Rice LM, Ziemek J, Stratton EA, McLaughlin SR, Padilla CM, Mathes AL, et al. A longitudinal biomarker for the extent of skin disease in patients with diffuse cutaneous systemic sclerosis. Arthritis Rheumatol 2015;67:3004–15.
12. Milano A, Pendergrass SA, Sargent JL, George LK, McCalmont TH, Connolly MK, et al. Molecular subsets in the gene expression signatures of scleroderma skin. PloS One 2008;3:e2696.
13. Assassi S, Swindell WR, Wu M, Tan FD, Khanna D, Furst DE, et al. Dissecting the heterogeneity of skin gene expression patterns in systemic sclerosis. Arthritis Rheumatol 2015;67:3016–26.
14. Ah Kioon MD, Tripodo C, Fernandez D, Kirou KA, Spiera RF, Crow MK, et al. Plasmacytoid dendritic cells promote systemic sclerosis with a key role for TLR8. Sci Transl Med 2018;10:eaam8458.
15. Fleming JN, Nash RA, McLeod DO, Fiorentino DF, Shulman HM, Connolly MK, et al. Capillary regeneration in scleroderma: stem cell therapy reverses phenotype? PloS One 2008;3:e1452.
16. Van Bon L, Affandi AJ, Broen J, Christmann RB, Marijnissen RJ, Stawski L, et al. Proteome-wide analysis and CXCL4 as a biomarker in systemic sclerosis. N Engl J Med 2014;370:433–43.
17. Xue D, Tabib T, Morse C, Lafyatis R. Transcriptome landscape of myeloid cells in human skin reveals diversity, rare populations and putative DC progenitors. J Dermatol Sci 2020;97:41–9.
18. Tabib T, Morse C, Wang T, Chen W, Lafyatis R. SFRP2/DPP4 and FMO1/LSP1 define major fibroblast populations in human skin. J Invest Dermatol 2018;138:802–10.
19. Tabib T, Huang M, Morse N, Papazoglou A, Behera R, Jia M. Myofibroblast transcriptome indicates SFRP2(hi) fibroblast progenitors in systemic sclerosis skin. Nat Commun 2021;12:4384.
20. Villani AC, Satija R, Reynolds G, Sarkizova S, Shekhar K, Fletcher J, et al. Single-cell RNA-seq reveals new types of human blood dendritic cells, monocytes, and progenitors. Science 2017;356:eaah4573.
21. Korsunsky I, Millard N, Fan J, Slowikowski K, Zhang F, Wei K, et al. Fast, sensitive and accurate integration of single-cell data with Harmony. Nat Methods 2019;16:1289–96.
22. Ivashkiv LB. IFNγ: signalling, epigenetics and roles in immunity, metabolism, disease and cancer immunotherapy [review]. Nat Rev Immunol 2018;18:545–58.
23. Stifano G, Sornasse T, Rice LM, Na L, Chen-Harris H, Khanna D, et al. Skin gene expression is prognostic for the trajectory of skin disease in patients with diffuse cutaneous systemic sclerosis. Arthritis Rheumatol 2018;70:912–9.
24. Trapnell C, Cacchiarelli D, Grimsby J, Pokharel P, Li S, Morse M, et al. The dynamics and regulators of cell fate decisions are revealed by pseudotemporal ordering of single cells [letter]. Nat Biotechnol 2014;32:381–6.
25. Butler A, Hoffman P, Smibert P, Papalexi E, Satija R. Integrating single-cell transcriptomic data across different conditions, technologies, and species. Nat Biotechnol 2018;36:411–20.

26. Collin M, Bigley V. Human dendritic cell subsets: an update [review]. Immunology 2018;154:3–20.
27. Stifano G, Affandi AJ, Mathes AL, Rice LM, Nakerakanti S, Nazari B, et al. Chronic Toll-like receptor 4 stimulation in skin induces inflammation, macrophage activation, transforming growth factor β signature gene expression, and fibrosis. Arthritis Res Ther 2014;16: R136.
28. Bhattacharyya S, Wang W, Qin W, Cheng K, Coulup S, Chavez S, et al. TLR4-dependent fibroblast activation drives persistent organ fibrosis in skin and lung. JCI Insight 2018;3:e98850.
29. Skaug B, Assassi S. Type I interferon dysregulation in systemic sclerosis [review]. Cytokine 2019:154635.
30. Kashem SW, Haniffa M, Kaplan DH. Antigen-presenting cells in the skin [review]. Annu Rev Immunol 2017;35:469–99.
31. Chen YL, Gomes T, Hardman CS, Braga FA, Gutowska-Owsiak D, Salimi M, et al. Re-evaluation of human BDCA-2+ DC during acute sterile skin inflammation. J Exp Med 2020;217;e20190811.
32. Pendergrass SA, Lemaire R, Francis IP, Mahoney JM, Lafyatis R, Whitfield ML. Intrinsic gene expression subsets of diffuse cutaneous systemic sclerosis are stable in serial skin biopsies. J Invest Dermatol 2012;132:1363–73.
33. Bhattacharyya S, Midwood KS, Yin H, Varga J. Toll-like receptor-4 signaling drives persistent fibroblast activation and prevents fibrosis resolution in scleroderma [review]. Adv Wound Care (New Rochelle) 2017;6:356–69.
34. Farina G, York M, Collins C, Lafyatis R. dsRNA activation of endothelin-1 and markers of vascular activation in endothelial cells and fibroblasts. Ann Rheum Dis 2011;70:544–50.
35. Farina GA, York MR, Di Marzio M, Collins CA, Meller S, Homey B, et al. Poly(I:C) drives type I IFN- and TGFβ-mediated inflammation and dermal fibrosis simulating altered gene expression in systemic sclerosis. J Invest Dermatol 2010;130:2583–93.
36. Khanna D, Denton CP, Jahreis A, van Laar JM, Frech TM, Anderson ME, et al. Safety and efficacy of subcutaneous tocilizumab in adults with systemic sclerosis (faSScinate): a phase 2, randomised, controlled trial. Lancet 2016;387:2630–40.
37. Morse C, Tabib T, Sembrat J, Buschur KL, Bittar HT, Valenzi E, et al. Proliferating SPP1/MERTK-expressing macrophages in idiopathic pulmonary fibrosis. Eur Respir J 2019;54:1802441.
38. Valenzi E, Bulik M, Tabib T, Morse C, Sembrat J, Bittar HT, et al. Single-cell analysis reveals fibroblast heterogeneity and myofibroblasts in systemic sclerosis-associated interstitial lung disease. Ann Rheum Dis 2019;78:1379–87.
39. Lande R, Lee EY, Palazzo R, Marinari B, Pietraforte I, Santos GS, et al. CXCL4 assembles DNA into liquid crystalline complexes to amplify TLR9-mediated interferon-α production in systemic sclerosis. Nat Commun 2019;10:1731.
40. Rodrigues PF, Alberti-Servera L, Eremin A, Grajales-Reyes GE, Ivanek R, Tussiwand R. Distinct progenitor lineages contribute to the heterogeneity of plasmacytoid dendritic cells. Nat Immunol 2018;19:711–22.
41. Musumeci A, Lutz K, Winheim E, Krug AB. What makes a pDC: recent advances in understanding plasmacytoid DC development and heterogeneity [review]. Front Immunol 2019;10:1222.
42. Brancato SK, Albina JE. Wound macrophages as key regulators of repair: origin, phenotype, and function [review]. Am J Pathol 2011; 178:19–25.

Arthritis & Rheumatology
Vol. 74, No. 2, February 2022, pp 342–352
DOI 10.1002/art.41929

American College of Rheumatology
Empowering Rheumatology Professionals

Contribution of Rare Genetic Variation to Disease Susceptibility in a Large Scandinavian Myositis Cohort

Matteo Bianchi,[1] Sergey V. Kozyrev,[1] Antonella Notarnicola,[2] Lina Hultin Rosenberg,[1] Åsa Karlsson,[1] Pascal Pucholt,[3] Simon Rothwell,[4] Andrei Alexsson,[3] Johanna K. Sandling,[3] Helena Andersson,[5] Robert G. Cooper,[6] Leonid Padyukov,[2] Anna Tjärnlund,[2] Maryam Dastmalchi,[2] The ImmunoArray Development Consortium, The DISSECT Consortium, Jennifer R. S. Meadows,[1] Louise Pyndt Diederichsen,[7] Øyvind Molberg,[8] Hector Chinoy,[9] Janine A. Lamb,[4] Lars Rönnblom,[3] Kerstin Lindblad-Toh,[10] and Ingrid E. Lundberg[2]

Objective. Idiopathic inflammatory myopathies (IIMs) are a heterogeneous group of complex autoimmune conditions characterized by inflammation in skeletal muscle and extramuscular compartments, and interferon (IFN) system activation. We undertook this study to examine the contribution of genetic variation to disease susceptibility and to identify novel avenues for research in IIMs.

Methods. Targeted DNA sequencing was used to mine coding and potentially regulatory single nucleotide variants from ~1,900 immune-related genes in a Scandinavian case–control cohort of 454 IIM patients and 1,024 healthy controls. Gene-based aggregate testing, together with rare variant– and gene-level enrichment analyses, was implemented to explore genotype–phenotype relations.

Results. Gene-based aggregate tests of all variants, including rare variants, identified *IFI35* as a potential genetic risk locus for IIMs, suggesting a genetic signature of type I IFN pathway activation. Functional annotation of the *IFI35* locus highlighted a regulatory network linked to the skeletal muscle–specific gene *PTGES3L*, as a potential candidate for IIM pathogenesis. Aggregate genetic associations with *AGER* and *PSMB8* in the major histocompatibility complex locus were detected in the antisynthetase syndrome subgroup, which also showed a less marked genetic signature of the type I IFN pathway. Enrichment analyses indicated a burden of synonymous and noncoding rare variants in IIM patients, suggesting increased disease predisposition associated with these classes of rare variants.

Conclusion. Our study suggests the contribution of rare genetic variation to disease susceptibility in IIM and specific patient subgroups, and pinpoints genetic associations consistent with previous findings by gene expression profiling. These features highlight genetic profiles that are potentially relevant to disease pathogenesis.

Supported by an AstraZeneca-Science for Life Laboratory Research Collaboration grant (DISSECT) (to Dr. Rönnblom), the Swedish Research Council for Medicine and Health (grants Dnr 2018-02399, 2018-02535, and 2016-01254), the Swedish Rheumatism Association, King Gustav V's 80-year Foundation, Karolinska Institutet KID, and Region Stockholm (ALF project). Dr. Meadows' work was partially supported by the Swedish Research Council (FORMAS grant Dnr 2012-1531). Dr. Lindblad-Toh's work was supported by a Wallenberg Scholar award.

[1]Matteo Bianchi, PhD, Sergey V. Kozyrev, PhD, Lina Hultin Rosenberg, PhD, Åsa Karlsson, BSc, Jennifer R. S. Meadows, PhD: Science for Life Laboratory and Uppsala University, Uppsala, Sweden; [2]Antonella Notarnicola, MD, PhD, Leonid Padyukov, MD, PhD, Anna Tjärnlund, PhD, Maryam Dastmalchi, MD, PhD, Ingrid E. Lundberg, MD, PhD: Karolinska Institutet and Karolinska University Hospital, Stockholm, Sweden; [3]Pascal Pucholt, PhD, Andrei Alexsson, MSc, Johanna K. Sandling, PhD, Lars Rönnblom, MD, PhD: Uppsala University, Uppsala, Sweden; [4]Simon Rothwell, PhD, Janine A. Lamb, PhD: The University of Manchester, Manchester, UK; [5]Helena Andersson, MD, PhD: Oslo University Hospital, Oslo, Norway; [6]Robert G. Cooper, MD, PhD: Aintree University Hospital, MRC-Arthritis Research UK Centre for integrated Research into Musculoskeletal Ageing, and University of Liverpool, Liverpool, UK; [7]Louise Pyndt Diederichsen, MD, PhD: Rigshospitalet, Copenhagen, Denmark, and Odense University Hospital, Odense, Denmark; [8]Øyvind Molberg, MD, PhD: Oslo University Hospital and University of Oslo, Oslo, Norway; [9]Hector Chinoy, MD, PhD: National Institute for Health Research Manchester Biomedical Research Centre, Manchester University NHS Foundation Trust, Manchester Academic Health Science Centre, University of Manchester, and Manchester Academic Health Science Centre, Manchester, UK, and Salford Royal NHS Foundation Trust, Salford, UK; [10]Kerstin Lindblad-Toh, PhD: Science for Life Laboratory and Uppsala University, Uppsala, Sweden, and Broad Institute of MIT and Harvard, Cambridge, Massachusetts.

Drs. Lindblad-Toh and Lundberg contributed equally to this work.

Author disclosures are available at https://onlinelibrary.wiley.com/action/downloadSupplement?doi=10.1002%2Fart.41929&file=art41929-sup-0001-Disclosureform.pdf.

Address correspondence to Matteo Bianchi, PhD, Uppsala University, Department of Medical Biochemistry and Microbiology, BMC, D11:3, Uppsala, Sweden (email: matteo.bianchi@imbim.uu.se) or to Ingrid E. Lundberg, MD, PhD, Karolinska Institutet, Division of Rheumatology, D2:01, Solna, S-171 76 Stockholm, Sweden (email: ingrid.lundberg@ki.se).

Submitted for publication May 14, 2021; accepted in revised form July 13, 2021.

INTRODUCTION

Idiopathic inflammatory myopathies (IIMs), also collectively known as myositis, are a heterogeneous group of rare chronic inflammatory autoimmune diseases with a multifactorial etiology (1). Inflammation mainly affects the skeletal muscle, but it can also occur in the lungs, skin, joints, heart, and gastrointestinal tract. IIMs can be categorized into major subgroups, including polymyositis (PM) and dermatomyositis (DM), which are defined by distinct clinical and histopathologic features (2–4). Taking serologic profiles into account, 2 additional subgroups have been identified: antisynthetase syndrome (ASyS), of which the anti–Jo-1–positive subgroup is the most prevalent, and immune-mediated necrotizing myopathy (5). IIMs are characterized by an interferon (IFN) signature, with the type I IFN and type II IFN pathways differentially activated in muscle tissues in different disease subgroups (6,7). While transcriptomic studies on muscle tissue have provided substantial evidence of distinctive IFN gene signatures in different types of IIMs, genetic studies have not achieved the same level of resolution mainly due to the small sample size of IIM patient cohorts and of clinically and serologically defined disease subgroups.

In recent years, classical genetic association studies have implicated, in addition to the HLA region, noncoding potentially regulatory common variation at several risk loci in IIM and specific disease subgroups (8,9). For complex disorders such as IIM, rare variation has also been implicated as contributing to the genetic architecture of the disease (1). However, for IIM, comprehensive studies investigating this class of genetic variation are lacking. Large-scale targeted sequencing of patient cohorts now represents a valid and accessible approach to explore genetic variation at the lower range of allele frequency (10). Moreover, the tailored implementation of statistical algorithms based on the aggregation of rare variants into specific analysis units allows for accurate modeling of these variants, thus resulting in increased discovery power (11).

Here, we present a next-generation sequencing-based study of IIM, designed to explore the contribution of rare (minor allele frequency [MAF] <0.01) single nucleotide variants (SNVs) to disease susceptibility and to identify novel candidate loci. We performed targeted DNA sequencing of coding and potentially regulatory regions of a set of ~1,900 immune-related genes in a Scandinavian IIM case–control cohort. We implemented gene-based aggregate testing in the whole patient cohort to maximize the power to explore the genetic underpinnings of the disease. This approach was also extended to examine the genetic background of subgroups of clinically and serologically distinct patients. To further characterize the genetic landscape of IIMs, we performed comprehensive functional annotation of candidate loci, as well as investigating differential allelic burden for specific rare variant categories and the genes potentially driving that burden. In summary, we comprehensively evaluated genetic variation underlying IIMs for the full allele frequency spectrum to gain novel insights into disease susceptibility and biology.

PATIENTS AND METHODS

Study patients. The Scandinavian IIM discovery cohort consisted of patients recruited in Sweden, Denmark, and Norway, as well as Swedish and Norwegian healthy blood donors and population controls. The Bohan and Peter criteria (2,3) were applied for the diagnosis of possible, probable, or definite PM or DM, and the Connors criteria (12) were used to evaluate ASyS. Patients with inclusion body myositis (IBM) were excluded (13). After quality control, the final data set included 454 IIM patients and 1,024 control samples. Patient characteristics and serologic profiles are summarized in Supplementary Tables 1 and 2 (http://onlinelibrary.wiley.com/doi/10.1002/art.41929/abstract). For detailed descriptions of the methods, see Supplementary Methods (available on the *Arthritis & Rheumatology* website at http://onlinelibrary.wiley.com/doi/10.1002/art.41929/abstract). See Appendix A for a list of members of the DISSECT Consortium and the ImmunoArray Development Consortium.

Ethics approval. All subjects provided informed consent to participate in the study, and the study was approved by the regional ethics board in Uppsala (Dnr 2015/450 and 2016/155) and by the local research ethics committee for the UK Myositis Network (MREC North West [Haydock Park], 98/8/86).

Targeted DNA sequencing and bioinformatics analysis. Targeted DNA sequencing was performed on the same technology platform on the Scandinavian IIM case–control cohort using an Illumina HiSeq 2500. An average sequencing read depth of >30× per sample was achieved. The targeted array comprised ~1,900 genes involved in immune function and immunologic diseases, for which both coding and potentially regulatory sequences were captured, as outlined elsewhere (14). As detailed in Supplementary Figure 1 (http://onlinelibrary.wiley.com/doi/10.1002/art.41929/abstract), bioinformatics analyses comprised mapping, genotype calling, variant-based and individual-based quality control (including relatedness and ancestry estimation [Supplementary Figure 2]), and generated a high-quality data set containing 264,956 SNVs characterized by high call rates (i.e., ≥98%).

Genetic association analyses. Single-marker association analysis of common SNVs (MAF ≥0.05) was performed with PLINK version 1.9 using a logistic regression model and assuming additive effects. Following classical HLA alleles imputation using SNP2HLA, the same statistical model was applied for conditional analysis on *DRB1*0301*. Aggregate association testing using all SNVs and analysis units defined as RefSeq gene body coordinates (+2 Kb upstream and +2 Kb downstream) was first

performed using SKAT-O (15). For this analysis, we used a weighted kernel with default settings and higher weight for rare variants. Employing the same analysis units, gene-based aggregate testing with all SNVs and with the inclusion of metrics defining variant functional potential was implemented using GenePy, version 1.2 (16). Gene- and region-based annotations were set according to Annovar, and the functional metrics included in the algorithm was based on the Combined Annotation Dependent Depletion (CADD) version 1.3 annotation (17). The gene score distributions between the patient and the control groups, including relevant patient subgroups (Supplementary Tables 1 and 2, http://onlinelibrary.wiley.com/doi/10.1002/art.41929/abstract), were modeled through logistic regression using the glm function with the "binomial" parameter in R.

All implemented association analyses and statistical models incorporated the most significant population principal components (PCs; PC1, PC2, and PC3) (Supplementary Figure 3, http://onlinelibrary.wiley.com/doi/10.1002/art.41929/abstract) and sex as covariates. The population PCs were generated in PLINK version 1.90 (--pca) after excluding long-range linkage disequilibrium (LD) regions (18), variants with MAF <0.05, and variants in LD ($r^2 > 0.2$). The significance of the generated PCs was assessed by evaluating the corresponding overall eigenvalues in a scree plot and identifying where the characteristic plateau occurs. PCs were also projected onto a 2-dimensional scatter plot to assess their convergence to a homogenous structure without any apparent cluster or batch effect (Supplementary Figure 3). The correlation between disease status and sex distribution was evaluated using Fisher's exact test, which identified a statistically significant sex imbalance between IIM patients and control subjects ($P < 1 \times 10^{-16}$). Statistical significance was based on Bonferroni and false discovery rate (FDR) corrections ($\alpha = 0.05$).

Variant annotation and enrichment analyses. Rare SNVs (MAF <0.01) were partitioned into relevant functional categories, for which the allelic burden between IIM patients and controls was evaluated globally using Mann-Whitney U test and at the gene level using GenePy. For the rare variant functional categories showing a statistically significant increased allelic burden in patients, we performed gene set enrichment analyses using the corresponding representative set of variants. An exhaustive variant functional annotation was performed using publicly available database resources and software, such as ENCODE, Roadmap Epigenomics, GTEx, and SnpEff (19–22).

Data generation and gene-based aggregate testing results in the replication cohort. The replication cohort consisted of IIM patients only, recruited through the UK Myositis Network (n = 397). Patients met the Bohan and Peter criteria for probable or definite PM or DM, or the Connors criteria for ASyS, and no patients had IBM. We did not have matched UK controls available for targeted sequencing. The UK IIM patients were subjected to sequence capture, targeted DNA sequencing, and subsequent bioinformatic analysis of the generated reads following the same procedures described for the discovery data set. An average individual sequencing read depth of >30× was achieved. The same criteria were also used for the individual- and variant-based quality controls. The resulting quality-controlled data set composed of patients only was employed as a replication data set (n = 348) (Supplementary Tables 2 and 3, http://onlinelibrary.wiley.com/doi/10.1002/art.41929/abstract).

Importantly, we explored the possibility of including out-of-study matched controls by utilizing the UK10K Avon Longitudinal Study of Parents and Children (ALSPAC) data set (23), which includes low read depth (~7×) whole-genome sequences of 1,927 control individuals from the UK. Despite implementing extensive and rigorous quality control procedures for data set harmonization, the substantially lower read depth of the ALSPAC controls prevented an unbiased and equivalent calling of rare variant alleles compared to the IIM UK patients. This precluded use of the ALSPAC cohort as a control population for the aggregate testing results replication. An alternative out-of-study source of matched controls could be the UK Biobank, for which genotype array-based and recently generated whole exome sequencing data (but no whole genome sequencing) are currently available (24,25). Nevertheless, neither of these technologies can provide full capture of the whole spectrum of rare variation detectable by our targeted array. For these reasons, to replicate the rare variation analysis results, we implemented an alternative method, intended to be fully unbiased and free from any confounders derived from systematic biases or technical artefacts, especially when focusing on rare variation.

First, for all UK patients, we generated CADD-based gene scores using GenePy. For all phenotypic contrasts, we then compared the distribution of the GenePy-derived gene scores for the patients in the discovery and replication cohorts using logistic regression, including the data set–specific most significant population PCs (as previously described) and sex as covariates. Assuming that a difference in the score of the same genes between the 2 groups of patients is likely to reflect ancestry or technical dissimilarities, we excluded genes that showed a significant difference ($P < 0.05$). This is a very conservative and low-sensitivity approach, which may also remove potentially relevant genes whose difference in score underlies a true involvement in disease etiology. However, by excluding these significantly different genes, we ensure harmonization and homogeneity of the data and minimize the risk of reporting erroneous results. Finally, we considered genes to be replicated if they matched the significantly associated genes (5% FDR) resulting from the GenePy aggregate analyses in the discovery data set.

Data availability. The data sets generated and/or analyzed in the present study are not publicly available due to the

inclusion of information that could compromise research participant privacy and consent. However, they are available from the corresponding authors upon reasonable request and on a collaborative basis.

RESULTS

In this study, we performed targeted DNA sequencing of coding and regulatory regions of immunologic genes to collectively explore the contribution of genetic variants to IIM. Outlines of these analyses can be found in Supplementary Figure 4 (http://onlinelibrary.wiley.com/doi/10.1002/art.41929/abstract).

Confirmation of HLA as a major risk locus in IIM by single-variant association analysis. In a single-variant association analysis performed on 69,110 common variants, an experiment-wide statistical threshold of $P < 7.2 \times 10^{-7}$ was exclusively reached by variants located in the major histocompatibility complex (MHC) region. The strongest association was detected for an intronic variant of *HLA–DQA1* (rs9272729-A; raw $P = 3.1 \times 10^{-31}$; odds ratio 4.0 [95% confidence interval 3.2–5.1]). No loci outside the MHC region exceeded the suggestive statistical significance threshold for single marker analysis ($P = 1 \times 10^{-5}$) (Supplementary Figure 5, http://onlinelibrary.wiley.com/doi/10.1002/art.41929/abstract). After analysis conditioning on rs9272729, no additional statistically significant signals

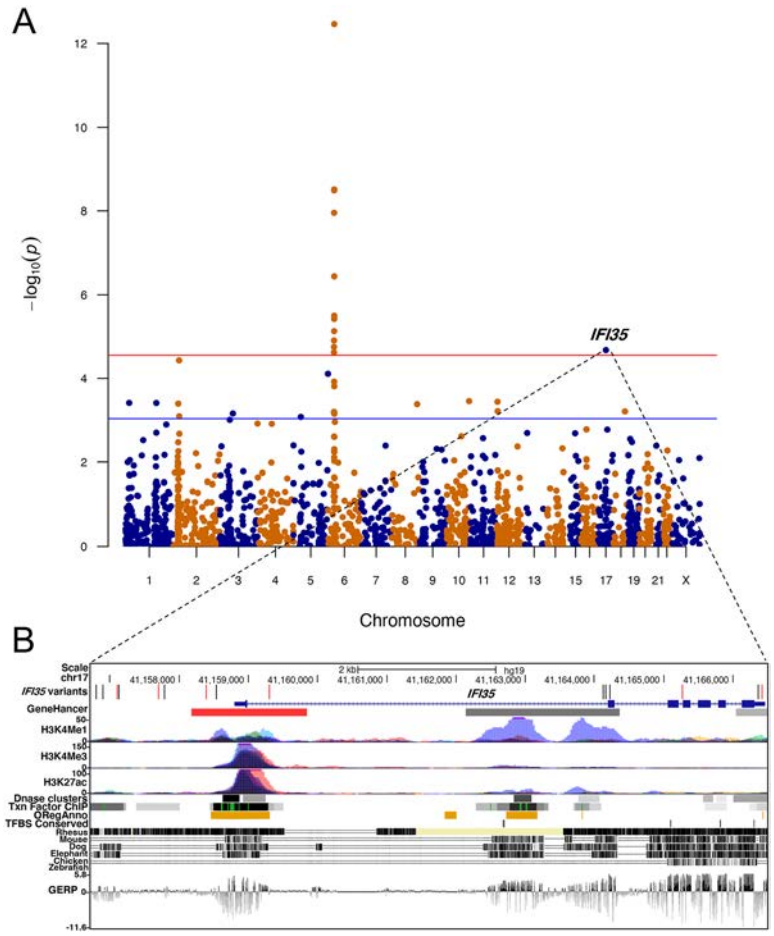

Figure 1. GenePy case–control gene-based association analysis of idiopathic inflammatory myopathies (IIMs) and "zoom in" of the associated locus. **A**, Manhattan plot showing the results of case–control gene-based association analysis (using GenePy) for IIM. Every point represents a gene region, with their associated *P* values plotted against chromosome location. Red line indicates the Bonferroni statistical significance threshold ($P = 2.9 \times 10^{-5}$), and blue line represents the 5% false discovery rate ($P = 8.7 \times 10^{-4}$). **B**, UCSC genome browser view of *IFI35*, i.e., the non–major histocompatibility complex, Bonferroni-corrected associated gene in the GenePy case–control aggregate association test for IIM. *IFI35* variants detected and tested in this study are indicated and are color-coded red if they represent GTEx expression quantitative trait loci. The *IFI35* locus overlaps with strong regulatory marks, including GeneHancer promoter (red bar) and enhancer (grey bars) regions, ENCODE histone modifications (H3K4Me1, H3K4Me3, H3K27ac), DNase I hypersensitivity sites (DNase clusters), transcription factor binding sites (Txn Factor ChIP), open regulatory region associated with active gene expression (ORegAnno), conserved transcription factor binding sites (TFBS conserved), as well as region of evolutionary constraint across 100 vertebrates and defined by Genomic Evolutionary Rate Profiling rejection submission scores.

remained (Supplementary Figure 6, http://onlinelibrary.wiley.com/doi/10.1002/art.41929/abstract). The same effect was obtained using imputed classical HLA alleles and conditioning on the well-established *DRB1*0301* IIM risk allele.

Suggestion of *IFI35* as a novel IIM genetic risk locus via aggregate association testing. To test for association between IIM and variants covering the full spectrum of allele frequency, as well as aggregating in genes, we first performed gene-based analysis using the SKAT-O software (15). In this gene-based analysis between all patients and controls, only 2 MHC genes were significantly associated with IIM after Bonferroni correction: *NOTCH4* (Bonferroni-adjusted $P = 0.022$) and *MICB* (Bonferroni-adjusted $P = 0.035$).

In addition to a classical aggregate test, we performed a gene-based analysis incorporating variant functional potential using GenePy (16). This analysis focused on the 1,737 gene units derived from the integrated Annovar variant annotation and constituted by a minimum of 2 genetic variants for which a CADD score was available. These 1,737 gene units were also used for stringent multiple-testing Bonferroni correction. Consistent with its sample size–independent increased discovery potential, this algorithm detected statistically significant associations with IIM exceeding Bonferroni correction in the MHC region (11 genes, top hit *HLA–DQA1*; Bonferroni-adjusted $P = 5.98 \times 10^{-10}$), and in *IFI35* on chromosome 17 (Bonferroni-adjusted $P = 0.036$) (Supplementary Table 4, http://onlinelibrary.wiley.com/doi/10.1002/art.41929/abstract). The association with *IFI35* derives from 16 variants spanning ~10 Kb (hg19-chr17:41,156,792–41,166,417) (Figure 1 and Supplementary Table 5, http://onlinelibrary.wiley.com/doi/10.1002/art.41929/abstract). A Kruskal-Wallis test for each of the *IFI35* rare variants (MAF <0.01) demonstrated that the difference in *IFI35* gene score distribution was not driven by any country-of-origin–specific subset of patients or controls showing unique population-specific alleles. With a less conservative statistical threshold (i.e., 5% FDR), we detected significant associations with non-MHC genes, including *PRDX3*, *SLAMF1*, *ZFAT*, and *PTPN6*, which further showed evidence of replication in downstream analyses (Supplementary Table 4).

Functional annotation of the *IFI35*-associated locus suggests *PTGES3L* as a potentially novel candidate gene for IIM. To functionally annotate the *IFI35* locus (the only non-MHC gene significant after Bonferroni correction), we used the GTEx Portal to investigate whether any of the variants contributing to the aggregate association overlapped with expression quantitative trait locus (eQTL) markers ($P < 1 \times 10^{-4}$) in relevant tissues. Of the 16 analyzed variants, 7 variants colocalized with eQTLs for *IFI35* and/or for other genes in the vicinity (Supplementary Tables 6 and 7, http://onlinelibrary.wiley.com/doi/10.1002/art.41929/abstract).

Overall, we observed strong pleiotropic effects on nearby genes, indicating the presence of considerable coregulatory mechanisms. In skeletal muscle tissue, *PTGES3L* and *NBR2* were the most significant eQTL gene targets ($P < 1 \times 10^{-6}$). Strikingly, in the 1000 Genomes Project European population, we observed high LD ($r^2 > 0.95$) between the strongest eQTLs for *PTGES3L* (rs34638441-T and rs10840-A, located in the *IFI35* gene) and 1 variant located in *PTGES3L* (rs35444712-A), suggesting their occurrence on a single haplotype. Moreover, these regions show evidence of a long-distance interaction (GeneHancer Regulatory Interactions marks GH17J043006/GH17J042979 and GH17J043014/GH17J042979), confirming a potentially shared regulatory control at this locus (Figure 2 and Supplementary Table 8, http://onlinelibrary.wiley.com/doi/10.1002/art.41929/abstract). Of note, the genes are localized within a common topologically associating domain (TAD) region (hg19-chr17:41,080,000–41,160,000) in the psoas muscle, as shown in the 3DIV web resource. Additionally, the expression of *PTGES3L* appears to be skeletal muscle–specific, with rs35444712 (1.2×10^{-16}) being a strong eQTL in this tissue (Supplementary Figure 7, http://onlinelibrary.wiley.com/doi/10.1002/art.41929/abstract).

Distinct genetic signature in patients with ASyS revealed by aggregate testing. To further dissect the IIM genetic landscape, we extended GenePy case–control aggregate testing to the major clinical subgroups: PM (n = 170) and DM (n = 133). The vast majority of the genes significantly associated with PM and DM were located in the MHC region (top hits *C2* [FDR-corrected $P = 0.0036$] and *HLA–DQA1* [FDR-corrected $P = 0.0035$], respectively).

Additionally, we restricted this analysis to clinically defined and autoantibody-specific patient subgroups, and focused on the most prevalent subgroup, the ASyS patients (n = 142) (Supplementary Tables 1 and 2, http://onlinelibrary.wiley.com/doi/10.1002/art.41929/abstract). Besides the most significant association with *AGER* (FDR-corrected $P = 5.56 \times 10^{-6}$), in these patients we detected, among others, aggregate associations with *PSMB8* (FDR-corrected $P = 0.0018$) and *PSMB9* (FDR-corrected $P = 0.021$). These genes are all located in the MHC region. Supplementary Table 9 summarizes the GenePy aggregate testing results in the patient subgroups (http://onlinelibrary.wiley.com/doi/10.1002/art.41929/abstract). Using Fisher's exact test on allele counts, we observed that the ASyS patients interestingly also showed a marginal underrepresentation ($P = 0.054$) of minor alleles for the 16 collectively associated *IFI35* variants when compared to the rest of the patients (Figure 3).

Replication of the aggregate testing results. Considering that the replication cohort included UK IIM patients only, and matched controls were not available for targeted DNA sequencing or technically amenable for inclusion in the replication stage after retrieval from publicly available resources, we implemented a strategy based on the comparison of the GenePy-derived gene scores between the patients in the

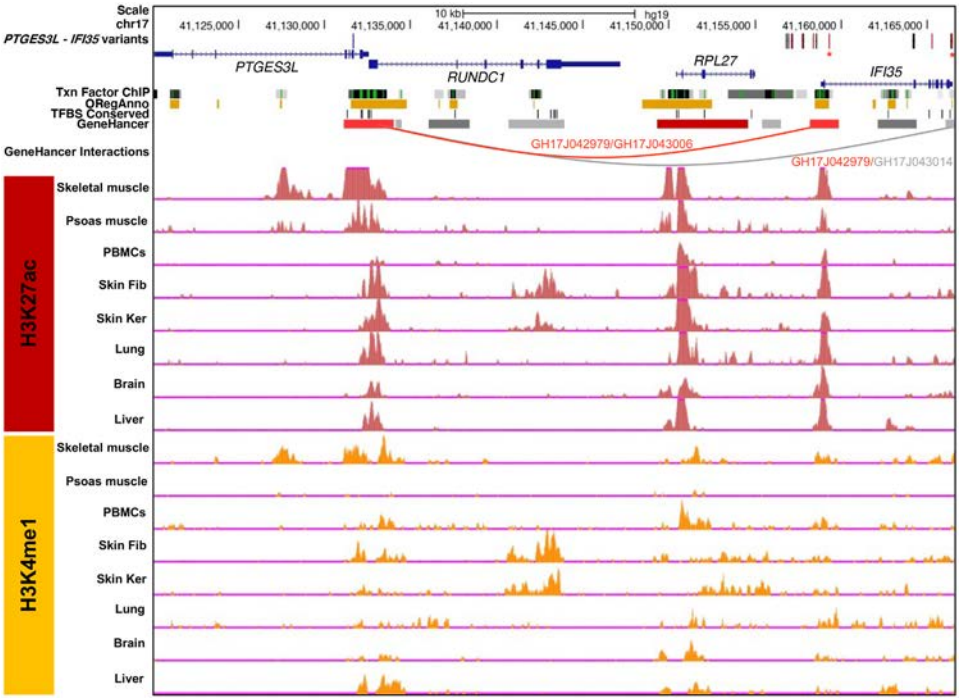

Figure 2. Functional annotation of the extended *IFI35* region. The *PTGES3L/IFI35* variants track shows the *PTGES3L* and *IFI35* variants detected and tested in this study. In this locus, a *PTGES3L* variant (rs35444712, hg19-chr17:41,131,645) (blue) shows high linkage disequilibrium (LD) ($r^2 > 0.95$) with 2 *IFI35* variants (rs34638441, hg19-chr17:41,159,301; rs10840, hg19-chr17:41,166,417) (red asterisks). These *IFI35* variants represent GTEx eQTLs (red) and are located in GeneHancer promoter (GH17J043006) and enhancer (GH17J043014) regions interacting with the *PTGE3L* promoter (GH17J042979). The histone modification marks (H3K27ac, H3K4me1) associated with active enhancers and mapped for different tissues according to Roadmap Epigenomics indicate the presence of skeletal muscle–specific enhancers. PBMCs = peripheral blood mononuclear cells; skin fib = skin fibroblasts; skin ker = skin keratinocytes (see Figure 1 for other definitions).

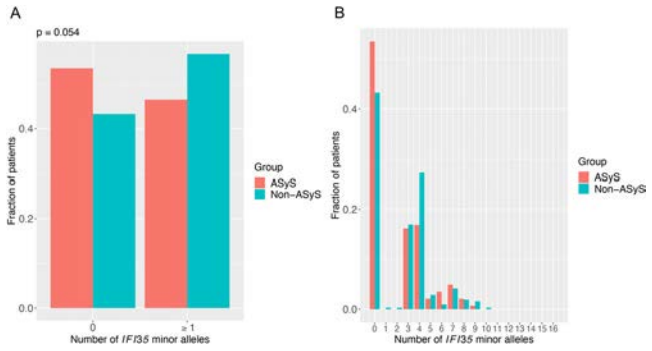

Figure 3. Enrichment of *IFI35* minor alleles in antisynthetase syndrome (ASyS) patients and those without ASyS (non-ASyS). **A**, Summed minor allele distribution for the 16 *IFI35* variants collectively associated with idiopathic inflammatory myopathies via GenePy. The number of patients with 0 alleles versus those with ≥1 allele was compared among the ASyS patients and the group without ASyS. The *P* value was obtained using Fisher's exact test on the parent contingency table composed of ASyS patients with 0 alleles (n = 76), non-ASyS patients with 0 alleles (n = 135), ASyS patients with ≥1 allele (n = 66), and non-ASyS patients with ≥1 allele (n = 177). **B**, Bar graph showing the breakdown of the differential minor allele distribution for all 16 *IFI35* variants total allele count bins in the ASyS and non-ASyS patients.

replication and discovery cohorts. A logistic regression model was implemented to compare the GenePy-derived gene scores between patients in the UK replication cohort (n = 348) and Scandinavian discovery cohort (n = 454) for all of the previously tested phenotypic comparisons. The genes showing evidence of heterogeneity ($P < 0.05$) were conservatively excluded. We considered genes to be replicated if they matched the discovery GenePy-based significantly associated (5% FDR) gene list. Using this approach, among the non-MHC genes significantly associated with IIM, *PRDX3*, *SLAMF1*, *ZFAT*, and *PTPN6* replicated, whereas *IFI35* did not show evidence of replication. Furthermore, the ASyS-associated genes *AGER*, *PSMB8*, and *PSMB9* all showed evidence of replication in the UK ASyS patients. Information on the associated genes in the Scandinavian discovery cohort and whether they showed evidence of aggregate testing replication is provided in Supplementary Table 4 and Supplementary Table 9 (http://onlinelibrary.wiley.com/doi/10.1002/art.41929/abstract).

Evidence of an increased regulatory rare variant allelic burden in IIM patients. Our data set offers the possibility to explore the extent to which rare variation contributes to

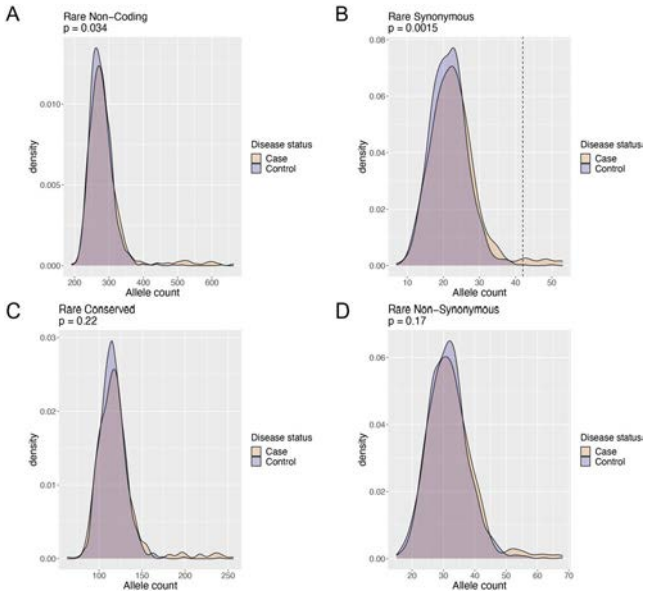

Figure 4. Distribution of single nucleotide variant functional categories in idiopathic inflammatory myopathy (IIM) patients and controls. **A**, Rare noncoding variants. **B**, Rare synonymous variants. Dashed line indicates the 2.5% right tail of the distribution in cases. **C**, Rare conserved variants (Genomic Evolutionary Rate Profiling rejection submission score >2). **D**, Rare nonsynonymous variants. *P* values indicate differences in allele burden between IIM patients and controls. Raw *P* values are shown (Bonferroni-corrected significance threshold of $P = 0.012$).

disease risk. After grouping all rare variants (MAF <0.01) into 4 functional categories, we sought to examine whether there was an increased allelic burden in IIM patients compared to controls, and whether this was driven by enrichment in specific genes or simply reflected a generalized cumulative effect across all the analyzed genomic regions.

For the 101,712 rare noncoding variants detected in the whole cohort, we found statistical evidence of increased allele burden in patients ($P = 0.034$) (Figure 4A), which is consistent with the finding that the majority of autoimmune complex disease–associated variants are located in regulatory regions (26). Although the enrichment was not robust to the conservative correction for multiple testing (i.e., correction for the 4 functional categories tested), 5 genes were significant when considering the allelic burden at the specific gene level: *ITIH4* (FDR-corrected $P = 0.018$), *PXN* (FDR-corrected $P = 0.024$), *TH* (FDR-corrected $P = 0.025$), *IFI35* (FDR-corrected $P = 0.034$), and *VRK1* (FDR-corrected $P = 0.047$).

Next, we detected a significant difference in allele burden in IIM patients when examining synonymous variants (n = 6,898; $P = 0.0015$) (Figure 4B). Although no individual gene was found to drive this enrichment, the gene set harboring these variants in the clinically heterogeneous patients representing the 2.5% right tail of the distribution showed a major enrichment for the JAK/STAT signaling pathway (adjusted $P = 1.4 \times 10^{-5}$). Conversely, the genes from the residual distribution were primarily enriched for the general immune system pathway (Figure 5 and Supplementary Table 10, http://onlinelibrary.wiley.com/doi/10.1002/art.41929/abstract). Interestingly, the predicted likely pathogenic case-only synonymous variants from the right tail of the distribution included a number of candidates in genes with known skeletal muscle–related function (Supplementary Table 11 and Supplementary Methods, http://onlinelibrary.wiley.com/doi/10.1002/art.41929/abstract).

Following the assumption that rare variants located in evolutionary constrained elements (Genomic Evolutionary Rate Profiling [GERP] rejection submission [RS] score >2) (27) have functional potential, we evaluated these variants (n = 42,448) and found no enrichment in cases ($P = 0.22$) (Figure 4C). No

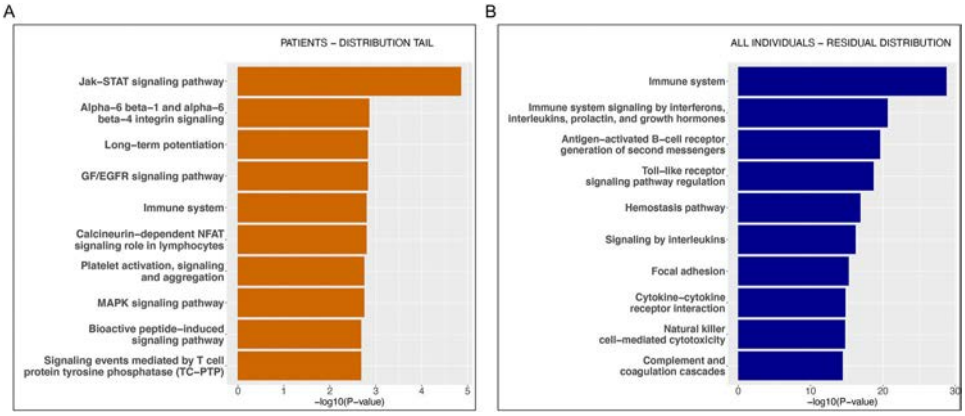

Figure 5. Gene set/pathway enrichment analysis of rare synonymous variants. **A**, Top 10 enriched gene sets/pathways derived from the rare synonymous variants with ≥1 minor allele detected in the patients constituting the 2.5% right tail of the distribution depicted in Figure 4B. The top 3 enriched gene sets/pathways here are respectively ranked 13th, 91st, and 343rd in the enrichment ranking from the analysis in **B**. **B**, Top 10 enriched gene sets/pathways derived from the rare synonymous variants with ≥1 minor allele detected in all individuals from the residual distribution indicated in Figure 4B. The top 3 enriched gene sets/pathways here are respectively ranked 5th, 221st, and 294th in the enrichment ranking from the analysis in **A**. Adjusted *P* values are shown.

evidence of allelic enrichment was detected for rare missense coding variants (n = 12,247) in patients ($P = 0.17$) (Figure 4D).

DISCUSSION

Targeted DNA sequencing, used here for the first time to study the genetic underpinnings of IIM, provides a valuable framework for exploring the genetic contribution to complex diseases characterized by effects from the full spectrum of allele frequencies, including common, low-frequency, and rare variations.

Our study confirmed that the strongest genetic risk for IIM exists within the HLA locus. The single-variant analysis top signal in *HLA–DQA1* presumably reflects the association with the 8.1 ancestral haplotype, as demonstrated by the loss of the whole association signal after conditional analysis on the well-established *DRB1*0301* IIM risk allele.

To effectively investigate rare variation, aggregate association testing algorithms that incorporate variants' functional annotations have recently been proposed to boost discovery power (16,28). Using GenePy, the gene-based aggregate analysis of all variants in the whole patient cohort identified the *IFI35* gene as a potential genetic risk locus for IIM. *IFI35* is preferentially induced by type I IFN and regulates the innate immune response (29). Type I IFN–inducible genes have been found to be overexpressed in the blood, muscle, and skin of DM and/or PM patients (30–32), and blockade of the type I IFN pathway has been investigated as a potential treatment option in such patients (33). Recently, *IFI35* overexpression has been detected and type I IFN pathway activation confirmed in muscle tissue from patients with DM and ASyS (6). Likely due to limited sample size, in the present study, we could only detect a nominal *IFI35* aggregate genetic association with the DM subgroup (raw $P = 0.0024$, FDR-corrected $P = 0.25$), which is also the clinical subgroup with strongest links to type I IFN in blood and tissues. ASyS did not show any association with *IFI35* (raw $P = 0.092$), which could also be due to a less strong association to type I IFN, as discussed below. Nevertheless, consistent with those findings that indicate a key role of type I IFN in the pathogenesis of certain subgroups of IIM, our study corroborates and provides additional evidence of its involvement in IIM at the genetic level.

It is well established that clinical and autoantibody-specific subgroups of IIM have distinct molecular pathway activation profiles. Here, we detected, among others, aggregate genetic associations in the *AGER*, *PSMB8*, and *PSMB9* genes with the ASyS subgroup. *AGER* encodes a multiligand cell surface receptor (receptor for advanced glycation end products [RAGE]) largely expressed in the lung. This gene has previously been associated with lung function and disease (34,35). It is noteworthy that interstitial lung disease is one of the key detrimental phenotypes associated with ASyS (12). *PSMB8* and *PSMB9* are interferonopathy genes involved in the proteasomal degradation pathway and are associated with proteasome-associated autoinflammatory syndromes (36). Interestingly, *PSMB8* has been indicated as the most significantly up-regulated gene in muscle tissue of ASyS patients (6). A reduced activation of the type I IFN pathway compared to the type II IFN pathway has also been described in ASyS patients (6,7). Consistently, our data suggest lower levels of genetic association with the type I IFN pathway in these patients compared to the rest of the IIM patients in our cohort. In fact, compared to all other patients, ASyS patients showed a suggestive depletion of minor alleles for the 16 collectively associated *IFI35* variants.

Autoimmune complex diseases have been largely associated with common noncoding genetic variation, but rare variants may also contribute to disease risk (37). In this study, we present evidence that rare variant alleles located in functionally important regulatory regions are enriched in IIM patients. Interestingly, this disease-driven overrepresentation was more pronounced for rare synonymous variants, which can be generally involved in gene expression, splicing, messenger RNA structure stability, and protein translation and folding. Gene set enrichment analysis indicated that the synonymous variant alleles showing overrepresentation in a clinically heterogeneous subset of patients do cluster in the JAK/STAT signaling pathway. Notably, JAK/STAT pathway inhibition has been proposed as a therapeutic target for DM (38,39). Intriguingly, when focusing on the subset of overrepresented case-only variants, a number of these were located in genes associated with muscular dysfunction. *TTN*, *EXOSC10*, *CDC42BPB*, and *CARM1* have been associated with Mendelian forms of myopathies, muscular atrophies, and motor neurodevelopmental disorders (40). Additionally, *COL1A1* and *COL4A5* could account for impaired collagen metabolism leading to muscle pain. Consistent with the genetic architecture of other polygenic disorders, IIM exhibits rare genetic variants that have the potential to exert monogenic effects in the relevant corresponding organ systems (41).

Despite not surviving multiple test correction, we also observed enrichment of rare noncoding regulatory variant alleles in IIM patients, with *IFI35* among the main gene drivers. It is interesting how 2 aggregate analyses based on different, albeit not fully independent, variant sets (i.e., all variants and all rare noncoding variants) implicate the *IFI35* locus as a potential genetic risk factor for IIM, thus cross-verifying each other.

When examining the potentially regulatory variants in the *IFI35* locus, we found from published chromatin immunoprecipitation sequencing data (20,21) that specific transcription factors active in immune signaling bind to several regions with variants and presumably regulate *IFI35* expression. These transcription factors include Bcl-3, which is crucial in controlling both innate and adaptive immunity (42), and FoxA1, which establishes a T cell regulatory population involved in inflammatory diseases (43).

Nearly half of the variants contributing to the *IFI35* aggregate association represent eQTLs in multiple tissues. Interestingly, these variants not only modulate *IFI35* expression but can also affect the level of several nearby gene transcripts, including

PTGES3L and *NBR2*. Our study suggests that the skeletal muscle–specific gene regulatory network, linking *IFI35* and *PTGES3L*, potentially contributes to the etiology of IIM. We hypothesize that, within this regulatory circuit, which is defined by direct across-gene enhancer– and promoter–promoter interactions, bordered by a distinct TAD in skeletal muscle, and characterized by high levels of LD, cumulative genetic contribution of eQTLs at the *IFI35* locus might also alter *PTGES3L* expression. Intriguingly, *PTGES3L* is predominantly expressed in skeletal muscle (Supplementary Figure 7, http://onlinelibrary.wiley.com/doi/10.1002/art.41929/abstract), which is supported by strong tissue-specific enhancers and the promoter for this gene. Notably, *PTGES3L* is associated with type 2A distal arthrogryposis (40). Arthrogryposis is a rare disorder characterized by systemic muscle weakness at birth and stiffness, thus showing some similarities with the IIM phenotype. Therefore, *PTGES3L* emerges as an attractive target for research in IIM, although further experiments and mechanistic evidence are required to confirm our hypothesis.

The *IFI35* locus eQTLs can also strongly affect *NBR2* expression in skeletal muscle. Interestingly, *NBR2* encodes a long noncoding RNA involved in metabolic and energy stress response (44), a process perturbed in muscle undergoing IIM pathogenic events (45). The non-MHC genes associated with IIM by gene-based aggregate testing, as well as showing evidence of replication (i.e., *PRDX3*, *SLAMF1*, *ZFAT*, and *PTPN6*), represent potentially novel genetic risk factors pointing to immune- and nonimmune-mediated mechanisms implicated in the development of muscle weakness and damage, such as oxidative stress (46), autophagy (47), and Toll-like receptor signaling (48,49). These mechanisms have all been suggested to contribute to the pathophysiology of IIM (1).

This study has the limitation of applying the old classification criteria for IIM, as samples were collected before the approval of the new European Alliance of Associations for Rheumatology/American College of Rheumatology classification criteria (50). Some patients might therefore be reclassified based on these more recent criteria. We also recognize that *IFI35* failed in our attempt to replicate the discovery aggregate testing results in the UK cohort. This could be due to the limited statistical power derived from the replication cohort size, the ancestry-specific aggregate effect of this gene (for which contribution of rare variation is key), or alternatively to the unique and overconservative strategy we used for replication in our study due to the lack of analogously sequenced UK controls. A further limitation is that our array targets mainly immune-related genes and covers only a fraction of the genome, thus preventing the investigation of additional genes and noncoding regions potentially involved in IIM pathogenesis.

In summary, aggregate genetic association suggests a potential role for *IFI35* and *PTGES3L* in the pathogenesis of IIM. We found a genetic signature indicating type I IFN pathway activation in IIM and highlighted specific genetic associations in patients with ASyS that are consistent with previous findings on their gene expression profile in muscle tissue and with lung involvement. Overall, these findings and the indication that genetic perturbations of the JAK/STAT pathway might occur in a subset of patients independently of the myositis subtype suggest that inhibitors of this pathway might be beneficial in a broader spectrum of patients. Our study highlights the contribution of rare genetic variation to disease susceptibility in a Scandinavian myositis cohort and in specific patient subgroups. These findings may collectively inform disease treatment options in the context of future personalized medicine practice.

ACKNOWLEDGMENTS

We would like to thank all patients and controls taking part in this study for making this research possible. We would also like to thank the UK Myositis Network for providing samples and relevant patient data. We thank Michael Dong for providing the 200 mammals' PhyloP evolutionary constraint scores. DNA sequencing and genotyping was performed at the SNP&SEQ Technology Platform in Uppsala. The facility is part of the National Genomics Infrastructure Sweden and Science for Life Laboratory. Computations were performed on resources provided by the Swedish National Infrastructure for Computing (SNIC) through Uppsala Multidisciplinary Center for Advanced Computational Science under projects SNIC SENS 2017142 and 2017107. A preliminary description of the project was presented at the 2019 Global Conference of Myositis 2019 (https://doi.org/10.1186/s41927-019-0078-3).

AUTHOR CONTRIBUTIONS

All authors were involved in drafting the article or revising it critically for important intellectual content, and all authors approved the final version to be published. Dr. Bianchi had full access to all of the data in the study and takes responsibility for the integrity of the data and the accuracy of the data analysis.

Study conception and design. Bianchi, Kozyrev, Notarnicola, Rönnblom, Lindblad-Toh, Lundberg, with contributions from members of the ImmunoArray Development Consortium.

Acquisition of data. Bianchi, Kozyrev, Notarnicola, Karlsson, Andersson, Cooper, Padyukov, Tjärnlund, Dastmalchi, Pyndt Diederichsen, Molberg, Chinoy, with contributions from members of the DISSECT Consortium.

Analysis and interpretation of data. Bianchi, Kozyrev, Notarnicola, Hultin Rosenberg, Pucholt, Rothwell, Alexsson, Sandling, Meadows, Lamb, Rönnblom, Lindblad-Toh, Lundberg, with contributions from members of the DISSECT Consortium.

ROLE OF THE STUDY SPONSOR

AstraZeneca had no role in the study design or in the collection, analysis, or interpretation of the data, the writing of the manuscript, or the decision to submit the manuscript for publication. Publication of this article was not contingent upon approval by AstraZeneca.

ADDITIONAL DISCLOSURES

Authors Hultin Rosenberg and Pucholt are employees of Olink Proteomics. Author Alexsson is an employee of Qiagen.

REFERENCES

1. Miller FW, Lamb JA, Schmidt J, Nagaraju K. Risk factors and disease mechanisms in myositis [review]. Nat Rev Rheumatol 2018;14:255–68.
2. Bohan A, Peter JB. Polymyositis and dermatomyositis: second of two parts [review]. N Engl J Med 1975;292:403–7.
3. Bohan A, Peter JB. Polymyositis and dermatomyositis: first of two parts [review]. N Engl J Med 1975;292:344–7.
4. Mammen AL, Casciola-Rosen L, Christopher-Stine L, Lloyd TE, Wagner KR. Myositis-specific autoantibodies are specific for myositis compared to genetic muscle disease. Neurol Neuroimmunol Neuroinflamm 2015;2:e172.
5. Lundberg IE. Myositis in 2016: new tools for diagnosis and therapy [review]. Nat Rev Rheumatol 2017;13:74–6.
6. Pinal-Fernandez I, Casal-Dominguez M, Derfoul A, Pak K, Plotz P, Miller FW, et al. Identification of distinctive interferon gene signatures in different types of myositis. Neurology 2019;93:e1193–204.
7. Rigolet M, Hou C, Amer YB, Aouizerate J, Periou B, Gherardi RK, et al. Distinct interferon signatures stratify inflammatory and dysimmune myopathies. RMD Open 2019;5:e000811.
8. Rothwell S, Chinoy H, Lamb JA, Miller FW, Rider LG, Wedderburn LR, et al. Focused HLA analysis in Caucasians with myositis identifies significant associations with autoantibody subgroups. Ann Rheum Dis 2019;78:996–1002.
9. Rothwell S, Cooper RG, Lundberg IE, Miller FW, Gregersen PK, Bowes J, et al. Dense genotyping of immune-related loci in idiopathic inflammatory myopathies confirms HLA alleles as the strongest genetic risk factor and suggests different genetic background for major clinical subgroups. Ann Rheum Dis 2016;75:1558–66.
10. Sandling JK, Pucholt P, Rosenberg LH, Farias FH, Kozyrev SV, Eloranta ML, et al. Molecular pathways in patients with systemic lupus erythematosus revealed by gene-centred DNA sequencing. Ann Rheum Dis 2021;80:109–17.
11. Lee S, Abecasis GR, Boehnke M, Lin XH. Rare-variant association analysis: study designs and statistical tests. Am J Hum Genet 2014;95:5–23.
12. Connors GR, Christopher-Stine L, Oddis CV, Danoff SK. Interstitial lung disease associated with the idiopathic inflammatory myopathies: what progress has been made in the past 35 years? [review]. Chest 2010;138:1464–74.
13. Griggs RC, Askanas V, DiMauro S, Engel A, Karpati G, Mendell JR, et al. Inclusion body myositis and myopathies [review]. Ann Neurol 1995;38:705–13.
14. Eriksson D, Bianchi M, Landegren N, Nordin J, Dalin F, Mathioudaki A, et al. Extended exome sequencing identifies BACH2 as a novel major risk locus for Addison's disease. J Intern Med 2016;280:595–608.
15. Lee S, Emond MJ, Bamshad MJ, Barnes KC, Rieder MJ, Nickerson DA, et al. Optimal unified approach for rare-variant association testing with application to small-sample case-control whole-exome sequencing studies. Am J Hum Genet 2012;91:224–37.
16. Mossotto E, Ashton JJ, O'Gorman L, Pengelly RJ, Beattie RM, MacArthur BD, et al. GenePy: a score for estimating gene pathogenicity in individuals using next-generation sequencing data. BMC Bioinformatics 2019;20:254.
17. Rentzsch P, Witten D, Cooper GM, Shendure J, Kircher M. CADD: predicting the deleteriousness of variants throughout the human genome. Nucleic Acids Res 2019;47:D886–94.
18. Price AL, Weale ME, Patterson N, Myers SR, Need AC, Shianna KV, et al. Long-range LD can confound genome scans in admixed populations [letter]. Am J Hum Genet 2008;83:132–5.
19. Cingolani P, Platts A, Wang LL, Coon M, Nguyen T, Wang L, et al. A program for annotating and predicting the effects of single nucleotide polymorphisms, SnpEff: SNPs in the genome of Drosophila melanogaster strain w^{1118}; iso-2; iso-3. Fly (Austin) 2012;6:80–92.
20. Roadmap Epigenomics Consortium, Kundaje A, Meuleman W, Ernst J, Bilenky M, Yen A, et al. Integrative analysis of 111 reference human epigenomes. Nature 2015;518:317–30.
21. The ENCODE Project Consortium. An integrated encyclopedia of DNA elements in the human genome. Nature 2012;489:57–74.
22. The GTEx Consortium. The Genotype-Tissue Expression (GTEx) project. Nat Genet 2013;45:580–5.
23. Walter K, Min JL, Huang J, Crooks L, Memari Y, McCarthy S, et al. The UK10K project identifies rare variants in health and disease. Nature 2015;526:82–90.
24. Bycroft C, Freeman C, Petkova D, Band G, Elliott LT, Sharp K, et al. The UK Biobank resource with deep phenotyping and genomic data. Nature 2018;562:203–9.
25. Van Hout CV, Tachmazidou I, Backman JD, Hoffman JD, Liu D, Pandey AK, et al. Exome sequencing and characterization of 49,960 individuals in the UK Biobank. Nature 2020;586:749–56.
26. Cano-Gamez E, Trynka G. From GWAS to function: using functional genomics to identify the mechanisms underlying complex diseases [review]. Front Genet 2020;11:424.
27. Cooper GM, Stone EA, Asimenos G, Program NC, Green ED, Batzoglou S, et al. Distribution and intensity of constraint in mammalian genomic sequence. Genome Res 2005;15:901–13.
28. Li XH, Li ZL, Zhou HF, Gaynor SM, Liu YW, Chen H, et al. Dynamic incorporation of multiple in silico functional annotations empowers rare variant association analysis of large whole genome sequencing studies at scale. Nat Genet 2020;52:969–83.
29. Jassal B, Matthews L, Viteri G, Gong C, Lorente P, Fabregat A, et al. The reactome pathway knowledgebase. Nucleic Acids Res 2020;48:D498–503.
30. Cappelletti C, Baggi F, Zolezzi F, Biancolini D, Beretta O, Severa M, et al. Type I interferon and Toll-like receptor expression characterizes inflammatory myopathies. Neurology 2011;76:2079–88.
31. Greenberg SA. Type 1 interferons and myositis [review]. Arthritis Res Ther 2010;12 Suppl 1:S4.
32. Greenberg SA, Pinkus JL, Pinkus GS, Burleson T, Sanoudou D, Tawil R, et al. Interferon-α/β-mediated innate immune mechanisms in dermatomyositis. Ann Neurol 2005;57:664–78.
33. Higgs BW, Zhu W, Morehouse C, White WI, Brohawn P, Guo X, et al. A phase 1b clinical trial evaluating sifalimumab, an anti-IFN-α monoclonal antibody, shows target neutralisation of a type I IFN signature in blood of dermatomyositis and polymyositis patients. Ann Rheum Dis 2014;73:256–62.
34. Hancock DB, Eijgelsheim M, Wilk JB, Gharib SA, Loehr LR, Marciante KD, et al. Meta-analyses of genome-wide association studies identify multiple loci associated with pulmonary function. Nat Genet 2010;42:45–52.
35. Repapi E, Sayers I, Wain LV, Burton PR, Johnson T, Obeidat M, et al. Genome-wide association study identifies five loci associated with lung function. Nat Genet 2010;42:36–44.
36. Arimochi H, Sasaki Y, Kitamura A, Yasutomo K. Dysfunctional immunoproteasomes in autoinflammatory diseases [review]. Inflamm Regen 2016;36:13.
37. Farias FH, Dahlqvist J, Kozyrev SV, Leonard D, Wilbe M, Abramov SN, et al. A rare regulatory variant in the MEF2D gene affects gene regulation and splicing and is associated with a SLE subphenotype in Swedish cohorts. Eur J Hum Genet 2019;27:432–41.
38. Ladislau L, Suarez-Calvet X, Toquet S, Landon-Cardinal O, Amelin D, Depp M, et al. JAK inhibitor improves type I interferon induced damage: proof of concept in dermatomyositis. Brain 2018;141:1609–21.
39. Paik JJ, Casciola-Rosen L, Shin JY, Albayda J, Tiniakou E, Leung DG, et al. Study of tofacitinib in refractory dermatomyositis: an open label pilot study of ten patients. Arthritis Rheumatol 2020;73:858–65.

40. Rappaport N, Twik M, Plaschkes I, Nudel R, Stein TI, Levitt J, et al. MalaCards: an amalgamated human disease compendium with diverse clinical and genetic annotation and structured search [review]. Nucleic Acids Res 2017;45:D877–87.
41. Katsanis N. The continuum of causality in human genetic disorders. Genome Biol 2016;17:233.
42. Tassi I, Claudio E, Wang H, Tang W, Ha HL, Saret S, et al. The NF-κB regulator Bcl-3 governs dendritic cell antigen presentation functions in adaptive immunity. J Immunol 2014;193: 4303–11.
43. Liu Y, Carlsson R, Comabella M, Wang J, Kosicki M, Carrion B, et al. FoxA1 directs the lineage and immunosuppressive properties of a novel regulatory T cell population in EAE and MS. Nat Med 2014;20: 272–82.
44. Liu X, Xiao ZD, Han L, Zhang J, Lee SW, Wang W, et al. LncRNA NBR2 engages a metabolic checkpoint by regulating AMPK under energy stress. Nat Cell Biol 2016;18:431–42.
45. Manole E, Bastian AE, Butoianu N, Goebel HH. Myositis non-inflammatory mechanisms: an up-dated review. J Immunoassay Immunochem 2017;38:115–26.
46. Lightfoot AP, Nagaraju K, McArdle A, Cooper RG. Understanding the origin of non-immune cell-mediated weakness in the idiopathic inflammatory myopathies: potential role of ER stress pathways [review]. Curr Opin Rheumatol 2015;27:580–5.
47. Cappelletti C, Galbardi B, Kapetis D, Vattemi G, Guglielmi V, Tonin P, et al. Autophagy, inflammation and innate immunity in inflammatory myopathies. PLoS One 2014;9:e111490.
48. Croker BA, Lawson BR, Rutschmann S, Berger M, Eidenschenk C, Blasius AL, et al. Inflammation and autoimmunity caused by a SHP1 mutation depend on IL-1, MyD88, and a microbial trigger. Proc Natl Acad Sci U S A 2008;105:15028–33.
49. Yurchenko M, Skjesol A, Ryan L, Richard GM, Kandasamy RK, Wang NH, et al. SLAMF1 is required for TLR4-mediated TRAM-TRIF–dependent signaling in human macrophages. J Cell Biol 2018; 217:1411–29.
50. Lundberg IE, Tjarnlund A, Bottai M, Werth VP, Pilkington C, Visser M, et al. 2017 European League Against Rheumatism/American College of Rheumatology classification criteria for adult and juvenile idiopathic inflammatory myopathies and their major subgroups. Arthritis Rheumatol 2017;76:2271–82.

APPENDIX A: THE DISSECT CONSORTIUM AND THE IMMUNOARRAY DEVELOPMENT CONSORTIUM COLLABORATORS

Members of the DISSECT Consortium are as follows: Matteo Bianchi, Sergey V. Kozyrev, Lina Hultin Rosenberg, Pascal Pucholt, Andrei Alexsson, Johanna K. Sandling, Lars Rönnblom, Maija-Leena Eloranta, Ann-Christine Syvänen, Dag Leonard, Jonas Carlsson Almlöf, Johanna Dahlqvist, Niklas Hagberg, Maria Lidén, Argyri Mathioudaki, Jennifer R. S. Meadows, Jessika Nordin, Gunnel Nordmark, Sule Yavuz (Uppsala University, Uppsala, Sweden); Ingrid E. Lundberg, Leonid Padyukov, Iva Gunnarsson, Elisabet Svenungsson, Daniel Eriksson (Karolinska Institutet and Karolinska University Hospital, Stockholm, Sweden); Øyvind Molberg (Oslo University Hospital and Institute of Clinical Medicine, University of Oslo, Oslo, Norway); Kerstin Lindblad-Toh (Uppsala University, Uppsala, Sweden and Broad Institute of MIT and Harvard, Cambridge, MA); Fabiana H. G. Farias (Uppsala University, Uppsala, Sweden, and Washington University, St. Louis, MO); Christine Bengtsson, Solbritt Rantapää-Dahlqvist (Umeå University, Umeå, Sweden); Roland Jonsson (University of Bergen, Bergen, Norway); Roald Omdal (Stavanger University Hospital, Stavanger, Norway, and University of Bergen, Bergen, Norway); Andreas Jönsen, Anders A. Bengtsson (Lund University and Skane University Hospital, Lund, Sweden); Christopher Sjöwall, Thomas Skogh (Linköping University, Linköping, Sweden); Marie Wahren-Herlenius (Karolinska Institutet and Karolinska University Hospital, Stockholm, Sweden, and University of Bergen, Norway); Awat Jalal (Örebro University Hospital, Örebro, Sweden); Balsam Hanna (Sahlgrenska University Hospital, Gothenburg, Sweden); Helena Hellström, Tomas Husmark (Falun Hospital, Falun, Sweden); Åsa Häggström (Kalmar Hospital, Kalmar, Sweden); and Anna Svärd (Falun Hospital, Falun, Sweden, and Uppsala University, Uppsala, Sweden).

Members of the ImmunoArray Development Consortium are as follows: Kerstin Lindblad-Toh (Uppsala University, Uppsala, Sweden, and Broad Institute of MIT and Harvard, Cambridge, MA); Gerli Rosengren Pielberg, Anna Lobell, Åsa Karlsson, Eva Murén, Kerstin M. Ahlgren, Lars Rönnblom; Maija-Leena Eloranta (Uppsala University, Uppsala, Sweden); Göran Andersson (Swedish University of Agricultural Sciences, Uppsala, Sweden); Nils Landegren (Karolinska Institutet, Stockholm, Sweden, and Uppsala University, Uppsala, Sweden); Olle Kämpe (Karolinska Institutet and Karolinska University Hospital, Stockholm, Sweden, Uppsala University, Uppsala, Sweden, and University of Bergen, Norway); and Peter Söderkvist (Linköping University, Linköping, Sweden).

Arthritis & Rheumatology
Vol. 74, No. 2, February 2022, pp 353–357
DOI 10.1002/art.41976

American College of Rheumatology
Empowering Rheumatology Professionals

BRIEF REPORT

Excess Serum Interleukin-18 Distinguishes Patients With Pathogenic Mutations in *PSTPIP1*

Deborah L. Stone,[1] Amanda Ombrello,[1] Juan I. Arostegui,[2] Corinne Schneider,[3] Vinh Dang,[4] Adriana de Jesus,[5] Charlotte Girard-Guyonvarc'h,[6] Cem Gabay,[6] Wonyong Lee,[1] Jae Jin Chae,[1] Ivona Aksentijevich,[1] Raphaela T. Goldbach-Mansky,[5] Daniel L. Kastner,[1] and Scott W. Canna[4]

Objective. Dominantly inherited *PSTPIP1* mutations cause a spectrum of autoinflammatory manifestations epitomized by PAPA syndrome (pyogenic sterile arthritis, pyoderma gangrenosum, and acne (PAPA) syndrome.). The connections between *PSTPIP1* and PAPA syndrome are poorly understood, although evidence suggests involvement of pyrin inflammasome activation. Interleukin-18 (IL-18) is an inflammasome-activated cytokine associated with susceptibility to macrophage activation syndrome (MAS). This study was undertaken to investigate an association of IL-18 with PAPA syndrome.

Methods. Clinical and genetic data and serum samples were obtained from patients referred to institutions due to symptoms indicative of PAPA syndrome. Serum IL-18, IL-18 binding protein (IL-18BP), and CXCL9 levels were assessed by bead-based assay, and free IL-18 levels were assessed by enzyme-linked immunosorbent assay.

Results. The symptoms of *PSTPIP1*-positive patients with PAPA syndrome overlapped with those of mutation-negative patients with PAPA-like conditions, but mutation-positive patients had earlier onset and a greater proportion had a history of arthritis. We found uniform elevation of total serum IL-18 in treated PAPA syndrome patients at levels nearly as high as those seen in NLRC4-associated autoinflammation with infantile enterocolitis patients, and well above levels found in most familial Mediterranean fever patients. Serum IL-18 elevation in PAPA syndrome patients persisted despite fluctuations in disease activity. Levels of the soluble IL-18 antagonist IL-18BP were modestly elevated, and PAPA syndrome patients had detectable free IL-18. PAPA syndrome was rarely associated with elevation of CXCL9, an indicator of interferon-γ activity, but no PAPA syndrome patients had a history of MAS.

Conclusion. PAPA syndrome is a refractory and often disabling monogenic autoinflammatory disease associated with chronic and unopposed elevation of serum IL-18 levels but not with risk of MAS. These findings affect our understanding of the diseases in which IL-18 is overproduced and suggest a link between pyrin inflammasome activation, IL-18, and autoinflammation, without susceptibility to MAS.

INTRODUCTION

PAPA syndrome (pyogenic sterile arthritis, pyoderma gangrenosum, and acne) was first shown to be associated with dominant mutations in *PSTPIP1* in 2002 (1), but since that time, the links between such mutations and the protean clinical manifestations have been challenging to elucidate. *PSTPIP1* mutations are now known to cause an array of manifestations that includes systemic features, early-onset (sterile) neutrophilic arthritis, and variable cutaneous involvement. Skin manifestations include simple

Supported by Intramural Research Programs of the National Human Genome Research Institute and National Institute of Allergy and Infectious Disease, NIH, the University Hospital of Geneva, the Institut d'Investigacions Biomediques August Pi i Sunyer, the RK Mellon Institute for Pediatric Research, and extramural funding from the National Institute of Allergy and Infectious Disease and Eunice Kennedy Shriver National Institute of Child Health and Human Development, NIH.

[1]Deborah L. Stone, MD, Amanda Ombrello, MD, Wonyong Lee, PhD, Jae Jin Chae, PhD, Ivona Aksentijevich, MD, Daniel L. Kastner, MD, PhD: National Human Genome Research Institute, NIH, Bethesda, Maryland; [2]Juan I. Arostegui, MD: Hospital Clínic de Barcelona, Institut d'Investigacions Biomédiques August Pi i Sunyer, Barcelona, Spain; [3]Corinne Schneider, BS: University of Pittsburgh and UPMC Children's Hospital of Pittsburgh, Pittsburgh, Pennsylvania; [4]Vinh Dang, BS, Scott W. Canna, MD: University of Pittsburgh and UPMC Children's Hospital of Pittsburgh, Pittsburgh, Pennsylvania, and The Children's Hospital of Philadelphia, Philadelphia, Pennsylvania; [5]Adriana de Jesus, MD, PhD, Raphaela T. Goldbach-Mansky, MD, MHS: National Institute of Allergy and Infectious Diseases, NIH, Bethesda, Maryland; [6]Charlotte Girard-Guyonvarc'h, MD, PhD, Cem Gabay, MD: University of Geneva, Geneva, Switzerland.

Author disclosures are available at https://onlinelibrary.wiley.com/action/downloadSupplement?doi=10.1002%2Fart.41976&file=art41976-sup-0001-Disclosureform.pdf.

Address correspondence to Scott W. Canna, MD, 1110A Abramson Research Center, 3615 Civic Center Boulevard, Philadelphia, PA 19104. Email: cannas@chop.edu.

Submitted for publication February 2, 2021; accepted in revised form September 2, 2021.

ulceration, pyoderma gangrenosum, cystic acne, and hidradenitis suppurativa (2). Other clinical findings can include cytopenias, lymphadenopathy, and hepatosplenomegaly, particularly in the context of high serum zinc levels and extremely elevated S100 protein levels (3). This spectrum has been collectively termed *PSTPIP1*-associated inflammatory diseases (2). Causative mutations operate in a dominant inheritance pattern and include both missense mutations and potentially, promotor microsatellite expansions (4).

Mechanistically, several *PSTPIP1* mutations have been shown to increase binding to pyrin (the protein mutated in familial Mediterranean fever [FMF]) and to activate both the pyrin and NLRP3 inflammasomes. *PSTPIP1* also interacts with the actin cytoskeleton and regulates the Wiskott-Aldrich Syndrome protein, and *PSTPIP1* mutants potentially alter actin dynamics, pyrin inflammasome activation, and innate immune cell motility (5,6).

Interleukin-18 (IL-18) is expressed by macrophages and by epithelia of the skin and intestine. It requires proteolytic activation, usually via inflammasome-dependent caspase 1 activation, and is thought to escape the cytosol through gasdermin D–mediated pyroptosis. Active IL-18 has a high-affinity soluble inhibitor called IL-18 binding protein (IL-18BP), which is itself induced by interferon-γ (IFNγ) signaling (7). IL-18 canonically acts on natural killer and activated T cells to promote production of type 1 cytokines and granule-mediated cytotoxicity. It usually acts in concert with cytokines of the JAK/STAT pathway such as IL-12 or IL-15. However, it may play homeostatic roles at tissue sites. Reports of serum IL-18 elevation have been published across a wide variety of infectious, malignant, and rheumatic diseases. However, the extraordinarily high serum levels necessary to overcome inhibition by IL-18BP and generate "free IL-18" appear restricted to diseases with the highest risk of macrophage activation syndrome (MAS), including systemic juvenile idiopathic arthritis (JIA), adult-onset Still's disease (AOSD), and monogenic disorders such as the NLRC4 inflammasomopathy autoinflammation with infantile enterocolitis (AIFEC; OMIM no. 616050) and C-terminal mutations in the Rho GTPase CDC42 (7–10).

PATIENTS AND METHODS

Patients were recruited and evaluated as part of natural history protocols ongoing in the intramural programs of the National Human Genome Research Institute and the National Institute of Allergy and Infectious Diseases, as well as the University of Pittsburgh and Hospital Clinic, Barcelona. All patients referred for evaluation of autoinflammatory disease indicative of PAPA syndrome (arthritis with suggestive skin findings, idiopathic pyoderma gangrenosum, severe acne/hidradenitis suppurativa, or known pathogenic mutation in *PSTPIP1*) and with serum available for study were included. PAPA syndrome patients (n = 20) were defined as those with a known mutation in *PSTPIP1*. Patients with "PAPA-like" conditions (n = 11) had refractory, idiopathic pyoderma gangrenosum and often other symptoms (Table 1), but no pathogenic mutation (in *PSTPIP1* or other genes) was detected. Samples from treated FMF patients (n = 18) and NLRC4-associated AIFEC patients (n = 3 [2 with distant enterocolitis]) were included as pyrin inflammasome and high IL-18 disease controls, respectively.

Total serum IL-18, IL-18BP, and CXCL9 levels were measured as described by Weiss et al (7). Briefly, serum was diluted 25-fold and assayed on a Magpix or Flexmap 3-D multiplex instrument per the instructions of the manufacturer (Luminex). Recombinant IL-18 (MBL International) and CXCL9 (PeproTech) were used to generate their respective standard curves. The standard curve for IL-18BP was generated using human IL-18BPa-Fc (R&D Systems) and run separately given its interaction with recombinant IL-18 (7). IL-18 and IL-18BPa beads were generated by conjugating capture antibody to magnetic beads per the instructions of the manufacturer (Bio-Rad), whereas CXCL9 beads (Bio-Rad) were purchased. Free IL-18 was measured in some samples by enzyme-linked immunosorbent assay as

Table 1. Clinical characteristics of the patients with PAPA syndrome and those with PAPA-like conditions*

Feature	PAPA (n = 20)	PAPA-like (n = 11)	Univariate *P*
Female sex	9 (45)	7 (64)	NS†
Age at onset, median (range) years‡	2.3 (0.2–45)	8.5 (3–19)	0.04§
Arthritis	16 (80)	1 (9)	0.0004†
Cystic acne	11 (55)	6 (55)	NS†
Mild	4 (20)	1 (9)	–
Moderate	1 (5)	0	–
Severe	6 (30)	5 (45)	–
Pyoderma gangrenosum	13 (65)	11 (100)	NS†
Mild	3 (15)	1 (9)	–
Moderate	3 (15)	2 (18)	–
Severe	7 (35)	8 (73)	–
Maximum CRP, median (range) mg/dl‡	2.4 (0.2–21.2)	1.15 (0.4–7.2)	0.03§

* Except where indicated otherwise, values are the number (%) of patients. PAPA = pyogenic sterile arthritis, pyoderma gangrenosum, and acne syndrome; NS = not significant; CRP = C-reactive protein.
† By Fisher's exact test.
‡ Based on records available for time points associated with biomarker measurements.
§ By Welch's *t*-test.

previously described (10). Minimal variation between plates and runs was verified using bridging controls.

RESULTS

This study originated, while assessing autoinflammatory disease controls for an MAS study (7), from the observation of highly elevated total serum IL-18 levels in 2 patients with PAPA syndrome. Subsequently, a total of 31 patients were identified as having been referred to institutions for symptoms suggestive of PAPA syndrome. Twenty patients were found to have heterozygous mutations in *PSTPIP1*, with the p.Ala230Thr (11 of 20 patients) and p.Glu250Gln (6 of 20 patients) occurring as the most prevalent (Supplementary Table 1, https://onlinelibrary.wiley.com/doi/10.1002/art.41976). In contrast, 11 patients with PAPA-like conditions did not carry mutations in *PSTPIP1*. One patient with a PAPA-like condition (with pyoderma gangrenosum) carried a heterozygous Arg405Cys variant, while a patient with an undifferentiated autoinflammatory disease (recurrent fevers) carried a heterozygous p.Gly258Ala variant, both of which we classified as benign.

Clinical features overlapped substantially between patients with and those without *PSTPIP1* mutations, consistent with the pattern of their referrals. However, PAPA syndrome patients carrying *PSTPIP1* mutations were, on average, younger at disease onset, more had a history of arthritis, and fewer had a history of pyoderma gangrenosum (Table 1). Both groups' treatment history reflected the often recalcitrant nature of these symptoms, with many patients having been treated with glucocorticoids and >1 biologic medicine (Supplementary Table 1). Two patients had clinical features of PAPA syndrome in addition to cytopenias, organomegaly, and mutations associated with the hyperzincemia/hypercalprotectinemia syndrome (11). No patients with PAPA syndrome or PAPA-like conditions had a history of MAS.

As part of an effort to determine the distribution of serum IL-18 across autoinflammatory diseases (7), stored sera from enrolled patients were assayed retrospectively and compared with that of relevant disease controls. These controls included patients with activating mutations causing NLRC4 inflammasome–induced AIFEC as well as patients with FMF, all of whom were undergoing antiinflammatory treatment (Supplementary Table 1). Previous work has demonstrated that dramatically elevated serum IL-18 and detectable free IL-18 levels were unique to patients at significant risk for MAS and not for other inflammasomopathies, type I IFN–mediated diseases, or other autoinflammatory diseases (7). Contradicting this, we observed highly elevated serum IL-18 levels in the group of patients with mutations in *PSTPIP1* (Figure 1A). Serum IL-18 levels in patients with PAPA-like conditions were largely in the normal range. As expected, AIFEC serum IL-18 levels were highly elevated. Sera from ~50% of the FMF patients showed above-average levels, but only a few samples showed elevations in the range routinely observed in PAPA syndrome. This did not appear to correlate with

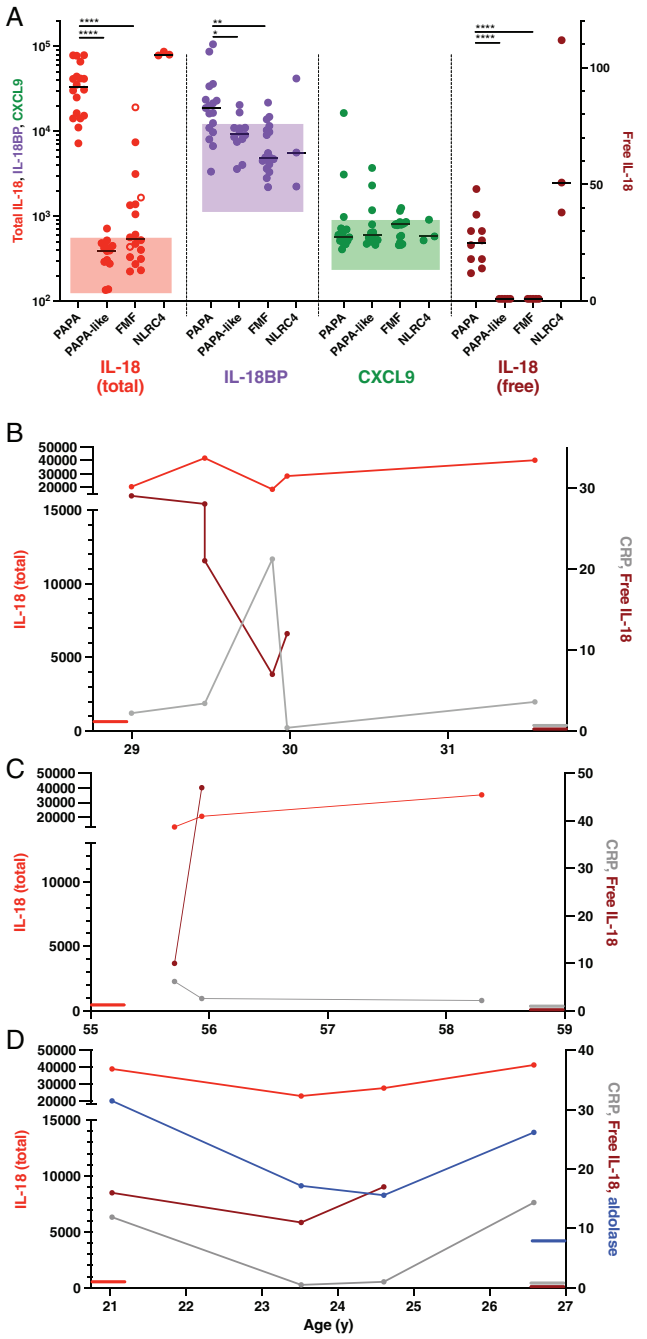

Figure 1. Association of PAPA syndrome (pyogenic sterile arthritis, pyoderma gangrenosum, and acne) with elevated levels of total and free interleukin-18 (IL-18). **A**, Serum was assayed for the indicated cytokines. Each symbol represents the first available sample from each patient. Shaded bars indicate the normal range. PAPA syndrome, PAPA-like conditions, and familial Mediterranean fever (FMF) groups were compared. Open circles in the total IL-18 graph represent p.Met694Val-homozygous FMF patients. * = $P < 0.05$; ** = $P < 0.01$; **** = $P < 0.0001$, by one-way analysis of variance with Tukey's post hoc test. **B–D**, Longitudinal measurements of IL-18, free IL-18, and C-reactive protein (CRP) from 3 PAPA syndrome patients carrying *PSTPIP1* mutations are shown. IL-18BP = IL-18 binding protein.

genotype, even in patients carrying homozygous p.Met694Val mutations in *MEFV* (12) (Figure 1A and Supplementary Table 1, https://onlinelibrary.wiley.com/doi/10.1002/art.41976). CXCL9 levels were not consistently elevated in any group. Although IL-18BP levels were significantly higher in patients with PAPA syndrome than in those with PAPA-like conditions, we were nevertheless able to detect free IL-18 in samples from PAPA syndrome patients.

In several patients, we were also able to analyze serial samples. Though we observed some variation in total and free IL-18 levels, the degree of this variation was minor in comparison to the degree of C-reactive protein variation (Figures 1B–D). All patients who were followed up longitudinally showed dramatic elevations of total IL-18 and detectable free IL-18 levels at all time points.

DISCUSSION

Many infectious, oncologic, or rheumatic causes of systemic inflammation have been associated with elevated peripheral levels of IL-18, and even very small differences have been independently associated with worse outcomes in chronic inflammatory diseases such as atherosclerosis (13). However, IL-18 has an extraordinary dynamic range of >4 logs in human serum, and extremely high total IL-18 levels have heretofore been observed almost exclusively in diseases associated with MAS, including systemic JIA, AOSD, and a few rare monogenic immune dysregulation disorders such as AIFEC/NLRC4-associated MAS (7). This has prompted investigation of IL-18 as a fundamental cause of MAS, and clinical trials of IL-18 blockade in genetically mediated MAS are in progress (ClinicalTrials.gov identifiers: NCT03113760, NCT04641442).

Though PAPA syndrome patients do not appear to be at risk for MAS, we found highly and chronically elevated total serum IL-18 levels and detectable free IL-18 in mutation-positive patients with PAPA syndrome. Disease activity can be challenging to quantitate in PAPA syndrome, but IL-18 levels did not clearly correlate with acute-phase reactants or with arthritis-, pyoderma-, or acne-predominant patients (Supplementary Table 1, https://onlinelibrary.wiley.com/doi/10.1002/art.41976). This suggests a direct pathogenic link between *PSTPIP1* and increased IL-18 levels, likely through pyrin inflammasome activation. Supporting this notion, we have corroborated others' findings that IL-18 can be significantly elevated in the serum of some FMF patients, possibly related to disease activity and/or p.Met694Val homozygosity (12). Likewise, mutations in *WDR1* causing periodic fever, immunodeficiency, or thrombocytopenia (PFIT) syndrome may also cause unopposed IL-18 elevation (14). However, IL-18 levels in most FMF patients are not significantly elevated, nor are those in pyrin-associated autoinflammation with neutrophilic dermatosis (7). The specific genetic, cellular, and environmental circumstances driving IL-18 through the pyrin inflammasome remain unclear.

IL-18 may be significantly elevated in PAPA syndrome without increasing MAS risk for a variety of reasons. First, although ample animal experiments and preliminary case reports suggest otherwise (7,15), it is possible that IL-18 elevation is associated with autoinflammatory diseases such as PAPA syndrome, PFIT syndrome, and MAS, but is not contributory to the pathology. Second, IL-18 typically functions by amplifying the effects of other cytokines; the inflammatory milieu of systemic JIA/MAS and AIFEC/NLRC4-associated MAS may be substantively different than that of PAPA syndrome. Third, though both are associated with detectable free IL-18, it may be that only the highest levels of IL-18 activity are sufficient to promote MAS. Finally, the source of IL-18 may dramatically alter its effects. The sources of extreme and chronic IL-18 elevation remain unclear. Macrophages are the canonical sites of inflammasome activation and IL-18 production, and *PSTPIP1* mutations have been shown to activate the pyrin inflammasome in macrophages in vitro (16). However, recent work in *Nlrc4*-hyperactive mice suggests that (intestinal) epithelial cells have both inflammasome machinery and abundant pro–IL-18 as a substrate (7). Notably, skin epithelium is also a substantial source of *Il18* transcript (7,13).

Measurement of peripheral IL-18 may be diagnostically useful in the evaluation of PAPA syndrome regardless of its pathogenic role. The difference in IL-18 between *PSTPIP1* mutation–positive patients and *PSTPIP1* mutation–negative patients appeared binary and helped confirm the p.Arg405Cys and p.Gly258Ala variants as likely nonpathogenic. Serum was available from only 1 patient carrying a mutation associated with *PSTPIP1*-associated myeloid-related proteinemia inflammatory syndrome and was elevated similarly to the elevations in other PAPA syndrome patients. Some patients in our cohort had almost exclusively cutaneous or articular disease, suggesting that IL-18 elevation correlates with *PSTPIP1* mutations rather than specific phenotypic features. Thus, serum IL-18 appears to reliably distinguish patients carrying true *PSTPIP1* mutations from patients with suspicious clinical findings or rare variants. Elucidating what connects specific autoinflammatory genes with dramatic elevations of S100 proteins, IL-18, and possibly zinc remains an important area of future research (2,3).

Although we included 20 PAPA syndrome patients from various institutions, our study was limited by its relatively small size and retrospective nature. Future studies would benefit from multicenter prospective enrollment and concomitant measurement of other PAPA syndrome–associated biomarkers (e.g., aldolase, zinc, S100 proteins). Nevertheless, our observations add a puzzling diversity to the group of disorders characterized by chronic elevation of total and free IL-18, and outline a path for studying the pathogenic effects of IL-18 beyond MAS.

AUTHOR CONTRIBUTIONS

All authors were involved in drafting the article or revising it critically for important intellectual content, and all authors approved the final

version to be published. Dr. Canna had full access to all of the data in the study and takes responsibility for the integrity of the data and the accuracy of the data analysis.

Study conception and design. Stone, Goldbach-Mansky, Kastner, Canna.

Acquisition of data. Stone, Ombrello, Arostegui, Schneider, Dang, de Jesus, Girard-Guyonvarc'h, Aksentijevich, Canna.

Analysis and interpretation of data. Gabay, Lee, Chae, Aksentijevich, Goldbach-Mansky, Kastner, Canna.

REFERENCES

1. Wise CA, Gillum JD, Seidman CE, Lindor NM, Veile R, Bashiardes S, et al. Mutations in CD2BP1 disrupt binding to PTP PEST and are responsible for PAPA syndrome, an autoinflammatory disorder. Hum Mol Genet 2002;11:961–9.
2. Holzinger D, Roth J. Alarming consequences: autoinflammatory disease spectrum due to mutations in proline-serine-threonine phosphatase-interacting protein 1 [review]. Curr Opin Rheumatol 2016;28:550–9.
3. Holzinger D, Fassl SK, de Jager W, Lohse P, Rohrig UF, Gattorno M, et al. Single amino acid charge switch defines clinically distinct proline-serine-threonine phosphatase-interacting protein 1 (PSTPIP1)-associated inflammatory diseases. J Allergy Clin Immunol 2015;136: 1337–45.
4. Demidowich AP, Freeman AF, Kuhns DB, Aksentijevich I, Gallin JI, Turner ML, et al. Genotype, phenotype, and clinical course in five patients with PAPA syndrome (pyogenic sterile arthritis, pyoderma gangrenosum, and acne). Arthritis Rheum 2012;64:2022–7.
5. Cortesio CL, Wernimont SA, Kastner DL, Cooper KM, Huttenlocher A. Impaired podosome formation and invasive migration of macrophages from patients with a PSTPIP1 mutation and PAPA syndrome. Arthritis Rheum 2010;62:2556–8.
6. Akkaya-Ulum YZ, Balci-Peynircioglu B, Purali N, Yilmaz E. Pyrin-PSTPIP1 colocalises at the leading edge during cell migration. Cell Biol Int 2015;39:1384–94.
7. Weiss ES, Girard-Guyonvarc'h C, Holzinger D, de Jesus AA, Tariq Z, Picarsic J, et al. Interleukin-18 diagnostically distinguishes and pathogenically promotes human and murine macrophage activation syndrome. Blood 2018;131:1442–55.
8. Gernez Y, de Jesus AA, Alsaleem H, Macaubas C, Roy A, Lovell D, et al. Severe autoinflammation in 4 patients with C-terminal variants in cell division control protein 42 homolog (CDC42) successfully treated with IL-1β inhibition. J Allergy Clin Immunol 2019;144:1122–25.
9. Lam MT, Coppola S, Krumbach OH, Prencipe G, Insalaco A, Cifaldi C, et al. A novel disorder involving dyshematopoiesis, inflammation, and HLH due to aberrant CDC42 function. J Exp Med 2019;216:2778–99.
10. Girard C, Rech J, Brown M, Allali D, Roux-Lombard P, Spertini F, et al. Elevated serum levels of free interleukin-18 in adult-onset Still's disease. Rheumatology (Oxford) 2016;55:2237–47.
11. Laberko A, Burlakov V, Maier S, Abinun M, Skinner R, Kozlova A, et al. HSCT is effective in patients with PSTPIP1-associated myeloid-related proteinemia inflammatory (PAMI) syndrome. J Allergy Clin Immunol 2021;148:250–5.
12. Stoler I, Freytag J, Orak B, Unterwalder N, Henning S, Heim K, et al. Gene-dose effect of MEFV gain-of-function mutations determines ex vivo neutrophil activation in familial Mediterranean fever. Front Immunol 2020;11:716.
13. Kaplanski G. Interleukin-18: Biological properties and role in disease pathogenesis [review]. Immunol Rev 2018;281:138–53.
14. Standing AS, Malinova D, Hong Y, Record J, Moulding D, Blundell MP, et al. Autoinflammatory periodic fever, immunodeficiency, and thrombocytopenia (PFIT) caused by mutation in actin-regulatory gene WDR1. J Exp Med 2017;214:59–71.
15. Tsoukas P, Rapp E, Van Der Kraak L, Weiss ES, Dang V, Schneider C, et al. Interleukin-18 and cytotoxic impairment are independent and synergistic causes of murine virus-induced hyperinflammation. Blood 2020;136:2162–74.
16. Yu JW, Fernandes-Alnemri T, Datta P, Wu J, Juliana C, Solorzano L, et al. Pyrin activates the ASC pyroptosome in response to engagement by autoinflammatory PSTPIP1 mutants. Mol Cell 2007;28: 214–27.

Arthritis & Rheumatology
Vol. 74, No. 2, February 2022, pp 358–364
DOI 10.1002/art.41931

American College of Rheumatology
Empowering Rheumatology Professionals

BRIEF REPORT

Anti-Cortactin Autoantibodies Are Associated With Key Clinical Features in Adult Myositis But Are Rarely Present in Juvenile Myositis

Iago Pinal-Fernandez,[1] Katherine Pak,[2] Albert Gil-Vila,[3] Andres Baucells,[4] Benjamin Plotz,[5] Maria Casal-Dominguez,[6] Assia Derfoul,[2] Maria Angeles Martinez-Carretero,[4] Albert Selva-O'Callaghan,[3] Sara Sabbagh,[7] Livia Casciola-Rosen,[8] Jemima Albayda,[8] Julie Paik,[8] Eleni Tiniakou,[8] Sonye K. Danoff,[8] Thomas E. Lloyd,[8] Frederick W. Miller,[9] Lisa G. Rider,[9] Lisa Christopher-Stine,[8] and Andrew L. Mammen,[6] on behalf of the Childhood Myositis Heterogeneity Collaborative Study Group

Objective. To define the prevalence and clinical phenotype of anti-cortactin autoantibodies in adult and juvenile myositis.

Methods. In this longitudinal cohort study, anti-cortactin autoantibody titers were assessed by enzyme-linked immunosorbent assay in 670 adult myositis patients and 343 juvenile myositis patients as well as in 202 adult healthy controls and 90 juvenile healthy controls. The prevalence of anti-cortactin autoantibodies was compared among groups. Clinical features of patients with and those without anti-cortactin autoantibodies were also compared.

Results. Anti-cortactin autoantibodies were more common in adult dermatomyositis (DM) patients (15%; $P = 0.005$), particularly those with coexisting anti–Mi-2 autoantibodies (24%; $P = 0.03$) or anti–NXP-2 autoantibodies (23%; $P = 0.04$). In adult myositis, anti-cortactin was associated with DM skin involvement (62% of patients with anti-cortactin versus 38% of patients without anti-cortactin; $P = 0.03$), dysphagia (36% versus 17%; $P = 0.02$) and coexisting anti–Ro 52 autoantibodies (47% versus 26%; $P = 0.001$) or anti-NT5c1a autoantibodies (59% versus 33%; $P = 0.001$). Moreover, the titers of anti-cortactin antibodies were higher in patients with interstitial lung disease (0.15 versus 0.12 arbitrary units; $P = 0.03$). The prevalence of anti-cortactin autoantibodies was not different in juvenile myositis patients (2%) or in any juvenile myositis subgroup compared to juvenile healthy controls (4%). Nonetheless, juvenile myositis patients with these autoantibodies had a higher prevalence of "mechanic's hands" (25% versus 7%; $P = 0.03$), a higher number of hospitalizations (2.9 versus 1.3; $P = 0.04$), and lower peak creatine kinase values (368 versus 818 IU/liter; $P = 0.02$) than those without anti-cortactin.

Conclusion. The prevalence of anti-cortactin autoantibodies is increased in adult DM patients with coexisting anti–Mi-2 or anti–NXP-2 autoantibodies. In adults, anti-cortactin autoantibodies are associated with dysphagia and interstitial lung disease.

Supported by the Intramural Research Program of the National Institute of Arthritis and Musculoskeletal and Skin Diseases and the National Institute of Environmental Health Sciences of the NIH, and Dr. Peter Buck. Dr. Pinal-Fernandez's work was supported by the Myositis Association.

[1]Iago Pinal-Fernandez, MD, PhD: National Institute of Arthritis and Musculoskeletal and Skin Diseases, NIH, Bethesda, Maryland, Johns Hopkins University School of Medicine, Baltimore, Maryland, and Universitat Oberta de Catalunya, Barcelona, Spain; [2]Katherine Pak, MD, Assia Derfoul, PhD: National Institute of Arthritis and Musculoskeletal and Skin Diseases, NIH, Bethesda, Maryland; [3]Albert Gil-Vila, MD, Albert Selva-O'Callaghan, MD, PhD: Vall d'Hebron Hospital and Autonomous University of Barcelona, Barcelona, Spain; [4]Andres Baucells, MD, Maria Angeles Martinez-Carretero, PhD: Sant Pau Hospital, Barcelona, Spain; [5]Benjamin Plotz, MD: New York University Langone Health, New York, New York; [6]Maria Casal-Dominguez MD, PhD, Andrew L. Mammen, MD, PhD: National Institute of Arthritis and Musculoskeletal and Skin Diseases, NIH, Bethesda, Maryland, and Johns Hopkins University School of Medicine, Baltimore, Maryland; [7]Sara Sabbagh, DO: Medical College of Wisconsin, Milwaukee, Wisconsin; [8]Livia Casciola-Rosen, PhD, Jemima Albayda, MD, Julie Paik, MD, MHS, Eleni Tiniakou, MD, Sonye K. Danoff, MD, PhD, Thomas E. Lloyd, MD, PhD, Lisa Christopher-Stine, MD, MPH: Johns Hopkins University School of Medicine, Baltimore, Maryland; [9]Frederick W. Miller, MD, PhD, Lisa G. Rider, MD: National Institute of Environmental Health Sciences, NIH, Bethesda, Maryland.

Drs. Pinal-Fernandez, Pak, Gil-Vila, Baucells, and Plotz contributed equally to this work.

Author disclosures are available at https://onlinelibrary.wiley.com/action/downloadSupplement?doi=10.1002%2Fart.41931&file=art41931-sup-0001-Disclosureform.pdf.

Address correspondence to Andrew L. Mammen, MD, PhD, Muscle Disease Unit, Laboratory of Muscle Stem Cells and Gene Regulation, National Institute of Arthritis and Musculoskeletal and Skin Diseases, NIH, 50 South Drive, Building 50, Room 1141, MSC 8024, Bethesda, MD 20892 (e-mail: andrew.mammen@nih.gov); or to Iago Pinal-Fernandez, MD, PhD, Muscle Disease Unit, Laboratory of Muscle Stem Cells and Gene Regulation, National Institute of Arthritis and Musculoskeletal and Skin Diseases, NIH, 50 South Drive, Building 50, Room 1141, MSC 8024, Bethesda, MD 20892 (e-mail: iago.pinalfernandez@nih.gov).

Submitted for publication September 20, 2020; accepted in revised form June 22, 2021.

INTRODUCTION

Idiopathic inflammatory myopathies (IIMs) are a heterogeneous group of diseases, and patients may be classified as having dermatomyositis (DM), polymyositis (PM), immune-mediated necrotizing myopathy (IMNM), or overlap myositis based on clinical and muscle biopsy features (1). In older adults, inclusion body myositis (IBM) represents another important type of IIM (2). In addition to these clinicopathologic categories, myositis-specific autoantibodies (MSAs) define distinct subtypes of myositis with unique clinical features. Furthermore, many myositis patients have myositis-associated autoantibodies (MAAs) that may be found in patients with other autoimmune disorders as well (3).

In 2014, autoantibodies targeting cortactin, a ubiquitous cytoplasmic protein that regulates polymerization of the actin cytoskeleton, were identified in adult patients with myositis (4) and those with myasthenia gravis (5). In a Spanish cohort of 162 adult myositis patients, these MAAs were present in 7 of 34 (20%) PM patients, 9 of 117 (7.6%) DM patients, 2 of 7 (28%) IMNM patients, and 0 of 4 (0%) IBM patients (4). Moreover, only 1 of 29 patients with noninflammatory myopathies tested positive. Anti-cortactin autoantibodies were not associated with distinct clinical features in this relatively small cohort of myositis patients (4). Furthermore, the prevalence and clinical features of anti-cortactin autoantibodies in juvenile myositis have not been described.

We undertook the present study to define the prevalence and clinical characteristics of adult and pediatric myositis patients with anti-cortactin autoantibodies. To accomplish this, we utilized large cohorts of patients with well-characterized adult and juvenile myositis that included significant numbers of patients with each of the major MSA-defined subtypes of myositis.

PATIENTS AND METHODS

Adult patients and sera. Six hundred seventy patients enrolled in the Johns Hopkins Myositis Center Longitudinal Cohort study between 2002 to 2015 were included in the study. These patients were classified as having IBM if they fulfilled the Lloyd-Greenberg criteria (6), having DM or PM according to the Bohan and Peter criteria (7), or having clinically amyopathic dermatomyositis according to Sontheimer's criteria (8). The clinical features of anti-cortactin–positive patients were compared to anti-cortactin–negative patients in the subset of 409 patients that had IBM or were positive for autoantibodies recognizing Mi-2, NXP-2, transcription intermediary factor 1γ (TIF1γ), melanoma differentiation–associated protein 5 (MDA-5), Jo-1, signal recognition particle, or hydroxymethylglutaryl-coenzyme A reductase (HMGCR) by ≥2 immunologic techniques from among the following: enzyme-linked immunosorbent assay (ELISA), in vitro transcription and translation followed by immunoprecipitation (IP), line blotting (EuroLine myositis profile), or IP from S35-labeled HeLa cell lysates (9,10). Data on demographic characteristics and clinical and laboratory features were collected prospectively at each visit. Dysphagia was defined by patient report as any type of difficulty swallowing, and interstitial lung disease (ILD) was defined through a multidisciplinary approach as suggested by the American Thoracic Society (11). Sera samples from 202 healthy adult donors to the National Institutes of Health (NIH) blood bank were also included in the study as controls.

Juvenile myositis patients and sera. Three hundred forty-three patients from the Childhood Myositis Heterogeneity Collaborative Study (12,13) enrolled in the NIH studies between 1989 and 2016 with probable or definite juvenile-onset myositis according to the Bohan and Peter criteria (7) were included. Sera from 90 healthy children enrolled in the same studies as controls were available. A physician questionnaire captured demographic data, clinical and laboratory features, and therapeutic usage (13). Patient sera from the time of enrollment were tested for myositis autoantibodies by validated methods, including protein and RNA IP using radiolabeled HeLa or K562 cell extracts, double immunodiffusion, immunoblot, or ELISA (13–15). For anti-TIF1γ, anti–NXP-2, and anti–MDA-5 autoantibodies, serum samples were screened by IP, with confirmation testing by IP blotting (16).

Anti-cortactin autoantibody testing. For the anti-cortactin autoantibody ELISA, the earliest available serum sample for each patient was used. Ninety-six–well ELISA plates were coated overnight at 4°C with 100 μg of recombinant cortactin protein (no. TP710315; OriGene) diluted in phosphate buffered saline (PBS). After washing the plates, human serum samples, diluted 1:100 in PBS with 5% nonfat milk and 0.05% Tween (PBS–Tween), were added to the wells (1 hour at room temperature). After washing, the horseradish peroxidase–labeled goat anti-human antibody (1:10,000 dilution) (no. 109-036-088; Jackson ImmunoResearch) was added to each well (40 minutes at room temperature). Color development was performed using SureBlue peroxidase reagent (KPL), and absorbances at 450 nm were determined. Test sample absorbances were normalized to the sera of an arbitrarily selected patient positive for anti-cortactin, a reference serum included in every ELISA. The cutoff for a normal anti-cortactin autoantibody titer was set at 0.21 arbitrary units (AU), calculated as 2 SD above the mean of the normalized absorbances in the 90 healthy juvenile controls. This cutoff was determined to be optimal based on a graphical analysis of the curve of normalized absorbances (17) (Supplementary Figure 1, available on the *Arthritis & Rheumatology* website at http://onlinelibrary.wiley.com/doi/10.1002/art.41931/abstract).

Standard protocol approvals and patient consent. This study was approved by the Johns Hopkins and NIH institutional review boards. Written informed consent was obtained from each participant.

Statistical analysis. Dichotomous variables are expressed as absolute frequencies and percentages, and continuous variables are reported as the mean ± SD. Bootstrapping with 1,000 replicates using the first-order normal approximation was used to statistically validate our key estimates using the boot R library version 1.3 for dichotomous variables and command bootstrap in Stata for continuous variables. Results are shown as 95% confidence intervals (95% CIs). Comparisons between groups were made using chi-square test, Fisher's exact test, or Student's *t*-test. Logistic and linear regression was used to adjust comparisons for the length of follow-up, and MSAs (or MSAs and IBM in adult patients). As previously described, indirect standardization was used to calculate the mortality (standardized mortality rate [SMR]) and rate of cancer (standardized cancer rate [SCR]) in adult myositis patients compared to the general population (10). Statistical analyses were performed using Stata/MP 14.1 and R version 4.0.3. A 2-sided *P* value less than 0.05 was considered significant with no correction for multiple comparisons.

RESULTS

Prevalence of anti-cortactin autoantibodies in adult myositis patients. Overall, the prevalence of anti-cortactin autoantibodies in the 670 adult myositis patients (11% [95% CI 9–13%]) (Table 1) was not different than that in 202 adult healthy controls (8% [95% CI 4–11%]; $P = 0.2$). However, anti-cortactin autoantibodies were more prevalent among adult DM patients (15% [95% CI 11–19%]) compared to either healthy adults ($P = 0.02$) or to the combined group of non-DM adult myositis patients (8% [95% CI 6–11%]; $P = 0.005$). Among the autoantibody subgroups of adult DM patients, the only 2 groups with a higher prevalence of anti-cortactin autoantibodies compared to adult healthy controls were patients positive for anti–Mi-2 (24% [95% CI 8–40%]; $P = 0.01$) and those positive for anti–NXP-2 (23% [95% CI 9–36%]; $P = 0.01$). Although the prevalence of anti-cortactin autoantibodies was lower in IBM patients (4% [95% CI 1–7%]; $P = 0.002$) and the anti-HMGCR autoantibody–positive subgroup (3% [95% CI 0–8%]; $P = 0.05$) than in other myositis patients, anti-cortactin autoantibodies were not significantly decreased in these 2 groups compared to the adult healthy controls (Table 1 and Supplementary Figure 2, http://onlinelibrary.wiley.com/doi/10.1002/art.41931/abstract). Anti-cortactin antibodies were also found in 18% [95% CI 3–33%] of the 28 anti-Pm/Scl–positive patients and 22% [95% CI 0–50%] of the 9 anti–U1 RNP–positive patients tested. There was an increased level of muscle weakness in the arm abductors of the patients positive for anti-cortactin with anti-Pm/Scl autoantibodies, but the rest of the clinical features were similar for anti-Pm/Scl and anti-Ku antibodies.

The epidemiologic features were similar between groups, except for a lower prevalence of anti-cortactin antibodies in white adult myositis patients (59% [95% CI 48–71%] versus 75% [95% CI 72–78%]; $P = 0.02$) (Table 2).

Clinical features of adult myositis patients with anti-cortactin autoantibodies. To determine whether anti-cortactin autoantibodies are associated with specific clinical features, we first performed a multivariate analysis comparing patients

Table 1. Prevalence of anti-cortactin autoantibodies in the adult and juvenile myositis patients*

	Adult myositis			Juvenile myositis		
	No./total no. tested (%)	*P*†	*P*‡	No./total no. tested (%)	*P*†	*P*‡
Clinical group						
DM	42/279 (15)	0.005	0.02	8/282 (3)	NS	NS
CADM	4/21 (19)	NS	NS	–	–	–
PM	23/231 (10)	NS	NS	0/23 (0)	NS	NS
IBM	5/139 (4)	0.002	NS	–	–	–
Overlap myositis	–	–	–	0/38 (0)	NS	NS
Autoantibody group						
Anti–Mi-2	7/29 (24)	0.03	0.01	1/15 (7)	NS	NS
Anti–Nxp-2	8/35 (23)	0.04	0.01	4/83 (5)	NS	NS
Anti-TIF1γ	6/46 (13)	NS	NS	2/24 (2)	NS	NS
Anti–MDA-5	4/25 (16)	NS	NS	0/28 (0)	NS	NS
Anti–Jo-1	5/49 (10)	NS	NS	1/6 (17)	NS	NS
Anti-SRP	5/27 (19)	NS	NS	0/6 (0)	NS	NS
Anti-HMGCR	2/59 (3)	0.05	NS	0/3 (0)	NS	NS
Total	74/670 (11)	–	–	8/343 (2)	–	–

* DM = dermatomyositis; NS = not significant; CADM = clinically amyopathic dermatomyositis; PM = polymyositis; IBM = inclusion body myositis; anti-TIF1γ = anti–transcription intermediary factor 1γ; anti–MDA-5 = anti–melanoma differentiation–associated protein 5; anti-SRP = anti–signal recognition particle; anti-HMGCR = anti–hydroxymethylglutaryl-coenzyme A reductase.
† Versus other myositis patients.
‡ Versus healthy controls.

Table 2. Epidemiologic features, MAA type, and clinical features of adult and juvenile myositis patients according to anti-cortactin autoantibody status*

	Adult myositis				Juvenile myositis			
	Anti-cortactin–positive (n = 74)	Anti-cortactin–negative (n = 596)	Univariate *P*	Multivariate *P*	Anti-cortactin–positive (n = 8)	Anti-cortactin–negative (n = 335)	Univariate *P*	Multivariate *P*
Epidemiologic features and MAA								
Female sex	53 (72)	369 (62)	NS	NS	5 (62)	238 (71)	NS	NS
Race								
White	44 (59)	447 (75)	0.004	0.02	6 (75)	215 (64)	NS	NS
Black	20 (27)	99 (17)	0.03	NS	1 (13)	53 (16)	NS	NS
Other races	10 (14)	50 (8)	NS	NS	1 (13)	67 (20)	NS	NS
Age at onset, mean ± SD years	45.8 ± 14.6	50.5 ± 14.7	0.01	NS	10.8 ± 5.5	8.9 ± 4.2	NS	NS
Duration of follow-up, mean ± SD years	2.8 ± 3.3	2.8 ± 3.3	NS	NS	5.2 ± 4.8	6.1 ± 7.2	NS	NS
Cancer associated myositis	5 (7)	67 (12)	NS	NS	0 (0)	0 (0)	NS	NS
Death during follow-up	0 (0)	27 (5)	NS	NS	0 (0)	12 (4)	NS	NS
MAA†								
Anti–Ro 52	35 (47)	156 (26)	<0.001	0.001	0 (0)	50 (16)	NS	NS
Anti-NT5c1a	10 (59)	70 (33)	0.03	0.001	2 (25)	86 (28)	NS	NS
Clinical features‡								
Muscle weakness	40 (95)	354 (96)	NS	NS	8 (100)	333 (99)	NS	NS
Skin involvement								
DM-specific skin involvement§	26 (62)	141 (38)	0.003	0.03	8 (100)	305 (91)	NS	NS
RP	9 (21)	51 (14)	NS	NS	2 (25)	48 (14)	NS	NS
Mechanic's hands	8 (19)	66 (18)	NS	NS	2 (25)	24 (7)	NS	0.03
Calcinosis	5 (12)	36 (10)	NS	NS	4 (50)	98 (29)	NS	NS
ILD	10 (24)	58 (16)	NS	NS	1 (12)	30 (9)	NS	NS
Esophageal involvement								
Dysphagia	15 (36)	61 (17)	0.003	0.02	4 (50)	137 (41)	NS	NS
Gastroesophageal reflux disease	28 (67)	174 (47)	0.02	0.02	1 (12)	73 (22)	NS	NS
Arthritis	7 (17)	60 (16)	NS	NS	4 (50)	173 (52)	NS	NS
Fever	8 (19)	33 (9)	0.05	NS	1 (14)	101 (30)	NS	NS

* Except where indicated otherwise, values are the number (%) of patients. Comparisons of continuous variables were made using Student's *t*-test, while dichotomous variables were compared using either the chi-square test or Fisher's exact test, as appropriate. Multivariate comparisons were performed using linear regression for continuous variables and logistic regression for dichotomous variables. All multivariate comparisons were adjusted by the patient group (IBM or autoantibody group) for the epidemiologic comparisons, and by time of follow-up and patient group for the comparisons of clinical features. RP = Raynaud's phenomenon; ILD = interstitial lung disease (see Table 1 for other definitions).
† Testing for myositis-associated autoantibody (MAA) type was performed in a subset of 227 adult myositis patients (mostly IBM [n = 139] and DM [n = 50]). In children, testing for both anti–Ro 52 and anti-NT5c1a was performed in 314 patients.
‡ In the adult myositis group, 42 patients with anti-cortactin, and 367 patients without anti-cortactin were assessed for clinical features.
§ Either heliotrope, Gottron's sign, or papules.

with and those without these autoantibodies, while controlling for follow-up time and patient group (Table 2). This revealed an increased prevalence of dysphagia and gastroesophageal reflux among anti-cortactin–positive patients compared to anti-cortactin–negative patients (36% [95% CI 21–50%] versus 17% [95% CI 13–20%] for dysphagia, and 67% [95% CI 52–81%] versus 47% [95% CI 42–52%] for gastroesophageal reflux; $P = 0.02$ for both) (Table 2). Of note, dysphagia was substantially more common in anti–Mi-2–positive patients with anti-cortactin autoantibodies than in anti–Mi-2–positive patients without them (100% versus 41% [95% CI 20–62%]; $P = 0.008$). Interestingly, the MAAs anti–Ro 52 and anti-NT5c1a were more likely to be present in the sera of adult myositis patients with anti-cortactin autoantibodies (47% [95% CI 36–59%] versus 26% [95% CI 23–30%] for anti–Ro 52, and 59% [95% CI 35–82%] versus 33% [95% CI 27–40%]; $P = 0.001$ for both) (Table 2). Among the 10 patients positive for both for anti-cortactin and anti-NT5c1a antibodies, 4 had IBM and 6 had DM. Of those 10 patients, 6 had dysphagia (4 DM).

Given their association with DM, there was an expected increased prevalence of DM skin features in adult myositis patients with anti-cortactin autoantibodies (62% [95% CI 47–77%] versus 38% [95% CI 33–43%]; $P = 0.03$) (Table 2). Otherwise, the clinical features of adult myositis patients with and those without anti-cortactin autoantibodies were remarkably similar. For instance, there were no differences in the pattern or severity of weakness, muscle enzyme levels, severity of lung disease, thigh magnetic resonance imaging features, or treatments received (Supplementary Tables 1–5, http://onlinelibrary.wiley.com/doi/10.1002/art.41931/abstract). Furthermore, compared to the general population, there were no differences in the survival rate (SMR 0 [95% CI 0–2]) or cancer rate (SCR 1.3 [95% CI 0.4–3) in anti-cortactin–positive patients.

Next, we explored whether anti-cortactin autoantibody titers were associated with specific clinical features. The multivariate analysis comparing anti-cortactin autoantibody titers in patients with and those without each clinical feature, while controlling for follow-up time and patient group, demonstrated that titers were higher in patients with DM skin features (0.14 [95% CI 0.12–0.16] versus 0.11 [95% CI 0.09–0.12]; $P = 0.008$) and dysphagia (0.14 [95% CI 0.12–0.16] versus 0.11 [95% CI 0.1–0.12]; $P = 0.005$). Furthermore, patients with ILD also had higher anti-cortactin autoantibody titers than those without ILD (0.14 [95% CI 0.11–0.19] versus 0.11 [95% CI 0.10–0.13]; $P = 0.005$) (Supplementary Table 6, http://onlinelibrary.wiley.com/doi/10.1002/art.41931/abstract).

Of note, at the onset of the disease, the presence of dysphagia was also more prevalent in patients with anti-cortactin autoantibodies compared to those without (29% [95% CI 15–42%] versus 10% [95% CI 7–13%]; $P = 0.01$) (data not shown). Likewise, the presence of ILD at the onset of the disease showed a trend toward being more frequent in patients with anti-cortactin antibodies (10% [95% CI 1–18%] versus 2% [95% CI 1–4%]; $P = 0.06$).

Prevalence of anti-cortactin autoantibodies in juvenile myositis patients and clinical features of this patient group. Overall, anti-cortactin autoantibodies were not more prevalent in juvenile myositis patients compared to juvenile healthy controls (2% [95% CI 1–4%] versus 4% [95% CI 0–9%]; $P = 0.3$) (Table 1). Notably, anti-cortactin antibodies were only found in patients with juvenile DM, which also accounted for the majority (82%) of the cohort. Unlike in adults, no differences were found in the prevalence of anti-cortactin autoantibodies among the different autoantibody subgroups in juvenile myositis. Also, anti-cortactin antibodies were not found in any of the anti-Pm/Scl–positive patients (n = 13) or anti–U1 RNP–positive patients (n = 24) who were tested. Anti-cortactin autoantibody–positive juvenile myositis patients did not show any significant differences in terms of clinical features compared to anti-cortactin–negative patients, except for a higher prevalence of "mechanic's hands" (25% [95% CI 0–54%] versus 7% [95% CI 4–10%]; $P = 0.03$), higher number of hospitalizations (2.9 [95% CI 0–6] versus 1.3 [95% CI 1–1.5]; $P = 0.04$), and lower peak creatine kinase (CK) values (368 [95% CI 0–1,800] versus 818 [95% CI 534–1,101]; $P = 0.02$) (Table 2 and Supplementary Tables 7 and 8, http://onlinelibrary.wiley.com/doi/10.1002/art.41931/abstract). Importantly, juvenile myositis patients with mechanic's hands had higher anti-cortactin autoantibody titers (0.1 [95% CI 0.05–0.14] versus 0.07 [95% CI 0.07–0.08]; $P = 0.04$) (Supplementary Table 6). There were no differences between these groups in disease course, mortality, or treatments received (Supplementary Tables 6 and 7).

DISCUSSION

In this study utilizing a large cohort of adult myositis patients, we demonstrate an increased prevalence of anti-cortactin autoantibodies in DM patients compared to those with PM or IBM or adult healthy controls. Surprisingly, among all adult DM patients studied, only those with anti–Mi-2 or anti–NXP-2 autoantibodies had an increased prevalence of anti-cortactin autoantibodies. Anti-cortactin antibodies fall into the category of MAA, since they were 1) previously found in myasthenia gravis (5), 2) not associated with a specific myositis phenotype (e.g., DM) but only with isolated clinical features, and 3) found in a significant proportion of healthy individuals. To the best of our knowledge, anti-cortactin is the only MAA exclusively associated with MSA-defined DM subtypes.

We also found that anti-cortactin autoantibodies were strongly associated with dysphagia in adults. Since we previously demonstrated an increased risk of dysphagia in anti–NXP-2–positive DM patients (18), we considered the possibility that dysphagia could be more common in anti-cortactin–positive patients because of the high number of such patients with coexisting anti–NXP-2 autoantibodies. However, dysphagia was associated with anti-cortactin autoantibodies even in a multivariate analysis controlling for MSAs, including anti–NXP-2. Additionally, we found

that adult myositis patients with ILD also had higher titers of anti-cortactin autoantibodies than patients without this clinical feature.

Interestingly, anti-cortactin autoantibodies were not more common in any type of juvenile myositis compared to juvenile healthy controls. This makes anti-cortactin the only known MAA with an increased prevalence in adult, but not juvenile, forms of myositis. Nonetheless, anti-cortactin autoantibodies were still associated with increased prevalence of mechanic's hands, a higher number of hospitalizations, and lower peak CK values in juvenile myositis patients. This observation suggests that anti-cortactin autoantibodies could still be associated with specific disease manifestations in children with myositis.

In the single prior report describing anti-cortactin autoantibodies in adult myositis (4), this MAA was more common in PM than DM. Furthermore, no MSA or clinical features were found to be associated with anti-cortactin autoantibodies in the prior study. While we cannot fully account for these differences, we expect that by including more than 4 times as many adult myositis patients, the current study is more highly powered to accurately determine the prevalence of this MAA and any relevant clinical or serologic associations. Future studies will be required to determine why the prevalence of anti-cortactin autoantibodies is only increased in adult DM patients with anti–NXP-2 or anti–Mi-2 autoantibodies and why such patients have an increased risk of developing dysphagia.

Notably, anti-cortactin autoantibodies were more common in adult patients who were also positive for the MAAs anti–Ro 52 and anti-NT5c1a. This suggests a potential association between the development of these 3 different MAAs. In this regard, it is of interest that anti–Ro 52, anti-NT5c1a, and anti-cortactin autoantibodies each seem to be associated with more severe disease manifestations (15,19,20). However, it remains to be determined whether the development of these MAAs contributes to more severe tissue damage or whether they are simply the byproduct of a more robust immune response.

The current study has several limitations. First, most of the conclusions of this study are based on signs and symptoms that were recorded prospectively from natural history studies that have been ongoing since 2002 for adults and since 1989 for children. Consequently, we could not include classification strategies (e.g., the European Alliance of Associations for Rheumatology/American College of Rheumatology 2017 myositis classification criteria [21]) or activity and damage tools that were not available when the studies started. Second, anti-cortactin antibodies were only tested by ELISA according to the original assay proposed by Labrador-Horrillo et al (4). Finally, while most of the autoantibodies were systematically tested in all patients, only 227 of the adult patients were tested for anti-NT5c1a, and only 314 juvenile cases were tested for anti–Ro 52 and anti-NT5c1a.

In conclusion, we have shown the following: 1) the prevalence of anti-cortactin autoantibodies is increased in adult DM patients with coexisting anti–Mi-2 or anti–NXP-2 autoantibodies; 2) in adults, anti-cortactin autoantibodies are associated with dysphagia and ILD; and 3) anti-cortactin autoantibodies are associated with other MAAs, specifically anti–Ro 52 and anti-NT5c1a, suggesting that the presence of these autoantibodies may be part of a broader, and largely uncharacterized, immunologic response in patients with myositis.

ACKNOWLEDGMENT

We would like to thank the Childhood Myositis Heterogeneity Collaborative Study Group (see Appendix A).

AUTHOR CONTRIBUTIONS

All authors were involved in drafting the article or revising it critically for important intellectual content, and all authors approved the final version to be published. Dr. Mammen had full access to all of the data in the study and takes responsibility for the integrity of the data and the accuracy of the data analysis.

Study conception and design. Pinal-Fernandez, Mammen.

Acquisition of data. Pak, Gil-Vila, Baucells, Plotz, Casal-Dominguez, Derfoul, Selva-O'Callaghan, Sabbagh, Casciola-Rosen, Albayda, Paik, Tiniakou, Danoff, Lloyd, Rider, Christopher-Stine, Mammen.

Analysis and interpretation of data. Pinal-Fernandez, Martinez-Carretero, Miller, Mammen.

REFERENCES

1. Selva-O'Callaghan A, Pinal-Fernandez I, Trallero-Araguas E, Milisenda JC, Grau-Junyent JM, Mammen AL. Classification and management of adult inflammatory myopathies [review]. Lancet Neurol 2018;17:816–28.
2. Griggs RC, Askanas V, DiMauro S, Engel A, Karpati G, Mendell JR, et al. Inclusion body myositis and myopathies [review]. Ann Neurol 1995;38:705–13.
3. McHugh NJ, Tansley SL. Autoantibodies in myositis [review]. Nat Rev Rheumatol 2018;14:290–302.
4. Labrador-Horrillo M, Martinez MA, Selva-O'Callaghan A, Trallero-Araguas E, Grau-Junyent JM, Vilardell-Tarres M, et al. Identification of a novel myositis-associated antibody directed against cortactin. Autoimmun Rev 2014;13:1008–12.
5. Gallardo E, Martinez-Hernandez E, Titulaer MJ, Huijbers MG, Martinez MA, Ramos A, et al. Cortactin autoantibodies in myasthenia gravis. Autoimmun Rev 2014;13:1003–7.
6. Lloyd TE, Mammen AL, Amato AA, Weiss MD, Needham M, Greenberg SA. Evaluation and construction of diagnostic criteria for inclusion body myositis [review]. Neurology 2014;83:426–33.
7. Bohan A, Peter JB. Polymyositis and dermatomyositis (first of two parts) [review]. N Engl J Med 1975;292:344–7.
8. Sontheimer RD. Would a new name hasten the acceptance of amyopathic dermatomyositis (dermatomyositis sine myositis) as a distinctive subset within the idiopathic inflammatory dermatomyopathies spectrum of clinical illness? J Am Acad Dermatol 2002;46:626–36.
9. Mammen AL, Chung T, Christopher-Stine L, Rosen P, Rosen A, Doering KR, et al. Autoantibodies against 3-hydroxy-3-methylglutaryl-coenzyme A reductase in patients with statin-associated autoimmune myopathy. Arthritis Rheum 2011;63:713–21.
10. Pinal-Fernandez I, Casal-Dominguez M, Huapaya JA, Albayda J, Paik JJ, Johnson C, et al. A longitudinal cohort study of the antisynthetase syndrome: increased severity of interstitial lung disease in black patients and patients with anti-PL7 and anti-PL12 autoantibodies. Rheumatology (Oxford) 2017;56:999–1007.

11. Travis WD, Costabel U, Hansell DM, King TE Jr, Lynch DA, Nicholson AG, et al. An official American Thoracic Society/European Respiratory Society statement: update of the international multidisciplinary classification of the idiopathic interstitial pneumonias. Am J Respir Crit Care Med 2013;188:733–48.
12. Rider LG, Shah M, Mamyrova G, Huber AM, Rice MM, Targoff IN, et al. The myositis autoantibody phenotypes of the juvenile idiopathic inflammatory myopathies. Medicine (Baltimore) 2013;92:223–43.
13. Shah M, Mamyrova G, Targoff IN, Huber AM, Malley JD, Rice MM, et al. The clinical phenotypes of the juvenile idiopathic inflammatory myopathies. Medicine (Baltimore) 2013;92:25–41.
14. Yeker RM, Pinal-Fernandez I, Kishi T, Pak K, Targoff IN, Miller FW, et al. Anti-NT5C1A autoantibodies are associated with more severe disease in patients with juvenile myositis. Ann Rheum Dis 2018;77:714–9.
15. Sabbagh S, Pinal-Fernandez I, Kishi T, Targoff IN, Miller FW, Rider LG, et al. Anti-Ro52 autoantibodies are associated with interstitial lung disease and more severe disease in patients with juvenile myositis. Ann Rheum Dis 2019;78:988–95.
16. Targoff IN, Mamyrova G, Trieu EP, Perurena O, Koneru B, O'Hanlon TP, et al. A novel autoantibody to a 155-kd protein is associated with dermatomyositis. Arthritis Rheum 2006;54:3682–9.
17. Lardeux F, Torrico G, Aliaga C. Calculation of the ELISA's cut-off based on the change-point analysis method for detection of Trypanosoma cruzi infection in Bolivian dogs in the absence of controls. Mem Inst Oswaldo Cruz 2016;111:501–4.
18. Albayda J, Pinal-Fernandez I, Huang W, Parks C, Paik J, Casciola-Rosen L, et al. Antinuclear matrix protein 2 sutoantibodies and edema, muscle disease, and malignancy risk in dermatomyositis patients. Arthritis Care Res (Hoboken) 2017;69:1771–6.
19. Goyal NA, Cash TM, Alam U, Enam S, Tierney P, Araujo N, et al. Seropositivity for NT5c1A antibody in sporadic inclusion body myositis predicts more severe motor, bulbar and respiratory involvement. J Neurol Neurosurg Psychiatry 2016;87:373–8.
20. Marie I, Hatron PY, Dominique S, Cherin P, Mouthon L, Menard JF, et al. Short-term and long-term outcome of anti-Jo1-positive patients with anti-Ro52 antibody. Semin Arthritis Rheum 2012;41:890–9.
21. Lundberg IE, Tjärnlund A, Bottai M, Werth VP, Pilkington C, de Visser M, et al. 2017 European League Against Rheumatism/American College of Rheumatology classification criteria for adult and juvenile idiopathic inflammatory myopathies and their major subgroups [published correction appears in Arthritis Rheumatol 2018;70:1532]. Arthritis Rheumatol 2017;69:2271–82.

APPENDIX A: THE CHILDHOOD MYOSITIS HETEROGENEITY COLLABORATIVE STUDY GROUP

Members of the Childhood Myositis Heterogeneity Collaborative Study Group who contributed to this study included Heinrike Schmeling, Bita Arabshahi, Imelda Balboni, Susan Ballinger, Lilliana Barillas-Arias, Mara Becker, Catherine April Bingham, John F. Bohnsack, Ruy Carrasco, Victoria Cartwright, Gail D. Cawkwell, Rodolfo Curiel, Jason Dare, Marietta M. DeGuzman, Kaleo Eade, Barbara Anne Ebernardt, Barbara S. Edelheit, Moussa El-Hallak, Terri H. Finkel, Stephen W. George, Ellen A. Goldmuntz, Beth Gottlieb, Brent Graham, William Hannan, Michael Henrickson, Gloria C. Higgins, Patricia Hobday, Alice Hoftman, Sandy Hong, Adam Huber, Lisa Imundo, Christi Inman, Anna Jansen, James Jarvis, Lawrence Jung, Philip Kahn, Ildy M. Katona, Yukiko Kimura, Daniel J. Kingsbury, W. Patrick Knibbe, Bianca A. Lang, Maureen Leffler, Melissa Lerman, Carol B. Lindsley, Katherine L. Madson, Gulnara Mamyrova, Diana Milojevic, Stephen R. Mitchell, Renee Modica, Linda Myers, Kabita Nanda, Simona Nativ, Terrance O'Hanlon, Judyann C. Olson, Lauren M. Pachman, Murray H. Passo, Maria D. Perez, Donald A. Person, Marilyn G. Punaro, Linda I. Ray, Robert M. Rennebohm, Rafael F. Rivas-Chacon, Tova Ronis, Margalit Rosenkranz, Deborah Rothman, Adam Schiffenbauer, Bracha Shaham, Susan Shenoi, David Sherry, David Siegel, Abigail Smukler, Jennifer Soep, Matthew Stoll, Sangeeta H. Sule, Robert Sundel, Stacey Tarvin, Melissa Tesher, Scott A. Vogelgesang, Rita Volochayev, Dawn Wahezi, Jennifer C. Wargula, Peter Weiser, Pamela Weiss, Patience H. White, Andrew Zeft, Lawrence S. Zemel, and Yongdong Zhao.

Arthritis & Rheumatology
Vol. 74, No. 2, February 2022, pp 365–372

AMERICAN COLLEGE of RHEUMATOLOGY
Empowering Rheumatology Professionals

LETTERS

DOI 10.1002/art.41977

Safety and tolerability of the COVID-19 messenger RNA vaccine in adolescents with juvenile idiopathic arthritis treated with tumor necrosis factor inhibitors

To the Editor:

Patients with rheumatic and musculoskeletal diseases (RMDs) who are taking immunosuppressants have been considered to be at increased risk of developing SARS–CoV-2 infection during the COVID-19 pandemic, and vaccination is the mainstay for the prevention of this infection (1). To date, recommendations and data for COVID-19 vaccination in adolescent patients with RMDs are lacking (2). Reports from international societies and post-authorization safety studies of the novel messenger RNA (mRNA) COVID-19 vaccines are generally reassuring; however, in adolescent RMD patients treated with immunomodulators, the safely profile of mRNA COVID-19 vaccines is unknown because adolescents with RMD were excluded from the vaccine trials (3–5). Furthermore, there is a theoretical risk of RMD flare related to the mRNA COVID-19 vaccines (1,2). Nevertheless, the estimated risks and benefits clearly favor vaccination (1,2). In a population of adult RMD patients receiving non–B cell–depleting therapy, it was demonstrated that after 2 doses of a COVID-19 mRNA vaccine, the vast majority of patients developed a positive antibody response (though data on relative amount of antibody responses are still lacking) and experienced only minor side effects with no apparent disease exacerbation/flare (6).

Recently we performed a study that aimed to evaluate the safety and tolerability of the BNT162b2 COVID-19 vaccine (BioNTech; Pfizer) in adolescents with juvenile idiopathic arthritis (JIA) treated with tumor necrosis factor (TNF) inhibitors. This single-center study included adolescent patients (ages 16–21 years) with stable JIA who had been receiving treatment with TNF inhibitors for at least 1 year following the diagnosis. Written informed consent was obtained at enrollment. The patients received 2 doses of the COVID-19 mRNA vaccine intramuscularly, with the initial dose and follow-up dose administered between April 15 and May 15, 2021 (designated 0 weeks and 3 weeks, respectively). Follow-up visits were planned for 1, 2, and 3 months after vaccination. All participants were observed for 30 minutes after the injection and were given a diary card to record the occurrence of local or systemic symptoms for the following 14 days. Adverse reactions were defined as any reaction that lasted for >7 days after vaccination, and serious adverse reactions were defined as any reaction requiring medical attention or hospitalization. Disease activity was evaluated using the Juvenile Arthritis Disease Activity Score in 27 joints (JADAS-27) (7). Data were analyzed using SPSS version 18.0 software. *P* values less than 0.05 were considered significant.

A total of 21 adolescent patients were enrolled in our study. Demographic and clinical characteristics are shown in Table 1. Both doses of the vaccine were well tolerated by all of the participants. Local reactions were frequent in the majority of participants (74%) (Table 1). No difference in reaction was noted between the patients taking etanercept versus those taking adalimumab (71% versus 75%, respectively; $P = 0.09$) or in patients with different JIA types. In addition, systemic reactions were relatively infrequent (19%) (Table 1). There were no differences in the rates of systemic reactions according to the type of JIA or the medication received. Most localized and systemic reactions were noted after the second dose of the vaccine ($P = 0.02$). One patient developed hives after the second dose, which was alleviated with antihistamines. JIA was in clinical remission in all patients at the time of

Table 1. Baseline characteristics, treatments, and frequency of AEs occurring after immunization with the COVID-19 messenger RNA vaccine among adolescent patients with JIA treated with TNF inhibitors*

Demographic and clinical characteristics (n = 21)	
Age, median (IQR) years	17 (16–21)
Sex	
Male	5 (24)
Female	16 (76)
Polyarticular JIA	8 (38)
Psoriatic JIA	7 (33)
ERA	6 (29)
Treatment (n = 21)	
TNF inhibitors	
Adalimumab	10 (48)
Etanercept	11 (52)
Other concurrent treatment, methotrexate	15 (71)
Postvaccination AEs (n = 21 patients, n = 42 vaccine doses)	
Local	31 (74)
Erythema	21 (50)
Pain	32 (76)
Swelling	12 (29)
Systemic	8 (19)
Headache	7 (17)
Myalgias	5 (12)
Fatigue	6 (14)
Transient arthralgia	5 (12)
Allergic reaction	1 (2)
Exacerbation of JIA	0 (0)
Serious AEs	0 (0)

* Except where indicated otherwise, values are the number (%). AEs = adverse events; JIA = juvenile idiopathic arthritis; TNF = tumor necrosis factor; IQR = interquartile range; ERA = enthesitis-related arthritis.

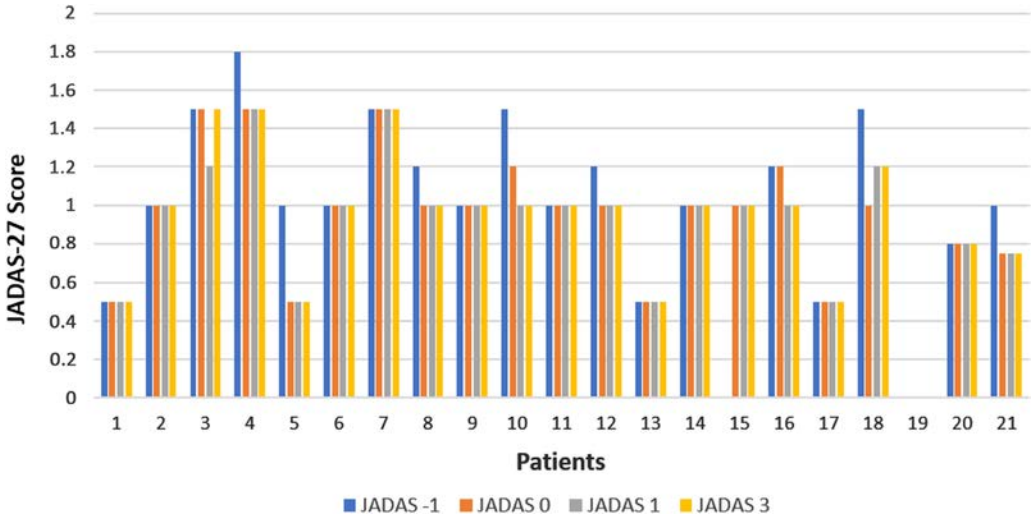

Figure 1. Disease Activity Score in 27 joints (JADAS-27) after vaccination with the BNT162b2 COVID-19 messenger RNA vaccine (BioNTech; Pfizer) in 21 adolescent patients with juvenile idiopathic arthritis treated with tumor necrosis factor inhibitors. No significant changes in the JADAS-27 were noted at 1 month prior to the vaccination (JADAS −1), at the time of vaccination (JADAS 0), 1 month after vaccination (JADAS 1), or 3 months after vaccination (JADAS 3) ($P = 0.417$ by Kruskal-Wallis H test).

vaccination. No exacerbation of underlying disease was noted, based on evaluation of the JADAS-27 at 1 month before the vaccination, as well as at 1 and 3 months after the second dose of vaccination (Figure 1). There were no significant changes in the JADAS-27 ($P = 0.417$) or in laboratory test results (C-reactive protein, erythrocyte sedimentation rate, and white blood cell count) at follow-up over a period of 3 months ($P = 0.1$, $P = 0.09$, and $P = 0.4$, respectively) (data not shown). None of the participants discontinued treatment with TNF inhibitors at the time of vaccine administration or during the follow-up period.

This is the first study demonstrating that mRNA vaccines appear to be safe and well tolerated in adolescents with JIA receiving treatment with TNF inhibitors. Although our sample size was small and a limited number of patients were included within each JIA type and treatment group, it may be concluded that the vaccine has an adequate safety and tolerability profile and does not provoke disease flare. As there are no studies examining the safety and effectiveness of COVID-19 vaccines in this population, further studies are needed to evaluate the immune response, analyze the immunogenicity of the 2-dose schedule, and determine the real duration of immune protection.

Author disclosures are available at https://onlinelibrary.wiley.com/action/downloadSupplement?doi=10.1002%2Fart.41977&file=art41977-sup-0001-Disclosureform.pdf.

Dimitra Dimopoulou, MD, PhD
Nikos Spyridis, MD, PhD
George Vartzelis, MD, PhD
Maria N. Tsolia, MD, PhD
Despoina N. Maritsi, MD, PhD
National and Kapodistrian University of Athens and Children's Hospital "Panagioti and Aglaia Kyriakou" Athens, Greece

1. Schulze-Koops H, Specker C, Skapenko A. Vaccination of patients with inflammatory rheumatic diseases against SARS-CoV-2: considerations before widespread availability of the vaccines. RMD Open 2021; 7:e001553.
2. Furer V, Rondaan C, Agmon-Levin N, van Assen S, Bijl M, Kapetanovic MC, et al. Point of view on the vaccination against COVID-19 in patients with autoimmune inflammatory rheumatic diseases. RMD Open 2021;7:e001594.
3. Curtis JR, Johnson SR, Anthony DD, Arasaratnam RJ, Baden LR, Bass AR, et al. American College of Rheumatology guidance for COVID-19 vaccination in patients with rheumatic and musculoskeletal diseases: version 1. Arthritis Rheumatol 2021;73:1093–107.
4. Bijlsma JW. EULAR December 2020 view-points on SARS-CoV-2 vaccination in patients with RMDs. Ann Rheum Dis 2021;80:411–2.
5. Paediatric Rheumatology European Association (PRES). Guidelines and recommendations. PRES update regarding COVID-19 vaccines in pediatric rheumatic patients. December 2020. URL: https://www.pres.eu/clinical-affairs/guidelines.html.
6. Braun-Moscovici Y, Kaplan M, Braun M, Markovits D, Giryes S, Toledano K, et al. Disease activity and humoral response in patients with inflammatory rheumatic diseases after two doses of the Pfizer mRNA vaccine against SARS-CoV2. Ann Rheum Dis 2021;80: 1317–21.
7. Consolaro A, Ruperto N, Bazso A, Pistorio A, Magni-Manzoni S, Filocamo G, et al. Development and validation of a composite disease activity score for juvenile idiopathic arthritis. Arthritis Rheum 2009;61: 658–66.

DOI 10.1002/art.41952

Sjögren disease, not Sjögren's: comment on the article by Baer and Hammitt

To the Editor:

I read with great interest the recent correspondence in *Arthritis & Rheumatology* discussing the naming standards for

"Sjögren's syndrome," in which Drs. Baer and Hammitt suggested that the terminology of "Sjögren's syndrome" be changed to "Sjögren's disease" (1). The main argument in favor of using the term "disease" is that this condition is now very well characterized and identified within the group of connective tissue diseases with autoimmune pathogenesis. In a very insightful article, Scadding commented on semantic problems in medicine and stated that there were 4 main classes of characteristics by which diseases could be defined: the clinical description (syndrome), a disorder of structure with recognizable morbid-anatomic change, an identified disorder of function (in morbid-anatomic or pathophysiologic terms), and/or when the cause of a disease becomes known (etiology) (2). The suggested new terminology of "Sjögren's disease" meets several of the above-mentioned criteria. However, Scadding further wrote: "One can speak of the syndrome of any disease with which a consistently recognisable pattern of symptoms and signs is associated. Whether a category definable only in clinical-descriptive terms is called a syndrome or a disease does not matter, provided that verbal usages are made explicit and applied consistently" (2).

While there should be no impediment in accepting the change from Sjögren's "syndrome" to "disease," the use of eponyms in medicine is debated. Eponymic terms should generally be replaced by descriptive terms (3). In rheumatology, the terms "Reiter's syndrome" and "Wegener's disease" were abandoned for historical reasons (3), and "eosinophilic granulomatosis with polyangiitis" was preferred to "Churg-Strauss syndrome" as it better describes this condition. Also, some eponyms may have 2 different diseases attached to them. Some diseases have different eponyms in different countries, and in fact Sjögren's disease is called "Gougerot Sjögren syndrome" in France.

Finally, if the eponym of "Sjögren" is here to stay because it is considered better than alternative descriptors, the possessive form should no longer be used (i.e., the eponym should no longer be shown with the apostrophe s, as in "Sjögren's"). The style manual of the Council of Science Editors states that "it is recommended that the possessive form be eliminated altogether from eponymic terms so that they can clearly be differentiated from true possessives" (4). This is because the person behind the eponym has no proprietary claim on the entity (5). Although it may be unfeasible to eliminate all eponyms, the nonpossessive form "Sjögren disease" should be preferred.

Author disclosures are available at https://onlinelibrary.wiley.com/action/downloadSupplement?doi=10.1002%2Fart.41952&file=art41952-sup-0001-Disclosureform.pdf.

Vincent Cottin, MD
National Reference Centre for Rare Pulmonary Diseases
Louis Pradel Hospital
Infections Virales et Pathologie Comparée, INRAE
Hospices Civils de Lyon
Claude Bernard University Lyon 1
and Radico-ILD and ERN-LUNG
Lyon, France

1. Baer AN, Hammitt KM. Sjögren's disease, not syndrome [letter]. Arthritis Rheumatol 2021;73:1347–8.
2. Scadding JG. Health and disease: what can medicine do for philosophy? J Med Ethics 1988;14:118–24.
3. Woywodt A, Matteson E. Should eponyms be abandoned? Yes. BMJ 2007;335:424.
4. Council of Science Editors, editors. Scientific style and format: the CSE manual for authors, editors, and publishers. 8th ed. New York: Cambridge University Press; 2014.
5. Cheng TO. No apostrophe s after an eponym [editorial]. Int J Cardiol 2010;140:259.

DOI 10.1002/art.41954

Reply

To the Editor:

We thank Dr. Cottin for supporting our call to adopt the term "disease" in lieu of "syndrome" when referring to the distinct systemic disease described by Henrik Sjögren in a comprehensive 150-page monograph published in 1933 (1). However, Dr. Cottin has questioned the continued use of an eponym for this disease. We appreciate the advantages of a noneponymic term for this disease, including avoidance of the attribution of disease discovery or description to one person, when in fact others also provided earlier descriptions. In addition, a noneponymic name can highlight a key clinical or pathophysiologic attribute of the disease (2). However, eponyms continue to be used widely in medicine to describe physical findings, instruments, surgical techniques, and diseases that were discovered, designed, or described in a comprehensive or compelling manner by one or more key individuals. As was pointed out by Castillo Aleman, eponyms provide a "valuable linguistic means of very succinct transmission of complex medical concepts" and fulfill a human need to honor seminal contributions of specific individuals to the medical craft (3).

We do not contest the logic of abandoning the possessive in favor of simply "Sjögren disease." The use of nonpossessive eponyms has been encouraged by prominent medical organizations and has been mandated by the editors of some medical journals and textbooks (4). Despite this, the possessive form remains in common use; "Sjögren's syndrome" was used 7,326 times compared to 1,748 times for "Sjögren syndrome" in articles published during the years 2010–2020 (analysis performed with PubMed).

Finally, our call for a name change for Sjögren's needs international acceptance. We note the success of past efforts in reaching international consensus with regard to the nomenclature of systemic vasculitides (5), IgG4-related disease (6), and antineutrophil cytoplasmic antibody–associated vasculitis (7). Thus, we plan to initiate an effort to achieve international consensus on the nomenclature of Sjögren's disease, in which collaborators could discuss not only a proper standardized term for this disease, but

also outmoded terms applied to its principal subsets, such as "primary" and "secondary" Sjögren's (8,9).

Dr. Baer's work was supported by the Jerome L. Greene Foundation.

Alan N. Baer, MD
Johns Hopkins University School of Medicine
Baltimore, MD
Katherine M. Hammitt, MA
Sjögren's Foundation
Reston, VA

1. Sjögren H. Zur Kenntnis der Keratoconjunctivitis sicca (Keratitis filiformis bei Hypofunktion der Tränendrüsen). Acta Ophthalmol (Copenh) 1933;11 Suppl 2:1–151.
2. Jennette JC. Nomenclature and classification of vasculitis: lessons learned from granulomatosis with polyangiitis (Wegener's granulomatosis). Clin Exp Immunol 2011;164 Suppl 1:7–10.
3. Castillo Aleman YM. Medical eponyms: redeeming or not the long-standing tradition. Postgrad Med J 2021;97:498–500.
4. Ayesu K, Nguyen B, Harris S, Carlan S. The case for consistent use of medical eponyms by eliminating possessive forms. J Med Libr Assoc 2018;106:127–9.
5. Jennette JC, Falk RJ, Andrassy K, Bacon PA, Churg J, Gross WL, et al. Nomenclature of systemic vasculitides: proposal of an international consensus conference. Arthritis Rheum 1994;37:187–92.
6. Stone JH, Khohahi A, Deshpande V, Chan JK, Heathcote JG, Aalberse R, et al. Recommendations for the nomenclature of IgG4-related disease and its individual organ system manifestations. Arthritis Rheum 2012;64:3061–7.
7. Falk RJ, Gross WL, Guillevin L, Hof GS, Jayne DR, Jennette JC, et al. Granulomatosis with polyangiitis (Wegener's): an alternative name for Wegener's granulomatosis. Arthritis Rheum 2011;63:863–4.
8. Kollert F, Fisher BA. Equal rights in autoimmunity: is Sjögren's syndrome ever 'secondary'? Rheumatology (Oxford) 2020;59:1218–25.
9. Mavragani CP, Moutsopoulos HM. Primary versus secondary Sjögren syndrome: is it time to reconsider these terms? [editorial]. J Rheumatol 2019;46:665–6.

DOI 10.1002/art.41945

Long-term risk of cancer development among anti-Th/To antibody–positive systemic sclerosis patients: comment on the article by Mecoli et al

To the Editor:

We read with great interest the article by Dr. Mecoli and colleagues on the relationship between cancer and anti-Th/To antibodies in patients with systemic sclerosis (SSc) (1). Interestingly, the presence of anti-Th/To antibodies was reported to confer a protective effect against the development of cancer in patients with SSc. However, cancer development in anti-Th/To antibody–positive patients was significantly suppressed only within the first 3 years after SSc onset, and there was no significant difference in the number of deceased patients between the anti-Th/To antibody–positive and the anti-Th/To antibody–negative groups.

In our own study on the development of cancer in SSc patients with anti-Th/To antibodies, we retrospectively analyzed data from 1,252 patients with various conditions seen at the Nagoya University Hospital Department of Dermatology between 1994 and 2020, and from 244 patients with idiopathic interstitial pneumonia (IIP) seen at the Tosei General Hospital Department of Respiratory Medicine between 2007 and 2015 (2). We investigated anti-Th/To antibodies in serum samples by enzyme-linked immunosorbent assay and immunoprecipitation using the recombinant RPP25 and human pyrin only protein 1 (hPOP-1) proteins produced by in vitro transcription/translation according to our established protocol (2). Seventeen patients had antibodies to RPP25 and/or hPOP-1, including 6 of 249 patients with SSc, 3 of 244 patients with IIP, 2 of 12 patients with overlap syndrome without overlapping SSc, 2 of 141 patients with systemic lupus erythematosus, 1 of 134 patients with primary Sjögren's syndrome, 1 of 187 patients with dermatomyositis, 1 of 33 patients with rheumatoid arthritis, and 1 of 23 patients with Raynaud's disease. These results demonstrate that anti-Th/To antibodies can be present in the setting of various autoimmune conditions.

The clinical features of the SSc patients with anti-Th/To antibodies are shown in Table 1. Two patients also had anticentromere antibodies, although none of the anti-Th/To antibody–positive patients had other SSc-related antinucleolar antibodies (anti-PM/Scl, anti–U3 RNP, or anti–NOR 90), anti–RNA polymerase III antibodies, or anti–topoisomerase I antibodies. Four of the anti-Th/To antibody–positive SSc patients had interstitial lung disease (ILD), but the complication rate of ILD was not significantly higher in SSc patients with anti-Th/To antibodies than in those without (4 of 6 patients versus 74 of 196 patients experiencing ILD-related complications; $P < 0.215$).

Only 1 anti-Th/To antibody–positive SSc patient developed cancer within 3 years of SSc onset; however, there was no significant difference in the rate of cancer development within 3 years of disease onset between the anti-Th/To antibody–positive and anti-Th/To antibody–negative SSc patients (1 of 6 patients versus 6 of 197 patients developing cancer within 3 years; $P < 0.193$). Moreover, 5 anti-Th/To antibody–positive SSc patients had a history of cancer, and cancer incidence was higher in the SSc patients with anti-Th/To antibodies versus those without (5 of 6 patients versus 31 of 197 patients with incident cancer; $P < 0.00072$). The duration of follow-up did not differ significantly between the anti-Th/To antibody–positive and anti-Th/To antibody–negative groups (median follow-up 10.8 years [interquartile range 3.3–31] versus 18.6 years [interquartile range 0.1–46]; $P < 0.282$). One anti-Th/To antibody–positive SSc patient did not have cancer, although he had been followed up for only 2 years.

One of our major concerns regarding the study by Mecoli et al (1) is that it lacks a description of the causes of death in the anti-Th/To antibody–positive SSc patients. Although none of the anti-Th/To antibody–positive SSc patients from our study have died to date, 8 (27.6%) of 29 deaths in our SSc cohort were cancer-related. Our study suggests that anti-Th/To antibody–positive patients need long-term follow-up.

Table 1. Clinical features of the SSc patients with anti-Th/To antibodies*

Patient/age (years)/sex	SSc subtype	IIF pattern†	Anti-RPP25/ anti–hPOP-1	Other SSc-related antibodies	ILD/ PAH	Cancer (age at onset, years)	Years from SSc onset to cancer development	Years of observation
1/38/F	Limited	AC-3; AC-8	+/+	ACA	+/–	Colon (55)	7	31
2/44/F	Limited	AC-8	+/+	–	–/–	Right breast (44), left breast (62)	0 (right), 18 (left)	27
3/58/M	Diffuse	AC-8	+/+	–	–/–	–	–	2
4/42/F	Limited	AC-8	+/+	–	+/–	Lung (63)	21	23
5/60/F	Limited	AC-3; AC-8; AC-21	–/+	ACA	+/–	Lung (73)	13	13
6/56/F	Limited	AC-8	+/+	–	+/–	Endometrial (54)	–2‡	4

* SSc = systemic sclerosis; IIF = indirect immunofluorescence; hPOP-1 = human pyrin only protein 1; ILD = interstitial lung disease; PAH = pulmonary arterial hypertension; AC = anti-cell; ACA = anticentromere antibody.
† Evaluation of IIF pattern is based on the International Consensus on Antinuclear Antibody Patterns.
‡ Patient 6 was diagnosed as having cancer 2 years before the onset of SSc.

Author disclosures are available at https://onlinelibrary.wiley.com/action/downloadSupplement?doi=10.1002%2Fart.41945&file=art41945-sup-0001-Disclosureform.docx.

Yuta Yamashita, MD
Yoshinao Muro, MD, PhD
Haruka Koizumi, MD
Takuya Takeichi, MD, PhD
Nagoya University Graduate School of Medicine
Nagoya, Japan
Yasuhiko Yamano, MD, PhD
Yasuhiro Kondoh, MD, PhD
Tosei General Hospital
Seto, Japan
Masashi Akiyama, MD, PhD
Nagoya University Graduate School of Medicine
Nagoya, Japan

1. Mecoli CA, Adler BL, Yang Q, Hummers LK, Rosen A, Casciola-Rosen L, et al. Cancer in systemic sclerosis: analysis of antibodies against components of the Th/To complex. Arthritis Rheumatol 2021; 73:315–23.
2. Yamashita Y, Yamano Y, Muro Y, Ogawa-Momohara M, Takeichi T, Kondoh Y, et al. Clinical significance of anti-NOR90 antibodies in systemic sclerosis and idiopathic interstitial pneumonia. Rheumatology (Oxford) 2021. doi: 10.1093/rheumatology/keab/575. E-pub ahead of print.

DOI 10.1002/art.41957

VEXAS syndrome with systemic lupus erythematosus: expanding the spectrum of associated conditions

To the Editor:

An article recently published in *The New England Journal of Medicine* reports the use of a genotype-driven approach to identify VEXAS syndrome (vacuoles, E1 enzyme, X-lined, autoinflammatory, somatic) (1). VEXAS syndrome is characterized by the presence of somatic mutations affecting p.Met41 in the *UBA1* gene. In the study by Dr. Beck and colleagues, all of the patients identified as having *UBA1* mutations were adult men who had recurrent fevers, cytopenias, dysplastic bone marrow with vacuoles in myeloid and erythroid precursors, and neutrophilic skin and lung tissue inflammation, and often had treatment-refractory and fatal disease courses. The various conditions occurring in conjunction with VEXAS syndrome (i.e., comprising a potential phenotype for VEXAS syndrome) included relapsing polychondritis, giant cell arteritis, polyarteritis nodosa, Sweet syndrome, myelodysplastic syndrome, and multiple myeloma.

To further clarify these disease traits, we would like to describe a previously unreported case of VEXAS syndrome in association with a diagnosis of systemic lupus erythematosus (SLE). In February 2020, a 70-year-old man presented to our hospital with an 8-month history of recurrent fevers, polyarthralgia, erythematous skin rash over the trunk, left leg venous thrombosis, and weight loss. Laboratory tests revealed macrocytic anemia, leukopenia, and neutropenia, as well as an increased erythrocyte sedimentation rate (99 mm/hour) and C-reactive protein level (33 mg/liter). The patient was positive for antinuclear antibodies (titer 1:80 in a fine speckled pattern) and anti–Scl-70 antibodies. His serum C3 level was below the normal range (73 mg/dl), while the serum C4 level was in the lower range of normal (23 mg/dl). Test results for anti–double-stranded DNA, anti-Ro, anti-La, and antiphospholipid antibodies were negative. Bone marrow examination showed hypercellular marrow with borderline megakaryocytic dysplasia. The patient was diagnosed as having late-onset SLE, accompanied by disease manifestations of cytopenias and polyarthralgia, and oral treatment with glucocorticoids (0.5.mg/kg/day) was initiated. Subsequently, the patient's fever subsided, and improvements in the cytopenias and arthralgia were observed.

In August 2020, the patient developed fever and lung nodules while receiving prednisolone at a dosage of 5 mg/day.

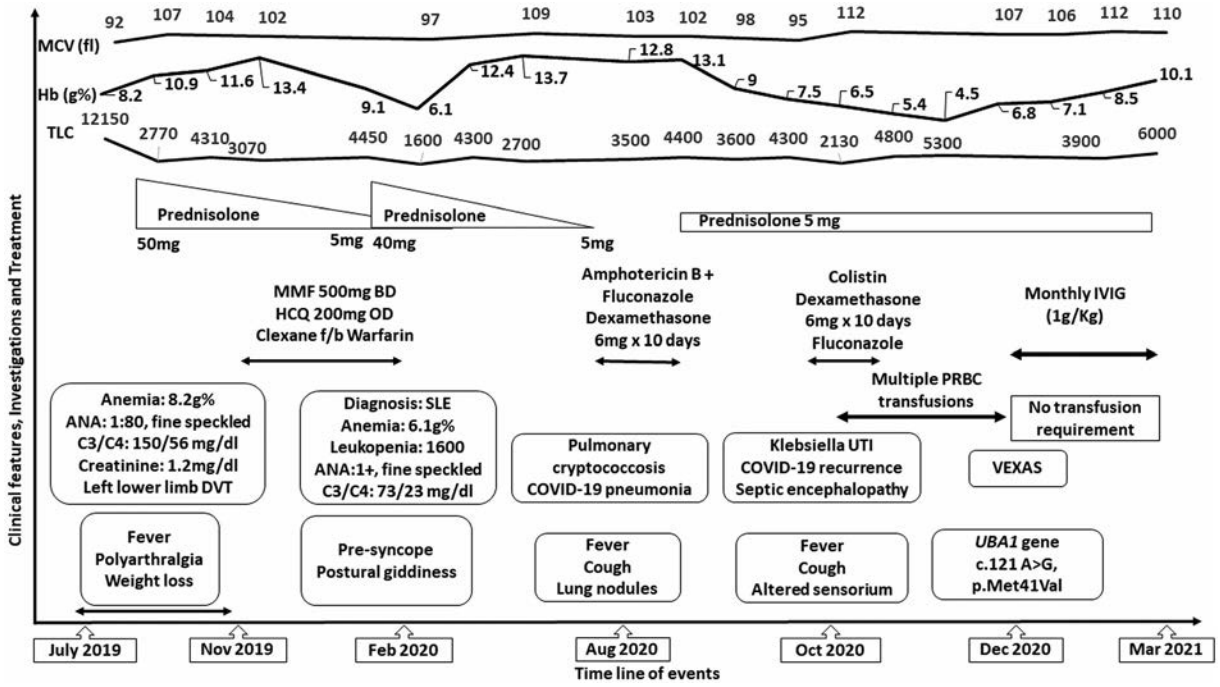

Figure 1. Time course of the clinical manifestations and response to therapy in a patient with a diagnosis of VEXAS syndrome in association with systemic lupus erythematosus (SLE). MCV = mean corpuscular volume; Hb = hemoglobin; TLC = total leukocyte count; MMF = mycophenolate mofetil; BD = twice per day; HCQ = hydroxychloroquine; OD = once per day; f/b = followed by; IVIG = intravenous immunoglobulin; PRBC = packed red blood cell; ANA = antinuclear antibodies; DVT = deep vein thrombosis; UTI = urinary tract infection; VEXAS = vacuoles, E1 enzyme, X-linked, autoinflammatory, somatic syndrome.

Fine-needle aspiration of the nodules revealed cryptococcal organisms. The patient was started on amphotericin B and fluconazole for pulmonary cryptococcosis, after which his fever subsided. However, while he was hospitalized, his fever and dry cough recurred, and testing for SARS–CoV-2 with nasopharyngeal swab and polymerase chain reaction (PCR) yielded positive findings for SARS–CoV-2 infection. In accordance with the hospital's COVID-19 protocols, the patient received treatment with glucocorticoids and heparin, and was subsequently discharged after 20 days. In October 2020, he again developed fever, breathlessness, and altered mental status and was found to have a *Klebsiella pneumoniae*–associated urinary tract infection. He received intravenous antibiotics but experienced respiratory failure. Mechanical ventilation was instituted, and subsequently, the patient again tested positive for SARS–CoV-2 by PCR. Treatment with intravenous dexamethasone was started, and thereafter the patient's symptoms improved and he was discharged from the hospital.

A potential diagnosis of VEXAS syndrome was considered for this patient, based on his clinical profile, older age, and history of fevers, neutropenia, skin lesions, and treatment-refractory symptoms. Slides of bone marrow samples that had been collected previously were reviewed and showed the presence of megakaryocytic dysplasia, toxic granulations, and vacuoles in myeloid precursors in the bone marrow. VEXAS syndrome was confirmed based on detection of a c.121A>G, p.Met41Val mutation in the *UBA1* gene. Monthly intravenous immunoglobulin (1 gm/kg/month) was initiated in December 2020. At the patient's last visit, in March 2021, his hemoglobin level had increased and he did not require a blood transfusion. Fever and leukopenia also resolved. Figure 1 shows the details of the patient's clinical course and response to treatment.

This is, to our knowledge, the first reported case of VEXAS syndrome in association with SLE, thus expanding the list of autoimmune diseases associated with VEXAS syndrome. While this patient met the 2019 European Alliance of Associations for Rheumatology/American College of Rheumatology classification criteria for SLE and the Systemic Lupus International Collaborating Clinics classification criteria for SLE (2,3), whether he has true SLE or an SLE-like phenotype might become clearer with follow-up.

Aman Sharma, MD, FRCP
Gsrsnk Naidu, DM
Prateek Deo, MD
Post Graduate Institute of Medical Education and Research
Chandigarh, India
David B. Beck, MD, PhD
National Human Genome Research Institute
NIH
Bethesda, MD

1. Beck DB, Ferrada MA, Sikora KA, Ombrello AK, Collins JC, Pei W, et al. Somatic mutations in UBA1 and severe adult-onset autoinflammatory disease. N Engl J Med 2020;383:2628–38.
2. Aringer M, Costenbader K, Daikh D, Brinks R, Mosca M, Ramsey-Goldman R, et al. 2019 European League Against Rheumatism/American College of Rheumatology classification criteria for systemic lupus erythematosus. Arthritis Rheumatol 2019;71:1400–12.
3. Petri M, Orbai AM, Alarcón GS, Gordon C, Merrill JT, Fortin PR, et al. Derivation and validation of the Systemic Lupus International Collaborating Clinics classification criteria for systemic lupus erythematosus. Arthritis Rheum 2012;64:2677–86.

DOI 10.1002/art.41944

Long-term extension study of tofacitinib in refractory dermatomyositis

To the Editor:

In our study evaluating the 12-week outcomes of tofacitinib treatment in patients with refractory dermatomyositis (DM) in a prospective, open-label clinical trial, as recently reported in *Arthritis & Rheumatology* (1), we demonstrated that tofacitinib was effective in treating skin-predominant refractory DM at 12 weeks. We now want to report the results from the long-term extension phase evaluating the durability of the efficacy of tofacitinib at 96 weeks in patients with refractory DM. In this extension study, we applied the same inclusion criteria and outcome measures as were used in the 12-week parent study (1). Patients were assessed at weeks 20, 72, and 96. The baseline demographic features of all 10 trial patients were reported previously (1).

All 10 patients continued treatment with tofacitinib for 20 weeks. The median total improvement score according to the 2016 American College of Rheumatology/European Alliance of Associations for Rheumatology myositis response criteria (2) at week 20 was 35 (interquartile range [IQR] 32.5–37.5) (Figure 1A). This represented a sustained moderate response given that the median total improvement score at week 12 (the primary end point of the original trial) was 35 (IQR 25–55). Methotrexate was added to the treatment regimen of 1 subject with refractory DM, in whom inflammatory arthritis had developed.

After the week 20 visit, 7 patients (70%) continued to receive tofacitinib treatment for a mean ± SD of 1.2 ± 0.47 years and then entered a follow-up period of up to 96 weeks. At 72 weeks and 96 weeks, median total improvement score values were 35 (IQR 25–37.5) and 25 (IQR 20–37.5), respectively. The lower median total improvement score was driven by 1 patient whose score dropped to 15. Two patients continued combination therapy with methotrexate. Throughout the 96-week extension study, no additional glucocorticoids were required to treat disease flares. Of note, all patients had full muscle strength at baseline; this remained unchanged for the duration of the study.

Compared to baseline, the Cutaneous Dermatomyositis Disease Area and Severity Index score (3) declined significantly at 96 weeks (mean ± SD 25.4 ± 15.0 at baseline to 4.71 ± 2.63 at 96 weeks; $P = 0.02$), and a notable resolution of cutaneous clinical symptoms was observed in all patients (a representative patient is shown in Figure 1B). Chemokine (CXCL9/CXCL10) levels also decreased by 72 weeks, but were trending upward at 96 weeks. Among all 10 patients, the median level of CXCL9 was 98.2 pg/ml (IQR 67.2–176) at baseline; this dropped to a median of 50.7 pg/ml (IQR 38.6–111) at 72 weeks ($P = 0.04$) and a median of 65.5 pg/ml (IQR 31.1–156) at 96 weeks ($P = 0.07$). The median levels of CXCL10 at each time point were as follows: 190 pg/ml (IQR 105–4,067) at baseline, 130 pg/ml (IQR 79.3–224) at 72 weeks ($P = 0.06$), and 185 pg/ml (IQR 87.3–354) at 96 weeks ($P = 0.07$). No serious adverse events occurred, and no patient discontinued treatment with tofacitinib.

These results indicate tofacitinib was safe and clinically beneficial in refractory DM for up to 96 weeks. Overall, all 7 patients met the International Myositis Assessment and Clinical Studies definition of improvement at 20 weeks and 72 weeks, while 6 (86%) of 7 patients met this at 96 weeks (4). The median total improvement score was 35 at both 20 weeks and 72 weeks, demonstrating an overall moderate response in the 7 patients.

Limitations of this study are the open-label design and small sample size. Nevertheless, the prospective design of the study, which included the standardized collection of data on validated outcome measures and long-term follow-up of ~2 years, highlights the durable therapeutic potential of JAK inhibitors in the treatment of DM.

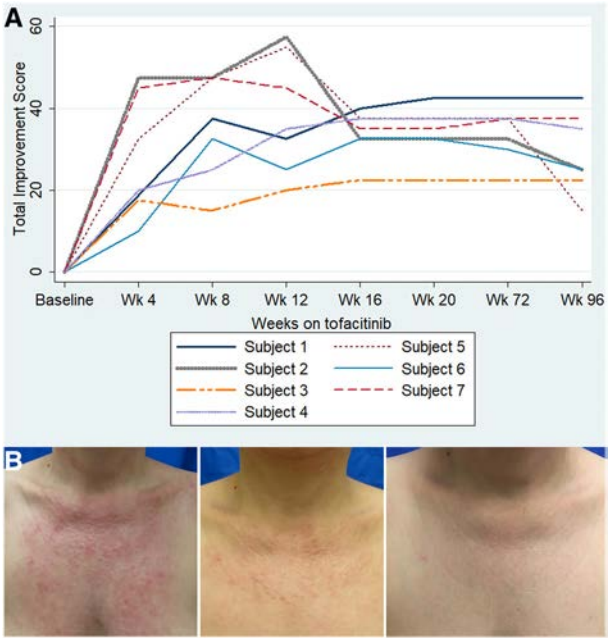

Figure 1. **A**, Change in total improvement score over the 96-week study period, as assessed using the 2016 American College of Rheumatology/European Alliance of Associations for Rheumatology myositis response criteria in 7 subjects with active dermatomyositis treated with tofacitinib. **B**, Assessment of skin disease activity in a representative subject with dermatomyositis showing improvement of clinical symptoms in the chest skin from baseline (left) to 12 weeks (middle) and 96 weeks (right) after tofacitinib treatment.

The Rheumatic Diseases Research Core Center, where antibodies and chemokines were assayed, is supported by NIH grant P30-AR-070254. Dr. Paik's work was supported in part by NIH grant K23-AR-073927 and by Pfizer. Drs. Albayada and Tiniakou's work was supported by the Jerome L. Greene Foundation. Dr. D. Leung's work was supported by the National Institute of Neurological Disorders and Stroke, NIH (Mentored Patient-Oriented Research Career Development award 5K23-NS-091379). Dr. Christopher-Stine's work was supported in part by the Donald B. and Dorothy L. Stabler Foundation and by Pfizer. Author disclosures are available at https://onlinelibrary.wiley.com/action/downloadSupplement?doi=10.1002%2Fart.41944&file=art41944-sup-0001-Disclosureform.pdf.

Julie J. Paik, MD, MHS
Matthew Shneyderman
Laura Gutierrez-Alamillo, MD
Jemima Albayda, MD
Eleni Tiniakou, MD
Jamie Perin, PhD
Grazyna Purwin, BA
Sherry Leung, BA
Doris Leung, MD, PhD
Livia Casciola-Rosen, PhD
Johns Hopkins University
Baltimore, MD

Andrew S. Koenig, DO
CSL Behring
King of Prussia, PA
Lisa Christopher-Stine, MD, MPH
Johns Hopkins University
Baltimore, MD

1. Paik JJ, Casciola-Rosen L, Shin JY, Albayda J, Tiniakou E, Leung DG, et al. Study of tofacitinib in refractory dermatomyositis: an open-label pilot study of 10 patients. Arthritis Rheumatol 2021;73:858–65.
2. Aggarwal R, Rider LG, Ruperto N, Bayat N, Erman B, Feldman BM, et al. 2016 American College of Rheumatology/European League Against Rheumatism criteria for minimal, moderate, and major clinical response in adult dermatomyositis and polymyositis: an International Myositis Assessment and Clinical Studies Group/Paediatric Rheumatology International Trials Organisation collaborative initiative. Arthritis Rheumatol 2017;69:898–910.
3. Anyanwu CO, Fiorentino DF, Chung L, Dzuong C, Wang Y, Okawa J, et al. Validation of the Cutaneous Dermatomyositis Disease Area and Severity Index: characterizing disease severity and assessing responsiveness to clinical change. Br J Dermatol 2015;173:969–74.
4. Rider LG, Giannini EH, Brunner HI, Ruperto N, James-Newton L, Reed AM, et al, for the International Myositis Assessment and Clinical Studies Group. International consensus on preliminary definitions of improvement in adult and juvenile myositis. Arthritis Rheum 2004;50:2281–90.